UNIVERSITÉ DE STRASBOURG

ÉCOLE DOCTORALE MSII n°269

UMR 7501

THÈSE présentée par :

Mathieu Lutz

soutenue le : **24 octobre 2013**

pour obtenir le grade de : **Docteur de l'université de Strasbourg**

Discipline/ Spécialité : Mathématiques Appliquées

Étude mathématique et numérique d'un modèle gyrocinétique incluant des effets électromagnétiques pour la simulation d'un plasma de Tokamak.

THÈSE dirigée par :

M. Sonnendrücker Éric	Professeur, université de Strasbourg
M. Frénod Emmanuel	Professeur, université de Bretagne-Sud

RAPPORTEURS :

M. Bostan Mihaï	Professeur, université Aix-Marseille
M. Méhats Florian	Professeur, université de Rennes 1

AUTRES MEMBRES DU JURY :

Mme. Audin Michèle	Professeur, université de Strasbourg
M. Helluy Philippe	Professeur, université de Strasbourg

Remerciements

Je tiens à adresser mes premiers remerciements à Emmanuel Frénod et à Éric Sonnendrücker qui ont co-encadré ma thèse durant ces trois années avec beaucoup de disponibilité et de gentillesse. Je remercie Emmanuel d'avoir été si présent et de m'avoir encouragé en toutes circonstances. J'ai pu bénéficier de ses larges connaissances, son esprit critique et sa vivacité d'esprit pour avancer toujours plus loin dans mes recherches. Il m'a guidé avec bienveillance tout au long de cette thèse et je lui en suis très reconnaissant. Je remercie Eric de m'avoir orienté d'abord pour mon mémoire de Master puis durant ces trois années. Il a toujours été disponible pour partager sa grande expérience et son savoir. Merci pour la confiance qu'il m'a accordée.

J'aimerais ensuite remercier Mihaï Bostan et Florian Méhats qui m'ont fait l'honneur de rapporter ce manuscrit. Ils ont accordé de leur précieux temps à la relecture attentive de ma thèse.

J'aimerais également exprimer ma gratitude à Michèle Audin, Philippe Helluy et Bruno Després d'avoir accepté de faire partie de mon jury. Je remercie une deuxième fois Michèle Audin pour nos discussions sur la géométrie symplectique.

Je remercie de tout coeur Sever Hirstoaga pour sa gentillesse, sa disponibilité, sa patiente ainsi que pour les nombreuses discussions que nous avons eu sur la physique des plasmas. Je le remercie également pour tout les conseils qu'il m'a donné. De plus, c'est un réel plaisir de travailler avec lui.

Je remercie également Olivier Lader pour sa disponibilité et son aide pour quelques preuves du second chapitre.

Les enseignements ont toujours été un moment agréable en grande partie grâce à ceux avec qui je les ai partagé : merci à Ambroise, Thomas et Viktoria.

C'est l'équipe EDP de l'IRMA qui m'a accueillie durant ces trois années. Son dynamisme et son ambiance très sympathique m'ont offert un cadre de travail idéal, c'est pourquoi je souhaite en remercier tous les membres actuels et anciens.

Je remercie les doctorants avec qui j'ai partagé de très bons moments à faire autre chose que des maths. Merci à Olivier, Ambroise, Anais, Christophe, Nhung, Ahmed et ceux que j'oublie. Merci à Anais d'avoir répondu à mes nombreuses questions d'ordre administrative. Je remercie particulièrement Jonathan avec qui j'ai partagé mon bureau, quelques centaines de RU, et de nombreuses discussions.

J'en profite pour remercier toutes les personnes que j'ai rencontré au cours de conférences et de séminaires. La liste serait beaucoup trop longue mais ils ont chacun à leur manière fait partie de cette histoire ...

Je suis également très reconnaissant envers le personnel administratif et technique de de l'IRMA et de l'UFR, les ingénieurs informatiques, les agents de la bibliothèque et les secrétaires qui font tous un travail remarquable.

Je n'oublie pas mes amis. Merci à Francois et Cécile pour leur bonne humeur perpétuelle et communicative. Merci à Emmanuel, Guilhème, Nicolas, Muriel et Jérémy pour leur

soutien avant l'oral de cette thèse.

Je souhaite enfin remercier ma famille à qui je dois énormément. Cousins, cousines, oncles, tantes et grand-parents, merci de votre présence qui est très importante pour moi. Je remercie enfin mes parents pour leur soutien moral sans faille pendant toutes ces années.

Enfin, une page de remerciements serait nécessaire mais je vais faire court, merci pour tout Auriane.

Résumé

Cette thèse propose différentes méthodes théoriques et numériques dont l'objectif est de simuler à coût réduit le comportement des plasmas ou des faisceaux de particules chargées sous l'action d'un champ magnétique fort. Le plan de cette thèse est le suivant.

Chapitre 1

Cette thèse s'ouvre sur une introduction à la modélisation des plasmas et des faisceaux de particules chargées. Dans un premier temps, je décris le contexte physique qui est de confiner un faisceau de particules chargées grâce à un champ magnétique fort, dans une structure de forme toroïdale appelée Tokamak. Puis je présente quelques trajectoires d'une particule chargée sous l'action d'un champ magnétique fort. Par ces exemples, j'introduis les concepts fondamentaux d'adimensionnement et de recherche d'invariants pour réduire la dimension du problème. En outre, bien que ces trajectoires ne tiennent pas compte des effets collectifs, elles donnent de nombreuses informations lorsque l'effet du champ magnétique est prépondérant sur l'effet collectif. Je présente ensuite les équations de Vlasov-Poisson qui décrivent l'évolution d'un faisceau de particules chargées sous l'action d'un champ magnétique externe. Je rappelle quelques estimations classiques, ainsi que les principaux résultats d'existence et d'unicité. J'expose également les principales difficultés liées à la simulation numérique d'un faisceau de particules chargées, notamment sous l'action d'un champ magnétique fort, et je décris une méthode numérique classique appelée la méthode PIC (Particle In Cell). Finalement, je rappelle le principe de deux méthodes permettant d'aboutir à des modèles réduits : la méthode d'homogénéisation basée sur la convergence à deux échelles, et la méthode Gyro-cinétique basée sur des changements de coordonnées permettant de réduire la dimension du problème.

Chapitre 2

Dans ce chapitre nous considérons un système dynamique hamiltonien décrivant le mouvement d'une particule chargée sous l'action d'un champ magnétique fort et nous construisons un changement de coordonnées pour réduire la dimension du système.

Considérons une variété différentielle $\mathcal{M}$. Un système dynamique hamiltonien (sur $\mathcal{M}$) est un système dynamique qui s'écrit dans tout système de coordonnées sous la forme :

$$\frac{\partial \mathbf{R}}{\partial t} = \mathcal{P}\left(\mathbf{R}\right) \nabla_{\mathbf{r}} H\left(\mathbf{R}\right). \tag{0.0.1}$$

Dans la formule (0.0.1) $\mathcal{P}$ est une matrice antisymétrique appelée la matrice du crochet de Poisson, et H est une fonction régulière appelée hamiltonien du système dynamique. Bien évidemment, les expressions de $\mathcal{P}$ et de H dépendent du système de coordonnées.

L'objectif du changement de coordonnées que nous construisons est de déterminer un système de coordonnées proche du système de coordonnées centre guide historique :

$$\begin{aligned} y_1^{hgc} &= x_1 - \varepsilon \frac{v}{B(\mathbf{x})} \cos(\theta), \\ y_2^{hgc} &= x_2 + \varepsilon \frac{v}{B(\mathbf{x})} \sin(\theta), \\ \theta^{hgc} &= \theta, \\ \mu^{hgc} &= \frac{v^2}{2B(\mathbf{x})}, \end{aligned}$$

dans lequel la matrice de Poisson et le hamiltonien satisfont les hypothèses du théorème suivant :

Théorème 0.0.1. *Si dans un système de coordonnées* $\mathbf{r} = (r_1, r_2, r_3, r_4)$, *la matrice de Poisson est sous la forme :*

$$\mathcal{P}(\mathbf{r}) = \left(\begin{array}{c|cc} \mathbb{M}_{(\mathbf{r})} & \begin{matrix} 0 & 0 \\ 0 & 0 \end{matrix} \\ \hline \begin{matrix} 0 & 0 \\ 0 & 0 \end{matrix} & \begin{matrix} 0 & 1 \\ -1 & 0 \end{matrix} \end{array}\right), \tag{0.0.2}$$

et si le hamiltonien ne dépend pas de l'avant dernière variable, i.e.

$$\frac{\partial H}{\partial r_3} = 0, \tag{0.0.3}$$

alors la matrice $\mathtt{M}$ *ne dépend pas des deux dernières variables, i.e.*

$$\frac{\partial \mathtt{M}}{\partial r_3} = 0 \text{ and } \frac{\partial \mathtt{M}}{\partial r_4} = 0. \tag{0.0.4}$$

Par conséquent l'évolution des deux premières composantes de la trajectoire $\mathbf{R}_1, \mathbf{R}_2$ *est indépendante de l'avant dernière composante* $\mathbf{R}_3$ *; et la dernière composante de la trajectoire* $\mathbf{R}_4$ *ne dépend pas du temps, i.e.*

$$\frac{\partial \mathbf{R}_4}{\partial t} = 0. \tag{0.0.5}$$

La succession de changement de coordonnées conduisant au système de coordonnées satisfaisant les hypothèses du Théorème 0.0.1 est donnée dans la Figure 1. Ce système de coordonnées est appelé le système de coordonnées Gyro-cinétique.

Le système dynamique de départ est donné dans la Figure 1 en haut à gauche. La première étape (flèche 1) consiste à vérifier que ce système dynamique est hamiltonien. La seconde étape (flèche 2) consiste à réécrire le système dynamique originel sous forme hamiltonienne. Puis (flèche 3), on fait un changement de coordonnées polaire en vitesse. La quatrième étape (flèche 4) consiste à déterminer un système de coordonnées proche du système de coordonnées centre guide historique dans lequel la matrice de Poisson a la forme requise pour appliquer le Théorème 0.0.1. Pour déterminer ce changement de coordonnées, on utilise les formules de changement de coordonnées pour la matrice de Poisson (à priori) afin de se ramener à la résolution d'un système d'équations aux dérivées partielles hyperboliques. Au terme de la troisième étape, la matrice de Poisson est sous la forme requise pour appliquer le Théorème 0.0.1. Cependant, le hamiltonien $\overline{H}_\varepsilon$ dépend (à partir de l'ordre 1 en ε) de la variable d'oscillation θ. Ainsi, la dernière étape (flèche 5) consiste à faire un

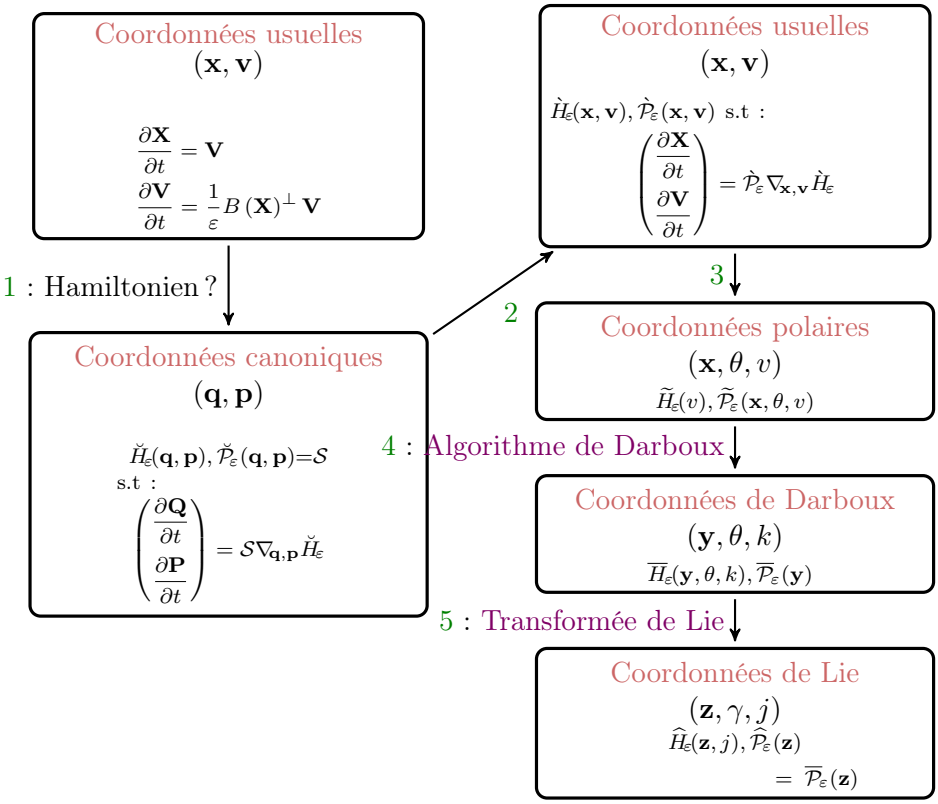

FIGURE 1 – Description schématique de la méthode qui aboutit aux coordonnées Gyrocinétique.

changement de coordonnées infinitésimal qui ne modifie pas la matrice de Poisson, de sorte que dans le nouveau système de coordonnées $(\mathbf{z}, \gamma, j)$ le hamiltonien ne dépende pas de la variable d'oscillation γ. Détaillons les étapes 4 et 5.

En notant $\boldsymbol{\Upsilon} = (\boldsymbol{\Upsilon}_1, \boldsymbol{\Upsilon}_2, \boldsymbol{\Upsilon}_3, \boldsymbol{\Upsilon}_4)$ le changement de coordonnées symbolisé par la flèche 4, les formules de changement de coordonnées impliquent que l'entrée (i, j) de la matrice de Poisson $\overline{\mathcal{P}}_\varepsilon$ est donnée par :

$$\left(\overline{\mathcal{P}}_\varepsilon\right)_{i,j}(\mathbf{y}, \theta, k) = \left\{\boldsymbol{\Upsilon}_i, \boldsymbol{\Upsilon}_j\right\}_{\mathbf{x},\theta,\mathbf{v}}\left(\boldsymbol{\Upsilon}^{-1}(\mathbf{x}, \theta, v)\right). \tag{0.0.6}$$

Pour déterminer ce changement de coordonnées, il suffit de trouver une fonction $\boldsymbol{\Upsilon}$ qui satisfasse les équations aux dérivées partielles :

$$\begin{aligned} &\{\boldsymbol{\Upsilon}_1, \boldsymbol{\Upsilon}_4\} = 0, \qquad &&\{\boldsymbol{\Upsilon}_1, \boldsymbol{\Upsilon}_3\} = 0, \\ &\{\boldsymbol{\Upsilon}_2, \boldsymbol{\Upsilon}_4\} = 0, \qquad &&\{\boldsymbol{\Upsilon}_2, \boldsymbol{\Upsilon}_3\} = 0, \\ &\{\boldsymbol{\Upsilon}_3, \boldsymbol{\Upsilon}_4\} = 1/\varepsilon, \end{aligned} \tag{0.0.7}$$

puis de vérifier que la fonction obtenue est bien un difféomorphisme. A noter que dans le but de gérer le petit paramètre ε, nous avons remplacé 1 par $1/\varepsilon$ dans (0.0.2). Pour résoudre ces équations, on pose $\boldsymbol{\Upsilon}_3 = \theta$ et on impose les conditions aux limites de sorte que en $v = 0$, le système de coordonnées centre guide historique et le système de coordonnées de Darboux coïncident ; i.e.

$$\boldsymbol{\Upsilon}_1(\mathbf{x}, \theta, v = 0) = x_1, \tag{0.0.8}$$
$$\boldsymbol{\Upsilon}_2(\mathbf{x}, \theta, v = 0) = x_2, \tag{0.0.9}$$
$$\boldsymbol{\Upsilon}_4(\mathbf{x}, \theta, v = 0) = 0. \tag{0.0.10}$$

La principale nouveauté que nous avons introduit dans cette étape correspond à la façon dont nous avons résolu ces équations. En effet, nous avons basé la résolution de ces équations sur la résolution d'une autre EDP :

$$-\varepsilon \boldsymbol{\Lambda}^1 \cdot \varphi - \frac{\partial \varphi}{\partial v} = 0, \tag{0.0.11}$$
$$\varphi(\mathbf{x}, \theta, 0) = \frac{1}{B(\mathbf{x})}, \tag{0.0.12}$$

où $\boldsymbol{\Lambda}$ est le champ de vecteur définit par :

$$\boldsymbol{\Lambda}(\mathbf{x}, \theta) = \frac{\cos(\theta)}{B(\mathbf{x})}\frac{\partial}{\partial x_1} - \frac{\sin(\theta)}{B(\mathbf{x})}\frac{\partial}{\partial x_2}. \tag{0.0.13}$$

En utilisant une méthode des caractéristiques géométriques, nous avons alors montré que cette EDP admettait pour unique solution la fonction

$$\varphi(\mathbf{x}, \theta, v) = \frac{1}{B\left(\mathcal{G}^1_{-\varepsilon v}(\mathbf{x}, \theta), \mathcal{G}^2_{-\varepsilon v}(\mathbf{x}, \theta)\right)}, \tag{0.0.14}$$

où $\mathcal{G}_\lambda$ correspond au flot du champ de vecteur $\boldsymbol{\Lambda}$. Nous avons ainsi montré que $\boldsymbol{\Upsilon}$ était donnée par

$$\boldsymbol{\Upsilon}_1(\mathbf{x}, \theta, v) = x_1 - \varepsilon \cos(\theta)\, \psi(\mathbf{x}, \theta, v), \tag{0.0.15}$$
$$\boldsymbol{\Upsilon}_2(\mathbf{x}, \theta, v) = x_2 + \varepsilon \sin(\theta)\, \psi(\mathbf{x}, \theta, v), \tag{0.0.16}$$
$$\boldsymbol{\Upsilon}_4(\mathbf{x}, \theta, v) = \int_0^v \psi(\mathbf{x}, \theta, s)\, ds, \tag{0.0.17}$$

où

$$\psi(\mathbf{x},\theta,v)=\int_0^v \varphi(\mathbf{x},\theta,s)\,ds. \tag{0.0.18}$$

En procédant ainsi nous avons pu montrer que le changement de coordonnées de Darboux, qui jusqu'à présent a toujours été considéré comme un changement de coordonnées formel, est un difféomorphisme de $\mathbb{R}^3\times(0,+\infty)$ sur lui-même. De plus, ceci nous a permis de montrer que le changement de coordonnées ainsi que son inverse étaient réguliers par rapport au petit paramètre ε. Nous avons ainsi été en mesure de déterminer les développements limités du changement de coordonnées, de son inverse, du hamiltonien, et ceci tout en contrôlant les restes !

Comme je l'ai dit plus tôt, et quitte à me répéter, la dernière étape consiste à déterminer un changement de coordonnées symplectique (qui préserve la matrice de Poisson) et infinitésimal (proche de l'identité). Là encore, la principale nouveauté a été de transformer un changement de coordonnées formel en un changement de coordonnées bien posé.

Expliquons dans un premier temps le principe de la méthode formelle. Notons $\boldsymbol{\chi}_\varepsilon$ le changement de coordonnées, et $\boldsymbol{\lambda}_\varepsilon=\boldsymbol{\chi}_\varepsilon^{-1}$ son inverse. Soit $\mathbf{d}$ un champ de vecteur sur $\mathbb{R}^4$. On peut alors associer une fonction à ce champ de vecteurs en posant $\mathbf{d}(\mathbf{r})=(\mathbf{d}\cdot\mathbf{r}_1(\mathbf{r}),\mathbf{d}\cdot\mathbf{r}_2(\mathbf{r}),\mathbf{d}\cdot\mathbf{r}_3(\mathbf{r}),\mathbf{d}\cdot\mathbf{r}_4(\mathbf{r}))$, où les $\mathbf{r}_i$ correspondent aux fonctions $\mathbf{r}=(r_1,r_2,r_3,r_4)\mapsto r_i$. On appelle série de Lie associée au champ de vecteurs $\mathbf{d}$ la série formelle :

$$\mathbf{ls}_\varepsilon=\sum_{n\geq 0}\varepsilon^n\frac{\mathbf{d}^n}{n!}, \tag{0.0.19}$$

où $\mathbf{d}^n=\mathbf{d}\cdot(\mathbf{d}\cdot(\ldots))$. Lorsque $\mathbf{d}$ est un champ de vecteurs hamiltonien, la série formelle $\mathbf{ls}_\varepsilon$ satisfait les propriétés remarquables suivantes :

- $f(\mathbf{ls}_\varepsilon(\mathbf{r}))=(\mathbf{ls}_\varepsilon\cdot f)(\mathbf{r})$, pour toutes fonctions analytiques f.
- En temps que fonction, l'inverse de $\mathbf{ls}_\varepsilon$ est donnée par $\mathbf{ls}_{-\varepsilon}$.

Dans une méthode de transformée de Lie usuelle, le changement de coordonnées $\boldsymbol{\chi}_\varepsilon$ est une composition infinie de séries de Lie :

$$\boldsymbol{\chi}_\varepsilon=\ldots\circ\mathbf{ls}_{2,-\varepsilon^2}\circ\mathbf{ls}_{1,-\varepsilon^1}. \tag{0.0.20}$$

Par la suite nous noterons $\mathbf{d}_i$ le champ de vecteurs hamiltonien associé à $\mathbf{ls}_{i,\varepsilon}$. L'inverse de $\boldsymbol{\chi}_\varepsilon$ est donnée par

$$\boldsymbol{\lambda}_\varepsilon=\mathbf{ls}_{1,\varepsilon^1}\circ\mathbf{ls}_{2,\varepsilon^2}\circ\ldots \tag{0.0.21}$$

Le principe de l'algorithme formel est le suivant :

1. Les formules de changements de coordonnées pour le hamiltonien donnent $\widehat{H}_\varepsilon=\overline{H}_\varepsilon\circ\boldsymbol{\lambda}_\varepsilon$.
2. On en déduit que $\widehat{H}_\varepsilon=\overline{H}_\varepsilon\circ\boldsymbol{\lambda}_\varepsilon=\ldots\cdot\mathbf{ls}_{2,\varepsilon^2}\cdot\mathbf{ls}_{1,\varepsilon^1}\cdot\overline{H}_\varepsilon$.
3. On développe $\widehat{H}_\varepsilon$ et $\overline{H}_\varepsilon$ en série de Hilbert, puis on injecte les développements dans la formule obtenue à l'étape précédente.
4. En identifiant les termes du même ordre (en ε), on aboutit à une succession d'EDP dont les inconnues sont les fonctions qui génèrent les champs de vecteurs hamiltonien $\mathbf{d}_i$ et les coefficients du DSH de $\widehat{H}_\varepsilon$.
5. On résout ces EDP en imposant principalement aux coefficients du DSH de $\widehat{H}_\varepsilon$ de ne pas dépendre de la variable d'oscillation γ et aux fonctions qui génèrent les champs de vecteurs hamiltonien d'être périodiques par rapport à γ.

Dans le chapitre 2 nous nous sommes fixés un entier N et nous avons construit un changement de coordonnées $\boldsymbol{\chi}_\varepsilon^N$ (flèche 5) qui permet d'obtenir le hamiltonien sous la forme souhaitée jusqu'à l'ordre N. Au lieu de considérer des séries de Lie formelles, nous avons utilisé des sommes de Lie partielles. La construction d'un tel changement de coordonnées a nécessité que les variables $(\mathbf{y}, \theta, k)$ soient dans un ensemble $\mathcal{D}_{\boldsymbol{\chi}} = K \times \mathbb{R} \times (c, d)$ où K est un compact et $c > 0$. Deux problèmes sont alors apparus. Premièrement, le changement de coordonnée $\boldsymbol{\chi}_\varepsilon^N$ n'est pas symplectique. D'autre part, il a fallu déterminer les conditions initiales du système originel (en haut à gauche dans la figure 1) pour lesquelles l'image des trajectoires (image par les flèches 3 et 4) est dans le domaine $\mathcal{D}_{\boldsymbol{\chi}}$. Pour régler ces deux problèmes, nous avons montré que $\boldsymbol{\chi}_\varepsilon^N$ est symplectique (la matrice de Poisson n'est pas modifiée) jusqu'à l'ordre $N-1$, et que si on considère des conditions initiales $(\mathbf{x}_0, \mathbf{v}_0)$ telles que $(\mathbf{x}_0, |\mathbf{v}_0|) \in K' \times (a, b)$, où K' est un compact inclus dans K et $\left[\frac{a^2}{2|B|_\infty}, \frac{c^2}{2}\right] \subset (c, d)$, alors pendant un intervalle de temps d'amplitude $1/\varepsilon$ l'image des trajectoires par les flèches 3 et 4 est dans $\mathcal{D}_{\boldsymbol{\chi}}$.

Finalement, nous avons montré que le système dynamique obtenu en tronquant le Hamiltonien à l'ordre N et la matrice de Poisson à l'ordre $N-1$ satisfaisait les hypothèses du théorème 0.0.1. De plus, nous avons montré que $\left\| \left(\mathbf{Z}_\varepsilon^T, \mathcal{J}_\varepsilon^T\right) - \left(\mathbf{Z}_\varepsilon, \mathcal{J}_\varepsilon\right) \right\| \leq C\varepsilon^{N-1}$, où $\left(\mathbf{Z}_\varepsilon^T, \mathcal{J}_\varepsilon^T\right)$ correspond à la trajectoire tronquée.

Chapitre 3

Dans ce chapitre nous considérons un système dynamique hamiltonien correspondant aux caractéristiques de l'équation de Vlasov qui modélise un faisceau de particules long et fin. On suppose que le faisceau est confiné par un champ électrique fort dans la direction radiale (voir Figure 2). Nous construisons alors un changement de coordonnées formel pour réduire la dimension du système. Ensuite, nous élaborons un schéma numérique pour simuler une approximation de l'équation de Vlasov-Poisson dans ce système de coordonnées.

Soit un faisceau de particules, non-relativiste, long et fin se propageant à vitesse constante v_b dans la direction (Ox_3) (voir Figure 2). Au lieu de modéliser ce faisceau par le système de Vlasov-Maxwell, nous considérons l'approximation paraxiale de ce système. Ce modèle simplifié des équations de Vlasov-Maxwell est particulièrement adapté lorsque, en plus d'être long et fin, le faisceau est dans un état stationnaire. Dans le cadre de l'approximation paraxiale, les effets du champ électromagnétique auto-consistant sont pris en compte en résolvant une équation de Poisson. Le modèle obtenu est alors similaire à un système de Vlasov-Poisson $2D$ dans lequel le temps correspond à la coordonnée x_3. En faisant l'hypothèse additionnelle que le faisceau est axisymétrique (c'est-à-dire invariant par rotation d'angle θ), et que la fonction de distribution est concentrée dans le moment

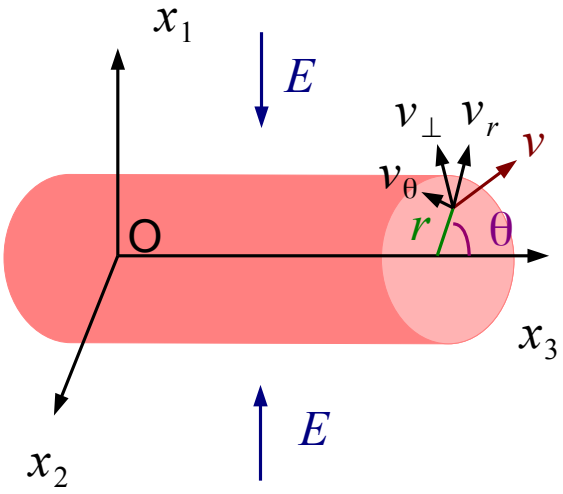

FIGURE 2 – Faisceau axisymétrique.

angulaire $rv_\theta = 0$, un adimensionnement des équations conduit au système suivant :

$$\frac{\partial f_\varepsilon}{\partial t} + \frac{v_r}{\varepsilon}\frac{\partial f_\varepsilon}{\partial r} + \left(E^\varepsilon + \Xi^\varepsilon\right)\frac{\partial f_\varepsilon}{\partial v_r} = 0, \tag{0.0.22}$$

$$-\frac{1}{r}\frac{\partial}{\partial r}\left(r\frac{\partial \phi_\varepsilon}{\partial r}\right) = \rho_\varepsilon\left(t,r\right), \quad E_\varepsilon = -\frac{\partial \phi^\varepsilon}{\partial r}, \tag{0.0.23}$$

$$\rho_\varepsilon\left(t,r\right) = \int_{\mathbb{R}} f_\varepsilon\left(t,r,v_r\right) dv_r, \tag{0.0.24}$$

$$E_\varepsilon\left(t,r=0\right) = 0, \quad \phi_\varepsilon\left(t,r=0\right) = 0, \tag{0.0.25}$$

$$f_\varepsilon\left(t=0,r,v_r\right) = f_0\left(r,v_r\right), \tag{0.0.26}$$

où le champ électrique externe est donné par $\Xi^\varepsilon = -r/\varepsilon$. Les caractéristiques de l'équation de Vlasov (0.0.22) sont obtenues en résolvant le système dynamique hamiltonien :

$$\frac{\partial \mathbf{R}^\varepsilon}{\partial t} = \partial_{v_r} H_\varepsilon\left(\mathbf{R}^\varepsilon, \mathbf{V}_r^\varepsilon, t\right), \qquad \mathbf{R}^\varepsilon\left(0,r,v_r\right) = r, \tag{0.0.27}$$

$$\frac{\partial \mathbf{V}_r^\varepsilon}{\partial t} = -\partial_r H_\varepsilon\left(\mathbf{R}^\varepsilon, \mathbf{V}_r^\varepsilon, t\right), \qquad \mathbf{V_r}^\varepsilon\left(0,r,v_r\right) = v_r. \tag{0.0.28}$$

où H_ε est défini par :

$$H_\varepsilon(r,v_r,t) = \frac{v_r^2 + r^2}{2\varepsilon} + \phi_\varepsilon(r,t). \tag{0.0.29}$$

Pour étudier ce système on se place sur la variété $\mathcal{M} = \mathbb{R}^2 \times \mathbb{R}$ munie de l'atlas $\mathcal{A}$ définit par :

- $\mathcal{A}$ contient la carte "identité" $\mathfrak{G} : \mathcal{M} \to \mathbb{R}^3; (r,v_r,t) \mapsto (r,v_r,t)$.
- $\mathcal{A}$ contient toutes les cartes $(\mathcal{U},\varphi)$ compatibles avec la carte identité et qui vérifient $\varphi_3(r,v_r,t) = t$, où φ_3 est la troisième composante de φ.

On construit le champ de vecteurs $\boldsymbol{\tau}_H^\varepsilon$ sur $\mathcal{M}$ dont l'expression dans la carte identité est donnée par :

$$\mathbf{X}_H^\varepsilon = \partial_{v_r} H_\varepsilon \partial_r - \partial_r H_\varepsilon \partial_{v_r} + \partial_t. \tag{0.0.30}$$

L'équation de Vlasov est alors caractérisée de façon intrinsèque par ce champ de vecteurs. En effet, nous montrons que dans tout système de coordonnées $(\tilde{r}, \tilde{v}_r, t)$, l'équation de Vlasov est donnée par

$$i_{\tilde{\mathbf{X}}_H^\varepsilon} d\tilde{f}^\varepsilon = \frac{\partial \tilde{f}^\varepsilon}{\partial t} + \left(\tilde{X}_H^\varepsilon\right)_1 \frac{\partial \tilde{f}^\varepsilon}{\partial \tilde{r}} + \left(\tilde{X}_H^\varepsilon\right)_2 \frac{\partial \tilde{f}^\varepsilon}{\partial \tilde{v}_r} = 0, \tag{0.0.31}$$

où $\tilde{\mathbf{X}}_H^\varepsilon$ et $\tilde{f}^\varepsilon$ correspondent aux expressions du champ de vecteurs $\boldsymbol{\tau}_H^\varepsilon$ et de la fonction de distribution dans le système de coordonnées $(\tilde{r}, \tilde{v}_r, t)$. Ensuite, nous introduisons la relation d'équivalence suivante sur l'espace des 1-formes : $\boldsymbol{\alpha} \sim \boldsymbol{\beta}$ si et seulement si $\boldsymbol{\alpha} - \boldsymbol{\beta}$ est exacte. Nous montrons alors que le champ de vecteurs $\boldsymbol{\tau}_H^\varepsilon$ est caractérisé de façon intrinsèque par la classe d'équivalence de la 1-forme de Poincaré-Cartan dont l'expression dans le système de coordonnées (r, v_r, t) est donnée par :

$$\boldsymbol{\Gamma}_H^\varepsilon (r, v_r, t) = v_r dr - H_\varepsilon dt. \tag{0.0.32}$$

En effet, nous montrons que $\forall \boldsymbol{\beta}_H^\varepsilon \in [\boldsymbol{\gamma}_H^\varepsilon]$, où $[\boldsymbol{\gamma}_H^\varepsilon]$ correspond à la classe d'équivalence de $\boldsymbol{\gamma}_H^\varepsilon$, le champ de vecteurs $\boldsymbol{\tau}_H^\varepsilon$ est caractérisé par $i_{\boldsymbol{\tau}_H^\varepsilon} d\boldsymbol{\beta}_H^\varepsilon = 0$ et $\boldsymbol{\tau}_{H,3}^\varepsilon = 1$.

Le changement de coordonnées est alors construit comme suit :
- La première étape consiste à effectuer le changement de coordonnées $(r, v_r, t) \mapsto (\mu, \theta, t)$ définit par $r = \sqrt{2\mu}\cos(\theta)$ et $v_r = \sqrt{2\mu}\sin(\theta)$.
- La seconde étape consiste à effectuer un changement de coordonnées infinitésimal de sorte que, dans le nouveau système de coordonnées, $(\tilde{\mu}, \tilde{\theta}, t)$ la première composante $\boldsymbol{\tau}_H^\varepsilon$ soit nulle et la seconde ne dépende pas de la variable d'oscillation.

Pour réaliser la seconde étape, nous introduisons une théorie des formes normales pour la classe d'équivalence de la 1-forme de Poincaré-Cartan. A l'issu de ce changement de coordonnées, nous obtenons les expressions des changements de coordonnées directs et réciproques, ainsi que le système différentiel définissant les caractéristiques sous forme de séries de Hilbert.

Après avoir tronqué le système dynamique et le changement de coordonnées, nous construisons un schéma numérique permettant de résoudre le système tronqué. Le principe de résolution approché du système (0.0.22)-(0.0.26) est alors le suivant :
- En utilisant les formules de changement de coordonnées, on détermine les conditions initiales dans le système de coordonnées $(\tilde{\mu}, \tilde{\theta}, t)$.
- On résout l'équation tronqué jusqu'au temps final de simulation.
- En utilisant les formules de changement de coordonnées réciproque, on obtient une approximation de la fonction de distribution à l'instant final de simulation.

Chapitre 4

Dans ce chapitre nous introduisons un nouveau schéma numérique pour étudier l'équation d'évolution :

$$\begin{aligned} &\partial_t f^\varepsilon + \mathbf{v} \cdot \nabla_{\mathbf{x}} f^\varepsilon + \left(\boldsymbol{\Xi}^\varepsilon + \frac{1}{\varepsilon}\mathbf{v}^\perp\right) \cdot \nabla_{\mathbf{v}} f^\varepsilon = 0, \\ &f^\varepsilon (\mathbf{x}, \mathbf{v}, t = 0) = f_0 (\mathbf{x}, \mathbf{v}), \end{aligned}$$

où $\mathbf{x} = (x_1, x_2)$ correspond à la variable de position, $\mathbf{v} = (v_1, v_2)$ à la variable de vitesse, $\mathbf{v}^\perp = (v_2, -v_1)$, $f^\varepsilon \equiv f^\varepsilon(\mathbf{x}, \mathbf{v}, t)$ est la fonction de distribution, f_0 est donnée, $\boldsymbol{\Xi}^\varepsilon \equiv \boldsymbol{\Xi}^\varepsilon(\mathbf{x}, t)$

correspond au champ électrique, et ε est un petit paramètre. Cette équation d'évolution peut être obtenue à partir de l'équation de Vlasov $6D$ dans le régime Drift-Kinetic en prenant un champ magnétique constant dans la direction x_3 et un champ électrique orthogonal au champ magnétique.

La résolution numérique est basée sur une méthode particulaire. Ce type de méthode consiste à approximer la fonction de distribution par un nombre N de macro particules dont les trajectoires sont données par :

$$\frac{\mathrm{d}\mathbf{X}^{\varepsilon}}{\mathrm{d}t} = \mathbf{V}^{\varepsilon}, \qquad \mathbf{X}^{\varepsilon}(0) = \mathbf{x}_0, \tag{0.0.33}$$

$$\frac{\mathrm{d}\mathbf{V}^{\varepsilon}}{\mathrm{d}t} = \frac{1}{\varepsilon}\left(\mathbf{V}^{\varepsilon}\right)^{\perp} + \mathbf{\Xi}^{\varepsilon}\left(\mathbf{X}^{\varepsilon}, t\right), \qquad \mathbf{V}^{\varepsilon}(0) = \mathbf{v}_0. \tag{0.0.34}$$

Lorsque le champ électrique est nul, la trajectoire d'une macro particule est un cercle de centre $\mathbf{c}_0 = \mathbf{x}_0 + \varepsilon \mathbf{v}_0^{\perp}$ et de rayon $\varepsilon |\mathbf{v}_0|$. Dans le cas général, c'est à dire en présence d'un champ électrique dépendant du temps et de la position, le système dynamique (0.0.33)-(0.0.34) correspond à une perturbation du système obtenu lorsque le champ électrique est nul. L'évolution en temps de la position d'une macro particule est alors une combinaison disparate de deux mouvements : un mouvement lent de la position qui correspondait au centre du cercle lorsque le champ électrique était nul, et une oscillation rapide autour de celui-ci. Ainsi, pour qu'un schéma classique soit suffisamment précis il est nécessaire de prendre un pas de temps plus petit que la période d'oscillation.

La nouveauté introduite dans ce chapitre est de proposer un schéma numérique permettant de résoudre de façon précise le système (0.0.33)-(0.0.34) en utilisant un pas de temps Δt nettement plus grand que la période d'oscillation.

Ce schéma est basé sur un intégrateur exponentiel en vitesse. Un intégrateur exponentiel consiste à résoudre de façon exacte le terme de raideur d'une équation du type :

$$u'(t) = \frac{u^{\perp}(t)}{\varepsilon} + F\left(t, u(t)\right), \qquad u(0) = u_0 \tag{0.0.35}$$

où ε est un petit paramètre, en effectuant une intégration par parties. La solution est alors donnée par

$$u(t) = e^{\frac{tM}{\varepsilon}} u_0 + \int_0^t e^{(t-\tau)/\varepsilon} F\left(\tau, u(\tau)\right) d\tau \tag{0.0.36}$$

où M est la matrice défini par :

$$M = \begin{bmatrix} 0 & 1 \\ -1 & 0 \end{bmatrix}. \tag{0.0.37}$$

L'algorithme de passage du temps t_n au temps $t_{n+1} = t_n + \Delta t$ est donné par :

Algorithme 0.0.2. *Supposons la solution* $(\mathbf{X}_n^{\varepsilon}, \mathbf{V}_n^{\varepsilon})$ *du système* (0.0.33)-(0.0.34) *au temps* t_n *donnée.*

1. *Calculer* $\left(\mathbf{X}^{\varepsilon}(t_n + 2\pi\varepsilon), \mathbf{V}^{\varepsilon}(t_n + 2\pi\varepsilon)\right)$ *en utilisant un solveur Runge-Kutta avec un petit pas de temps et la condition initiale* $(\mathbf{X}_n^{\varepsilon}, \mathbf{V}_n^{\varepsilon})$.
2. *Calculer* $\left(\mathbf{X}^{\varepsilon}(t_n + N \cdot (2\pi\varepsilon)), \mathbf{V}^{\varepsilon}(t_n + N \cdot (2\pi\varepsilon))\right)$ *en posant*

$$\begin{pmatrix} \mathbf{X}^{\varepsilon}(t_n + N \cdot (2\pi\varepsilon)) \\ \mathbf{V}^{\varepsilon}(t_n + N \cdot (2\pi\varepsilon)) \end{pmatrix} = \begin{pmatrix} \mathbf{X}_n^{\varepsilon} \\ \mathbf{V}_n^{\varepsilon} \end{pmatrix} + N \cdot \begin{pmatrix} \mathbf{X}^{\varepsilon}(t_n + 2\pi\varepsilon) - \mathbf{X}_n^{\varepsilon} \\ \mathbf{V}^{\varepsilon}(t_n + 2\pi\varepsilon) - \mathbf{V}_n^{\varepsilon} \end{pmatrix}. \tag{0.0.38}$$

3. *Calculer* $(\mathbf{X}^\varepsilon, \mathbf{V}^\varepsilon)$ *au temps* t_{n+1} *en utilisant un solveur Runge-Kutta avec un petit pas de temps et la condition initiale* $(\mathbf{X}^\varepsilon, \mathbf{V}^\varepsilon)$ *au temps* $t_n + N \cdot (2\pi\varepsilon)$*, obtenu à l'étape précédente.*

Cet algorithme est validé sur plusieurs cas tests. Dans un premier temps, nous avons étudié le cas où le champ électrique est donné par :

$$\mathbf{\Xi}^\varepsilon(\mathbf{x}, t) = \begin{pmatrix} 2x_1 + x_2 \\ x_1 + 2x_2 \end{pmatrix}. \tag{0.0.39}$$

Nous avons alors déterminé une expression analytique de la variété lente (conditions initiales pour lesquelles il n'y a pas d'oscillations), et nous avons comparé, pour plusieurs valeurs de ε et de Δt, notre algorithme avec une solution de référence dans les cas suivant :

- la condition initiale se réduit à une particule qui est alternativement dans, proche, et loin de la variété lente,
- la condition initiale est un faisceau de particules.

Nous avons observé que plus on s'éloigne de la variété lente plus l'erreur augmente. Néanmoins, même loin de la variété lente les résultats sont très probants. Par exemple, pour un temps final de simulation $t = 10$, $\varepsilon = 10^{-4}$, et un pas de temps Δt de l'ordre de 1500 fois la période d'oscillation, on obtient une erreur de l'ordre de $2,5 \cdot 10^{-7}$. De plus, pour tous ces cas tests, nous avons observé que de manière uniforme, plus ε est petit, plus l'erreur est petite. Nous avons ensuite testé notre algorithme lorsque l'équation de Vlasov est posée sur un tore et que le champ électrique est donné par l'équation de Poisson :

$$\mathbf{E}^\varepsilon = -\nabla\phi^\varepsilon, -\Delta\phi^\varepsilon = \int_{\mathbb{R}^2} f^\varepsilon d\mathbf{v} - 1. \tag{0.0.40}$$

A nouveau les courbes d'erreurs étaient très concluantes et nous avons observé que de manière uniforme plus ε est petit, plus l'erreur est petite.

Articles

Cette thèse est basée principalement sur les trois articles qui en sont issus :

E. Frénod, **M. Lutz**, *On the Geometrical Gyro-kinetic Theory*, (Soumis).

M. Lutz, *Application of Lie Transform Techniques for simulation of a charged particle beam*, DCDS-S Special Issue on "Numerical Methods Based on Two-Scale Convergence and Homogenization" (Accepté).

E. Frénod, **S. Hirstoaga**, **M. Lutz**, **E. Sonnendrücker** *An exponential integrator for a Vlasov-Poisson system with strong magnetic field*, (En finition).

Table des matières

Chapitre 1

Inroduction

Sommaire

1.1 Contexte physique

1.1.1 Physique des plasmas

Dans notre environnement proche la matière se décline principalement sous trois formes : solide, liquide et gazeuse. Le plasma est un autre état de la matière qui est constitué d'un mélange globalement neutre d'ions et d'électrons libres. L'ensemble des concepts, méthodes et résultats propres à l'étude de cet état de la matière constitue la physique des plasmas.

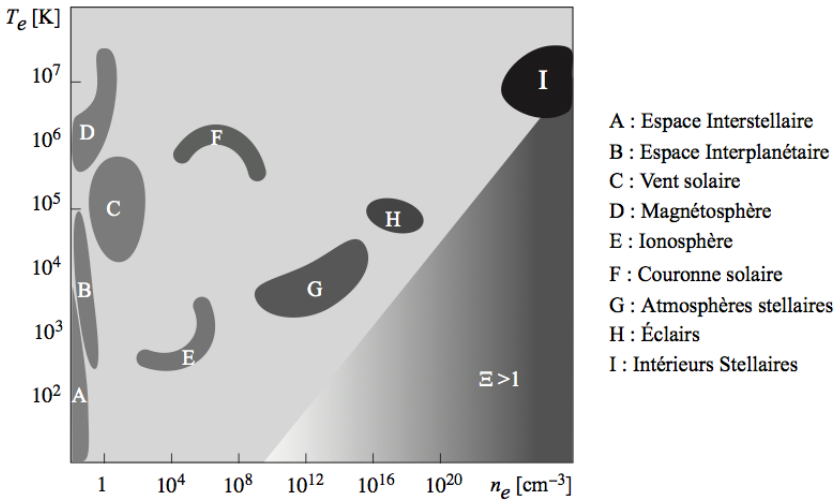

FIGURE 1.1 – Densités et températures électroniques des principaux plasmas naturels (Source : Physique des Plasmas [57]).

Cet état de la matière peut être obtenu en chauffant très fortement un gaz. Les électrons quittent alors l'orbite du noyau de l'atome auquel ils sont rattachés. Le plasma peut également se former à basse température. C'est par exemple le cas de l'ionosphère, cette couche élevée de l'atmosphère terrestre qui subit en permanence un intense bombardement ionisant de particules venant du soleil.

Bien qu'absent à l'état naturel sur terre (hormis les aurores boréales aux pôles), le plasma représente plus de $99,9\%$ de la matière visible de notre Univers. Les étoiles entre autres, quel que soit leur type, sont essentiellement des sphères de plasma. Ainsi la physique des plasmas se révèle comme étant l'outil de référence pour l'étude des problèmes d'astrophysique et de physique spatiale.

Actuellement la recherche en physique des plasmas se décline sous trois formes : la physique des plasmas industriels (les tubes à néon, les écrans plasma, les satellites de communication, la production de rayons X, la gravure par plasma en micro-électronique, etc...), la physique des plasmas thermonucléaires, et la physique des plasmas naturels, spatiaux et astrophysiques. Sur les figures 4.1 et 3.2 on peut observer les densités et températures électroniques de quelques plasmas. Dans cette thèse nous nous intéresserons exclusivement à la physique des plasmas thermonucléaires.

1.1.2 La fusion thermonucléaire contrôlée

La fusion thermonucléaire est un processus où deux noyaux atomiques légers s'assemblent pour former un noyau plus lourd. Cette réaction dégage une grande quantité d'énergie. Elle se produit par exemple dans le soleil et la plupart des étoiles de l'univers. Théoriquement, à masse de combustible égale, la fusion produit entre 3 à 4 fois plus d'énergie que la fission.

L'obtention d'une réaction de fusion entre deux particules chargées positivement est très difficile à réaliser. Deux types d'interactions entrent en jeu : la répulsion coulombienne et l'interaction forte. La répulsion coulombienne traduit le fait que deux particules de même charge ont une tendance naturelle à se repousser. Cette répulsion est intense et à longue portée. L'interaction forte est la force responsable de la cohésion d'un noyau atomique ; elle

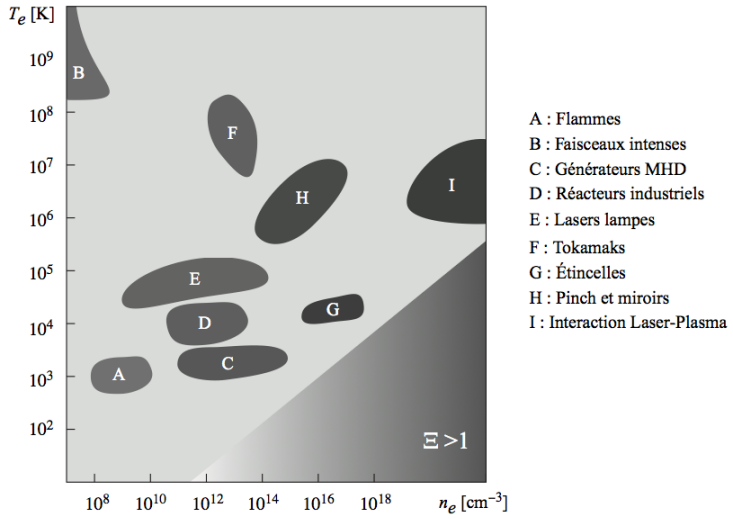

FIGURE 1.2 – Densités et températures électroniques de quelques plasmas thermonucléaires et industriels (Source : Physique des Plasmas [57]).

agit à courte distance (de l'ordre de 10^{-15} m) et tend à unir les deux noyaux. La réaction de fusion a alors lieu lorsque l'interaction forte domine la répulsion coulombienne c'est à dire à une distance de quelques fermis. Dans une description à l'aide des niveaux d'énergie la répulsion électrostatique se présente comme une barrière : la barrière coulombienne. La hauteur de la barrière coulombienne est alors de l'ordre de plusieurs centaines de keV. Ainsi les réactions de fusion apparaissent comme un phénomène extrêmement rare. Néanmoins on peut observer de façon expérimentale que des noyaux franchissent la barrière coulombienne avec une énergie inférieure à celle-ci. Ce phénomène est appelé effet tunnel et il peut être justifié avec des arguments de mécanique quantique.

Enfin, pour une énergie donnée la probabilité de passage de la barrière coulombienne dépend des espèces chimiques mises en jeu. La réaction de fusion la plus accessible est celle impliquant le deutérium et le tritium :

$$D + T \longrightarrow {}^4He + n, \tag{1.1.1}$$

où n est un neutron très énergétique. C'est en ralentissant ces neutrons dans un milieu adéquat que l'on transforme l'énergie cinétique en énergie thermique convertie en électricité. Par ailleurs, les océans contiennent naturellement suffisamment de deutérium pour alimenter en énergie la planète pendant 100 millions d'années. Contrairement à la fission nucléaire, les produits de la fusion (principalement de l'hélium 4) ne sont que très peu radioactifs. C'est sur cette réaction que se concentrent actuellement les recherches sur la fusion contrôlée.

La température requise pour une telle réaction est si élevée que les électrons se détachent de leur atome, le mélange gazeux obtenu est un plasma. Dans ce plasma, la grande agitation des ions et des électrons produit de nombreuses collisions entre les particules. Pour que ces collisions soient suffisamment violentes et entrainent une fusion, trois grandeurs interviennent : la densité n du plasma, la température T et le temps t_E de confinement. Le facteur d'amplification Q, qui est le rapport de la puissance produite à la puissance extérieure fournie, est relié à ces trois quantités via le critère de Lawson. Celui-ci stipule que Q est proportionnel au produit nTt_E.

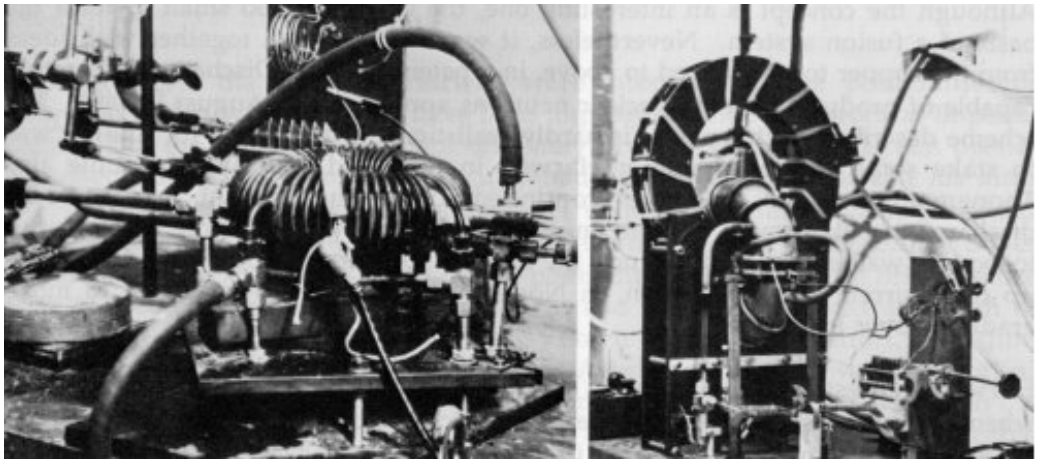

FIGURE 1.3 – Les dispositifs de confinement magnétique testés par Thoneman en 1946 (tores en verre et en métal), au laboratoire Clarendon (Oxford, Royaume-Uni).

Actuellement deux voies sont envisagées : la fusion par confinement inertiel et la fusion par confinement magnétique. La fusion par confinement inertiel consiste à atteindre une densité très élevée pendant un temps relativement court en tirant sur une capsule de Deutérium et de Tritium avec des faisceaux laser. Dans cette thèse je m'intéresserai exclusivement à la fusion par confinement magnétique. Comme je l'ai dit dans la section 1.1.1 le plasma est constitué de particules chargées. Si on applique un champ électromagnétique externe, le plasma va donc interagir avec celui-ci. La fusion par confinement magnétique consiste à trouver une structure et un champ électromagnétique adéquat de sorte à confiner le plasma dans cette structure. Le plasma est confiné plus longtemps et à une densité moins élevée que pour le confinement inertiel. Le premier brevet pour un réacteur de fusion a été déposé en 1946 par Thomson et Blackman (voir Figure 3.3). En 1968 les scientifiques russes parviennent à faire fusionner des atomes d'hydrogène en produisant un plasma à une température de l'ordre d'une dizaine de millions de degrés. Il l'ont confiné dans une chambre de forme toroïdale appelé Tokamak.

L'histoire de la fusion nucléaire contrôlée démarre dans les années 1920 lorsque le physicien Aston mesure le défaut de masse de l'Hélium et en conclut qu'il est possible de récupérer une importante quantité d'énergie en fabriquant un noyau d'hélium à partir d'éléments plus légers. Suite à cela l'anglais Eddington suggère que l'énergie des étoiles est produite par une réaction de ce type et qu'il serait intéressant d'arriver à reproduire et à contrôler cette façon de produire de l'énergie. Néanmoins, à ce jour aucune application industrielle de la fusion à la production d'énergie n'a encore abouti. Le record actuel de puissance d'un réacteur à fusion fonctionnant au deutérium et au tritium est atteint par la centrale JET en Angleterre (voir Figure 1.4). Son facteur de qualité est de 0.64. Afin d'obtenir un facteur de qualité supérieur à 1 il est nécessaire de construire une centrale plus grande. Le projet international ITER, lancé en 2006 et basé dans le sud est de la France à Cadarache, consiste a construire un Tokamak ayant un facteur de qualité supérieur à 1, démontrant ainsi la faisabilité à l'échelle industrielle de telles centrales. De façon plus précise le facteur d'amplification prévu devrait être supérieur à 10. Une vue d'artiste de ce Tokamak est donnée dans la Figure 1.5.

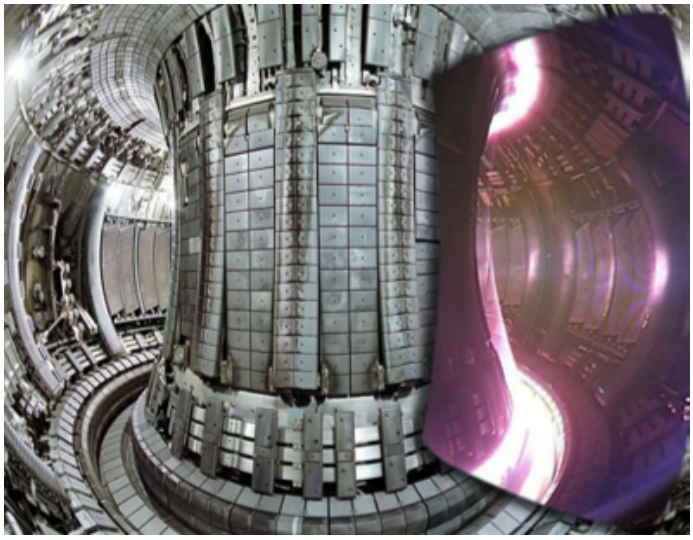

FIGURE 1.4 – Tokamak JET.

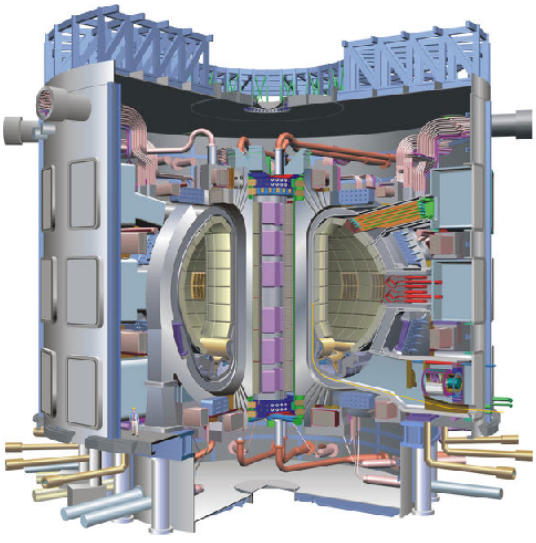

FIGURE 1.5 – Tokamak ITER en construction à Cadarache.

1.2 Confinement d'une particule chargée à l'aide d'un champ magnétique externe

Comme nous venons de le voir la fusion par confinement magnétique consiste à confiner un plasma, c'est à dire un ensemble de particules chargées, à l'aide d'un champ électromagnétique externe. Chaque particule est alors soumise au champ électromagnétique externe et au champ électromagnétique crée par les particules elles-mêmes. Dans cette thèse je vais principalement m'intéresser à des "régimes" pour lesquels la composante externe du champ magnétique est prédominante. Il est donc indispensable de comprendre comment une particule chargée évolue sous l'action d'un champ magnétique externe fort. L'hypothèse champ magnétique fort sera traduite par un adimensionnement des équations. De plus dans cette section je vais introduire certains mécanismes basés sur des changements de coordonnées et des recherches d'invariants qui permettent de simplifier la résolution numérique des problèmes initiaux. Le fil conducteur de cette section sera d'illustrer ces techniques en répondant à la question : "Comment confiner une particule chargée à l'aide d'un champ magnétique fort ?"

Considérons donc une particule chargée sous l'action d'un champ magnétique. Le modèle de base correspond aux équations de Newton dans $\mathbb{R}^3$:

$$\frac{\partial^2 \mathbf{X}}{\partial t^2}(t, \mathbf{x}_0, \mathbf{v}_0) = \frac{q}{m} \frac{\partial \mathbf{X}}{\partial t}(t, \mathbf{x}_0, \mathbf{v}_0) \times \mathbf{B}\left(\mathbf{X}(t, \mathbf{x}_0, \mathbf{v}_0)\right), \tag{1.2.1}$$

$$\mathbf{X}(0, \mathbf{x}_0, \mathbf{v}_0) = \mathbf{x}_0, \qquad \frac{\partial \mathbf{X}}{\partial t}(0, \mathbf{x}_0, \mathbf{v}_0) = \mathbf{v}_0, \tag{1.2.2}$$

où m est la masse de la particule, q sa charge, $\mathbf{X}(t, \mathbf{x}_0, \mathbf{v}_0)$ la position au temps t de la particule qui à l'instant $t = 0$ avait pour position $\mathbf{x}_0$ et pour vitesse $\mathbf{v}_0$, et $\mathbf{B}$ correspond au champ magnétique.

1.2.1 Cas d'un champ magnétique constant

Supposons dans un premier temps que le champ magnétique est constant dans la direction x_3, c'est à dire que $\mathbf{B} = B_0 \mathbf{e}_{x_3}$. En introduisant les quantités r_L et ω_c définit par

$$\omega_c = \frac{|q| B_0}{m} \quad \text{et} \quad r_L = \frac{v_\perp}{\omega_c}, \tag{1.2.3}$$

où $v_\perp = \sqrt{v_{0,1}^2 + v_{0,2}^2}$, les trajectoires sont données par :

$$X_1(t, \mathbf{x}_0, \mathbf{v}_0) = x_{0,1} + \frac{|q| v_\perp}{q\omega_c} \sin\left(\frac{q}{|q|}\omega_c t\right), \tag{1.2.4}$$

$$X_2(t, \mathbf{x}_0, \mathbf{v}_0) = x_{0,2} + \frac{|q| v_\perp}{q\omega_c} \cos\left(\frac{q}{|q|}\omega_c t\right), \tag{1.2.5}$$

$$X_3(t, \mathbf{x}_0, \mathbf{v}_0) = x_{0,3} + v_{0,3} t. \tag{1.2.6}$$

Les trajectoires obtenues sont donc des trajectoires hélicoïdales (voir figure 1.6) d'axe $(M_0 x_3)$ et de rayon r_L, où M_0 est le point de coordonnées $\mathbf{x}_0$. Le rayon de giration r_L est appelé rayon de Larmor et la pulsation ω_c est appelée la fréquence cyclotronique. Au vu des formules (1.2.3) le rayon de Larmor dépend de la masse de la particule, de l'intensité du champ magnétique, et de la composante orthogonale au champ magnétique de la vitesse.

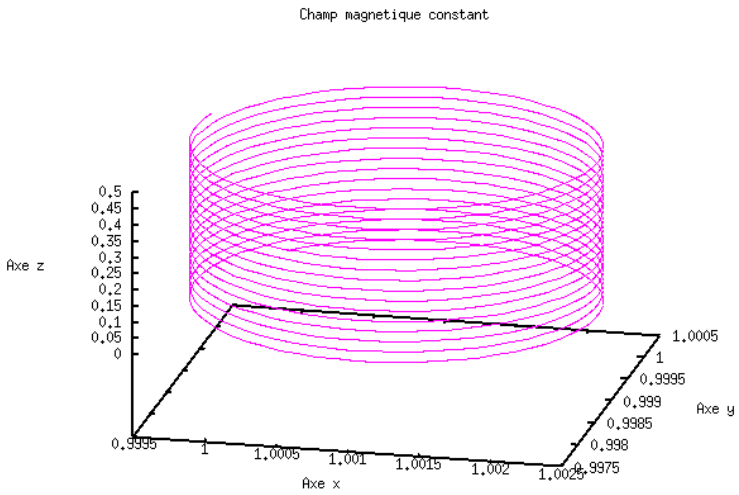

FIGURE 1.6 – Trajectoire d'une particule sous l'action d'un champ constant dans la direction x_3.

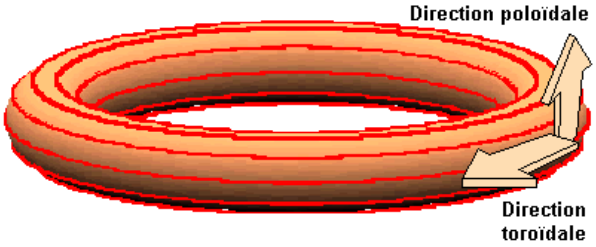

FIGURE 1.7 – Source : Site du CEA

Pour une particule donnée, plus l'intensité du champ magnétique est forte, plus la particule est proche de la ligne de champ et plus elle oscille rapidement.

1.2.2 Cas d'un champ magnétique toroïdal

Au vu de la Section 1.2.1, l'idée naturelle pour confiner une particule serait donc de refermer les lignes de champ, c'est à dire de considérer un champ magnétique dans la direction toroïdale (voir Figure 1.7), et de confiner la particule dans une structure de forme toroïdale. On note R_0 le grand rayon de la structure toroïdale dans laquelle la particule est confinée. Soit $(\mathbf{e}_{x_1}, \mathbf{e}_{x_2}, \mathbf{e}_{x_3})$, une base orthonormée directe de $\mathbb{R}^3$. Considérons le champ magnétique toroïdal

$$\mathbf{B} = \mathbf{e}_\varphi, \tag{1.2.7}$$

où $\mathbf{e}_\varphi$ est définit par

$$\mathbf{e}_\varphi = -\sin(\varphi)\,\mathbf{e}_{x_1} + \cos(\varphi)\,\mathbf{e}_{x_2} \tag{1.2.8}$$

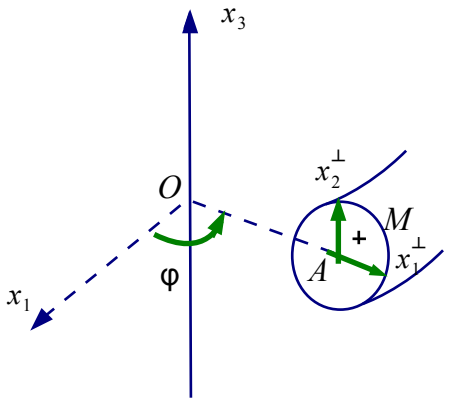

FIGURE 1.8 – En coordonnées toroïdales, la position M de la particule est définie par l'angle φ et les coordonnées $x_1^\perp$ et $x_2^\perp$ dans le plan $(Ax_1^\perp x_2^\perp)$.

(voir la figure 1.8 pour la définition de φ). En faisant la décomposition $\overrightarrow{OM} = \overrightarrow{OA} + \overrightarrow{AM}$ (voir Figure 1.8), avec $\overrightarrow{OA} = R_0 \mathbf{e}_{x_1^\perp}$ et $\overrightarrow{AM} = x_1^\perp \mathbf{e}_{x_1^\perp} + x_2^\perp \mathbf{e}_{x_2^\perp}$, où

$$\mathbf{e}_{x_1^\perp} = \cos(\varphi)\,\mathbf{e}_{x_1} + \sin(\varphi)\,\mathbf{e}_{x_2} \text{ et } \mathbf{e}_{x_2^\perp} = \mathbf{e}_{x_3}, \tag{1.2.9}$$

on est amené à considérer le changement de coordonnées $(x_1, x_2, x_3) \mapsto \left(x_1^\perp, x_2^\perp, \varphi\right)$ défini par

$$\begin{aligned} x_1 &= (R_0 + x_1^\perp)\cos(\varphi) \\ x_2 &= (R_0 + x_1^\perp)\sin(\varphi) \\ x_3 &= x_2^\perp. \end{aligned} \tag{1.2.10}$$

Dans ce système de coordonnées la vitesse de la particule est donnée par :

$$\frac{\partial \mathbf{X}}{\partial t} = \frac{\partial \mathbf{X}_1^\perp}{\partial t}\mathbf{e}_{x_1^\perp} + \left(R_0 + \mathbf{X}_1^\perp\right)\frac{\partial \boldsymbol{\varphi}}{\partial t}\mathbf{e}_\varphi + \frac{\partial \mathbf{X}_2^\perp}{\partial t}\mathbf{e}_{x_2^\perp}. \tag{1.2.11}$$

En utilisant la stratégie habituelle consistant à doubler les variables pour transformer un système différentiel d'ordre 2 en un système différentiel d'ordre 1, la formule (1.2.11) nous amène à considérer un espace de dimension 6 muni d'un système de variables que nous allons noter $\left(x_1^\perp, x_2^\perp, \varphi, v_1^\perp, v_2^\perp, v^{\shortparallel}\right)$ et dans lequel l'équation d'ordre 2 (1.2.1) écrite dans le

système de coordonnées $\left(x_1^\perp, x_2^\perp, \varphi\right)$, est équivalente à :

$$\frac{\partial \mathbf{X}_1^\perp}{\partial t} = \mathbf{V}_1^\perp, \tag{1.2.12}$$

$$\frac{\partial \mathbf{X}_2^\perp}{\partial t} = \mathbf{V}_2^\perp, \tag{1.2.13}$$

$$\frac{\partial \boldsymbol{\varphi}}{\partial t} = \frac{\mathbf{V}^{\shortparallel}}{R_0 + \mathbf{X}_1^\perp}, \tag{1.2.14}$$

$$\frac{\partial \mathbf{V}_1^\perp}{\partial t} - \frac{\left(\mathbf{V}^{\shortparallel}\right)^2}{R_0 + \mathbf{X}_1^\perp} = -\frac{q}{m}\mathbf{V}_2^\perp, \tag{1.2.15}$$

$$\frac{\partial \mathbf{V}_2^\perp}{\partial t} = \frac{q}{m}\mathbf{V}_1^\perp, \tag{1.2.16}$$

$$\frac{\partial \mathbf{V}^{\shortparallel}}{\partial t} + \frac{\mathbf{V}_1^\perp \mathbf{V}^{\shortparallel}}{R_0 + \mathbf{X}_1^\perp} = 0. \tag{1.2.17}$$

Nous allons maintenant adimensionner cette équation. Soit $\bar{t}$ une échelle de temps caractéristique, $\bar{L}$ une échelle de longueur caractéristique dans la direction orthogonale au champ magnétique, $\bar{v}$ une échelle de vitesse caractéristique, et $\bar{B}$ une échelle d'intensité caractéristique du champ magnétique. On définit alors de nouvelles variables $x_1'^\perp$, $x_2'^\perp$, $v_1'^\perp$, $v_2'^\perp$, $v'^{\shortparallel}$ et t' par $x_1^\perp = \bar{L}x_1'^\perp$, $x_2^\perp = \bar{L}x_2'^\perp$ $v_1 = \bar{v}v_1'^\perp$, $v_2 = \bar{v}v_2'^\perp$, $v^{\shortparallel} = \bar{v}v'^{\shortparallel}$ et $t = \bar{t}t'$. On définit également le vecteur sans dimension $\mathbf{B}'$ par $\mathbf{B}(\mathbf{x}) = \bar{B}\mathbf{B}'(\mathbf{x}')$. De même on définit les trajectoires adimensionnées par :

$$\mathbf{X}_1^\perp\left(\bar{t}t', \bar{L}x_1'^\perp, \bar{L}x_2'^\perp, \varphi, \bar{v}v_1'^\perp, \bar{v}v_2'^\perp\right) = \bar{L}\mathbf{X}_1'^\perp\left(t', x_1'^\perp, x_2'^\perp, \varphi, v_1'^\perp, v_2'^\perp\right), \tag{1.2.18}$$

$$\mathbf{X}_2^\perp\left(\bar{t}t', \bar{L}x_1'^\perp, \bar{L}x_2'^\perp, \varphi, \bar{v}v_1'^\perp, \bar{v}v_2'^\perp\right) = \bar{L}\mathbf{X}_2'^\perp\left(t', x_1'^\perp, x_2'^\perp, \varphi, v_1'^\perp, v_2'^\perp\right), \tag{1.2.19}$$

$$\mathbf{V}_1^\perp\left(\bar{t}t', \bar{L}x_1'^\perp, \bar{L}x_2'^\perp, \varphi, \bar{v}v_1'^\perp, \bar{v}v_2'^\perp\right) = \bar{v}\mathbf{V}_1'^\perp\left(t', x_1'^\perp, x_2'^\perp, \varphi, v_1'^\perp, v_2'^\perp\right), \tag{1.2.20}$$

$$\mathbf{V}_2^\perp\left(\bar{t}t', \bar{L}x_1'^\perp, \bar{L}x_2'^\perp, \varphi, \bar{v}v_1'^\perp, \bar{v}v_2'^\perp\right) = \bar{v}\mathbf{V}_2'^\perp\left(t', x_1'^\perp, x_2'^\perp, \varphi, v_1'^\perp, v_2'^\perp\right), \tag{1.2.21}$$

$$\mathbf{V}^{\shortparallel}\left(\bar{t}t', \bar{L}x_1'^\perp, \bar{L}x_2'^\perp, \varphi, \bar{v}v_1'^\perp, \bar{v}v_2'^\perp\right) = \bar{v}\mathbf{V}_1'^{\shortparallel}\left(t', x_1'^\perp, x_2'^\perp, \varphi, v_1'^\perp, v_2'^\perp\right). \tag{1.2.22}$$

En injectant ces variables dans le système d'équations (1.2.12)-(1.2.17), en identifiant les grandeurs caractéristiques $\bar{\omega}_c = q\bar{B}/m$, $\bar{a}_L = \bar{v}/\bar{\omega}_c$, et en imposant

$$\bar{\omega}_c\bar{t} = \frac{1}{\varepsilon}, \tag{1.2.23}$$

$$\frac{\bar{a}_L}{\bar{L}} = \varepsilon \quad \text{et} \quad \frac{\bar{L}}{R_0} = \varepsilon, \tag{1.2.24}$$

on obtient :

$$\frac{\partial \mathbf{X}_1'^{\perp}}{\partial t'} = \mathbf{V}_1'^{\perp}, \tag{1.2.25}$$

$$\frac{\partial \mathbf{X}_2'^{\perp}}{\partial t'} = \mathbf{V}_2'^{\perp}, \tag{1.2.26}$$

$$\frac{\partial \boldsymbol{\varphi}}{\partial t'} = \varepsilon \frac{\mathbf{V}'^{\shortparallel}}{1+\varepsilon \mathbf{X}_1'^{\perp}}, \tag{1.2.27}$$

$$\frac{\partial \mathbf{V}_1'^{\perp}}{\partial t'} - \frac{\varepsilon \left(\mathbf{V}'^{\shortparallel}\right)^2}{1+\varepsilon \mathbf{X}_1'^{\perp}} = -\frac{1}{\varepsilon}\mathbf{V}_2'^{\perp}, \tag{1.2.28}$$

$$\frac{\partial \mathbf{V}_2'^{\perp}}{\partial t'} = \frac{1}{\varepsilon}\mathbf{V}_1'^{\perp}, \tag{1.2.29}$$

$$\frac{\partial \mathbf{V}'^{\shortparallel}}{\partial t'} + \varepsilon \frac{\mathbf{V}_1'^{\perp}\mathbf{V}'^{\shortparallel}}{1+\varepsilon \mathbf{X}_1'^{\perp}} = 0. \tag{1.2.30}$$

Remarque 1.2.1. *La formule* (1.2.23) *signifie qu'à l'échelle de temps à laquelle on se place la période caractéristique d'oscillation autour des lignes de champ est petite. D'autre part la formule* (1.2.24) *signifie qu'à l'échelle spatiale à laquelle on observe le système le rayon de Larmor caractéristique est petit.*

On pose

$$\mathbf{P}_\varphi(x_1'^{\perp}, x_2'^{\perp}, \varphi, v_1'^{\perp}, v_2'^{\perp}, v'^{\shortparallel}) = (1+\varepsilon x_1'^{\perp})v'^{\shortparallel}. \tag{1.2.31}$$

On remarque alors que $\mathbf{P}_\varphi$ est constant le long des trajectoires. En effet, en multipliant (1.2.30) par $(1+\varepsilon \mathbf{X}_1'^{\perp})$ on obtient :

$$\frac{\partial}{\partial t'}\mathbf{P}_\varphi\left(\mathbf{X}_1'^{\perp}, \mathbf{X}_2'^{\perp}, \boldsymbol{\varphi}, \mathbf{V}_1'^{\perp}, \mathbf{V}_2'^{\perp}, \mathbf{V}'^{\shortparallel}\right) = 0. \tag{1.2.32}$$

Ainsi pour résoudre le système différentiel (1.2.25)-(1.2.30) il suffit de résoudre le système différentiel

$$\frac{\partial \mathbf{X}_1'^{\perp}}{\partial t'} = \mathbf{V}_1'^{\perp}, \tag{1.2.33}$$

$$\frac{\partial \mathbf{X}_2'^{\perp}}{\partial t'} = \mathbf{V}_2'^{\perp}, \tag{1.2.34}$$

$$\frac{\partial \mathbf{V}_1'^{\perp}}{\partial t'} = -\frac{1}{\varepsilon}\mathbf{V}_2'^{\perp} + \frac{\varepsilon \mathbf{P}_\varphi^2}{\left(1+\varepsilon \mathbf{X}_1'^{\perp}\right)^3}, \tag{1.2.35}$$

$$\frac{\partial \mathbf{V}_2'^{\perp}}{\partial t'} = \frac{1}{\varepsilon}\mathbf{V}_1'^{\perp}. \tag{1.2.36}$$

Les quantités $\boldsymbol{\varphi}$ et $\mathbf{V}'^{\shortparallel}$ sont alors obtenues via :

$$\frac{\partial \boldsymbol{\varphi}}{\partial t'} = \frac{\varepsilon \mathbf{P}_\varphi}{\left(1+\varepsilon \mathbf{X}_1'^{\perp}\right)^2}, \tag{1.2.37}$$

$$\mathbf{V}'^{\shortparallel} = \frac{\mathbf{P}_\varphi}{1+\varepsilon \mathbf{X}_1'^{\perp}}. \tag{1.2.38}$$

Enfin, pour obtenir les trajectoires dans le système de coordonnées initial (mais adimensionné), il suffit d'adimensionner le changement de coordonnées (1.2.10), c'est à dire de poser $x_1' = (1+\varepsilon x_1'^{\perp})\cos(\varphi)$, $x_2' = (1+\varepsilon x_1'^{\perp})\sin(\varphi)$ et $x_3' = x_2'^{\perp}$.

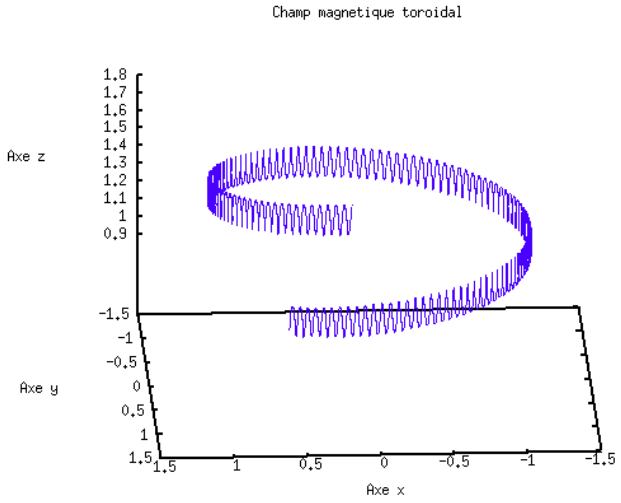

FIGURE 1.9 – Trajectoire d'une particule sous l'action d'un champ constant dans la direction toroidale.

Remark 1.2.2. *La détermination de l'invariant* $\mathbf{P}_\varphi$*, défini par* (1.2.31)*, nous a donc permis de passer d'un système différentiel dans* $\mathbb{R}^6$ *a un système différentiel dans* $\mathbb{R}^4$ *réduisant ainsi la dimension du problème.*

Dans ce cas la particule n'est pas confinée. En effet, comme on peut le voir sur la figure 1.9, la particule subit une lente dérive transverse. La figure 1.9 a été obtenu avec un solveur Runge-Kutta d'ordre quatre, $\varepsilon = 0.1$, $\left(x_1'^{\perp}\right)_0 = 1$, $\left(x_2'^{\perp}\right)_0 = 1$, $\varphi_0 = 1$, $\left(v_1'^{\perp}\right)_0 = 0.5$, $\left(v_2'^{\perp}\right)_0 = 0.7$ et $\left(v'^{\parallel}\right)_0 = 0.4$.

1.2.3 Cas d'un champ magnétique ayant des composantes toroïdales et poloïdales

Comme nous venons de le voir dans la section 1.2.2 un champ purement toroïdal ne permet pas de confiner une particule chargée. L'idée est alors d'ajouter au champ magnétique une composante poloïdale (voir figure 1.7). Les lignes de champ sont alors des hélices s'enroulant autour de surfaces toriques que l'on appelle des surfaces magnétiques. De cette manière, les effets de dérives transverses se compensent. De façon plus précise, considérons le champ magnétique

$$\begin{aligned}\mathbf{B} &= \frac{B_0 r}{f_q\left(R_0 + r\cos\left(\theta\right)\right)}\mathbf{e}_\theta + \frac{B_0 R_0}{R_0 + r\cos\left(\theta\right)}\mathbf{e}_\varphi \\ &= -\frac{B_0 x_2^\perp}{f_q\left(R_0 + x_1^\perp\right)}\mathbf{e}_{x_1^\perp} + \frac{B_0 x_1^\perp}{f_q\left(R_0 + x_1^\perp\right)}\mathbf{e}_{x_2^\perp} + \frac{B_0 R_0}{R_0 + x_1^\perp}\mathbf{e}_\varphi,\end{aligned} \tag{1.2.39}$$

où

$$\mathbf{e}_\theta = -\sin\left(\theta\right)\mathbf{e}_{x_1^\perp} + \cos\left(\theta\right)\mathbf{e}_{x_2^\perp} \tag{1.2.40}$$

(voir la figure 1.10 pour la définition de θ), et où f_q est appelé le facteur de qualité. f_q correspond au nombre de tours toroïdaux effectués par une ligne de champ pour faire un tour poloïdale.

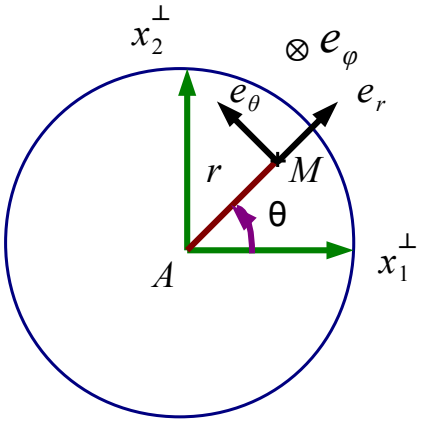

FIGURE 1.10 – Section toroïdales de la figure 1.8

En procédant comme dans la section précédente, et en utilisant l'expression (1.2.39) du champ magnétique, on obtient que l'équation d'ordre 2 (1.2.1) écrite dans le système de coordonnées $\left(x_1^\perp, x_2^\perp, \varphi\right)$ défini par (1.2.10) est équivalente à :

$$\frac{\partial \mathbf{X}_1^\perp}{\partial t} = \mathbf{V}_1^\perp, \tag{1.2.41}$$

$$\frac{\partial \mathbf{X}_2^\perp}{\partial t} = \mathbf{V}_2^\perp, \tag{1.2.42}$$

$$\frac{\partial \boldsymbol{\varphi}}{\partial t} = \frac{\mathbf{V}^{\shortparallel}}{R_0 + \mathbf{X}_1^\perp}, \tag{1.2.43}$$

$$\frac{\partial \mathbf{V}_1^\perp}{\partial t} - \frac{\left(\mathbf{V}^{\shortparallel}\right)^2}{R_0 + \mathbf{X}_1^\perp} = \frac{qB_0}{m}\left(-\frac{\mathbf{V}_2^\perp R_0}{R_0 + \mathbf{X}_1^\perp} + \frac{\mathbf{V}^{\shortparallel}\mathbf{X}_1^\perp}{f_q\left(R_0 + \mathbf{X}_1^\perp\right)}\right), \tag{1.2.44}$$

$$\frac{\partial \mathbf{V}_2^\perp}{\partial t} = \frac{qB_0}{m}\left(\frac{\mathbf{V}^{\shortparallel}\mathbf{X}_2^\perp}{f_q\left(R_0 + \mathbf{X}_1^\perp\right)} + \frac{\mathbf{V}_1^\perp R_0}{R_0 + \mathbf{X}_1^\perp}\right), \tag{1.2.45}$$

$$\frac{\partial \mathbf{V}^{\shortparallel}}{\partial t} + \frac{\mathbf{V}_1^\perp \mathbf{V}^{\shortparallel}}{R_0 + \mathbf{X}_1^\perp} = -\frac{qB_0}{m}\left(\frac{\mathbf{V}_2^\perp \mathbf{X}_2^\perp}{f_q\left(R_0 + \mathbf{X}_1^\perp\right)} + \frac{\mathbf{V}_1^\perp \mathbf{X}_1^\perp}{f_q\left(R_0 + \mathbf{X}_1^\perp\right)}\right). \tag{1.2.46}$$

Sous le même adimensionnement que dans la section précédente on obtient :

$$\frac{\partial \mathbf{X}_1'^{\perp}}{\partial t'} = \mathbf{V}_1'^{\perp}, \tag{1.2.47}$$

$$\frac{\partial \mathbf{X}_2'^{\perp}}{\partial t'} = \mathbf{V}_2'^{\perp}, \tag{1.2.48}$$

$$\frac{\partial \boldsymbol{\varphi}}{\partial t'} = \varepsilon \frac{\mathbf{V}'^{\shortparallel}}{1+\varepsilon \mathbf{X}_1'^{\perp}}, \tag{1.2.49}$$

$$\frac{\partial \mathbf{V}_1'^{\perp}}{\partial t'} - \frac{\varepsilon \left(\mathbf{V}'^{\shortparallel}\right)^2}{1+\varepsilon \mathbf{X}_1'^{\perp}} = -\frac{\mathbf{V}_2'^{\perp}}{\varepsilon\left(1+\varepsilon \mathbf{X}_1'^{\perp}\right)} + \frac{1}{f_q}\frac{\mathbf{V}'^{\shortparallel}\mathbf{X}_1'^{\perp}}{\left(1+\varepsilon \mathbf{X}_1'^{\perp}\right)}, \tag{1.2.50}$$

$$\frac{\partial \mathbf{V}_2'^{\perp}}{\partial t'} = \frac{\mathbf{V}_1'^{\perp}}{\varepsilon\left(1+\varepsilon \mathbf{X}_1'^{\perp}\right)} + \frac{1}{f_q}\frac{\mathbf{V}'^{\shortparallel}\mathbf{X}_2'^{\perp}}{\left(1+\varepsilon \mathbf{X}_1'^{\perp}\right)}, \tag{1.2.51}$$

$$\frac{\partial \mathbf{V}'^{\shortparallel}}{\partial t'} + \varepsilon \frac{\mathbf{V}_1'^{\perp}\mathbf{V}'^{\shortparallel}}{1+\varepsilon \mathbf{X}_1'^{\perp}} = -\frac{1}{f_q}\left(\frac{\mathbf{V}_2'^{\perp}\mathbf{X}_2'^{\perp}}{\left(1+\varepsilon \mathbf{X}_1'^{\perp}\right)} + \frac{\mathbf{V}_1'^{\perp}\mathbf{X}_1'^{\perp}}{\left(1+\varepsilon \mathbf{X}_1'^{\perp}\right)}\right). \tag{1.2.52}$$

On pose

$$\mathbf{P}_{\varphi}(x_1'^{\perp}, x_2'^{\perp}, \varphi, v_1'^{\perp}, v_2'^{\perp}, v'^{\shortparallel}) = (1+\varepsilon x_1'^{\perp})v'^{\shortparallel} + \frac{1}{2f_q}\left(\left(x_1'^{\perp}\right)^2 + \left(x_2'^{\perp}\right)^2\right). \tag{1.2.53}$$

On remarque alors que $\mathbf{P}_{\varphi}$ est constant le long des trajectoires. En effet, en multipliant (1.2.52) par $(1+\varepsilon \mathbf{X}_1'^{\perp})$ on obtient :

$$\frac{\partial}{\partial t'}\mathbf{P}_{\varphi}\left(\mathbf{X}_1'^{\perp}, \mathbf{X}_2'^{\perp}, \boldsymbol{\varphi}, \mathbf{V}_1'^{\perp}, \mathbf{V}_2'^{\perp}, \mathbf{V}'^{\shortparallel}\right) = 0. \tag{1.2.54}$$

Ainsi pour résoudre le système différentiel (1.2.25)-(1.2.30) il suffit de résoudre le système différentiel

$$\frac{\partial \mathbf{X}_1'^{\perp}}{\partial t'} = \mathbf{V}_1'^{\perp}, \tag{1.2.55}$$

$$\frac{\partial \mathbf{X}_2'^{\perp}}{\partial t'} = \mathbf{V}_2'^{\perp}, \tag{1.2.56}$$

$$\begin{aligned}\frac{\partial \mathbf{V}_1'^{\perp}}{\partial t'} &= -\frac{\mathbf{V}_2'^{\perp}}{\varepsilon\left(1+\varepsilon \mathbf{X}_1'^{\perp}\right)} \\ &+ \frac{\mathbf{X}_1'^{\perp}}{f_q\left(1+\varepsilon \mathbf{X}_1'^{\perp}\right)}\Big(\frac{\mathbf{P}_{\varphi}}{1+\varepsilon \mathbf{X}_1'^{\perp}} - \frac{\left(\left(\mathbf{X}_1'^{\perp}\right)^2 + \left(\mathbf{X}_2'^{\perp}\right)^2\right)}{2f_q\left(1+\varepsilon \mathbf{X}_1'^{\perp}\right)}\Big) \\ &+ \frac{\varepsilon}{\left(1+\varepsilon \mathbf{X}_1'^{\perp}\right)}\Big(\frac{\mathbf{P}_{\varphi}}{1+\varepsilon \mathbf{X}_1'^{\perp}} - \frac{\left(\left(\mathbf{X}_1'^{\perp}\right)^2 + \left(\mathbf{X}_2'^{\perp}\right)^2\right)}{2f_q\left(1+\varepsilon \mathbf{X}_1'^{\perp}\right)}\Big)^2,\end{aligned} \tag{1.2.57}$$

$$\begin{aligned}\frac{\partial \mathbf{V}_2'^{\perp}}{\partial t'} &= \frac{\mathbf{V}_1'^{\perp}}{\varepsilon\left(1+\varepsilon \mathbf{X}_1'^{\perp}\right)} \\ &+ \frac{\mathbf{X}_2'^{\perp}}{f_q\left(1+\varepsilon \mathbf{X}_1'^{\perp}\right)}\Big(\frac{\mathbf{P}_{\varphi}}{1+\varepsilon \mathbf{X}_1'^{\perp}} - \frac{\left(\left(\mathbf{X}_1'^{\perp}\right)^2 + \left(\mathbf{X}_2'^{\perp}\right)^2\right)}{2f_q\left(1+\varepsilon \mathbf{X}_1'^{\perp}\right)}\Big).\end{aligned} \tag{1.2.58}$$

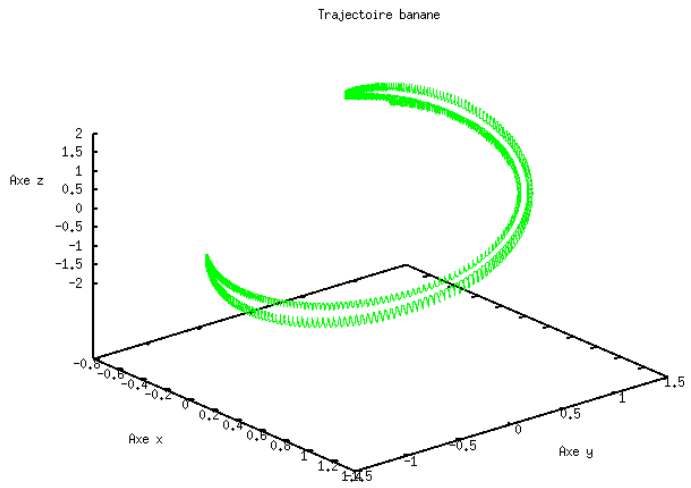

FIGURE 1.11 – Trajectoire d'une particule sous l'action d'un champ ayant des composantes toroïdales et poloïdales.

Les quantités $\boldsymbol{\varphi}$ et $\mathbf{V}'^{\parallel}$ sont alors obtenues via :

$$\frac{\partial \boldsymbol{\varphi}}{\partial t'} = \frac{\varepsilon}{1+\varepsilon \mathbf{X}_1'^{\perp}} \Big(\frac{\mathbf{P}_\varphi}{1+\varepsilon \mathbf{X}_1'^{\perp}} - \frac{\left(\left(\mathbf{X}_1'^{\perp}\right)^2 + \left(\mathbf{X}_2'^{\perp}\right)^2\right)}{2 f_q \left(1+\varepsilon \mathbf{X}_1'^{\perp}\right)} \Big), \tag{1.2.59}$$

$$\mathbf{V}'^{\parallel} = \frac{\mathbf{P}_\varphi}{1+\varepsilon \mathbf{X}_1'^{\perp}} - \frac{\left(\left(\mathbf{X}_1'^{\perp}\right)^2 + \left(\mathbf{X}_2'^{\perp}\right)^2\right)}{2 f_q \left(1+\varepsilon \mathbf{X}_1'^{\perp}\right)}. \tag{1.2.60}$$

Enfin, pour obtenir les trajectoires dans le système de coordonnées initial (mais adimensionné), il suffit de poser $x_1' = (1+\varepsilon x_1'^{\perp})\cos(\varphi)$, $x_2' = (1+\varepsilon x_1'^{\perp})\sin(\varphi)$ et $x_3' = x_2'^{\perp}$.

En utilisant un solveur Runge Kutta d'ordre 4 j'ai obtenu les figures 1.11 et 1.12. Pour réaliser ces deux figures j'ai pris $\varepsilon = 0.1$, un facteur de qualité $f_q = 1$ et un temps final de simulation $t = 350$. Les autres paramètres utilisés sont données dans le tableau 4.1. Les

	$\left(x_1'^{\perp}\right)_0$	$\left(x_2'^{\perp}\right)_0$	φ_0	$\left(v_1'^{\perp}\right)_0$	$\left(v_2'^{\perp}\right)_0$	$\left(v'^{\parallel}\right)_0$
Figure 1.11	1	1	1	0.5	0.7	0.4
Figure 1.12	1	1	1	0.5	0.7	0.8

TABLE 1.1 –

figures 1.11 et 1.12 illustrent le fait que la nature des trajectoires est fortement liée à la vitesse parallèle initiale. Sur la figure 1.11 la particule semble rebondir entre deux points. Ces deux points sont appelés des points miroirs. En utilisant des arguments heuristiques on peut montrer l'existence d'un cône, appelé cône de perte du miroir, tel que toutes les particules à l'extérieur de ce cône sont réfléchies. De façon plus précise, en notant α_0 l'angle entre la vitesse et sa composante parallèle à l'instant initial, on peut montrer qu'il existe une valeur α_c tel que si $\sin^2(\alpha_0) > \sin^2(\alpha_c)$ la particule est piégée. Ces arguments heuristiques sont présentés dans la section 1.2.5.

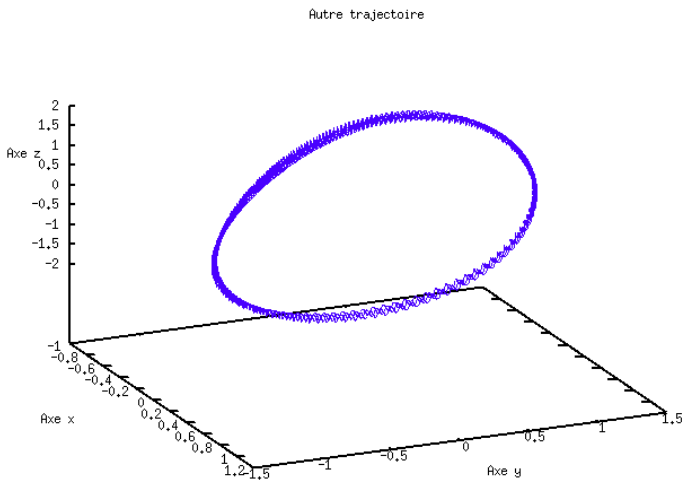

FIGURE 1.12 – Trajectoire d'une particule sous l'action d'un champ ayant des composantes toroïdales et poloïdales.

1.2.4 Moment magnétique

Soit $\mathbf{V}(t, \mathbf{x}_0, \mathbf{v}_0)$ la vitesse au temps t de la particule qui à l'instant $t = 0$ avait pour position $\mathbf{x}_0$ et pour vitesse $\mathbf{v}_0$. Par définition la vitesse vérifie

$$\frac{\partial \mathbf{X}}{\partial t} = \mathbf{V}, \tag{1.2.61}$$

où $\mathbf{X}$ est donnée par (1.2.1)-(1.2.2). On décompose alors la vitesse en sa composante orthogonale au champ magnétique et sa composante parallèle :

$$\mathbf{V} = \mathbf{V}_\perp + \mathbf{V}_{||}. \tag{1.2.62}$$

Le moment magnétique μ est alors définit par :

$$\mu = \frac{m v_\perp^2}{2 \left\| \mathbf{B}(\mathbf{x}) \right\|_2}. \tag{1.2.63}$$

Lorsqu'à l'échelle spatial du mouvement de la particule le champ magnétique varie peu (en espace), le moment magnétique varie peu. En effet, dans ce cas tout se passe localement comme si le champ magnétique était constant. Or lorsque le champ magnétique est constant la norme de la composante orthogonale au champ magnétique de la vitesse est constante (voir section 1.2.1). Nous reviendrons longuement sur cette condition par la suite (voir Chapitre 2). On dit alors que le moment magnétique est un invariant adiabatique.

1.2.5 Effet miroir magnétique

Un premier exemple d'effet mirroir est donné dans la section précédente dans le cas où l'orbite de la particule est en forme de banane (Figure 1.11). De manière générale il s'agit d'une configuration dans laquelle la particule semble "rebondir" entre deux points. Comme nous l'avons observé dans la section précédente l'existence de cet effet dépend des conditions initiales. Dans cette section nous allons exposer les arguments heuristiques

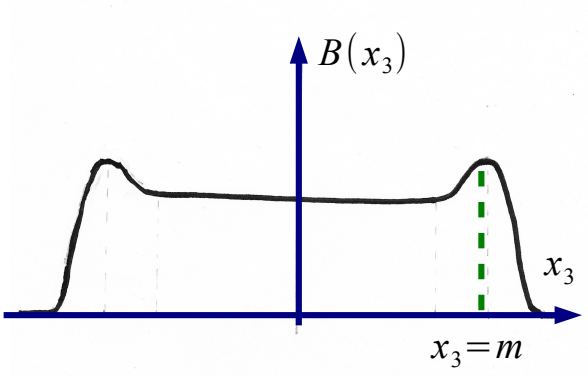

FIGURE 1.13 – Profil du champ magnétique

permettant de déterminer le cône de perte.

La vitesse $\mathbf{V}$ de la particule, définie par (1.2.61), vérifie :

$$\frac{\partial \mathbf{V}}{\partial t} = \frac{q}{m}\mathbf{V} \times \mathbf{B}(\mathbf{X}). \tag{1.2.64}$$

En faisant le produit scalaire de (1.2.64) avec $\mathbf{V}$ on obtient l'équation de conservation de l'énergie cinétique :

$$\frac{\partial}{\partial t}\left(\frac{1}{2}m\left\|\mathbf{V}\right\|_2^2\right) = 0. \tag{1.2.65}$$

Plaçons-nous dans le cadre où le champ magnétique varie peu à l'échelle spatiale du mouvement de la particule. On fait alors l'approximation que le moment magnétique et le rayon de Larmor sont des invariants. Dans ce cas le champ magnétique ne dépend que de la coordonnée x_3. Supposons en outre que le champ magnétique a le profil donné dans la figure 1.13. En injectant le moment magnétique dans l'équation de conservation de l'énergie cinétique on obtient :

$$\frac{1}{2}m\left\|\mathbf{V}_{\shortparallel}\right\|_2^2 + \mu\left\|\mathbf{B}(\mathbf{X}_3)\right\|_2 = \text{constante}. \tag{1.2.66}$$

Si à l'instant initial la particule se trouve dans le plan $x_3 = 0$ et qu'elle se déplace dans le sens des x_3 croissant alors $\left\|\mathbf{B}(\mathbf{X}_3)\right\|_2$ va augmenter jusqu'à atteindre son maximum dans le plan $x_3 = m$. La conservation de l'énergie cinétique implique alors que la vitesse parallèle va diminuer. Si celle-ci vaut 0 avant d'arriver au plan $x_3 = m$ la particule va repartir dans l'autre sens. En effet $\left\|\mathbf{B}(\mathbf{X}_3)\right\|_2$ ne peut plus augmenter.

Ecrivons cette condition à partir de l'angle α_0 que fait la vitesse initiale avec sa composante parallèle. La conservation du moment magnétique donne :

$$\frac{\sin^2(\alpha)}{\left\|\mathbf{B}(\mathbf{X}_3)\right\|_2} = \frac{\sin^2(\alpha_0)}{\left\|\mathbf{B}_0\right\|_2}, \tag{1.2.67}$$

où α correspond à l'angle entre la vitesse à l'instant t et sa composante parallèle. En se déplaçant dans le sens des x_3 croissant à partir de l'origine, la norme du champ magnétique augmente de B_0 à B_m, ce qui implique que l'angle α augmente à partir de sa valeur initiale α_0. On voit donc que si la situation initiale est telle que α atteint $\pi/2$ avant d'atteindre le plan $x_3 = m$, la particule sera réfléchie. Si $\sin^2(\alpha) > B_0/B_m$ la particule est piégée et sinon elle s'échappe. La relation $\sin^2(\alpha_0) = B_0/B_m$ définit le cône de perte.

1.3 Modélisation du plasma

Le modèle à N corps est le modèle le plus précis et le plus complet pour décrire l'évolution d'un plasma. Néanmoins, comme nous allons le voir dans la section 1.3.1 ce modèle est inutilisable en pratique. Il existe alors toute une hiérarchie de modèles dérivant du problème à N corps. On peut classer ces modèles selon deux catégories : les modèles cinétiques et les modèles fluides. Les modèles macroscopiques, ou fluides, sont moins précis que les modèles cinétiques. Ils constituent une bonne approximation lorsque les particules sont proche de l'équilibre thermodynamique. Ces modèles consistent à assimiler chaque espèce de particules d'un plasma à un fluide caractérisé par sa densité, sa vitesse et son énergie. En outre, ils peuvent être obtenus à partir des équations cinétiques en calculant les moments de l'équation de Vlasov, puis en fermant le système par une condition d'équilibre thermodynamique (voir [60]). Dans cette section je vais présenter les modèles à N corps, qui sont finalement à la base de tous les autres modèles, et les modèles cinétiques.

1.3.1 Modèle à N corps

Comme nous l'avons vu dans la section 1.1.1 le plasma est un gaz constitué de particules chargées. Dans le cadre du confinement de ce plasma par un champ électromagnétique externe, nous sommes donc intéressés par des modèles décrivant l'interaction de ces particules sous l'effet d'un champ électromagnétique externe. Le modèle le plus basique pour simuler l'évolution de ces particules consiste à appliquer pour chaque particule les lois de Newton. En notant N le nombre de particules, en négligeant les collisions entre les particules, et en supposant que le poids est faible devant la force de Lorentz, on est donc amené à résoudre le système constitué des N équations vectorielles :

$$m_k \frac{d^2\mathbf{x}^k}{dt^2}(t) = \Big(\sum_{j\in\{1,\dots,N\},\ j\neq k} \mathbf{F}_{j\to k} \Big) + \mathbf{F}_e^k, \tag{1.3.1}$$

$$\mathbf{x}^k(0) = \mathbf{x}_0^k, \qquad \frac{d\mathbf{x}^k}{dt}(0) = \mathbf{v}_0^k, \tag{1.3.2}$$

où m_k et q_k correspondent respectivement à la masse et à la charge de la particule k,

$$\mathbf{F}_e^k = q_k \left(\mathbf{E}_e(\mathbf{x}^k, t) + \frac{d\mathbf{x}^k}{dt} \times \mathbf{B}_e\left(\mathbf{x}^k, t\right) \right) \tag{1.3.3}$$

est la force de Lorentz due au champ électromagnétique externe $(\mathbf{E}_e, \mathbf{B}_e)$, et pour tout $j \neq k$

$$\mathbf{F}_{j\to k} = q_k \left(\frac{d\mathbf{x}^k}{dt} \times \mathbf{B}_j\left(\mathbf{x}^k\right) + \mathbf{E}_j\left(\mathbf{x}^k\right) \right) \tag{1.3.4}$$

correspond à la force de Lorentz due au champ électromagnétique $(\mathbf{E}_j, \mathbf{B}_j)$ créé par la particule j.

Cette modélisation du plasma, appelée modèle à N corps, n'est pas utilisable en pratique pour faire des simulations numériques. En effet, dans un plasma l'ordre de grandeur du nombre de particules est $N \simeq 10^{20}$. Il faudrait donc résoudre un système de $3N$ équations d'ordre 2.

1.3.2 Modèle cinétique

Dans cette thèse je vais m'intéresser exclusivement aux modèles cinétiques. Un modèle cinétique consiste à représenter chaque espèce s de particule par une fonction $f_s =$

$f_s(\mathbf{x}, \mathbf{v}, t)$ appelée fonction de distribution. Elle correspond à une moyenne statistique de la répartition des particules dans l'espace des phases pour un grand nombre de réalisations du système physique considéré. Le produit $f_s d\mathbf{x} d\mathbf{v}$ correspond à la moyenne du nombre de particules de l'espèce s dont la position et la vitesse sont dans une boîte de volume $d\mathbf{x}d\mathbf{v}$ centrée en $(\mathbf{x}, \mathbf{v})$. En négligeant les collisions entre particules et en se plaçant dans un cadre non relativiste (c'est à dire lorsque les vitesses des particules sont faibles devant la vitesse de la lumière), des techniques de physique statistique permettent de passer du modèle à N corps au système d'équations aux dérivées partielles :

$$\frac{\partial f_s}{\partial t} + \mathbf{v} \cdot \nabla_{\mathbf{x}} f_s + \frac{q_s}{m_s} \left(\mathbf{E}(\mathbf{x}, t) + \mathbf{v} \times \mathbf{B}(\mathbf{x}, t) \right) \cdot \nabla_{\mathbf{v}} f_s = 0, \tag{1.3.5}$$

où q_s et m_s correspondent respectivement à la charge et à la masse d'une particule d'espèce s. Les champs électriques et magnétiques $\mathbf{E}$ et $\mathbf{B}$ vérifient les équations de Maxwell :

$$\frac{\partial \mathbf{E}}{\partial t} - c^2 \nabla \times \mathbf{B} = -\frac{\mathbf{J}}{\varepsilon_0}, \tag{1.3.6}$$

$$\frac{\partial \mathbf{B}}{\partial t} + \nabla \times \mathbf{E} = 0, \tag{1.3.7}$$

$$\nabla \cdot \mathbf{E} = \frac{\rho}{\varepsilon_0}, \tag{1.3.8}$$

$$\nabla \cdot \mathbf{B} = 0 \tag{1.3.9}$$

qui sont reliées aux fonctions de distribution par les densités de charges et de courants dont les expressions sont données par :

$$\rho(\mathbf{x}, t) = \sum_s q_s \int_{\mathbb{R}^3} f_s(\mathbf{x}, \mathbf{v}, t) \, d\mathbf{v}, \tag{1.3.10}$$

$$\mathbf{J}(\mathbf{x}, t) = \sum_s q_s \int_{\mathbb{R}^3} \mathbf{v} f_s(\mathbf{x}, \mathbf{v}, t) \, d\mathbf{v}, \tag{1.3.11}$$

où c est la vitesse de la lumière dans le vide et ε_0 la permittivité diélectrique du vide. On peut décomposer le champ électromagnétique en deux parties : la partie externe, notée $(\mathbf{E}_e, \mathbf{B}_e)$, et la partie créé par les particules elles-mêmes, notée $(\mathbf{E}_c, \mathbf{B}_c)$. Cette dernière est appelée la partie auto-consistante du champ électromagnétique. En procédant ainsi et en utilisant la linéarité des équations de Maxwell on peut supposer que la partie externe satisfait les équations de Maxwell dans le vide (c'est à dire avec des densités de charge et de courant qui sont nulles) et que la partie auto consistante satisfait les équations (1.3.6)-(1.3.9) avec les densités de charges et de courants données par (1.3.10)-(1.3.11).

Dans le cas non-relativiste on peut supposer que le champ magnétique auto-consistant est stationnaire. Dans ce cas l'équation (1.3.7) se réduit à $\nabla \times \mathbf{E} = 0$. On aboutit alors au système de Vlasov-Poisson dans lequel le champ électrique vérifie l'équation de Poisson (1.3.8) ou de façon équivalente le problème de Laplace :

$$\mathbf{E} = -\nabla \phi, \qquad -\Delta \phi = \frac{\rho}{\varepsilon_0}. \tag{1.3.12}$$

Remarque 1.3.1. *Même lorsque l'on ne considère qu'une seule espèce de particule et que l'on ne tient compte que des interactions électrostatiques entre les particules, le passage mathématique du modèle à N corps aux équations de Vlasov Poisson, via la théorie des champs moyens, n'est pas encore justifié. Pour plus de détails sur ce problème je conseille*

la lecture du cours [62]. Le principal obstacle concerne le fait que le potentiel électrostatique créé par une particule, c'est à dire

$$\phi(r) = \frac{q}{4\pi\varepsilon_0 r}, \tag{1.3.13}$$

où $r = \|\mathbf{r} - \mathbf{r}_q\|_2$ *correspond à la distance entre le point* $\mathbf{r}$ *où on calcule le potentiel et la position* $\mathbf{r}_q$ *de la particule, présente une singularité à l'origine.*

Par la suite, nous nous placerons dans le cas d'un plasma contenant uniquement une espèce d'ions et des électrons. Les ions étant plus lourds que les électrons, leur inertie est plus grande. Si bien que les ions peuvent être considérés immobiles. En notant n_i leur densité, cette hypothèse se traduit par :

$$\partial_t n_i = 0. \tag{1.3.14}$$

Concernant leur distribution dans l'espace des phases, on considérera qu'ils sont à l'équilibre thermodynamique. Ils sont alors répartis selon une gaussienne et la densité est donnée par $n_i = \int f_i d\mathbf{x} d\mathbf{v} = 1$. Le système d'équations à résoudre se réduit alors à :

$$\frac{\partial f}{\partial t} + \mathbf{v}\cdot\nabla_{\mathbf{x}} f + \frac{e}{m}\left(\mathbf{E}(\mathbf{x},t) + \mathbf{v}\times\mathbf{B}(\mathbf{x},t)\right)\cdot\nabla_{\mathbf{v}} f = 0, \tag{1.3.15}$$

$$\mathbf{E} = -\nabla\phi, \qquad -\Delta\phi = \frac{1}{\varepsilon_0}\left(1 - \int_{\mathbb{R}^3} f(\mathbf{x},\mathbf{v},t)\, d\mathbf{v}\right), \tag{1.3.16}$$

$$f(t=0,\mathbf{x},\mathbf{v}) = f_0(\mathbf{x},\mathbf{v}), \tag{1.3.17}$$

où f correspond à la fonction de distribution des électrons et f_0 à la répartition initiale des électrons. Je considérerai souvent le cas où le champ magnétique $\mathbf{B}$ est uniquement externe et où le champ électrique $\mathbf{E}$ se réduit à un champ auto-consistant.

Remarque 1.3.2. *Les plasmas font intervenir différentes échelles déterminées par certaines grandeurs caractéristiques, telles que la longueur de Debye, la fréquence plasma ou encore le nombre de Knudsen (voir le livre Rax [57], le proceeding Frénod Lutz [16], ou les thèses Crestetto [9], Filbet [12]).*

L'équation de Vlasov est fortement liée aux équations de Newton. Elle exprime que la fonction de distribution f est conservée le long des trajectoires d'une particule qui évoluerait sous l'action du champ électromagnétique "moyen" $(\mathbf{E},\mathbf{B})$.

1.4 Quelques outils pour les équations de Vlasov Poisson

Par souci de simplicité et de lisibilité je vais considérer dans cette section le système de Vlasov Poisson pour une espèce de particule. En normalisant les constantes à 1 on obtient :

$$\frac{\partial f}{\partial t} + \mathbf{v}\cdot\nabla_{\mathbf{x}} f + \mathbf{E}(\mathbf{x},t)\cdot\nabla_{\mathbf{v}} f = 0, \tag{1.4.1}$$

$$\mathbf{E} = -\nabla\phi, \qquad -\Delta\phi = \rho, \tag{1.4.2}$$

$$\rho = \int_{\mathbb{R}^3} f(\mathbf{x},\mathbf{v},t)\, d\mathbf{v}, \tag{1.4.3}$$

$$f(t=0,\mathbf{x},\mathbf{v}) = f_0(\mathbf{x},\mathbf{v}). \tag{1.4.4}$$

Les résultats sont alors facilement généralisables au cas où l'on considère un champ magnétique externe suffisamment régulier.

1.4.1 Quelques estimations à priori.

J'ai choisi dans cette section de présenter quelques estimations et quelques propriétés de conservation classique. Ces estimations sont d'une importance capitale d'un point de vue numérique et d'un point de vue théorique. D'un point de vue numérique il est important de s'assurer que les méthodes numériques conservent exactement, ou au moins approximativement, ces propriétés de conservation. D'un point de vue théorique ces résultats sont à la base de nombreux théorèmes d'existences et d'unicités de solutions de l'équation de Vlasov Poisson. Elles permettent également de montrer des résultats essentiels dans les différentes théories d'homogénéisation.

Nous allons démontrer ces propriétés de façon formelle. Plus précisément nous allons appliquer les formules de Green :

$$\int_{\mathbf{\Omega}} (\nabla \cdot \mathbf{F})\, g + \int_{\mathbf{\Omega}} \mathbf{F} \cdot \nabla g = \int_{\partial \mathbf{\Omega}} (\mathbf{F} \cdot \mathbf{n})\, g, \tag{1.4.5}$$

$$\int_{\mathbf{\Omega}} (\Delta u)\, v + \int_{\mathbf{\Omega}} \nabla u \cdot \nabla v = \int_{\partial \mathbf{\Omega}} \frac{\partial u}{\partial \mathbf{n}} v. \tag{1.4.6}$$

et nous allons systématiquement supposer que les intégrandes tendent suffisamment vite vers 0, de sorte à ce que :

$$\int_{\mathbb{R}^3 \times \mathbb{R}^3} (\nabla \cdot \mathbf{F})\, g + \int_{\mathbb{R}^3 \times \mathbb{R}^3} \mathbf{F} \cdot \nabla g = 0, \tag{1.4.7}$$

$$\int_{\mathbb{R}^3 \times \mathbb{R}^3} (\Delta u)\, v + \int_{\mathbb{R}^3 \times \mathbb{R}^3} \nabla u \cdot \nabla v = 0. \tag{1.4.8}$$

Remarque 1.4.1. *D'un point de vue pratique cela signifie que la distribution de particules, la densité de particules, le potentiel électrique et le champ électrique tendent suffisamment vite vers* 0. *On peut obtenir ces résultats de façon rigoureuse en procédant à une étape de régularisation et en passant à la limite.*

Principe du maximum

Pour obtenir le principe du maximum nous allons introduire les caractéristiques de l'équation de Vlasov (1.4.1) et utiliser le fait que la fonction de distribution f est constante le long de ces caractéristiques.

Definition 1.4.2. *Les caractéristiques de l'équation de Vlasov* (1.4.1) *sont les fonctions* $\mathbf{X}\big(s; t,\, \mathbf{x}, \mathbf{v}\big)$ *et* $\mathbf{V}\,(s; t, \mathbf{x}, \mathbf{v})$ *solutions du système différentiel :*

$$\frac{\partial \mathbf{X}}{\partial t}\,(s; t, \mathbf{x}, \mathbf{v}) = \mathbf{V}\,(s; t, \mathbf{x}, \mathbf{v})\,, \tag{1.4.9}$$

$$\frac{\partial \mathbf{V}}{\partial t}\,(s; t, \mathbf{x}, \mathbf{v}) = \mathbf{E}\,(\mathbf{X}\,(s; t, \mathbf{x}, \mathbf{v})\,, t)\,, \tag{1.4.10}$$

$$\mathbf{X}\,(s; s, \mathbf{x}, \mathbf{v}) = \mathbf{x}, \qquad \mathbf{V}\,(s; s, \mathbf{x}, \mathbf{v}) = \mathbf{v}. \tag{1.4.11}$$

La fonction f est alors constante le long des caractéristiques. En effet, par définition des caractéristiques, on a :

$$\frac{\partial}{\partial t} f\,(\mathbf{X}\,(s; t, \mathbf{x}, \mathbf{v})\,, \mathbf{V}\,(s; t, \mathbf{x}, \mathbf{v})\,, t) \tag{1.4.12}$$

$$= \left(\frac{\partial f}{\partial t} + \frac{\partial \mathbf{X}}{\partial t} \cdot \nabla_{\mathbf{x}} f + \frac{\partial \mathbf{V}}{\partial t} \cdot \nabla_{\mathbf{v}} f\right)(\mathbf{X}\,(s; t, \mathbf{x}, \mathbf{v})\,, \mathbf{V}\,(s; t, \mathbf{x}, \mathbf{v})\,, t) \tag{1.4.13}$$

$$= 0. \tag{1.4.14}$$

On en déduit que f est donnée par

$$f(t,\mathbf{x},\mathbf{v}) = f(\mathbf{X}(t;0,\mathbf{x},\mathbf{v}),\mathbf{V}(t;0,\mathbf{x},\mathbf{v}),0) \tag{1.4.15}$$
$$= f_0(\mathbf{X}(t;0,\mathbf{x},\mathbf{v}),\mathbf{V}(t;0,\mathbf{x},\mathbf{v})). \tag{1.4.16}$$

Ainsi si f_0 est bornée on obtient le principe du maximum :

$$0 \leq f(t,\mathbf{x},\mathbf{v}) \leq \sup_{(\mathbf{x},\mathbf{v})} f_0(\mathbf{x},\mathbf{v}). \tag{1.4.17}$$

Conservation de la charge

En intégrant l'équation de Vlasov (1.4.1) par rapport à $\mathbf{v}$ et en utilisant une formule de green appropriée on obtient l'équation de conservation de la charge :

$$\frac{\partial \rho}{\partial t} + \nabla_{\mathbf{x}} \cdot \mathbf{J} = 0, \tag{1.4.18}$$

où ρ est la densité de charge définie par (1.4.3) et $\mathbf{J}$ la densité de courant définie par

$$\mathbf{J}(\mathbf{x},t) = \int_{\mathbb{R}^3} f(\mathbf{x},\mathbf{v},t)\, d\mathbf{v}. \tag{1.4.19}$$

En intégrant l'équation de conservation de la charge par rapport à $\mathbf{x}$ on obtient la conservation de la charge :

$$\frac{\partial}{\partial t} \int_{\mathbb{R}^3 \times \mathbb{R}^3} f(\mathbf{x},\mathbf{v},t)\, d\mathbf{x} d\mathbf{v} = 0. \tag{1.4.20}$$

Remarque 1.4.3. *En multipliant l'équation de Vlasov par f^{q-1}, où q est un entier supérieur à 1, et en intégrant par rapport à $\mathbf{x}$ et $\mathbf{v}$ on obtient de façon similaire la conservation de la norme L^q de f*

Conservation de l'énergie

En multipliant l'équation de Vlasov par $|\mathbf{v}|^2$ et en intégrant par rapport à $\mathbf{x}$ et $\mathbf{v}$ on obtient :

$$\frac{\partial}{\partial t} \int_{\mathbb{R}^3 \times \mathbb{R}^3} |\mathbf{v}|^2 f(\mathbf{x},\mathbf{v},t)\, d\mathbf{x} d\mathbf{v} - 2\int_{\mathbb{R}^3} \mathbf{E} \cdot \mathbf{J}(\mathbf{x},t)\, d\mathbf{x} = 0. \tag{1.4.21}$$

En utilisant l'équation de conservation de la charge (1.4.18) on obtient :

$$\int_{\mathbb{R}^3} \mathbf{J} \cdot \mathbf{E} d\mathbf{x} = -\int_{\mathbb{R}^3} \mathbf{J} \cdot \nabla_{\mathbf{x}} \phi d\mathbf{x} = \int_{\mathbb{R}^3} (\nabla_{\mathbf{x}} \cdot \mathbf{J})\, \phi d\mathbf{x} = -\int_{\mathbb{R}^3} \frac{\partial \rho}{\partial t} \phi d\mathbf{x} \tag{1.4.22}$$

En utilisant maintenant l'équation de Poisson (1.4.2) on obtient :

$$\begin{aligned} \frac{1}{2}\frac{d}{dt}\int_{\mathbb{R}^3} \nabla_{\mathbf{x}}\phi \cdot \nabla_{\mathbf{x}}\phi d\mathbf{x} &= \int_{\mathbb{R}^3} \nabla_{\mathbf{x}}\phi \cdot \nabla_{\mathbf{x}} \frac{\partial \phi}{\partial t} d\mathbf{x} \\ &= -\int_{\mathbb{R}^3} \phi \frac{\partial}{\partial t} \Delta_{\mathbf{x}} \phi d\mathbf{x} \\ &= \int_{\mathbb{R}^3} \phi \frac{\partial \rho}{\partial t} d\mathbf{x}. \end{aligned} \tag{1.4.23}$$

En injectant (1.4.23) dans (1.4.22), puis en injectant le résultat dans (1.4.21), on obtient l'équation de conservation de l'énergie :

$$\frac{\partial}{\partial t}\left(\int_{\mathbb{R}^3 \times \mathbb{R}^3} |\mathbf{v}|^2 f d\mathbf{x} d\mathbf{v} + \int_{\mathbb{R}^3} |\nabla_{\mathbf{x}}\phi|^2 d\mathbf{x} \right) = 0. \tag{1.4.24}$$

Remarque 1.4.4. *En supposant que* $\int_{\mathbb{R}^6} f_0 \left|\mathbf{v}\right|^2 d\mathbf{x}d\mathbf{v} < +\infty$*, et en appliquant le lemme de Grönwall ,on déduit directement de* (1.4.24) *que pour tout réel* $T > 0$ *il existe une constante* C *telle que*

$$\left\| \left|\mathbf{v}\right|^2 f \right\|_{L^\infty(0,T;L^1(\mathbb{R}^6))} \leq C. \tag{1.4.25}$$

Estimation sur la densité de charge

Supposons que $f_0 \in L^2(\mathbb{R}^3 \times \mathbb{R}^3)$ et que $\int_{\mathbb{R}^6} f_0 \left|\mathbf{v}\right|^2 d\mathbf{x}d\mathbf{v} < +\infty$. D'après la remarque 1.4.3 et en utilisant que $f_0 \in L^2(\mathbb{R}^3 \times \mathbb{R}^3)$, on obtient la conservation de la norme L^2 de f. Soit R un réel strictement positif. On fait alors la décomposition suivante de la densité de charge :

$$\rho\left(\mathbf{x},t\right) = \int_{|\mathbf{v}|>R} f d\mathbf{v} + \int_{|\mathbf{v}|\leq R} f d\mathbf{v}. \tag{1.4.26}$$

D'une part on a

$$\int_{|\mathbf{v}|>R} f d\mathbf{v} \leq \int_{|\mathbf{v}|>R} \frac{\left|\mathbf{v}\right|^2}{R^2} f d\mathbf{v} \leq \frac{1}{R^2} \int_{\mathbb{R}^3} \left|\mathbf{v}\right|^2 f d\mathbf{v}, \tag{1.4.27}$$

et d'autre part, en utilisant l'inégalité de Cauchy Schwartz, on obtient :

$$\int_{|\mathbf{v}|\leq R} f d\mathbf{v} \leq \left(\int_{\mathbb{R}^3} f^2 d\mathbf{v} \right)^{1/2} \left(\int_{\mathbb{R}^3} 1_{\{|\mathbf{v}|\leq R\}} d\mathbf{v} \right)^{1/2} \leq C_1 R^{3/2} \left(\int_{\mathbb{R}^3} f^2 d\mathbf{v} \right)^{1/2}. \tag{1.4.28}$$

Ainsi pour tout $R > 0$ on a :

$$\rho\left(\mathbf{x},t\right) \leq \frac{1}{R^2} \int_{\mathbb{R}^3} \left|\mathbf{v}\right|^2 f d\mathbf{v} + C_1 R^{3/2} \left(\int_{\mathbb{R}^3} f^2 d\mathbf{v} \right)^{1/2}. \tag{1.4.29}$$

En minimisant le membre de droite par rapport à R on obtient :

$$\rho\left(\mathbf{x},t\right) \leq C_2 \left(\int_{\mathbb{R}^3} \left|\mathbf{v}\right|^2 f d\mathbf{v} \right)^{3/7} \left(\int_{\mathbb{R}^3} f^2 d\mathbf{v} \right)^{2/7}. \tag{1.4.30}$$

Finalement en appliquant l'inégalité d'Hölder on obtient :

$$\int_{\mathbb{R}^3} \left|\rho\left(\mathbf{x},t\right)\right|^{7/5} d\mathbf{x} \leq \int_{\mathbb{R}^3} C_3 \left(\int_{\mathbb{R}^3} \left|\mathbf{v}\right|^2 f d\mathbf{v} \right)^{3/5} \left(\int_{\mathbb{R}^3} f^2 d\mathbf{v} \right)^{2/5} d\mathbf{x} \tag{1.4.31}$$

$$\leq C_3 \left(\int_{\mathbb{R}^3} \left|\mathbf{v}\right|^2 f d\mathbf{x}d\mathbf{v} \right)^{3/5} \left(\int_{\mathbb{R}^3} f^2 d\mathbf{x}d\mathbf{v} \right)^{2/5}. \tag{1.4.32}$$

En d'autres termes, la densité est bornée dans $L^\infty\left(0,T;L^{7/5}\left(\mathbb{R}^3\right)\right)$.

Remarque 1.4.5. *De la même façon on obtient une estimation sur la densité de courant.*

1.4.2 Existence de solution pour le problème de Vlasov Poisson.

Intéressons-nous maintenant à la pertinence d'un point de vue mathématique du système (1.4.1)-(1.4.4). En d'autres termes, le système est-il bien posé pour une condition initiale donnée ? Il existe trois célèbres théorèmes pour ce problème.

Le premier est dû a Ukai et Okabe [61] :

Theorem 1.4.6. *Soit $f_0 \in \mathcal{C}^1\left(\mathbb{R}^d \times \mathbb{R}^d\right)$ positive telle qu'il existe $\kappa,\ \kappa' > 0$ et $\gamma > d$ tels que*

$$|f_0(\mathbf{x},\mathbf{v})| \leq \kappa\left(1+|\mathbf{x}|\right)^{-\gamma-1}\left(1+|\mathbf{v}|\right)^{-\gamma-1}, \tag{1.4.33}$$

$$|\nabla_{\mathbf{x},\mathbf{v}} f_0(\mathbf{x},\mathbf{v})| \leq \kappa'\left(1+|\mathbf{x}|\right)^{-\gamma}\left(1+|\mathbf{v}|\right)^{-\gamma}. \tag{1.4.34}$$

- *Si $d = 2$ alors $\forall T > 0$ l'équation* (1.4.1)-(1.4.4) *admet une unique solution $f \in \mathcal{C}^1\left([0,T], \mathcal{C}^1\left(\mathbb{R}^2 \times \mathbb{R}^2\right)\right)$.*
- *Si $d = 3$ alors $\exists T_0 > 0$ tel que l'équation* (1.4.1)-(1.4.4) *admet une unique solution $f \in \mathcal{C}^1\left([0,T_0], \mathcal{C}^1\left(\mathbb{R}^3 \times \mathbb{R}^3\right)\right)$.*

De plus ce théorème est généralisable lorsque les équations (1.4.1)-(1.4.4) sont posées sur le tore $\mathbb{T}^2$ ou $\mathbb{T}^3$.

Le second résultat est dû à Pfaffelmoser [53] :

Theorem 1.4.7. *Soit $f_0 \in \mathcal{C}^1\left(\mathbb{R}^3 \times \mathbb{R}^3\right)$ une fonction positive et à support compact. Alors le système* (1.4.1)-(1.4.4) *admet une unique solution $f \in \mathcal{C}^1\left(\mathbb{R}_+, \mathcal{C}^1\left(\mathbb{R}^3 \times \mathbb{R}^3\right)\right)$.*

Ce théorème est également généralisable sur le tore $\mathbb{T}^2$ ou $\mathbb{T}^3$.

Ces deux résultats sont les principaux résultats concernant les solutions régulières du système (1.4.1)-(1.4.4). Dans le premier cas la solution n'est pas définie pour $t \in \mathbb{R}_+$ et dans le second cas l'hypothèse support compact est très restrictive. Elle n'inclut notamment pas la distribution initiale la plus importante en physique des plasmas : la gaussienne, qui correspond à la distribution d'équilibre dans un plasma. Dans [58] l'auteur suggère que cette hypothèse est essentiellement technique et qu'elle peut être remplacée par des propriétés de décroissance rapide à l'infini (voir également [33]).

Remarque 1.4.8. *Dans [2], C. Bardos et P. Degond ont montré que lorsque les données initiales sont localisées et assez petites il existe une solution globale en temps et que celle-ci est unique.*

Nous allons terminer cette section par le principal résultat concernant les solutions faibles (c'est à dire au sens des distribution) du système (1.4.1)-(1.4.4). La théorie a été principalement élaborée par P.L. Lions et B. Perthame [39].

Theorem 1.4.9. *Soit $f_0 \in L^1 \cap L^\infty\left(\mathbb{R}^3 \times \mathbb{R}^3\right)$ une fonction positive. Supposons que*

$$\int_{\mathbb{R}^3\times\mathbb{R}^3} |\mathbf{v}|^m f_0(\mathbf{x},\mathbf{v})\, d\mathbf{x}d\mathbf{v} < +\infty \text{ si } m < m_0 \tag{1.4.35}$$

où $m_0 > 3$. Alors le système (1.4.1)-(1.4.4) *admet une solution $f \in \mathcal{C}\left(\mathbb{R}_+; L^p\left(\mathbb{R}^3 \times \mathbb{R}^3\right)\right) \cap L^\infty\left(\mathbb{R}_+; L^\infty\left(\mathbb{R}^3 \times \mathbb{R}^3\right)\right)$ (pour tout $1 \leq p < +\infty$) qui vérifie*

$$\sup_{t\in[0,T]} \int_{\mathbb{R}^3\times\mathbb{R}^3} |\mathbf{v}|^m f(t,\mathbf{x},\mathbf{v})\, d\mathbf{x}d\mathbf{v} < +\infty, \tag{1.4.36}$$

pour tout $T < +\infty$ et $m < m_0$.

Remarque 1.4.10. *L'unicité a été démontré par G. Loeper [43] sous l'hypothèse que $f_0 \in \mathcal{M}^+(\mathbb{R}^3\times\mathbb{R}^3)$, où $\mathcal{M}^+(\mathbb{R}^3\times\mathbb{R}^3)$ correspond à l'espace des mesures positives et bornées sur $\mathbb{R}^3 \times \mathbb{R}^3$.*

Remarque 1.4.11. *Dans [49] C. Pallard a montré que les résultats d'existence et d'unicité étaient toujours valable pour $m_0 > 2$. De plus, l'auteur a montrer l'existence de solution dans le cas du tore $\mathbb{T}^3$ lorsque $m_0 > 14/3$.*

1.5 Résolution numérique de l'équation de Vlasov-Poisson.

1.5.1 Difficultés liées à la dimension élevée et au couplage non-linéaire.

La résolution numérique des équations de Vlasov Poisson ou de Vlasov Maxwell est un défi important vu la complexité du problème. En effet, la fonction de distribution dépend de la position $\mathbf{x} = (x_1, x_2, x_3)$, de la vitesse $\mathbf{v} = (v_1, v_2, v_3)$, et du temps t. De plus, il est nécessaire de résoudre un couplage non linéaire entre les équations de Vlasov et de Poisson ou de Maxwell.

L'évolution des méthodes numériques utilisées pour la résolution de ces équations est fortement liée à l'évolution des moyens informatiques. Au cours de cette évolution, des situations de plus en plus complexes ont pu être traitées. Ceci, a nécessité le développement de nouvelles méthodes numériques. Ainsi dans les années 60 et 70 on ne pouvait traiter que des problèmes $1D$. Dans les années 80 et 90 la méthode PIC (Particle In Cell), que nous allons présenter dans la section 1.5.3, était quasiment la seule utilisée pour les simulations numériques. En effet, elle fournit de bons résultats physiques pour un coût de calcul raisonnable car elle ne nécessite pas la construction d'un maillage de l'espace des phases.

Depuis la fin des années 90 l'évolution de la puissance de calcul a permis d'envisager des méthodes plus précises utilisant un maillage de l'espace des phases. Parmis ces méthodes on trouve principalement les méthodes semi-Lagrangiennes et les méthodes de volumes finis (voir [60]). Les méthodes semi-Lagrangiennes utilisent le fait que la fonction de distribution est constante le long des caractéristiques et consistent à résoudre ces équations sur un maillage de l'espace des phases. Cependant ces deux méthodes ne sont utilisées qu'en petite dimension ($2D$ ou $4D$) et il n'est pas encore possible de résoudre les équations sur une grille $6D$.

Actuellement, les méthodes numériques et les moyens informatiques sont toujours fortement liés. Depuis le début des années 2000, la puissance de calcul des cartes graphiques est devenue tellement importante, pour un coût finalement très réduit (100 à 700 euros pour les modèles grand public), que les chercheurs en physique des plasmas sont de plus en plus nombreux à vouloir en exploiter le potentiel. L'objectif recherché est alors de répartir les tâches d'un même programme informatique sur plusieurs processeurs de la carte graphique permettant ainsi de réduire le temps de simulation, et de produire des simulations en temps réel.

1.5.2 Difficulté spécifique aux plasmas fortement magnétisés.

Outre les problèmes liés à la dimension élevée et au couplage non linéaire entre Vlasov et Maxwell ou Vlasov et Poisson, un autre problème apparait lorsque l'on souhaite simuler l'évolution du plasma dans le cadre du confinement magnétique. En effet, nous allons nous intéresser à des régimes dont la principale caractéristique est l'intensité du champ magnétique. En notant $\bar{t}$ le temps caractéristique d'observation et $\bar{T}_c$ la période cyclotron caractéristique (la période caractéristique de rotation autour des lignes de champ magnétique) l'hypothèse champ magnétique fort se traduit par :

$$\frac{\bar{T}_c}{\bar{t}} = \varepsilon \tag{1.5.1}$$

où ε est un petit paramètre. D'un point de vue numérique cela signifie que pour une méthode numérique classique le pas de temps doit être très petit, notamment plus petit que la période cyclotron qui à l'échelle d'observation est déjà de l'ordre de ε.

1.5.3 La méthode PIC.

D'un point de vue numérique j'ai principalement utilisé des méthodes PIC, notamment dans les chapitres 3 et 4. Pour terminer cette section, je vais donc exposer le principe de cette méthode dans le cadre de la résolution numérique des équations de Vlasov Poisson. Une application à l'amortissement Landau est proposé dans l'annexe A.3. Le principe de la méthode est d'approcher la fonction de distribution, solution de l'équation de Vlasov, par une combinaison linéaire de N masses de Dirac. Ces masses de Dirac sont centrées en les positions dans l'espace des phases d'un nombre N de macro-particules. Les coefficients affectés aux masses de Dirac sont appelés poids des macro particules. En d'autres termes, on approche la fonction de distribution par :

$$f_N(\mathbf{x}, \mathbf{v}, t) = \sum_{k=1}^{N} \omega_k \delta(\mathbf{x} - \mathbf{x}_k(t)) \delta(\mathbf{v} - \mathbf{v}_k(t)), \tag{1.5.2}$$

où $\left\{\left(\mathbf{x}^k, \mathbf{v}^k\right)\right\}_{k=1}^N$ correspond aux N macro particules et où pour tout $k = 1, \ldots, N$, $\mathbf{x}_k(0) = \mathbf{x}_0^k$, et $\mathbf{v}_k(0) = \mathbf{v}_0^k$. L'algorithme est donné dans le schéma ci-dessous.

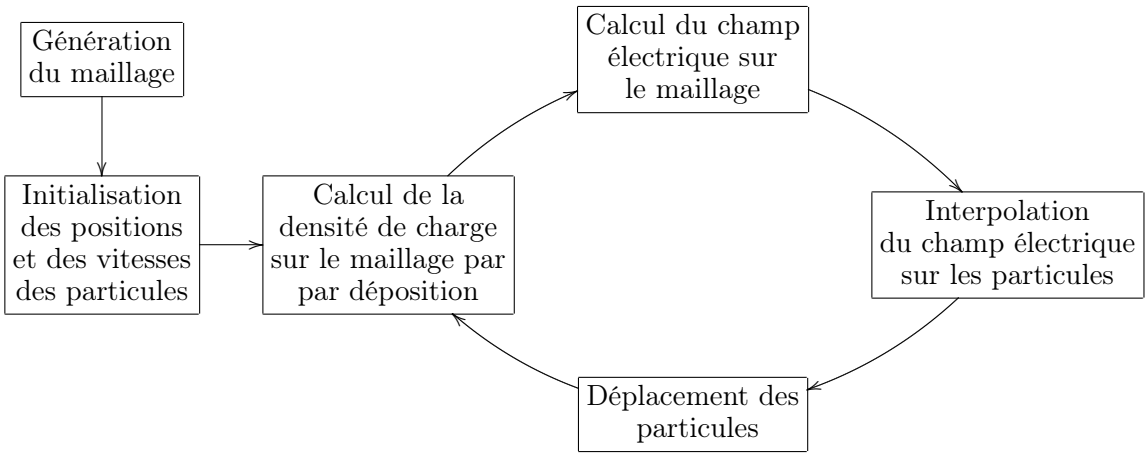

Détaillons ces étapes :

Choix des conditions initiales

Il existe principalement deux types de méthodes pour générer les conditions initiales $\left\{\left(\mathbf{x}_0^k, \mathbf{v}_0^k\right)\right\}_{k=1}^N$:

- Méthode déterministe : on construit un maillage de l'espace des phases et on place les particules aux barycentres des mailles. Les poids correspondent alors aux intégrales de la condition initiale sur les mailles.
- Méthode de type Monte Carlo : les positions et vitesses des particules sont choisies aléatoirement ou pseudo-aléatoirement selon la densité de probabilité associée à f_0. Il est alors fréquent de prendre des poids égaux à $1/N$.

Génération du maillage

Le maillage correspond à un maillage de l'espace des positions. Considérons donc un domaine $\mathbf{\Omega_x}$ et supposons ce domaine suffisamment grand de sorte que les macro particules restent dans ce domaine durant les simulations. Une autre alternative consiste à supposer que les particules se déplacent dans un tore. Dans ce cas, cette condition devient obsolète. Pour fixer les idées supposons que $\mathbf{x} \in \mathbb{R}^2$, $\mathbf{v} \in \mathbb{R}^2$ et que

$$\mathbf{\Omega_x} = [0, T_{x_1}] \times [0, T_{x_2}], \tag{1.5.3}$$

où T_{x_1} et T_{x_2} sont deux réels strictement positifs. L'option la plus simple consiste alors à construire un maillage uniforme

$$\begin{aligned} x_1^i &= i\Delta x_1, \quad i = 0, \ldots, N_1, \\ x_2^j &= j\Delta x_2, \quad i = 0, \ldots, N_2, \end{aligned} \tag{1.5.4}$$

où N_1 et N_2 sont deux entiers positifs et où $\Delta x_1 = T_{x_1}/N_1$ et $\Delta x_2 = T_{x_2}/N_2$.

Remarque 1.5.1. *Le choix du pas d'espace est un point clé de l'algorithme. Il faut par exemple s'assurer qu'il y ait au moins* 100 *particules par maille.*

Couplage particules maillage

On définit la densité de charge discrète par

$$\rho_N(\mathbf{x}, t) = q \int_{\mathbb{R}^2} f_N(\mathbf{x}, \mathbf{v}, t)\, d\mathbf{v} = q \sum_{k=1}^{N} \omega_k \delta(\mathbf{x} - \mathbf{x}_k(t)). \tag{1.5.5}$$

Cette approximation particulaire de ρ ne permet pas d'avoir les valeurs de ρ sur le maillage. Ainsi dans le but de coupler cette approximation avec un solveur de l'équation de Poisson il est nécessaire de procéder à une étape de régularisation. Cette étape est alors réalisée à l'aide d'un noyau de convolution S. On définit alors la régularisée ρ_h de ρ_N comme étant le produit de convolution entre ρ_N et S :

$$\rho_h(\mathbf{x}, t) = \int_{\mathbb{R}^2} S(\mathbf{x} - \mathbf{x}')\, \rho_N(\mathbf{x}', \mathbf{v}, t)\, d\mathbf{v} = q \sum_{k=1}^{N} \omega_k S(\mathbf{x} - \mathbf{x}_k(t)). \tag{1.5.6}$$

Un bon choix consiste à prendre des splines. Dans cette thèse je prendrai en général des splines d'ordre 1. Elles sont définies par :

$$S_{\Delta x}(x) = \begin{cases} \frac{1}{\Delta x}\left(1 - \frac{|x|}{\Delta x}\right) & \text{si } |x| < \Delta x \\ 0 & \text{sinon,} \end{cases} \tag{1.5.7}$$

lorsqu'on est en dimension 1, par $S^{2D}(x_1, x_2) = S_{\Delta x_1}(x_1)\, S_{\Delta x_2}(x_2)$ en dimension 2, etc... L'expression de ρ_h sur le maillage Poisson est alors donnée par

$$\rho_h(\mathbf{x}^{i,j}, t) = q \sum_{k=1}^{N} \omega_k S^{2D}(\mathbf{x}^{i,j} - \mathbf{x}_k(t)), \tag{1.5.8}$$

où $\mathbf{x}^{i,j} = (x_1^i, x_2^j)$. Le choix des splines comme noyau de convolution permet notamment d'avoir une conservation numérique de la masse.

En résolvant l'équation de Poisson on aboutit a l'expression du champ électrique sur le maillage. On peut formaliser ceci par l'expression suivante :

$$\mathbf{E}(\mathbf{x},t)=\sum_{k=1}^{N}\mathbf{E}_{i,j}\delta\left(\mathbf{x}-\mathbf{x}^{i,j}\right). \tag{1.5.9}$$

A nouveau, pour obtenir l'expression du champ électrique au niveau des particules, il est nécessaire de régulariser cette expression. On procède alors comme pour l'étape précédente. L'expression du champ au niveau des particules est alors donnée par :

$$\mathbf{E}\left(\mathbf{x}_k(t),t\right)=\Delta x_1\Delta x_2\sum_{k=1}^{N}\mathbf{E}_{i,j}S^{2D}\left(\mathbf{x}-\mathbf{x}^{i,j}\right) \tag{1.5.10}$$

Remarque 1.5.2. *Afin d'éviter des problèmes numériques il est impératif de choisir le même noyau de convolution que celui utilisé pour la déposition des particules.*

Advection

Les particules sont déplacées en suivant les caractéristique de l'équation de Vlasov. Pour résoudre ces caractéristiques on peut par exemple utliser la méthode de Runge Kutta d'ordre 4. Pour une équation du type $dy/dt=K(t,y)$ le schéma numérique permettant de passer du temps t_n au temps $t_{n+1}=t_n+\Delta t$ s'écrit :

$$\begin{aligned}
&t_{n,1}=t_n,\quad y^{n,1}=y^n\\
&t_{n,2}=t_n+\frac{\Delta t}{2},\quad y^{n,2}=y^n+\frac{1}{2}I^1,\ \text{avec } I^1=\Delta tK(t_{n,1},y^{n,1}),\\
&t_{n,3}=t_n+\frac{\Delta t}{2},\quad y^{n,3}=y^n+\frac{1}{2}I^2,\ \text{avec } I^2=\Delta tK(t_{n,2},y^{n,2}),\\
&t_{n,4}=t_n+\Delta t,\quad y^{n,4}=y^n+I^3,\ \text{avec } I^3=\Delta tK(t_{n,3},y^{n,3}),\\
&y^{n+1}=y^n+\frac{1}{6}I^1+\frac{1}{3}I^2+\frac{1}{3}I^3+\frac{1}{6}I^4,\ \text{avec } I^4=\Delta tK(t_{n,4},y^{n,4}).
\end{aligned} \tag{1.5.11}$$

Il est donc nécessaire de résoudre numériquement l'équation de Poisson aux étapes 2, 3, 4, et 5. Il existe bien évidemment d'autres schémas pour avancer les particules. Le principal défaut de cette méthode est que celle-ci ne conserve pas les volumes. Par exemple, si on considère les équations de la section 1.2.3, et en effectuant des simulations en temps long, les trajectoires semblent s'écraser sur elles mêmes (voir [56]). Il est donc en général plus intéressant d'utiliser des méthodes symplectiques. Le schéma de Verlet est de loin le plus utilisé (voir [60]). Mais on peut également utiliser des intégrateurs symplectiques variationnels ([56]), ou des schémas Runge Kutta symplectiques.

1.6 Gyrocinétique et méthodes d'homogénéisations.

Dans la section précédente (section 1.5) nous avons observé que la simulation numérique d'un plasma ou d'un faisceau de particules fortement magnétisé se heurtait à deux principaux problèmes : la dimension élevée du problème ainsi que la nécessité de choisir un petit pas de temps. Il peut ainsi s'avérer très intéressant d'avoir recours à des modèles réduits.

Comme nous l'avons vu dans la section 1.2.1, la trajectoire d'une particule chargée dans un champ magnétique constant est hélicoïdale le long des lignes de champ avec un rayon

proportionnel à l'inverse de la norme du champ magnétique. Lorsque cette norme est très grande la particule est piégée le long de la ligne de champ. Le mouvement apparent de la particule, appelé mouvement du centre guide, est alors donné par

$$\mathbf{C}_1(t, \mathbf{x}_0, \mathbf{v}_0) = x_{0,1}, \tag{1.6.1}$$
$$\mathbf{C}_2(t, \mathbf{x}_0, \mathbf{v}_0) = x_{0,2}, \tag{1.6.2}$$
$$\mathbf{C}_3(t, \mathbf{x}_0, \mathbf{v}_0) = x_{0,3} + v_{0,3}t. \tag{1.6.3}$$

Lorsque le champ magnétique varie, où lorsque l'on considère un faisceau de particules, les choses sont moins triviales. En particulier, la question de savoir si l'influence mutuelle des particules peut être exprimée en terme de leur mouvement apparent ou si l'oscillation génère des effets supplémentaires est importante. L'un des principaux objectifs est de trouver un modèle approché permettant d'éliminer les oscillations rapides. Toutes les théories d'homogénéisations des équations de Vlasov Poisson sont basées sur ce point.

1.6.1 Régimes Drift-Kinetic et Rayon de Larmor Fini.

D'un point de vue mathématique la première étape consiste à quantifier ce que signifie se placer dans le cadre d'un champ magnétique fort. Cette étape est réalisée via un adimensionnement des équations. Pour simplifier, plaçons nous dans le cadre où : $\mathbf{B} = B(x_1, x_2)\mathbf{e}_{x_3}$, $\mathbf{E} = \mathbf{E}(x_1, x_2)$, et $\mathbf{E} \cdot \mathbf{B} = 0$. Dans ce cas en notant $\mathbf{x} = (x_1, x_2) \in \mathbb{R}^2$ et $\mathbf{v} = (v_1, v_2) \in \mathbb{R}^2$, les équations de Vlasov Poisson, écrites dans le plan orthogonal au champ magnétique, sont données par

$$\frac{\partial f}{\partial t} + \mathbf{v} \cdot \nabla_{\mathbf{x}} f + \frac{q}{m}\left(\mathbf{E}(\mathbf{x}, t) + \mathbf{v}^{\perp} B(\mathbf{x})\right) \cdot \nabla_{\mathbf{v}} f = 0, \tag{1.6.4}$$
$$\mathbf{E} = -\nabla\phi, \quad -\Delta\phi = \frac{\rho}{\varepsilon_0} = \frac{q}{\varepsilon_0}\int_{\mathbb{R}^2} f(t, \mathbf{x}, \mathbf{v})\, d\mathbf{v}, \tag{1.6.5}$$
$$f(t = 0, \mathbf{x}, \mathbf{v}) = f_0(\mathbf{x}, \mathbf{v}), \tag{1.6.6}$$

où $\mathbf{v}^{\perp} = (v_2, -v_1)$.

Pour adimensionner ces équations on procède comme dans les sections 1.2.2 et 1.2.3. Soit $\bar{t}$ une échelle de temps caractéristique, $\bar{L}$ une échelle de longueur caractéristique, $\bar{v}$ une échelle de vitesse caractéristique, $\bar{B}$ une échelle d'intensité caractéristique du champ magnétique, $\bar{E}$ une échelle d'intensité caractéristique du champ électrique et $\bar{f}$ un facteur d'échelle pour f. On définit alors de nouvelles variables $\mathbf{x}'$, $\mathbf{v}'$ et t' par $\mathbf{x} = \bar{L}\mathbf{x}'$, $\mathbf{v} = \bar{v}\mathbf{v}'$ et $t = \bar{t}t'$. On définit également les quantités sans dimensions $\mathbf{E}'$, B', et f' par :

$$\begin{aligned} &\mathbf{E}(\mathbf{x}, t) = \bar{E}\mathbf{E}'(\mathbf{x}', t'), \\ &B(\mathbf{x}) = \bar{B}B'(\mathbf{x}', t), \\ &f(\mathbf{x}, \mathbf{v}, t) = \bar{f}f'(\mathbf{x}', \mathbf{v}', t'). \end{aligned} \tag{1.6.7}$$

En injectant ces quantités dans (1.6.4), en identifiant les grandeurs caractéristiques $\bar{\omega}_c = q\bar{B}/m$ et $\bar{a}_L = \bar{v}/\bar{\omega}_c$, puis en imposant

$$\bar{\omega}_c\bar{t} = \frac{1}{\varepsilon}, \quad \frac{\bar{a}_L}{\bar{L}} = \varepsilon, \quad \text{et} \quad \frac{\bar{E}}{\bar{v}\bar{B}} = \varepsilon, \tag{1.6.8}$$

on obtient l'équation de Vlasov $2D$ dans *le régime Drift Kinetic* :

$$\frac{\partial f'}{\partial t'} + \mathbf{v}' \cdot \nabla_{\mathbf{x}'} f' + \left(\mathbf{E}'(\mathbf{x}', t') + \frac{B'(\mathbf{x}')\,\mathbf{v}^{\perp}}{\varepsilon}\right) \cdot \nabla_{\mathbf{v}'} f' = 0. \tag{1.6.9}$$

Remarque 1.6.1. *Les formules* (1.6.8) *signifient dans l'ordre énuméré que : à l'échelle temporelle caractéristique la période d'oscillation est petite, à l'échelle de longueur caractéristique le rayon de Larmor est petit, et que la force électrique caractéristique est petite devant la force magnétique caractéristique,*

Pour la condition initiale nous allons supposer que ses échelles de variation (avant la mise à l'échelle) sont du même ordre de grandeur que les échelles caractéristiques utilisées c'est à dire que $f'(t'=0,\mathbf{x}',\mathbf{v}') = f'_0(\mathbf{x}',\mathbf{v}')$.

Concernant l'équation de Poisson on va imposer que $\bar{E} = \bar{\phi}/\bar{L}$ et que $\bar{f} = \frac{\bar{\phi}}{q\bar{L}^2\bar{v}^2}$, de sorte que ces équations se réécrivent :

$$\mathbf{E}' = -\nabla_{\mathbf{x}'}\phi', \qquad -\Delta_{\mathbf{x}'}\phi' = \int_{\mathbb{R}^2} f'\left(t',\mathbf{x}',\mathbf{v}'\right) d\mathbf{v}'. \tag{1.6.10}$$

Dans la suite par souci de lisibilité, et puisque je travaillerai toujours dans des régimes adimensionnés, j'enlèverai les $'$.

1.6.2 Méthode d'homogénéisation basée sur la convergence à deux échelles

Cette méthode est largement développée dans les articles Frénod Sonnendrücker [19] et Frénod Sonnendrücker [21]. Je me contenterai d'en expliquer les principales étapes. Homogénéiser le système de Vlasov Poisson consiste à déterminer un système d'équations limites lorsque le petit paramètre ε, introduit dans l'adimensionnement, tend vers 0. L'intérêt d'un système limite est qu'il ne dépend pas du petit paramètre ε, ce qui permet d'augmenter le pas de temps lors de la résolution numérique.

Les différentes méthodes d'homogénéisation se distinguent par le cadre de convergence choisi. Le cadre de la convergence à deux échelles est particulièrement adapté à notre problème puisque il y a principalement deux échelles de temps : une petite échelle à laquelle se produisent les oscillations rapides et une autre échelle plus lente à laquelle se produit le mouvement apparent.

Par la suite nous noterons W un espace de Banach, dont le dual est un espace séparable, et qui est inclus de façon compact dans $\mathcal{D}'(\mathbb{R}^2_{\mathbf{x}}\times\mathbb{R}^2_{\mathbf{v}})$. Commençons par définir la convergence deux-échelles.

Definition 1.6.2. *On dit qu'une suite de fonction $f_\varepsilon \in L^\infty(0,T;W)$ converge à deux échelles vers une fonction 2π-périodique $F \in L^\infty(0,T;L^\infty_{2\pi}(\mathbb{R}_\tau;W))$, si pour toutes fonctions $\psi = \psi(t,\tau,\mathbf{x},\mathbf{v})$ régulières, à support compact par rapport à $(t,\mathbf{x},\mathbf{v})$, et 2π-périodiques par rapport à τ on a :*

$$\int_{\mathcal{Q}} f^\varepsilon\left(t,\mathbf{x},\mathbf{v}\right)\psi\left(t,\frac{t}{\varepsilon},\mathbf{x},\mathbf{v}\right) dtd\mathbf{x}d\mathbf{v} \to \int_{\mathcal{Q}}\int_0^{2\pi} F\psi d\tau dtd\mathbf{x}d\mathbf{v} \tag{1.6.11}$$

lorsque ε tend vers 0, où $\mathcal{Q} = [0,T)\times\mathbb{R}^2_{\mathbf{x}}\times\mathbb{R}^2_{\mathbf{v}}$.

En général, une preuve directe de la convergence à deux échelle d'une suite de fonctions est complexe. Heureusement, il existe d'autres méthodes pour prouver la convergence à deux échelles. En général on utilise le théorème suivant :

Theorem 1.6.3. *Si une suite f_ε est bornée dans $L^\infty(0,T;W)$ alors il existe une fonction 2π-périodique $F \in L^\infty(0,T;L^\infty_{2\pi}(\mathbb{R}_\tau;W))$ et une sous-suite de f_ε qui converge à deux-échelles vers F.*

Ainsi en utilisant une propriété de conservation de la norme L^2 de la fonction de distribution, il est facile de montrer qu'il existe une sous-suite de f^ε qui converge à deux échelles vers une fonction $F \in L^\infty(0,T;L^\infty_{2\pi}(\mathbb{R}_\tau;L^2(\mathbb{R}^2_{\mathbf{x}}\times\mathbb{R}^2_{\mathbf{v}})))$. Pour fixer les idées considérons l'équation de Vlasov-Poisson (1.6.4)-(1.6.6) dans le régime Drift-Kinetic avec un champ magnétique B constant égal à 1, c'est à dire

$$\frac{\partial f^\varepsilon}{\partial t} + \mathbf{v}\cdot\nabla_{\mathbf{x}} f^\varepsilon + \left(\mathbf{E}^\varepsilon(\mathbf{x},t) + \frac{1}{\varepsilon}\mathbf{v}^\perp\right)\cdot\nabla_{\mathbf{v}} f = 0, \tag{1.6.12}$$

$$\mathbf{E}^\varepsilon = -\nabla_{\mathbf{x}}\phi^\varepsilon, \quad -\Delta_{\mathbf{x}}\phi^\varepsilon = \int_{\mathbb{R}^2} f^\varepsilon d\mathbf{v}, \tag{1.6.13}$$

$$f^\varepsilon(t=0) = f_0. \tag{1.6.14}$$

L'objectif est maintenant de déterminer une équation limite caractérisant la fonction F. En multipliant l'équation de Vlasov (1.6.12) par les fonctions tests suggérées dans la définition 1.6.2 et en faisant des intégrations par parties on obtient la formulation faible suivante :

$$\begin{aligned} &-\int_{\mathcal{Q}} f^\epsilon\left(\left[\frac{\partial\psi}{\partial t}\right]^\epsilon + \frac{1}{\epsilon}\left[\frac{\partial\psi}{\partial\tau}\right]^\epsilon + \mathbf{v}\cdot[\nabla_{\mathbf{x}}\psi]^\epsilon + \left(\mathbf{E}^\epsilon + \frac{1}{\epsilon}\mathbf{v}^\perp\right)\cdot[\nabla_{\mathbf{v}}\psi]^\epsilon\right) d\mathbf{x}d\mathbf{v}dt \\ &= \int_{\mathcal{O}} f_0(\mathbf{x},\mathbf{v})\,\psi(0,0,\mathbf{x},\mathbf{v})\,d\mathbf{x}d\mathbf{v}, \end{aligned} \tag{1.6.15}$$

où pour toutes fonctions $\varphi = \varphi(t,\tau,\mathbf{x},\mathbf{v})$ on a noté

$$[\varphi]^\varepsilon(t,\mathbf{x},\mathbf{v}) = \varphi(t,t/\varepsilon,\mathbf{x},\mathbf{v}), \tag{1.6.16}$$

et où

$$\mathcal{O} = \mathbb{R}^2_{\mathbf{x}}\times\mathbb{R}^2_{\mathbf{v}}, \tag{1.6.17}$$

$$\mathcal{Q} = [0,T)\times\mathbb{R}^2_{\mathbf{x}}\times\mathbb{R}^2_{\mathbf{v}}. \tag{1.6.18}$$

En utilisant une estimation sur la densité de charge, l'équation de Poisson, et un argument de compacité (Théorème 1.6.3), il est facile de montrer que le champ et le potentiel électrique convergent à deux échelles (modulo une sous-suite) vers des fonctions 2π-périodiques Φ et $\boldsymbol{\mathcal{E}}$. La principale difficulté technique de la méthode est concentrée dans le passage à la limite dans l'intégrale contenant le produit $f^\varepsilon\mathbf{E}^\varepsilon$. Il s'agit alors de se placer dans les conditions d'application du théorème suivant :

Theorem 1.6.4. *Soit u_ε une suite de fonctions dans $L^\infty(0,T;W)$ qui converge à deux échelles vers une fonction U. Si une suite v^ε converge fortement vers une fonctions v dans un second espace de Banach W' (qui satisfait les mêmes propriétés que W), et si le produit $u_\varepsilon v^\varepsilon$ a du sens dans un troisième espace de Banach W'', alors le produit $u_\varepsilon v^\varepsilon$ converge à deux échelles vers $Uv \in L^\infty(0,T;L^\infty_{2\pi}(\mathbb{R}_\tau;W''))$.*

On peut alors, par exemple, montrer que le champ électrique converge fortement. On utilise le Théorème d'Aubin-Lions (voir [59]) :

Theorem 1.6.5. *Soient W et W' deux espaces de Banach, et W'' un espace de Hausdorff métrisable et localement convexe tels que $W \subseteq W' \subseteq W''$. Supposons également que la première inclusion est compact, que la seconde est continue, et que W soit un espaces séparable et réflexif. Pour $1 < p < \infty$, et $1 \le q \le \infty$ on définit*

$$\mathcal{S} = \left\{ u \in L^p([0,T],W), \frac{\partial u}{\partial t} \in L^q\left([0,T],W''\right)\right\}. \tag{1.6.19}$$

Alors l'inclusion $\mathcal{S} \subseteq L^p([0,T],W'')$ est compact.

En estimant la densité de courant et en utilisant les équations de conservation de la charge et de Poisson (notamment les propriétés régularisante du laplacien), on obtient une estimation de $\partial_t \mathbf{E}$ et on se place ainsi dans les conditions d'applications du Théorème 1.6.5. On en déduit alors la convergence forte du champ électrique. On note $\mathbf{E}$ la limite forte.

Remarque 1.6.6. *La limite forte* $\mathbf{E}$ *de* $\mathbf{E}^\varepsilon$ *est relié à la limite deux échelles par la formule*

$$\boldsymbol{\mathcal{E}} = \frac{1}{2\pi}\mathbf{E}. \tag{1.6.20}$$

En particulier, la limite deux échelles ne dépend pas de τ*.*

En multipliant (1.6.15) par ε, puis en passant à la limite, on obtient l'équation de contrainte suivante :

$$\frac{\partial F}{\partial \tau} + \mathbf{v}^\perp \cdot \nabla_{\mathbf{v}} F = 0. \tag{1.6.21}$$

L'équation de contrainte ne permet pas de caractériser la limite deux échelles F. En particulier cette équation ne permet pas de relier F à la condition initiale f_0. Néanmoins, en utilisant la méthode des caractéristiques (voir section 1.4.1), cette équation donne la forme que doit avoir F :

$$F(t,\tau,\mathbf{x},\mathbf{v}) = G(t,\mathbf{x},\mathbf{u}(\mathbf{v},\tau)), \text{ où } \mathbf{u}(\mathbf{v},\tau) = \begin{bmatrix} \cos(\tau) & -\sin(\tau) \\ \sin(\tau) & \cos(\tau) \end{bmatrix} \mathbf{v}. \tag{1.6.22}$$

La dernière étape de la méthode consiste à caractériser la fonction G. On procède alors comme suit : on définit la fonction g^ε par $g^\varepsilon(t,\mathbf{x},\mathbf{v}) = f^\varepsilon(t,\mathbf{x},\mathbf{u}(\mathbf{v},-t/\varepsilon))$, puis on écrit une formulation faible de l'équation de Vlasov en terme de g^ε.

Remarque 1.6.7. *La fonction* g^ε *correspond à la fonction* f^ε *à laquelle on aurait "retirée" l'oscillation rapide.*

Soit $\varphi = \varphi(t,\mathbf{x},\mathbf{u})$ une fonction test, régulière et à support compact. Posons $\psi(t,\tau,\mathbf{x},\mathbf{v}) = \varphi(t,\mathbf{x},\mathbf{u}(\mathbf{v},\tau))$. En utilisant cette classe de fonction test dans l'équation (1.6.15), puis en faisant le changement de variables $\mathbf{u} = \mathbf{u}(\mathbf{v},t/\varepsilon)$ on aboutit à la formulation faible suivante :

$$\begin{aligned} &\int_{\mathcal{Q}'} g^\epsilon(t,\mathbf{x},\mathbf{u}) \left(\frac{\partial \varphi}{\partial t} + e^{\frac{t}{\varepsilon}M}\mathbf{u} \cdot \nabla_{\mathbf{x}}\varphi + \mathbf{E}^\epsilon \cdot \left(e^{\frac{t}{\varepsilon}M} \nabla_{\mathbf{u}}\varphi \right) \right) d\mathbf{x}d\mathbf{u}dt \\ &= -\int_{\mathcal{O}} f_0(\mathbf{x},\mathbf{v})\,\varphi(0,\mathbf{x},\mathbf{v})\,d\mathbf{x}d\mathbf{v} = 0. \end{aligned} \tag{1.6.23}$$

Remarque 1.6.8. *En écrivant l'équation satisfaite par* g^ε *et en utilisant des arguments similaires à ceux utilisés pour montrer la convergence forte du champ électrique, on peut montrer que* g^ε *converge fortement vers la fonction* $2\pi G$*.*

En passant à la limite dans 1.6.23 on obtient l'équation caractérisant G :

$$\frac{\partial G}{\partial t} = 0, \tag{1.6.24}$$

$$G_{t=0} = \frac{1}{2\pi} f_0. \tag{1.6.25}$$

On en déduit donc que F est donnée par

$$F(t,\tau,\mathbf{x},\mathbf{v}) = \frac{1}{2\pi} f_0(\mathbf{x},\mathbf{u}(\mathbf{v},\tau)). \tag{1.6.26}$$

On peut alors approximer f^ε par $f^\varepsilon(t,\mathbf{x},\mathbf{v}) \simeq F(t,t/\varepsilon,\mathbf{x},\mathbf{v})$.

Remarque 1.6.9. *La limite deux échelles du système* (1.6.12)-(1.6.14) *ne tient pas compte du champ électrique auto-consistant. Pour obtenir un modèle plus précis il faut déterminer l'ordre suivant dans la développement asymptotique deux échelles de* f^ε *(voir [14]).*

Remarque 1.6.10. *Dans d'autre cas, comme par exemple ceux traités dans [19] et [21], l'équation caractérisant* G *dépend de la limite deux-échelles du champ électrique. Pour obtenir l'équation satisfaite par la limite deux échelles du champ électrique il suffit de multiplier l'équation de Poisson par une fonction test appropriée et passer à la limite.*

1.6.3 Méthodes géométriques

Les méthodes géométriques que je vais présenter dans cette section opèrent lorsque le moment magnétique est un invariant adiabatique. Comme nous l'avons observé dans la section 1.2.4 le moment magnétique est un invariant adiabatique lorsqu'à l'échelle du mouvement de la particule le champ magnétique varie peu c'est à dire lorsque

$$\frac{\bar{a}_L}{\bar{L}} \frac{\nabla_{\mathbf{x}} B}{B} \sim \varepsilon. \tag{1.6.27}$$

Remarque 1.6.11. *Dans la formule* (1.6.27)*,* B *correspond au champ magnétique adimensionné et* $\mathbf{x}$ *à la variable de position adimensionnée.*

Dans le régime Drift-Kinetic $\bar{a}_L/\bar{L} \sim \varepsilon$ et la condition (1.6.27) est toujours satisfaite. Dans le régime Rayon de Larmor Fini le rayon de Larmor est de magnitude 1. Ainsi pour qu'une particule perçoive de faible variation du champ magnétique il est nécessaire que le champ magnétique adimensionné varie peu, c'est à dire que $\nabla_{\mathbf{x}} B/B \sim \varepsilon$.

Definition 1.6.12. *On appel système de coordonnées centre-guide historique le système de coordonnées définit par :*

$$y_1^{hgc} = x_1 - \frac{\bar{a}_L}{\bar{L}} \frac{v}{B(\mathbf{x})} \cos(\theta), \tag{1.6.28}$$

$$y_2^{hgc} = x_2 + \frac{\bar{a}_L}{\bar{L}} \frac{v}{B(\mathbf{x})} \sin(\theta), \tag{1.6.29}$$

$$\theta^{hgc} = \theta, \tag{1.6.30}$$

$$\mu^{hgc} = \frac{v^2}{2B(\mathbf{x})}, \tag{1.6.31}$$

où θ *et* v *sont tels que* $v = |\mathbf{v}|$ *et* $\mathbf{v} = v(-\sin(\theta), -\cos(\theta))$.

Remarque 1.6.13. *Supposons que le champ magnétique est constant égal à* B_0*. Dans ce cas, dans les régimes Drift-Kinetic et Rayon de Larmor Fini, les caractéristiques de l'équation de Vlasov écrites dans le système de coordonnées centre guide historique sont données par :*

$$\begin{aligned} \frac{\partial \mathbf{Y}^{hgc}}{\partial t} &= 0, \\ \frac{\partial \Theta^{hgc}}{\partial t} &= \frac{B_0}{\varepsilon}, \\ \frac{\partial K^{hgc}}{\partial t} &= 0. \end{aligned} \tag{1.6.32}$$

De manière générale les méthodes géométriques consistent à déterminer un système de coordonnées infinitésimalement proche du système de coordonnées centre-guide historique dans lequel la coordonnée proche du moment magnétique est un invariant et dans lequel l'évolution des autres variables ne dépend pas de la variable d'oscillation. Le système de coordonnées obtenu est appelé le système de coordonnée gyrocinétique. Ainsi, si on s'intéresse uniquement au mouvement de la particule dans l'espace physique, la résolution du système dynamique dans le système de coordonnées gyrocinétique se réduit à trouver une trajectoire dans $\mathbb{R}^2$, au lieu d'une trajectoire dans $\mathbb{R}^4$ lorsque le système est résolu dans le système de coordonnées initial.

Chapitre 2

On the Geometrical Gyro-kinetic Theory

Sommaire

2.1 Introduction

At the end of the 70', Littlejohn [40, 41, 42] shed new light on what is called *the Guiding Center Approximation.* His approach incorporated high level mathematical concepts from Hamiltonian Mechanics, Differential Geometry and Symplectic Geometry into a physical affordable theory in order to clarify what has been done for years in the domain (see Kruskal [37], Gardner [24], Northrop [46], Northrop & Rome [47]). This theory is a nice success. It has been beeing widely used by physicists to deduce related models (*Finite Larmor Radius Approximation, Drift-Kinetic Model, Quasi-Neutral Gyro-Kinetic Model, etc.*, see for instance Brizard [5], Dubin *et al.* [11], Frieman & Chen [22], Hahm [29], Hahm, Lee & Brizard [31], Parra & Catto [50, 51, 52]) making up the *Gyro-Kinetic Approximation Theory*, which is the basis of all kinetic codes used to simulate Plasma Turbulence emergence and evolution in Tokamak and Stellarators (see for instance Brizard [5], Quin *et al* [54, 55], Kawamura & Fukuyama [35], Hahm [30], Hahm, Wang & Madsen [32], Grandgirard *et al.* [27, 28], and the review of Garbet *et al.* [23]).
Yet, the resulting Geometrical Gyro-Kinetic Approximation Theory remains a physical theory which is formal from the mathematical point of view and not directly affordable for mathematicians. The present paper is a first step towards providing a mathematical affordable theory, particularly for the analysis, the applied mathematics and computer sciences communities.

Notice that, beside this Geometrical Gyro-Kinetic Approximation Theory, an alternative approach, based on Asymptotic Analysis and Homogenization Methods was developed by Frénod & Sonnendrücker [19, 20, 21], Frénod, Raviart & Sonnendrücker [17], Golse & Saint-Raymond [26] and Ghendrih, Hauray & Nouri [25].

Summarizing, the Geometrical Gyro-Kinetic Approximation Theory consists in building a change of coordinates in order to make two components of a dynamical system disappear. The method to achieve this goal involves, in a intricate way, elements of Hamiltonian Dynamical System Theory, Symplectic Geometry, Non-Linear Hyperbolic PDE, Hilbert Theory of Operators and Asymptotic Analysis.

In order to clarify the purpose and put things in context, notice that the domain of validity of the Gyro-Kinetic Approximation Theory is that of charged particles under the action of a strong magnetic field. Hence, we begin by considering a non-relativistic charged particle moving in a static magnetic field. It is well known that, in usual coordinates $(\underline{\mathbf{x}}, \underline{\mathbf{v}}) = (x_1, x_2, x_3, v_1, v_2, v_3)$, where $\underline{\mathbf{x}}$ stands for the position variable and $\underline{\mathbf{v}}$ for the velocity variable, the position $\underline{\mathbf{X}}(t; \underline{\mathbf{x}}, \underline{\mathbf{v}})$ and the velocity $\underline{\mathbf{V}}(t; \underline{\mathbf{x}}, \underline{\mathbf{v}})$ at time t of the particle which is in $\underline{\mathbf{x}}$ with velocity $\underline{\mathbf{v}}$ at time $t = 0$ are solutions to

$$\frac{\partial \underline{\mathbf{X}}}{\partial t} = \underline{\mathbf{V}}, \qquad \underline{\mathbf{X}}(0) = \underline{\mathbf{x}}, \tag{2.1.1}$$

$$\frac{\partial \underline{\mathbf{V}}}{\partial t} = \frac{q}{m} \underline{\mathbf{V}} \times \mathbf{B}(\underline{\mathbf{X}}), \qquad \underline{\mathbf{V}}(0) = \underline{\mathbf{v}}. \tag{2.1.2}$$

In this dynamical system, $\underline{\mathbf{X}}$ has three components $(\mathbf{X}_1, \mathbf{X}_2, \mathbf{X}_3)$, as $\underline{\mathbf{V}} : (\mathbf{V}_1, \mathbf{V}_2, \mathbf{V}_3)$.

For the purpose of this paper, we restrict to magnetic fields of the form

$$\mathbf{B}\left(\underline{\mathbf{x}}\right) = (0, 0, B(x_1, x_2)), \tag{2.1.3}$$

and furthermore, we consider only the projection of the particle motion onto the x_1, x_2-plan. So writing $\mathbf{x} = (x_1, x_2)$ and $\mathbf{v} = (v_1, v_2)$, the bi-dimensional dynamical system for $\mathbf{X}(t; \mathbf{x}, \mathbf{v})$ ($\mathbf{X} = (\mathbf{X}_1, \mathbf{X}_2)$) and $\mathbf{V}(t; \mathbf{x}, \mathbf{v})$ ($\mathbf{V} = (\mathbf{V}_1, \mathbf{V}_2)$) resulting from (3.1.6) and (3.1.7) reads

$$\frac{\partial \mathbf{X}}{\partial t} = \mathbf{V}, \qquad \mathbf{X}(0) = \mathbf{x}, \tag{2.1.4}$$

$$\frac{\partial \mathbf{V}}{\partial t} = \frac{q}{m} B(\mathbf{X})\, {}^{\perp}\mathbf{V}, \qquad \mathbf{V}(0) = \mathbf{v}, \tag{2.1.5}$$

where, for any $\mathbf{u} = (u_1, u_2)$ in $\mathbb{R}^2$, the notation ${}^{\perp}\mathbf{u}$ stands for $(u_2, -u_1)$. Throughout the rest of this paper, we will be interested in trajectory $(\mathbf{X}, \mathbf{V})$ and in dynamical system (2.1.4) and (2.1.5).
Finally, we suppose that the sign of B remains constant and that B is nowhere close to 0.

Now we make precise the context of strong magnetic field we work within. It is well known that the norm $|\mathbf{V}|$ of the velocity $\mathbf{V}$ solution to (2.1.5) is constant and that if the magnetic field B is uniform, the trajectory $\mathbf{X}$ of the considered charged particle is a circle. The radius a_L of the circle, which is called the Larmor radius in the context of Tokamak and Stellarator plasma, equals the norm of the velocity times the particle charge divided by the particle mass times the norm of the magnetic field, i.e.

$$a_L = \frac{|\mathbf{V}|}{\omega_c} \quad \text{where} \quad \omega_c = \frac{q|B|}{m}, \tag{2.1.6}$$

is the cyclotron frequency. The center of the circle, which is called the guiding center, equals

$$\mathbf{C} = \mathbf{X}(t) - \boldsymbol{\rho}(t), \tag{2.1.7}$$

where

$$\boldsymbol{\rho}(t) = -a_L \frac{{}^{\perp}\mathbf{V}(t)}{|\mathbf{V}|}. \tag{2.1.8}$$

Here, we do not consider a uniform B. Nevertheless, at any time t_0 when the position of the particle is $\mathbf{X}(t_0)$, we can consider the local values of the Larmor radius, the cyclotron frequency and the guiding center

$$a_L(t_0) = \frac{|\mathbf{V}|}{\omega_c(t_0)}, \tag{2.1.9}$$

$$\omega_c(t_0) = \frac{q|B(\mathbf{X}(t_0)|}{m}, \tag{2.1.10}$$

$$\mathbf{C}(t_0) = \mathbf{X}(t_0) - \boldsymbol{\rho}(t_0), \tag{2.1.11}$$

$$\boldsymbol{\rho}(t_0) = -a_L(t_0) \frac{{}^{\perp}\mathbf{V}(t_0)}{|\mathbf{V}|}. \tag{2.1.12}$$

With the help of those quantities, we can say that considering a small Larmor Radius consists in considering that the magnetic field applied to the particle position $\mathbf{X}(t_0)$ is close to the magnetic field applied to the guiding center position $\mathbf{C}(t_0)$. Now, as the magnetic field is strong, the local value of the period of rotation

$$T_c(t_0) = (2\pi/\omega_c(t_0)) \approx (2\pi m/q|B(\mathbf{C}(t_0)|), \tag{2.1.13}$$

is small. Considering that $a_L(t)$ and $T_c(t)$ have the same magnitude and that they are both small implies that $(a_L(t))^2\omega_c(t)$ is small and hence that

$$\frac{\partial \mathbf{C}}{\partial t}(t) = (a_L(t))^2\omega_c(t)\,\frac{{}^{\perp}\mathbf{V}(t)}{|\mathbf{V}|}\,\frac{\nabla_{\mathbf{x}}B(\mathbf{X}(t))\cdot(\mathbf{V}(t)/|\mathbf{V}|)}{B(\mathbf{X}(t))}$$

is small. As

$$a_L(t) \approx \frac{m|\mathbf{V}|}{q|B(\mathbf{C}(t)|}, \tag{2.1.14}$$

the fact that $\mathbf{C}(t)$ vary slowly has for consequence that the Larmor Radius vary slowly. To summarize, for any time t belonging to a time interval of length of order $(2\pi m/q|B(\mathbf{C}(t_0)|)$ the values of $a_L(t)$ and of $\mathbf{C}(t)$ remain almost constant, so that the particle trajectory is close to a circle of radius $m|\mathbf{V}|/qB(\mathbf{C}(t_0))$ traveled in a time close to $(2\pi m/q|B(\mathbf{C}(t_0)|)$.

To reexplain this within a rigorous modeling procedure, called scaling, and to introduce rigorously the small and large quantities, we need to define some characteristic scales : $\bar{t}$ stands for a characteristic time, $\bar{L}$ for a characteristic length and $\bar{v}$ for a characteristic velocity. We now define new variables t', $\mathbf{x}'$ and $\mathbf{v}'$ by $t = \bar{t}t'$, $\mathbf{x} = \bar{L}\mathbf{x}'$, and $\mathbf{v} = \bar{v}\mathbf{v}'$, making the characteristic scales the units. In the same way, we define the scaling factor $\bar{B}$ for the magnetic field :

$$\mathbf{B}\left(\bar{L}\mathbf{x}'\right) = \bar{B}\mathcal{B}\left(\mathbf{x}'\right). \tag{2.1.15}$$

Using those dimensionless variables and magnetic field, we obtain from dynamical system (2.1.4)–(2.1.5) that dimensionless trajectory $(\mathbf{X}', \mathbf{V}')$ defined by

$$\mathbf{X}(\bar{t}t'; \bar{L}\mathbf{x}', \bar{v}\mathbf{v}') = \bar{L}\mathbf{X}'(t'; \mathbf{x}', \mathbf{v}'), \tag{2.1.16}$$
$$\mathbf{V}(\bar{t}t'; \bar{L}\mathbf{x}', \bar{v}\mathbf{v}') = \bar{v}\mathbf{V}'(t'; \mathbf{x}', \mathbf{v}'), \tag{2.1.17}$$

is solution to

$$\frac{\bar{L}}{\bar{t}}\frac{\partial \mathbf{X}'}{\partial t'} = \bar{v}\mathbf{V}', \qquad \mathbf{X}'(0) = \mathbf{x}', \tag{2.1.18}$$
$$\frac{\bar{v}}{\bar{t}}\frac{\partial \mathbf{V}'}{\partial t'} = \frac{q\bar{B}\bar{v}}{m}\mathcal{B}\left(\mathbf{X}'\right)\ {}^{\perp}\mathbf{V}', \qquad \mathbf{V}'(0) = \mathbf{v}'. \tag{2.1.19}$$

We introduce the characteristic cyclotron frequency and Larmor radius :

$$\bar{\omega}_c = \frac{q\bar{B}}{m} \quad \text{and} \quad \bar{a}_L = \frac{\bar{v}}{\bar{\omega}_c}. \tag{2.1.20}$$

Using those physical characteristic quantities, system (2.1.18)–(2.1.19) becomes

$$\frac{\partial \mathbf{X}'}{\partial t'} = \bar{t}\bar{\omega}_c\frac{\bar{a}_L}{\bar{L}}\mathbf{V}', \qquad \mathbf{X}'(0) = \mathbf{x}', \tag{2.1.21}$$
$$\frac{\partial \mathbf{V}'}{\partial t'} = \bar{t}\bar{\omega}_c\mathcal{B}\left(\mathbf{X}'\right)\ {}^{\perp}\mathbf{V}', \qquad \mathbf{V}'(0) = \mathbf{v}'. \tag{2.1.22}$$

Once this dimensionless system written, saying that the magnetic field is strong means that the characteristic time $\bar{t}$ is large when compared to the characteristic period $\bar{T}_c = 2\pi/\bar{\omega}_c$. Introducing a small parameter ε, this can be translated into :

$$\bar{t}\bar{\omega}_c = \frac{1}{\varepsilon}. \tag{2.1.23}$$

Now, saying that the Larmor radius is small when compared to the characteristic scale length consists in considering that

$$\frac{\bar{a}_L}{\bar{L}} = \varepsilon, \tag{2.1.24}$$

Hence, the dimensionless dynamical system is rewritten as :

$$\frac{\partial \mathbf{X}'}{\partial t'} = \mathbf{V}', \qquad \mathbf{X}'(0) = \mathbf{x}', \tag{2.1.25}$$

$$\frac{\partial \mathbf{V}'}{\partial t'} = \frac{1}{\varepsilon}\mathcal{B}\left(\mathbf{X}'\right)^{\perp}\mathbf{V}', \qquad \mathbf{V}'(0) = \mathbf{v}'. \tag{2.1.26}$$

Yet, we have enough material to precise, within this framework, our intuition that, with accuracy of the order of ε, for any time t' belonging to a time interval $[t'_0, t'_1]$ of length of the order ε, $\mathbf{X}'$ draws a circle of radius $\varepsilon\left|\mathbf{v}'\right|/\mathcal{B}\left(\mathbf{X}'\left(t'_0\right)\right)$ over a time $2\pi\varepsilon/\mathcal{B}(\mathbf{X}'\left(t'_0\right))$. We let,

$$\mathbf{X}'\left(t'\right) = \mathbf{C}'\left(t'\right) + \boldsymbol{\rho}'\left(t'\right), \tag{2.1.27}$$

$$\boldsymbol{\rho}'\left(t'\right) = -\frac{\varepsilon}{\mathcal{B}\left(\mathbf{X}'\left(t'\right)\right)}{}^{\perp}\mathbf{V}'\left(t'\right), \tag{2.1.28}$$

$$\boldsymbol{\rho}'\left(t'\right) = \left|\boldsymbol{\rho}'\left(t'\right)\right|\left(\cos\left(\Theta'\left(t'\right)\right), -\sin\left(\Theta'\left(t'\right)\right)\right), \tag{2.1.29}$$

where $\Theta'\left(t'\right)$ is the angle between the x_1-axis and $\boldsymbol{\rho}'\left(t'\right)$ mesured in the clockwise sense.

Using the usual mobile orthonormal frame $(\hat{\mathbf{c}}(\theta), \hat{\mathbf{a}}(\theta))$, where $\hat{\mathbf{c}}(\theta) = (-\sin(\theta), -\cos(\theta))$ and $\hat{\mathbf{a}}\left(\theta\right) = \left(\cos\left(\theta\right), -\sin\left(\theta\right)\right)$, equations (2.1.28) and (2.1.29) yield the expression of $\mathbf{V}'$ in this frame and the ODE it satisfies :

$$\mathbf{V}'\left(t'\right) = \left|\mathbf{V}'\right|\hat{\mathbf{c}}\left(\Theta'\left(t'\right)\right), \tag{2.1.30}$$

$$\frac{\partial \mathbf{V}'}{\partial t'} = \left|\mathbf{V}'\right|\frac{\partial}{\partial t'}\hat{\mathbf{c}}\left(\Theta'\left(t'\right)\right) = -\left|\mathbf{V}'\right|\frac{\partial \Theta'}{\partial t'}\left(t'\right)\hat{\mathbf{a}}\left(\Theta'\left(t'\right)\right). \tag{2.1.31}$$

Injecting (2.1.31) in (2.1.26) and using the fact that, in frame $(\hat{\mathbf{c}}\left(\theta\right), \hat{\mathbf{a}}\left(\theta\right))$, ${}^{\perp}\mathbf{V}'\left(t'\right)$ writes :

$${}^{\perp}\mathbf{V}'\left(t'\right) = -\left|\mathbf{V}'\right|\hat{\mathbf{a}}\left(\Theta'\left(t'\right)\right),$$

we obtain the equation satisfied by $\Theta'\left(t'\right)$.

In the case of a constant magnetic field, we have :

$$\frac{\partial \mathbf{C}'}{\partial t'}\left(t'\right) = 0, \tag{2.1.32}$$

$$\frac{\partial}{\partial t'}\left|\boldsymbol{\rho}'\left(t'\right)\right| = 0, \tag{2.1.33}$$

$$\frac{\partial \Theta'}{\partial t'}\left(t'\right) = \frac{1}{\varepsilon}\mathcal{B}, \tag{2.1.34}$$

and the particle draws a circle of center $\mathbf{C}'$, of radius $|\rho'|$ over a time $2\pi\varepsilon/\mathcal{B}$.
When the magnetic field is not constant the ODEs satisfied by $\mathbf{C}'$, $|\rho'|$, and Θ' are

$$\frac{\partial \mathbf{C}'}{\partial t'}\left(t'\right) = -\varepsilon\,{}^{\perp}\mathbf{V}'\left(t\right)\frac{\nabla_{\mathbf{x}'}\mathcal{B}\left(\mathbf{X}'\left(t'\right)\right)\cdot\mathbf{V}'\left(t'\right)}{\left(\mathcal{B}\left(\mathbf{X}'\left(t'\right)\right)\right)^2}, \tag{2.1.35}$$

$$\frac{\partial}{\partial t'}\left|\boldsymbol{\rho}'\left(t'\right)\right| = \varepsilon\left|\mathbf{V}'\right|\frac{\nabla_{\mathbf{x}'}\mathcal{B}\left(\mathbf{X}'\left(t'\right)\right)\cdot\mathbf{V}'\left(t'\right)}{\left(\mathcal{B}\left(\mathbf{X}'\left(t'\right)\right)\right)^2}, \tag{2.1.36}$$

$$\frac{\partial \Theta'}{\partial t'}\left(t'\right) = \frac{1}{\varepsilon}\mathcal{B}\left(\mathbf{X}'\left(t'\right)\right) \underset{\varepsilon\to 0}{\sim} \frac{1}{\varepsilon}\mathcal{B}\left(\mathbf{C}'\left(t'\right)\right), \tag{2.1.37}$$

Hence, for any time t' belonging to a time interval $[t'_0, t'_1]$ of length of the order of ε, the usual Taylor inequality leads to $|\mathcal{B}(\mathbf{C}'(t')) - \mathcal{B}(\mathbf{C}'(t'_0))| = O(\varepsilon^2)$ and hence

$$\frac{\partial \Theta'}{\partial t'}(t') \underset{\varepsilon \to 0}{\sim} \frac{1}{\varepsilon}\mathcal{B}(\mathbf{C}'(t'_0)) \text{ and } \Theta'\left(t' + \frac{2\pi\varepsilon}{\mathcal{B}(\mathbf{C}'(t'_0))}\right) - \Theta'(t') \text{ is close to } 2\pi. \quad (2.1.38)$$

Moreover, for any time t belonging to $[t'_0, t'_1]$, from (2.1.35)–(2.1.37) we obtain

$$\left|\mathbf{C}'(t') - \mathbf{C}'(t'_0)\right| = O(\varepsilon^2), \left|\left|\boldsymbol{\rho}'(t')\right| - \left|\boldsymbol{\rho}'(t'_0)\right|\right| = O(\varepsilon^2). \quad (2.1.39)$$

Writing $\mathbf{X}'(t') = \mathbf{C}'(t') + \rho'(t')$, (2.1.39) and (2.1.38) say nothing but that $\mathbf{X}'$ draws a circle of radius $\varepsilon|\mathbf{v}'|/\mathcal{B}(\mathbf{C}'(t'_0))$ around $\mathbf{C}'(t'_0)$ over a time $2\pi\varepsilon/\mathcal{B}(\mathbf{C}'(t'_0))$ with accuracy of the order of ε.

The regime in which dynamical system (2.1.25)–(2.1.26) is written is called the drift-kinetic regime.

Subsequently, we will work exclusively with dimensionless variables. Since no confusion is possible, to simplify the notations, we will remove the ' and replace $\mathcal{B}$ by B. Hence, for $\mathbf{x}_0 = (x_{10}, x_{20}) \in \mathbb{R}^2$ and $\mathbf{v} = (v_{10}, v_{20}) \in \mathbb{R}^2$ we consider $\mathbf{X}(t, \mathbf{x}_0, \mathbf{v}_0) = (\mathbf{X}_1(t, \mathbf{x}_0, \mathbf{v}_0), \mathbf{X}_2(t, \mathbf{x}_0, \mathbf{v}_0))$ and $\mathbf{V}(t, \mathbf{x}_0, \mathbf{v}_0) = (\mathbf{V}_1(t, \mathbf{x}_0, \mathbf{v}_0), \mathbf{V}_2(t, \mathbf{x}_0, \mathbf{v}_0))$ solutions to the following dynamical system

$$\frac{\partial \mathbf{X}}{\partial t} = \mathbf{V}, \qquad \mathbf{X}(0) = \mathbf{x}_0, \quad (2.1.40)$$

$$\frac{\partial \mathbf{V}}{\partial t} = \frac{1}{\varepsilon} B(\mathbf{X})^{\perp}\mathbf{V}, \qquad \mathbf{V}(0) = \mathbf{v}_0, \quad (2.1.41)$$

and we make the following assumptions on B :

$$B(\mathbf{x}) = \frac{\partial A_2}{\partial x_1} - \frac{\partial A_1}{\partial x_2}. \quad (2.1.42)$$

with $\mathbf{A} = (A_1, A_2)$ an analytic function on $\mathbb{R}^2$ and

$$\inf_{\mathbf{x} \in \mathbb{R}^2} B(\mathbf{x}) > 1. \quad (2.1.43)$$

Remark 2.1.1. *In this remark, we will evoke issues related to the numerical simulation of system* (2.1.40)–(2.1.41). *What we learn from* (2.1.27) *is that the solution of* (2.1.40)–(2.1.41) *is made of two parts : a strongly oscillating one, related to the strong oscillations of* $\boldsymbol{\rho}$*, and, the guiding center motion, i.e. the motion of* $\mathbf{C}$*. Because of the oscillation part, direct numerical simulation of* (2.1.40)–(2.1.41) *requires a very small time step, and then is not considered. One could think that a good option to compute an approximate solution of* (2.1.40)–(2.1.41) *would be to compute* $\mathbf{C}$*. Yet, the resolution of EDO* (2.1.35) $\mathbf{C}$ *is solution to, requires the knowledge of trajectory* $\mathbf{X}$ *and consequently the resolution of* (2.1.40)-(2.1.41). *This option seems then to be a dead end. The interest of the Gyro-Kinetic Approximation is that it yields a dynamical system for something which is close to* $\mathbf{X}$ *and* $\mathbf{C}$*, but which can be solved as a stand-alone system.*

Now, we give a detailed summarize of what the present paper contains. In the geometric formalism, in any system of coordinates on a manifold $\mathcal{M}$, a Hamiltonian dynamical system, which solution is $\mathbf{R} = \mathbf{R}(t, \mathbf{r}_0)$ in the considered system of coordinates, can be written in the following form

$$\frac{\partial \mathbf{R}}{\partial t} = \mathcal{P}(\mathbf{R}) \nabla_{\mathbf{r}} H(\mathbf{R}), \quad \mathbf{R}(0, \mathbf{r}_0) = \mathbf{r}_0, \tag{2.1.44}$$

where $\mathcal{P}(\mathbf{r})$ is a skew-symmetric matrix called the matrix of the Poisson Bracket (or Poisson Matrix in short), and $H(\mathbf{r})$ is called the Hamiltonian function. Moreover, a sufficient condition for a dynamical system to be Hamiltonian is that the dynamical system writes in the form (2.1.44) in one system of coordinates which is global on $\mathcal{M}$. Roughly speaking, the goal of the Geometrical Gyro-Kinetic Theory is to make a succession of change of coordinates in order to satisfy the assumptions of the following theorem.

Theorem 2.1.2. *If, in a given coordinate system* $\mathbf{r} = (r_1, r_2, r_3, r_4)$*, the Poisson Matrix has the following form :*

$$\mathcal{P}(\mathbf{r}) = \left(\begin{array}{c|cc} \mathbb{M}_{(\mathbf{r})} & \begin{array}{c} 0 \\ 0 \end{array} & \begin{array}{c} 0 \\ 0 \end{array} \\ \hline \begin{array}{cc} 0 & 0 \end{array} & 0 & 1 \\ \begin{array}{cc} 0 & 0 \end{array} & -1 & 0 \end{array} \right), \tag{2.1.45}$$

and if the Hamiltonian function does not depend on the penultimate variable, i.e.

$$\frac{\partial H}{\partial r_3} = 0, \tag{2.1.46}$$

then, submatrix $\mathtt{M}$ *does not depend on the two last variables, i.e.*

$$\frac{\partial \mathtt{M}}{\partial r_3} = 0 \text{ and } \frac{\partial \mathtt{M}}{\partial r_4} = 0. \tag{2.1.47}$$

Consequently, the time-evolution of the two first components $\mathbf{R}_1, \mathbf{R}_2$ *is independent of the penultimate component* $\mathbf{R}_3$ *; and, the last component* $\mathbf{R}_4$ *of the trajectory is not time-evolving, i.e.*

$$\frac{\partial \mathbf{R}_4}{\partial t} = 0. \tag{2.1.48}$$

Proof. When the Poisson Matrix has the form given by (2.1.45), the last line of (2.1.44) reads

$$\frac{\partial \mathbf{R}_4}{\partial t} = -\frac{\partial H}{\partial r_3}(\mathbf{R}).$$

Hence, if the Hamiltonian function does not depend on the penultimate variable, then, the last component $\mathbf{R}_4$ of the trajectory is not time-evolving. Now, introducing the Poisson Bracket of two functions $f \equiv f(\mathbf{r})$ and $g \equiv g(\mathbf{r})$ defined by

$$\{f, g\}_{\mathbf{r}}(\mathbf{r}) = [\nabla_{\mathbf{r}} f(\mathbf{r})]^T \mathcal{P}(\mathbf{r}) \nabla_{\mathbf{r}} g(\mathbf{r}), \tag{2.1.49}$$

where $\mathcal{P}(\mathbf{r})$ is the Poisson Matrix, we have

$$\mathcal{P}_{i,j} = \{\mathbf{r}_i, \mathbf{r}_j\}_{\mathbf{r}} \text{ for } i, j = 1, 2, 3, 4, \tag{2.1.50}$$

where $\mathbf{r}_i$ is the i-th coordinate function $\mathbf{r} \mapsto r_i$ and a direct computation leads to

$$\left\{\left\{\mathbf{r}_1, \mathbf{r}_2\right\}_{\mathbf{r}}, \mathbf{r}_3\right\}_{\mathbf{r}}(\mathbf{r}) = -\frac{\partial \mathcal{P}_{1,2}}{\partial r_4}(\mathbf{r}) \text{ and } \left\{\left\{\mathbf{r}_1, \mathbf{r}_2\right\}_{\mathbf{r}}, \mathbf{r}_4\right\}_{\mathbf{r}}(\mathbf{r}) = \frac{\partial \mathcal{P}_{1,2}}{\partial r_3}(\mathbf{r}). \tag{2.1.51}$$

Using the Jacobi identity saying that for any regular function f, g, h,

$$\left\{\left\{f, g\right\}_{\mathbf{r}}, h\right\}_{\mathbf{r}} + \left\{\left\{h, f\right\}_{\mathbf{r}}, g\right\}_{\mathbf{r}} + \left\{\left\{g, h\right\}_{\mathbf{r}}, f\right\}_{\mathbf{r}} = 0, \tag{2.1.52}$$

and the facts that $\mathcal{P}_{3,1} = \mathcal{P}_{2,3} = \mathcal{P}_{4,1} = \mathcal{P}_{2,4} = 0$, we obtain

$$\left\{\left\{\mathbf{r}_1, \mathbf{r}_2\right\}_{\mathbf{r}}, \mathbf{r}_3\right\}_{\mathbf{r}} = -\left\{\left\{\mathbf{r}_3, \mathbf{r}_1\right\}_{\mathbf{r}}, \mathbf{r}_2\right\}_{\mathbf{r}} - \left\{\left\{\mathbf{r}_2, \mathbf{r}_3\right\}_{\mathbf{r}}, \mathbf{r}_1\right\}_{\mathbf{r}} = 0, \tag{2.1.53}$$

$$\left\{\left\{\mathbf{r}_1, \mathbf{r}_2\right\}_{\mathbf{r}}, \mathbf{r}_4\right\}_{\mathbf{r}} = -\left\{\left\{\mathbf{r}_4, \mathbf{r}_1\right\}_{\mathbf{r}}, \mathbf{r}_2\right\}_{\mathbf{r}} - \left\{\left\{\mathbf{r}_2, \mathbf{r}_4\right\}_{\mathbf{r}}, \mathbf{r}_1\right\}_{\mathbf{r}} = 0. \tag{2.1.54}$$

and consequently, since $\mathcal{P}_{1,1} = \mathcal{P}_{2,2} = 0$, (2.1.51) brings (2.1.47), ending the proof of the theorem. □

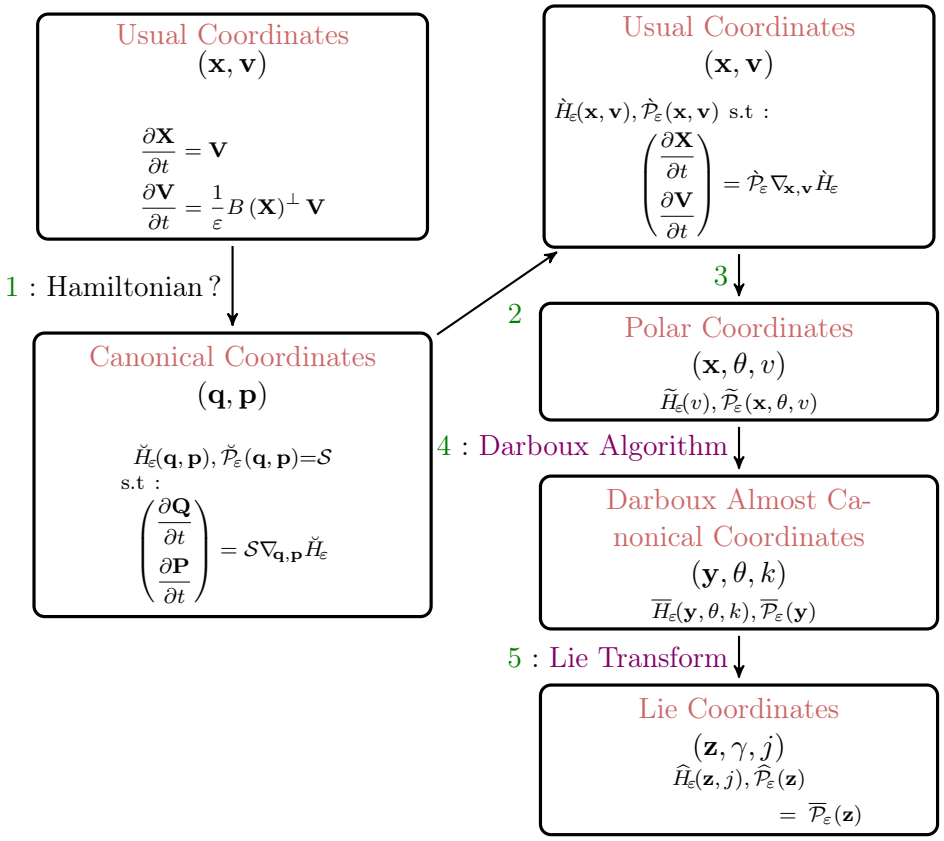

FIGURE 2.1 – A schematic description of the method leading the Gyro-Kinetic Approximation.

Theorem 2.1.2 is the Key Result that brings the understanding of the Geometrical Gyro-Kinetic Theory. Skipping most of the details, we can say that the Gyro-Kinetic Approximation of dynamical system (2.1.40)–(2.1.41) consists in writing it within a system of coordinates, called the Gyro-Kinetic coordinate system, that satisfies the assumptions of Theorem 2.1.2 and which is close to the Historic Guiding-Center Coordinates which is

such that :

$$y_1^{hgc} = x_1 - \varepsilon \frac{v}{B(\mathbf{x})} \cos(\theta), \tag{2.1.55}$$

$$y_2^{hgc} = x_2 + \varepsilon \frac{v}{B(\mathbf{x})} \sin(\theta), \tag{2.1.56}$$

$$\theta^{hgc} = \theta, \tag{2.1.57}$$

$$k^{hgc} = \frac{v^2}{2B(\mathbf{x})}, \tag{2.1.58}$$

where $v = |\mathbf{v}|$ and where θ is such that (v, θ) is a Polar Coordinate System for the velocity variable and is defined precisely by formula (2.2.21).

Once this done, our attempts will be satisfied : the two first components of the resulting dynamical system will give raise to a good approximation of the evolution of the Guiding Center motion and hence of the evolution of the particle in the physical space, and, the dynamical system that needs to be solved will be easier. In particular, it will not involve the strong oscillations. Moreover, the last component of the solution will be constant and the evolution of the two firsts will not depend on the third component. As a consequence, if we are just interested in the motion of the particle in the physical space, i.e. just in the evolution of the two first components, solving the dynamical system in the new system of coordinates, reduces to find a trajectory in $\mathbb{R}^2$, in place of a trajectory in $\mathbb{R}^4$ when it is solved in the original system of coordinates.
To be more precise writing dynamical system (2.1.40)–(2.1.41) in a form satisfying the assumptions of Theorem 2.1.2 can only be done in a formal way using formal series expansion. Then, in fact, we will use a variant of Theorem 2.1.2 which result is the same, up to any order of ε. This variant is given in Theorem 2.4.1. From this variant, we can set dynamical system (2.1.40)– (2.1.41) in a form from which we can, for instance, prove the following theorem.

Theorem 2.1.3. *Assume that the magnetic field B satisfies assumptions* (2.1.42) *and* (2.1.43) *and that all its derivatives are bounded. Let N be a positive integer. Then, for any of open subsets $\mathcal{O}(\mathbf{x}_0, R_{\mathbf{x}_0}; a, b)$ (see formula* (2.1.70)*), for any real number $R'_{\mathbf{x}_0}$ such that $R'_{\mathbf{x}_0} > R_{\mathbf{x}_0}$, and for any open interval (c, d) such that $\left[\frac{a^2}{2\|B\|_\infty}, \frac{b^2}{2}\right] \subset (c, d)$, there exists a positive real number η, such that for any $\varepsilon \in (-\eta, \eta)$, there exists a map $\mathcal{C}^k G_\varepsilon = \boldsymbol{\chi}_\varepsilon^{N,\circ} \circ \boldsymbol{\Upsilon}^\circ \circ \mathfrak{Pol}$, one to one from*

$$\boldsymbol{\mathcal{U}_\mathcal{D}} = (\boldsymbol{\Upsilon}^\circ \circ \mathfrak{Pol})^{-1}\left(\mathfrak{b}^2\left(\mathbf{x}_0, R'_{\mathbf{x}_0}\right) \times (\mathbb{R}/(2\pi\mathbb{Z})) \times (c, d)\right) \supset \mathcal{O}(\mathbf{x}_0, R_{\mathbf{x}_0}; a, b) \tag{2.1.59}$$

onto $\mathcal{C}^k G_\varepsilon(\boldsymbol{\mathcal{U}_\mathcal{D}})$; a system of coordinates $(\mathbf{z}, \gamma, j) = \mathcal{C}^k G_\varepsilon(\mathbf{x}, \mathbf{v})$ on $\mathcal{C}^k G_\varepsilon(\boldsymbol{\mathcal{U}_\mathcal{D}})$; and for any $\varepsilon \in (0, \eta)$ a real t_e^ε, with $t_e^\varepsilon > \frac{\alpha_0}{\varepsilon}$, where α_0 is a positive real number that does not depend on ε, such that the solution

$$\left(\mathbf{Z}^T, \Gamma^T, \mathcal{J}^T\right) = \left(\mathbf{Z}^T(t, \mathbf{z}_0, \gamma_0, j_0), \Gamma^T(t, \mathbf{z}_0, \gamma_0, j_0), \mathcal{J}^T(t, \mathbf{z}_0, \gamma_0, j_0)\right) \tag{2.1.60}$$

of the following dynamical system, written within system of coordinates $(\mathbf{z},\gamma,j)$*,*

$$\frac{\partial \mathbf{Z}^T}{\partial t} = -\frac{\varepsilon}{B\left(\mathbf{Z}^T\right)} \begin{pmatrix} \dfrac{\partial \hat{H}^N_{\varepsilon,T}}{\partial z_2}\left(\mathbf{Z}^T, j_0\right) \\ -\dfrac{\partial \hat{H}^N_{\varepsilon,T}}{\partial z_1}\left(\mathbf{Z}^T, j_0\right) \end{pmatrix}, \qquad \mathbf{Z}^T\left(0;\mathbf{z}_0,j_0\right) = \mathbf{z}_0, \tag{2.1.61}$$

$$\frac{\partial \Gamma^T}{\partial t} = -\frac{1}{\varepsilon}\frac{\partial \hat{H}^N_{\varepsilon,T}}{\partial j}\left(\mathbf{Z}^T, j_0\right), \qquad \mathbf{\Gamma}^T\left(0;\mathbf{z}_0,j_0,\gamma_0\right) = \gamma_0, \tag{2.1.62}$$

$$\frac{\partial \mathcal{J}^T}{\partial t} = 0, \qquad \mathcal{J}^T\left(0;\mathbf{z}_0,j_0\right) = j_0, \tag{2.1.63}$$

where $\hat{H}^N_{\varepsilon,T}$ *is the function obtained by Algorithm 2.5.11 , satisfies*

$$\left\|(\mathbf{Z},\mathcal{J}) - (\mathbf{Z}^T,\mathcal{J}^T)\right\|_{\infty,\mathbf{init}} \leq C\varepsilon^{N-1} \tag{2.1.64}$$

for any $t \in (-t^\varepsilon_e, t^\varepsilon_e)$*. In* (2.1.64)*,* $\|g\|_{\infty,\mathbf{init}}$ *stands for*

$$\|g\|_{\infty,\mathbf{init}} = \sup_{(\mathbf{z}_0,\gamma_0,j_0)\in \mathscr{C}\!\mathscr{G}_\varepsilon\left(\mathcal{O}\left(\mathbf{x}_0,R_{\mathbf{x}_0};a,b\right)\right)} |g(\mathbf{z}_0,\gamma_0,j_0)|; \tag{2.1.65}$$

$$(\mathbf{Z}(t,\mathbf{z}_0,\gamma_0,j_0),\Gamma(t,\mathbf{z}_0,\gamma_0,j_0),\mathcal{J}(t,\mathbf{z}_0,\gamma_0,j_0)) = \mathscr{C}\!\mathscr{G}_\varepsilon\left(\mathbf{X}(t,\mathbf{x}_0,\mathbf{v}_0),\mathbf{V}(t,\mathbf{x}_0,\mathbf{v}_0)\right), \tag{2.1.66}$$

with $(\mathbf{X},\mathbf{V})$ *the solution of dynamical system* (2.1.40)–(2.1.41) *and* $(\mathbf{x}_0,\mathbf{v}_0) = \mathscr{C}\!\mathscr{G}^{-1}_\varepsilon(\mathbf{z}_0,\gamma_0, j_0)$*; and,* C *that does not depend on* ε*.*

The map $\mathscr{C}\!\mathscr{G}_\varepsilon$ *giving coordinate system* $(\mathbf{z},\gamma,j)$ *is a composition of several ones :* $\mathfrak{Pol}$*,* $\mathbf{\Upsilon}^\circ$*, and* $\boldsymbol{\chi}^{N,\circ}_\varepsilon$*. A detailed summarize of these maps is given in the beginning of section 2.6 in Theorem* (2.6.1) *and in subsection 2.6.1.*

When $N = 2$*, system* (2.1.61)–(2.1.63) *reads*

$$\frac{\partial \mathbf{Z}^T}{\partial t} = -\frac{\varepsilon \mathcal{J}^T}{B\left(\mathbf{Z}^T\right)}\,{}^\perp\nabla B\left(\mathbf{Z}^T\right), \qquad \mathbf{Z}^T(0) = \mathbf{z}_0, \tag{2.1.67}$$

$$\frac{\partial \Gamma^T}{\partial t} = \frac{B\left(\mathbf{Z}^T\right)}{\varepsilon} + \varepsilon\frac{\mathcal{J}^T}{2B\left(\mathbf{Z}^T\right)^2}\left(B\left(\mathbf{Z}^T\right)\nabla^2 B\left(\mathbf{Z}^T\right) - 3\left(\nabla B\left(\mathbf{Z}^T\right)\right)^2\right), \quad \Gamma^T(0) = \gamma_0, \tag{2.1.68}$$

$$\frac{\partial \mathcal{J}^T}{\partial t} = 0, \qquad \mathcal{J}^T(0) = j_0. \tag{2.1.69}$$

In this theorem and in the sequel, $\mathcal{O}\left(\mathbf{x}_0,R_{\mathbf{x}_0};a,b\right)$ stands for the open subset defined by :

$$\mathcal{O}\left(\mathbf{x}_0,R_{\mathbf{x}_0};a,b\right) = \mathfrak{b}^2(\mathbf{x}_0,R_{\mathbf{x}_0}) \times \mathfrak{C}\left(a;b\right), \tag{2.1.70}$$

where $\mathfrak{b}^2(\mathbf{x}_0,R_{\mathbf{x}_0}) \subset \mathbb{R}^2$ is the open Euclidian ball of radius $R_{\mathbf{x}_0}$ and of center $\mathbf{x}_0$, and $\mathfrak{C}\left(a;b\right)$ is the open crown of $\mathbb{R}^2$ defined by

$$\mathfrak{C}\left(a;b\right) = \left\{\mathbf{v}\in\mathbb{R}^2,\ |\mathbf{v}| \in (a,b)\right\}, \tag{2.1.71}$$

where $[a,b] \subset (0,+\infty)$.

If we are not interested in the evolution of Γ, since (2.1.63) is obviously solved, in this system of coordinates solving dynamical system (2.1.40)–(2.1.41) reduces to compute a bidimensionnal trajectory by solving (2.1.61).

Definition 2.1.4. *The coordinate system $(\mathbf{z}, \gamma, j)$ obtained in Theorem 2.1.3 is called the Gyro-Kinetic coordinate system of order N.*

Remark 2.1.5. *After having obtained the coordinate system given by Theorem 2.1.3, if, to make numerical simulations of the evolution of the particle, we compute $\mathbf{Z}^T$ in place of the particle trajectory $\mathbf{X}$, then the global error is given by :*

$$\textit{global error} \;=\; \textit{Series Truncation Error} \;+\; \textit{Numerical Error}\,. \tag{2.1.72}$$

The Series Truncation Error is made of two parts. As regard to the first part which is the error done when approximating $\mathbf{Z}$ by $\mathbf{Z}^T$, inequality (2.1.64) of Theorem 2.1.3 claims that it can be pushed up to any order of ε. As regard to its second part which is related to the fact that the change of coordinates giving $\mathbf{Z}$ from $\mathbf{X}$ is not exactly known, the method for its construction allows also us to also push this expression to any order of ε. As a consequence, and because the numerical method (which is the one induced by the numerical scheme used to compute approximatted solution to (2.1.61)) can be as accurate as needed, our result claims that from the Geometrical Gyro-Kinetic Approximation numerical methods with any desired accuracy can be built to solve dynamical system (2.1.40)–(2.1.41).

As illustrated in Figure 2.1, the method to build the desired change of coordinates is made of 5 steps. The first one consists in checking that dynamical system (2.1.40)–(2.1.41) is well Hamiltonian. This is symbolized by arrow 1 in the top of the figure. Once this is done, we can go back into the Usual Coordinate System but knowing that the dynamical system writes as in the square which is in the top-right of the figure, i.e., involving the Poisson Matrix $\grave{\mathcal{P}}_\varepsilon$ and the gradient $\nabla_{\mathbf{x},\mathbf{v}}\grave{H}_\varepsilon$ of Hamiltonian function $\grave{H}_\varepsilon$. It may be written in that form in any coordinates system, and formulas give how to transform the Hamiltonian function and the Poisson Matrix while changing of coordinates. The goal of the third step is to introduce a Polar in velocity Coordinate System. In the fourth step, we make another change of coordinates, based on a Darboux Algorithm, in order to get the form of the Poisson Matrix allowing the application of the Key Result. This step consists essentially in solving a hyperbolic non-linear system of Partial Differential Equations (PDEs) for which a specific well adapted method of characteristics, in a spirit inspired by Abraham [1], is set out. We obtain a coordinate system close to the Historical Guiding-Center Coordinates of [37], [24], [46] and [47] involving the magnetic moment and the gyro-angle around the magnetic direction. In the fifth step, we make a last change of coordinates based on a Partial Lie Transform Method that we introduce in the present paper, leaving the form of the Poisson Matrix unchanged up to any desired order N of ε and bringing the Hamiltonian function independent of the last variable up to order $N+1$, allowing the proof of Theorem 2.1.3.

Remark 2.1.6. *The method in itself is complex and call upon concepts coming from several mathematical theories. Besides, as the method consists in building a succession of changes of coordinates, each of them being defined via a complex protocol, we have to check that what we build are well changes of coordinates, i.e. that they are well one to one, that they have the required regularity to be real changes of coordinates and that their inverse transformations have also the required regularity. Since moreover some of the domains on which those changes of coordinates are built are not straightforwardly comprehensible, those checks add a level of technical complexity.*

The motivation for introducing the Polar in velocity Coordinates $(\mathbf{x}, \theta, v)$ in the third step is not obvious. Indeed, whatever the system of coordinates chosen as point-of-departure, the resolution of the non-linear set of hyperbolic PDEs involved in the Darboux Algorithm is possible. Hence, we may wonder why taking this specific one. On another hand, the change of coordinates based on the Partial Lie Transform, which is a perturbation method, gives a system of coordinates close to the Historical Guiding Center-Coordinate System (2.1.55)–(2.1.58). Hence, we may also wonder if there is an a priori argument suggesting that method, starting from the Polar in velocity Coordinates and leading to a coordinate system close to the Historical Guiding-Center Coordinate System, generates a coordinate system satisfying the assumptions of Theorem 2.1.2. As a mater of fact, a few words are needed to attempt at providing some answers to those questions and, as a by-product, to explain this motivation.

Helping to provide some answers calls upon geometrical arguments put into the perspective of the regime under consideration. In a first place, the Darboux Algorithm needs to select a component of the coordinates which is left unchanged while doing the change of coordinates. This component plays the role of a pivot on which the change of coordinates leans to be defined.
If we look at what happens in the case of a constant magnetic field, we observe that the particle trajectory is a circle and obviously rotations of angle θ are its associated symmetries. Invoking the Noether's Theorem, which relates symmetries and invariants of the particle trajectory, yields that the magnetic moment, which is the product of the Larmor Radius by the norm of the velocity, is the invariant associated with those symmetries. Hence, a well adapted coordinate system to study the motion of a particle is such that its two first components give the position of the center of the circle and its two lasts are related to the symmetries and the invariant linked by the Noether's Theorem. This coordinate system is exactly the Historical Guiding-Center Coordinate System. Notice that, in the mathematical literature, the coordinate related to the invariant is called "action" and the coordinate related to the symmetries is called "angle". Consequently, the best order 0 change of coordinate, before a method leading to a coordinate system close to the Historical Guiding-Center Coordinate System, is the one leading to the Polar in velocity Coordinates. With this point-of-departure, and with θ as pivot, the Darboux Algorithm gives the Historical Guiding-Center Coordinate System. Moreover the Hamiltonian function is independent of θ, bringing the conditions of application of the Key Result.
Going back to our concerns where the magnetic field $B = B(\mathbf{x})$ depends on the position, but under the assumptions of the drift-kinetic regime, in view of what we said while explaining this regime and in particular that the particle's trajectory is close to a circle, rotations of angles θ are close to symmetries, the Noether's Theorem allows us to hope that there exists a coordinate system close to the Historical Guiding-Center Coordinate System with a component related to an invariant close to the magnetic moment. Hence, the Polar in velocity Coordinate System is the best choice as point-of-departure. As we will see, with the Polar in velocity Coordinates System as point-of-departure, and with θ as pivot, the Darboux Algorithm gives a coordinate system close to the Historical Guiding-Center Coordinate System. This helps to provide answers to the two above questions : since the sought system of coordinates is, with accuracy of the order of ε, the Historical Guiding-Center Coordinates, and since the result of the Darboux algorithm is, with accuracy of the order of ε, the Historical Guiding-Center Coordinates, it can be obtained from the Darboux Algorithm result using a perturbation method like a Lie Transform Method.

Another remarkable fact is that in the Polar in velocity Coordinate System the Hamiltonian function does not depend on θ. As the Darboux algorithm gives a coordinate system

close to the Historical Guiding-Center Coordinate System, and the Lie algorithm is close to the identity, this fact is indispensable. Indeed, this leads that the θ-dependency of the Hamiltonian function in the Darboux Coordinates System, appears only at the first order in ε. Consequently the Partial Lie Transform method has finally the ability to eliminate this θ-dependency up to any order N.

The context of the Gyro-Kinetic Approximation is Tokamak and Stellarator Plasma Physics. An artist vision of ITER, which is a Tokamak, is given in figure 1. The Vessel of a Tokamak is the interior of a torus with vertical axis of symmetry which, along the torus, electromagnets can generate a large magnetic field. At first sight, a Stellarator is similar but with a more complicated shape.

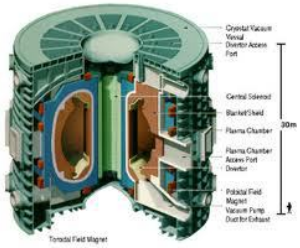

FIGURE 2.2 – Artist vision of Iter.

Clearly, dynamical system (2.1.25)–(2.1.26) is too simplified to be consider in a Tokamak or a Stellarator. Nevertheless, this model is simple enough to well understand the method and contains enough complexity to convince that it may be generalized to the genuine Dynamical System involved for particles in a Tokamak or a Stellarator.

The paper is organized as fallows : in section 2.2, we will construct a symplectic structure well adapted to the study of (2.1.40)–(2.1.41) and we will give the mathematical tools necessary for the comprehension of the Geometrical Gyro-Kinetic Theory we develop then. As a by-product of this section we obtain that the dynamical system we work with is a Hamiltonian one. In the third section, we will set out the method of characteristics and we will use it in order to derive the Darboux Coordinate System. In the fourth and fifth section, we will introduce the concept of Partial Lie Sum and develop the Partial Lie Transform Method in the case of a Poisson Matrix that depends on ε. This method is a mathematically rigorous version of the Lie Transform Method developed by Littlejohn [40, 41, 42]. In this new framework, we do not use formal Lie Series, we use Partial Lie Sums and we control the rests all along the method development. Then in section 2.6 we will derive the Gyro-Kinetic Coordinate System and prove Theorem 2.1.3.

2.2 Construction of the symplectic structure

We start by recalling the manifold that is used in order to study the motion of a charged particle. To avoid confusions, we will introduce the notation $\mathcal{M}$ for $\mathbb{R}^4$ endowed with its usual Cartesian coordinate system and with its usual Euclidian topology. As $\mathcal{M}$ is flat the first chart we choose is the global chart $(\mathcal{M}, \boldsymbol{\tau})$ where $\boldsymbol{\tau} \ : \ \mathcal{M} \to \mathbb{R}^4 \, ; \, \boldsymbol{\tau}(\mathbf{x}, \mathbf{v}) = (\mathbf{x}, \mathbf{v})$. Afterwards, we choose the maximal atlas containing this coordinate chart.

The first step of the construction of the symplectic structure consists in defining the Symplectic Two-Form. In the non-dimensionless case and within the general framework, the electromagnetic Lagrangian reads :

$$L(\mathbf{x},\mathbf{v},t)=\frac{|\mathbf{v}|^2}{2}-\frac{q}{m}\phi(\mathbf{x},t)+\frac{q}{m}\mathbf{v}\cdot\mathbf{A}(\mathbf{x},t), \tag{2.2.1}$$

where ϕ is the usual scalar potential and $\mathbf{A}$ is the usual vector potential. In the context of the present paper, where $\phi=0$ and where the drift-kinetic regime is considered, the dimensionless electromagnetic Lagrangian reads

$$L_\varepsilon(\mathbf{x},\mathbf{v})=\frac{|\mathbf{v}|^2}{2}+\frac{1}{\varepsilon}\mathbf{v}\cdot\mathbf{A}(\mathbf{x}), \tag{2.2.2}$$

where $\mathbf{A}$ is given by (2.1.42). The Canonical Coordinates $(\mathbf{q},\mathbf{p})$ are given by

$$\mathbf{q}=\mathbf{x}\text{ and }\mathbf{p}=\frac{\partial L_\varepsilon}{\partial\mathbf{v}}(\mathbf{x},\mathbf{v}); \tag{2.2.3}$$

i.e. :

$$\mathbf{q}=\mathbf{x}\text{ and }\mathbf{p}=\mathbf{v}+\frac{1}{\varepsilon}\mathbf{A}(\mathbf{x}). \tag{2.2.4}$$

The Symplectic Two-Form $\mathbf{\Omega}_\varepsilon$ on $\mathcal{M}$ that is considered is the unique Two-Form which expression in the Canonical Coordinate chart is given by

$$\breve{\omega}_\varepsilon=d\mathbf{q}\wedge d\mathbf{p}. \tag{2.2.5}$$

Now, $\underline{a}$ Poisson Matrix $\mathcal{P}$ on an open subset is a skew-symmetric matrix satisfying :

$$\forall i,j,k\in\{1,\ldots,4\},\ \{\{\mathbf{r}_i,\mathbf{r}_j\},\mathbf{r}_k\}+\{\{\mathbf{r}_k,\mathbf{r}_i\},\mathbf{r}_j\}+\{\{\mathbf{r}_j,\mathbf{r}_k\},\mathbf{r}_i\}=0, \tag{2.2.6}$$

where for smooth functions f and g the Poisson Bracket $\{f,g\}$ is defined by (2.1.49), and in the case of a symplectic manifold, $\underline{the}$ Poisson Matrix in a given coordinate system is defined as follow : it is the inverse of the transpose of the matrix of the expression of the Symplectic Two-Form in this coordinate system. Notice that the Jacoby identities (2.2.6) are direct consequences of the closure of the Symplectic Two-Form.
For our purpose, in the Canonical Coordinates, the matrix associated with the Symplectic Two-Form is given by

$$\breve{\mathcal{K}}_\varepsilon(\mathbf{q},\mathbf{p})=\mathcal{S}=\begin{pmatrix}0_2 & I_2\\ -I_2 & 0_2\end{pmatrix}, \tag{2.2.7}$$

and then the Poisson Matrix is given by

$$\breve{\mathcal{P}}_\varepsilon(\mathbf{q},\mathbf{p})=\left(\breve{\mathcal{K}}_\varepsilon(\mathbf{q},\mathbf{p})\right)^{-T}=\mathcal{S} \tag{2.2.8}$$

We now turn to the change-of-coordinates rule for the Poisson Matrix. Firstly, if in a given coordinate chart $\overset{\star}{\mathbf{r}}$, the matrix associated with the Symplectic Two-Form $\mathbf{\Omega}_\varepsilon$ reads $\overset{\star}{\mathcal{K}}_\varepsilon\left(\overset{\star}{\mathbf{r}}\right)$, then, according to the previous definition, the Poisson Matrix is given by

$$\overset{\star}{\mathcal{P}}_\varepsilon\left(\overset{\star}{\mathbf{r}}\right)=\left(\overset{\star}{\mathcal{K}}_\varepsilon\left(\overset{\star}{\mathbf{r}}\right)\right)^{-T}. \tag{2.2.9}$$

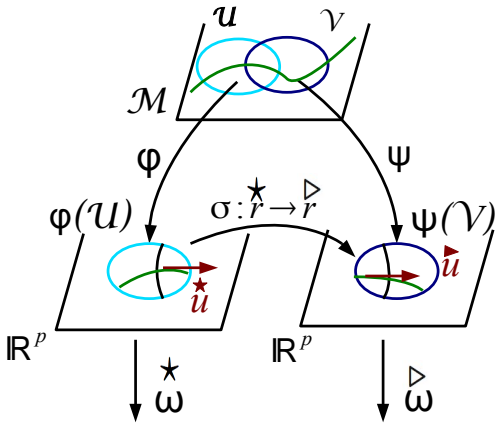

FIGURE 2.3 – General change of coordinates rule for the expression of a Two-Form. The Two-Form $\overset{\triangleright}{\omega}_\varepsilon$ is the pull-back of $\overset{\star}{\omega}_\varepsilon$ by σ : $\overset{\triangleright}{\omega}_\varepsilon = \sigma^\star \overset{\star}{\omega}_\varepsilon$

If we make the change of coordinates σ : $\overset{\star}{\mathbf{r}} \mapsto \overset{\triangleright}{\mathbf{r}}$, then the usual change-of-coordinates rule for the expression of the Symplectic Two-Form (see Figure 2.3) leads to the following change of coordinates rule for the Poisson Matrix

$$\overset{\triangleright}{\mathcal{P}}_\varepsilon \left(\overset{\triangleright}{\mathbf{r}} \right) = \nabla_{\overset{\star}{\mathbf{r}}} \sigma \left(\sigma^{-1} \left(\overset{\triangleright}{\mathbf{r}} \right) \right) \overset{\star}{\mathcal{P}}_\varepsilon \left(\sigma^{-1} \left(\overset{\triangleright}{\mathbf{r}} \right) \right) \left[\nabla_{\overset{\star}{\mathbf{r}}} \sigma \left(\sigma^{-1} \left(\overset{\triangleright}{\mathbf{r}} \right) \right) \right]^T . \tag{2.2.10}$$

Using the Poisson Bracket defined in formula (2.1.49), the change-of-coordinates rule for the Poisson Matrix reads

$$\left(\overset{\triangleright}{\mathcal{P}}_\varepsilon \right)_{i,j} \left(\overset{\triangleright}{\mathbf{r}} \right) = \left\{ \overset{\triangleright}{\mathbf{r}}_i, \overset{\triangleright}{\mathbf{r}}_j \right\}_{\overset{\star}{\mathbf{r}}} \left(\sigma^{-1} \left(\overset{\triangleright}{\mathbf{r}} \right) \right) . \tag{2.2.11}$$

A Hamiltonian function is a smooth function on $\mathcal{M}$ and the Hamiltonian vector field associated with Hamiltonian function $\mathcal{G}$ is the unique vector field $\boldsymbol{\mathcal{X}}^\varepsilon_{\mathcal{G}}$ satisfying

$$i_{\boldsymbol{\mathcal{X}}^\varepsilon_{\mathcal{G}}} d\boldsymbol{\Omega}_\varepsilon = d\mathcal{G}, \tag{2.2.12}$$

where $i_{\boldsymbol{\mathcal{X}}^\varepsilon_{\mathcal{G}}} d\boldsymbol{\Omega}_\varepsilon$ is the interior product of differential two-form $d\boldsymbol{\Omega}_\varepsilon$ by vector field $\boldsymbol{\mathcal{X}}^\varepsilon_{\mathcal{G}}$. The expression of the Hamiltonian vector field associated with the Hamiltonian function $\mathcal{G}$, in the coordinate system $\overset{\star}{\mathbf{r}}$, is the vector field which reads :

$$\overset{\star}{\mathbf{X}}{}^{\varepsilon}_{\overset{\star}{G}} \left(\overset{\star}{\mathbf{r}} \right) = \overset{\star}{\mathcal{P}}_\varepsilon \left(\overset{\star}{\mathbf{r}} \right) \nabla_{\overset{\star}{\mathbf{r}}} \overset{\star}{G} \left(\overset{\star}{\mathbf{r}} \right) , \tag{2.2.13}$$

where $\overset{\star}{G}$ is the representative of $\mathcal{G}$ in this coordinate system. In fact, we can consider Hamiltonian vector fields on $\mathcal{M}$, which requires that the Hamiltonian functions are smooth functions on $\mathcal{M}$, or just Hamiltonian vector fields on an open subset of $\mathcal{M}$, which requires that the Hamiltonian functions are defined on this open subset.

The Hamiltonian dynamical system associated with Hamiltonian function $\mathcal{G}$ on $\mathcal{M}$ is the dynamical system which reads

$$\frac{\partial \boldsymbol{\mathcal{R}}}{\partial t} (t) = \boldsymbol{\mathcal{X}}^\varepsilon_{\mathcal{G}} \left(\boldsymbol{\mathcal{R}} (t) \right) , \tag{2.2.14}$$

or equivalently as said in the introduction, the dynamical system whose expression in every coordinate system $\overset{\star}{\mathbf{r}}$ is given by

$$\frac{\partial \overset{\star}{\mathbf{R}}}{\partial t} = \overset{\star}{\mathcal{P}}_{\varepsilon}\left(\overset{\star}{\mathbf{R}}\right) \nabla_{\overset{\star}{\mathbf{r}}} \overset{\star}{G}\left(\overset{\star}{\mathbf{R}}\right). \tag{2.2.15}$$

In particular, if we check that on a global coordinate chart, a dynamical system is Hamiltonian, then the dynamical system is Hamiltonian on $\mathcal{M}$ and its expression in every coordinate chart $\overset{\star}{\mathbf{r}}$ is given by (2.2.15).

Going back to dynamical system (2.1.40)–(2.1.41), we can easily check that in coordinate system $(\mathbf{q}, \mathbf{p})$ defined by (2.2.4) trajectory $(\mathbf{Q}, \mathbf{P})$ defined by

$$\mathbf{Q}(s) = \mathbf{X}(s) \text{ and } \mathbf{P}(s) = \mathbf{V}(s) + \frac{1}{\varepsilon}\mathbf{A}(\mathbf{X}(s)), \tag{2.2.16}$$

is solution to

$$\begin{pmatrix} \dfrac{\partial \mathbf{Q}}{\partial t} \\ \dfrac{\partial \mathbf{P}}{\partial t} \end{pmatrix} = \mathcal{S} \nabla_{\mathbf{q},\mathbf{p}} \breve{H}(\mathbf{Q}, \mathbf{P}), \tag{2.2.17}$$

where $\mathcal{S}$ is defined by (2.2.7) and $\breve{H}(\mathbf{q}, \mathbf{p}) = \frac{1}{2}\left|\mathbf{p} - \frac{1}{\varepsilon}\mathbf{A}(\mathbf{q})\right|^2$, insuring that it is Hamiltonian. And, using (2.2.10) or (2.2.11), we obtain the expression of the Poisson Matrix in the Cartesian Coordinate System :

$$\grave{\mathcal{P}}_{\varepsilon}(\mathbf{x}, \mathbf{v}) = \begin{pmatrix} 0 & 0 & 1 & 0 \\ 0 & 0 & 0 & 1 \\ -1 & 0 & 0 & \frac{B(\mathbf{x})}{\varepsilon} \\ 0 & -1 & -\frac{B(\mathbf{x})}{\varepsilon} & 0 \end{pmatrix}, \tag{2.2.18}$$

and of the Hamiltonian function :

$$\grave{H}_{\varepsilon}(\mathbf{x}, \mathbf{v}) = \frac{|\mathbf{v}|^2}{2}. \tag{2.2.19}$$

Since the above coordinate charts are both global, dynamical system (2.1.40)–(2.1.41) is Hamiltonian on $\mathcal{M}$. We will denote by $\mathcal{H}_{\varepsilon} : \mathcal{M} \to \mathbb{R}$ the Hamiltonian function on the manifold.

Now, we will perform the third step (see Figure 2.1) which consists in setting the dynamical system (2.1.40)-(2.1.41) in a Polar in velocity Coordinate System $(\mathbf{x}, \theta, v = |\mathbf{v}|)$. To be consistent with the physical literature, we define θ as the angle between the x_1-axis and the gyro-radius vector $\boldsymbol{\rho}_{\varepsilon}(\mathbf{x}, \mathbf{v}) = -\frac{\varepsilon}{B(\mathbf{x})}{}^{\perp}\mathbf{v}$, measured in a clockwise sense ; i.e.

$$\boldsymbol{\rho}_{\varepsilon}(\mathbf{x}, \mathbf{v}) = |\boldsymbol{\rho}_{\varepsilon}(\mathbf{x}, \mathbf{v})| \begin{pmatrix} \cos(\theta) \\ -\sin(\theta) \end{pmatrix}. \tag{2.2.20}$$

The change of coordinates leading to the Polar in velocity Coordinate System is then given by :

$$\begin{array}{rccc} \mathfrak{Pol}: & \mathbb{R}^2 \times \mathbb{R}^2 & \to & \mathbb{R}^2 \times (\mathbb{R}/(2\pi\mathbb{Z})) \times (0, +\infty) \\ & (\mathbf{x}, \mathbf{v}) & \mapsto & (\mathbf{x}, \theta, v) \end{array} \quad \text{with } \mathbf{v} = v \begin{pmatrix} -\sin(\theta) \\ -\cos(\theta) \end{pmatrix}. \tag{2.2.21}$$

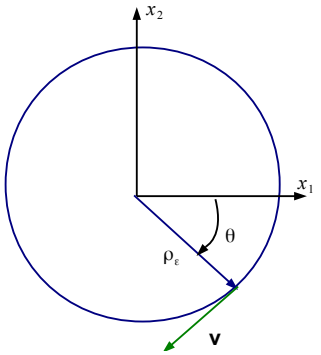

FIGURE 2.4 – Polar coordinates for the velocity variable.

Using the change-of-coordinates formula we deduce from (2.2.19) that the expression of Hamiltonian function $\mathcal{H}_\varepsilon$ in the Polar in velocity Coordinate System is :

$$\tilde{H}_\varepsilon(\mathbf{x},\theta,v) = \frac{v^2}{2}, \tag{2.2.22}$$

and, using (2.2.11), the expression of the Poisson Matrix in this system is

$$\tilde{\mathcal{P}}_\varepsilon(\mathbf{x},\theta,v) = \begin{pmatrix} 0 & 0 & -\frac{\cos(\theta)}{v} & -\sin(\theta) \\ 0 & 0 & \frac{\sin(\theta)}{v} & -\cos(\theta) \\ \frac{\cos(\theta)}{v} & -\frac{\sin(\theta)}{v} & 0 & \frac{B(\mathbf{x})}{\varepsilon v} \\ \sin(\theta) & \cos(\theta) & -\frac{B(\mathbf{x})}{\varepsilon v} & 0 \end{pmatrix}. \tag{2.2.23}$$

According to formula (2.2.15), in this system, the characteristic $(\mathbf{X}^\varepsilon_{\mathfrak{Pol}}, \Theta^\varepsilon, \mathcal{V}^\varepsilon)(t;\mathbf{x},\theta,v)$ laying on $\mathbb{R}^2\times(\mathbb{R}/(2\pi\mathbb{Z}))\times(0,+\infty)$ and satisfying initial condition $(\mathbf{X}^\varepsilon_{\mathfrak{Pol}}, \Theta^\varepsilon, \mathcal{V}^\varepsilon)(0;\mathbf{x},\theta,v) = (\mathbf{x},\theta,v) \in \mathbb{R}^2\times(\mathbb{R}/(2\pi\mathbb{Z}))\times(0,+\infty)$ is defined by

$$\mathbf{X}^\varepsilon_{\mathfrak{Pol}}(t;\mathbf{x},\theta,v) = \mathbf{X}^\varepsilon\left(t;\mathfrak{Pol}^{-1}(\mathbf{x},\theta,v)\right), \tag{2.2.24}$$

$$\Theta^\varepsilon(t;\mathbf{x},\theta,v) = \mathfrak{Pol}_3\left(\mathbf{X}^\varepsilon\left(t;\mathfrak{Pol}^{-1}(\mathbf{x},\theta,v)\right), \mathbf{V}^\varepsilon\left(t;\mathfrak{Pol}^{-1}(\mathbf{x},\theta,v)\right)\right), \tag{2.2.25}$$

$$\mathcal{V}^\varepsilon(t;\mathbf{x},\theta,v) = \sqrt{\left(X^\varepsilon_1\left(t;\mathfrak{Pol}^{-1}(\mathbf{x},\theta,v)\right)\right)^2 + \left(X^\varepsilon_2\left(t;\mathfrak{Pol}^{-1}(\mathbf{x},\theta,v)\right)\right)^2}, \tag{2.2.26}$$

and is solution to

$$\frac{\partial X^\varepsilon_{\mathfrak{Pol},1}}{\partial t}(t;\mathbf{x},\theta,v) = -\sin\left(\Theta^\varepsilon(t;\mathbf{x},\theta,v)\right)\mathcal{V}^\varepsilon(t;\mathbf{x},\theta,v), \tag{2.2.27}$$

$$\frac{\partial X^\varepsilon_{\mathfrak{Pol},2}}{\partial t}(t;\mathbf{x},\theta,v) = -\cos\left(\Theta^\varepsilon(t;\mathbf{x},\theta,v)\right)\mathcal{V}^\varepsilon(t;\mathbf{x},\theta,v), \tag{2.2.28}$$

$$\frac{\partial \Theta^\varepsilon}{\partial t}(t;\mathbf{x},\theta,v) = \frac{B\left(\mathbf{X}^\varepsilon_{\mathfrak{Pol}}(t;\mathbf{x},\theta,v)\right)}{\varepsilon}, \tag{2.2.29}$$

$$\frac{\partial \mathcal{V}^\varepsilon}{\partial t}(t;\mathbf{x},\theta,v) = 0. \tag{2.2.30}$$

In particular, for any $t \in (0,+\infty)$ and for any $(\mathbf{x},\theta,v)$, the characteristic $\mathcal{V}^\varepsilon$ satisfies $\mathcal{V}^\varepsilon(t;\mathbf{x},\theta,v) = v$.

In the next subsection we will rather consider that the range of $\mathfrak{Pol}$ is $\mathbb{R}^2\times\mathbb{R}\times(0,+\infty)$ instead of $\mathbb{R}^2\times(\mathbb{R}/(2\pi\mathbb{Z}))\times(0,+\infty)$. This is not a big issue, nevertheless, for purposes

linked to what we will do in the fifth step, we need to define properly the periodic extensions of the characteristics expressed in the Polar in Velocity coordinate system as follows :

Definition 2.2.1. *Function* $(\mathbf{X}^{\varepsilon,\#}_{\mathfrak{Pol}}, \Theta^{\varepsilon,\#}, \mathcal{V}^{\varepsilon,\#})$ *ranging in* $\mathbb{R}^2 \times \mathbb{R} \times (0,+\infty)$*, solution of dynamical system* (2.2.27)–(2.2.30) *and satisfying initial conditions*

$$\mathbf{X}^{\varepsilon,\#}_{\mathfrak{Pol}}(0,\mathbf{x},\theta,v) = \mathbf{x},\ \Theta^{\varepsilon,\#}(0,\mathbf{x},\theta,v) = \theta,\ \mathcal{V}^{\varepsilon,\#}(0,\mathbf{x},\theta,v) = v, \tag{2.2.31}$$

where $(\mathbf{x},\theta,v) \in \mathbb{R}^2 \times \mathbb{R} \times (0,+\infty)$*, is called the periodic extension of characteristic* $(\mathbf{X}^{\varepsilon}_{\mathfrak{Pol}}, \Theta^{\varepsilon}, \mathcal{V}^{\varepsilon})$.

Lemma 2.2.2. *Let* $\mathfrak{p} : \mathbb{R}^2 \times \mathbb{R} \times (0,+\infty) \to \mathbb{R}^2 \times (\mathbb{R}/(2\pi\mathbb{Z})) \times (0,+\infty)$ *be the canonical projection. Then, the periodic extension* $(\mathbf{X}^{\varepsilon,\#}_{\mathfrak{Pol}}, \Theta^{\varepsilon,\#}, \mathcal{V}^{\varepsilon,\#})$ *of* $(\mathbf{X}^{\varepsilon}_{\mathfrak{Pol}}, \Theta^{\varepsilon}, \mathcal{V}^{\varepsilon})$ *satisfies*

$$\mathfrak{p} \circ \left(\mathbf{X}^{\varepsilon,\#}_{\mathfrak{Pol}}, \Theta^{\varepsilon,\#}, \mathcal{V}^{\varepsilon,\#}\right)(t,\cdot) = \left(\mathbf{X}^{\varepsilon}_{\mathfrak{Pol}}, \Theta^{\varepsilon}, \mathcal{V}^{\varepsilon}\right)(t,\cdot) \circ \mathfrak{p}, \tag{2.2.32}$$

for any $t \in \mathbb{R}$.

Proof. Let $\left(\widetilde{\mathbf{X}^{\varepsilon,\#}_{\mathfrak{Pol}}}(t;\mathbf{x},\theta,v), \widetilde{\Theta^{\varepsilon,\#}}(t;\mathbf{x},\theta,v), \widetilde{\mathcal{V}^{\varepsilon,\#}}(t;\mathbf{x},\theta,v)\right)$ be the function defined by

$$\left(\widetilde{\mathbf{X}^{\varepsilon,\#}_{\mathfrak{Pol}}}, \widetilde{\Theta^{\varepsilon,\#}}, \widetilde{\mathcal{V}^{\varepsilon,\#}}\right)(t;\mathbf{x},\theta,v) = \left(\mathbf{X}^{\varepsilon,\#}_{\mathfrak{Pol}}, \Theta^{\varepsilon,\#} - 2\pi, \mathcal{V}^{\varepsilon,\#}\right)(t;\mathbf{x},\theta+2\pi,v). \tag{2.2.33}$$

Then, $\left(\widetilde{\mathbf{X}^{\varepsilon,\#}_{\mathfrak{Pol}}}, \widetilde{\Theta^{\varepsilon,\#}}, \widetilde{\mathcal{V}^{\varepsilon,\#}}\right)(t;\mathbf{x},\theta,v)$ satisfies (2.2.27)–(2.2.30) and

$$\left(\widetilde{\mathbf{X}^{\varepsilon,\#}_{\mathfrak{Pol}}}, \widetilde{\Theta^{\varepsilon,\#}}, \widetilde{\mathcal{V}^{\varepsilon,\#}}\right)(0;\mathbf{x},\theta,v) = (\mathbf{x},\theta,v). \tag{2.2.34}$$

Consequently, the Cauchy-Lipschitz Theorem yields that

$$\left(\mathbf{X}^{\varepsilon,\#}_{\mathfrak{Pol}}, \Theta^{\varepsilon,\#}, \mathcal{V}^{\varepsilon,\#}\right)(t;\mathbf{x},\theta+2\pi,v) = \left(\mathbf{X}^{\varepsilon,\#}_{\mathfrak{Pol}}, \Theta^{\varepsilon,\#} + 2\pi, \mathcal{V}^{\varepsilon,\#}\right)(t;\mathbf{x},\theta,v). \tag{2.2.35}$$

This ends the proof of Lemma 2.2.2. □

Having this geometrical material on hand, we end this section by clarifying our comments about the Noether's Theorem done in the introduction. For this we first make precise the Noether's Theorem statement. Consider the following definitions :

Definition 2.2.3. *Let* F *be a Hamiltonian function on* $\mathbb{R}^4$ *and* ψ_t *be the flow associated with the Hamiltonian vector field of* F*. Let* H *be another Hamiltonian function, we say that* ψ_t *is a symplectic symmetry for* H *if*

$$\forall t \in \mathbb{R}, \forall \mathbf{r} \in \mathbb{R}^4,\ H(\mathbf{r}) = H(\psi_t(\mathbf{r})). \tag{2.2.36}$$

Definition 2.2.4. *Let* φ_t *be the flow of the Hamiltonian system with Hamiltonian* H*. We say that a function* G *is an invariant of the Hamiltonian system with Hamiltonian* H *if*

$$\forall t \in \mathbb{R}, \forall \mathbf{r} \in \mathbb{R}^4,\ G(\mathbf{r}) = G(\varphi_t(\mathbf{r})). \tag{2.2.37}$$

The Noether's Theorem links symmetry and invariants in the following way :

Theorem 2.2.5. *If the flow ψ_t associated with Hamiltonian function F is a symplectic symmetry of H, then F is an invariant of the Hamiltonian system of Hamiltonian H.*

Now, turning to dynamical system (2.1.40)–(2.1.41) assuming that the magnetic field is constant, if we make the Historical Guiding-Center change of coordinates ; i.e. if we apply (2.1.55)– (2.1.58), using (2.2.11), we obtain the following expression of the Poisson Matrix in this Historical Guiding-Center Coordinate System

$$\bar{\mathcal{P}}_\varepsilon\left(\mathbf{y}^{hgc},\theta^{hgc},k^{hgc}\right)=\begin{pmatrix}0&-\frac{\varepsilon}{B}&0&0\\ \frac{\varepsilon}{B}&0&0&0\\ 0&0&0&\frac{1}{\varepsilon}\\ 0&0&-\frac{1}{\varepsilon}&0\end{pmatrix} \tag{2.2.38}$$

and the Hamiltonian function (2.2.22) becomes $\bar{H}_\varepsilon\left(\mathbf{y}^{hgc},\theta^{hgc},k^{hgc}\right)=k^{hgc}B$. The vector field $\frac{\partial}{\partial\theta^{hgc}}$ is clearly hamiltonian. Indeed, its related Hamiltonian function is εk^{hgc}. As $\bar{H}_\varepsilon$ does not depend on θ^{hgc}, the flow of $\frac{\partial}{\partial\theta^{hgc}}$ is a symplectic symmetry. The Noether's Theorem ensures us that εk^{hgc} is an invariant for the Hamiltonian system with Hamiltonian $\bar{H}_\varepsilon$. Notice also that this coordinate system satisfies the assumptions of Theorem 2.1.2. Now, if the magnetic field is not constant, the trajectory of a particle is close to a circle. Hence, the flow of $\frac{\partial}{\partial\theta^{hgc}}$ is close to a symmetry and εk^{hgc} defined by (2.1.58) is close to an invariant.

2.3 The Darboux algorithm

2.3.1 Objectives

The fourth step (see Figure 2.1) on the way to build the Gyro-Kinetic Approximation is the application of the mathematical algorithm, so called the Darboux Algorithm, to build a global Coordinate System (y_1,y_2,θ,k) close to the Historic Guiding-Center Coordinate System (2.1.55)–(2.1.58), and in which the Poisson Matrix has the required form (2.1.45) to apply the Key Result (Theorem 2.1.2). In fact, in order to manage the small parameter ε, we will build the Coordinate System (y_1,y_2,θ,k) in order to have $\bar{\mathcal{P}}_\varepsilon(\mathbf{y},\theta,k)$ with the following form :

$$\bar{\mathcal{P}}_\varepsilon(\mathbf{y},\theta,k)=\left(\begin{array}{c|cc}\mathbb{M}_\varepsilon(\mathbf{y})&\begin{matrix}0&0\\0&0\end{matrix}\\ \hline \begin{matrix}0&0\end{matrix}&\begin{matrix}0&\frac{1}{\varepsilon}\end{matrix}\\ \begin{matrix}0&0\end{matrix}&\begin{matrix}-\frac{1}{\varepsilon}&0\end{matrix}\end{array}\right), \tag{2.3.1}$$

An important and constitutive fact in the Darboux Algorithm is that the θ-variable is left unchanged.

We first introduce the following notations : we will denote by

$$\boldsymbol{\Upsilon}(\mathbf{x},\theta,v)=\left(\boldsymbol{\Upsilon}_1(\mathbf{x},\theta,v),\boldsymbol{\Upsilon}_2(\mathbf{x},\theta,v),\boldsymbol{\Upsilon}_3(\mathbf{x},\theta,v),\boldsymbol{\Upsilon}_4(\mathbf{x},\theta,v)\right), \tag{2.3.2}$$

the mapping, defined on a subset of $\mathbb{R}^2\times\mathbb{R}\times(0,+\infty)$, (which will be built) giving the coordinates $(\mathbf{y},\theta,k)$ and by

$$\boldsymbol{\kappa}=\boldsymbol{\Upsilon}^{-1}, \tag{2.3.3}$$

its inverse map (which existence will be set out). Then, the change of coordinates write $(\mathbf{y},\theta,k)=\boldsymbol{\Upsilon}(\mathbf{x},\theta,v)$ and $(\mathbf{x},\theta,v)=\boldsymbol{\kappa}(\mathbf{y},\theta,k)$.

Applying formula (2.2.11), the matrix entries of (2.3.1) can be rewritten for $i = 1, \dots, 4$ and $j = 1, \dots, 4$ as

$$(\overline{\mathcal{P}}_\varepsilon(\mathbf{y}, \theta, k))_{ij} = \{\boldsymbol{\Upsilon}_i, \boldsymbol{\Upsilon}_j\}_{\mathbf{x},\theta,v}(\boldsymbol{\kappa}(\mathbf{y}, \theta, k)), \quad \{\boldsymbol{\Upsilon}_i, \boldsymbol{\Upsilon}_j\}_{\mathbf{x},\theta,v} = (\nabla \boldsymbol{\Upsilon}_i) \cdot (\widetilde{\mathcal{P}}_\varepsilon(\nabla \boldsymbol{\Upsilon}_j)), \tag{2.3.4}$$

with $\tilde{\mathcal{P}}_\varepsilon$ given by (2.2.23). Hence, the bottom-right of matrix form given in (2.3.1), results from :

$$\{\boldsymbol{\Upsilon}_4, \boldsymbol{\Upsilon}_3\} = -\frac{1}{\varepsilon}. \tag{2.3.5}$$

In the sequel, we will use the following notations :

$$\boldsymbol{\Upsilon}_1 = \boldsymbol{\Upsilon}_{y_1}, \ \boldsymbol{\Upsilon}_2 = \boldsymbol{\Upsilon}_{y_2}, \ \boldsymbol{\Upsilon}_3 = \boldsymbol{\Upsilon}_\theta \text{ and } \boldsymbol{\Upsilon}_4 = \boldsymbol{\Upsilon}_k. \tag{2.3.6}$$

Remark 2.3.1. *If we use those notations,* (2.3.5) *may be also read* $\{\boldsymbol{\Upsilon}_k, \boldsymbol{\Upsilon}_\theta\} = -\frac{1}{\varepsilon}$. *In papers of physicists, this last equation reads* $\{k, \theta\} = -\frac{1}{\varepsilon}$.

In the same way, the fact that the two last lines (or columns) contain only zeros results from :

$$\{\boldsymbol{\Upsilon}_1, \boldsymbol{\Upsilon}_3\} = 0, \tag{2.3.7}$$
$$\{\boldsymbol{\Upsilon}_1, \boldsymbol{\Upsilon}_4\} = 0, \tag{2.3.8}$$
$$\{\boldsymbol{\Upsilon}_2, \boldsymbol{\Upsilon}_3\} = 0, \tag{2.3.9}$$
$$\{\boldsymbol{\Upsilon}_2, \boldsymbol{\Upsilon}_4\} = 0. \tag{2.3.10}$$

Remark 2.3.2. *Using notations* (2.3.6), (2.3.7)–(2.3.10) *may also read*

$$\begin{array}{ll} \{\boldsymbol{\Upsilon}_{y_1}, \boldsymbol{\Upsilon}_k\} = 0, (or\ \{y_1, k\} = 0), & \{\boldsymbol{\Upsilon}_{y_1}, \boldsymbol{\Upsilon}_\theta\} = 0, (or\ \{y_1, \theta\} = 0), \\ \{\boldsymbol{\Upsilon}_{y_2}, \boldsymbol{\Upsilon}_k\} = 0, (or\ \{y_2, k\} = 0), & \{\boldsymbol{\Upsilon}_{y_2}, \boldsymbol{\Upsilon}_\theta\} = 0, (or\ \{y_2, \theta\} = 0). \end{array} \tag{2.3.11}$$

Equations (2.3.5) and (2.3.7)–(2.3.10) make a non linear hyperbolic system of PDEs that needs to be solved to build mapping $\boldsymbol{\Upsilon}$ and consequently the desired change of coordinates. In the perspective of the fifth step (see Figure 2.1), mapping $\boldsymbol{\Upsilon}$ needs to be close to the Historic Guiding-Center Coordinate System (2.1.55)–(2.1.58).

The non-linear nature of (2.3.5) and (2.3.7)–(2.3.10) is balanced by the fact that θ is left unchanged by $\boldsymbol{\Upsilon}$ and then that $\boldsymbol{\Upsilon}_3 = \boldsymbol{\Upsilon}_\theta$ is known. As a consequence, (2.3.5), (2.3.7) and (2.3.9) may be solved by an ad-hoc method of characteristics.

Besides, the choice of the boundary conditions, that need to be set to make system (2.3.5) and (2.3.7)–(2.3.10) to be well-posed, makes that (2.3.8) and (2.3.10) are consequences of (2.3.7) and (2.3.9). This choice is compatible with the constraint to get a system of coordinates close to the Historic Guiding-Center System which requires, among others, k to be close to the magnetic moment. As the magnetic moment is 0 when velocity v is 0, we choose to set the boundary conditions in $v = 0$, and for $\boldsymbol{\Upsilon}_k = \boldsymbol{\Upsilon}_4$ we set

$$\boldsymbol{\Upsilon}_k(\mathbf{x}, \theta, 0) = 0. \tag{2.3.12}$$

This choice to set the boundary condition in $v = 0$ generates a small difficulty because $\tilde{\mathcal{P}}_\varepsilon(\mathbf{x}, \theta, v)$ has a singularity in $v = 0$. To overcome this difficulty, we use that entry $(3, 4)$ of matrix $\tilde{\mathcal{P}}_\varepsilon$ satisfies :

$$(\tilde{\mathcal{P}}_\varepsilon(\mathbf{x}, \theta, v))_{3,4} = (\tilde{\mathcal{P}}_\varepsilon(\mathbf{x}, \theta, v))_{\theta,v} = \frac{B(\mathbf{x})}{\varepsilon v} > 0, \tag{2.3.13}$$

for all $(\mathbf{x}, \theta, v)$ belonging to $\mathbb{R}^2 \times \mathbb{R} \times (0, +\infty)$ because of (2.1.43). We will denote :

$$\frac{B(\mathbf{x})}{\varepsilon v} = \omega_\varepsilon(\mathbf{x}, v). \tag{2.3.14}$$

That allows us to introduce the matrix $\tilde{\mathcal{Q}}_\varepsilon(\mathbf{x}, \theta, v)$ defined by

$$\tilde{\mathcal{P}}_\varepsilon(\mathbf{x}, \theta, v) = \omega_\varepsilon(\mathbf{x}, v)\, \tilde{\mathcal{Q}}_\varepsilon(\mathbf{x}, \theta, v) \tag{2.3.15}$$

Using this matrix, (2.3.5) and (2.3.7)–(2.3.10) are equivalent, for $v \neq 0$, to equations involving $\tilde{\mathcal{Q}}_\varepsilon$:

$$(\nabla \boldsymbol{\Upsilon}_k) \cdot (\tilde{\mathcal{Q}}_\varepsilon(\nabla \boldsymbol{\Upsilon}_\theta)) = -\frac{v}{B(\mathbf{x})}, \tag{2.3.16}$$

and

$$(\nabla \boldsymbol{\Upsilon}_{y_1}) \cdot (\tilde{\mathcal{Q}}_\varepsilon(\nabla \boldsymbol{\Upsilon}_\theta)) = 0, \tag{2.3.17}$$
$$(\nabla \boldsymbol{\Upsilon}_{y_1}) \cdot (\tilde{\mathcal{Q}}_\varepsilon(\nabla \boldsymbol{\Upsilon}_k)) = 0, \tag{2.3.18}$$
$$(\nabla \boldsymbol{\Upsilon}_{y_2}) \cdot (\tilde{\mathcal{Q}}_\varepsilon(\nabla \boldsymbol{\Upsilon}_\theta)) = 0, \tag{2.3.19}$$
$$(\nabla \boldsymbol{\Upsilon}_{y_2}) \cdot (\tilde{\mathcal{Q}}_\varepsilon(\nabla \boldsymbol{\Upsilon}_k)) = 0. \tag{2.3.20}$$

that have no singularity in $v = 0$. Consequently in place of solving (2.3.5) and (2.3.7)–(2.3.10) we will solve (2.3.16)–(2.3.20) which is provided with boundary condition (2.3.12) and, with regard to (2.3.17)–(2.3.20), with :

$$\boldsymbol{\Upsilon}_{y_1}(\mathbf{x}, \theta, 0) = x_1, \tag{2.3.21}$$
$$\boldsymbol{\Upsilon}_{y_2}(\mathbf{x}, \theta, 0) = x_2. \tag{2.3.22}$$

Obviously in these PDEs the variable v belongs to $(0, +\infty)$. Nevertheless, in subsections 2.3.2 to 2.3.5 we will solve PDEs (2.3.17)–(2.3.20) on $\mathbb{R}^4$. Afterwards, in subsection 2.3.6, we will take the restriction of $\boldsymbol{\Upsilon}$ to $\mathbb{R}^2 \times \mathbb{R} \times (0, +\infty)$ and we will show that this restriction is a diffeomorphisms from $\mathbb{R}^2 \times \mathbb{R} \times (0, +\infty)$ onto itself.

2.3.2 First equation processing

In this subsection we deduce $\boldsymbol{\Upsilon}_k$ from equation (2.3.16). Since the θ-variable is left unchanged by $\boldsymbol{\Upsilon}$,

$$\nabla \boldsymbol{\Upsilon}_\theta = (0, 0, 1, 0)^T, \tag{2.3.23}$$

we deduce $\tilde{\mathcal{Q}}_\varepsilon(\nabla \boldsymbol{\Upsilon}_\theta)$ is the penultimate column of $\tilde{\mathcal{Q}}_\varepsilon$. Hence, in view of (2.3.16), (2.3.15) and (2.2.23), we have the following lemma

Lemma 2.3.3. *The last component $\boldsymbol{\Upsilon}_4 = \boldsymbol{\Upsilon}_k$ of mapping $\boldsymbol{\Upsilon}$ that gives the Darboux Coordinates in terms of the Polar in velocity Coordinates is the unique solution to*

$$-\varepsilon \frac{\cos(\theta)}{B(\mathbf{x})} \frac{\partial \boldsymbol{\Upsilon}_k}{\partial x_1} + \varepsilon \frac{\sin(\theta)}{B(\mathbf{x})} \frac{\partial \boldsymbol{\Upsilon}_k}{\partial x_2} - \frac{\partial \boldsymbol{\Upsilon}_k}{\partial v} = -\frac{v}{B(\mathbf{x})}, \tag{2.3.24}$$
$$\boldsymbol{\Upsilon}_k(\mathbf{x}, \theta, 0) = 0. \tag{2.3.25}$$

Moreover, when $\varepsilon = 0$, $\boldsymbol{\Upsilon}_k(\mathbf{x}, \theta, v) = v^2/(2B(\mathbf{x}))$ is the rescaled magnetic moment associated with the trajectory solution to (2.1.40)–(2.1.41).

Proof. As already said the boundary value problem $\boldsymbol{\Upsilon}_k$ is solution to is a consequence of (2.3.16) and of the choice concerning the boundary condition. Problem (2.3.24)–(2.3.25) is clearly well-posed as a consequence of the linearity of (2.3.24) and of the regularity of its coefficients. Uniqueness of the solution is obvious. The remark concerning the case when $\varepsilon = 0$ is easily obtained by solving (2.3.24)–(2.3.25) with $\varepsilon = 0$. □

We now turn to the resolution of (2.3.24)–(2.3.25). And, as already mentioned, we will solve this equation on $\mathbb{R}^4$. Defining vector field $\boldsymbol{\Lambda}$ of $\mathbb{R}^3$ as

$$\boldsymbol{\Lambda}(\mathbf{x},\theta) = \frac{\cos(\theta)}{B(\mathbf{x})}\frac{\partial}{\partial x_1} - \frac{\sin(\theta)}{B(\mathbf{x})}\frac{\partial}{\partial x_2}, \tag{2.3.26}$$

$\boldsymbol{\Lambda}^n\cdot$ its iterated application acting on regular functions f as

$$\boldsymbol{\Lambda}^0 \cdot f = f, \qquad \boldsymbol{\Lambda}^1 \cdot f = \frac{\cos(\theta)}{B(\mathbf{x})}\frac{\partial f}{\partial x_1} - \frac{\sin(\theta)}{B(\mathbf{x})}\frac{\partial f}{\partial x_2}, \tag{2.3.27}$$

$$\boldsymbol{\Lambda}^n \cdot f = \boldsymbol{\Lambda}\cdot\left(\boldsymbol{\Lambda}^{n-1}\cdot f\right) \qquad \forall n \geq 2. \tag{2.3.28}$$

and $\mathcal{G}_\lambda = \mathcal{G}_\lambda(\mathbf{x},\theta)$ its flow, we obtain the following expansion of $\boldsymbol{\Upsilon}_k$.

Theorem 2.3.4. *Under assumptions* (2.1.42) *and* (2.1.43)*, for any* $n \geq 0$*, for any* $\varepsilon \in \mathbb{R}$*, and for any* $(\mathbf{x},\theta,v) \in \mathbb{R}^4$*,*

$$\begin{aligned}\boldsymbol{\Upsilon}_k(\mathbf{x},\theta,v) = &\sum_{l=0}^{n}\frac{(-\varepsilon)^l v^{l+2}}{(l+2)!}\left(\boldsymbol{\Lambda}^l\cdot\frac{1}{B}\right)(\mathbf{x},\theta)\\ &+\frac{(-\varepsilon)^{n+1}}{(n+2)!}\int_0^v (v-u)^{n+2}\left(\boldsymbol{\Lambda}^{n+1}\cdot\frac{1}{B}\right)\circ\mathcal{G}_{-\varepsilon u}(\mathbf{x},\theta)\,du,\end{aligned} \tag{2.3.29}$$

with $\boldsymbol{\Lambda}^n\cdot$ *defined by* (2.3.28)*. Moreover, for any* $l \in \mathbb{N}$*,* $\left(\boldsymbol{\Lambda}^l\cdot\frac{1}{B}\right)$ *is in* $\mathcal{C}^\infty_{\#}\left(\mathbb{R}^4\right)$*; for any* $n \in \mathbb{N}$*,* $(\varepsilon,\mathbf{x},\theta,v) \mapsto \int_0^v (v-u)^{n+2}\left(\boldsymbol{\Lambda}^{n+1}\cdot\frac{1}{B}\right)\circ\mathcal{G}_{-\varepsilon u}(\mathbf{x},\theta)\,du$ *is in* $\mathcal{C}^\infty_{\#}\left(\mathbb{R}^5\right)$*; for any* $l \in \mathbb{N}$*,* $\left(\boldsymbol{\Lambda}^l\cdot\frac{1}{B}\right)$ *is in* $\mathcal{C}^\infty_b\left(\mathbb{R}^3\right)$*; and, for any* $v \in \mathbb{R}$ *and for any* $n \in \mathbb{N}$*,* $(\varepsilon,\mathbf{x},\theta) \mapsto \int_0^v (v-u)^{n+2}\left(\boldsymbol{\Lambda}^{n+1}\cdot\frac{1}{B}\right)\circ\mathcal{G}_{-\varepsilon u}(\mathbf{x},\theta)\,du$ *is bounded by* $C_n^{\boldsymbol{\Upsilon}_k}(v) = \frac{|v|^{n+3}}{n+3}\left\|\boldsymbol{\Lambda}^{n+1}\cdot\frac{1}{B}\right\|_\infty$*.*

Here and hereafter, $\mathcal{C}^\infty_b(\mathbb{R}^m)$ (where $m \in \mathbb{N}$) stands of the space of functions being in $\mathcal{C}^\infty(\mathbb{R}^m)$ and with their derivatives at any order which are bounded. For a 2π-periodic set $I^\#$ included in $\mathbb{R}$, $\mathcal{C}^\infty_{\mathrm{per}}\left(I^\#\right)$ stands of the space of functions being in $\mathcal{C}^\infty(I^\#)$ and 2π-periodic. For a set $\mathfrak{M}^\#$ included in $\mathbb{R}^m$ (where $m \in \mathbb{N}$ and $m \geq 2$) which is 2π-periodic with respect to the l-th variable ($l \leq m$); meaning that there exists a set $\mathfrak{I}^\flat \subset \{(r_1,\ldots,r_{l-1},r_{l+1},\ldots,r_m) \in \mathbb{R}^{m-1}\}$ and, for any $(r_1,\ldots,r_{l-1},r_{l+1},\ldots,r_m) \in \mathfrak{I}^\flat$, another 2π-periodic set $\mathfrak{I}^\sharp(r_1,\ldots,r_{l-1},r_{l+1},\ldots,r_m)$ included in $\mathbb{R}$, such that $\mathfrak{M}^\# = \{\mathbf{r},(r_1,\ldots,r_{l-1},r_{l+1},\ldots,r_m) \in \mathfrak{I}^\flat, r_l \in \mathfrak{I}^\sharp(r_1,\ldots,r_{l-1},r_{l+1},\ldots,r_m)\}$; we denote

$$\begin{aligned}\mathcal{C}^\infty_{\#,l}\left(\mathfrak{M}^\#\right) = \Big\{&f \in \mathcal{C}^\infty\left(\mathfrak{M}^\#\right) \text{ such that } r_l \mapsto f(\mathbf{r})\\ &\in \mathcal{C}^\infty_{per}(\mathfrak{I}^\sharp(r_1,\ldots,r_{l-1},r_{l+1},\ldots,r_m)),\ \forall (r_1,\ldots,r_{l-1},r_{l+1},\ldots,r_m) \in \mathfrak{I}^\flat\Big\}.\end{aligned} \tag{2.3.30}$$

Since the case when the variable with respect to which periodicity occurs is the penultimate happens very often in the following, we define

$$\mathcal{C}^\infty_{\#}\left(\mathfrak{M}^\#\right) = \mathcal{C}^\infty_{\#,(m-1)}\left(\mathfrak{M}^\#\right) \tag{2.3.31}$$

The proof of Theorem 2.3.4 is based on a method of characteristics that we will develop now.

2.3.3 The method of Characteristics

In this subsection we will set out a method of characteristics which brings the capability of building solution to a PDE, related to (2.3.24), (2.3.17) and (2.3.19), on which the resolution of (2.3.24), (2.3.17) and (2.3.19) themselves will be based in the next subsection. This method of characteristics is in the same spirit as the method developed in Abraham [1, page 233].
In a first place, we give the regularity property of the flow $\mathcal{G}_\lambda$ of vector field $\mathbf{\Lambda}$ defined by (2.3.26).

Lemma 2.3.5. *Flow $\mathcal{G}_\lambda = \mathcal{G}_\lambda(\mathbf{x},\theta)$ of vector field $\mathbf{\Lambda}$ defined by (2.3.26) is complete, in $\mathcal{C}^\infty(\mathbb{R}^3)$, $\left(\mathcal{G}^1_\lambda, \mathcal{G}^2_\lambda\right)$ is in $\mathcal{C}^\infty_{\#,3}(\mathbb{R}^3)$ and $\mathcal{G}^3_\lambda(\mathbf{x},\theta) = \theta$.*

Proof. The fact that $\mathcal{G}_\lambda$ is complete is obvious. The regularity of $\mathcal{G}_\lambda$ comes from the assumed regularity of B (see (2.1.42) and (2.1.43)). Integrating $\frac{\partial \mathcal{G}^3_\lambda}{\partial \lambda}(\mathbf{x},\theta) = 0$ with initial condition $\mathcal{G}^3_0(\mathbf{x},\theta) = \theta$ yields $\mathcal{G}^3_\lambda(\mathbf{x},\theta) = \theta$. Finally, let $\tilde{\mathcal{G}}_\lambda$ be defined by $\tilde{\mathcal{G}}_\lambda(\mathbf{x},\theta) = \mathcal{G}_\lambda(\mathbf{x},\theta+2\pi)$. Then, the two first components of $\mathcal{G}_\lambda$ and $\tilde{\mathcal{G}}_\lambda$ satisfy the same dynamical system. Furthermore, since

$$\left(\tilde{\mathcal{G}}^1_0(\mathbf{x},\theta), \tilde{\mathcal{G}}^2_0(\mathbf{x},\theta)\right) = \mathbf{x} = \left(\mathcal{G}^1_0(\mathbf{x},\theta), \mathcal{G}^2_0(\mathbf{x},\theta)\right),$$

the Cauchy-Lipschitz Theorem allows us to conclude that

$$\left(\tilde{\mathcal{G}}^1_\lambda(\mathbf{x},\theta), \tilde{\mathcal{G}}^2_\lambda(\mathbf{x},\theta)\right) = \left(\mathcal{G}^1_\lambda(\mathbf{x},\theta), \mathcal{G}^2_\lambda(\mathbf{x},\theta)\right)$$

and consequently that the two first components of $\mathcal{G}_\lambda$ are 2π-periodic. □

Secondly, we define vector field $\boldsymbol{\xi}$ on $\mathbb{R}^5$ by :

$$\boldsymbol{\xi}(\mathbf{x},\theta,v,x_5) = -\varepsilon \mathbf{\Lambda}(\mathbf{x},\theta) - \frac{\partial}{\partial v}, \tag{2.3.32}$$

with $\mathbf{\Lambda}$ given by (2.3.26), and its flow $\mathcal{F}_\lambda \equiv \mathcal{F}_\lambda(\mathbf{x},\theta,v,x_5)$ which is such that

$$\frac{d\mathcal{F}_\lambda(\mathbf{x},\theta,v,x_5)}{d\lambda} = \boldsymbol{\xi}\left(\mathcal{F}_\lambda(\mathbf{x},\theta,v,x_5)\right), \tag{2.3.33}$$

$$\mathcal{F}_0(\mathbf{x},\theta,v,x_5) = (\mathbf{x},\theta,v,x_5). \tag{2.3.34}$$

Since the function

$$(\mathbf{x},\theta,v,x_5) \mapsto \left(-\varepsilon\frac{\cos(\theta)}{B(\mathbf{x})}, \varepsilon\frac{\sin(\theta)}{B(\mathbf{x})}, 0, -1, 0\right),$$

is Lipschitz continuous on $\mathbb{R}^5$, the flow is complete and we can consider the manifolds

$$\Gamma = \left\{(\mathbf{x},\theta,v,x_5) \in \mathbb{R}^5,\ v = 0,\ x_5 = \frac{1}{B(\mathbf{x})}\right\},$$

and $P = \underset{\lambda\in\mathbb{R}}{\cup} \mathcal{F}_\lambda(\Gamma)$.
The following lemma holds true.

Lemma 2.3.6. *If there exists a function $\varphi \equiv \varphi(\mathbf{x},\theta,v)$, from $\mathbb{R}^4$ to $\mathbb{R}$, which is in $\mathcal{C}^1\left(\mathbb{R}^4\right)$ such that P writes*

$$P = \left\{(\mathbf{x},\theta,v,x_5),\ x_5 = \varphi(\mathbf{x},\theta,v)\right\}, \tag{2.3.35}$$

then φ is solution to the following PDE

$$-\varepsilon \mathbf{\Lambda}^1 \cdot \varphi - \frac{\partial \varphi}{\partial v} = 0, \tag{2.3.36}$$

$$\varphi(\mathbf{x}, \theta, 0) = \frac{1}{B(\mathbf{x})}. \tag{2.3.37}$$

Proof. By construction, $\boldsymbol{\xi}$ is a vector field tangent to manifold P. On another hand, if P writes as in formula (2.3.35), then the vector field

$$\mathbf{n}(\mathbf{x}, \theta, v) = \frac{\partial \varphi}{\partial x_1}\frac{\partial}{\partial x_1} + \frac{\partial \varphi}{\partial x_2}\frac{\partial}{\partial x_2} + \frac{\partial \varphi}{\partial \theta}\frac{\partial}{\partial \theta} + \frac{\partial \varphi}{\partial v}\frac{\partial}{\partial v} - \frac{\partial}{\partial x_5} \tag{2.3.38}$$

is orthogonal to P in every point of P. Then, using $\boldsymbol{\xi}(\mathbf{x}, \theta, v, x_5) \cdot \mathbf{n}(\mathbf{x}, \theta, v) = 0$ yields (2.3.36). Moreover the boundary condition of (2.3.37) is obviously satisfied by φ. □

Using this lemma we obtain the following theorem.

Theorem 2.3.7. *The unique solution φ to* (2.3.36)–(2.3.37) *is given by*

$$\varphi(\mathbf{x}, \theta, v) = \frac{1}{B\left(\mathcal{G}^1_{-\varepsilon v}(\mathbf{x}, \theta), \mathcal{G}^2_{-\varepsilon v}(\mathbf{x}, \theta)\right)}, \tag{2.3.39}$$

where $\mathcal{G}_\lambda = \mathcal{G}_\lambda(\mathbf{x}, \theta)$ is the flow of $\mathbf{\Lambda}$. Moreover, φ is in $\mathcal{C}^\infty_\#(\mathbb{R}^4)$ and is bounded (see (2.3.31) *for notation).*

Proof. By definition, the flow $\mathcal{G}_\lambda$ of $\mathbf{\Lambda}$ is solution to :

$$\begin{aligned} &\frac{d\mathcal{G}_\lambda(\mathbf{x}, \theta)}{d\lambda} = \mathbf{\Lambda}\left(\mathcal{G}_\lambda(\mathbf{x}, \theta)\right), \\ &\mathcal{G}_0(\mathbf{x}, \theta) = (\mathbf{x}, \theta). \end{aligned} \tag{2.3.40}$$

As

$$\left[\frac{d\mathcal{G}}{d\lambda}\right]_{-\varepsilon\lambda}(\mathbf{x}, \theta) = -\varepsilon \frac{d(\mathcal{G}_{-\varepsilon\lambda})}{d\lambda}(\mathbf{x}, \theta) = -\varepsilon \mathbf{\Lambda}\left(\mathcal{G}_{-\varepsilon\lambda}(\mathbf{x}, \theta)\right), \tag{2.3.41}$$

we deduce that the flow of $\boldsymbol{\xi}$ writes :

$$\mathcal{F}_\lambda(\mathbf{x}, \theta, v, x_5) = \left(\mathcal{G}_{-\varepsilon\lambda}(\mathbf{x}, \theta), -\lambda + v, x_5\right). \tag{2.3.42}$$

Now, using the following parametric representation of Γ :

$$\Gamma = \left\{ x_1 = t_1,\ x_2 = t_2,\ \theta = t_3,\ v = 0,\ x_5 = \frac{1}{B(t_1, t_2)};\ (t_1, t_2, t_3) \in \mathbb{R}^3 \right\}, \tag{2.3.43}$$

for any $\mathbf{z}$ $(= (z_1, z_2, z_3, z_4, z_5)) \in P$, there exists $\lambda \in \mathbb{R}$ and $\mathbf{m}$ $\left(= \left(t_1, t_2, t_3, 0, \frac{1}{B(t_1,t_2)}\right)\right) \in \Gamma$ such that

$$\mathbf{z} = \mathcal{F}_\lambda(\mathbf{m}) \text{ or } \mathbf{m} = \mathcal{F}_{-\lambda}(\mathbf{z}). \tag{2.3.44}$$

This last equality reads also

$$(t_1, t_2, t_3) = \mathcal{G}_{\varepsilon\lambda}(z_1, z_2, z_3), \tag{2.3.45}$$

$$\lambda + z_4 = 0, \tag{2.3.46}$$

$$z_5 = \frac{1}{B(t_1, t_2)}. \tag{2.3.47}$$

Hence,

$$\lambda = -z_4, \tag{2.3.48}$$

$$(t_1, t_2) = \left(\mathcal{G}^1_{-\varepsilon z_4}(z_1, z_2, z_3), \mathcal{G}^2_{-\varepsilon z_4}(z_1, z_2, z_3)\right), \tag{2.3.49}$$

$$z_5 = \frac{1}{B\left(\mathcal{G}^1_{-\varepsilon z_4}(z_1, z_2, z_3), \mathcal{G}^2_{-\varepsilon z_4}(z_1, z_2, z_3)\right)}. \tag{2.3.50}$$

In view of the expression of z_5 in this formula, applying Lemma 2.3.6, the solution $\varphi = \varphi(\mathbf{x}, \theta, v)$ of (2.3.36)–(2.3.37) is given by (2.3.39). Uniqueness of the solution of problem (2.3.36)–(2.3.37) is obvious. Since the regularity and periodicity of φ is a direct consequence of Lemma 2.3.5 and of assumptions (2.1.42) and (2.1.43), this ends the proof of Theorem 2.3.7. □

Now, we will look for an asymptotic expansion, with respect to ε, of the solution φ to (2.3.36)–(2.3.37). This will be based on a Lie expansion of the flow $\mathcal{G}_\lambda$.

Definition 2.3.8. *If $\mathbf{\Lambda}$ is a vector field of $\mathbb{R}^3$ with coefficients which are in $\mathcal{C}^\infty_b(\mathbb{R}^3)$, then we define the Lie Series $S^\infty_L(\mathbf{\Lambda})\cdot$ associated with $\mathbf{\Lambda}$ by*

$$S^\infty_L(\mathbf{\Lambda})\cdot = \sum_{l\geq 0} \frac{(\mathbf{\Lambda})^l \cdot}{l!}, \tag{2.3.51}$$

where $(\mathbf{\Lambda})^l$ is defined by (2.3.27) *and* (2.3.28)*, and the partial Lie Sum of order n :*

$$S^n_L(\mathbf{\Lambda})\cdot = \sum_{l=0}^{n} \frac{(\mathbf{\Lambda})^l \cdot}{l!}. \tag{2.3.52}$$

It is known that, formally, the flow $\mathcal{G}_\lambda$ associated with $\mathbf{\Lambda}$ may be expressed in terms of the Lie Series of $\mathbf{\Lambda}$:

$$\mathcal{G}_\lambda = S^\infty_L(\lambda\mathbf{\Lambda})\cdot = \sum_{l\geq 0} \frac{(\lambda\mathbf{\Lambda})^l \cdot}{l!}. \tag{2.3.53}$$

More rigorously, as the flow is complete, using its partial Lie Sum we have

$$f\circ\mathcal{G}_\lambda = \sum_{l=0}^{n} \frac{\lambda^l (\mathbf{\Lambda})^l \cdot}{l!} f + \int_0^\lambda \frac{(\lambda-u)^n}{n!} \left(\mathbf{\Lambda}^{n+1}\cdot f\right)\circ\mathcal{G}_u du, \tag{2.3.54}$$

for any function $f:\ \mathbb{R}^3 \to \mathbb{R}$ being $\mathcal{C}^\infty(\mathbb{R}^3)$. Taking now $\frac{1}{B}$ as function f in (2.3.54), we obtain

$$\varphi(\mathbf{x}, \theta, v) = \sum_{l=0}^{n} \frac{(-\varepsilon v)^l}{l!} \left(\mathbf{\Lambda}^l \cdot \frac{1}{B}\right)(\mathbf{x}, \theta) + \int_0^{-\varepsilon v} \frac{(-\varepsilon v - u)^n}{n!} \left(\mathbf{\Lambda}^{n+1}\cdot\frac{1}{B}\right)\circ\mathcal{G}_u(\mathbf{x}, \theta)\, du.$$

Hence we have proven the following lemma

Lemma 2.3.9. *Function φ, solution to* (2.3.36)–(2.3.37)*, admits for any $n \in \mathbb{N}$, for any $\varepsilon \in \mathbb{R}$ and for any $(\mathbf{x}, \theta, v) \in \mathbb{R}^4$ the following expansion in power of ε*

$$\begin{aligned}\varphi(\mathbf{x}, \theta, v) = &\sum_{l=0}^{n} \frac{(-\varepsilon v)^l}{l!} \left(\mathbf{\Lambda}^l \cdot \frac{1}{B}\right)(\mathbf{x}, \theta) \\ &+ \frac{(-\varepsilon)^{n+1}}{n!} \int_0^v \frac{(v-u)^n}{n!} \left(\mathbf{\Lambda}^{n+1}\cdot\frac{1}{B}\right)\circ\mathcal{G}_{-\varepsilon u}(\mathbf{x}, \theta)\, du.\end{aligned} \tag{2.3.55}$$

Moreover, for any $l \in \mathbb{N}$, $\left(\mathbf{\Lambda}^l \cdot \frac{1}{B}\right)$ *is in* $\mathcal{C}^\infty_{\#,3}(\mathbb{R}^3) \cap \mathcal{C}^\infty_b\left(\mathbb{R}^3\right)$ *; for any* $n \in \mathbb{N}$, $(\varepsilon, \mathbf{x}, \theta, v) \mapsto \int_0^v \frac{(v-u)^n}{n!} \left(\mathbf{\Lambda}^{n+1} \cdot \frac{1}{B}\right) \circ \mathcal{G}_{-\varepsilon u}(\mathbf{x}, \theta)\, du$ *is in* $\mathcal{C}^\infty_{\#}(\mathbb{R}^5)$ *; and for any* $v \in \mathbb{R}$ *and any* $n \in \mathbb{N}$, $(\varepsilon, \mathbf{x}, \theta) \mapsto \int_0^v \frac{(v-u)^n}{n!} \left(\mathbf{\Lambda}^{n+1} \cdot \frac{1}{B}\right) \circ \mathcal{G}_{-\varepsilon u}(\mathbf{x}, \theta)\, du$ *is bounded by* $C^\varphi_n(v) = \frac{|v|^{n+1}}{(n+1)!} \left\|\mathbf{\Lambda}^{n+1} \cdot \frac{1}{B}\right\|_\infty$.

This ends this subsection. We will now use these results to solve (2.3.24)–(2.3.25) and consequently prove Theorem 2.3.4.

2.3.4 Proof of Theorem 2.3.4

For φ being given by (2.3.39), let

$$\psi(\mathbf{x}, \theta, v) = \int_0^v \varphi(\mathbf{x}, \theta, s)\, ds. \tag{2.3.56}$$

Integrating (2.3.36) between 0 and v, using (2.3.37) and expression (2.3.27) of $\mathbf{\Lambda}^1 \cdot$, we obtain that ψ satisfies $-\varepsilon \mathbf{\Lambda}^1 \cdot \psi(\mathbf{x}, \theta, v) - \varphi(\mathbf{x}, \theta, v) = -\varphi(\mathbf{x}, \theta, 0)$ and then is the unique solution to

$$-\varepsilon \frac{\cos(\theta)}{B(\mathbf{x})} \frac{\partial \psi}{\partial x_1} + \varepsilon \frac{\sin(\theta)}{B(\mathbf{x})} \frac{\partial \psi}{\partial x_2} - \frac{\partial \psi}{\partial v} = -\frac{1}{B(\mathbf{x})}, \tag{2.3.57}$$

$$\psi(\mathbf{x}, \theta, 0) = 0. \tag{2.3.58}$$

Integrating now (2.3.57) between 0 and v and using (2.3.58) we obtain that $\int_0^v \psi(\mathbf{x}, \theta, s)\, ds$ is the unique solution of (2.3.24)–(2.3.25), from which we deduce that

$$\mathbf{\Upsilon}_k(\mathbf{x}, \theta, v) = \int_0^v \psi(\mathbf{x}, \theta, s)\, ds. \tag{2.3.59}$$

Moreover, integrating between 0 and v the expansion of φ given by Lemma 2.3.9, we obtain

$$\begin{aligned} \psi(\mathbf{x}, \theta, v) = &\sum_{l=0}^{n} \frac{(-\varepsilon)^l v^{l+1}}{(l+1)!} \left(\mathbf{\Lambda}^l \cdot \frac{1}{B}\right)(\mathbf{x}, \theta) \\ &+ \frac{(-\varepsilon)^{n+1}}{(n+1)!} \int_0^v (v-u)^{n+1} \left(\mathbf{\Lambda}^{n+1} \cdot \frac{1}{B}\right) \circ \mathcal{G}_{-\varepsilon u}(\mathbf{x}, \theta)\, du, \end{aligned} \tag{2.3.60}$$

and integrating the expansion of ψ given by (2.3.60) we obtain the expansion (2.3.29). This ends the proof of Theorem 2.3.4. □

2.3.5 The other equations

Equation (2.3.16) was processed and gave expression of $\mathbf{\Upsilon}_k$. Equations (2.3.17), (2.3.18), (2.3.19) and (2.3.20) will be processed using results of the previous sections. Here, there is an additional difficulty which is that $\mathbf{\Upsilon}_{y_1}$ and $\mathbf{\Upsilon}_{y_2}$ are simultaneously solutions of two PDEs ; one involving $\mathbf{\Upsilon}_\theta$ and another one involving $\mathbf{\Upsilon}_k$.

We have the following theorem.

Theorem 2.3.10. *The first component* $\mathbf{\Upsilon}_1 = \mathbf{\Upsilon}_{y_1}$ *of mapping* $\mathbf{\Upsilon}$ *which is solution to* (2.3.18) *and* (2.3.17) *and which satisfies* (2.3.21) *is given by*

$$\mathbf{\Upsilon}_{y_1}(\mathbf{x}, \theta, v) = x_1 - \varepsilon \cos(\theta)\, \psi(\mathbf{x}, \theta, v), \tag{2.3.61}$$

where ψ is defined by formula (2.3.56). For any $n \geq 1$, for any $\varepsilon \in \mathbb{R}$, and for any $(\mathbf{x}, \theta, v) \in \mathbb{R}^4$ we have the following expansion for $\boldsymbol{\Upsilon}_{y_1}$

$$\begin{aligned}\boldsymbol{\Upsilon}_{y_1}(\mathbf{x}, \theta, v) = x_1 + \cos(\theta) \sum_{l=1}^{n} \frac{v^l (-\varepsilon)^l}{l!} \left(\boldsymbol{\Lambda}^{l-1} \cdot \frac{1}{B}\right)(\mathbf{x}, \theta) + \\ \cos(\theta) \frac{(-\varepsilon)^{n+1}}{n!} \int_0^v (v-u)^n \left(\boldsymbol{\Lambda}^n \cdot \frac{1}{B}\right)(\mathcal{G}_{-\varepsilon u}(\mathbf{x}, \theta))\, du.\end{aligned} \tag{2.3.62}$$

Moreover, $(\varepsilon, \mathbf{x}, \theta, v) \mapsto \boldsymbol{\Upsilon}_{y_1}(\mathbf{x}, \theta, v)$ and $(\varepsilon, \mathbf{x}, \theta, v) \mapsto \psi(\mathbf{x}, \theta, v)$ are in $\mathcal{C}^\infty_\#(\mathbb{R}^5)$; ψ is bounded by $C^\psi(v) = |v|^2 \left\|\frac{1}{B}\right\|_\infty$; for any $l \in \mathbb{N}$, $\left(\boldsymbol{\Lambda}^l \cdot \frac{1}{B}\right)$ is in $\mathcal{C}^\infty_b\left(\mathbb{R}^3\right) \cap \mathcal{C}^\infty_\#\left(\mathbb{R}^4\right)$; $(\varepsilon, \mathbf{x}, \theta, v) \mapsto \int_0^v (v-u)^n \left(\boldsymbol{\Lambda}^n \cdot \frac{1}{B}\right)(\mathcal{G}_{-\varepsilon u}(\mathbf{x}, \theta))\, du$ is in $\mathcal{C}^\infty_\#\left(\mathbb{R}^5\right)$, and for any $v \in \mathbb{R}$ and any $n \in \mathbb{N}$, it is bounded by $C_n^{\boldsymbol{\Upsilon}_{y_1}}(v) = \frac{|v|^{n+1}}{n+1} \left\|\boldsymbol{\Lambda}^n \cdot \frac{1}{B}\right\|_\infty$.

Proof. In a first place, by definition, $\psi(\mathbf{x}, \theta, 0) = 0$ and hence $\boldsymbol{\Upsilon}_{y_1}$ given by (2.3.61) satisfies $\boldsymbol{\Upsilon}_{y_1}(\mathbf{x}, \theta, 0) = x_1$. Moreover ψ satisfies $\left(-\varepsilon\boldsymbol{\Lambda} - \frac{\partial}{\partial v}\right) \cdot \psi = -\frac{1}{B}$ and hence by linearity $\boldsymbol{\Upsilon}_{y_1}$ given by (2.3.61) is solution of (2.3.17). On another hand from expansion (2.3.60) of ψ we deduce expansion (2.3.62) of $\boldsymbol{\Upsilon}_{y_1}$.

Secondly we show that $\{\boldsymbol{\Upsilon}_{y_1}, \boldsymbol{\Upsilon}_k\}$, which is defined (with worth 0) for $v \neq 0$ because of the singularity of $\tilde{\mathcal{P}}_\varepsilon$, can be extended smoothly by 0 in $v = 0$. Using expansion (2.3.62) of $\boldsymbol{\Upsilon}_{y_1}$ for $n = 1$ we obtain

$$\boldsymbol{\Upsilon}_{y_1}(\mathbf{x}, \theta, v) = x_1 - \frac{\varepsilon \cos(\theta)\, v}{B(\mathbf{x})} + \varepsilon^2 \cos(\theta) \int_0^v (v-u) \left(\boldsymbol{\Lambda} \cdot \frac{1}{B}\right)(\mathcal{G}_{-\varepsilon u}(\mathbf{x}, \theta))\, du. \tag{2.3.63}$$

In the same way, applying formula (2.3.29) with $n = 0$ we obtain :

$$\boldsymbol{\Upsilon}_k(\mathbf{x}, \theta, v) = \frac{v^2}{2B(\mathbf{x})} - \frac{\varepsilon}{2} \int_0^v (v-u) \left(\boldsymbol{\Lambda} \cdot \frac{1}{B}\right)(\mathcal{G}_{-\varepsilon u}(\mathbf{x}, \theta))\, du. \tag{2.3.64}$$

Differentiating (2.3.63) with respect to x_1 yields

$$\begin{aligned}\frac{\partial \boldsymbol{\Upsilon}_{y_1}}{\partial x_1}(\mathbf{x}, \theta, v) = 1 - \varepsilon \cos(\theta)\, v \left(\frac{\partial}{\partial x_1}\left(\frac{1}{B}\right)\right)(\mathbf{x}) \\ + \varepsilon^2 \cos(\theta) \int_0^v (v-u) \left[\left(\frac{\partial}{\partial x_1}\left(\boldsymbol{\Lambda} \cdot \frac{1}{B}\right)\right)(\mathcal{G}_{-\varepsilon u}(\mathbf{x}, \theta)) \frac{\partial \mathcal{G}^1_{-\varepsilon u}}{\partial x_1}(\mathbf{x}, \theta)\right. \\ \left. + \left(\frac{\partial}{\partial x_2}\left(\boldsymbol{\Lambda} \cdot \frac{1}{B}\right)\right)(\mathcal{G}_{-\varepsilon u}(\mathbf{x}, \theta)) \frac{\partial \mathcal{G}^2_{-\varepsilon u}}{\partial x_1}(\mathbf{x}, \theta)\right] du.\end{aligned} \tag{2.3.65}$$

As $\frac{1}{B}$ and all its derivatives are bounded and as $\frac{\partial \mathcal{G}^1_\lambda}{\partial x_1}$ and $\frac{\partial \mathcal{G}^2_\lambda}{\partial x_1}$ are continuous with respect to λ we obtain the following estimate :

$$\begin{aligned}\left|\frac{\partial \boldsymbol{\Upsilon}_{y_1}}{\partial x_1}(\mathbf{x}, \theta, v)\right| \leq 1 + \varepsilon |v| \left\|\frac{\partial}{\partial x_1}\frac{1}{B}\right\|_\infty \\ + \frac{\varepsilon^2 |v|^2}{2} \left[\left\|\frac{\partial}{\partial x_1}\left(\boldsymbol{\Lambda} \cdot \frac{1}{B}\right)\right\|_\infty \sup_{u \in [-|v|, |v|]} \left|\frac{\partial \mathcal{G}^1_{-\varepsilon u}}{\partial x_1}\right|(\mathbf{x}, \theta)\right. \\ \left. + \left\|\frac{\partial}{\partial x_2}\left(\boldsymbol{\Lambda} \cdot \frac{1}{B}\right)\right\|_\infty \sup_{u \in [-|v|, |v|]} \left|\frac{\partial \mathcal{G}^2_{-\varepsilon u}}{\partial x_1}\right|(\mathbf{x}, \theta)\right].\end{aligned}$$

Hence $\frac{\partial \boldsymbol{\Upsilon}_{y_1}}{\partial x_1}(\mathbf{x},\theta,v) = \epsilon_{y_1}^{x_1}(\mathbf{x},\theta,v)$ with $\epsilon_{y_1}^{x_1}(\mathbf{x},\theta,v)$ such that for any $(\mathbf{x},\theta)$, $v \mapsto \epsilon_{y_1}^{x_1}(\mathbf{x},\theta,v)$ is smooth, and is bounded in the neighborhood of $v=0$. In the same way we can show that

$$\begin{aligned}
&\frac{\partial \boldsymbol{\Upsilon}_{y_1}}{\partial x_2}(\mathbf{x},\theta,v) = v\epsilon_{y_1}^{x_2}(\mathbf{x},\theta,v), \qquad &&\frac{\partial \boldsymbol{\Upsilon}_{y_1}}{\partial \theta}(\mathbf{x},\theta,v) = v\epsilon_{y_1}^{\theta}(\mathbf{x},\theta,v),\\
&\frac{\partial \boldsymbol{\Upsilon}_{y_1}}{\partial v}(\mathbf{x},\theta,v) = \epsilon_{y_1}^{v}(\mathbf{x},\theta,v), \qquad &&\frac{\partial \boldsymbol{\Upsilon}_{k}}{\partial x_1}(\mathbf{x},\theta,v) = v^2\epsilon_{k}^{x_1}(\mathbf{x},\theta,v),\\
&\frac{\partial \boldsymbol{\Upsilon}_{k}}{\partial x_2}(\mathbf{x},\theta,v) = v^2\epsilon_{k}^{x_2}(\mathbf{x},\theta,v), \qquad &&\frac{\partial \boldsymbol{\Upsilon}_{k}}{\partial \theta}(\mathbf{x},\theta,v) = v^3\epsilon_{k}^{\theta}(\mathbf{x},\theta,v),\\
&\frac{\partial \boldsymbol{\Upsilon}_{k}}{\partial v}(\mathbf{x},\theta,v) = v\epsilon_{k}^{v}(\mathbf{x},\theta,v).
\end{aligned} \tag{2.3.66}$$

with $\epsilon_{y_1}^{x_2}(\mathbf{x},\theta,v)$, $\epsilon_{y_1}^{\theta}(\mathbf{x},\theta,v)$, $\epsilon_{y_1}^{v}(\mathbf{x},\theta,v)$, $\epsilon_{k}^{x_1}(\mathbf{x},\theta,v)$, $\epsilon_{k}^{x_2}(\mathbf{x},\theta,v)$, $\epsilon_{k}^{\theta}(\mathbf{x},\theta,v)$, $\epsilon_{k}^{v}(\mathbf{x},\theta,v)$ such that for any $(\mathbf{x},\theta)$, the functions $v \mapsto \epsilon_{\bullet}^{\bullet}(\mathbf{x},\theta,v)$ are smooth, and are bounded in the neighborhood of $v=0$. Injecting these expressions in $\{\boldsymbol{\Upsilon}_{y_1},\boldsymbol{\Upsilon}_k\}(\mathbf{x},\theta,v) = (\nabla \boldsymbol{\Upsilon}_{y_1}) \cdot \left(\tilde{\mathcal{P}}_\varepsilon \nabla \boldsymbol{\Upsilon}_k\right)$ we obtain $\{\boldsymbol{\Upsilon}_{y_1},\boldsymbol{\Upsilon}_k\}(\mathbf{x},\theta,v) = v\epsilon_{y_1,k}(\mathbf{x},\theta,v)$ with $\epsilon_{y_1,k}(\mathbf{x},\theta,v)$ such that $v \mapsto \epsilon_{y_1,k}(\mathbf{x},\theta,v)$ is smooth, and is bounded in the neighborhood of $v=0$ leading that $\{\boldsymbol{\Upsilon}_{y_1},\boldsymbol{\Upsilon}_k\}$ can be smoothly extended by 0 in $v=0$.

As the last step of this proof, because of the Jacobi identity we have

$$\forall v \neq 0, \quad \{\{\boldsymbol{\Upsilon}_{y_1},\boldsymbol{\Upsilon}_k\},\boldsymbol{\Upsilon}_\theta\} + \{\{\boldsymbol{\Upsilon}_\theta,\boldsymbol{\Upsilon}_{y_1}\},\boldsymbol{\Upsilon}_k\} + \{\{\boldsymbol{\Upsilon}_k,\boldsymbol{\Upsilon}_\theta\},\boldsymbol{\Upsilon}_{y_1}\} = 0, \tag{2.3.67}$$

which reads, because the gradient of a constant is zero, because, according to (2.3.5), $\{\boldsymbol{\Upsilon}_k,\boldsymbol{\Upsilon}_\theta\} = \frac{1}{\varepsilon}$ and, as we just saw, because $\boldsymbol{\Upsilon}_{y_1}$ given by (2.3.61) satisfies $\{\boldsymbol{\Upsilon}_\theta,\boldsymbol{\Upsilon}_{y_1}\} = 0$,

$$\{\{\boldsymbol{\Upsilon}_{y_1},\boldsymbol{\Upsilon}_k\},\boldsymbol{\Upsilon}_\theta\} = 0. \tag{2.3.68}$$

Dividing (2.3.68) by $\omega_\varepsilon(\mathbf{x},\theta)$ defined by (2.3.14), we obtain that for $v \neq 0$, $\{\boldsymbol{\Upsilon}_{y_1},\boldsymbol{\Upsilon}_k\}$ is solution to

$$(\nabla\{\boldsymbol{\Upsilon}_{y_1},\boldsymbol{\Upsilon}_k\}) \cdot \left(\tilde{\mathcal{Q}}_\varepsilon(\nabla \boldsymbol{\Upsilon}_\theta)\right) = 0. \tag{2.3.69}$$

By continuity of the left hand side of (2.3.69) on $\mathbb{R}^4$, we deduce that equality (2.3.69) is valid on $\mathbb{R}^4$. As $\{\boldsymbol{\Upsilon}_{y_1},\boldsymbol{\Upsilon}_k\}$ may be smoothly extended by 0 in $v=0$, and as (2.3.69) admits an unique solution satisfying the boundary condition $\{\boldsymbol{\Upsilon}_{y_1},\boldsymbol{\Upsilon}_k\}(\mathbf{x},\theta,0) = 0$, we deduce that $\boldsymbol{\Upsilon}_{y_1}$ given by (2.3.61) satisfies $\{\boldsymbol{\Upsilon}_{y_1},\boldsymbol{\Upsilon}_k\} = 0$ for all $(\mathbf{x},\theta,v)$. Hence (2.3.18) follows and we deduce that $\boldsymbol{\Upsilon}_{y_1}$ given by (2.3.61) is well $\boldsymbol{\Upsilon}_{y_1}$. This ends the proof of Theorem 2.3.10. □

In the same way we can prove :

Theorem 2.3.11. *The second component $\boldsymbol{\Upsilon}_2 = \boldsymbol{\Upsilon}_{y_2}$ of mapping $\boldsymbol{\Upsilon}$ that gives the Darboux Coordinates in terms of the Polar in velocity Coordinates is given by*

$$\boldsymbol{\Upsilon}_{y_2}(\mathbf{x},\theta,v) = x_2 + \varepsilon \sin(\theta)\,\psi(\mathbf{x},\theta,v), \tag{2.3.70}$$

where ψ is defined by formula (2.3.56). For any $n \geq 1$, for any $\varepsilon \in \mathbb{R}$, and for any $(\mathbf{x},\theta,v) \in \mathbb{R}^4$ we have the following expansion for $\boldsymbol{\Upsilon}_{y_2}$

$$\begin{aligned}
\boldsymbol{\Upsilon}_{y_2}(\mathbf{x},\theta,v) = x_2 &- \sin(\theta)\sum_{l=1}^{n}\frac{v^l(-\varepsilon)^l}{l!}\left(\boldsymbol{\Lambda}^{l-1}\cdot\frac{1}{B}\right)(\mathbf{x},\theta)\\
&- \sin(\theta)\frac{(-\varepsilon)^{n+1}}{n!}\int_0^v (v-u)^n\left(\boldsymbol{\Lambda}^n\cdot\frac{1}{B}\right)(\mathcal{G}_{-\varepsilon u}(\mathbf{x},\theta))\,du.
\end{aligned} \tag{2.3.71}$$

Moreover, $(\varepsilon,\mathbf{x},\theta,v) \mapsto \boldsymbol{\Upsilon}_{y_2}(\mathbf{x},\theta,v)$ is $\mathcal{C}^\infty_{\#}(\mathbb{R}^5)$.

2.3.6 The Darboux Coordinates System

In subsection 2.3.2 and 2.3.5 we solved equations (2.3.5) and (2.3.7)–(2.3.10) on $\mathbb{R}^4$. Now, we need to check that the restriction of $\boldsymbol{\Upsilon}$ to $\mathbb{R}^2 \times \mathbb{R} \times (0, +\infty)$, also denoted by $\boldsymbol{\Upsilon}$, is a diffeomorphism (onto $\mathbb{R}^2 \times \mathbb{R} \times (0, +\infty)$) and hence that $(\mathbf{y}, \theta, k)$ makes a true coordinate system on $\mathbb{R}^2 \times \mathbb{R} \times (0, +\infty)$. We will also prove that function $\boldsymbol{\kappa}$ defined by $\boldsymbol{\kappa} = \boldsymbol{\Upsilon}^{-1}$ is smooth with respect to the small parameter ε and we will give its expansion in power of ε.

Firstly, using expressions (2.3.61) and (2.3.70) of $\boldsymbol{\Upsilon}_{y_1}$ and $\boldsymbol{\Upsilon}_{y_2}$, formula (2.3.39) that gives the expression of $\varphi = \partial_v \psi$, expression (2.3.26) of $\boldsymbol{\Lambda}$ and the definition (2.3.40) of its flow $\mathcal{G}_\lambda$, we deduce that

$$\frac{\partial \boldsymbol{\Upsilon}_{y_1}}{\partial v}(\mathbf{x}, \theta, v) = \frac{\partial}{\partial v} \mathcal{G}^1_{-\varepsilon v}(\mathbf{x}, \theta), \tag{2.3.72}$$

$$\frac{\partial \boldsymbol{\Upsilon}_{y_2}}{\partial v}(\mathbf{x}, \theta, v) = \frac{\partial}{\partial v} \mathcal{G}^2_{-\varepsilon v}(\mathbf{x}, \theta), \tag{2.3.73}$$

$$\frac{\partial \boldsymbol{\Upsilon}_{\theta}}{\partial v}(\mathbf{x}, \theta, v) = \frac{\partial}{\partial v} \mathcal{G}^3_{-\varepsilon v}(\mathbf{x}, \theta). \tag{2.3.74}$$

Hence, since $\boldsymbol{\Upsilon}_{y_1}(\mathbf{x}, \theta, 0) = x_1$, $\boldsymbol{\Upsilon}_{y_2}(\mathbf{x}, \theta, 0) = x_2$ and $\boldsymbol{\Upsilon}_{\theta}(\mathbf{x}, \theta, 0) = \theta$ we obtain that

$$\left(\boldsymbol{\Upsilon}_{y_1}(\mathbf{x}, \theta, v), \boldsymbol{\Upsilon}_{y_2}(\mathbf{x}, \theta, v), \boldsymbol{\Upsilon}_{\theta}(\mathbf{x}, \theta, v)\right) = \mathcal{G}_{-\varepsilon v}(\mathbf{x}, \theta). \tag{2.3.75}$$

From this, it is clear that $(\mathbf{y}, \theta, v)$ makes a coordinate system and that the reciprocal change of coordinates is given by $(\mathbf{x}, \theta, v) = (\mathcal{G}_{\varepsilon v}(\mathbf{y}, \theta), v)$.

In order to show that $(\mathbf{y}, \theta, k)$ makes also a coordinate system we will proceed as follows : we will express $\boldsymbol{\Upsilon}_k$ in the $(\mathbf{y}, \theta, v)$-coordinate system and using this expression, we will express v in terms of $\mathbf{y}$ and θ and the yielding expression of $\boldsymbol{\Upsilon}_k$ in the $(\mathbf{y}, \theta, v)$-coordinate system.

Lemma 2.3.12. *The representative of $\boldsymbol{\Upsilon}_k$ in the $(\mathbf{y}, \theta, v)$-coordinate system is given by*

$$\tilde{\boldsymbol{\Upsilon}}_k(\mathbf{y}, \theta, v) = \int_0^v \frac{u}{B\left(\mathcal{G}^1_{\varepsilon u}(\mathbf{y}, \theta), \mathcal{G}^2_{\varepsilon u}(\mathbf{y}, \theta)\right)} du. \tag{2.3.76}$$

Proof. Using function φ involved in the expression of $\boldsymbol{\Upsilon}_k$ (see (2.3.59) and (2.3.56)), we obtain :

$$\begin{aligned} \boldsymbol{\Upsilon}_k(\mathbf{x}, \theta, v) &= \int_0^v \left(\int_0^s \varphi(\mathbf{x}, \theta, u)\, du \right) ds \\ &= \int_0^v \left(\int_u^v \varphi(\mathbf{x}, \theta, u)\, ds \right) du \\ &= \int_0^v (v - u)\, \varphi(\mathbf{x}, \theta, u)\, du. \end{aligned} \tag{2.3.77}$$

Now, using expressions (2.3.39) of φ and (2.3.75) of $(\boldsymbol{\Upsilon}_{y_1}, \boldsymbol{\Upsilon}_{y_2}, \boldsymbol{\Upsilon}_{\theta})$, we obtain

$$\begin{aligned} \boldsymbol{\Upsilon}_k(\mathbf{x}, \theta, v) &= \int_0^v \frac{(v - u)}{B\left(\mathcal{G}^1_{-\varepsilon u}(\mathbf{x}, \theta), \mathcal{G}^2_{-\varepsilon u}(\mathbf{x}, \theta)\right)} du \\ &= \int_0^v \frac{(v - u)}{B\left(\mathcal{G}^1_{\varepsilon(v-u)}\left(\mathcal{G}_{-\varepsilon v}(\mathbf{x}, \theta)\right), \mathcal{G}^2_{\varepsilon(v-u)}\left(\mathcal{G}_{-\varepsilon v}(\mathbf{x}, \theta)\right)\right)} du \\ &= \int_0^v (v - u)\, \varphi(\mathcal{G}_{-\varepsilon v}(\mathbf{x}, \theta), u - v)\, du, \\ &= \int_0^v u \varphi\left(\boldsymbol{\Upsilon}_{y_1}(\mathbf{x}, \theta, v), \boldsymbol{\Upsilon}_{y_2}(\mathbf{x}, \theta, v), \boldsymbol{\Upsilon}_{\theta}(\mathbf{x}, \theta, v), -u\right) du, \end{aligned} \tag{2.3.78}$$

implying (2.3.76) and consequently proving the lemma. □

Having expression (2.3.76) of $\tilde{\boldsymbol{\Upsilon}}_k$ on hand, for all $(\mathbf{y},\theta)\in\mathbb{R}^3$ we can define the parametrized smooth function $\eta=[\eta(\mathbf{y},\theta)]$ of v by

$$[\eta(\mathbf{y},\theta)](v)=\tilde{\boldsymbol{\Upsilon}}_k(\mathbf{y},\theta,v). \tag{2.3.79}$$

Lemma 2.3.13. *For any $(\mathbf{y},\theta)\in\mathbb{R}^2\times\mathbb{R}$, function $[\eta(\mathbf{y},\theta)]$ is a $\mathcal{C}^\infty$-diffeomorphism from $(0,+\infty)$ onto itself and function $\tilde{\eta}=\tilde{\eta}(\mathbf{y},\theta,k)$ defined by :*

$$\tilde{\eta}(\mathbf{y},\theta,k)=[\eta(\mathbf{y},\theta)]^{-1}(k) \tag{2.3.80}$$

which gives the expression of v, is $\mathcal{C}^\infty_{\#}(\mathbb{R}^2\times\mathbb{R}\times(0,+\infty))$.

Proof. As

$$\left[\frac{d[\eta(\mathbf{y},\theta)]}{dv}\right](v)=\frac{v}{B(\mathcal{G}^1_{\varepsilon v}(\mathbf{y},\theta),\mathcal{G}^2_{\varepsilon v}(\mathbf{y},\theta))}>0,$$

$[\eta(\mathbf{y},\theta)]$ is a $\mathcal{C}^\infty$-diffeomorphism from $(0,+\infty)$ onto

$$\left(\lim_{v\to 0}[\eta(\mathbf{y},\theta)](v),\lim_{v\to+\infty}[\eta(\mathbf{y},\theta)](v)\right) \tag{2.3.81}$$

for all $(\mathbf{y},\theta)$. Moreover, according to formula (2.3.76) we have for any $v>0$ the following estimates :

$$\frac{v^2}{2\|B\|_\infty}\leq[\eta(\mathbf{y},\theta)](v)\leq\frac{v^2}{2}, \tag{2.3.82}$$

and consequently for any $(\mathbf{y},\theta)\in\mathbb{R}^3$

$$[\eta(\mathbf{y},\theta)]((0,+\infty))=(0,+\infty). \tag{2.3.83}$$

Particularly, for any $v\in(0,+\infty)$ there exists $k\in(0,+\infty)$ such that

$$v=[\eta(\mathbf{y},\theta)]^{-1}(k). \tag{2.3.84}$$

The regularity of $\tilde{\eta}$ with respect to k is easily obtained from the fact that $[\eta(\mathbf{y},\theta)]$ is a $\mathcal{C}^\infty$-diffeomorphism. The $\mathcal{C}^\infty$-nature of $\tilde{\eta}$ with respect to $\mathbf{y}$ and θ is obtained by computing the successive derivatives of $[\eta(\mathbf{y},\theta)]\circ[\eta(\mathbf{y},\theta)]^{-1}=id$ and using the regularity of η that comes from the regularity of $\tilde{\boldsymbol{\Upsilon}}_k$ and then from the regularity of B and flow $\mathcal{G}_\lambda$. Moreover, the periodicity of $\tilde{\eta}$ with respect to θ comes from the fact that $\theta\mapsto\left(\mathcal{G}^1_\lambda(\mathbf{x},\theta),\mathcal{G}^2_\lambda(\mathbf{x},\theta)\right)$ is in $\mathcal{C}^\infty_{\mathrm{per}}(\mathbb{R})$ for any $\mathbf{x}\in\mathbb{R}^2$ as set out in Lemma 2.3.5. □

Hence we have proven the following theorem.

Theorem 2.3.14. *$(\mathbf{y},\theta,k)$ makes a coordinate system on $\mathbb{R}^2\times\mathbb{R}\times(0,+\infty)$ and function $\boldsymbol{\kappa}$ defined by* (2.3.3) *is given by*

$$\boldsymbol{\kappa}(\mathbf{y},\theta,k)=\left(\mathcal{G}_{\varepsilon\tilde{\eta}(\mathbf{y},\theta,k)}(\mathbf{y},\theta),\tilde{\eta}(\mathbf{y},\theta,k)\right), \tag{2.3.85}$$

where $\tilde{\eta}$ is defined by (2.3.80).

Now, we will focus on the ε-dependency of $\boldsymbol{\kappa}$. For this purpose, we will introduce the functions $\alpha = [\alpha(\mathbf{y},\theta)](v)$, which is defined for $v \in \mathbb{R}_+$, $\beta = [\beta(\mathbf{y},\theta,k)](\varepsilon)$, which is defined for $\varepsilon \in (0,+\infty)$, and $\gamma = [\gamma(\mathbf{y},\theta,k)](\varepsilon)$, which is defined for $\varepsilon \in \mathbb{R}_+$ by

$$[\alpha(\mathbf{y},\theta)](v) = \int_0^v \frac{s}{B(\mathcal{G}_s^1(\mathbf{y},\theta), \mathcal{G}_s^2(\mathbf{y},\theta))} ds, \tag{2.3.86}$$

$$[\beta(\mathbf{y},\theta,k)](\varepsilon) = [\alpha(\mathbf{y},\theta)]^{-1}(\varepsilon^2 k), \tag{2.3.87}$$

$$[\gamma(\mathbf{y},\theta,k)](\varepsilon) = \sqrt{\frac{[\alpha(\mathbf{y},\theta)](\varepsilon)}{k}}. \tag{2.3.88}$$

With their help, we can state the following lemma.

Lemma 2.3.15. *Function β defined by formula* (2.3.87) *admits a smooth continuation to $\mathbb{R}_+$ such that*

$$[\beta(\mathbf{y},\theta,k)](0) = 0, \tag{2.3.89}$$

Moreover, for any $\varepsilon > 0$ we have

$$[\beta(\mathbf{y},\theta,k)]'(\varepsilon) = \frac{1}{[\gamma(\mathbf{y},\theta,k)]'([\beta(\mathbf{y},\theta,k)](\varepsilon))}, \tag{2.3.90}$$

where γ is defined by (2.3.88).

Proof. By definition, function $\varepsilon \mapsto [\beta(\mathbf{y},\theta,k)](\varepsilon)$ is in $\mathcal{C}^\infty(\mathbb{R}_+^\star)$ for every $(\mathbf{y},\theta,k) \in \mathbb{R}^2 \times \mathbb{R} \times (0,+\infty)$. Moreover function γ is such that

$$\forall \varepsilon > 0,\ [\gamma(\mathbf{y},\theta,k)](\varepsilon) = [\beta(\mathbf{y},\theta,k)]^{-1}(\varepsilon). \tag{2.3.91}$$

Hence, in order to show that β admits a smooth continuation on $\mathbb{R}_+$ we just have to show that γ admits a smooth inverse function in the neighborhood of 0 in $\mathbb{R}_+$. And yet, for all $\varepsilon \geq 0$, we have

$$[\gamma(\mathbf{y},\theta,k)](\varepsilon) = \varepsilon \sqrt{\frac{1}{k}\int_0^1 \frac{u}{B(\mathcal{G}_{\varepsilon u}^1(\mathbf{y},\theta), \mathcal{G}_{\varepsilon u}^2(\mathbf{y},\theta))} du}. \tag{2.3.92}$$

This function is in $\mathcal{C}^\infty(\mathbb{R}_+)$ and

$$\left[\frac{d\gamma(\mathbf{y},\theta,k)}{d\varepsilon}\right](0) = \frac{1}{\sqrt{2kB(\mathbf{y})}} \neq 0. \tag{2.3.93}$$

Hence, there exists a neighborhood I of 0 and a smooth function $\delta = [\delta(\mathbf{y},\theta,k)](\varepsilon)$ defined on $J = [\gamma(\mathbf{y},\theta,k)](I \cap \mathbb{R}_+)$ such that $[\gamma(\mathbf{y},\theta,k)] \circ [\delta(\mathbf{y},\theta,k)] = id$. Hence we have shown that the smooth function β defined on $\mathbb{R}_+^\star$ admits a smooth continuation to $\mathbb{R}_+$. Then, since (2.3.90) follows directly (2.3.91), Lemma 2.3.15 is proven □

Lemma 2.3.16. *Function*

$$(\mathbf{y},\theta,k,\varepsilon) \mapsto [\beta(\mathbf{y},\theta,k)](\varepsilon) \tag{2.3.94}$$

is in $\mathcal{C}^\infty_{\#,3}\big(\mathbb{R}^2 \times \mathbb{R} \times (0,+\infty) \times \mathbb{R}_+\big)$ (see (2.3.30) *for the definition of this space).*

The proof of the periodicity with respect to the third variable is similar to the one of Lemma 2.3.13.

We will now use Lemmas 2.3.15 and 2.3.16 to deduce an expression of the expansion with respect to ε of the v-component of $\boldsymbol{\kappa} = \boldsymbol{\Upsilon}^{-1}$.

Lemma 2.3.17. *For any $n \in \mathbb{N}^\star$, there exists $P_n \in \mathbb{R}_{n-1}[X_1, \ldots, X_n]$ (where $\mathbb{R}_{n-1}[X_1, \ldots, X_n]$ stands for the space of the homogeneous polynomial of degree $n-1$ in n variables) such that*

$$[\beta(\mathbf{y}, \theta, k)]^{(n)}(\varepsilon) = \frac{P_n\left([\gamma(\mathbf{y}, \theta, k)]^{(1)}(\beta(\varepsilon)), \ldots, [\gamma(\mathbf{y}, \theta, k)]^{(n)}(\beta(\varepsilon))\right)}{\left([\gamma(\mathbf{y}, \theta, k)]^{(1)}(\beta(\varepsilon))\right)^{2n-1}}. \tag{2.3.95}$$

Proof. For $n = 1$ it is just formula (2.3.90). For $n \geq 2$, we will prove formula (2.3.95) by induction.

Differentiating (2.3.90) we obtain

$$[\beta(\mathbf{y}, \theta, k)]^{(2)}(\varepsilon) = \frac{P_2\left([\gamma(\mathbf{y}, \theta, k)]^{(1)}(\beta(\varepsilon)), [\gamma(\mathbf{y}, \theta, k)]^{(2)}(\beta(\varepsilon))\right)}{\left([\gamma(\mathbf{y}, \theta, k)]^{(1)}(\beta(\varepsilon))\right)^{3}}, \tag{2.3.96}$$

where $P_2(X_1, X_2) = -X_2$.

Now, assume that formula (2.3.95) is true for some given $n \geq 2$. Differentiating (2.3.95) yields :

$$[\beta(\mathbf{y}, \theta, k)]^{(n+1)}(\varepsilon) = \frac{P_{n+1}\left([\gamma(\mathbf{y}, \theta, k)]^{(1)}(\beta(\varepsilon)), \ldots, [\gamma(\mathbf{y}, \theta, k)]^{(n+1)}(\beta(\varepsilon))\right)}{\left([\gamma(\mathbf{y}, \theta, k)]^{(1)}(\beta(\varepsilon))\right)^{2n+1}},$$

where

$$P_{n+1}(X_1, \ldots, X_{n+1}) = -(2n-1) X_2 P_n(X_1, \ldots, X_n) + \sum_{k=1}^{n} X_1 X_{k+1} \frac{\partial P_n}{\partial X_k}(X_1, \ldots, X_n).$$

This ends the proof of Lemma 2.3.17. □

Lemma 2.3.18. *For any $l \in \mathbb{N}^\star$, there exists $a_l \in \mathcal{O}^\infty_{T,b}$ such that*

$$[\beta(\mathbf{y}, \theta, k)]^{(l)}(0) = \sqrt{k}^{\,l} a_l(\mathbf{y}, \theta). \tag{2.3.97}$$

Here and hereafter, $\mathcal{O}^\infty_{T,b}$ stands of the algebra of functions spanned by the functions of the form

$$(\mathbf{y}, \theta) \mapsto f_1(\mathbf{y}) \cos(\theta) + f_2(\mathbf{y}) \sin(\theta), \tag{2.3.98}$$

where $f_1, f_2 \in \mathcal{C}^\infty_b(\mathbb{R}^2)$.

Proof. On the one hand, for any $(\mathbf{y},\theta,k)$ and for any $n\in\mathbb{N}$, $[\gamma(\mathbf{y},\theta,k)]$ admits a Taylor-MacLaurin expansion of order n.

$$[\gamma(\mathbf{y},\theta,k)](\varepsilon)=[\gamma(\mathbf{y},\theta,k)](0)+\varepsilon[\gamma(\mathbf{y},\theta,k)]^{(1)}(0)+\ldots+\frac{\varepsilon^n}{n!}[\gamma(\mathbf{y},\theta,k)]^{(n)}(0)+\int_0^{\varepsilon}\frac{[\gamma(\mathbf{y},\theta,k)]^{(n+1)}(t)}{n!}(t-\varepsilon)^n\,dt. \tag{2.3.99}$$

On the other hand, applying formula (2.3.54) with $\frac{1}{B}$, multiplying by λ and integrating between 0 and ε yields :

$$[\alpha(\mathbf{y},\theta)](\varepsilon)=\varepsilon^2\Big(\sum_{l=0}^{n}\frac{\varepsilon^l}{(l+2)\,l!}\left(\mathbf{\Lambda}^l\cdot\frac{1}{B}\right)(\mathbf{y},\theta)+\frac{\varepsilon^{n+1}}{(n+1)!}\int_0^1(1-u)^{n+1}(n+1+u)\left(\mathbf{\Lambda}^{n+1}\cdot\frac{1}{B}\right)\circ\mathcal{G}_{\varepsilon u}du\Big). \tag{2.3.100}$$

Injecting formula (2.3.100) in (2.3.88) yields :

$$[\gamma(\mathbf{y},\theta,k)](\varepsilon)=\frac{\varepsilon}{\sqrt{k}}\sqrt{\left(\sum_{l=0}^{n}\frac{\varepsilon^l}{(l+2)\,l!}\left(\mathbf{\Lambda}^l\cdot\frac{1}{B}\right)(\mathbf{y},\theta)+\frac{\varepsilon^{n+1}}{(n+1)!}\int_0^1(1-u)^{n+1}(n+1+u)\left(\mathbf{\Lambda}^{n+1}\cdot\frac{1}{B}\right)\circ\mathcal{G}_{\varepsilon u}du\right)}. \tag{2.3.101}$$

Expanding formula (2.3.101) with respect to ε, up to order n, by using the usual expansion of $s\mapsto\sqrt{1+s}$, and identifying with formula (2.3.99) yields that for any $l\in\{0,\ldots,n\}$, $\sqrt{k}\,[\gamma(\mathbf{y},\theta,k)]^{(l)}(0)\in\mathcal{O}_{T,b}^{\infty}$.

Finally, using formula (2.3.95) we obtain formula (2.3.97). This ends the proof of Lemma 2.3.18. □

Theorem 2.3.19. *The v-component $\boldsymbol{\kappa}_v$ of $\boldsymbol{\kappa}=\mathbf{\Upsilon}^{-1}$ admits the following expansion in power of ε :*

$$\boldsymbol{\kappa}_v(\mathbf{y},\theta,k)=\sum_{i=0}^{n}\sqrt{k}^{i+1}a_{i+1}(\mathbf{y},\theta)\frac{\varepsilon^i}{(i+1)!}+\frac{\varepsilon^{n+1}}{(n+1)!}\int_0^1(1-u)^{n+1}[\beta(\mathbf{y},\theta,k)]^{(n+2)}(\varepsilon u)\,du, \tag{2.3.102}$$

where the terms a_i of the expansion are defined in Lemma 2.3.18 and are easily obtained by using formulas (2.3.89) *and* (2.3.90)*. Moreover,*

$$(\mathbf{y},\theta,k,\varepsilon)\mapsto\int_0^1(1-u)^{n+1}[\beta(\mathbf{y},\theta,k)]^{(n+2)}(\varepsilon u)\,du\in\mathcal{C}^{\infty}_{\#,3}(\mathbb{R}^2\times\mathbb{R}\times(0,+\infty)\times\mathbb{R}_+), \tag{2.3.103}$$

(see (2.3.30) *for the definition of this space).*

Proof. We just have to notice that, because of expression (2.3.78) of $\mathbf{\Upsilon}_k$, or more precisey of expression (2.3.76) of $\tilde{\mathbf{\Upsilon}}_k$ and of (2.3.86), we have

$$\tilde{\mathbf{\Upsilon}}_k(\mathbf{y},\theta,v)=\frac{1}{\varepsilon^2}[\alpha(\mathbf{y},\theta)](\varepsilon v)\ \text{ or }\ \varepsilon v=[\alpha(\mathbf{y},\theta)]^{-1}(\varepsilon^2\tilde{\mathbf{\Upsilon}}_k(\mathbf{y},\theta,v)), \tag{2.3.104}$$

and consequently, in view of (2.3.87), function $\boldsymbol{\kappa}_v$ expresses as

$$\forall \varepsilon > 0,\ \boldsymbol{\kappa}_v(\mathbf{y},\theta,k) = \frac{1}{\varepsilon}\left[\beta(\mathbf{y},\theta,k)\right](\varepsilon). \tag{2.3.105}$$

Hence equality (2.3.102) follows directly from a Taylor expansion and using (2.3.97) and (2.3.89).
Property (2.3.103) is a direct consequence of the regularity of function β. Hence, the theorem is proven. □

Applying Theorem 2.3.19, up to order 2, we obtain

$$\begin{aligned}\boldsymbol{\kappa}_v(\mathbf{y},\theta,k) = &\sqrt{2kB(\mathbf{y})} + \varepsilon\frac{2kB(\mathbf{y})}{3}\hat{\mathbf{a}}(\theta)\cdot\nabla_{\mathbf{x}}B(\mathbf{y})\\ &-\varepsilon^2 k\sqrt{\frac{kB(\mathbf{y})}{2}}\left[\frac{7}{18B(\mathbf{y})^3}\left(\hat{\mathbf{a}}(\theta)\cdot\nabla_{\mathbf{x}}B(\mathbf{y})\right)^2 - \frac{\hat{\mathbf{a}}(\theta)^T\mathcal{H}_B(\mathbf{y})\hat{\mathbf{a}}(\theta)}{2B(\mathbf{y})^2}\right] +\\ &\frac{\varepsilon^3}{3!}\int_0^1 (1-u)^3\left[\beta(\mathbf{y},\theta,k)\right]^{(4)}(\varepsilon u)\,du\end{aligned} \tag{2.3.106}$$

where $\hat{\mathbf{a}} = \hat{\mathbf{a}}(\theta)$, already used in the introduction, is defined by

$$\hat{\mathbf{a}}(\theta) = \begin{pmatrix}\cos(\theta)\\ -\sin(\theta)\end{pmatrix} \tag{2.3.107}$$

and where $\mathcal{H}_B$ is the Hessian Matrix of B.

2.3.7 Expression of the Poisson Matrix

We have solved Equations (2.3.5) and (2.3.7)–(2.3.10) and obtained the change-of-coordinates mapping $\boldsymbol{\Upsilon}$. Furthermore, by construction, from formula (2.1.50), we know all the Poisson Matrix entries, except its entry number $(1,2)$: $\{\boldsymbol{\Upsilon}_{y_1},\boldsymbol{\Upsilon}_{y_2}\}_{\mathbf{x},\theta,v}(\boldsymbol{\kappa}(\mathbf{y},\theta,k))$. Its expression is given by the following theorem.

Theorem 2.3.20. *The Poisson Bracket between the two first components $\boldsymbol{\Upsilon}_{y_1}$ and $\boldsymbol{\Upsilon}_{y_2}$ of mapping $\boldsymbol{\Upsilon}$ is given by*

$$\{\boldsymbol{\Upsilon}_{y_1},\boldsymbol{\Upsilon}_{y_2}\}_{\mathbf{x},\theta,v}(\mathbf{x},\theta,v) = -\frac{\varepsilon}{B\left(\boldsymbol{\Upsilon}_{y_1}(\mathbf{x},\theta,v),\boldsymbol{\Upsilon}_{y_2}(\mathbf{x},\theta,v)\right)}. \tag{2.3.108}$$

Proof. The proof consists in identifying the Poisson Bracket between $\boldsymbol{\Upsilon}_{y_1}$ and $\boldsymbol{\Upsilon}_{y_2}$ as the unique solution of the PDE of unknown u

$$-\varepsilon\boldsymbol{\Lambda}^1\cdot u - \frac{\partial u}{\partial v} = 0, \tag{2.3.109}$$

$$u(\mathbf{x},\theta,0) = \frac{-\varepsilon}{B(\mathbf{x})}. \tag{2.3.110}$$

In a first place, as function φ defined by (2.3.39) is the unique solution of (2.3.36)–(2.3.37), the unique solution of (2.3.109)–(2.3.110) is given by

$$u(\mathbf{x},\theta,v) = -\varepsilon\varphi(\mathbf{x},\theta,v);$$

i.e. by (2.3.108).

On an another hand as for any $v \neq 0$, $\{\boldsymbol{\Upsilon}_\theta, \boldsymbol{\Upsilon}_{y_1}\}_{\mathbf{x},\theta,v} = 0$ and $\{\boldsymbol{\Upsilon}_{y_2}, \boldsymbol{\Upsilon}_\theta\}_{\mathbf{x},\theta,v} = 0$, the Jacobi identity ensures that

$$\forall v \neq 0,\ \{\{\boldsymbol{\Upsilon}_{y_1}, \boldsymbol{\Upsilon}_{y_2}\}, \boldsymbol{\Upsilon}_\theta\}_{\mathbf{x},\theta,v} = 0. \tag{2.3.111}$$

Hence, dividing (2.3.111) by $\omega_\varepsilon(\mathbf{x}, v)$, we obtain that for $v \neq 0$, $\{\boldsymbol{\Upsilon}_{y_1}, \boldsymbol{\Upsilon}_{y_2}\}$ is solution of (2.3.109). Using now the same method as when proving Theorem 2.3.10, we obtain

$$\{\boldsymbol{\Upsilon}_{y_1}, \boldsymbol{\Upsilon}_{y_2}\}_{\mathbf{x},\theta,v}(\mathbf{x}, \theta, v) = -\frac{\varepsilon}{B(\mathbf{x})} + v\epsilon_{y_1,y_2}(\mathbf{x}, \theta, v), \tag{2.3.112}$$

with $\epsilon_{y_1,y_2}(\mathbf{x}, \theta, v)$ such that for any $(\mathbf{x}, \theta)$, $v \mapsto \epsilon_{y_1,y_2}(\mathbf{x}, \theta, v)$ is bounded in the neighborhood of $v = 0$ and consequently that $\{\boldsymbol{\Upsilon}_{y_1}, \boldsymbol{\Upsilon}_{y_2}\}_{\mathbf{x},\theta,v}(\mathbf{x}, \theta, 0) = \frac{-\varepsilon}{B(\mathbf{x})}$.

As a conclusion, $\{\boldsymbol{\Upsilon}_{y_1}, \boldsymbol{\Upsilon}_{y_2}\}_{\mathbf{x},\theta,v} = u$, and u is given by (2.3.108). Hence the theorem is proven. □

Since the entries $\left(\bar{\mathcal{P}}_\varepsilon\right)_{i,j}$ of $\bar{\mathcal{P}}_\varepsilon$ are given by $\left(\bar{\mathcal{P}}_\varepsilon\right)_{i,j} = \{\boldsymbol{\Upsilon}_i, \boldsymbol{\Upsilon}_j\}$ and since we used the convention (2.3.6) we have enough information to state the following Corollary.

Corollary 2.3.21. *The Poisson Matrix in the Darboux Coordinate System is given by*

$$\bar{\mathcal{P}}_\varepsilon(\mathbf{y}, \theta, k) = \begin{pmatrix} 0 & -\frac{\varepsilon}{B(\mathbf{y})} & 0 & 0 \\ \frac{\varepsilon}{B(\mathbf{y})} & 0 & 0 & 0 \\ 0 & 0 & 0 & \frac{1}{\varepsilon} \\ 0 & 0 & -\frac{1}{\varepsilon} & 0 \end{pmatrix}. \tag{2.3.113}$$

2.3.8 Expression of the Hamiltonian in the Darboux Coordinate System

In the Darboux Coordinate System, the Hamiltonian is given by $\bar{H}_\varepsilon(\mathbf{y}, \theta, k) = \tilde{H}_\varepsilon\big(\boldsymbol{\kappa}(\mathbf{y}, \theta, k)\big)$. Since $\tilde{H}_\varepsilon(\mathbf{x}, \theta, v) = \frac{v^2}{2}$, we have

$$\bar{H}_\varepsilon(\mathbf{y}, \theta, k) = \frac{\boldsymbol{\kappa}_v^2(\mathbf{y}, \theta, k)}{2}. \tag{2.3.114}$$

Hence, according to Theorem 2.3.19, Hamiltonian function $\bar{H}_\varepsilon$ is regular with respect to ε on $\mathbb{R}_+$ and it admits an expansion in power of ε. More precisely, using expansion (2.3.102), we obtain the following corollaries.

Corollary 2.3.22. *The Hamiltonian function in the Darboux Coordinate System admits the following expansion in power of ε :*

$$\bar{H}_\varepsilon(\mathbf{y}, \theta, k) = \bar{H}_0(\mathbf{y}, k) + \sum_{n=1}^{N} \varepsilon^n \bar{H}_n(\mathbf{y}, \theta, k) + \varepsilon^{N+1} \iota_{N+1}(\varepsilon, \mathbf{y}, \theta, k), \tag{2.3.115}$$

where function ι_{N+1} is in $\mathcal{C}^\infty_{\#}(\mathbb{R}_+ \times \mathbb{R}^2 \times \mathbb{R} \times (0, +\infty))$. Moreover, for any $n \in \{1, \ldots, N\}$ there exists a function $b_n \in \mathcal{O}^\infty_{T,b}$ such that

$$\bar{H}_n(\mathbf{y}, \theta, k) = \sqrt{k}^{n+2} b_n(\mathbf{y}, \theta), \tag{2.3.116}$$

with $\mathcal{O}^\infty_{T,b}$ defined by (2.3.98).

Here and hereafter, $\mathcal{Q}^{\infty}_{T,b}$ stands of the space of functions

$$\mathcal{Q}^{\infty}_{T,b} = \left\{ f \in \mathcal{C}^{\infty}\left(\mathbb{R}^3 \times (0,+\infty)\right),\ f(\mathbf{y},\theta,k) = \sum_{n\in\mathbb{I}_f} c_n(\mathbf{y},\theta)\sqrt{k}^n \right. \\ \left. \text{where } \mathbb{I}_f \subset \mathbb{Z} \text{ is finite and } \forall n \in \mathbb{I}_f,\ c_n \in \mathcal{O}^{\infty}_{T,b} \right\}. \tag{2.3.117}$$

Corollary 2.3.23. *The Hamiltonian function in the Darboux Coordinate System admits, up to order two, the following expansion in power of ε :*

$$\begin{aligned} \bar{H}_{\varepsilon}(\mathbf{y},\theta,k) = {} & B(\mathbf{y})\,k + \varepsilon \frac{\hat{\mathbf{a}}(\theta)\cdot\nabla_{\mathbf{x}}B(\mathbf{y})}{3B(\mathbf{y})^2}\left(2B(\mathbf{y})\,k\right)^{\frac{3}{2}} + \\ & \varepsilon^2 \frac{\left(2B(\mathbf{y})\,k\right)^2}{24B(\mathbf{y})^2}\left[-\hat{\mathbf{a}}(\theta)\cdot\nabla_{\mathbf{x}}B(\mathbf{y}) + 3B(\mathbf{y})\,\hat{\mathbf{a}}(\theta)^T\mathcal{H}_B(\mathbf{y})\,\hat{\mathbf{a}}(\theta)\right] + \\ & \varepsilon^3 \iota_3(\mathbf{y},\theta,k,\varepsilon), \end{aligned} \tag{2.3.118}$$

where $\hat{\mathbf{a}}$ is defined by (2.3.107)*, function ι_3 is in $\mathcal{C}^{\infty}_{\#,3}(\mathbb{R}^2\times\mathbb{R}\times(0,+\infty)\times\mathbb{R}_+)$, and where $\mathcal{H}_B$ stands for the Hessian matrix associated with B.*

In expression (2.3.115), there is an important fact for the setting out of the to come Lie Transform based Method : the first term is independent of θ.

2.3.9 Characteristics in the Darboux Coordinate System

We denote by $(\mathbf{Y}^{\varepsilon}(t;\mathbf{y},\theta,k), \Theta^{\varepsilon}_{\mathfrak{Dar}}(t;\mathbf{y},\theta,k), \boldsymbol{\mathcal{K}}^{\varepsilon}_{\mathfrak{Dar}}(t;\mathbf{y},\theta,k))$ the characteristics expressed in the Darboux coordinate system. According to formula (2.2.15), these characteristics satisfy

$$\frac{\partial\begin{pmatrix}\mathbf{Y}^{\varepsilon}\\ \Theta^{\varepsilon}_{\mathfrak{Dar}}\\ \boldsymbol{\mathcal{K}}^{\varepsilon}_{\mathfrak{Dar}}\end{pmatrix}}{\partial t} = \bar{\mathcal{P}}_{\varepsilon}(\mathbf{Y}^{\varepsilon})\,\nabla\bar{H}_{\varepsilon}(\mathbf{Y}^{\varepsilon},\Theta^{\varepsilon}_{\mathfrak{Dar}},\boldsymbol{\mathcal{K}}^{\varepsilon}_{\mathfrak{Dar}}), \tag{2.3.119}$$

equipped with $(\mathbf{Y}^{\varepsilon}(0;\mathbf{y},\theta,k), \Theta^{\varepsilon}_{\mathfrak{Dar}}(0;\mathbf{y},\theta,k), \boldsymbol{\mathcal{K}}^{\varepsilon}_{\mathfrak{Dar}}(0;\mathbf{y},\theta,k)) = (\mathbf{y},\theta,k)$, where $\bar{\mathcal{P}}_{\varepsilon}$ is the Poisson matrix expressed in the Darboux coordinate system and given by formula (2.3.113), and $\bar{H}_{\varepsilon}$ is the Hamiltonian function expressed in the Darboux Coordinate System and given by (2.3.114). The characteristic expressed in the Darboux Coordinate System is related with the periodic extension of the characteristic expressed in the Polar in velocity Coordinate System (see Definition 2.2.1 and Lemma 2.2.2) by

$$Y^{\varepsilon}_1(t;\mathbf{y},\theta,k) = \boldsymbol{\Upsilon}_{y_1}\left(\mathbf{X}^{\varepsilon,\#}_{\mathfrak{Pol}}(t,\boldsymbol{\kappa}(\mathbf{y},\theta,k)), \Theta^{\varepsilon,\#}(t,\boldsymbol{\kappa}(\mathbf{y},\theta,k)), \mathcal{V}^{\varepsilon,\#}(t,\boldsymbol{\kappa}(\mathbf{y},\theta,k))\right), \tag{2.3.120}$$

$$Y^{\varepsilon}_2(t;\mathbf{y},\theta,k) = \boldsymbol{\Upsilon}_{y_2}\left(\mathbf{X}^{\varepsilon,\#}_{\mathfrak{Pol}}(t,\boldsymbol{\kappa}(\mathbf{y},\theta,k)), \Theta^{\varepsilon,\#}(t,\boldsymbol{\kappa}(\mathbf{y},\theta,k)), \mathcal{V}^{\varepsilon,\#}(t,\boldsymbol{\kappa}(\mathbf{y},\theta,k))\right), \tag{2.3.121}$$

$$\Theta^{\varepsilon}_{\mathfrak{Dar}}(t;\mathbf{y},\theta,k) = \Theta^{\varepsilon,\#}(t,\boldsymbol{\kappa}(\mathbf{y},\theta,k)), \tag{2.3.122}$$

$$\boldsymbol{\mathcal{K}}^{\varepsilon}_{\mathfrak{Dar}}(t;\mathbf{y},\theta,k) = \boldsymbol{\Upsilon}_{k}\left(\mathbf{X}^{\varepsilon,\#}_{\mathfrak{Pol}}(t,\boldsymbol{\kappa}(\mathbf{y},\theta,k)), \Theta^{\varepsilon,\#}(t,\boldsymbol{\kappa}(\mathbf{y},\theta,k)), \mathcal{V}^{\varepsilon,\#}(t,\boldsymbol{\kappa}(\mathbf{y},\theta,k))\right). \tag{2.3.123}$$

The purpose of this subsection is the two following theorems :

Theorem 2.3.24. *Let $[a,b]$ be an interval such that $[a,b] \subset (0,+\infty)$. Then, for any $(\mathbf{y},\theta) \in \mathbb{R}^3$ and for any $v \in [a,b]$, $\boldsymbol{\Upsilon}_k(\mathbf{x},\theta,v) \in \left[\frac{a^2}{2\|B\|_\infty}, \frac{b^2}{2}\right]$. And, for any $(\mathbf{y},\theta,k) \in \boldsymbol{\Upsilon}\left(\mathbb{R}^3 \times [a,b]\right)$, for any $\varepsilon \in (0,+\infty)$, and for any $t \in \mathbb{R}$, $\boldsymbol{\mathcal{K}}^{\varepsilon}_{\mathfrak{Dar}}(t;\mathbf{y},\theta,k) \in \left[\frac{a^2}{2\|B\|_\infty}, \frac{b^2}{2}\right]$.*

Theorem 2.3.25. *Let $[a,b]$ be an interval such that $[a,b] \subset (0,+\infty)$, $\mathbf{x}_0 \in \mathbb{R}^2$, and $R_{\mathbf{x}_0}$ and $R'_{\mathbf{x}_0}$ be two real numbers satisfying $0 < R_{\mathbf{x}_0} < R'_{\mathbf{x}_0}$. Then, for any $\varepsilon \in \left(-\frac{R'_{\mathbf{x}_0}-R_{\mathbf{x}_0}}{b}, \frac{R'_{\mathbf{x}_0}-R_{\mathbf{x}_0}}{b}\right)$,*

$$\boldsymbol{\Upsilon}\left(\overline{\mathfrak{b}^2(\mathbf{x}_0,R_{\mathbf{x}_0})} \times \mathbb{R} \times [a,b]\right) \subset \mathfrak{b}^2\big(\mathbf{x}_0,R'_{\mathbf{x}_0}\big) \times \mathbb{R} \times \left[\frac{a^2}{2\|B\|_\infty}, \frac{b^2}{2}\right]. \tag{2.3.124}$$

Moreover, there exists two positive real numbers α_0 and η, such that for any $\varepsilon \in (0,\eta)$, there exists a real number $t^{\varepsilon}_e > \frac{\alpha_0}{\varepsilon}$, such that for any $t \in (-t^{\varepsilon}_e, t^{\varepsilon}_e)$ and for any $(\mathbf{y},\theta,k) \in \boldsymbol{\Upsilon}\left(\overline{\mathfrak{b}^2(\mathbf{x}_0,R_{\mathbf{x}_0})} \times \mathbb{R} \times [a,b]\right)$,

$$\mathbf{Y}^{\varepsilon}(t;\mathbf{y},\theta,k) \in \mathfrak{b}^2\big(\mathbf{x}_0,R'_{\mathbf{x}_0}\big). \tag{2.3.125}$$

We will prove Theorems 2.3.24 and 2.3.25 in subsection 2.3.10.

2.3.10 Proof of Theorems 2.3.24 and 2.3.25

By definition $\boldsymbol{\Upsilon}_k(\mathbf{x},\theta,v) = \int_0^v \psi(\mathbf{x},\theta,s)\,ds$, and $\psi(\mathbf{x},\theta,s) = \int_0^s \varphi(\mathbf{x},\theta,u)\,du$ where ψ is defined by (2.3.56) and where φ is given by Theorem 2.3.7. Hence,

$$\psi(\mathbf{x},\theta,s) = \int_0^s \varphi(\mathbf{x},\theta,u)\,du = \int_0^s \frac{1}{B\left(\mathcal{G}^1_{-\varepsilon u}(\mathbf{x},\theta),\mathcal{G}^2_{-\varepsilon u}(\mathbf{x},\theta)\right)}du \geq \frac{s}{\|B\|_\infty}, \tag{2.3.126}$$

and consequently, for any $v \in [a,b]$ and for any $(\mathbf{x},\theta) \in \mathbb{R}^2 \times \mathbb{R}$, we obtain

$$\boldsymbol{\Upsilon}_k(\mathbf{x},\theta,v) = \int_0^v \psi(\mathbf{x},\theta,s)\,ds \geq \frac{v^2}{2\|B\|_\infty} \geq \frac{a^2}{2\|B\|_\infty}. \tag{2.3.127}$$

On another hand, since $\inf\limits_{\mathbf{x}\in\mathbb{R}^2} B(\mathbf{x}) \geq 1$, we obtain $\psi(\mathbf{x},\theta,s) \leq s$, and consequently for any $v \in [a,b]$ and for any $(\mathbf{x},\theta)$, we obtain

$$\boldsymbol{\Upsilon}_k(\mathbf{x},\theta,v) \leq \frac{v^2}{2} \leq \frac{b^2}{2}. \tag{2.3.128}$$

According to Lemma 2.2.2 and formula (2.2.30), for any $(\mathbf{x},\theta,v) \in \mathbb{R}^2\times\mathbb{R}\times(0,+\infty)$ and for any $t \in \mathbb{R}$, $\mathcal{V}^{\varepsilon,\#}(t;\mathbf{x},\theta,v) = v$, and consequently for any $(\mathbf{y},\theta,k) \in \mathbb{R}^2 \times \mathbb{R} \times (0,+\infty)$ and for any $t \in \mathbb{R}$, formula (2.3.123) can be rewritten :

$$\boldsymbol{\mathcal{K}}^{\varepsilon}_{\mathfrak{Dar}}(t;\mathbf{y},\theta,k) = \boldsymbol{\Upsilon}_k\left(\mathbf{X}^{\varepsilon,\#}_{\mathfrak{Pol}}(t,\boldsymbol{\kappa}(\mathbf{y},\theta,k)),\Theta^{\varepsilon,\#}(t,\boldsymbol{\kappa}(\mathbf{y},\theta,k)),\boldsymbol{\kappa}_v(\mathbf{y},\theta,k)\right). \tag{2.3.129}$$

Now, for any $(\mathbf{y},\theta,k) \in \boldsymbol{\Upsilon}\left(\mathbb{R}^2 \times \mathbb{R} \times [a,b]\right)$, $\boldsymbol{\kappa}_v(\mathbf{y},\theta,k) \in [a,b]$ and estimates (2.3.127) and (2.3.128) yield that $\boldsymbol{\mathcal{K}}^{\varepsilon}_{\mathfrak{Dar}}(t;\mathbf{y},\theta,k) \in \left[\frac{a^2}{2\|B\|_\infty}, \frac{b^2}{2}\right]$. This ends the proof of Theorem 2.3.24. □

Concerning Theorem 2.3.25, firstly, for any $(\mathbf{x},\theta)\in\mathbb{R}^2\times\mathbb{R}$ and for any $v\in[a,b]$, function ψ satisfies $|\psi(\mathbf{x},\theta,v)|\leq b$. Consequently, for any $(\mathbf{x},\theta,v)\in\overline{\mathfrak{b}^2(\mathbf{x}_0,R_{\mathbf{x}_0})}\times\mathbb{R}\times[a,b]$ and for any $\varepsilon\in\mathbb{R}$ we have :

$$|(\boldsymbol{\Upsilon}_{y_1}(\mathbf{x},\theta,v),\boldsymbol{\Upsilon}_{y_2}(\mathbf{x},\theta,v))-\mathbf{x}_0|\leq R_{\mathbf{x}_0}+|\varepsilon|\,b. \tag{2.3.130}$$

Eventually, since for any $\varepsilon\in\mathbb{R}$, $\boldsymbol{\Upsilon}_k$ satisfies (2.3.127) and (2.3.128), and since $(\boldsymbol{\Upsilon}_{y_1},\boldsymbol{\Upsilon}_{y_2})$ satisfies (2.3.130), we obtain (2.3.124).

Applying formula (2.3.62) with $n=1$ yields :

$$\boldsymbol{\Upsilon}_{y_1}(\mathbf{x},\theta,v)=\boldsymbol{\Upsilon}^s_{y_1}(\mathbf{x},\theta,v)+\boldsymbol{\Upsilon}^b_{y_1}(\mathbf{x},\theta,v), \tag{2.3.131}$$

where

$$\begin{aligned}&\boldsymbol{\Upsilon}^s_{y_1}(\mathbf{x},\theta,v)=x_1-\varepsilon v\frac{\cos(\theta)}{B(\mathbf{x})},\\&\boldsymbol{\Upsilon}^b_{y_1}(\mathbf{x},\theta,v)=-\varepsilon^2\cos(\theta)\int_0^v(v-u)\left(\boldsymbol{\Lambda}\cdot\frac{1}{B}\right)(\mathcal{G}_{-\varepsilon u}(\mathbf{x},\theta))\,du.\end{aligned} \tag{2.3.132}$$

For any $(\mathbf{x},\theta)\in\mathbb{R}^2\times\mathbb{R}$, for any $v\in[a,b]$ and for any $\varepsilon\in\mathbb{R}$ we have :

$$\left|\boldsymbol{\Upsilon}^b_{y_1}(\mathbf{x},\theta,v)\right|\leq\frac{\varepsilon^2b^2}{2}\left\|\boldsymbol{\Lambda}\cdot\frac{1}{B}\right\|_\infty, \tag{2.3.133}$$

and consequently for any $(\mathbf{x},\theta)\in\mathbb{R}^2\times\mathbb{R}$, for any $v\in[a,b]$, for any $\varepsilon\in\mathbb{R}^\star$ and for any $t\in\mathbb{R}$

$$\left|\boldsymbol{\Upsilon}^b_{y_1}\left(\mathbf{X}^{\varepsilon,\#}_{\mathfrak{Pol}}(t,\mathbf{x},\theta,v),\Theta^{\varepsilon,\#}(t,\mathbf{x},\theta,v),v\right)\right|\leq\frac{\varepsilon^2b^2}{2}\left\|\boldsymbol{\Lambda}\cdot\frac{1}{B}\right\|_\infty. \tag{2.3.134}$$

On another hand, evaluating $\boldsymbol{\Upsilon}^s_{y_1}$ in $\left(\mathbf{X}^{\varepsilon,\#}_{\mathfrak{Pol}}(t,\mathbf{x},\theta,v),\Theta^{\varepsilon,\#}(t,\mathbf{x},\theta,v),v\right)$ and differentiating with respect to t yields :

$$\frac{\partial}{\partial t}\left(\boldsymbol{\Upsilon}^s_{y_1}\left(\mathbf{X}^{\varepsilon,\#}_{\mathfrak{Pol}},\Theta^{\varepsilon,\#},v\right)\right)=\varepsilon v^2\cos\left(\Theta^{\varepsilon,\#}\right)\frac{\hat{\mathbf{c}}\left(\Theta^{\varepsilon,\#}\right)\cdot\nabla_{\mathbf{x}}B\left(\mathbf{X}^{\varepsilon,\#}_{\mathfrak{Pol}}\right)}{B\left(\mathbf{X}^{\varepsilon,\#}_{\mathfrak{Pol}}\right)^2}, \tag{2.3.135}$$

where

$$\hat{\mathbf{c}}(\theta)=\begin{pmatrix}-\sin(\theta)\\-\cos(\theta)\end{pmatrix}, \tag{2.3.136}$$

was already used in the introduction, and consequently

$$\left|\frac{\partial}{\partial t}\left(\boldsymbol{\Upsilon}^s_{y_1}\left(\mathbf{X}^{\varepsilon,\#}_{\mathfrak{Pol}},\Theta^{\varepsilon,\#},v\right)\right)\right|\leq|\varepsilon|\,b^2\sup_{(\mathbf{x},\theta)\in\mathbb{R}^3}\left|\frac{\hat{\mathbf{c}}(\theta)\cdot\nabla_{\mathbf{x}}B(\mathbf{x})}{B(\mathbf{x})^2}\right|. \tag{2.3.137}$$

Combining estimates (2.3.133), (2.3.134) and (2.3.137) yields that for any $(\mathbf{x},\theta)\in\mathbb{R}^2\times\mathbb{R}$, for any $v\in[a,b]$, for any $\varepsilon\in\mathbb{R}^\star$ and for any $t\in\mathbb{R}$

$$\begin{aligned}&\left|\boldsymbol{\Upsilon}_{y_1}\left(\mathbf{X}^{\varepsilon,\#}_{\mathfrak{Pol}}(t,\mathbf{x},\theta,v),\Theta^{\varepsilon,\#}(t,\mathbf{x},\theta,v),v\right)-\boldsymbol{\Upsilon}_{y_1}(\mathbf{x},\theta,v)\right|\\&\qquad\leq|t|\,|\varepsilon|\,b^2\sup_{(\mathbf{x},\theta)\in\mathbb{R}^3}\left|\frac{\hat{\mathbf{c}}(\theta)\cdot\nabla_{\mathbf{x}}B(\mathbf{x})}{B(\mathbf{x})^2}\right|+\varepsilon^2b^2\left\|\boldsymbol{\Lambda}\cdot\frac{1}{B}\right\|_\infty.\end{aligned} \tag{2.3.138}$$

The same estimate holds true by replacing $\boldsymbol{\Upsilon}_{y_1}$ by $\boldsymbol{\Upsilon}_{y_2}$.

Using estimates (2.3.138) and (2.3.130), we obtain for any $(\mathbf{x},\theta,v) \in \overline{\mathfrak{b}^2(\mathbf{x}_0, R_{\mathbf{x}_0})} \times \mathbb{R} \times [a,b]$, for any $t \in \mathbb{R}$ and for any $\varepsilon \in \mathbb{R}^\star$

$$\left|\left(\boldsymbol{\Upsilon}_{y_1}\left(\mathbf{X}^{\varepsilon,\#}_{\mathfrak{Pol}}(t,\mathbf{x},\theta,v),\Theta^{\varepsilon,\#}(t,\mathbf{x},\theta,v),v\right),\boldsymbol{\Upsilon}_{y_2}\left(\mathbf{X}^{\varepsilon,\#}_{\mathfrak{Pol}}(t,\mathbf{x},\theta,v),\Theta^{\varepsilon,\#}(t,\mathbf{x},\theta,v),v\right)\right)-\mathbf{x}_0\right|$$
$$\leq \sqrt{2}\left(|t|\,|\varepsilon|\,b^2\alpha_1+\varepsilon^2 b^2\alpha_2\right)+\left(R_{\mathbf{x}_0}+|\varepsilon|\,b\right),$$

where $\alpha_1 = \sup_{(\mathbf{x},\theta)\in\mathbb{R}^3}\left|\frac{\hat{\mathbf{c}}(\theta)\cdot\nabla_{\mathbf{x}}B(\mathbf{x})}{B(\mathbf{x})^2}\right|$ and $\alpha_2 = \left\|\boldsymbol{\Lambda}\cdot\frac{1}{B}\right\|_\infty$. The right hand side of the above estimate is smaller than $R'_{\mathbf{x}_0}$ if and only if t satisfies

$$|t| < \frac{R'_{\mathbf{x}_0}-R_{\mathbf{x}_0}}{\sqrt{2}\,|\varepsilon|\,b^2\alpha_1} - \frac{1}{\sqrt{2}b\alpha_1} - |\varepsilon|\,\frac{\alpha_2}{\alpha_1}. \tag{2.3.139}$$

Let $\eta \in (0,+\infty)$ be such that

$$\frac{R'_{\mathbf{x}_0}-R_{\mathbf{x}_0}}{\sqrt{2}b^2\alpha_1} - \frac{\eta}{\sqrt{2}b\alpha_1} - \eta^2\frac{\alpha_2}{\alpha_1} > 0. \tag{2.3.140}$$

Hence, setting

$$\alpha_0 = \frac{R'_{\mathbf{x}_0}-R_{\mathbf{x}_0}}{\sqrt{2}b^2\alpha_1} - \frac{\eta}{\sqrt{2}b\alpha_1} - \eta^2\frac{\alpha_2}{\alpha_1} \tag{2.3.141}$$

yields that for any ε in $(-\eta,\eta)\setminus\{0\}$,

$$\frac{\alpha_0}{|\varepsilon|} \leq \frac{R'_{\mathbf{x}_0}-R_{\mathbf{x}_0}}{\sqrt{2}\,|\varepsilon|\,b^2\alpha_1} - \frac{1}{\sqrt{2}b\alpha_1} - |\varepsilon|\,\frac{\alpha_2}{\alpha_1}, \tag{2.3.142}$$

and consequently formulas (2.3.120) and (2.3.121) yield (2.3.125). Notice that the restriction of ε to $(0,\eta)$ in Formula (2.3.125) is due to the fact that the function $\boldsymbol{\kappa}$ is only defined for $\varepsilon \in \mathbb{R}_+$. This ends the proof of Theorem 2.3.25. □

2.3.11 Consistency with the Torus

The change of coordinate map $\boldsymbol{\Upsilon} = (\boldsymbol{\Upsilon}_{y_1}, \boldsymbol{\Upsilon}_{y_1}, \boldsymbol{\Upsilon}_\theta, \boldsymbol{\Upsilon}_k)$ is such that components 1, 2 and 4 are 2π-periodic with respect to θ, and the penultimate component is given by $\boldsymbol{\Upsilon}_\theta(\mathbf{x},\theta,v) = \theta$. Hence the map $\mathfrak{p}\circ\boldsymbol{\Upsilon}$, where $\mathfrak{p}$ is the canonical projection on the torus, induces a $\mathcal{C}^\infty$-diffeomorphism

$$\boldsymbol{\Upsilon}^\circ :\ \mathbb{R}^2\times(\mathbb{R}/2\pi\mathbb{Z})\times\mathbb{R} \to \mathbb{R}^2\times(\mathbb{R}/2\pi\mathbb{Z})\times\mathbb{R}, \tag{2.3.143}$$

such that $\mathfrak{p}\circ\boldsymbol{\Upsilon} = \boldsymbol{\Upsilon}^\circ\circ\mathfrak{p}$. We denote by $\mathbf{Y}^{\varepsilon,\circ}$, $\Theta^{\varepsilon,\circ}_{\mathfrak{Dar}}$ and $\boldsymbol{\mathcal{K}}^{\varepsilon,\circ}_{\mathfrak{Dar}}$ the expression of the characteristics solution to (2.1.40)–(2.1.41) and expressed in the coordinate system $(\mathbf{y},\theta,v) = \boldsymbol{\Upsilon}^\circ(\mathbf{x},\theta,v)$. Then, these characteristics are solutions to the dynamical system (2.3.120)–(2.3.123) (viewed as a dynamical system on $\mathbb{R}^2\times\mathbb{R}/2\pi\mathbb{Z}\times(0,+\infty)$), and they satisfy

$$\mathfrak{p}\circ(\mathbf{Y}^\varepsilon,\Theta^\varepsilon_{\mathfrak{Dar}},\boldsymbol{\mathcal{K}}^\varepsilon_{\mathfrak{Dar}})(t,\cdot) = \left(\mathbf{Y}^{\varepsilon,\circ},\Theta^{\varepsilon,\circ}_{\mathfrak{Dar}},\boldsymbol{\mathcal{K}}^{\varepsilon,\circ}_{\mathfrak{Dar}}\right)(t,\cdot)\circ\mathfrak{p}. \tag{2.3.144}$$

2.4 The Partial Lie Sums

2.4.1 Objectives

As a result of the Darboux Algorithm, we obtained a Poisson Matrix $\bar{\mathcal{P}}_\varepsilon(\mathbf{y},\theta,k)$ (see (2.3.113)) with the required form to apply the Key Result (Theorem 2.1.2), but the resulting Hamiltonian Function given by (2.3.115) depends on θ. In order to be under the assumptions of the Key Result, we would need to make this dependency to vanish. Since $\bar{H}_0$ does not depend on θ, it seems to be possible to make the penultimate coordinate vanish using a mapping parametrized by ε and close to the identity map for small ε.

Moreover, we would like to build this mapping in such a way that it does not change the Poisson Matrix expression. This means that, as regarded as functions, $\bar{\mathcal{P}}_\varepsilon$ and the expression $\hat{\mathcal{P}}_\varepsilon$ of the Poisson Matrix in the sought coordinate system would need to be the same ; i.e. :

$$\bar{\mathcal{P}}_\varepsilon(\mathbf{z},\gamma,j)=\hat{\mathcal{P}}_\varepsilon(\mathbf{z},\gamma,j)\ \text{ or }\ \bar{\mathcal{P}}_\varepsilon(\mathbf{y},\theta,k)=\hat{\mathcal{P}}_\varepsilon(\mathbf{y},\theta,k) \tag{2.4.1}$$

for any $(\mathbf{z},\gamma,j)$ or $(\mathbf{y},\theta,k)$. Changes of variables having this property are called symplectic. It is well-known that, in the case of a Poisson Matrix that does not depend on ε, flows of Hamiltonian vector fields, parametrized by ε, are symplectic and moreover close to the identity map for small values of their parameter.
In the case we are dealing with, the Poisson Matrix depends on ε. In general, as illustrated by the example of Appendix B.1, flows of Hamiltonian vector fields are no longer symplectic.

In order to avoid this problem, in Littlejohn [40, 41, 42], $\bar{H}_\varepsilon$ is formally expanded as a series. Then a Lie Transform method based on the use of Lie Series

$$S_L^\infty\left(\varepsilon\bar{\mathbf{X}}^\varepsilon_{\varepsilon\bar{f}}\right)\cdot=\sum_{n\geq 0}\frac{\varepsilon^n}{n!}\left(\bar{\mathbf{X}}^\varepsilon_{\varepsilon\bar{f}}\right)^n\cdot, \tag{2.4.2}$$

where $\bar{f}=\bar{f}(\mathbf{y},\theta,k)$ is a smooth function and where $\bar{\mathbf{X}}^\varepsilon_{\varepsilon\bar{f}}$ is the smooth Hamiltonian vector field defined by

$$\bar{\mathbf{X}}^\varepsilon_{\varepsilon\bar{f}}=\varepsilon\bar{\mathcal{P}}_\varepsilon\nabla\bar{f}, \tag{2.4.3}$$

is developed. Notice that $\bar{\mathbf{X}}^\varepsilon_{\varepsilon\bar{f}}$ is the Hamiltonian vector field associated with Hamiltonian Function $\varepsilon\bar{f}$. Formally, i.e. if convergence of the series are not considered, the map $(\mathbf{y},\theta,k)\mapsto S_L^\infty\left(\varepsilon\bar{\mathbf{X}}^\varepsilon_{\varepsilon\bar{f}}\right)\cdot(\mathbf{y},\theta,k)$ is symplectic and from this Lie Series, a symplectic and close-to-identity change-of-coordinates mapping may be built such that, in the resulting coordinate system, the Hamiltonian function, which is expressed as a series, does not depend on the penultimate variable. The drawback of using such a formal Lie Series method is that its convergence is neither ensured nor controlled.

Unfortunately, building a coordinate system that satisfies the assumptions of the Key Theorem can only be led in a formal way and not in a mathematical rigorous way. Hence, in order to insure its existence, we will rather build a coordinate system satisfying the assumption of the following variant of Theorem 2.1.2 :

Theorem 2.4.1. *Let $\mathbf{z}_0\in\mathbb{R}^2$ and $\mathfrak{b}^2\left(\mathbf{z}_0,R^\bullet_{\mathbf{z}_0}\right)\subset\mathbb{R}^2$ be the open ball of radius $R^\bullet_{\mathbf{z}_0}$; $\mathcal{O}^{\mathfrak{D},\bullet}_{\mathfrak{Int}}$ be the open subset of $\mathbb{R}^4$ defined by $\mathcal{O}^{\mathfrak{D},\bullet}_{\mathfrak{Int}}=\mathfrak{b}^2\left(\mathbf{z}_0,R^\bullet_{\mathbf{z}_0}\right)\times\mathbb{R}\times(c^\bullet,d^\bullet)$, where $[c^\bullet,d^\bullet]\subset(0,+\infty)$; and $\mathcal{O}'$ be an open subset such that $\overline{\mathcal{O}'}\subset\mathfrak{b}^2\left(\mathbf{z}_0,R^\star_{\mathbf{z}_0}\right)\times\mathbb{R}\times(c^\star,d^\star)$, where $0<R^\star_{\mathbf{z}_0}<R^\bullet_{\mathbf{z}_0}$ and $[c^\star,d^\star]\subset(c^\bullet,d^\bullet)$. If, there exists a real number η such that for any $\varepsilon\in(0,\eta)$ there*

exists a coordinate system $\mathbf{r} = (r_1, r_2, r_3, r_4)$ *on* $\mathcal{O}^{\mathfrak{D},\bullet}_{\mathfrak{Int}}$ *in which the Poisson Matrix has the following form for* $N \in \mathbb{N}^*$ *:*

$$\mathcal{P}_\varepsilon(\mathbf{r}) = \bar{\mathcal{P}}_\varepsilon(\mathbf{r}) + \varepsilon^N \boldsymbol{\rho}^N_{\mathcal{P}}(\varepsilon, \mathbf{r}), \tag{2.4.4}$$

where

$$\bar{\mathcal{P}}_\varepsilon(\mathbf{r}) = \left(\begin{array}{cc|cc} 0 & -\dfrac{\varepsilon}{B(r_1,r_2)} & 0 & 0 \\ \dfrac{\varepsilon}{B(r_1,r_2)} & 0 & 0 & 0 \\ \hline 0 & 0 & 0 & \dfrac{1}{\varepsilon} \\ 0 & 0 & -\dfrac{1}{\varepsilon} & 0 \end{array}\right), \tag{2.4.5}$$

and where $\boldsymbol{\rho}^N_{\mathcal{P}}$ *is in* $\mathcal{C}^\infty_\#([0,\eta) \times \mathcal{O}^{\mathfrak{D},\bullet}_{\mathfrak{Int}})$ *(see* (2.3.31)*); if for any* $\varepsilon \in [0,\eta)$ *the Hamiltonian function* H_ε*, expressed in the coordinate system* $\mathbf{r}$*, writes*

$$H_\varepsilon(\mathbf{r}) = H_{\varepsilon,T}(r_1, r_2, r_4) + \varepsilon^{N+1} \rho_H(\varepsilon, \mathbf{r}), \tag{2.4.6}$$

where ρ_H *is in* $\mathcal{C}^\infty_\#([0,\eta) \times \mathcal{O}^{\mathfrak{D},\bullet}_{\mathfrak{Int}})$ *; if*

$$H_{\varepsilon,T}(r_1, r_2, r_4) = H_0(r_1, r_2, r_4) + \ldots + \varepsilon^N H_N(r_1, r_2, r_4), \tag{2.4.7}$$

where H_i*,* $i = 0 \ldots N-1$ *are in* $\mathcal{Q}^\infty_{T,b}$ *(see* (2.3.117)*); if*

$$R^\bullet_{\mathbf{z}_0} > 1 + R^\star_{\mathbf{z}_0} + \sqrt{2} \sup_{\varepsilon \in [-\eta,\eta]} \frac{\|\nabla H_{\varepsilon,T}\|_\infty}{\|B\|_\infty}; \tag{2.4.8}$$

and if for any $\varepsilon \in (0,\eta)$ *there exists a time* $t^\varepsilon_e > \frac{\alpha_0}{\varepsilon}$*, where* $\alpha_0 \in (0,+\infty)$ *does not depend* ε*, such that for any* $t \in (-t^\varepsilon_e, t^\varepsilon_e)$ *and for any* $\mathbf{r} \in \overline{\mathcal{O}'}$*, the trajectory* $\mathbf{R}^\varepsilon(t;\mathbf{r})$ *solution to dynamical system :*

$$\frac{\partial \mathbf{R}^\varepsilon}{\partial t} = \mathcal{P}_\varepsilon(\mathbf{R}^\varepsilon) \nabla H_\varepsilon(\mathbf{R}^\varepsilon), \quad \mathbf{R}^\varepsilon(0) = \mathbf{r}, \tag{2.4.9}$$

belongs to $\mathcal{O}^{\mathfrak{D},\bullet}_{\mathfrak{Int}}$ *; then, the following truncated dynamical system*

$$\frac{\partial \mathbf{R}^\varepsilon_T}{\partial t} = \bar{\mathcal{P}}_\varepsilon(\mathbf{R}^\varepsilon_T) \nabla H_{\varepsilon,T}(\mathbf{R}^\varepsilon_T), \quad \mathbf{R}^\varepsilon_T(0) = \mathbf{r}, \tag{2.4.10}$$

is Hamiltonian of Hamiltonian function $H_{\varepsilon,T}(r_1, r_2, r_4)$ *and satisfies the assumptions of Theorem 2.1.2, so that* $\mathbf{R}^\varepsilon_T$ *satisfies the conclusions of this same Theorem 2.1.2.*

Moreover, $\underline{\mathbf{R}^\varepsilon} = (\mathbf{R}^\varepsilon_1, \mathbf{R}^\varepsilon_2, \mathbf{R}^\varepsilon_4)$ *a priori defined for* $\varepsilon \in (0,\eta)$ *is extensible to* $[0,\eta)$ *and this extension, also denoted by* $\underline{\mathbf{R}^\varepsilon}$*, belongs to* $\mathcal{C}^{N-1}([0,\eta))$ *for any* $\mathbf{r} \in \overline{\mathcal{O}'}$ *; and, for any* $\varepsilon \in (0,\eta)$*, for any* $t \in \left(-\frac{\min(1,\alpha_0)}{\varepsilon}, \frac{\min(1,\alpha_0)}{\varepsilon}\right)$ *and for any* $\mathbf{r} \in \overline{\mathcal{O}'}$*,* $\underline{\mathbf{L}^\varepsilon} = (\mathbf{L}^\varepsilon_1, \mathbf{L}^\varepsilon_2, \mathbf{L}^\varepsilon_4)$ *defined by*

$$\underline{\mathbf{L}^\varepsilon} = \frac{\underline{\mathbf{R}^\varepsilon} - \underline{\mathbf{R}^\varepsilon_T}}{\varepsilon^{N-1}} \tag{2.4.11}$$

is extensible to $[0,\eta)$ *and this extension, also denoted by* $\underline{\mathbf{L}^\varepsilon}$*, is smooth and continuous with respect to* ε*. Eventually, for any* $\alpha \in (0,\eta)$*, we have, for any* $\varepsilon \in [0,\alpha]$ *and for any* $t \in \left(-\frac{\min(1,\alpha_0)}{\varepsilon}, \frac{\min(1,\alpha_0)}{\varepsilon}\right)$*,*

$$\left\|\underline{\mathbf{R}^\varepsilon} - \underline{\mathbf{R}^\varepsilon_T}\right\|_{\infty,\mathcal{O}'} \leq |\varepsilon|^{N-1} \sup_{\varepsilon \in [0,\alpha]} \|\underline{\mathbf{L}^\varepsilon}\|_{\infty,\overline{\mathcal{O}'}}, \tag{2.4.12}$$

where $\underline{\mathbf{R}_T^\varepsilon} = ((\mathbf{R}_T^\varepsilon)_1, (\mathbf{R}_T^\varepsilon)_2, (\mathbf{R}_T^\varepsilon)_4)$ *and where* $\|g\|_{\infty,\mathcal{O}'}$ *stands for*

$$\|g\|_{\infty,\mathcal{O}'} = \sup_{\mathbf{r}\in\mathcal{O}'} |g(\mathbf{r})|. \tag{2.4.13}$$

.

Proof. In a first place, since $\bar{\mathcal{P}}_\varepsilon$ is a Poisson Matrix and since $H_{\varepsilon,T}$ is smooth, dynamical system (2.4.10) is Hamiltonian of Hamiltonian function $H_{\varepsilon,T}$.

Setting

$$\boldsymbol{\rho}_{\mathcal{P}}^N(\varepsilon,\mathbf{r}) = \begin{pmatrix} \left(\boldsymbol{\rho}_{\mathcal{P}}^N(\varepsilon,\mathbf{r})\right)^{\mathrm{TL}} & \left(\boldsymbol{\rho}_{\mathcal{P}}^N(\varepsilon,\mathbf{r})\right)^{\mathrm{TR}} \\ \left(\boldsymbol{\rho}_{\mathcal{P}}^N(\varepsilon,\mathbf{r})\right)^{\mathrm{BL}} & \left(\boldsymbol{\rho}_{\mathcal{P}}^N(\varepsilon,\mathbf{r})\right)^{\mathrm{BR}} \end{pmatrix} = \left(\left(\boldsymbol{\rho}_{\mathcal{P}}^N(\varepsilon,\mathbf{r})\right)^{i,j}\right)_{i,j=1,\dots 4}, \tag{2.4.14}$$

and using the skew-symmetry of $\mathcal{P}_\varepsilon$ in (2.4.4) yields :

$$\mathcal{P}_\varepsilon(\mathbf{r}) = \begin{pmatrix} 0 & \bar{\mathcal{P}}_\varepsilon^{1,2} + \varepsilon^N\left(\boldsymbol{\rho}_{\mathcal{P}}^N\right)^{1,2} & \varepsilon^N\left(\boldsymbol{\rho}_{\mathcal{P}}^N\right)^{1,3} & \varepsilon^N\left(\boldsymbol{\rho}_{\mathcal{P}}^N\right)^{1,4} \\ -\bar{\mathcal{P}}_\varepsilon^{1,2} - \varepsilon^N\left(\boldsymbol{\rho}_{\mathcal{P}}^N\right)^{1,2} & 0 & \varepsilon^N\left(\boldsymbol{\rho}_{\mathcal{P}}^N\right)^{2,3} & \varepsilon^N\left(\boldsymbol{\rho}_{\mathcal{P}}^N\right)^{2,4} \\ -\varepsilon^N\left(\boldsymbol{\rho}_{\mathcal{P}}^N\right)^{1,3} & -\varepsilon^N\left(\boldsymbol{\rho}_{\mathcal{P}}^N\right)^{2,3} & 0 & \frac{1}{\varepsilon} + \varepsilon^N\left(\boldsymbol{\rho}_{\mathcal{P}}^N\right)^{3,4} \\ -\varepsilon^N\left(\boldsymbol{\rho}_{\mathcal{P}}^N\right)^{1,4} & -\varepsilon^N\left(\boldsymbol{\rho}_{\mathcal{P}}^N\right)^{2,4} & -\frac{1}{\varepsilon} - \varepsilon^N\left(\boldsymbol{\rho}_{\mathcal{P}}^N\right)^{3,4} & 0 \end{pmatrix}. \tag{2.4.15}$$

The second part of the proof consists essentially in checking that $\underline{\mathbf{R}}^\varepsilon$ is in $\mathcal{C}^{N-1}([0,\eta))$. In order to check this, we define for any $\varepsilon \in (0,\eta)$, for any $t \in \left(-\frac{t_e^\varepsilon}{\varepsilon}, \frac{t_e^\varepsilon}{\varepsilon}\right)$, and for any $\mathbf{r} \in \overline{\mathcal{O}'}$, $\widetilde{\mathbf{R}^\varepsilon} = \widetilde{\mathbf{R}^\varepsilon}(t,\mathbf{r})$ by

$$\widetilde{\mathbf{R}^\varepsilon}(t,\mathbf{r}) = \mathbf{R}^\varepsilon(\varepsilon t,\mathbf{r}). \tag{2.4.16}$$

It satisfies

$$\frac{\partial\widetilde{\mathbf{R}^\varepsilon}}{\partial t}(t) = \varepsilon\mathcal{P}_\varepsilon(\widetilde{\mathbf{R}^\varepsilon}(t))\nabla H_\varepsilon\left(\widetilde{\mathbf{R}^\varepsilon}(t)\right), \tag{2.4.17}$$

Since $\varepsilon \mapsto \varepsilon\mathcal{P}_\varepsilon(\mathbf{r})$ is in $\mathcal{C}^\infty([0,\eta))$ for any $\mathbf{r} \in \mathcal{O}_{\mathfrak{Int}}^{\mathfrak{D},\bullet}$, the solution of (2.4.17) depends smoothly on the parameter ε. In particular function $\widetilde{\mathbf{R}^\varepsilon}$, defined by (2.4.16), is smoothly extensible at $\varepsilon = 0$. Notice that for $\varepsilon = 0$, we obtain

$$\widetilde{\mathbf{R}^0}(t,\mathbf{r}) = \left(r_1, r_2, r_3 + t\frac{\partial H_0}{\partial r_4}(r_1,r_2,r_4), r_4\right). \tag{2.4.18}$$

On another hand, for any $\varepsilon \in (0,\eta)$, for any $\mathbf{r} \in \overline{\mathcal{O}'}$, and for any $t \in (-t_e^\varepsilon, t_e^\varepsilon)$, $\underline{\mathbf{R}^\varepsilon}(t,\mathbf{r}) =$

$(\mathbf{R}_1^\varepsilon, \mathbf{R}_2^\varepsilon, \mathbf{R}_4^\varepsilon)(t,\mathbf{r})$ is solution to

$$\begin{aligned}
&\frac{\partial \begin{pmatrix} \mathbf{R}_1^\varepsilon \\ \mathbf{R}_2^\varepsilon \end{pmatrix}}{\partial t} = \mathtt{M}_\varepsilon(\mathbf{R}_1^\varepsilon, \mathbf{R}_2^\varepsilon) \begin{pmatrix} \dfrac{\partial H_{\varepsilon,T}}{\partial r_1} \\ \dfrac{\partial H_{\varepsilon,T}}{\partial r_2} \end{pmatrix} (\underline{\mathbf{R}^\varepsilon}) + \\
&\varepsilon^N \left[\varepsilon \mathtt{M}_\varepsilon \begin{pmatrix} \dfrac{\partial \rho_H}{\partial r_1} \\ \dfrac{\partial \rho_H}{\partial r_2} \end{pmatrix} + \left(\boldsymbol{\rho}_{\mathcal{P}}^N(\varepsilon,.)\right)^{\mathrm{TL}} \begin{pmatrix} \dfrac{\partial H_\varepsilon}{\partial r_1} \\ \dfrac{\partial H_\varepsilon}{\partial r_2} \end{pmatrix} + \left(\boldsymbol{\rho}_{\mathcal{P}}^N(\varepsilon,.)\right)^{\mathrm{TR}} \begin{pmatrix} \dfrac{\partial H_\varepsilon}{\partial r_3} \\ \dfrac{\partial H_\varepsilon}{\partial r_4} \end{pmatrix} \right] \left(\mathbf{R}_1^\varepsilon, \mathbf{R}_2^\varepsilon, \widetilde{\mathbf{R}_3^\varepsilon}\left(\frac{t}{\varepsilon}, \mathbf{r}\right), \mathbf{R}_4^\varepsilon\right), \\
&\frac{\partial \mathbf{R}_4^\varepsilon}{\partial t} = -\varepsilon^N \left[\left(\boldsymbol{\rho}_{\mathcal{P}}^N(\varepsilon,.)\right)^{1,4} \frac{\partial H_\varepsilon}{\partial r_1} + \left(\boldsymbol{\rho}_{\mathcal{P}}^N(\varepsilon,.)\right)^{2,4} \frac{\partial H_\varepsilon}{\partial r_2} + \left(\boldsymbol{\rho}_{\mathcal{P}}^N(\varepsilon,.)\right)^{3,4} \frac{\partial H_\varepsilon}{\partial r_3} + \frac{\partial \rho_H}{\partial r_3}(\varepsilon,.) \right] \\
&\qquad\qquad \left(\mathbf{R}_1^\varepsilon, \mathbf{R}_2^\varepsilon, \widetilde{\mathbf{R}_3^\varepsilon}\left(\frac{t}{\varepsilon}, \mathbf{r}\right), \mathbf{R}_4^\varepsilon\right),
\end{aligned} \tag{2.4.19}$$

where

$$\mathtt{M}_\varepsilon(r_1, r_2) = \begin{pmatrix} 0 & -\dfrac{\varepsilon}{B(r_1, r_2)} \\ \dfrac{\varepsilon}{B(r_1, r_2)} & 0 \end{pmatrix}. \tag{2.4.20}$$

Notice that, in this system, $\widetilde{\mathbf{R}_3^\varepsilon}$ is known and then considered as given. Beside this,

$$\varepsilon \mathtt{M}_\varepsilon \begin{pmatrix} \dfrac{\partial \rho_H}{\partial r_1} \\ \dfrac{\partial \rho_H}{\partial r_2} \end{pmatrix} + \left(\boldsymbol{\rho}_{\mathcal{P}}^N(\varepsilon,.)\right)^{\mathrm{TL}} \begin{pmatrix} \dfrac{\partial H_\varepsilon}{\partial r_1} \\ \dfrac{\partial H_\varepsilon}{\partial r_2} \end{pmatrix} + \left(\boldsymbol{\rho}_{\mathcal{P}}^N(\varepsilon,.)\right)^{\mathrm{TR}} \begin{pmatrix} \dfrac{\partial H_\varepsilon}{\partial r_3} \\ \dfrac{\partial H_\varepsilon}{\partial r_4} \end{pmatrix}, \tag{2.4.21}$$

and

$$\left(\boldsymbol{\rho}_{\mathcal{P}}^N(\varepsilon,.)\right)^{1,4} \frac{\partial H_\varepsilon}{\partial r_1} + \left(\boldsymbol{\rho}_{\mathcal{P}}^N(\varepsilon,.)\right)^{2,4} \frac{\partial H_\varepsilon}{\partial r_2} + \left(\boldsymbol{\rho}_{\mathcal{P}}^N(\varepsilon,.)\right)^{3,4} \frac{\partial H_\varepsilon}{\partial r_3} + \frac{\partial \rho_H}{\partial r_3}(\varepsilon,.) \tag{2.4.22}$$

are 2π-periodic and smooth, and consequently $\mathcal{C}_b^\infty(\mathbb{R})$ with respect to the third variable r_3. Hence, computing the successive derivatives of (2.4.19) with respect to ε, we obtain that $\varepsilon \mapsto \underline{\mathbf{R}^\varepsilon}(t)$ is $\mathcal{C}^{N-1}$ in the neighborhood of $\varepsilon = 0$.
Moreover, as $\underline{\mathbf{R}_T^\varepsilon} = ((\mathbf{R}_T^\varepsilon)_1, (\mathbf{R}_T^\varepsilon)_2, (\mathbf{R}_T^\varepsilon)_4)$ is solution to

$$\begin{aligned}
&\frac{\partial \begin{pmatrix} (\mathbf{R}_T^\varepsilon)_1 \\ (\mathbf{R}_T^\varepsilon)_2 \end{pmatrix}}{\partial t} = \mathtt{M}_\varepsilon((\mathbf{R}_T^\varepsilon)_1, (\mathbf{R}_T^\varepsilon)_2) \begin{pmatrix} \dfrac{\partial H_{\varepsilon,T}}{\partial r_1} \\ \dfrac{\partial H_{\varepsilon,T}}{\partial r_2} \end{pmatrix} \left(\underline{\mathbf{R}_T^\varepsilon}\right), \\
&\frac{\partial (\mathbf{R}_T^\varepsilon)_4}{\partial t} = 0,
\end{aligned} \tag{2.4.23}$$

$\underline{\mathbf{R}_T^\varepsilon}$ is smooth with respect to ε, for any $t \in \mathbb{R}$ and for any $\mathbf{r} \in \mathbb{R}^3 \times (0, +\infty)$. Moreover, for any $\mathbf{r} = (\mathbf{z}, r_3, r_4)$, we have

$$\left| \begin{pmatrix} (\mathbf{R}_T^\varepsilon)_1 \\ (\mathbf{R}_T^\varepsilon)_2 \end{pmatrix} (t, \mathbf{r}) - \mathbf{z} \right| \leq \sqrt{2}\, |\varepsilon|\, |t|\, \frac{\|\nabla H_{\varepsilon,T}\|_\infty}{\|B\|_\infty}. \tag{2.4.24}$$

Consequently, assumption (2.4.8) yields that for any $\varepsilon \in (-\eta,\eta)$, for any $t \in \left(-\frac{1}{|\varepsilon|},\frac{1}{|\varepsilon|}\right)$ (By convention if $\varepsilon = 0$, $\left(-\frac{1}{|\varepsilon|},\frac{1}{|\varepsilon|}\right) = \mathbb{R}$) and for any $\mathbf{r} \in \overline{\mathcal{O}'}$,

$$\begin{pmatrix} (\mathbf{R}_T^\varepsilon)_1 \\ (\mathbf{R}_T^\varepsilon)_2 \end{pmatrix}(t;\mathbf{r}) \in \mathfrak{b}^2\big(\mathbf{z}_0, R^\bullet_{\mathbf{z}_0}\big)\,, \tag{2.4.25}$$

and consequently, $\mathbf{R}_T^\varepsilon$ remains in $\mathcal{O}^{\mathfrak{D},\bullet}_{\mathfrak{Int}}$.

Now, we will show that $\underline{\mathbf{L}^\varepsilon}$ defined for $\varepsilon \in (0,\eta)$ by (2.4.11) is extensible to $[0,\eta)$ and that the yielding extension is continuous with respect to ε. By definition for any $\varepsilon \in (0,\eta)$, for any $t \in (-t_e^\varepsilon, t_e^\varepsilon)$, and for any $\mathbf{r} \in \overline{\mathcal{O}'}$, $\mathbf{L}^\varepsilon$ is smooth on $\overline{\mathcal{O}'}$ and $\mathcal{C}^{N-1}((0,\eta))$ with respect to ε. So, we just have to show that $\varepsilon \mapsto \underline{\mathbf{L}^\varepsilon}$ is extensible as a continuous function on $[0,\eta)$, and particularly, that $\varepsilon = 0$ is not a singularity.
In a first place, for any $\varepsilon \in (0,\eta)$, we will explicit the dynamical system $\underline{\mathbf{L}^\varepsilon}$ satisfies. Injecting

$$\underline{\mathbf{R}^\varepsilon}\,(t,\mathbf{r}) = \underline{\mathbf{R}_T{}^\varepsilon}\,(t,\mathbf{r}) + \varepsilon^{N-1}\underline{\mathbf{L}^\varepsilon}\,(t,\mathbf{r})\,, \tag{2.4.26}$$

in (2.4.19) gives

$$\begin{aligned}
&\frac{\partial \begin{pmatrix} (\mathbf{R}_T^\varepsilon)_1 + \varepsilon^{N-1}\mathbf{L}_1^\varepsilon \\ (\mathbf{R}_T^\varepsilon)_2 + \varepsilon^{N-1}\mathbf{L}_2^\varepsilon \end{pmatrix}}{\partial t} \\
&\quad = \mathtt{M}_\varepsilon\big((\mathbf{R}_T^\varepsilon)_1 + \varepsilon^{N-1}\mathbf{L}_1^\varepsilon, (\mathbf{R}_T^\varepsilon)_2 + \varepsilon^{N-1}\mathbf{L}_2^\varepsilon\big)\begin{pmatrix} \dfrac{\partial H_{\varepsilon,T}}{\partial r_1} \\ \dfrac{\partial H_{\varepsilon,T}}{\partial r_2} \end{pmatrix}\Big(\underline{\mathbf{R}_T^\varepsilon} + \varepsilon^{N-1}\underline{\mathbf{L}^\varepsilon}\Big) \\
&\qquad + \varepsilon^N\left[\varepsilon\mathtt{M}_\varepsilon\begin{pmatrix} \dfrac{\partial \rho_H}{\partial r_1} \\ \dfrac{\partial \rho_H}{\partial r_2} \end{pmatrix} + \big(\boldsymbol{\rho}^N_{\mathcal{P}}(\varepsilon,.)\big)^{\mathrm{TL}}\begin{pmatrix} \dfrac{\partial H_\varepsilon}{\partial r_1} \\ \dfrac{\partial H_\varepsilon}{\partial r_2} \end{pmatrix} + \big(\boldsymbol{\rho}^N_{\mathcal{P}}(\varepsilon,.)\big)^{\mathrm{TR}}\begin{pmatrix} \dfrac{\partial H_\varepsilon}{\partial r_3} \\ \dfrac{\partial H_\varepsilon}{\partial r_4} \end{pmatrix}\right] \\
&\qquad\qquad \Big((\mathbf{R}_T^\varepsilon)_1 + \varepsilon^{N-1}\mathbf{L}_1^\varepsilon, (\mathbf{R}_T^\varepsilon)_2 + \varepsilon^{N-1}\mathbf{L}_2^\varepsilon, \widetilde{\mathbf{R}_3^\varepsilon}\Big(\frac{t}{\varepsilon},\mathbf{r}\Big), (\mathbf{R}_T^\varepsilon)_4 + \varepsilon^{N-1}\mathbf{L}_4^\varepsilon\Big)\,, \\
&\frac{\partial(\mathbf{R}_T^\varepsilon)_4}{\partial t} + \varepsilon^{N-1}\frac{\partial \mathbf{L}_4^\varepsilon}{\partial t} \\
&\quad = -\varepsilon^N\left[\big(\boldsymbol{\rho}^N_{\mathcal{P}}(\varepsilon,.)\big)^{1,4}\frac{\partial H_\varepsilon}{\partial r_1} + \big(\boldsymbol{\rho}^N_{\mathcal{P}}(\varepsilon,.)\big)^{2,4}\frac{\partial H_\varepsilon}{\partial r_2} + \big(\boldsymbol{\rho}^N_{\mathcal{P}}(\varepsilon,.)\big)^{3,4}\frac{\partial H_\varepsilon}{\partial r_3} + \frac{\partial \rho_H}{\partial r_3}(\varepsilon,.)\right] \\
&\qquad\qquad \Big((\mathbf{R}_T^\varepsilon)_1 + \varepsilon^{N-1}\mathbf{L}_1^\varepsilon, (\mathbf{R}_T^\varepsilon)_2 + \varepsilon^{N-1}\mathbf{L}_2^\varepsilon, \widetilde{\mathbf{R}_3^\varepsilon}\Big(\frac{t}{\varepsilon},\mathbf{r}\Big), (\mathbf{R}_T^\varepsilon)_4 + \varepsilon^{N-1}\mathbf{L}_4^\varepsilon\Big)\,.
\end{aligned} \tag{2.4.27}$$

According to formula (2.4.25), and by assumption, for any $\varepsilon \in (0,\eta)$, for any $t \in \left(-\frac{\min(1,\alpha_0)}{\varepsilon}, \frac{\min(1,\alpha_0)}{\varepsilon}\right)$ and for any $\mathbf{r} \in \overline{\mathcal{O}'}$, $\mathbf{R}_T^\varepsilon$ and $\mathbf{R}^\varepsilon$ are both in $\mathcal{O}^{\mathfrak{D},\bullet}_{\mathfrak{Int}}$, which is a convex set. This allows us to use a Taylor expansion in

$$\mathtt{M}_\varepsilon\big((\mathbf{R}_T^\varepsilon)_1 + \varepsilon^{N-1}\mathbf{L}_1^\varepsilon, (\mathbf{R}_T^\varepsilon)_2 + \varepsilon^{N-1}\mathbf{L}_2^\varepsilon\big)\begin{pmatrix} \dfrac{\partial H_{\varepsilon,T}}{\partial r_1} \\ \dfrac{\partial H_{\varepsilon,T}}{\partial r_2} \end{pmatrix}\Big(\underline{\mathbf{R}_T^\varepsilon} + \varepsilon^{N-1}\underline{\mathbf{L}^\varepsilon}\Big)$$

leading to

$$\begin{aligned}
&\mathtt{M}_\varepsilon\big((\mathbf{R}_T^\varepsilon)_1+\varepsilon^{N-1}\mathbf{L}_1^\varepsilon,(\mathbf{R}_T^\varepsilon)_2+\varepsilon^{N-1}\mathbf{L}_2^\varepsilon\big)\begin{pmatrix}\dfrac{\partial H_{\varepsilon,T}}{\partial r_1}\\ \dfrac{\partial H_{\varepsilon,T}}{\partial r_2}\end{pmatrix}\Big(\underline{\mathbf{R}_T^\varepsilon}+\varepsilon^{N-1}\underline{\mathbf{L}^\varepsilon}\Big)\\
&\quad=\mathtt{M}_\varepsilon((\mathbf{R}_T^\varepsilon)_1,(\mathbf{R}_T^\varepsilon)_2)\begin{pmatrix}\dfrac{\partial H_{\varepsilon,T}}{\partial r_1}\\ \dfrac{\partial H_{\varepsilon,T}}{\partial r_2}\end{pmatrix}\Big(\underline{\mathbf{R}_T^\varepsilon}\Big)+\beta_1\left(\varepsilon,\underline{\mathbf{R}_T^\varepsilon},\underline{\mathbf{L}^\varepsilon}\right),
\end{aligned}\tag{2.4.28}$$

where $\beta_1=\beta_1(\varepsilon,\underline{\mathbf{r}},\underline{\mathbf{l}})$ belongs to $\mathcal{C}^\infty(\mathcal{U}_\eta^1)$, with

$$\begin{aligned}
\mathcal{U}_\eta^1=\Big\{&(\varepsilon,\underline{\mathbf{r}},\underline{\mathbf{l}})\in\mathbb{R}_+\times\mathbb{R}^3\times\mathbb{R}^3,\\
&\text{s.t. }\varepsilon\in[0,\eta)\ \text{ and }\underline{\mathbf{r}}+\varepsilon^{N-1}\underline{\mathbf{l}}\in\mathbf{b}\left(\mathbf{z}_0,R^\bullet_{\mathbf{z}_0}\right)\times(c^\bullet,d^\bullet)\Big\}.
\end{aligned}\tag{2.4.29}$$

Injecting (2.4.28) in (2.4.27) and using (2.4.23) yields

$$\frac{\partial\begin{pmatrix}\mathbf{L}_1^\varepsilon\\ \mathbf{L}_2^\varepsilon\end{pmatrix}}{\partial t}=\beta_1\Big(\varepsilon,\underline{\mathbf{L}^\varepsilon},\underline{\mathbf{R}_T^\varepsilon}\Big)+\varepsilon\beta_2\left(\varepsilon,\underline{\mathbf{L}^\varepsilon},\underline{\mathbf{R}_T^\varepsilon},\widetilde{\mathbf{R}_3^\varepsilon}\left(\frac{t}{\varepsilon},\mathbf{r}\right)\right),\tag{2.4.30}$$

and

$$\frac{\partial\mathbf{L}_4^\varepsilon}{\partial t}=\varepsilon\beta_3\left(\varepsilon,\underline{\mathbf{L}^\varepsilon},\underline{\mathbf{R}_T^\varepsilon},\widetilde{\mathbf{R}_3^\varepsilon}\left(\frac{t}{\varepsilon},\mathbf{r}\right)\right),\tag{2.4.31}$$

where β_2 and β_3 are in $\mathcal{C}^\infty(\mathcal{U}_\eta^2)$, with

$$\begin{aligned}
\mathcal{U}_\eta^2=\Big\{&(\varepsilon,\underline{\mathbf{r}},\underline{\mathbf{l}},r_3)\in\mathbb{R}_+\times\mathbb{R}^3\times\mathbb{R}^3\times\mathbb{R},\\
&\text{s.t. }\varepsilon\in[0,\eta)\,,\ \text{and }\underline{\mathbf{r}}+\varepsilon^{N-1}\underline{\mathbf{l}}\in\mathbf{b}\left(\mathbf{z}_0,R^\bullet_{\mathbf{z}_0}\right)\times(c^\bullet,d^\bullet)\Big\}.
\end{aligned}\tag{2.4.32}$$

Moreover, β_2 and β_3 are smooth and 2π-periodic with respect to r_3. Besides, the solutions of this dynamical system are continuous with respect to ε. Clearly the initial data for $\underline{\mathbf{L}^\varepsilon}$ is $\underline{\mathbf{L}^\varepsilon}(0)=0$. Hence, $\underline{\mathbf{L}^\varepsilon}$ is continuous with respect to ε. Since $\underline{\mathbf{R}^\varepsilon}-\underline{\mathbf{R}_T^\varepsilon}=\varepsilon^{N-1}\underline{\mathbf{L}^\varepsilon}$, estimate (2.4.12) follows. This ends the proof of Theorem 2.4.1. □

Theorem 2.4.1 means that we can approximate with accuracy ε^{N-1} dynamical system (2.4.9) by dynamical system (2.4.10).

Let us fix

$$N\in\mathbb{N}^\star.\tag{2.4.33}$$

In order to find a coordinate system satisfying the assumptions of Theorem 2.4.1, with this given N, we will introduce and develop a Partial Lie Transform Method of order N based on the use of the partial Lie Sums of order (i,j)

$$S_L^i\left(\varepsilon^j\bar{\mathbf{X}}^\varepsilon_{\varepsilon^{\bar{f}}}\right)\cdot=\sum_{n=0}^{i}\frac{\varepsilon^{jn}}{n!}\left(\bar{\mathbf{X}}^\varepsilon_{\varepsilon^{\bar{f}}}\right)^n\cdot,\tag{2.4.34}$$

where i and j are non-negative integers and where $\bar{\mathbf{X}}^{\varepsilon}_{\varepsilon\bar{f}}$ is defined by (2.4.3). For any positive integer N, the partial Lie Transform of order N will allow us to build a coordinate system satisfying at this order the assumptions of Theorem 2.4.1. The resulting coordinate system will be the Gyro-Kinetic Coordinate System of order N (see Definition 2.1.4) : $(\mathbf{z}, \gamma, j)$.
In the forthcoming subsections, we will introduce the Partial Lie Sums of order (i, j) and set out their properties. In the next section we will develop for any $N \in \mathbb{N}^\star$ the Partial Lie Transform Method of order N. This method will then be applied in section 2.6 to deduce Theorem 2.1.3 from Theorem 2.4.1.

2.4.2 The partial Lie Sums : definitions and properties

Firstly, to simplify notations to come, we introduce

$$\bar{\mathbf{r}} = (\bar{r}_1, \ldots, \bar{r}_4) \text{ defined on } \mathbb{R}^2 \times \mathbb{R} \times (0, +\infty), \tag{2.4.35}$$

as the Darboux Coordinates and the domain on which they are defined (notice that with this notation $\bar{r}_3 = \theta$) and we also introduce the set $\mathfrak{b}^{\#}(\bar{\mathbf{r}}_0, R_{\bar{\mathbf{r}}_0}) \subset \mathbb{R}^4$ defined by :

$$\mathfrak{b}^{\#}(\bar{\mathbf{r}}_0, R_{\bar{\mathbf{r}}_0}) = \left\{ \bar{\mathbf{r}} \in \mathbb{R}^4,\ |\bar{\mathbf{r}} - \bar{\mathbf{r}}_0|_{1,2,4} < R_{\bar{\mathbf{r}}_0} \right\}. \tag{2.4.36}$$

Here and hereafter, $|\bar{\mathbf{r}}|_{1,2,4}$ stands for $|(\bar{r}_1, \bar{r}_2, \bar{r}_4)|$, where $|\cdot|$ corresponds to the Euclidian norm on $\mathbb{R}^3$. We call such sets : open periodic balls. We then consider $\bar{\mathbf{r}}_0^*$ in $\mathbb{R}^2 \times \mathbb{R} \times (0, +\infty)$ and $R_0^* > 0$ such that

$$\overline{\mathfrak{b}^{\#}(\bar{\mathbf{r}}_0^*, R_0^*)} \subset \mathbb{R}^2 \times \mathbb{R} \times (0, +\infty). \tag{2.4.37}$$

We also recall properties of real analytic functions. For a positive integer p, let

$$S(\mathbf{Z}) = \sum_{\mathbf{l} \in \mathbb{N}^p} a_{\mathbf{l}} \mathbf{Z}^{\mathbf{l}}, \tag{2.4.38}$$

where $\mathbf{l} = (l_1, \ldots, l_p) \in \mathbb{N}^p$, $\mathbf{Z} = (Z_1, \ldots, Z_p) \in \mathbb{R}^p$ and $\mathbf{Z}^{\mathbf{l}} = Z_1^{l_1} \ldots Z_p^{l_p}$, be a formal power series of p variables. We can associate with this formal power series the numerical series

$$\sum_{\mathbf{l} \in \mathbb{N}^p} |a_{\mathbf{l}}|\, \mathbf{r}^{\mathbf{l}}, \tag{2.4.39}$$

where $\mathbf{r} = (r_1, \ldots, r_p) \in \mathbb{R}^p_+$. We denote by $\mathbf{\Gamma}_S$ the set

$$\mathbf{\Gamma}_S = \left\{ \mathbf{r} \in \mathbb{R}^p_+ \text{ such that } \sum_{\mathbf{l} \in \mathbb{N}^p} |a_{\mathbf{l}}|\, \mathbf{r}^{\mathbf{l}} < +\infty \right\}, \tag{2.4.40}$$

and the set $\overset{\circ}{\mathbf{\Gamma}}_S$ is called the "set of convergence" of this series. By abuse of language,

$$\mathbf{\Sigma}_S = \left\{ \mathbf{x} \in \mathbb{R}^p \text{ such that } \sum_{\mathbf{l} \in \mathbb{N}^p} |a_{\mathbf{l}}| \left|\mathbf{x}^{\mathbf{l}}\right| < \infty \right\}. \tag{2.4.41}$$

is also called "set of convergence". We recall that on $\mathbf{\Sigma}_S$, the series $S(\mathbf{r})$ is infinitely differentiable, that the set of convergence of the partial derivatives is the same as of S and that the derivatives are obtained by permuting sum and derivatives. Notice also that if the closure of a non-empty open ball is included in the set of convergence, then, the series converges normally on this ball.

Definition 2.4.2. *We say that a function f is a real analytic function on the open subset $U \subset \mathbb{R}^p$ if, for all $\mathbf{r}_0 \in U$, there exists a formal power series $S_{\mathbf{r}_0}$ and a real number $R_{\mathbf{r}_0} > 0$ such that the n-dimensional open ball $\mathfrak{b}^n(\mathbf{r}_0, R_{\mathbf{r}_0})$ is included in U, such that $\mathfrak{b}^n(0, R_{\mathbf{r}_0})$ is included in $\mathbf{\Sigma}_S$ and such that*

$$\forall \mathbf{r} \in \mathfrak{b}^n(\mathbf{r}_0, R_{\mathbf{r}_0}),\ f(\mathbf{r}) = S(\mathbf{r} - \mathbf{r}_0). \tag{2.4.42}$$

We denote by $\mathcal{A}(U)$ the space of real analytic functions on U.

We recall the two following theorems.

Theorem 2.4.3. *Let $\Omega \subset \mathbb{R}^p$ and $\Omega' \subset \mathbb{R}^q$ be two open subsets. Let $f : \Omega \to \mathbb{R}^q$ in $(\mathcal{A}(\Omega))^q$ and $g : \Omega' \to \mathbb{R}^p$ in $(\mathcal{A}(\Omega'))^p$ be such that $g(\Omega') \subset \Omega$. Then, $f \circ g$ is in $(\mathcal{A}(\Omega'))^q$.*

Theorem 2.4.4. *Let f be a real analytic function in a neighborhood of $a = (a_1, \ldots, a_p)$. If the differential $(df)_a$ of f in a is non-singular, then f^{-1} is defined and real analytic in a neighborhood of $f(a)$.*

For more details about the real analytic functions, or for the proofs of the two previous theorems, see Cartan [7] or Krantz & Park [36].

We also recall the following version of the global inversion Theorem :

Theorem 2.4.5. *Let E be a Banach space and F a normed vector space. Let $A : E \to F$ be a linear, continuous and invertible map such that A^{-1} is continuous. Let $\varphi : E \to F$ be a Lipshitz continuous map such that its Lipshitz constant $Lip(\varphi)$ satisfies $Lip(\varphi) < \left\|A^{-1}\right\|^{-1}$. Then,*

- *$h = A + \varphi$ is invertible.*
- *h^{-1} is Lipschitz continuous.*
- *If $U \subset E$ is an open subset, if $h \in \mathcal{C}^1(U)$ and if for any $x \in U$, $(dh)_x$ is an isomorphism from E onto F, then h^{-1} is $\mathcal{C}^1(h(U))$, and for any $x \in U$, $\left(dh^{-1}\right)_{h(x)} = (dh)_x^{-1}$.*

We will use the results just recalled. The Poisson Matrix $\bar{\mathcal{P}}_\varepsilon = \bar{\mathcal{P}}_\varepsilon(\bar{\mathbf{r}})$ in the coordinate system $\bar{\mathbf{r}}$ satisfies :

Lemma 2.4.6. *The Poisson matrix $\bar{\mathcal{P}}_\varepsilon = \bar{\mathcal{P}}_\varepsilon(\bar{\mathbf{r}})$ given by formula (2.3.113) and defined by construction on $\mathbb{R}^2 \times \mathbb{R} \times (0, +\infty)$, is extensible, with the same expression, as a Poisson Matrix to $\mathbb{R}^4$, the extension being also denoted $\bar{\mathcal{P}}_\varepsilon$. Moreover, all entries of $\bar{\mathcal{P}}_\varepsilon$ are independent of $\bar{r}_3$ and $\bar{r}_4$ and they can be viewed as functions in $\mathcal{A}\left(\mathbb{R}^2\right) \cap \mathcal{C}_b^\infty\left(\mathbb{R}^2\right)$.*

Proof. The symplectic Two-Form associated with $\bar{\mathcal{P}}_\varepsilon$

$$\bar{\omega}_\varepsilon(\bar{\mathbf{r}}) = \frac{\varepsilon}{B(\bar{r}_1, \bar{r}_2)} d\bar{r}_1 \wedge d\bar{r}_2 - \frac{1}{\varepsilon} d\bar{r}_3 \wedge d\bar{r}_4, \tag{2.4.43}$$

on the Darboux Coordinate chart is clearly extensible with the same expression to $\mathbb{R}^4$ and the yielding extension is clearly closed and non-degenerate. Hence the extension is a Poisson Matrix on $\mathbb{R}^4$. Moreover, as the magnetic field is defined on $\mathbb{R}^2$ and since it is by assumption bounded, larger than 1, and analytic on $\mathbb{R}^2$ so is $\frac{1}{B}$. Hence, all entries of $\bar{\mathcal{P}}_\varepsilon$ are analytic and in $\mathcal{C}_b^\infty\left(\mathbb{R}^2\right)$. This ends the proof of Lemma 2.4.6. □

In addition, $\bar{\mathcal{P}}_\varepsilon$ can be rewritten as

$$\bar{\mathcal{P}}_\varepsilon(\bar{\mathbf{r}}) = \frac{1}{\varepsilon}\bar{\mathcal{T}}_\varepsilon(\bar{\mathbf{r}}), \tag{2.4.44}$$

which define matrix $\bar{\mathcal{T}}_\varepsilon(\bar{\mathbf{r}})$.

We will now introduce the Partial Lie Sum of order (i,j) and the Partial Lie Sum Function as follows :

Definition 2.4.7. *Let $\mathfrak{C}^4$ be a convex subset of $\mathbb{R}^4$. For any $\bar{f} = \bar{f}(\bar{\mathbf{r}})$ in $\mathcal{C}^\infty(\mathfrak{C}^4)$, let $\boldsymbol{\vartheta}^{i,j}_{\varepsilon,\bar{f}}$ be the differential operator acting on functions $\bar{g} = \bar{g}(\bar{\mathbf{r}})$ of $\mathcal{C}^\infty(\mathfrak{C}^4)$ in the following way :*

$$\boldsymbol{\vartheta}^{i,j}_{\varepsilon,\bar{f}} \cdot \bar{g} = S^i_L\left(\varepsilon^j \bar{\mathbf{X}}^\varepsilon_{\varepsilon\bar{f}}\right) \cdot \bar{g}, \tag{2.4.45}$$

where S^i_L is defined by (2.4.34) and $\bar{\mathbf{X}}^\varepsilon_{\varepsilon\bar{f}}$ by (2.4.3). From operator $\boldsymbol{\vartheta}^{i,j}_{\varepsilon,\bar{f}}$ we define, with the same notation, function $\boldsymbol{\vartheta}^{i,j}_{\varepsilon,\bar{f}} = \boldsymbol{\vartheta}^{i,j}_{\varepsilon,\bar{f}}(\bar{\mathbf{r}})$ from $\mathfrak{C}^4$ to $\mathbb{R}$ by

$$\boldsymbol{\vartheta}^{i,j}_{\varepsilon,\bar{f}} = \boldsymbol{\vartheta}^{i,j}_{\varepsilon,\bar{f}}(\bar{\mathbf{r}}) = \left(\left(\boldsymbol{\vartheta}^{i,j}_{\varepsilon,\bar{f}} \cdot \bar{\mathbf{r}}_1\right)(\bar{\mathbf{r}}), \ldots, \left(\boldsymbol{\vartheta}^{i,j}_{\varepsilon,\bar{f}} \cdot \bar{\mathbf{r}}_4\right)(\bar{\mathbf{r}})\right), \tag{2.4.46}$$

where $\bar{\mathbf{r}}_i$ stands for $\bar{\mathbf{r}} \mapsto \bar{r}_i$.

Definition 2.4.8. *Viewed as a differential operator, $\boldsymbol{\vartheta}^{i,j}_{\varepsilon,\bar{f}}$ is called the Partial Lie Sum of order (i,j) generated by f, and view as a function $\boldsymbol{\vartheta}^{i,j}_{\varepsilon,\bar{f}}$ is called the Partial Lie Sum map generated by f.*

The first property that we will prove is the following theorem.

Theorem 2.4.9. *Let i,j be two positive integers, $\mathfrak{C}$ be a convex subset of $\mathbb{R}^3$ and $\mathfrak{C}^\#$ defined by :*

$$\mathfrak{C}^\# = \left\{\bar{\mathbf{r}} \in \mathbb{R}^4,\ (\bar{r}_1, \bar{r}_2, \bar{r}_4) \in \mathfrak{C} \text{ and } \bar{r}_3 \in \mathbb{R}\right\}, \tag{2.4.47}$$

and let $\bar{f} = \bar{f}(\bar{\mathbf{r}})$ be in $\mathcal{C}^\infty_\#\left(\mathfrak{C}^\#\right) \cap \mathcal{C}^\infty_b\left(\mathfrak{C}^\#\right)$. Then, there exists a real number $\bar{\eta}_1 > 0$ such that for any $\varepsilon \in [-\bar{\eta}_1, \bar{\eta}_1]$, function $\boldsymbol{\vartheta}^{i,j}_{\varepsilon,\bar{f}}$ defined by (2.4.46) is a diffeomorphism from $\mathfrak{C}^\#$ onto its range. We denote by $\boldsymbol{\Xi}^{i,j}_{\varepsilon,f}$ the inverse function of $\boldsymbol{\vartheta}^{i,j}_{\varepsilon,f}$.

Remark 2.4.10. *Thanks to Theorem 2.4.9, we will be able to consider change of coordinates $\hat{\mathbf{r}} = \boldsymbol{\vartheta}^{i,j}_{\varepsilon,\bar{f}}(\bar{\mathbf{r}})$ for $\bar{\mathbf{r}}$ in $\mathfrak{b}^\#(\bar{\mathbf{r}}^*_0, R^*_0)$ and $\bar{f}$ defined on $\mathfrak{b}^\#(\bar{\mathbf{r}}^*_0, R^*_0)$, where $\mathfrak{b}^\#(\bar{\mathbf{r}}^*_0, R^*_0)$ is defined by (2.4.36). We will denote by $\bar{\mathbf{r}} = \boldsymbol{\Xi}^{i,j}_{\varepsilon,\bar{f}}(\hat{\mathbf{r}})$ the reciprocal change of coordinates. In view of the Partial Lie Transform method, that we will construct in the next section, we need to express $\boldsymbol{\Xi}^{i,j}_{\varepsilon,\bar{f}}$ in terms of $\boldsymbol{\vartheta}^{i,j}_{\varepsilon,-\bar{f}}$. The problem to reach this goal, is that function $\bar{f}$ is not necessarily defined on $\boldsymbol{\vartheta}^{i,j}_{\varepsilon,\bar{f}}\left(\mathfrak{b}^\#(\bar{\mathbf{r}}^*_0, R^*_0)\right)$. In order to overcome this difficulty, we can choose among two options. The first option consists in restricting the method to an open subset $\mathfrak{V} \subset \mathfrak{b}^\#(\bar{\mathbf{r}}^*_0, R^*_0)$ such that $\boldsymbol{\vartheta}^{i,j}_{\varepsilon,\bar{f}}(\mathfrak{V}) \subset \mathfrak{b}^\#(\bar{\mathbf{r}}^*_0, R^*_0)$. But this option implies a restriction of the domain, and consequently, we do not choose it. The second option, which is the one we opt for, consists in taking an open subset $\mathfrak{U}$ containing $\mathfrak{b}^\#(\bar{\mathbf{r}}^*_0, R^*_0)$ and $\boldsymbol{\vartheta}^{i,j}_{\varepsilon,\bar{f}}\left(\mathfrak{b}^\#(\bar{\mathbf{r}}^*_0, R^*_0)\right)$ and defining an extension of function $\bar{f}$ to this set. Of course this option requires the Poisson Matrix to be extensible to $\mathfrak{U}$, which is the case because of Lemma 2.4.6.*

Remark 2.4.11. *Another restriction regarding the class of functions $\bar{f}$ generating the Partial Lie Sum of order N (see Definition 2.4.8) required by the Partial Lie Transform Method, is that their restriction to $\boldsymbol{\vartheta}^{i,j}_{\varepsilon,\bar{f}}\left(\mathfrak{b}^{\#}(\bar{\mathfrak{r}}^*_0, R^*_0)\right)$ will depend on the N first terms of the expansion in power of ε of the Hamiltonian function (see* (2.3.115)*). This implies that those N first terms need to be extensible to set $\boldsymbol{\vartheta}^{i,j}_{\varepsilon,\bar{f}}\left(\mathfrak{b}^{\#}(\bar{\mathfrak{r}}^*_0, R^*_0)\right)$. Hence, we could think that the best choice for $\mathfrak{U}$ is an open subset on which both the Poisson Matrix and the N first terms of the expansion in power of ε of the Hamiltonian function can be extended and such that $\boldsymbol{\vartheta}^{i,j}_{\varepsilon,\bar{f}}\left(\mathfrak{b}^{\#}(\bar{\mathfrak{r}}^*_0, R^*_0)\right) \subset \mathfrak{U}$.*

Remark 2.4.12. *In the context of the application of the Partial Lie Transform Method to the Gyro-Kinetic Coordinates, $\mathfrak{b}^{\#}(\bar{\mathfrak{r}}^*_0, R^*_0)$ (see* (2.4.36)*) is a set on which function $\boldsymbol{\kappa}$ is defined (see* (2.3.3)*,* (2.3.85) *and* (2.3.102)*), the Hamiltonian function is function $\bar{H}_\varepsilon$ defined by* (2.3.114) *and expanded in* (2.3.115) *and the Poisson Matrix is the matrix $\bar{\mathcal{P}}_\varepsilon$ defined by* (2.3.113)*. As already noticed, the Poisson matrix is clearly extensible to $\mathbb{R}^4$. The maximal open subset on which the N first terms of the Hamiltonian expansion in power of ε (see* (2.3.115)*) can be smoothly extended is $\mathbb{R}^2 \times \mathbb{R} \times (0, +\infty)$. Hence, one could think that a good choice for $\mathfrak{U}$ is $\mathbb{R}^2 \times \mathbb{R} \times (0, +\infty)$. Notice that $\mathfrak{b}^{\#}(\bar{\mathfrak{r}}^*_0, R^*_0) \subset \mathbb{R}^2 \times \mathbb{R} \times (0, +\infty)$. Yet with this choice, there is no reason for the requirement $\boldsymbol{\vartheta}^{i,j}_{\varepsilon,\bar{f}}\left(\mathfrak{b}^{\#}(\bar{\mathfrak{r}}^*_0, R^*_0)\right) \subset \mathbb{R}^2 \times \mathbb{R} \times (0, +\infty)$ to be satisfied.*
Nevertheless, according to the expression of the N first terms of the expansion in power of ε of the Hamiltonian function (see (2.3.115)*) we will be able to proceed as follows. We will choose functions $\bar{f}$ in $\mathcal{C}^\infty_{\#}\left(\mathbb{R}^2 \times \mathbb{R} \times (0, +\infty)\right)$. We will show that if $\overline{\mathfrak{b}^{\#}(\bar{\mathfrak{r}}^*_0, R^*_0)} \subset \mathbb{R}^2 \times \mathbb{R} \times (0, +\infty)$, then, for any $\mathfrak{r}_0$ in $\mathbb{R}^2 \times \mathbb{R} \times (0, +\infty)$ and any $R_0 > 0$ such that $\overline{\mathfrak{b}^{\#}(\bar{\mathfrak{r}}^*_0, R^*_0)} \subset \mathfrak{b}^{\#}(\mathfrak{r}_0, R_0)$ and $\overline{\mathfrak{b}^{\#}(\mathfrak{r}_0, R_0)} \subset \mathbb{R}^2 \times \mathbb{R} \times (0, +\infty)$, there exists a real number $\eta > 0$ such that for any $\varepsilon \in [-\eta, \eta]$, $\boldsymbol{\vartheta}^{i,j}_{\varepsilon,\bar{f}}\left(\mathfrak{b}^{\#}(\bar{\mathfrak{r}}^*_0, R^*_0)\right) \subset \mathfrak{b}^{\#}(\mathfrak{r}_0, R_0)$. Consequently, we will choose for $\mathfrak{U}$: $\mathfrak{b}^{\#}(\mathfrak{r}_0, R_0)$ with $\mathfrak{r}_0$ and R_0 properly chosen.*

Theorem 2.4.13. *Let i, j be two positive integers, $f \in \mathcal{C}^\infty_{\#}(\mathbb{R}^2 \times \mathbb{R} \times (0, +\infty))$, $\mathfrak{r}_0 \in \mathbb{R}^2 \times \mathbb{R} \times (0, +\infty)$, R_0 be such that $\overline{\mathfrak{b}^{\#}(\mathfrak{r}_0, R_0)} \subset \mathbb{R}^2 \times \mathbb{R} \times (0, +\infty)$ and R'_0 be such that $0 < R'_0 < R_0$. Then, there exists a real number $\eta > 0$ such, that for any $\varepsilon \in [-\eta, \eta]$, function $\boldsymbol{\vartheta}^{i,j}_{\varepsilon,f}$ is a diffeomorphism from $\mathfrak{b}^{\#}(\mathfrak{r}_0, R'_0)$ onto its range and such that*

$$\boldsymbol{\vartheta}^{i,j}_{\varepsilon,f}\left(\mathfrak{b}^{\#}(\mathfrak{r}_0, R'_0)\right) \subset \mathfrak{b}^{\#}(\mathfrak{r}_0, R_0). \tag{2.4.48}$$

The two following theorems are consequences of the previous one.

Theorem 2.4.14. *Let $\mathfrak{r}_0 \in \mathbb{R}^2 \times \mathbb{R} \times (0, +\infty)$ and $R_0 > 0$ be such that $\overline{\mathfrak{b}^{\#}(\bar{\mathfrak{r}}^*_0, R^*_0)} \subset \mathfrak{b}^{\#}(\mathfrak{r}_0, R_0)$, where $\bar{\mathfrak{r}}^*_0$, R^*_0 and $\mathfrak{b}^{\#}(\bar{\mathfrak{r}}^*_0, R^*_0)$ are set by* (2.4.37)*. Let $\bar{f} \in \mathcal{A}\big(\mathbb{R}^2 \times \mathbb{R} \times (0, +\infty)\big) \cap \mathcal{Q}^\infty_{T,b}$ (see definition* (2.3.117) *of $\mathcal{Q}^\infty_{T,b}$) and $i, j \in \mathbb{N}$ be such that $ij \geq N$, where N is fixed by* (2.4.33)*. Then, there exists a real number $\bar{\eta}_2 > 0$ such that for any $\varepsilon \in [-\bar{\eta}_2; \bar{\eta}_2]$*

$$\boldsymbol{\vartheta}^{i,j}_{\varepsilon,\bar{f}}\left(\mathfrak{b}^{\#}(\bar{\mathfrak{r}}^*_0, R^*_0)\right) \subset \mathfrak{b}^{\#}(\mathfrak{r}_0, R_0), \tag{2.4.49}$$

$\boldsymbol{\Xi}^{i,j}_{\varepsilon,f}$ is well defined and analytic on $\mathfrak{b}^{\#}(\mathfrak{r}_0, R_0)$, the components 1, 2 and 4 of $\boldsymbol{\Xi}^{i,j}_{\varepsilon,f}$ are in $\mathcal{C}^\infty_{\#}\left(\mathfrak{b}^{\#}(\mathfrak{r}_0, R_0)\right)$ and its penultimate component satisfies for any $\bar{\mathfrak{r}} \in \mathfrak{b}^{\#}(\mathfrak{r}_0, R_0)$:

$$\left(\boldsymbol{\Xi}^{i,j}_{\varepsilon,f}\right)_3(\bar{\mathfrak{r}}_1, \bar{\mathfrak{r}}_2, \bar{\mathfrak{r}}_3 + 2\pi, \bar{\mathfrak{r}}_4) = \left(\boldsymbol{\Xi}^{i,j}_{\varepsilon,f}\right)_3(\bar{\mathfrak{r}}_1, \bar{\mathfrak{r}}_2, \bar{\mathfrak{r}}_3, \bar{\mathfrak{r}}_4) + 2\pi. \tag{2.4.50}$$

Moreover, for any $\mathfrak{r} \in \mathfrak{b}^{\#}(\mathfrak{r}_0, R_0)$ *the following equality holds true :*

$$\Xi^{i,j}_{\varepsilon,\bar{f}}(\mathfrak{r}) = \vartheta^{i,j}_{\varepsilon,-\bar{f}}(\mathfrak{r}) + \varepsilon^{N+1}\boldsymbol{\rho}^{N}_{\Xi^{i,j}}(\varepsilon,\mathfrak{r}), \tag{2.4.51}$$

where $\boldsymbol{\rho}^{N}_{\Xi^{i,j}}$ *is in* $\mathcal{C}^{\infty}_{\#}\Big([-\bar{\eta}_2;\bar{\eta}_2]\times\mathfrak{b}^{\#}(\mathfrak{r}_0,R_0)\Big)$ *(see* (2.3.31)*).*

Theorem 2.4.15. *Let* $\mathfrak{r}_0 \in \mathbb{R}^2\times\mathbb{R}\times(0,+\infty)$ *and* $R_0 > 0$ *be such that* $\overline{\mathfrak{b}^{\#}(\mathfrak{r}_0,R_0)} \subset \mathbb{R}^2\times\mathbb{R}\times(0,+\infty)$*. Let* $\bar{f} \in \mathcal{A}\big(\mathbb{R}^2\times\mathbb{R}\times(0,+\infty)\big)\cap\mathcal{Q}^{\infty}_{T,b}$*,* $i,j\in\mathbb{N}$ *be such that* $ij \geq N$ *and* $\hat{\mathcal{P}}_\varepsilon$ *be the matrix whose entries are given, for* $k,l\in\{1,\dots,4\}$*, by*

$$\hat{\mathcal{P}}^{k,l}_{\varepsilon}(\mathfrak{r}) = \Big\{\Big(\vartheta^{i,j}_{\varepsilon,\bar{f}}\Big)_k, \Big(\vartheta^{i,j}_{\varepsilon,\bar{f}}\Big)_l\Big\}_{\bar{\mathfrak{r}}}\Big(\Xi^{i,j}_{\varepsilon,\bar{f}}(\mathfrak{r})\Big). \tag{2.4.52}$$

Then, for any $\mathfrak{b}^{\#}(\mathfrak{r}^{\star}_0,R^{\star}_{\mathfrak{r}_0})$ *such that* $\overline{\mathfrak{b}^{\#}(\mathfrak{r}^{\star}_0,R^{\star}_{\mathfrak{r}_0})}\subset\mathfrak{b}^{\#}(\mathfrak{r}_0,R_{\mathfrak{r}_0})$*, there exists a real number* $\bar{\eta}_3>0$ *such that for any* $\varepsilon\in[-\bar{\eta}_3,\bar{\eta}_3]$

$$\vartheta^{i,j}_{\varepsilon,\bar{f}}\Big(\mathfrak{b}^{\#}(\mathfrak{r}^{\star}_0,R^{\star}_{\mathfrak{r}_0})\Big)\subset\mathfrak{b}^{\#}(\mathfrak{r}_0,R_0), \tag{2.4.53}$$

and for any $\mathfrak{r}\in\mathfrak{b}^{\#}(\mathfrak{r}_0,R_0)$ *the following equality holds true :*

$$\forall k,l\in\{1,2,3,4\},\ \hat{\mathcal{T}}^{k,l}_{\varepsilon}(\mathfrak{r}) = \bar{\mathcal{T}}^{k,l}_{\varepsilon}(\mathfrak{r}) + \varepsilon^{N+1}\rho^{N,k,l}_{S}(\varepsilon,\mathfrak{r}), \tag{2.4.54}$$

where $\rho^{N,k,l}_{S}$ *is in* $\mathcal{C}^{\infty}_{\#}\Big([-\bar{\eta}_3,\bar{\eta}_3]\times\mathfrak{b}^{\#}(\mathfrak{r}_0,R_0)\Big)$ *and where* $\hat{\mathcal{T}}_\varepsilon$ *stands for the matrix which satisfies*

$$\hat{\mathcal{P}}_\varepsilon = \frac{1}{\varepsilon}\hat{\mathcal{T}}_\varepsilon. \tag{2.4.55}$$

Remark 2.4.16. *Formula* (2.4.54) *is written in terms of* $\hat{\mathcal{T}}_\varepsilon$ *because* $\hat{\mathcal{P}}_\varepsilon$ *has a singularity in* $\varepsilon=0$*. Considering* $\hat{\mathcal{T}}_\varepsilon$ *instead of* $\hat{\mathcal{P}}_\varepsilon$ *allows us to avoid having to distinguish between the cases* $\varepsilon=0$ *and* $\varepsilon\neq0$*. In formula* (2.4.52)*, we have rather written the formula using that* $\hat{\mathcal{P}}_\varepsilon$ *is the Poisson Matrix in the coordinate system* $\hat{\mathbf{r}}$*. This allows to understand why* $\hat{\mathcal{P}}_\varepsilon$ *is defined on a subset larger than* $\vartheta^{i,j}_{\varepsilon,\bar{f}}\Big(\mathfrak{b}^{\#}(\bar{\mathfrak{r}}^{*}_0,R^{*}_0)\Big)$*.*

The proof of these theorems are given in subsections 2.4.4, 2.4.5 and 2.4.6. They are essentially based on the basic properties of the Partial Lie Sums we will expose in the next subsection.

2.4.3 Basic Properties of the Partial Lie Sums

We will start this subsection with some topological properties.

Lemma 2.4.17. *Let* $\mathfrak{W}\subset\mathbb{R}^4$ *be an open set,* $f=f(\mathfrak{r})\in\mathcal{C}^{\infty}_{b}(\mathfrak{W})$ *and* $\mathbf{X}^{\varepsilon}_{\varepsilon f}$ *be the Hamiltonian vector field associated with* εf*. Then for any* $p\in\{1,\dots,4\}$ *and any* $k\geq1$*,* $\Big(\mathbf{X}^{\varepsilon}_{\varepsilon f}\Big)^k\cdot\mathbf{r}_p\in\mathcal{C}^{\infty}_{b}(\mathfrak{W})$*, where* $\mathbf{r}_p$ *is the p-th coordinate function and* $\Big(\mathbf{X}^{\varepsilon}_{\varepsilon f}\Big)^k\cdot$ *is the iterated application of* $\mathbf{X}^{\varepsilon}_{\varepsilon f}$ *as a differential operator acting on functions.*

Proof. By definition, $\mathbf{X}^{\varepsilon}_{\varepsilon f}=\bar{\mathcal{P}}_\varepsilon\nabla(\varepsilon f)$ and $\Big(\mathbf{X}^{\varepsilon}_{\varepsilon f}\Big)^1\cdot\mathbf{r}_p=\big(\bar{\mathcal{T}}_\varepsilon\nabla f\big)_p$. Hence, as all entries of $\bar{\mathcal{T}}_\varepsilon$ are in $\mathcal{C}^{\infty}_{b}\big(\mathbb{R}^4\big)$ and as f is in $\mathcal{C}^{\infty}_{b}(\mathfrak{W})$, so is $\Big(\mathbf{X}^{\varepsilon}_{\varepsilon f}\Big)^1\cdot\mathbf{r}_p$. An easy induction gives then the result. This ends the proof of Lemma 2.4.17. □

Lemma 2.4.18. *Let $\mathfrak{b}^{\#}(\mathfrak{r}_0, R_0)$ be an open periodic ball defined by (2.4.36), f be a function in $\mathcal{C}^{\infty}_{\#}\Big(\mathfrak{b}^{\#}(\mathfrak{r}_0, R_0)\Big)$ and i, j be two positive integers. Then, for every $R_0' > R_0$, there exists a real number $\eta_4 > 0$ such that*

$$\forall \varepsilon \in [-\eta_4, \eta_4]\,,\ \boldsymbol{\vartheta}^{i,j}_{\varepsilon,f}\left(\mathfrak{b}^{\#}(\mathfrak{r}_0, R_0)\right) \subset \mathfrak{b}^{\#}(\mathfrak{r}_0, R_0'). \tag{2.4.56}$$

Proof. From definitions (2.4.45) and (2.4.46), for any $\mathfrak{r} \in \mathfrak{b}^{\#}(\mathfrak{r}_0, R_0)$:

$$\begin{aligned}\boldsymbol{\vartheta}^{i,j}_{\varepsilon,f}(\mathfrak{r}) &= \left(\left(\sum_{k=0}^{i}\frac{\varepsilon^{jk}}{k!}\left(\mathbf{X}^{\varepsilon}_{\varepsilon f}\right)^k \cdot \mathbf{r}_1\right)(\mathfrak{r}), \ldots, \left(\sum_{k=0}^{i}\frac{\varepsilon^{jk}}{k!}\left(\mathbf{X}^{\varepsilon}_{\varepsilon f}\right)^k \cdot \mathbf{r}_4\right)(\mathfrak{r})\right) \\ &= \mathfrak{r} + \varepsilon \boldsymbol{\nu}^{i,j}_{\varepsilon,f}(\mathfrak{r}),\end{aligned} \tag{2.4.57}$$

where

$$\boldsymbol{\nu}^{i,j}_{\varepsilon,f}(\mathfrak{r}) = \left(\left(\sum_{k=1}^{i}\frac{\varepsilon^{jk-1}}{k!}\left(\mathbf{X}^{\varepsilon}_{\varepsilon f}\right)^k \cdot \mathbf{r}_1\right)(\mathfrak{r}), \ldots, \left(\sum_{k=1}^{i}\frac{\varepsilon^{jk-1}}{k!}\left(\mathbf{X}^{\varepsilon}_{\varepsilon f}\right)^k \cdot \mathbf{r}_4\right)(\mathfrak{r})\right). \tag{2.4.58}$$

According to Lemma 2.4.17, as f is in $\mathcal{C}^{\infty}_{b}\Big(\mathfrak{b}^{\#}(\mathfrak{r}_0, R_0)\Big)$, $\boldsymbol{\nu}^{i,j}_{\varepsilon,f}$ is in $\mathcal{C}^{\infty}_{b}\Big(\mathfrak{b}^{\#}(\mathfrak{r}_0, R_0)\Big)$, we can define

$$\left\|\boldsymbol{\nu}^{i,j}_{\varepsilon,f}\right\|_{\infty} = \sup_{\mathfrak{r}\in\mathfrak{b}^{\#}(\mathfrak{r}_0,R_0)}\left|\boldsymbol{\nu}^{i,j}_{\varepsilon,f}(\mathfrak{r})\right|. \tag{2.4.59}$$

Since $\varepsilon \mapsto \left\|\boldsymbol{\nu}^{i,j}_{\varepsilon,f}\right\|_{\infty}$ is smooth, $\varepsilon\left\|\boldsymbol{\nu}^{i,j}_{\varepsilon,f}\right\|_{\infty} \to 0$ when $\varepsilon \to 0$ and for all $c > 0$ there exists a real number η_4 such that for any $\varepsilon \in [-\eta_4, \eta_4]$, $\left|\varepsilon\left\|\boldsymbol{\nu}^{i,j}_{\varepsilon,f}\right\|_{\infty}\right| < c$. Let $c > 0$ such that $c < R_0' - R_0$, for any $\varepsilon \in [-\eta_4, \eta_4]$ and for any $\mathfrak{r} \in \mathfrak{b}^{\#}(\mathfrak{r}_0, R_0)$ we have

$$\left|\boldsymbol{\vartheta}^{i,j}_{\varepsilon,f}(\mathfrak{r}) - \mathfrak{r}_0\right|_{1,2,4} \leq |\mathfrak{r} - \mathfrak{r}_0|_{1,2,4} + \left|\varepsilon\boldsymbol{\nu}^{i,j}_{\varepsilon,f}(\mathfrak{r})\right|_{1,2,4} \leq R_0 + c < R_0' \tag{2.4.60}$$

This proves that $\boldsymbol{\vartheta}^{i,j}_{\varepsilon,f}\Big(\mathfrak{b}^{\#}(\mathfrak{r}_0, R_0)\Big) \subset \mathfrak{b}^{\#}(\mathfrak{r}_0, R_0')$ and ends the proof of Lemma 2.4.18. □

Lemma 2.4.19. *Let $\mathfrak{b}^{\#}(\mathfrak{r}_0, R_0)$ be an open periodic ball defined by (2.4.36), f be a function in $\mathcal{C}^{\infty}_{\#}\Big(\mathfrak{b}^{\#}(\mathfrak{r}_0, R_0)\Big)$ and i, j be two positive integers. Then, for any real number R_0' such that $0 < R_0' < R_0$, there exists a real number η such that for any $\varepsilon \in [-\eta, \eta]$*

$$\boldsymbol{\vartheta}^{i,j}_{\varepsilon,f}\Big(\mathfrak{b}^{\#}(\mathfrak{r}_0, R_0)\Big) \supset \mathfrak{b}^{\#}(\mathfrak{r}_0, R_0'). \tag{2.4.61}$$

Proof. Here again, we will use expression (2.4.57) of $\boldsymbol{\vartheta}^{i,j}_{\varepsilon,f}$. The proof of Lemma 2.4.19 is based on the Brouwer Theorem (see Brouwer [6] or Istratescu [34]). Let $R_0^{(2)}$, $R_0^{(3)}$, $\alpha_0^{(2)}$ and $\alpha_0^{(3)}$ be real numbers satisfying $R_0' < R_0^{(2)} < R_0^{(3)} < R_0$ and $0 < \alpha_0^{(2)} < \alpha_0^{(3)}$, l be an integer, and let $\mathfrak{K}^{l}_{\mathfrak{r}_0,R_0^{(2)},\alpha_0^{(2)}}$ and $\mathfrak{K}^{l}_{\mathfrak{r}_0,R_0^{(3)},\alpha_0^{(3)}}$ be the compact and convex subsets of $\mathbb{R}^4$ defined by

$$\mathfrak{K}^{l}_{\mathfrak{r}_0,R_0^{(2)},\alpha_0^{(2)}} = \left\{\mathfrak{r} \in \mathbb{R}^4,\ |\mathfrak{r} - \mathfrak{r}_0|_{1,2,4} \leq R_0^{(2)} \text{ and } \mathfrak{r}_3 \in \left[(l-1)\,\pi - \alpha_0^{(2)}, (l+1)\,\pi + \alpha_0^{(2)}\right]\right\} \tag{2.4.62}$$

and

$$\mathfrak{K}^l_{\mathfrak{r}_0,R_0^{(3)},\alpha_0^{(3)}}=\left\{\mathfrak{r}\in\mathbb{R}^4,\ \left|\mathfrak{r}-\mathfrak{r}_0\right|_{1,2,4}\leq R_0^{(3)}\text{ and }\mathfrak{r}_3\in\left[(l-1)\,\pi-\alpha_0^{(3)},(l+1)\,\pi+\alpha_0^{(3)}\right]\right\}. \tag{2.4.63}$$

Since $\varepsilon\left\|\boldsymbol{\nu}^{i,j}_{\varepsilon,f}\right\|_\infty\to 0$ when $\varepsilon\to 0$, we can define $\eta>0$ such that for any $\varepsilon\in[-\eta,\eta]$, for any $l\in\mathbb{Z}$, and for any $\mathfrak{r}'\in\mathfrak{K}^l_{\mathfrak{r}_0,R_0^{(2)},\alpha_0^{(2)}}$,

$$\left|\mathfrak{r}'-\mathfrak{r}_0\right|_{1,2,4}+|\varepsilon|\left\|\boldsymbol{\nu}^{i,j}_{\varepsilon,f}\right\|_\infty\leq R_0^{(3)}, \tag{2.4.64}$$

and

$$\left|\mathfrak{r}'_3-l\pi\right|+|\varepsilon|\left\|\boldsymbol{\nu}^{i,j}_{\varepsilon,f}\right\|_\infty\leq\alpha_0^{(3)}. \tag{2.4.65}$$

Now, for all $\mathfrak{r}'\in\mathfrak{K}^l_{\mathfrak{r}_0,R_0^{(2)},\alpha_0^{(2)}}$, we define the function $F^\varepsilon_{\mathfrak{r}'}$ by

$$F^\varepsilon_{\mathfrak{r}'}:\ \mathfrak{K}^l_{\mathfrak{r}_0,R_0^{(3)},\alpha_0^{(3)}}\to\mathbb{R}^4;\ \mathfrak{r}\mapsto\mathfrak{r}'-\varepsilon\boldsymbol{\nu}^{i,j}_{\varepsilon,f}(\mathfrak{r}). \tag{2.4.66}$$

By construction and because of the properties of $\boldsymbol{\nu}^{i,j}_{\varepsilon,f}$, $F^\varepsilon_{\mathfrak{r}'}$ is continuous on $\mathfrak{K}^l_{\mathfrak{r}_0,R_0^{(3)},\alpha_0^{(3)}}$ and for any $\varepsilon\in[-\eta,\eta]$ and any $\mathfrak{r}\in\mathfrak{K}^l_{\mathfrak{r}_0,R_0^{(3)},\alpha_0^{(3)}}$,

$$\left|F^\varepsilon_{\mathfrak{r}'}(\mathfrak{r})-\mathfrak{r}_0\right|_{1,2,4}\leq\left|\mathfrak{r}'-\mathfrak{r}_0\right|_{1,2,4}+|\varepsilon|\left|\boldsymbol{\nu}^{i,j}_{\varepsilon,f}(\mathfrak{r})\right|_{1,2,3}<R_0^{(3)}, \tag{2.4.67}$$

and

$$\left|(F^\varepsilon_{\mathfrak{r}'}(\mathfrak{r}))_3-l\pi\right|\leq\left|\mathfrak{r}'_3-l\pi\right|+|\varepsilon|\left|\left(\boldsymbol{\nu}^{i,j}_{\varepsilon,f}(\mathfrak{r})\right)_3\right|\leq\alpha_0^{(3)}, \tag{2.4.68}$$

meaning $F^\varepsilon_{\mathfrak{r}'}\left(\mathfrak{K}^l_{\mathfrak{r}_0,R_0^{(3)},\alpha_0^{(3)}}\right)\subset\mathfrak{K}^l_{\mathfrak{r}_0,R_0^{(3)},\alpha_0^{(3)}}$. Hence, invoking the Brouwer Theorem and more precisely its convex compact version, function $F^\varepsilon_{\mathfrak{r}'}$ has a fixed point in $\mathfrak{K}^l_{\mathfrak{r}_0,R_0^{(3)},\alpha_0^{(3)}}$. So we have proven that

$$\exists\eta>0,\ \forall\varepsilon,|\varepsilon|<\eta,\ \forall l\in\mathbb{Z},\ \forall\mathfrak{r}'\in\mathfrak{K}^l_{\mathfrak{r}_0,R_0^{(2)},\alpha_0^{(2)}},\ \exists\mathfrak{r}\in\mathfrak{K}^l_{\mathfrak{r}_0,R_0^{(3)},\alpha_0^{(3)}},\ \boldsymbol{\vartheta}^{i,j}_{\varepsilon,f}(\mathfrak{r})=\mathfrak{r}', \tag{2.4.69}$$

proving $\boldsymbol{\vartheta}^{i,j}_{\varepsilon,f}\left(\mathfrak{K}^l_{\mathfrak{r}_0,R_0^{(3)},\alpha_0^{(3)}}\right)\supset\mathfrak{K}^l_{\mathfrak{r}_0,R_0^{(2)},\alpha_0^{(2)}}$ and consequently, since η does not depend on l, that

$$\boldsymbol{\vartheta}^{i,j}_{\varepsilon,f}\left(\underset{l\in\mathbb{Z}}{\cup}\mathfrak{K}^l_{\mathfrak{r}_0,R_0^{(3)},\alpha_0^{(3)}}\right)\supset\underset{l\in\mathbb{Z}}{\cup}\mathfrak{K}^l_{\mathfrak{r}_0,R_0^{(2)},\alpha_0^{(2)}}. \tag{2.4.70}$$

Since $\overline{\mathfrak{b}^\#\left(\mathfrak{r}_0,R_0^{(3)}\right)}=\underset{l\in\mathbb{Z}}{\cup}\mathfrak{K}^l_{\mathfrak{r}_0,R_0^{(3)},\alpha_0^{(3)}}$ and $\overline{\mathfrak{b}^\#\left(\mathfrak{r}_0,R_0^{(2)}\right)}=\underset{l\in\mathbb{Z}}{\cup}\mathfrak{K}^l_{\mathfrak{r}_0,R_0^{(2)},\alpha_0^{(2)}}$, (2.4.70) can be rewritten as $\boldsymbol{\vartheta}^{i,j}_{\varepsilon,f}\left(\overline{\mathfrak{b}^\#\left(\mathfrak{r}_0,R_0^{(3)}\right)}\right)\supset\overline{\mathfrak{b}^\#\left(\mathfrak{r}_0,R_0^{(2)}\right)}$. Finally, since $\mathfrak{b}^\#(\mathfrak{r}_0,R'_0)\subset\overline{\mathfrak{b}^\#\left(\mathfrak{r}_0,R_0^{(2)}\right)}$ and $\overline{\mathfrak{b}^\#\left(\mathfrak{r}_0,R_0^{(3)}\right)}\subset\mathfrak{b}^\#(\mathfrak{r}_0,R_0)$ we obtain (2.4.61). This ends the proof of Lemma 2.4.19. □

Lemma 2.4.19 ensures that, if $\boldsymbol{\vartheta}^{i,j}_{\varepsilon,f}$ is invertible with $\boldsymbol{\Xi}^{i,j}_{\varepsilon,f}$ as inverse function, for sufficiently small ε we have :

$$\boldsymbol{\Xi}^{i,j}_{\varepsilon,f}\Big(\mathfrak{b}^{\#}(\mathfrak{r}_0, R_0')\Big) \subset \mathfrak{b}^{\#}(\mathfrak{r}_0, R_0). \tag{2.4.71}$$

Now, we will focus on more algebraic properties. In definition 2.4.7 we used Hamiltonian vector fields. The reason why chosing this class of vector fields is related to the following lemma and its consequences.

Lemma 2.4.20. *Let $f = f(\mathfrak{r})$, $g = g(\mathfrak{r})$ and $h = h(\mathfrak{r})$ be three smooth functions defined on an open subset $\mathfrak{M} \subset \mathbb{R}^4$. Then, for all $n \geq 1$, the following equality holds true on $\mathfrak{M}$:*

$$\left(\mathbf{X}^{\varepsilon}_{\varepsilon f}\right)^n \cdot \{g,h\} = \sum_{k=0}^{n} C_n^k \left\{ \left(\mathbf{X}^{\varepsilon}_{\varepsilon f}\right)^k \cdot g, \left(\mathbf{X}^{\varepsilon}_{\varepsilon f}\right)^{n-k} \cdot h \right\}, \tag{2.4.72}$$

where $\mathbf{X}^{\varepsilon}_{\varepsilon f}$ is the Hamiltonian vector field associated with εf, $\left(\mathbf{X}^{\varepsilon}_{\varepsilon f}\right)^n \cdot$ its iterated application as a differential operator and $\{g,h\}$ the Poisson Bracket between functions g and h.

Proof. This proof is easily obtained by induction. The key point of the proof is the following equality

$$\mathbf{X}^{\varepsilon}_{\varepsilon f} \cdot \{g,h\} = \left\{\mathbf{X}^{\varepsilon}_{\varepsilon f} \cdot g, h\right\} + \left\{g, \mathbf{X}^{\varepsilon}_{\varepsilon f} \cdot h\right\}, \tag{2.4.73}$$

which is a direct consequence of the Jacoby identity and which is specific to Hamiltonian vector fields. □

Another result, which does not require the Hamiltonian nature of the vector field, is the following lemma.

Lemma 2.4.21. *Let $g = g(\mathfrak{r})$ and $h = h(\mathfrak{r})$ be two smooth functions defined on an open subset $\mathfrak{M} \subset \mathbb{R}^4$ and $\mathfrak{X}$ be a smooth vector field defined on $\mathfrak{M}$. Then, for all $p \geq 0$, the following equality holds true on $\mathfrak{M}$:*

$$(\mathfrak{X})^p \cdot (gh) = \sum_{k=0}^{p} C_p^k \Big((\mathfrak{X})^k \cdot g\Big) \Big((\mathfrak{X})^{p-k} \cdot h\Big). \tag{2.4.74}$$

As consequence of the previous lemmas, we will now see that operator $\boldsymbol{\vartheta}^{i,j}_{\varepsilon,f}\cdot$ almost commutes with the Poisson Bracket and the product between two functions. More precisely, we have

Property 2.4.22. *Let $\mathfrak{M} \subset \mathbb{R}^4$ be an open subset, $f = f(\mathfrak{r})$, $g = g(\mathfrak{r})$ and $h = h(\mathfrak{r})$ be three functions in $\mathcal{C}^\infty(\mathfrak{M})$ and i,j be two positive integers. If $ij \geq N$, then the following equality holds true for every $\mathfrak{r}$ in $\mathfrak{M}$:*

$$\Big(\boldsymbol{\vartheta}^{i,j}_{\varepsilon,f} \cdot \{g,h\}\Big)(\mathfrak{r}) = \Big\{\boldsymbol{\vartheta}^{i,j}_{\varepsilon,f} \cdot g, \boldsymbol{\vartheta}^{i,j}_{\varepsilon,f} \cdot h\Big\}(\mathfrak{r}) + \varepsilon^N \rho^{N,i,j}_{PC}(\varepsilon, \mathfrak{r}), \tag{2.4.75}$$

where operator $\boldsymbol{\vartheta}^{i,j}_{\varepsilon,f}$ is defined by (2.4.45) and where $\rho^{N,i,j}_{PC}$ is in $\mathcal{C}^\infty(\mathbb{R} \times \mathfrak{M})$.

Proof. Firstly, we will define on $\mathfrak{M}$ the function $\{g,h\}^{\bar{\mathcal{T}}_\varepsilon} = \{g,h\}^{\bar{\mathcal{T}}_\varepsilon}(\mathfrak{r})$ by

$$\{g,h\}^{\bar{\mathcal{T}}_\varepsilon}(\mathfrak{r}) = \big(\bar{\mathcal{T}}_\varepsilon(\mathfrak{r})\,\nabla h(\mathfrak{r})\big)\cdot(\nabla g(\mathfrak{r}))\,, \tag{2.4.76}$$

and we notice that $\varepsilon \mapsto \{g,h\}^{\bar{\mathcal{T}}_\varepsilon}(\mathfrak{r})$ is in $\mathcal{C}^\infty(\mathbb{R})$ for any $\mathfrak{r}\in\mathfrak{M}$.

Now, expanding $\boldsymbol{\vartheta}^{i,j}_{\varepsilon,f}\cdot\{g,h\}$ using Lemma 2.4.20, expanding $\Big\{\boldsymbol{\vartheta}^{i,j}_{\varepsilon,f}\cdot g, \boldsymbol{\vartheta}^{i,j}_{\varepsilon,f}\cdot h\Big\}$, and making the difference between these two expansions yields (2.4.75) with

$$\rho^{N,i,j}_{PC}(\varepsilon,\mathfrak{r}) = -\sum_{k=i+1}^{2i}\varepsilon^{jk-(N+1)}\sum_{(m,p)\in\{1,\dots,i\}^2\ s.t.\ m+p=k}\frac{1}{m!p!}\left\{\left(\mathbf{X}^\varepsilon_{\varepsilon f}\right)^m\cdot g, \left(\mathbf{X}^\varepsilon_{\varepsilon f}\right)^p\cdot h\right\}^{\bar{\mathcal{T}}_\varepsilon}(\mathfrak{r})\,. \tag{2.4.77}$$

As $ij\geq N$, all $k\geq i+1$ satisfy $jk\geq N+1$. Hence $\varepsilon\mapsto\rho^{N,i,j}_{PC}(\varepsilon,\mathfrak{r})$ is in $\mathcal{C}^\infty(\mathbb{R})$ for any $\mathfrak{r}\in\mathfrak{M}$. In addition, $\mathfrak{r}\mapsto\rho^{N,i,j}_{PC}(\varepsilon,\mathfrak{r})$ is clearly in $\mathcal{C}^\infty(\mathfrak{M})$ for any $\varepsilon\in\mathbb{R}$. This ends the proof of Property 2.4.22. □

Property 2.4.23. *Let $\mathfrak{M}\subset\mathbb{R}^4$ be an open subset, $f=f(\mathfrak{r})$, $g=g(\mathfrak{r})$ and $h=h(\mathfrak{r})$ be three functions in $\mathcal{C}^\infty(\mathfrak{M})$ and i,j be two positive integers. Then, if $ij\geq N$, the following equality holds true on $\mathfrak{M}$:*

$$\Big(\boldsymbol{\vartheta}^{i,j}_{\varepsilon,f}\cdot(gh)\Big)(\mathfrak{r}) = \Big(\boldsymbol{\vartheta}^{i,j}_{\varepsilon,f}\cdot g\Big)(\mathfrak{r})\,\Big(\boldsymbol{\vartheta}^{i,j}_{\varepsilon,f}\cdot h\Big)(\mathfrak{r}) + \varepsilon^{N+1}\rho^{N,i,j}_{FP}(\varepsilon,\mathfrak{r})\,, \tag{2.4.78}$$

where $\rho^{N,i,j}_{FP}$ is in $\mathcal{C}^\infty(\mathbb{R}\times\mathfrak{M})$.

We will now end this subsection by giving the following important property claiming that $\boldsymbol{\vartheta}^{i,j}_{\varepsilon,f}\cdot$ and $\circ\,\boldsymbol{\vartheta}^{i,j}_{\varepsilon,f}$ almost commute.

Theorem 2.4.24. *Let $\mathfrak{N}\in\mathbb{R}^3$ be an open subset such that $\overline{\mathfrak{N}}$ is a compact subset of $\mathbb{R}^2\times(0,+\infty)$; $\mathfrak{M}^\#$ be the open subset of $\mathbb{R}^2\times\mathbb{R}\times(0,+\infty)$ defined by*

$$\mathfrak{M}^\# = \big\{\mathfrak{r}\in\mathbb{R}^2\times\mathbb{R}\times(0,+\infty)\,,\ (\mathfrak{r}_1,\mathfrak{r}_2,\mathfrak{r}_4)\in\mathfrak{N}\ \textit{and}\ \mathfrak{r}_3\in\mathbb{R}\big\}\,; \tag{2.4.79}$$

$\mathcal{O}\subset\mathbb{R}^2\times(0,+\infty)$ be an open subset such that $\overline{\mathfrak{N}}\subset\mathcal{O}$ and $\mathcal{O}^\#$ be the open subset of $\mathbb{R}^2\times\mathbb{R}\times(0,+\infty)$ defined by

$$\mathcal{O}^\# = \big\{\mathfrak{r}\in\mathbb{R}^2\times\mathbb{R}\times(0,+\infty)\,,\ (\mathfrak{r}_1,\mathfrak{r}_2,\mathfrak{r}_4)\in\mathcal{O}\ \textit{and}\ \mathfrak{r}_3\in\mathbb{R}\big\}\,; \tag{2.4.80}$$

$f=f(\mathfrak{r})\in\mathcal{C}^\infty_\#\big(\mathcal{O}^\#\big)$ (see (2.3.31)) ; $g_\varepsilon=g_\varepsilon(\mathfrak{r})\in\mathcal{A}\big(\mathbb{R}^3\times(0,+\infty)\big)\cap\mathcal{Q}^\infty_{T,b}$ (see Definition 2.4.2 and (2.3.117)) for every ε in some interval I containing 0 and $\varepsilon\mapsto g_\varepsilon(\mathfrak{r})$ be in $\mathcal{C}^\infty(I)$ for any $\mathfrak{r}\in\mathfrak{M}^\#$; and i,j be two positive integers such that $ij\geq N$. Then, there exists a real number $\bar\eta_5>0$ such that for any $\varepsilon\in[-\bar\eta_5,\bar\eta_5]\cap I$ the following equality holds true for any $\mathfrak{r}$ in $\mathfrak{M}^\#$:

$$\Big(g_\varepsilon\circ\boldsymbol{\vartheta}^{i,j}_{\varepsilon,f}\Big)(\mathfrak{r}) = \Big(\boldsymbol{\vartheta}^{i,j}_{\varepsilon,f}\cdot g_\varepsilon\Big)(\mathfrak{r}) + \varepsilon^{N+1}\rho^{N,i,j}_{FC}(\varepsilon,\mathfrak{r})\,, \tag{2.4.81}$$

where $\boldsymbol{\vartheta}^{i,j}_{\varepsilon,f}$ stands for the function defined by (2.4.46) in the left hand side of the equality and for operator defined by (2.4.45) in the right hand side and where $\rho^{N,i,j}_{FC}$ is in $\mathcal{C}^\infty_\#\big(([-\bar\eta_5,\bar\eta_5]\cap I)\times\mathfrak{M}^\#\big)$.

Proof. Since $g_\varepsilon \in \mathcal{Q}^\infty_{T,b}$, there exists a finite set $\mathbb{I}_{g_\varepsilon} \subset \mathbb{Z}$ and $(c^\varepsilon_n)_{n\in\mathbb{I}_{g_\varepsilon}} \in \left(\mathcal{O}^\infty_{T,b}\right)^{\mathbb{I}_{g_\varepsilon}}$ such that $g_\varepsilon(\mathfrak{r}) = \sum_{n\in\mathbb{I}_{g_\varepsilon}} c^\varepsilon_n(\mathfrak{r}_1,\mathfrak{r}_2,\mathfrak{r}_3)\sqrt{\mathfrak{r}_4}^n$. Moreover, for each $n \in \mathbb{I}_{g_\varepsilon}$, c^ε_n corresponds to a finite sum of terms of the form $\cos^{n_l}(\mathfrak{r}_3)\sin^{n_m}(\mathfrak{r}_3)\, d^\varepsilon_{n_p}(\mathfrak{r}_1,\mathfrak{r}_2)$, where $d^\varepsilon_{n_p} \in \mathcal{C}^\infty_b\big(\mathbb{R}^2\big)$. Now, as $g_\varepsilon \in \mathcal{A}\big(\mathbb{R}^2\times\mathbb{R}\times(0,+\infty)\big)$, the $d^\varepsilon_{n_p}$ belong to $\mathcal{A}\big(\mathbb{R}^2\big)$. Consequently, by linearity, the proof of the theorem reduces to prove formula (2.4.81) with function g_ε of the form $g_\varepsilon(\mathfrak{r}) = \cos^l(\mathfrak{r}_3)\sin^m(\mathfrak{r}_3)\, d^\varepsilon(\mathfrak{r}_1,\mathfrak{r}_2)\sqrt{\mathfrak{r}_4}^n$, where $d^\varepsilon = d^\varepsilon(\mathfrak{r}_1,\mathfrak{r}_2) \in \mathcal{A}\big(\mathbb{R}^2\big)\cap\mathcal{C}^\infty_b\left(\mathbb{R}^2\right)$. This is what we will do.

Let $\mathfrak{r}_0 \in \mathcal{O}^\#$. As $d^\varepsilon \in \mathcal{A}\big(\mathbb{R}^2\big)$, and as $(\mathfrak{r}_4 \mapsto \sqrt{\mathfrak{r}_4}^n) \in \mathcal{A}((0,+\infty))$, there exists a real number $R_{\mathfrak{r}_0} > 0$ and a formal power series $T_{\mathfrak{r}_0}$ of three variables which set of convergence contains the closure $\overline{\mathfrak{b}^3(0,R_{\mathfrak{r}_0})}$ of the Euclidian ball of dimension 3, which is such that $\mathfrak{b}^3(((\mathfrak{r}_0)_1,(\mathfrak{r}_0)_2,(\mathfrak{r}_0)_4),R_{\mathfrak{r}_0}) \subset \mathcal{O}$ and such that $\forall(\mathfrak{r}_1,\mathfrak{r}_2,\mathfrak{r}_4) \in \mathfrak{b}^3(((\mathfrak{r}_0)_1,(\mathfrak{r}_0)_2,(\mathfrak{r}_0)_4),R_{\mathfrak{r}_0})$,

$$\begin{aligned} d(\mathfrak{r}_1,\mathfrak{r}_2)\sqrt{\mathfrak{r}_4}^n =& T_{\mathfrak{r}_0}((\mathfrak{r}_1,\mathfrak{r}_2,\mathfrak{r}_4) - ((\mathfrak{r}_0)_1,(\mathfrak{r}_0)_2,(\mathfrak{r}_0)_4)) && (2.4.82)\\ =& \sum_{\mathbf{l}\in\mathbb{N}^3} a^{l,\mathfrak{r}_0}_\varepsilon\left((\mathfrak{r}_1,\mathfrak{r}_2,\mathfrak{r}_4) - ((\mathfrak{r}_0)_1,(\mathfrak{r}_0)_2,(\mathfrak{r}_0)_4)\right)^{\mathbf{l}}. && (2.4.83)\end{aligned}$$

In addition, since $\left(\mathfrak{r}_3 \mapsto \cos^l(\mathfrak{r}_3)\sin^m(\mathfrak{r}_3)\right)$ is a power series of radius $+\infty$ with respect to $\mathfrak{r}_3$, there exists a formal power series $S_{\mathfrak{r}_0}$ such that $\overline{\mathfrak{b}^\#(0,R_{\mathfrak{r}_0})} \subset \mathbf{\Sigma}_{S_{\mathfrak{r}_0}}$ (see (2.4.41)), $\mathfrak{b}^\#(\mathfrak{r}_0,R_{\mathfrak{r}_0}) \subset \mathcal{O}^\#$ and such that

$$\forall \mathfrak{r} \in \mathfrak{b}^\#(\mathfrak{r}_0,R_{\mathfrak{r}_0}),\ g_\varepsilon(\mathfrak{r}) = S_{\mathfrak{r}_0}(\mathfrak{r}-\mathfrak{r}_0) = \sum_{\mathbf{l}\in\mathbb{N}^4} g^{l,\mathfrak{r}_0}_\varepsilon\,(\mathfrak{r}-\mathfrak{r}_0)^{\mathbf{l}}. \tag{2.4.84}$$

Let $R'_{\mathfrak{r}_0} \in (0,R_{\mathfrak{r}_0})$. According to Lemma 2.4.18, there exists a real number $\eta_{R_{\mathfrak{r}_0},R'_{\mathfrak{r}_0}} > 0$ such that for any $\varepsilon \in \left[-\eta_{R_{\mathfrak{r}_0},R'_{\mathfrak{r}_0}},\eta_{R_{\mathfrak{r}_0},R'_{\mathfrak{r}_0}}\right]$, $\boldsymbol{\vartheta}^{i,j}_{\varepsilon,f}\left(\mathfrak{b}^\#\left(\mathfrak{r}_0,R'_{\mathfrak{r}_0}\right)\right) \subset \mathfrak{b}^\#(\mathfrak{r}_0,R_{\mathfrak{r}_0})$. Hence, for any $\mathfrak{r} \in \mathfrak{b}^\#\left(\mathfrak{r}_0,R'_{\mathfrak{r}_0}\right)$, we have

$$g_\varepsilon\left(\boldsymbol{\vartheta}^{i,j}_{\varepsilon,f}(\mathfrak{r})\right) = \sum_{\mathbf{l}\in\mathbb{N}^4} g^{l,\mathfrak{r}_0}_\varepsilon\left(\boldsymbol{\vartheta}^{i,j}_{\varepsilon,f}(\mathfrak{r}) - \mathfrak{r}_0\right)^{\mathbf{l}}. \tag{2.4.85}$$

On another hand, let $\Theta_\varepsilon = \Theta_\varepsilon(\mathfrak{r}) = (\Theta_{\varepsilon,\mathbf{m}}(\mathfrak{r}))_{\mathbf{m}\in\mathbb{N}^4\ s.t.\ |\mathbf{m}|\le i}$ be the smooth function satisfying for all smooth functions h_ε,

$$\left(\boldsymbol{\vartheta}^{i,j}_{\varepsilon,f}\cdot h_\varepsilon\right)(\mathfrak{r}) = \sum_{|\mathbf{m}|\le i} \Theta_{\varepsilon,\mathbf{m}}(\mathfrak{r})\,\frac{\partial h_\varepsilon}{\partial \mathfrak{r}^{\mathbf{m}}}(\mathfrak{r}). \tag{2.4.86}$$

We have, for any $\mathfrak{r} \in \mathfrak{b}^\#(\mathfrak{r}_0,R_{\mathfrak{r}_0})$,

$$\left(\boldsymbol{\vartheta}^{i,j}_{\varepsilon,f}\cdot g_\varepsilon\right)(\mathfrak{r}) = \sum_{|\mathbf{m}|\le i} \Theta_{\varepsilon,\mathbf{m}}(\mathfrak{r})\frac{\partial g_\varepsilon}{\partial \mathfrak{r}^{\mathbf{m}}}(\mathfrak{r}) = \left(\sum_{|\mathbf{m}|\le i}\Theta_{\varepsilon,\mathbf{m}}(\mathfrak{r})\,\frac{\partial}{\partial\mathfrak{r}^{\mathbf{m}}}\right)\left(\sum_{\mathbf{l}\in\mathbb{N}^4} g^{l,\mathfrak{r}_0}_\varepsilon\,\mathbf{r}^{\mathbf{l}}_{\mathfrak{r}_0}\right)(\mathfrak{r}), \tag{2.4.87}$$

where $\mathbf{r}^{\mathbf{l}}_{\mathfrak{r}_0}$ stand for the function $\mathfrak{r} \mapsto (\mathfrak{r}_1-(\mathfrak{r}_0)_1)^{l_1}(\mathfrak{r}_2-(\mathfrak{r}_0)_2)^{l_2}(\mathfrak{r}_3-(\mathfrak{r}_0)_3)^{l_3}(\mathfrak{r}_4-(\mathfrak{r}_0)_4)^{l_4}$.

Since $\mathfrak{b}^\#(0,R_{\mathfrak{r}_0}) \subset \mathbf{\Sigma}_{S_{\mathfrak{r}_0}}$, we can permute sum and derivatives and we obtain :

$$\left(\boldsymbol{\vartheta}^{i,j}_{\varepsilon,f}\cdot g_\varepsilon\right)(\mathfrak{r}) = \sum_{|\mathbf{m}|\le i}\Theta_{\varepsilon,\mathbf{m}}(\mathfrak{r})\sum_{\mathbf{l}\in\mathbb{N}^4} g^{l,\mathfrak{r}_0}_\varepsilon\frac{\partial \mathbf{r}^{\mathbf{l}}_{\mathfrak{r}_0}}{\partial\mathfrak{r}^m}(\mathfrak{r}) = \sum_{\mathbf{l}\in\mathbb{N}^4} g^{\mathbf{l},\mathfrak{r}_0}_\varepsilon\left(\boldsymbol{\vartheta}^{i,j}_{\varepsilon,f}\cdot\mathbf{r}^{\mathbf{l}}_{\mathfrak{r}_0}\right)(\mathfrak{r}). \tag{2.4.88}$$

Besides, using Property 2.4.23 and the link (2.4.46) between function $\boldsymbol{\vartheta}^{i,j}_{\varepsilon,f}$ and operator $\boldsymbol{\vartheta}^{i,j}_{\varepsilon,f}$, we obtain that, for any $\mathbf{l}\in\mathbb{N}^4$,

$$\begin{aligned}\left(\boldsymbol{\vartheta}^{i,j}_{\varepsilon,f}\cdot\mathbf{r}^{\mathbf{l}}_{\mathfrak{r}_0}\right)(\mathfrak{r}) &= \left(\boldsymbol{\vartheta}^{i,j}_{\varepsilon,f}\cdot(\mathbf{r}_1-(\mathfrak{r}_0)_1),\dots,\boldsymbol{\vartheta}^{i,j}_{\varepsilon,f}\cdot(\mathbf{r}_4-(\mathfrak{r}_0)_4)\right)^{\mathbf{l}}(\mathfrak{r})+\varepsilon^{N+1}\rho^{N,i,j}_{\mathbf{l},\mathfrak{r}_0}(\varepsilon,\mathfrak{r})\\ &= \left(\left(\boldsymbol{\vartheta}^{i,j}_{\varepsilon,f}\cdot\mathbf{r}_1,\dots,\boldsymbol{\vartheta}^{i,j}_{\varepsilon,f}\cdot\mathbf{r}_4\right)(\mathfrak{r})-\mathfrak{r}_0\right)^{\mathbf{l}}+\varepsilon^{N+1}\rho^{N,i,j}_{\mathbf{l},\mathfrak{r}_0}(\varepsilon,\mathfrak{r})\\ &= \left(\boldsymbol{\vartheta}^{i,j}_{\varepsilon,f}(\mathfrak{r})-\mathfrak{r}_0\right)^{\mathbf{l}}+\varepsilon^{N+1}\rho^{N,i,j}_{\mathbf{l},\mathfrak{r}_0}(\varepsilon,\mathfrak{r})\,.\end{aligned} \tag{2.4.89}$$

As both $\sum\limits_{\mathbf{l}\in\mathbb{N}^4} g^{l,\mathfrak{r}_0}_{\varepsilon}\left(\boldsymbol{\vartheta}^{i,j}_{\varepsilon,f}(\mathfrak{r})-\mathfrak{r}_0\right)^{\mathbf{l}}$ and $\sum\limits_{\mathbf{l}\in\mathbb{N}^4} g^{\mathbf{l},\mathfrak{r}_0}_{\varepsilon}\left(\boldsymbol{\vartheta}^{i,j}_{\varepsilon,f}\cdot\mathbf{r}^{\mathbf{l}}_{\mathfrak{r}_0}\right)(\mathfrak{r})$ converge normally on subset $\mathfrak{b}^{\#}\big(\mathfrak{r}_0,R'_{\mathfrak{r}_0}\big)\cap\big(\mathbb{R}^2\times[a,b]\times\mathbb{R}\big)$ for any compact set $[a,b]\subset\mathbb{R}$, their difference

$$\varepsilon^{N+1}\left(-\sum_{\mathbf{l}\in\mathbb{N}^4} g^{\mathbf{l},\mathfrak{r}_0}_{\varepsilon}\rho^{N,i,j}_{\mathbf{l},\mathfrak{r}_0}(\varepsilon,\mathfrak{r})\right) \tag{2.4.90}$$

also converges normally on this subset and we can deduce that, for any $\mathfrak{r}\in\mathfrak{b}^{\#}\big(\mathfrak{r}_0,R'_{\mathfrak{r}_0}\big)$,

$$\left(g_\varepsilon\circ\boldsymbol{\vartheta}^{i,j}_{\varepsilon,f}\right)(\mathfrak{r})=\left(\boldsymbol{\vartheta}^{i,j}_{\varepsilon,f}\cdot g_\varepsilon\right)(\mathfrak{r})+\varepsilon^{N+1}\left(-\sum_{\mathbf{l}\in\mathbb{N}^4} g^{\mathbf{l},\mathfrak{r}_0}_{\varepsilon}\rho^{N,i,j}_{\mathbf{l},\mathfrak{r}_0}(\varepsilon,\mathfrak{r})\right). \tag{2.4.91}$$

Finally, as

$$\overline{\mathfrak{N}}\subset\bigcup_{((\mathfrak{r}_0)_1,(\mathfrak{r}_0)_2,(\mathfrak{r}_0)_4)\in\mathfrak{O}}\mathfrak{b}^3\big(((\mathfrak{r}_0)_1,(\mathfrak{r}_0)_2,(\mathfrak{r}_0)_4),R'_{\mathfrak{r}_0}\big) \tag{2.4.92}$$

and as $\overline{\mathfrak{N}}$ is compact, there exists $\mathfrak{r}^1_0,\dots,\mathfrak{r}^p_0$ such that

$$\overline{\mathfrak{N}}\subset\bigcup_{i=1}^{p}\mathfrak{b}^3\Big(\big((\mathfrak{r}^i_0)_1,(\mathfrak{r}^i_0)_2,(\mathfrak{r}^i_0)_4\big),R'_{\mathfrak{r}^i_0}\Big). \tag{2.4.93}$$

Setting $\bar\eta_5=\min\limits_{i=1,\dots,p}\eta_{R_{\mathfrak{r}^i_0},R'_{\mathfrak{r}^i_0}}$, we obtain equality (2.4.81) for all $\mathfrak{r}\in\mathfrak{M}^{\#}$ and for all $\varepsilon\in[-\bar\eta_5,\bar\eta_5]\cap I$. This ends the proof of Theorem 2.4.24. □

2.4.4 Proof of Theorems 2.4.9 and 2.4.13

The proof of Theorem 2.4.9 consists in checking that there exists a real number $\bar\eta_1$ such that for any $\varepsilon\in[-\bar\eta_1,\bar\eta_1]$, the map $\bar{\mathbf{r}}\mapsto\boldsymbol{\vartheta}^{i,j}_{\varepsilon,\bar f}(\bar{\mathbf{r}})$, defined by (2.4.46), satisfies the assumptions of the global inversion Theorem (see Theorem 2.4.5) on $\mathfrak{C}^{\#}$.

In the first place, function $\boldsymbol{\nu}^{i,j}_{\varepsilon,\bar f}$, defined by (2.4.58), is differentiable and, according to Lemma 2.4.17, its differential is bounded. Moreover, according to formula (2.4.58), $\varepsilon\mapsto\boldsymbol{\nu}^{i,j}_{\varepsilon,\bar f}(\bar{\mathbf{r}})$ is clearly in $\mathcal{C}^\infty(\mathbb{R})$ for any $\bar{\mathbf{r}}\in\mathfrak{C}^{\#}$. Hence, we can define

$$\left\|\boldsymbol{\nu}^{i,j}_{\varepsilon,\bar f}\right\|_{1,\infty}=\sup_{\bar{\mathbf{r}}\in\mathfrak{C}^{\#}}\left|\left(d\boldsymbol{\nu}^{i,j}_{\varepsilon,\bar f}\right)_{\bar{\mathbf{r}}}\right|_\infty, \tag{2.4.94}$$

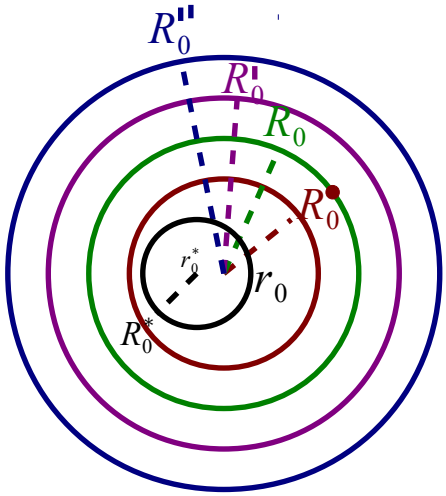

FIGURE 2.5 –

where, here, $|.|_\infty$ stands for norm infinity in $\mathbb{R}^{4\times 4}$, and function $\varepsilon \mapsto \left\|\boldsymbol{\nu}^{i,j}_{\varepsilon,\bar{f}}\right\|_{1,\infty}$ is clearly in $\mathcal{C}^\infty(\mathbb{R})$. Now, since $\varepsilon \left\|\boldsymbol{\nu}^{i,j}_{\varepsilon,\bar{f}}\right\|_{1,\infty} \to 0$ when $\varepsilon \to 0$, there exists a real number $\eta' > 0$ such that

$$\forall \varepsilon \in \left[-\eta', \eta'\right], \ \left|\varepsilon \left\|\boldsymbol{\nu}^{i,j}_{\varepsilon,\bar{f}}\right\|_{1,\infty}\right| < 1. \tag{2.4.95}$$

Hence, since $\mathfrak{C}^\#$ is convex, we deduce that $\varepsilon\boldsymbol{\nu}^{i,j}_{\varepsilon,\bar{f}}$ is Lipschitz continuous on $\mathfrak{C}^\#$ and that its Lipschitz constant is less than $\left\|id^{-1}\right\|_\infty^{-1}$.

The second step consists in checking that for any $\bar{\mathbf{r}} \in \mathfrak{C}^\#$, $\left(d\boldsymbol{\vartheta}^{i,j}_{\varepsilon,\bar{f}}\right)_{\bar{\mathbf{r}}}$ is an isomorphism. As

$$\left(d\boldsymbol{\vartheta}^{i,j}_{\varepsilon,\bar{f}}\right)_{\bar{\mathbf{r}}} = id + \varepsilon \left(d\boldsymbol{\nu}^{i,j}_{\varepsilon,\bar{f}}\right)_{\bar{\mathbf{r}}}, \tag{2.4.96}$$

the Jacobian Matrix of $\boldsymbol{\vartheta}^{i,j}_{\varepsilon,\bar{f}}$ in $\bar{\mathbf{r}} \in \mathfrak{C}^\#$ can be rewritten as

$$\mathrm{Jac}(\boldsymbol{\vartheta}^{i,j}_{\varepsilon,\bar{f}})\left(\bar{\mathbf{r}}\right) = 1 + \varepsilon\chi(\varepsilon, \bar{\mathbf{r}}), \tag{2.4.97}$$

where χ is bounded with respect to $\bar{\mathbf{r}} \in \mathfrak{C}^\#$ and $\varepsilon \mapsto \chi(\varepsilon, \bar{\mathbf{r}})$ is in $\mathcal{C}^\infty(\mathbb{R})$ for any $\bar{\mathbf{r}} \in \mathfrak{C}^\#$. Hence, there exists a real number $\eta'' > 0$ such that for any $\varepsilon \in [-\eta'', \eta'']$ $|\varepsilon \left\|\chi(\varepsilon, .)\right\|_\infty| < 1$.

Hence, for $|\varepsilon| < \bar{\eta}_1$, where $\bar{\eta}_1 = \min\left(\eta', \eta''\right)$, the assumptions of the global inversion Theorem are satisfied leading to the conclusion that $\boldsymbol{\vartheta}^{i,j}_{\varepsilon,\bar{f}}$ is a diffeomorphism on $\mathfrak{C}^\#$. This ends the proof of Theorem 2.4.9. □

Theorem 2.4.13 is a direct consequence of Theorem 2.4.9 and Lemma 2.4.18. □

2.4.5 Proof of Theorem 2.4.14

Once $\bar{\mathbf{r}}_0^*$, R_0^*, $\mathfrak{r}_0$ and R_0 are set, let $R_0^\bullet$, R_0' and R_0'' be three real numbers satisfying $0 < R_0^* < R_0^\bullet < R_0 < R_0' < R_0''$ and such that $\overline{\mathfrak{b}^\#(\bar{\mathbf{r}}_0^*, R_0^*)} \subset \mathfrak{b}^\#(\mathfrak{r}_0, R_0^\bullet)$ and

$\overline{\mathfrak{b}^{\#}(\mathfrak{r}_0, R_0'')} \subset \mathbb{R}^2 \times \mathbb{R} \times (0, +\infty)$ (see Figure 2.5).

In this proof, we will apply Theorem 2.4.24 with $f = -\bar{f}$ and $g_\varepsilon = \boldsymbol{\nu}^{i,j}_{\varepsilon,\bar{f}}$. Using this Theorem requires that $\boldsymbol{\nu}^{i,j}_{\varepsilon,\bar{f}} \in \mathcal{A}\big(\mathbb{R}^2 \times \mathbb{R} \times (0, +\infty)\big) \cap \mathcal{Q}^{\infty}_{T,b}$ and that $\varepsilon \mapsto \boldsymbol{\nu}^{i,j}_{\varepsilon,\bar{f}}$ is smooth on some interval I containing 0. Obviously $\varepsilon \mapsto \boldsymbol{\nu}^{i,j}_{\varepsilon,\bar{f}}$ is in $\mathcal{C}^{\infty}(\mathbb{R})$. On another hand, as $\bar{f}$ and all entries of the Poisson Matrix $\bar{\mathcal{P}}_\varepsilon$ are real analytic functions and as product and partial derivatives of real analytic functions are real analytic functions, function $\boldsymbol{\nu}^{i,j}_{\varepsilon,\bar{f}}$ is real analytic on $\mathbb{R}^2 \times \mathbb{R} \times (0, +\infty)$. In addition, since $\mathcal{Q}^{\infty}_{T,b}$ is an algebra, it is stable by addition, multiplication by a scalar and by product. Moreover, $\mathcal{Q}^{\infty}_{T,b}$ is clearly stable by derivation. Consequently, $\boldsymbol{\nu}^{i,j}_{\varepsilon,\bar{f}} \in \mathcal{Q}^{\infty}_{T,b}$.

In a first place, we will show that there exists a real number $\eta > 0$ such that for any $\varepsilon \in [-\eta, \eta]$:

$$\boldsymbol{\vartheta}^{i,j}_{\varepsilon,\bar{f}}\left(\mathfrak{b}^{\#}(\bar{\mathfrak{r}}_0^*, R_0^*)\right) \subset \mathfrak{b}^{\#}(\mathfrak{r}_0, R_0), \tag{2.4.98}$$

$$\boldsymbol{\Xi}^{i,j}_{\varepsilon,\bar{f}} \text{ is well defined and analytic on } \mathfrak{b}^{\#}(\mathfrak{r}_0, R_0). \tag{2.4.99}$$

According to Lemma 2.4.18, there exists a real number η_6 such that, for any $\varepsilon \in [-\eta_6, \eta_6]$, $\boldsymbol{\vartheta}^{i,j}_{\varepsilon,\bar{f}}\left(\mathfrak{b}^{\#}(\mathfrak{r}_0, R_0^{\bullet})\right) \subset \mathfrak{b}^{\#}(\mathfrak{r}_0, R_0)$ and hence such that, for any $\varepsilon \in [-\eta_6, \eta_6]$, (2.4.98) holds true.

According to Lemma 2.4.19, there exists a real number η_7 such that, for any $\varepsilon \in [-\eta_7, \eta_7]$,

$$\boldsymbol{\vartheta}^{i,j}_{\varepsilon,\bar{f}}\left(\mathfrak{b}^{\#}(\mathfrak{r}_0, R_0'')\right) \supset \mathfrak{b}^{\#}(\mathfrak{r}_0, R_0'). \tag{2.4.100}$$

Applying Theorem 2.4.5 as in the proof of Theorem 2.4.9, and applying Theorem 2.4.4, yields that there exists a real number η_8 such that for any $\varepsilon \in [-\eta_8, \eta_8]$, $\boldsymbol{\Xi}^{i,j}_{\varepsilon,\bar{f}}$ is well defined and analytic on $\boldsymbol{\vartheta}^{i,j}_{\varepsilon,\bar{f}}\left(\mathfrak{b}^{\#}(\mathfrak{r}_0, R_0'')\right)$. Hence, for any $\varepsilon \in [-\min(\eta_7, \eta_8), \min(\eta_7, \eta_8)]$, $\boldsymbol{\Xi}^{i,j}_{\varepsilon,\bar{f}}$ is well defined and analytic on $\mathfrak{b}^{\#}(\mathfrak{r}_0, R_0')$ and consequently on $\mathfrak{b}^{\#}(\mathfrak{r}_0, R_0)$. Setting $\eta = \min(\eta_6, \eta_7, \eta_8)$ yields (2.4.98) and (2.4.99) and the first part of the theorem.

Secondly, we will show that there exists a real number $\bar{\eta}_2 > 0$ such that $\forall \varepsilon \in [-\bar{\eta}_2, \bar{\eta}_2]$, and for any $\mathfrak{r} \in \mathfrak{b}^{\#}(\mathfrak{r}_0, R_0)$ equality (2.4.51) holds true. Applying Theorem 2.4.24 with $f = -\bar{f}$, $\mathfrak{N} = \mathfrak{b}^3\left((\mathfrak{r}_0)_1, (\mathfrak{r}_0)_2, (\mathfrak{r}_0)_3, R_0\right) \subset \mathbb{R}^3$ (the closure of $\mathfrak{N}$ is clearly compact) and $g_\varepsilon = \varepsilon\boldsymbol{\nu}^{i,j}_{\varepsilon,\bar{f}}$, we deduce that there exists a real number $\bar{\eta}_8$ such that for any $\varepsilon \in [-\bar{\eta}_8, \bar{\eta}_8]$ and any $\mathfrak{r} \in \mathfrak{b}^{\#}(\mathfrak{r}_0, R_0)$:

$$\varepsilon\boldsymbol{\nu}^{i,j}_{\varepsilon,\bar{f}}\left(\boldsymbol{\vartheta}^{i,j}_{\varepsilon,-\bar{f}}(\mathfrak{r})\right) = \left(\boldsymbol{\vartheta}^{i,j}_{\varepsilon,-\bar{f}} \cdot \varepsilon\boldsymbol{\nu}^{i,j}_{\varepsilon,\bar{f}}\right)(\mathfrak{r}) + \varepsilon^{N+1}\boldsymbol{\rho}^{N,i,j}_{FC}(\varepsilon, \mathfrak{r}). \tag{2.4.101}$$

Moreover, by definition of $\boldsymbol{\vartheta}^{i,j}_{\varepsilon,-\bar{f}}$,

$$id\left(\boldsymbol{\vartheta}^{i,j}_{\varepsilon,-\bar{f}}(\mathfrak{r})\right) = \left(\boldsymbol{\vartheta}^{i,j}_{\varepsilon,-\bar{f}} \cdot id\right)(\mathfrak{r}), \tag{2.4.102}$$

and consequently

$$\boldsymbol{\vartheta}^{i,j}_{\varepsilon,\bar{f}}\left(\boldsymbol{\vartheta}^{i,j}_{\varepsilon,-\bar{f}}(\mathfrak{r})\right) = \left(\boldsymbol{\vartheta}^{i,j}_{\varepsilon,-\bar{f}} \cdot \boldsymbol{\vartheta}^{i,j}_{\varepsilon,\bar{f}}\right)(\mathfrak{r}) + \varepsilon^{N+1}\boldsymbol{\rho}^{N,i,j}_{FC}(\varepsilon, \mathfrak{r}). \tag{2.4.103}$$

An easy computation leads to

$$\begin{aligned}\left(\boldsymbol{\vartheta}^{i,j}_{\varepsilon,-\bar{f}}\cdot\boldsymbol{\vartheta}^{i,j}_{\varepsilon,\bar{f}}\right)(\mathfrak{r}) &= \left(\sum_{l=0}^{i}\frac{\left(-\varepsilon^{j}\right)^{l}}{l!}\left(\bar{\mathbf{X}}^{\varepsilon}_{\varepsilon\bar{f}}\right)^{l}\cdot\right)\left(\sum_{k=0}^{i}\frac{\left(\varepsilon^{j}\right)^{k}}{k!}\left(\bar{\mathbf{X}}^{\varepsilon}_{\varepsilon\bar{f}}\right)^{k}\cdot\mathfrak{r}\right)(\mathfrak{r})\\ &= \mathfrak{r}+\varepsilon^{N+1}\boldsymbol{\rho}^{N,i,j}_{c}\left(\varepsilon,\mathfrak{r}\right),\end{aligned} \tag{2.4.104}$$

where $\boldsymbol{\rho}^{N,i,j}_{c}$ is in $\mathcal{C}^{\infty}_{\#}\Big(\mathbb{R}\times\mathfrak{b}^{\#}(\mathfrak{r}_0,R_0)\Big)$.
Hence, we have shown that for any $\varepsilon\in[-\bar{\eta}_8,\bar{\eta}_8]$ and for any $\mathfrak{r}\in\mathfrak{b}^{\#}(\mathfrak{r}_0,R_0)$ we have

$$\boldsymbol{\vartheta}^{i,j}_{\varepsilon,\bar{f}}\left(\boldsymbol{\vartheta}^{i,j}_{\varepsilon,-\bar{f}}(\mathfrak{r})\right)=\mathfrak{r}+\varepsilon^{N+1}\left(\boldsymbol{\rho}^{N,i,j}_{c}\left(\varepsilon,\mathfrak{r}\right)+\boldsymbol{\rho}^{N,i,j}_{FC}\left(\varepsilon,\mathfrak{r}\right)\right). \tag{2.4.105}$$

Now, there exists a real number $\eta_9>0$ such that for any $\varepsilon\in[-\eta_9,\eta_9]$,

$$\boldsymbol{\vartheta}^{i,j}_{\varepsilon,\bar{f}}\left(\boldsymbol{\vartheta}^{i,j}_{\varepsilon,-\bar{f}}\left(\mathfrak{b}^{\#}(\mathfrak{r}_0,R_0)\right)\right)\subset\mathfrak{b}^{\#}(\mathfrak{r}_0,R_0'). \tag{2.4.106}$$

Let $\bar{\eta}_2=\min\left(\bar{\eta}_8,\eta_9,\eta\right)$. Then, for any $\varepsilon\in[-\bar{\eta}_2,\bar{\eta}_2]$, $\boldsymbol{\Xi}^{i,j}_{\varepsilon,\bar{f}}$ is well defined and analytic on $\mathfrak{b}^{\#}(\mathfrak{r}_0,R_0')$ (see the first part of the proof) and applying $\boldsymbol{\Xi}^{i,j}_{\varepsilon,\bar{f}}$ to both sides of formula (2.4.105), we obtain for any $\mathfrak{r}\in\mathfrak{b}^{\#}(\mathfrak{r}_0,R_0)$:

$$\boldsymbol{\vartheta}^{i,j}_{\varepsilon,-\bar{f}}(\mathfrak{r})=\boldsymbol{\Xi}^{i,j}_{\varepsilon,\bar{f}}\left(\mathfrak{r}+\varepsilon^{N+1}\left(\boldsymbol{\rho}^{N,i,j}_{c}\left(\varepsilon,\mathfrak{r}\right)+\boldsymbol{\rho}^{N,i,j}_{FC}\left(\varepsilon,\mathfrak{r}\right)\right)\right). \tag{2.4.107}$$

As $\boldsymbol{\Xi}^{i,j}_{\varepsilon,\bar{f}}$ is well defined both on $\boldsymbol{\vartheta}^{i,j}_{\varepsilon,\bar{f}}\left(\boldsymbol{\vartheta}^{i,j}_{\varepsilon,-\bar{f}}\left(\mathfrak{b}^{\#}(\mathfrak{r}_0,R_0)\right)\right)$ and on $\mathfrak{b}^{\#}(\mathfrak{r}_0,R_0)$ and as for any $\varepsilon\in[-\bar{\eta}_2,\bar{\eta}_2]$, they are both included in $\mathfrak{b}^{\#}(\mathfrak{r}_0,R_0')$, which is convex, we can make a Taylor expansion of the right hand side of formula (2.4.107). Hence we obtain formula (2.4.51) for any $\varepsilon\in[-\bar{\eta}_2,\bar{\eta}_2]$ and for any $\mathfrak{r}\in\mathfrak{b}^{\#}(\mathfrak{r}_0,R_0)$.

Thirdly, we will show that the components 1, 2 and 4 of $\boldsymbol{\Xi}^{i,j}_{\varepsilon,f}$ are in $\mathcal{C}^{\infty}_{\#}\Big(\mathfrak{b}^{\#}(\mathfrak{r}_0,R_0)\Big)$ and that the penultimate coordinate satisfies (2.4.50). Let $\bar{\mathfrak{r}}\in\mathfrak{b}^{\#}(\mathfrak{r}_0,R_0)$. As $\boldsymbol{\vartheta}^{i,j}_{\varepsilon,\bar{f}}\left(\mathfrak{b}^{\#}(\mathfrak{r}_0,R_0'')\right)\supset\mathfrak{b}^{\#}(\mathfrak{r}_0,R_0)$, there exists $\bar{\mathfrak{r}}'\in\mathfrak{b}^{\#}(\mathfrak{r}_0,R_0'')$ satisfying $\bar{\mathfrak{r}}=\boldsymbol{\vartheta}^{i,j}_{\varepsilon,f}\left(\bar{\mathfrak{r}}'\right)$. We also define $\bar{\mathfrak{r}}^{\#}\in\mathfrak{b}^{\#}(\mathfrak{r}_0,R_0)$ and $\bar{\mathfrak{r}}'^{\#}\in\mathfrak{b}^{\#}(\mathfrak{r}_0,R_0'')$ by $\bar{\mathfrak{r}}^{\#}=(\bar{\mathfrak{r}}_1,\bar{\mathfrak{r}}_2,\bar{\mathfrak{r}}_3+2\pi,\bar{\mathfrak{r}}_4)$ and $\bar{\mathfrak{r}}'^{\#}=(\bar{\mathfrak{r}}'_1,\bar{\mathfrak{r}}'_2,\bar{\mathfrak{r}}'_3+2\pi,\bar{\mathfrak{r}}'_4)$. Since the components 1, 2 and 4 of $\boldsymbol{\vartheta}^{i,j}_{\varepsilon,f}$ are in $\mathcal{C}^{\infty}_{\#}\left(\mathfrak{b}^{\#}(\mathfrak{r}_0,R_0'')\right)$ and since the penultimate component satisfy

$$\left(\boldsymbol{\vartheta}^{i,j}_{\varepsilon,f}\right)_3\left(\bar{\mathfrak{r}}'^{\#}\right)=\left(\boldsymbol{\vartheta}^{i,j}_{\varepsilon,f}\right)_3\left(\bar{\mathfrak{r}}'\right)+2\pi, \tag{2.4.108}$$

we obtain :

$$\bar{\mathfrak{r}}^{\#}=\boldsymbol{\vartheta}^{i,j}_{\varepsilon,f}\left(\bar{\mathfrak{r}}'^{\#}\right), \tag{2.4.109}$$

and consequently

$$\boldsymbol{\Xi}^{i,j}_{\varepsilon,f}\left(\bar{\mathfrak{r}}^{\#}\right)=\boldsymbol{\Xi}^{i,j}_{\varepsilon,f}\left(\boldsymbol{\vartheta}^{i,j}_{\varepsilon,f}\left(\bar{\mathfrak{r}}'^{\#}\right)\right)=\bar{\mathfrak{r}}'^{\#}. \tag{2.4.110}$$

Eventually, to end this proof we need to show that $\boldsymbol{\rho}^N_{\boldsymbol{\Xi}^{i,j}}$ is in $\mathcal{C}^\infty_\#\Big([-\bar\eta_2;\bar\eta_2]\times\mathfrak{b}^\#(\mathfrak{r}_0,R_0)\Big)$. The components 1, 2 and 4 of $\boldsymbol{\Xi}^{i,j}_{\varepsilon,f}$ and $\boldsymbol{\vartheta}^{i,j}_{\varepsilon,-f}$ are 2π-periodic with respect to $\mathfrak{r}_3$. Consequently, the components 1, 2 and 4 of $\boldsymbol{\rho}^N_{\boldsymbol{\Xi}^{i,j}}$ are 2π-periodic with respect to $\mathfrak{r}_3$. Moreover, the penultimate component of $\boldsymbol{\Xi}^{i,j}_{\varepsilon,f}$ and $\boldsymbol{\vartheta}^{i,j}_{\varepsilon,-f}$ satisfy

$$\begin{aligned}\Big(\boldsymbol{\Xi}^{i,j}_{\varepsilon,f}\Big)_3(\mathfrak{r}_1,\mathfrak{r}_2,\mathfrak{r}_3+2\pi,\mathfrak{r}_4)&=\Big(\boldsymbol{\Xi}^{i,j}_{\varepsilon,f}\Big)_3(\mathfrak{r}_1,\mathfrak{r}_2,\mathfrak{r}_3,\mathfrak{r}_4)+2\pi,\\ \Big(\boldsymbol{\vartheta}^{i,j}_{\varepsilon,-f}\Big)_3(\mathfrak{r}_1,\mathfrak{r}_2,\mathfrak{r}_3+2\pi,\mathfrak{r}_4)&=\Big(\boldsymbol{\vartheta}^{i,j}_{\varepsilon,-f}\Big)_3(\mathfrak{r}_1,\mathfrak{r}_2,\mathfrak{r}_3,\mathfrak{r}_4)+2\pi.\end{aligned}$$

Consequently, the penultimate component of $\boldsymbol{\rho}^N_{\boldsymbol{\Xi}^{i,j}}$ is 2π-periodic. This ends the proof of Theorem 2.4.14. □

2.4.6 Proof of Theorem 2.4.15

Since (2.4.53) is a consequence of Theorem 2.4.14, for any $k,l\in\{1,\dots,4\}$, ones $\hat{\mathcal{P}}^{k,l}_\varepsilon$ is set by (2.4.52) the only thing to prove is (2.4.54). For this, let $R'_{\mathfrak{r}_0}$ and $R''_{\mathfrak{r}_0}$ be two real numbers such that $0<R_0<R'_{\mathfrak{r}_0}<R''_{\mathfrak{r}_0}$ and $\overline{\mathfrak{b}^\#\big(\mathfrak{r}_0,R''_{\mathfrak{r}_0}\big)}\subset\mathbb{R}^2\times\mathbb{R}\times(0,+\infty)$.

Applying Property 2.4.22 with $\mathfrak{M}=\mathfrak{b}^\#\big(\mathfrak{r}_0,R''_{\mathfrak{r}_0}\big)$, $f=\bar f$, $g=\bar{\mathbf{r}}_k$ and $h=\bar{\mathbf{r}}_l$ we obtain for any $\mathfrak{r}\in\mathfrak{b}^\#\big(\mathfrak{r}_0,R''_{\mathfrak{r}_0}\big)$

$$\Big[\boldsymbol{\vartheta}^{i,j}_{\varepsilon,\bar f}\cdot\{\bar{\mathbf{r}}_k,\bar{\mathbf{r}}_l\}_{\bar{\mathbf{r}}}\Big](\mathfrak{r})=\Big\{\boldsymbol{\vartheta}^{i,j}_{\varepsilon,\bar f}\cdot\bar{\mathbf{r}}_k,\boldsymbol{\vartheta}^{i,j}_{\varepsilon,\bar f}\cdot\bar{\mathbf{r}}_l\Big\}_{\bar{\mathbf{r}}}(\mathfrak{r})+\varepsilon^N\rho^{N,k,l}_{PC}(\varepsilon,\mathfrak{r})\,,\tag{2.4.111}$$

where $\rho^{N,k,l}_{PC}$ is $\mathcal{C}^\infty(\mathbb{R}\times\mathfrak{b}^\#\big(\mathfrak{r}_0,R''_{\mathfrak{r}_0}\big))$. Moreover, from expression (2.4.77) of the remainder $\rho^{N,k,l}_{PC}$ we obviously see that it is 2π-periodic with respect to $\mathfrak{r}_3=\theta$ and in $\mathcal{Q}^\infty_{T,b}$.

Applying Theorem 2.4.24 with $f=\bar f$, $\mathfrak{N}=\mathfrak{b}^3\big((\mathfrak{r}_0)_1,(\mathfrak{r}_0)_2,(\mathfrak{r}_0)_3,R'_{\mathfrak{r}_0}\big)\subset\mathbb{R}^3$ (the closure of $\mathfrak{N}$ is clearly compact) and $g_\varepsilon=\bar{\mathcal{T}}^{k,l}_\varepsilon$, there exists a real number $\bar\eta_8>0$ such that for any $\varepsilon\in[-\bar\eta_8,\bar\eta_8]$ and any $\mathfrak{r}\in\mathfrak{b}^\#\big(\mathfrak{r}_0,R'_{\mathfrak{r}_0}\big)$:

$$\Big(\bar{\mathcal{T}}^{k,l}_\varepsilon\circ\boldsymbol{\vartheta}^{i,j}_{\varepsilon,\bar f}\Big)(\mathfrak{r})=\Big[\boldsymbol{\vartheta}^{i,j}_{\varepsilon,\bar f}\cdot\bar{\mathcal{T}}^{k,l}_\varepsilon\Big](\mathfrak{r})+\varepsilon^{N+1}\rho^{N,k,l}_{FC}(\varepsilon,\mathfrak{r})\,,\tag{2.4.112}$$

where $\rho^{N,k,l}_{FC}$ is in $\mathcal{C}^\infty_\#([-\bar\eta_8,\bar\eta_8]\times\mathfrak{b}^\#\big(\mathfrak{r}_0,R'_{\mathfrak{r}_0}\big))$.

Combining equations (2.4.111) and (2.4.112) yields for any $\varepsilon\in[-\bar\eta_8,\bar\eta_8]$ and any $\mathfrak{r}\in\mathfrak{b}^\#\big(\mathfrak{r}_0,R'_{\mathfrak{r}_0}\big)$:

$$\varepsilon\Big\{\boldsymbol{\vartheta}^{i,j}_{\varepsilon,\bar f}\cdot\bar{\mathbf{r}}_k,\boldsymbol{\vartheta}^{i,j}_{\varepsilon,\bar f}\cdot\bar{\mathbf{r}}_l\Big\}_{\bar{\mathbf{r}}}(\mathfrak{r})=\bar{\mathcal{T}}^{k,l}_\varepsilon\Big(\boldsymbol{\vartheta}^{i,j}_{\varepsilon,\bar f}(\mathfrak{r})\Big)-\varepsilon^{N+1}\Big[\rho^{N,k,l}_{PC}(\varepsilon,\mathfrak{r})+\rho^{N,k,l}_{FC}(\varepsilon,\mathfrak{r})\Big]\,.\tag{2.4.113}$$

Now, according to Theorem 2.4.9, there exists a real number $\bar\eta_9>0$ such that for any $\varepsilon\in[-\bar\eta_9,\bar\eta_9]$, $\boldsymbol{\vartheta}^{i,j}_{\varepsilon,\bar f}$ is invertible on $\mathfrak{b}^\#\big(\mathfrak{r}_0,R'_{\mathfrak{r}_0}\big)$, and a real number $\bar\eta_{10}>0$ such that for any $\varepsilon\in[-\bar\eta_{10},\bar\eta_{10}]$,

$$\boldsymbol{\vartheta}^{i,j}_{\varepsilon,\bar f}\Big(\mathfrak{b}^\#\big(\mathfrak{r}_0,R'_{\mathfrak{r}_0}\big)\Big)\supset\mathfrak{b}^\#(\mathfrak{r}_0,R_0)\,.\tag{2.4.114}$$

Formula (2.4.114) also means that for any $\varepsilon\in[-\min(\bar\eta_9,\bar\eta_{10}),\min(\bar\eta_9,\bar\eta_{10})]$, $\boldsymbol{\Xi}^{i,j}_{\varepsilon,\bar f}\Big(\mathfrak{b}^\#(\mathfrak{r}_0,R_0)\Big)\subset\mathfrak{b}^\#\big(\mathfrak{r}_0,R'_{\mathfrak{r}_0}\big)$ and hence that $\boldsymbol{\vartheta}^{i,j}_{\varepsilon,\bar f}$ is well defined on $\boldsymbol{\Xi}^{i,j}_{\varepsilon,\bar f}\Big(\mathfrak{b}^\#(\mathfrak{r}_0,R_0)\Big)$

and that Formula (2.4.113) can be applied at $\boldsymbol{\Xi}^{i,j}_{\varepsilon,\bar{f}}(\mathfrak{r})$, where $\mathfrak{r} \in \mathfrak{b}^{\#}(\mathfrak{r}_0, R_0)$.

Let $\bar{\eta}_3 = \min(\bar{\eta}_8, \bar{\eta}_9, \bar{\eta}_{10})$, then for any $\varepsilon \in [-\bar{\eta}_3, \bar{\eta}_3]$ and any $\mathfrak{r} \in \mathfrak{b}^{\#}(\mathfrak{r}_0, R_0)$, we have

$$\hat{\mathcal{T}}^{k,l}_{\varepsilon}(\mathfrak{r}) = \bar{\mathcal{T}}^{k,l}_{\varepsilon}(\mathfrak{r}) - \varepsilon^{N+1}\left[\rho^{N,k,l}_{PC}\Big(\varepsilon, \boldsymbol{\Xi}^{i,j}_{\varepsilon,\bar{f}}(\mathfrak{r})\Big) + \rho^{N,k,l}_{FC}\Big(\varepsilon, \boldsymbol{\Xi}^{i,j}_{\varepsilon,\bar{f}}(\mathfrak{r})\Big)\right]. \tag{2.4.115}$$

Now, as $\rho^{N,k,l}_{PC}$ and $\rho^{N,k,l}_{FC}$ are smooth with respect to $\mathfrak{r} \in \mathfrak{b}^{\#}(\mathfrak{r}_0, R_0')$ and as $\boldsymbol{\Xi}^{i,j}_{\varepsilon,\bar{f}}$ is smooth with respect to $\mathfrak{r} \in \mathfrak{b}^{\#}(\mathfrak{r}_0, R_0)$ and with respect to ε, formula (2.4.115) can be rewritten for any $\mathfrak{r} \in \mathfrak{b}^{\#}(\mathfrak{r}_0, R_0)$ as

$$\hat{\mathcal{T}}^{k,l}_{\varepsilon}(\mathfrak{r}) = \bar{\mathcal{T}}^{k,l}_{\varepsilon}(\mathfrak{r}) + \varepsilon^{N+1}\rho^{N,k,l}_{S}(\varepsilon, \mathfrak{r}), \tag{2.4.116}$$

where $\rho^{N,k,l}_{S}(\varepsilon, \mathfrak{r}) = -\Big(\rho^{N,k,l}_{PC} + \rho^{N,k,l}_{FC}\Big)\Big(\varepsilon, \boldsymbol{\Xi}^{i,j}_{\varepsilon,\bar{f}}(\mathfrak{r})\Big)$ is in $\mathcal{C}^{\infty}([-\bar{\eta}_3, \bar{\eta}_3] \times \mathfrak{b}^{\#}(\mathfrak{r}_0, R_0))$. Moreover, since the 1, 2 and 4 components of $\boldsymbol{\Xi}^{i,j}_{\varepsilon,f}$ are 2π-periodic with respect to $\mathfrak{r}_3$, the penultimate component of $\boldsymbol{\Xi}^{i,j}_{\varepsilon,f}$ satisfies formula (2.4.50) and $\rho^{N,k,l}_{PC}$ and $\rho^{N,k,l}_{FC}$ are 2π-periodic with respect to $\mathfrak{r}_3$, the remainder $\rho^{N,k,l}_{S}$ is 2π-periodic with respect to $\mathfrak{r}_3$. This ends the proof of Theorem 2.4.15. □

2.4.7 Extension of Lemmas 2.4.18 and 2.4.19, Properties 2.4.22 and 2.4.23, and Theorem 2.4.24

The purpose of this subsection is to extend Lemmas 2.4.18 and 2.4.19, Properties 2.4.22 and 2.4.23, and Theorem 2.4.24 to $\boldsymbol{\vartheta}^{i_1,j_1}_{\varepsilon,f_1} \cdot \ldots \cdot \boldsymbol{\vartheta}^{i_k,j_k}_{\varepsilon,f_k}$. Notice also that viewed as a function $\boldsymbol{\vartheta}^{i_1,j_1}_{\varepsilon,f_1} \cdot \ldots \cdot \boldsymbol{\vartheta}^{i_k,j_k}_{\varepsilon,f_k}$ is defined by :

$$\boldsymbol{\vartheta}^{i_1,j_1}_{\varepsilon,f_1} \cdot \ldots \cdot \boldsymbol{\vartheta}^{i_k,j_k}_{\varepsilon,f_k} = \left(\left(\boldsymbol{\vartheta}^{i_1,j_1}_{\varepsilon,f_1} \cdot \ldots \cdot \boldsymbol{\vartheta}^{i_k,j_k}_{\varepsilon,f_k}\right) \cdot \mathfrak{r}_1, \ldots, \left(\boldsymbol{\vartheta}^{i_1,j_1}_{\varepsilon,f_1} \cdot \ldots \cdot \boldsymbol{\vartheta}^{i_k,j_k}_{\varepsilon,f_k}\right) \cdot \mathfrak{r}_4\right), \tag{2.4.117}$$

Lemma 2.4.25. *Let $k \in \mathbb{N}^{\star}$, f_1, $f_2, \ldots, f_k \in \mathcal{C}^{\infty}_{\#}\big(\mathbb{R}^2 \times \mathbb{R} \times (0, +\infty)\big)$, $i_1, \ldots, i_k$ and $j_1, \ldots, j_k$ be positive integers, $\mathfrak{r}_0 \in \mathbb{R}^2 \times \mathbb{R} \times (0, +\infty)$, and $R_0^{\bullet}$, R_0 and R_0' be three real numbers satisfying $R_0^{\bullet} < R_0 < R_0'$, and such that $\overline{\mathfrak{b}^{\#}(\mathfrak{r}_0, R_0')} \subset \mathbb{R}^2 \times \mathbb{R} \times (0, +\infty)$. Then, there exists a real number $\eta > 0$ such that for any $\varepsilon \in (-\eta, \eta)$:*

$$\mathfrak{b}^{\#}(\mathfrak{r}_0, R_0^{\bullet}) \subset \boldsymbol{\vartheta}^{i_1,j_1}_{\varepsilon,f_1} \cdot \ldots \cdot \boldsymbol{\vartheta}^{i_k,j_k}_{\varepsilon,f_k}\Big(\mathfrak{b}^{\#}(\mathfrak{r}_0, R_0)\Big) \subset \mathfrak{b}^{\#}\big(\mathfrak{r}_0, R_0'\big). \tag{2.4.118}$$

Proof. The proof of Lemma 2.4.25 is very similar to the proofs of Lemmas 2.4.18 and 2.4.19. In fact, we just have to replace in these proofs $\boldsymbol{\nu}^{i,j}_{\varepsilon,f}$ by $\boldsymbol{\nu}^{k}_{\varepsilon}$, where $\boldsymbol{\nu}^{k}_{\varepsilon}$ is such that

$$\boldsymbol{\vartheta}^{i_1,j_1}_{\varepsilon,f_1} \cdot \ldots \cdot \boldsymbol{\vartheta}^{i_k,j_k}_{\varepsilon,f_k}(\mathfrak{r}) = \mathfrak{r} + \varepsilon\boldsymbol{\nu}^{k}_{\varepsilon}(\mathfrak{r}). \tag{2.4.119}$$

This ends the proof of Lemma 2.4.25. □

Lemma 2.4.26. *Let $k \in \mathbb{N}^{\star}$, f_1, $f_2, \ldots, f_k \in \mathcal{C}^{\infty}_{\#}\big(\mathbb{R}^2 \times \mathbb{R} \times (0, +\infty)\big)$, $i_1, \ldots, i_k$ and $j_1, \ldots, j_k$ be positive integers such that for any $l \in \{1, \ldots, k\}$, $i_l j_l \geq N$, and $\mathfrak{b}^{\#}(\mathfrak{r}_0, R_0)$ such that $\mathfrak{b}^{\#}(\mathfrak{r}_0, R_0) \subset \mathbb{R}^2 \times \mathbb{R} \times (0, +\infty)$. Then, for any functions h and g in $\mathcal{C}^{\infty}_{\#}\big(\mathbb{R}^2 \times \mathbb{R} \times (0, +\infty)\big)$, the following equality holds true on $\mathfrak{b}^{\#}(\mathfrak{r}_0, R_0)$*

$$\begin{aligned}&\Big(\boldsymbol{\vartheta}^{i_1,j_1}_{\varepsilon,f_1} \cdot \ldots \cdot \boldsymbol{\vartheta}^{i_k,j_k}_{\varepsilon,f_k} \cdot \{g, h\}\Big)(\mathfrak{r})\\ &= \Big\{\boldsymbol{\vartheta}^{i_1,j_1}_{\varepsilon,f_1} \cdot \ldots \cdot \boldsymbol{\vartheta}^{i_k,j_k}_{\varepsilon,f_k} \cdot g, \boldsymbol{\vartheta}^{i_1,j_1}_{\varepsilon,f_1} \cdot \ldots \cdot \boldsymbol{\vartheta}^{i_k,j_k}_{\varepsilon,f_k} \cdot h\Big\}(\mathfrak{r}) + \varepsilon^{N}\rho^{N,k}_{PC}(\varepsilon, \mathfrak{r}),\end{aligned} \tag{2.4.120}$$

where $\rho^{N,k}_{PC}$ is $\mathcal{C}^{\infty}_{\#}\Big(\mathbb{R} \times \mathfrak{b}^{\#}(\mathfrak{r}_0, R_0)\Big)$.

Proof. For $k = 1$, formula (2.4.120) is given by Property 2.4.22. Moreover, since $f_1,\ g$ and h are in $\mathcal{C}^\infty_{\#}\left(\mathbb{R}^2 \times \mathbb{R} \times (0,+\infty)\right)$, and according to formula (2.4.77), the remainder is clearly 2π-periodic with respect to the penultimate variable. The rest of the proof is an easy induction. This ends the proof of Lemma 2.4.26. □

Lemma 2.4.27. *Let $k \in \mathbb{N}^\star,\ f_1,\ f_2, \ldots, f_k \in \mathcal{C}^\infty_{\#}\big(\mathbb{R}^2 \times \mathbb{R} \times (0,+\infty)\big),\ i_1, \ldots, i_k$ and $j_1, \ldots, j_k$ be positive integers such that for any $l \in \{1, \ldots, k\}$, $i_l j_l \geq N$, and $\mathfrak{b}^{\#}(\mathfrak{r}_0, R_0)$ such that $\mathfrak{b}^{\#}(\mathfrak{r}_0, R_0) \subset \mathbb{R}^2 \times \mathbb{R} \times (0,+\infty)$. Then, for any functions h and g in $\mathcal{C}^\infty_{\#}\left(\mathbb{R}^2 \times \mathbb{R} \times (0,+\infty)\right)$, the following equality holds true on $\mathfrak{b}^{\#}(\mathfrak{r}_0, R_0)$*

$$\Big(\boldsymbol{\vartheta}^{i_1,j_1}_{\varepsilon,f_1} \cdot \ldots \cdot \boldsymbol{\vartheta}^{i_k,j_k}_{\varepsilon,f_k} \cdot (gh)\Big)(\mathfrak{r}) = \Big(\boldsymbol{\vartheta}^{i_1,j_1}_{\varepsilon,f_1} \cdot \ldots \cdot \boldsymbol{\vartheta}^{i_k,j_k}_{\varepsilon,f_k} \cdot g\Big)(\mathfrak{r}) \Big(\boldsymbol{\vartheta}^{i_1,j_1}_{\varepsilon,f_1} \cdot \ldots \cdot \boldsymbol{\vartheta}^{i_k,j_k}_{\varepsilon,f_k} \cdot h\Big)(\mathfrak{r}) + \varepsilon^{N+1} \rho^{N,k}_{FP}(\varepsilon, \mathfrak{r}), \quad (2.4.121)$$

where $\rho^{N,k}_{FP}$ is in $\mathcal{C}^\infty_{\#}\Big(\mathbb{R} \times \mathfrak{b}^{\#}(\mathfrak{r}_0, R_0)\Big)$.

Proof. For $k = 1$, formula (2.4.121) is given by Property 2.4.23. Moreover, since $f_1,\ g$ and h are in $\mathcal{C}^\infty_{\#}\left(\mathbb{R}^2 \times \mathbb{R} \times (0,+\infty)\right)$, the remainder is clearly 2π-periodic with respect to the penultimate variable. The rest of the proof is an easy induction. This ends the proof of Lemma 2.4.27. □

Lemma 2.4.28. *Let $\mathfrak{N} \subset \mathbb{R}^3$ be an open set such that $\overline{\mathfrak{N}}$ is a compact subset of $\mathbb{R}^2 \times (0,+\infty)$; $\mathfrak{M}^{\#}$ the open subset of $\mathbb{R}^4$ defined by*

$$\mathfrak{M}^{\#} = \big\{\mathfrak{r} \in \mathbb{R}^4,\ (\mathfrak{r}_1, \mathfrak{r}_2, \mathfrak{r}_4) \in \mathfrak{N} \text{ and } \mathfrak{r}_3 \in \mathbb{R}\big\}; \quad (2.4.122)$$

$\mathcal{O} \subset \mathbb{R}^2 \times (0,+\infty)$ be an open subset such that $\overline{\mathfrak{N}} \subset \mathcal{O}$; $\mathcal{O}^{\#}$ the be open subset of $\mathbb{R}^4$ defined by

$$\mathcal{O}^{\#} = \big\{\mathfrak{r} \in \mathbb{R}^4,\ (\mathfrak{r}_1, \mathfrak{r}_2, \mathfrak{r}_4) \in \mathcal{O} \text{ and } \mathfrak{r}_3 \in \mathbb{R}\big\}; \quad (2.4.123)$$

$k \in \mathbb{N}^\star,\ f_1,\ f_2, \ldots, f_k \in \mathcal{C}^\infty_{\#}\left(\mathcal{O}^{\#}\right),\ i_1, \ldots, i_k$ and $j_1, \ldots, j_k$ be positive integers such that for any $l \in \{1, \ldots, k\}$, $i_l j_l \geq N$; and $g_\varepsilon = g_\varepsilon(\mathfrak{r}) \in \mathcal{A}\big(\mathbb{R}^2 \times \mathbb{R} \times (0,+\infty)\big) \cap \mathcal{Q}^\infty_{T,b}$ for every ε in some interval I containing 0 and $\varepsilon \mapsto g_\varepsilon(\mathfrak{r})$ be in $\mathcal{C}^\infty(I)$ for any $\mathfrak{r} \in \mathfrak{M}^{\#}$. Then, there exists a real number $\bar{\eta}_5 > 0$ such that for any $\varepsilon \in [-\bar{\eta}_5, \bar{\eta}_5] \cap I$ the following equality holds true for any $\mathfrak{r}$ in $\mathfrak{M}^{\#}$:

$$\Big(g_\varepsilon \circ \Big(\boldsymbol{\vartheta}^{i_1,j_1}_{\varepsilon,f_1} \cdot \ldots \cdot \boldsymbol{\vartheta}^{i_k,j_k}_{\varepsilon,f_k}\Big)\Big)(\mathfrak{r}) = \Big(\boldsymbol{\vartheta}^{i_1,j_1}_{\varepsilon,f_1} \cdot \ldots \cdot \boldsymbol{\vartheta}^{i_k,j_k}_{\varepsilon,f_k} \cdot g_\varepsilon\Big)(\mathfrak{r}) + \varepsilon^{N+1} \rho^{N,k}_{FC}(\varepsilon, \mathfrak{r}), \quad (2.4.124)$$

where $\rho^{N,k}_{FC}$ is in $\mathcal{C}^\infty_{\#}\big(([-\bar{\eta}_5, \bar{\eta}_5] \cap I) \times \mathfrak{M}^{\#}\big)$.

Proof. In order to prove Lemma 2.4.28, we only have to check that all the steps of the proof of Theorem 2.4.24 are valid with $\boldsymbol{\vartheta}^{i_1,j_1}_{\varepsilon,f_1} \cdot \ldots \cdot \boldsymbol{\vartheta}^{i_k,j_k}_{\varepsilon,f_k}$ instead of $\boldsymbol{\vartheta}^{i,j}_{\varepsilon,f}$.

Firstly, and with the same arguments as in the proof of Theorem 2.4.24, we have only to show formula (2.4.124) with functions g_ε of the form $g_\varepsilon(\mathfrak{r}) = \cos^l(\mathfrak{r}_3) \sin^m(\mathfrak{r}_3)\, d^\varepsilon(\mathfrak{r}_1, \mathfrak{r}_2) \sqrt{\mathfrak{r}_4}^n$, where $d^\varepsilon = d^\varepsilon(\mathfrak{r}_1, \mathfrak{r}_2) \in \mathcal{A}\big(\mathbb{R}^2\big) \cap \mathcal{C}^\infty_b\left(\mathbb{R}^2\right)$.

Since Lemma 2.4.18 is extended by Lemma 2.4.25, formula (2.4.85) is also valid with $\boldsymbol{\vartheta}^{i_1,j_1}_{\varepsilon,f_1} \cdot \ldots \cdot \boldsymbol{\vartheta}^{i_k,j_k}_{\varepsilon,f_k}$ instead of $\boldsymbol{\vartheta}^{i,j}_{\varepsilon,f}$.

Eventually, since Property 2.4.23 is extended by Lemma 2.4.27, and since $\boldsymbol{\vartheta}^{i_1,j_1}_{\varepsilon,f_1} \cdot \ldots \cdot \boldsymbol{\vartheta}^{i_k,j_k}_{\varepsilon,f_k}$ is defined by (2.4.117), formula (2.4.89) is also valid with $\boldsymbol{\vartheta}^{i_1,j_1}_{\varepsilon,f_1} \cdot \ldots \cdot \boldsymbol{\vartheta}^{i_k,j_k}_{\varepsilon,f_k}$ instead of $\boldsymbol{\vartheta}^{i,j}_{\varepsilon,f}$.

The rest of the proof is stricto-sensu the same. This ends the proof of Lemma 2.4.28 □

2.5 The Partial Lie Transform Method

In the previous section we introduced the partial Lie Sum functions and the Partial Lie Sums of order (i, j) and we have set out their properties. In this section, from these Sums, we will build for $N \in \mathbb{N}^\star$ fixed by (2.4.33), whatever its worth, a change of coordinates such that in the yielding coordinate system $(\mathbf{z}, \gamma, j)$, the Hamiltonian function does not depend on γ up to order N in ε. Moreover, thanks to Theorem 2.4.15, we will construct this change of coordinates such that the Poisson Matrix (regarded as a function) remains unchanged, up to order $N-1$ in ε, under this change of coordinates. More precisely, we will prove that such a coordinate system exists and give a constructive algorithm (Algorithm 2.5.11) in order to build it. In the first subsection, we will introduce the general Partial Lie Transform change of coordinates of order N (see formula (2.5.2)), and set out its properties. In the second subsection, we will give an algorithm to find the $\bar{g}_i$, for $i \in \{0, \ldots, N\}$ such that the Hamiltonian becomes under its partial normal form (see subsection 2.5.2 for a definition of the partial normal forms).

2.5.1 The Partial Lie Transform Change of Coordinates of order N

Let $N \in \mathbb{N}^*$ be set by (2.4.33). For $i \in \{1, \ldots, N\}$, we define the positive integer α_i by

$$\alpha_i = \min\{k \in \mathbb{N} \text{ s.t. } ki \geq N\} \left(= \mathbb{E}\left(\frac{N}{i}\right) + 1\right), \tag{2.5.1}$$

where $\mathbb{E}$ stands for the integer part, and let us state the following lemma which will allow us to define the change of coordinates.

Lemma 2.5.1. *Let $\mathfrak{r}_0 \in \mathbb{R}^2 \times \mathbb{R} \times (0, +\infty)$, $R_{\mathfrak{r}_0}$ be a positive real number; $\mathfrak{b}^{\#}(\mathfrak{r}_0, R_{\mathfrak{r}_0})$ be defined by (2.4.36) and satisfying $\mathfrak{b}^{\#}(\mathfrak{r}_0, R_{\mathfrak{r}_0}) \subset \mathbb{R}^2 \times \mathbb{R} \times (0, +\infty)$; $R'_{\mathfrak{r}_0}$ be a real number such that $0 < R'_{\mathfrak{r}_0} < R_{\mathfrak{r}_0}$; and $\bar{g}_1, \ldots, \bar{g}_N \in \mathcal{C}^\infty_{\#}\left(\mathbb{R}^2 \times \mathbb{R} \times (0, +\infty)\right)$. Then, there exists a real number η such that for any $\varepsilon \in [-\eta, \eta]$, the function $\boldsymbol{\chi}^N_\varepsilon$ defined by :*

$$\boldsymbol{\chi}^N_\varepsilon = \boldsymbol{\vartheta}^{\alpha_1,1}_{\varepsilon,-\bar{g}_1} \circ \boldsymbol{\vartheta}^{\alpha_2,2}_{\varepsilon,-\bar{g}_2} \circ \ldots \circ \boldsymbol{\vartheta}^{\alpha_N,N}_{\varepsilon,-\bar{g}_N}, \tag{2.5.2}$$

with the $\boldsymbol{\vartheta}^{\alpha_i,i}_{\varepsilon,-\bar{g}_i}$ defined by (2.4.46), is well defined on $\mathfrak{b}^{\#}(\mathfrak{r}_0, R_{\mathfrak{r}_0})$, and satisfies

$$\boldsymbol{\chi}^N_\varepsilon\Big(\mathfrak{b}^{\#}\left(\mathfrak{r}_0, R'_{\mathfrak{r}_0}\right)\Big) \subset \mathfrak{b}^{\#}(\mathfrak{r}_0, R_{\mathfrak{r}_0}), \tag{2.5.3}$$

and

$$\mathfrak{b}^{\#}\left(\mathfrak{r}_0, R'_{\mathfrak{r}_0}\right) \subset \boldsymbol{\chi}^N_\varepsilon\Big(\mathfrak{b}^{\#}(\mathfrak{r}_0, R_{\mathfrak{r}_0})\Big). \tag{2.5.4}$$

Proof. We will prove this lemma by induction on N. More precisely, we will show by induction on N, that for any $\mathfrak{b}^{\#}(\mathfrak{r}_0, R_{\mathfrak{r}_0}) \subset \mathbb{R}^2 \times \mathbb{R} \times (0, +\infty)$, for any $f_1, f_2, \ldots, f_N \in \mathcal{C}^\infty_{\#}\left(\mathbb{R}^2 \times \mathbb{R} \times (0, +\infty)\right)$, for any positive integers $\beta_1, \ldots, \beta_N$ and $\gamma_1, \ldots, \gamma_N$, for any $R'_{\mathfrak{r}_0}$ and $R^\bullet_{\mathfrak{r}_0}$ such that $0 < R'_{\mathfrak{r}_0} < R^\bullet_{\mathfrak{r}_0} < R_{\mathfrak{r}_0}$, there exists a real number $\bar{\eta}_N > 0$ such that for all $\varepsilon \in [-\bar{\eta}_N, \bar{\eta}_N]$ the function

$$\boldsymbol{\vartheta}^{\beta_1,\gamma_1}_{\varepsilon,f_1} \circ \boldsymbol{\vartheta}^{\beta_2,\gamma_2}_{\varepsilon,f_2} \circ \ldots \circ \boldsymbol{\vartheta}^{\beta_N,\gamma_N}_{\varepsilon,f_N}, \tag{2.5.5}$$

is well defined on $\mathfrak{b}^{\#}\left(\mathfrak{r}_0, R^\bullet_{\mathfrak{r}_0}\right)$ and is such that

$$\boldsymbol{\vartheta}^{\beta_1,\gamma_1}_{\varepsilon,f_1} \circ \boldsymbol{\vartheta}^{\beta_2,\gamma_2}_{\varepsilon,f_2} \circ \ldots \circ \boldsymbol{\vartheta}^{\beta_N,\gamma_N}_{\varepsilon,f_N}\left(\mathfrak{b}^{\#}\left(\mathfrak{r}_0, R^\bullet_{\mathfrak{r}_0}\right)\right) \subset \mathfrak{b}^{\#}(\mathfrak{r}_0, R_{\mathfrak{r}_0}), \tag{2.5.6}$$

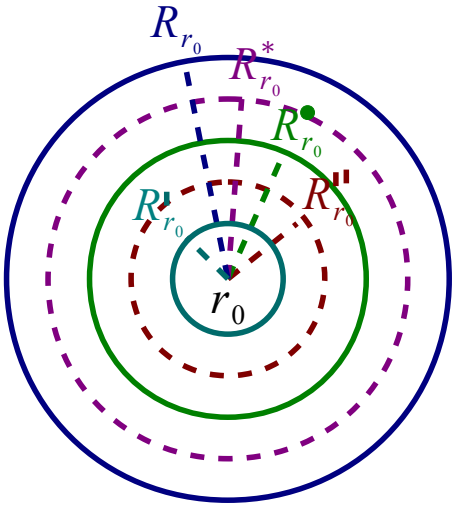

FIGURE 2.6 –

and

$$\mathfrak{b}^{\#}\left(\mathfrak{r}_0, R'_{\mathfrak{r}_0}\right) \subset \boldsymbol{\vartheta}^{\beta_1,\gamma_1}_{\varepsilon,f_1} \circ \boldsymbol{\vartheta}^{\beta_2,\gamma_2}_{\varepsilon,f_2} \circ \ldots \circ \boldsymbol{\vartheta}^{\beta_N,\gamma_N}_{\varepsilon,f_N} \left(\mathfrak{b}^{\#}\left(\mathfrak{r}_0, R^\bullet_{\mathfrak{r}_0}\right)\right). \tag{2.5.7}$$

For $N = 1$ it is simply Lemmas 2.4.18 and 2.4.19.

Now, we assume the result for some $N \geq 1$. Let $\mathfrak{b}^{\#}(\mathfrak{r}_0, R_{\mathfrak{r}_0}) \subset \mathbb{R}^2 \times \mathbb{R} \times (0, +\infty)$, $f_1, f_2, \ldots, f_{N+1} \in \mathcal{C}^\infty_{\#}\left(\mathbb{R}^2 \times \mathbb{R} \times (0, +\infty)\right)$, $\beta_1, \ldots, \beta_{N+1}$ and $\gamma_1, \ldots, \gamma_{N+1}$ be positive integers and $R'_{\mathfrak{r}_0}$, $R^\bullet_{\mathfrak{r}_0}$ be such that $0 < R'_{\mathfrak{r}_0} < R^\bullet_{\mathfrak{r}_0} < R_{\mathfrak{r}_0}$.

Let $R^\star_{\mathfrak{r}_0} \in (R^\bullet_{\mathfrak{r}_0}, R_{\mathfrak{r}_0})$ and $R''_{\mathfrak{r}_0} \in (R'_{\mathfrak{r}_0}, R^\bullet_{\mathfrak{r}_0})$ (see Figure 2.6). Then according to Lemmas 2.4.18 and 2.4.19, there exists a real number $\eta_0 > 0$ such that for all $\varepsilon \in [-\eta_0, \eta_0]$

$$\mathfrak{b}^{\#}\left(\mathfrak{r}_0, R''_{\mathfrak{r}_0}\right) \subset \boldsymbol{\vartheta}^{\beta_{N+1},\gamma_{N+1}}_{\varepsilon,f_{N+1}} \left(\mathfrak{b}^{\#}\left(\mathfrak{r}_0, R^\bullet_{\mathfrak{r}_0}\right)\right), \tag{2.5.8}$$

$$\boldsymbol{\vartheta}^{\beta_{N+1},\gamma_{N+1}}_{\varepsilon,f_{N+1}} \left(\mathfrak{b}^{\#}\left(\mathfrak{r}_0, R^\bullet_{\mathfrak{r}_0}\right)\right) \subset \mathfrak{b}^{\#}\left(\mathfrak{r}_0, R^\star_{\mathfrak{r}_0}\right). \tag{2.5.9}$$

By induction hypothesis (applied with the triplet of periodic balls of radius $(R^\bullet_{\mathfrak{r}_0},\ R^\star_{\mathfrak{r}_0},\ R_{\mathfrak{r}_0})$ and $(R'_{\mathfrak{r}_0},\ R''_{\mathfrak{r}_0},\ R^\bullet_{\mathfrak{r}_0})$), there exists a real number $\eta' > 0$ such that for all $\varepsilon \in [-\eta', \eta']$

$$\boldsymbol{\vartheta}^{\beta_1,\gamma_1}_{\varepsilon,f_1} \circ \boldsymbol{\vartheta}^{\beta_2,\gamma_2}_{\varepsilon,f_2} \circ \ldots \circ \boldsymbol{\vartheta}^{\beta_N,\gamma_N}_{\varepsilon,f_N} \tag{2.5.10}$$

is well defined on $\mathfrak{b}^{\#}\left(\mathfrak{r}_0, R^\star_{\mathfrak{r}_0}\right)$ and such that

$$\boldsymbol{\vartheta}^{\beta_1,\gamma_1}_{\varepsilon,f_1} \circ \boldsymbol{\vartheta}^{\beta_2,\gamma_2}_{\varepsilon,f_2} \circ \ldots \circ \boldsymbol{\vartheta}^{\beta_N,\gamma_N}_{\varepsilon,f_N} \left(\mathfrak{b}^{\#}\left(\mathfrak{r}_0, R^\star_{\mathfrak{r}_0}\right)\right) \subset \mathfrak{b}^{\#}(\mathfrak{r}_0, R_{\mathfrak{r}_0}), \tag{2.5.11}$$

and

$$\mathfrak{b}^{\#}\left(\mathfrak{r}_0, R'_{\mathfrak{r}_0}\right) \subset \boldsymbol{\vartheta}^{\beta_1,\gamma_1}_{\varepsilon,f_1} \circ \boldsymbol{\vartheta}^{\beta_2,\gamma_2}_{\varepsilon,f_2} \circ \ldots \circ \boldsymbol{\vartheta}^{\beta_N,\gamma_N}_{\varepsilon,f_N} \left(\mathfrak{b}^{\#}\left(\mathfrak{r}_0, R''_{\mathfrak{r}_0}\right)\right) \tag{2.5.12}$$

Let $\bar{\eta}_{N+1} = \min(\eta_0, \eta')$. For any $\varepsilon \in [-\bar{\eta}_{N+1}, \bar{\eta}_{N+1}]$,

$$\boldsymbol{\vartheta}_{\varepsilon,f_1}^{\beta_1,\gamma_1} \circ \boldsymbol{\vartheta}_{\varepsilon,f_2}^{\beta_2,\gamma_2} \circ \ldots \circ \boldsymbol{\vartheta}_{\varepsilon,f_{N+1}}^{\beta_{N+1},\gamma_{N+1}}, \tag{2.5.13}$$

is well defined on $\mathfrak{b}^{\#}\big(\mathfrak{r}_0, R_{\mathfrak{r}_0}^{\bullet}\big)$,

$$\boldsymbol{\vartheta}_{\varepsilon,f_1}^{\beta_1,\gamma_1} \circ \boldsymbol{\vartheta}_{\varepsilon,f_2}^{\beta_2,\gamma_2} \circ \ldots \circ \boldsymbol{\vartheta}_{\varepsilon,f_{N+1}}^{\beta_{N+1},\gamma_{N+1}} \Big(\mathfrak{b}^{\#}\big(\mathfrak{r}_0, R_{\mathfrak{r}_0}^{\bullet}\big)\Big) \subset \mathfrak{b}^{\#}(\mathfrak{r}_0, R_{\mathfrak{r}_0}), \tag{2.5.14}$$

and

$$\mathfrak{b}^{\#}\big(\mathfrak{r}_0, R'_{\mathfrak{r}_0}\big) \subset \boldsymbol{\vartheta}_{\varepsilon,f_1}^{\beta_1,\gamma_1} \circ \boldsymbol{\vartheta}_{\varepsilon,f_2}^{\beta_2,\gamma_2} \circ \ldots \circ \boldsymbol{\vartheta}_{\varepsilon,f_{N+1}}^{\beta_{N+1},\gamma_{N+1}} \Big(\mathfrak{b}^{\#}\big(\mathfrak{r}_0, R_{\mathfrak{r}_0}^{\bullet}\big)\Big). \tag{2.5.15}$$

This ends the proof of Lemma 2.5.1. □

In particular, Lemma 2.5.1 ensures that, if $\boldsymbol{\chi}_{\varepsilon}^{N}$ is invertible with $\boldsymbol{\lambda}_{\varepsilon}^{N}$ as inverse function, for sufficiently small ε we have : $\boldsymbol{\lambda}_{\varepsilon}^{N}\Big(\mathfrak{b}^{\#}\big(\mathfrak{r}_0, R'_{\mathfrak{r}_0}\big)\Big) \subset \mathfrak{b}^{\#}(\mathfrak{r}_0, R_{\mathfrak{r}_0})$.

Definition 2.5.2. *Function $\boldsymbol{\chi}_{\varepsilon}^{N}$ is called the Partial Lie Transform map of order N.*

The reason to choose $1, 2, \ldots, N$ as the indexes in $\boldsymbol{\vartheta}_{\varepsilon,-\bar{g}_i}^{\alpha_i,i}$ will be clarified in the next subsection. The first reason for the choice of α_i is that they satisfy $i\alpha_i \geq N$ for $i \in \{1, \ldots, N\}$. Hence, the theorems of the previous subsection may apply to functions $\boldsymbol{\vartheta}_{\varepsilon,-\bar{g}_i}^{\alpha_i,i}$. The second reason for this choice is that with this definition the number of terms in the sum that defines $\boldsymbol{\vartheta}_{\varepsilon,-\bar{g}_i}^{\alpha_i,i}$ is minimal.

We now give a theorem concerning the inverse of the Partial Lie Transform map.

Theorem 2.5.3. *Let $\bar{g}_1, \bar{g}_2, \ldots, \bar{g}_N \in \mathcal{C}_{\#}^{\infty}\big(\mathbb{R}^2 \times \mathbb{R} \times (0, +\infty)\big)$, $\mathfrak{r}_0 \in \mathbb{R}^2 \times \mathbb{R} \times (0, +\infty)$ and $R_{\mathbf{r}_0} > 0$ be a real number such that $\overline{\mathfrak{b}^{\#}(\mathfrak{r}_0, R_{\mathbf{r}_0})} \subset \mathbb{R}^2 \times \mathbb{R} \times (0, +\infty)$. Then, for any $R'_{\mathfrak{r}_0} > 0$ such that $0 < R_{\mathbf{r}_0} < R'_{\mathfrak{r}_0}$ and such that $\overline{\mathfrak{b}^{\#}\big(\mathfrak{r}_0, R'_{\mathfrak{r}_0}\big)} \subset \mathbb{R}^2 \times \mathbb{R} \times (0, +\infty)$, there exists a real number $\eta > 0$ such that for any $\varepsilon \in [-\eta, \eta]$, the restriction $\boldsymbol{\chi}_{\varepsilon}^{N}{}_{|\mathfrak{b}^{\#}(\mathfrak{r}_0, R_{\mathbf{r}_0})}$ of $\boldsymbol{\chi}_{\varepsilon}^{N}$ defined by (2.5.2) to $\mathfrak{b}^{\#}(\mathfrak{r}_0, R_{\mathbf{r}_0})$ is a diffeomorphism, $\boldsymbol{\chi}_{\varepsilon}^{N}\Big(\mathfrak{b}^{\#}(\mathfrak{r}_0, R_{\mathbf{r}_0})\Big) \subset \mathfrak{b}^{\#}\big(\mathfrak{r}_0, R'_{\mathfrak{r}_0}\big)$, and the inverse function $\boldsymbol{\lambda}_{\varepsilon}^{N} = \big(\boldsymbol{\chi}_{\varepsilon}^{N}\big)^{-1}$ of $\boldsymbol{\chi}_{\varepsilon}^{N}$ is well defined on $\mathfrak{b}^{\#}(\mathfrak{r}_0, R_{\mathbf{r}_0})$ and expresses as*

$$\boldsymbol{\lambda}_{\varepsilon}^{N} = \boldsymbol{\Xi}_{\varepsilon,-\bar{g}_N}^{\alpha_N,N} \circ \ldots \circ \boldsymbol{\Xi}_{\varepsilon,-\bar{g}_1}^{\alpha_1,1}. \tag{2.5.16}$$

where for $i = 1, \ldots, N$, $\boldsymbol{\Xi}_{\varepsilon,-\bar{g}_i}^{\alpha_i,i}$ is the inverse function of $\boldsymbol{\vartheta}_{\varepsilon,-\bar{g}_i}^{\alpha_i,i}$, given by Theorem 2.4.14 Moreover, the components 1, 2 and 4 of $\boldsymbol{\lambda}_{\varepsilon}^{N}$ are in $\mathcal{C}_{\#}^{\infty}\Big(\mathfrak{b}^{\#}(\mathfrak{r}_0, R_{\mathfrak{r}_0})\Big)$ and the penultimate component satisfies for any $\mathfrak{r} \in \mathfrak{b}^{\#}(\mathfrak{r}_0, R_{\mathfrak{r}_0})$ and for any $\varepsilon \in [-\eta, \eta]$:

$$\big(\boldsymbol{\lambda}_{\varepsilon}^{N}\big)_3(\mathfrak{r}_1, \mathfrak{r}_2, \mathfrak{r}_3 + 2\pi, \mathfrak{r}_4) = \big(\boldsymbol{\lambda}_{\varepsilon}^{N}\big)_3(\mathfrak{r}_1, \mathfrak{r}_2, \mathfrak{r}_3, \mathfrak{r}_4) + 2\pi. \tag{2.5.17}$$

Proof. Firstly, we will prove by induction that for any $N \in \mathbb{N}^{\star}$, any $f_1, \ldots, f_N \in \mathcal{C}_{\#}^{\infty}\Big(\mathbb{R}^2 \times \mathbb{R} \times (0, +\infty)\Big)$, any $\beta_1, \ldots, \beta_N \in \mathbb{N}^{\star}$, any $\gamma_1, \ldots, \gamma_N \in \mathbb{N}^{\star}$, any $\mathfrak{b}^{\#}(\mathfrak{r}_0, R_{\mathfrak{r}_0})$ such that $\overline{\mathfrak{b}^{\#}(\mathfrak{r}_0, R_{\mathfrak{r}_0})} \subset \mathbb{R}^2 \times \mathbb{R} \times (0, +\infty)$ and for any $R'_{\mathfrak{r}_0} > 0$ such that $\overline{\mathfrak{b}^{\#}\big(\mathfrak{r}_0, R'_{\mathfrak{r}_0}\big)} \subset \mathbb{R}^2 \times \mathbb{R} \times (0, +\infty)$ and such that $0 < R_{\mathfrak{r}_0} < R'_{\mathfrak{r}_0}$ there exists a real number $\eta_N > 0$ such that, for

any $\varepsilon \in [-\eta_N, \eta_N]$, $\Big(\boldsymbol{\vartheta}_{\varepsilon,f_N}^{\beta_N,\gamma_N} \circ \boldsymbol{\vartheta}_{\varepsilon,f_{N-1}}^{\beta_{N-1},\gamma_{N-1}} \circ \ldots \circ \boldsymbol{\vartheta}_{\varepsilon,f_1}^{\beta_1,\gamma_1}\Big)_{|\mathfrak{b}^{\#}\left(\mathfrak{r}_0,R_{\mathfrak{r}_0}\right)}$ is a diffeomorphism, such that

$$\Big(\boldsymbol{\vartheta}_{\varepsilon,f_N}^{\beta_N,\gamma_N} \circ \boldsymbol{\vartheta}_{\varepsilon,f_{N-1}}^{\beta_{N-1},\gamma_{N-1}} \circ \ldots \circ \boldsymbol{\vartheta}_{\varepsilon,f_1}^{\beta_1,\gamma_1}\Big)\Big(\mathfrak{b}^{\#}(\mathfrak{r}_0, R_{\mathfrak{r}_0})\Big) \subset \mathfrak{b}^{\#}\big(\mathfrak{r}_0, R'_{\mathfrak{r}_0}\big) \tag{2.5.18}$$

and such that $\Big(\boldsymbol{\vartheta}_{\varepsilon,f_N}^{\beta_N,\gamma_N} \circ \boldsymbol{\vartheta}_{\varepsilon,f_{N-1}}^{\beta_{N-1},\gamma_{N-1}} \circ \ldots \circ \boldsymbol{\vartheta}_{\varepsilon,f_1}^{\beta_1,\gamma_1}\Big)^{-1}$ expresses

$$\Big(\boldsymbol{\vartheta}_{\varepsilon,f_N}^{\beta_N,\gamma_N} \circ \boldsymbol{\vartheta}_{\varepsilon,f_{N-1}}^{\beta_{N-1},\gamma_{N-1}} \circ \ldots \circ \boldsymbol{\vartheta}_{\varepsilon,f_1}^{\beta_1,\gamma_1}\Big)^{-1} = \boldsymbol{\Xi}_{\varepsilon,f_1}^{\beta_1,\gamma_1} \circ \boldsymbol{\Xi}_{\varepsilon,f_2}^{\beta_2,\gamma_2} \circ \ldots \circ \boldsymbol{\Xi}_{\varepsilon,f_N}^{\beta_N,\gamma_N} \tag{2.5.19}$$

and is well defined on $\mathfrak{b}^{\#}(\mathfrak{r}_0, R_{\mathfrak{r}_0})$.

For $N = 1$: Let $R''_{\mathfrak{r}_0} > 0$ be such that $0 < R_{\mathfrak{r}_0} < R''_{\mathfrak{r}_0} < R'_{\mathfrak{r}_0}$. Applying Theorem 2.4.13 and Lemma 2.4.19 yield that there exists a real number $\eta_1 > 0$ such that $\forall \varepsilon \in [-\eta_1, \eta_1]$, $\boldsymbol{\vartheta}_{\varepsilon,f_1}^{\beta_1,\gamma_1}{}_{|\mathfrak{b}^{\#}\left(\mathfrak{r}_0,R''_{\mathfrak{r}_0}\right)}$ is a diffeomorphism and such that

$$\mathfrak{b}^{\#}(\mathfrak{r}_0, R_{\mathfrak{r}_0}) \subset \boldsymbol{\vartheta}_{\varepsilon,f_1}^{\beta_1,\gamma_1}\Big(\mathfrak{b}^{\#}\big(\mathfrak{r}_0, R''_{\mathfrak{r}_0}\big)\Big) \subset \mathfrak{b}^{\#}\big(\mathfrak{r}_0, R'_{\mathfrak{r}_0}\big).$$

Consequently, $\boldsymbol{\vartheta}_{\varepsilon,f_1}^{\beta_1,\gamma_1}\Big(\mathfrak{b}^{\#}(\mathfrak{r}_0, R_{\mathfrak{r}_0})\Big) \subset \mathfrak{b}^{\#}\big(\mathfrak{r}_0, R'_{\mathfrak{r}_0}\big)$, and $\boldsymbol{\Xi}_{\varepsilon,f_1}^{\beta_1,\gamma_1}$ is well defined on $\mathfrak{b}^{\#}(\mathfrak{r}_0, R_{\mathfrak{r}_0})$.

Now, we assume that the result is true for some $N \geq 1$. Let $f_1, \ldots, f_{N+1} \in \mathcal{C}^{\infty}_{\#}\Big(\mathbb{R}^2 \times \mathbb{R} \times (0, +\infty)\Big)$, $\beta_1, \ldots, \beta_{N+1} \in \mathbb{N}^{\star}$, $\gamma_1, \ldots, \gamma_{N+1} \in \mathbb{N}^{\star}$, $\mathfrak{b}^{\#}(\mathfrak{r}_0, R_{\mathfrak{r}_0})$ satisfying $\overline{\mathfrak{b}^{\#}(\mathfrak{r}_0, R_{\mathfrak{r}_0})} \subset \mathbb{R}^2 \times \mathbb{R} \times (0, +\infty)$, and $R'_{\mathfrak{r}_0} > 0$ a real number such that $\overline{\mathfrak{b}^{\#}\big(\mathfrak{r}_0, R'_{\mathfrak{r}_0}\big)} \subset \mathbb{R}^2 \times \mathbb{R} \times (0, +\infty)$ and such that $0 < R_{\mathfrak{r}_0} < R'_{\mathfrak{r}_0}$.
Let $R''_{\mathfrak{r}_0}$, $R^{(3)}_{\mathfrak{r}_0}$ and $R^{(4)}_{\mathfrak{r}_0}$ be such that $0 < R_{\mathfrak{r}_0} < R''_{\mathfrak{r}_0} < R^{(3)}_{\mathfrak{r}_0} < R'_{\mathfrak{r}_0} < R^{(4)}_{\mathfrak{r}_0}$, and $\overline{\mathfrak{b}^{\#}(\mathfrak{r}_0, R^{(4)}_{\mathfrak{r}_0})} \subset \mathbb{R}^2 \times \mathbb{R} \times (0, +\infty)$ (see Figure 2.7). By induction hypothesis (applied successively with the couples of ball of radius $(R'_{\mathfrak{r}_0}, R^{(4)}_{\mathfrak{r}_0})$, $(R_{\mathfrak{r}_0}, R''_{\mathfrak{r}_0})$, and again with $(R'_{\mathfrak{r}_0}, R^{(4)}_{\mathfrak{r}_0})$), there exists a real number $\eta_N > 0$ such that for any $\varepsilon \in [-\eta_N, \eta_N]$, function $\Big(\boldsymbol{\vartheta}_{\varepsilon,f_N}^{\beta_N,\gamma_N} \circ \boldsymbol{\vartheta}_{\varepsilon,f_{N-1}}^{\beta_{N-1},\gamma_{N-1}} \circ \ldots \circ \boldsymbol{\vartheta}_{\varepsilon,f_1}^{\beta_1,\gamma_1}\Big)_{\big|\mathfrak{b}^{\#}\left(\mathfrak{r}_0,R'_{\mathfrak{r}_0}\right)}$ is a diffeomorphism,

$$\Big(\boldsymbol{\vartheta}_{\varepsilon,f_N}^{\beta_N,\gamma_N} \circ \boldsymbol{\vartheta}_{\varepsilon,f_{N-1}}^{\beta_{N-1},\gamma_{N-1}} \circ \ldots \circ \boldsymbol{\vartheta}_{\varepsilon,f_1}^{\beta_1,\gamma_1}\Big)\Big(\mathfrak{b}^{\#}(\mathfrak{r}_0, R_{\mathfrak{r}_0})\Big) \subset \mathfrak{b}^{\#}\big(\mathfrak{r}_0, R''_{\mathfrak{r}_0}\big) \tag{2.5.20}$$

and

$$\Big(\boldsymbol{\vartheta}_{\varepsilon,f_N}^{\beta_N,\gamma_N} \circ \boldsymbol{\vartheta}_{\varepsilon,f_{N-1}}^{\beta_{N-1},\gamma_{N-1}} \circ \ldots \circ \boldsymbol{\vartheta}_{\varepsilon,f_1}^{\beta_1,\gamma_1}\Big)^{-1} = \boldsymbol{\Xi}_{\varepsilon,f_1}^{\beta_1,\gamma_1} \circ \boldsymbol{\Xi}_{\varepsilon,f_2}^{\beta_2,\gamma_2} \circ \ldots \circ \boldsymbol{\Xi}_{\varepsilon,f_N}^{\beta_N,\gamma_N} \tag{2.5.21}$$

is well defined on $\mathfrak{b}^{\#}\big(\mathfrak{r}_0, R'_{\mathfrak{r}_0}\big)$.

Applying Lemma 2.4.18, there exists a real number $\eta' > 0$ such that for any $\varepsilon \in [-\eta', \eta']$,

$$\boldsymbol{\vartheta}_{\varepsilon,f_{N+1}}^{\beta_{N+1},\gamma_{N+1}}\Big(\mathfrak{b}^{\#}\big(\mathfrak{r}_0, R''_{\mathfrak{r}_0}\big)\Big) \subset \mathfrak{b}^{\#}\Big(\mathfrak{r}_0, R^{(3)}_{\mathfrak{r}_0}\Big).$$

Let $\eta'' = \min(\eta_N, \eta')$, then for any $\varepsilon \in [-\eta'', \eta'']$,

$$\boldsymbol{\vartheta}_{\varepsilon,f_{N+1}}^{\beta_{N+1},\gamma_{N+1}}\Big(\Big(\boldsymbol{\vartheta}_{\varepsilon,f_N}^{\beta_N,\gamma_N} \circ \boldsymbol{\vartheta}_{\varepsilon,f_{N-1}}^{\beta_{N-1},\gamma_{N-1}} \circ \ldots \circ \boldsymbol{\vartheta}_{\varepsilon,f_1}^{\beta_1,\gamma_1}\Big)\Big(\mathfrak{b}^{\#}(\mathfrak{r}_0, R_{\mathfrak{r}_0})\Big)\Big) \subset \mathfrak{b}^{\#}\Big(\mathfrak{r}_0, R^{(3)}_{\mathfrak{r}_0}\Big). \tag{2.5.22}$$

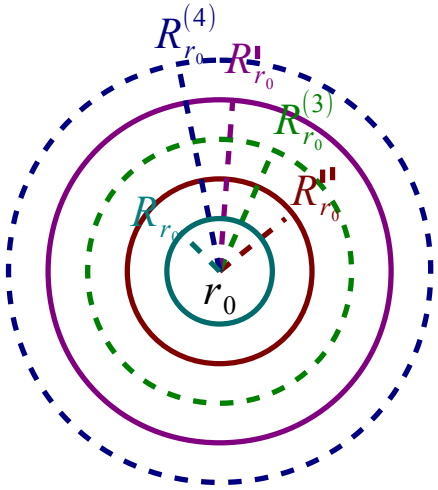

FIGURE 2.7 –

Applying Lemma 2.4.19 and Theorem 2.4.9, there exists a real number $\bar{\eta}_{12} > 0$ such that $\forall \varepsilon \in [-\bar{\eta}_{12}, \bar{\eta}_{12}]$,

$$\mathfrak{b}^{\#}\left(\mathfrak{r}_0, R^{(3)}_{\mathfrak{r}_0}\right) \subset \boldsymbol{\vartheta}^{\beta_{N+1},\gamma_{N+1}}_{\varepsilon,f_{N+1}}\left(\mathfrak{b}^{\#}\left(\mathfrak{r}_0, R'_{\mathfrak{r}_0}\right)\right) \tag{2.5.23}$$

and such that $\boldsymbol{\vartheta}^{\beta_{N+1},\gamma_{N+1}}_{\varepsilon,f_{N+1}}$ is invertible on $\mathfrak{b}^{\#}\left(\mathfrak{r}_0, R'_{\mathfrak{r}_0}\right)$. Consequently, for any $\varepsilon \in [-\min\left(\bar{\eta}_{12}, \eta''\right), \min\left(\bar{\eta}_{12}, \eta''\right)]$

$$\boldsymbol{\Xi}^{\beta_1,\gamma_1}_{\varepsilon,f_1} \circ \boldsymbol{\Xi}^{\beta_2,\gamma_2}_{\varepsilon,f_2} \circ \ldots \circ \boldsymbol{\Xi}^{\beta_N,\gamma_N}_{\varepsilon,f_N} \circ \boldsymbol{\Xi}^{\beta_{N+1},\gamma_{N+1}}_{\varepsilon,f_{N+1}} \tag{2.5.24}$$

is well defined on $\mathfrak{b}^{\#}\left(\mathfrak{r}_0, R^{(3)}_{\mathfrak{r}_0}\right)$.

Let $\eta_{N+1} = \min\left(\eta'', \bar{\eta}_{12}\right)$, then for any $\varepsilon \in [-\eta_{N+1}, \eta_{N+1}]$, the following equalities hold true on $\mathfrak{b}^{\#}(\mathfrak{r}_0, R_{\mathfrak{r}_0})$:

$$\begin{aligned}
&\left[\left(\boldsymbol{\Xi}^{\beta_1,\gamma_1}_{\varepsilon,f_1} \circ \ldots \circ \boldsymbol{\Xi}^{\beta_N,\gamma_N}_{\varepsilon,f_N}\right) \circ \boldsymbol{\Xi}^{\beta_{N+1},\gamma_{N+1}}_{\varepsilon,f_{N+1}}\right] \circ \left(\boldsymbol{\vartheta}^{\beta_{N+1},\gamma_{N+1}}_{\varepsilon,f_{N+1}} \circ \boldsymbol{\vartheta}^{\beta_N,\gamma_N}_{\varepsilon,f_N} \circ \ldots \circ \boldsymbol{\vartheta}^{\beta_1,\gamma_1}_{\varepsilon,f_1}\right) \\
&= \left(\boldsymbol{\Xi}^{\beta_1,\gamma_1}_{\varepsilon,f_1} \circ \ldots \circ \boldsymbol{\Xi}^{\beta_N,\gamma_N}_{\varepsilon,f_N}\right) \circ \left(\boldsymbol{\Xi}^{\beta_{N+1},\gamma_{N+1}}_{\varepsilon,f_{N+1}} \circ \boldsymbol{\vartheta}^{\beta_{N+1},\gamma_{N+1}}_{\varepsilon,f_{N+1}}\right) \circ \left(\boldsymbol{\vartheta}^{\beta_N,\gamma_N}_{\varepsilon,f_N} \circ \ldots \circ \boldsymbol{\vartheta}^{\beta_1,\gamma_1}_{\varepsilon,f_1}\right) \\
&= \left(\boldsymbol{\Xi}^{\beta_1,\gamma_1}_{\varepsilon,f_1} \circ \ldots \circ \boldsymbol{\Xi}^{\beta_N,\gamma_N}_{\varepsilon,f_N}\right) \circ \left(\boldsymbol{\vartheta}^{\beta_N,\gamma_N}_{\varepsilon,f_N} \circ \ldots \circ \boldsymbol{\vartheta}^{\beta_1,\gamma_1}_{\varepsilon,f_1}\right) \\
&= id_{|\mathfrak{b}^{\#}(\mathfrak{r}_0,R_{\mathfrak{r}_0})}.
\end{aligned} \tag{2.5.25}$$

Starting with the 2π-periodicity of the components 1, 2 and 4 of $\boldsymbol{\Xi}^{i,j}_{\varepsilon,f}$ and formula (2.4.50), the proofs of the 2π-periodicity of the components 1, 2 and 4 of $\boldsymbol{\lambda}^N_\varepsilon$ and formula (2.5.17) are easily obtained by induction. This ends the proof of Theorem 2.5.3. □

Theorem 2.5.4. *Let $\bar{g}_1, \dots, \bar{g}_N \in \mathcal{Q}^\infty_{T,b} \cap \mathcal{A}\big(\mathbb{R}^2 \times \mathbb{R} \times (0,+\infty)\big)$ (see Definition 2.4.2 and (2.3.117)), $\mathfrak{r}_0 \in \mathbb{R}^2 \times \mathbb{R} \times (0,+\infty)$ and $R_{\mathfrak{r}_0} > 0$ be a real number such that $\overline{\mathfrak{b}^\#(\mathfrak{r}_0, R_{\mathfrak{r}_0})} \subset \mathbb{R}^2 \times \mathbb{R} \times (0,+\infty)$. Then, for any $\mathfrak{b}^\#\big(\mathfrak{r}^\star_0, R^\star_{\mathfrak{r}_0}\big)$ such that $\overline{\mathfrak{b}^\#\big(\mathfrak{r}^\star_0, R^\star_{\mathfrak{r}_0}\big)} \subset \mathfrak{b}^\#(\mathfrak{r}_0, R_{\mathfrak{r}_0})$ there exists a real number $\bar{\eta}_{13} > 0$ such that for any $\varepsilon \in [-\bar{\eta}_{13}; \bar{\eta}_{13}]$*

$$\boldsymbol{\chi}^N_\varepsilon\Big(\mathfrak{b}^\#\big(\mathfrak{r}^\star_0, R^\star_{\mathfrak{r}_0}\big)\Big) \subset \mathfrak{b}^\#(\mathfrak{r}_0, R_{\mathfrak{r}_0}) \tag{2.5.26}$$

(where $\boldsymbol{\chi}^N_\varepsilon$ is defined by (2.5.2)), and such that the inverse function $\boldsymbol{\lambda}^N_\varepsilon = \big(\boldsymbol{\chi}^N_\varepsilon\big)^{-1}$ of $\boldsymbol{\chi}^N_\varepsilon$ is well defined and analytic on $\mathfrak{b}^\#(\mathfrak{r}_0, R_{\mathfrak{r}_0})$ and expresses as

$$\boldsymbol{\lambda}^N_\varepsilon(\mathfrak{r}) = \boldsymbol{\vartheta}^{\alpha_1,1}_{\varepsilon,\bar{g}_1} \cdot \boldsymbol{\vartheta}^{\alpha_2,2}_{\varepsilon,\bar{g}_2} \cdot \ldots \cdot \boldsymbol{\vartheta}^{\alpha_N,N}_{\varepsilon,\bar{g}_N}(\mathfrak{r}) + \varepsilon^{N+1}\boldsymbol{\rho}^N_{\boldsymbol{\lambda}}(\varepsilon, \mathfrak{r}), \tag{2.5.27}$$

where $\boldsymbol{\rho}^N_{\boldsymbol{\lambda}}$ is in $\mathcal{C}^\infty_\#\Big([-\bar{\eta}_{13}, \bar{\eta}_{13}] \times \mathfrak{b}^\#(\mathfrak{r}_0, R_{\mathfrak{r}_0})\Big)$.

Proof. We will start the proof of Theorem 2.5.4 by proving formula (2.5.26). Since $\overline{\mathfrak{b}^\#(\mathfrak{r}^\star_0, R^\star_{\mathfrak{r}_0})} \subset \mathfrak{b}^\#(\mathfrak{r}_0, R_{\mathfrak{r}_0})$, there exists a real number $R'_{\mathfrak{r}_0} > 0$ such that $0 < R'_{\mathfrak{r}_0} < R_{\mathfrak{r}_0}$ and $\overline{\mathfrak{b}^\#\big(\mathfrak{r}^\star_0, R^\star_{\mathfrak{r}_0}\big)} \subset \mathfrak{b}^\#\big(\mathfrak{r}_0, R'_{\mathfrak{r}_0}\big)$. Applying Theorem 2.5.3, there exists a real number $\bar{\eta} > 0$ such that for any $\varepsilon \in [-\bar{\eta}; \bar{\eta}]$, $\boldsymbol{\chi}^N_\varepsilon\Big(\mathfrak{b}^\#\big(\mathfrak{r}_0, R'_{\mathfrak{r}_0}\big)\Big) \subset \mathfrak{b}^\#(\mathfrak{r}_0, R_{\mathfrak{r}_0})$, and consequently such that formula (2.5.26) is satisfied.

The fact that there exists a real number $\bar{\eta}' > 0$ such that for any $\varepsilon \in [-\bar{\eta}'; \bar{\eta}']$, $\boldsymbol{\lambda}^N_\varepsilon$ is well defined on $\mathfrak{b}^\#(\mathfrak{r}_0, R_{\mathfrak{r}_0})$ is also obtained by applying Theorem 2.5.3.

Consequently, to end the proof of Theorem 2.5.4 we need to check that there exists a real number $\eta^\star_N > 0$ such that for any $\varepsilon \in [-\eta^\star_N; \eta^\star_N]$, $\boldsymbol{\lambda}^N_\varepsilon$ is analytic and satisfies formula (2.5.27) on $\mathfrak{b}^\#(\mathfrak{r}_0, R_{\mathfrak{r}_0})$. Consequently, we will prove by induction on $p \in \mathbb{N}^\star$ that for any $\mathfrak{b}^\#(\mathfrak{r}_0, R_{\mathfrak{r}_0})$ such that $\overline{\mathfrak{b}^\#(\mathfrak{r}_0, R_{\mathfrak{r}_0})} \subset \mathbb{R}^2 \times \mathbb{R} \times (0,+\infty)$; for any $\beta_1, \dots, \beta_p \in \mathbb{N}^\star$, for any $\gamma_1, \dots, \gamma_p \in \mathbb{N}^\star$, such that for any $i \in \{1, \dots, p\}$, $\beta_i\gamma_i \geq N$; for any $f_1,\ f_2, \dots,\ f_p \in \mathcal{A}\big(\mathbb{R}^3 \times (0,+\infty)\big) \cap \mathcal{Q}^\infty_{T,b}$; there exists a real number $\eta_p > 0$ such that for any $\varepsilon \in [-\eta_p, \eta_p]$, $\boldsymbol{\Xi}^{\beta_1,\gamma_1}_{\varepsilon,f_1} \circ \boldsymbol{\Xi}^{\beta_2,\gamma_2}_{\varepsilon,f_2} \circ \ldots \circ \boldsymbol{\Xi}^{\beta_p,\gamma_p}_{\varepsilon,f_p}$ is well defined and analytic on $\mathfrak{b}^\#(\mathfrak{r}_0, R_{\mathfrak{r}_0})$ and for any $\mathfrak{r} \in \mathfrak{b}^\#(\mathfrak{r}_0, R_{\mathfrak{r}_0})$

$$\Big(\boldsymbol{\Xi}^{\beta_1,\gamma_1}_{\varepsilon,f_1} \circ \boldsymbol{\Xi}^{\beta_2,\gamma_2}_{\varepsilon,f_2} \circ \ldots \circ \boldsymbol{\Xi}^{\beta_p,\gamma_p}_{\varepsilon,f_p}\Big)(\mathfrak{r}) = \Big(\boldsymbol{\vartheta}^{\beta_p,\gamma_p}_{\varepsilon,-f_p} \cdot \ldots \cdot \boldsymbol{\vartheta}^{\beta_1,\gamma_1}_{\varepsilon,-f_1}\Big)(\mathfrak{r}) + \varepsilon^{N+1}\boldsymbol{\rho}^{N,p}(\varepsilon, \mathfrak{r}), \tag{2.5.28}$$

where $\boldsymbol{\rho}^{N,p}$ is in $\mathcal{C}^\infty_\#\Big([-\eta_p, \eta_p] \times \mathfrak{b}^\#(\mathfrak{r}_0, R_{\mathfrak{r}_0})\Big)$.

The initialization of the induction is given by Theorem 2.4.14.

Now, we assume that the result is true for some fixed $p \geq 1$. Let $\mathfrak{b}^\#(\mathfrak{r}_0, R_{\mathfrak{r}_0})$ be such that $\overline{\mathfrak{b}^\#(\mathfrak{r}_0, R_{\mathfrak{r}_0})} \subset \mathbb{R}^2 \times \mathbb{R} \times (0,+\infty)$; $\beta_1, \dots, \beta_{p+1} \in \mathbb{N}$ and $\gamma_1, \dots, \gamma_{p+1} \in \mathbb{N}$ such that for any $i \in \{1, \dots, p+1\}$, $\beta_i\gamma_i \geq N$; and $f_1,\ f_2, \dots, f_{p+1} \in \mathcal{A}\big(\mathbb{R}^2 \times \mathbb{R} \times (0,+\infty)\big) \cap \mathcal{Q}^\infty_{T,b}$.

Let $R'_{\mathfrak{r}_0}$ be a positive real numbers such that $0 < R_{\mathfrak{r}_0} < R'_{\mathfrak{r}_0}$ and $\overline{\mathfrak{b}^\#\big(\mathfrak{r}_0, R'_{\mathfrak{r}_0}\big)} \subset \mathbb{R}^2 \times \mathbb{R} \times (0,+\infty)$. In a first place we will show that there exists a real number $\eta > 0$ such that for any $\varepsilon \in [-\eta, \eta]$, $\boldsymbol{\Xi}^{\beta_1,\gamma_1}_{\varepsilon,f_1} \circ \boldsymbol{\Xi}^{\beta_2,\gamma_2}_{\varepsilon,f_2} \circ \ldots \circ \boldsymbol{\Xi}^{\beta_{p+1},\gamma_{p+1}}_{\varepsilon,f_{p+1}}$ is well defined and analytic on $\mathfrak{b}^\#(\mathfrak{r}_0, R_{\mathfrak{r}_0})$. According to Theorem 2.4.14, there exists a real number $\bar{\eta}_1 > 0$ such that for any $\varepsilon \in [-\bar{\eta}_1, \bar{\eta}_1]$, $\boldsymbol{\Xi}^{\beta_{p+1},\gamma_{p+1}}_{\varepsilon,f_{p+1}}$ is well defined and analytic on $\mathfrak{b}^\#(\mathfrak{r}_0, R_{\mathfrak{r}_0})$. Moreover, according to Lemma 2.4.19, there exists a real number $\bar{\eta}_2 > 0$ such that for any $\varepsilon \in$

$[-\bar\eta_2,\bar\eta_2]$, $\boldsymbol{\vartheta}^{\beta_{p+1},\gamma_{p+1}}_{\varepsilon,f_{p+1}}\Big(\mathfrak{b}^{\#}\big(\mathfrak{r}_0,R'_{\mathfrak{r}_0}\big)\Big)\supset\mathfrak{b}^{\#}(\mathfrak{r}_0,R_{\mathfrak{r}_0})$. Let $\bar\eta_3=\min(\bar\eta_1,\bar\eta_2)$, then for any $\varepsilon\in[-\bar\eta_3,\bar\eta_3]$, $\boldsymbol{\Xi}^{\beta_{p+1},\gamma_{p+1}}_{\varepsilon,f_{p+1}}$ is well defined and analytic on $\mathfrak{b}^{\#}(\mathfrak{r}_0,R_{\mathfrak{r}_0})$ and

$$\boldsymbol{\Xi}^{\beta_{p+1},\gamma_{p+1}}_{\varepsilon,f_{p+1}}\Big(\mathfrak{b}^{\#}(\mathfrak{r}_0,R_{\mathfrak{r}_0})\Big)\subset\mathfrak{b}^{\#}\big(\mathfrak{r}_0,R'_{\mathfrak{r}_0}\big)\,. \tag{2.5.29}$$

By the induction hypothesis, there exists a real number $\eta_p>0$ such that for any $\varepsilon\in[-\eta_p,\eta_p]$, $\boldsymbol{\Xi}^{\beta_1,\gamma_1}_{\varepsilon,f_1}\circ\boldsymbol{\Xi}^{\beta_2,\gamma_2}_{\varepsilon,f_2}\circ\ldots\circ\boldsymbol{\Xi}^{\beta_p,\gamma_p}_{\varepsilon,f_p}$ is well defined and analytic on $\mathfrak{b}^{\#}\big(\mathfrak{r}_0,R'_{\mathfrak{r}_0}\big)$. Now, let $\eta=\min(\bar\eta_3,\eta_p)$. According to Theorem 2.4.3, for any $\varepsilon\in[-\eta,\eta]$, $\boldsymbol{\Xi}^{\beta_1,\gamma_1}_{\varepsilon,f_1}\circ\boldsymbol{\Xi}^{\beta_2,\gamma_2}_{\varepsilon,f_2}\circ\ldots\circ\boldsymbol{\Xi}^{\beta_{p+1},\gamma_{p+1}}_{\varepsilon,f_{p+1}}$ is well defined and analytic on $\mathfrak{b}^{\#}(\mathfrak{r}_0,R_{\mathfrak{r}_0})$.

On another hand, according to Lemma 2.5.1, there exists a real number η' such that for any $\varepsilon\in[-\eta',\eta']$

$$\boldsymbol{\Xi}^{\beta_2,\gamma_2}_{\varepsilon,f_2}\circ\ldots\circ\boldsymbol{\Xi}^{\beta_{p+1},\gamma_{p+1}}_{\varepsilon,f_{p+1}}\Big(\mathfrak{b}^{\#}(\mathfrak{r}_0,R_{\mathfrak{r}_0})\Big)\subset\mathfrak{b}^{\#}\big(\mathfrak{r}_0,R'_{\mathfrak{r}_0}\big)\,, \tag{2.5.30}$$

and such that $\boldsymbol{\Xi}^{\beta_1,\gamma_1}_{\varepsilon,f_1}$ is well defined on $\mathfrak{b}^{\#}\big(\mathfrak{r}_0,R'_{\mathfrak{r}_0}\big)$. Moreover, according to Lemma 2.4.25, there exists a real number $\eta''>0$ such that for any $\varepsilon\in[-\eta'',\eta'']$

$$\Big(\boldsymbol{\vartheta}^{\beta_{p+1},\gamma_{p+1}}_{\varepsilon,-f_{p+1}}\cdot\ldots\cdot\boldsymbol{\vartheta}^{\beta_2,\gamma_2}_{\varepsilon,-f_2}\Big)\Big(\mathfrak{b}^{\#}(\mathfrak{r}_0,R_{\mathfrak{r}_0})\Big)\subset\mathfrak{b}^{\#}\big(\mathfrak{r}_0,R'_{\mathfrak{r}_0}\big)\,. \tag{2.5.31}$$

Let $\eta_{p+1}=\min(\eta,\eta',\eta'')$. Then for any $\varepsilon\in[-\eta_{p+1},\eta_{p+1}]$ and for any $\mathfrak{r}\in\mathfrak{b}^{\#}(\mathfrak{r}_0,R_{\mathfrak{r}_0})$,

$$\begin{aligned}
&\boldsymbol{\Xi}^{\beta_1,\gamma_1}_{\varepsilon,f_1}\circ\boldsymbol{\Xi}^{\beta_2,\gamma_2}_{\varepsilon,f_2}\circ\ldots\circ\boldsymbol{\Xi}^{\beta_{p+1},\gamma_{p+1}}_{\varepsilon,f_{p+1}}(\mathfrak{r})\\
&=\boldsymbol{\Xi}^{\beta_1,\gamma_1}_{\varepsilon,f_1}\Big(\boldsymbol{\Xi}^{\beta_2,\gamma_2}_{\varepsilon,f_2}\circ\ldots\circ\boldsymbol{\Xi}^{\beta_p,\gamma_p}_{\varepsilon,f_p}\circ\boldsymbol{\Xi}^{\beta_{p+1},\gamma_{p+1}}_{\varepsilon,f_{p+1}}(\mathfrak{r})\Big)\\
&=\boldsymbol{\Xi}^{\beta_1,\gamma_1}_{\varepsilon,f_1}\Big(\Big(\boldsymbol{\vartheta}^{\beta_{p+1},\gamma_{p+1}}_{\varepsilon,-f_{p+1}}\cdot\ldots\cdot\boldsymbol{\vartheta}^{\beta_2,\gamma_2}_{\varepsilon,-f_2}\Big)(\mathfrak{r})+\varepsilon^{N+1}\boldsymbol{\rho}^{N,p}(\varepsilon,\mathfrak{r})\Big)\\
&=\boldsymbol{\Xi}^{\beta_1,\gamma_1}_{\varepsilon,f_1}\Big(\Big(\boldsymbol{\vartheta}^{\beta_{p+1},\gamma_{p+1}}_{\varepsilon,-f_{p+1}}\cdot\ldots\cdot\boldsymbol{\vartheta}^{\beta_2,\gamma_2}_{\varepsilon,-f_2}\Big)(\mathfrak{r})\Big)+\varepsilon^{N+1}\boldsymbol{\rho}^{N}_{int}(\varepsilon,\mathfrak{r})\\
&=\boldsymbol{\vartheta}^{\beta_1,\gamma_1}_{\varepsilon,-f_1}\Big(\Big(\boldsymbol{\vartheta}^{\beta_{p+1},\gamma_{p+1}}_{\varepsilon,-f_{p+1}}\cdot\ldots\cdot\boldsymbol{\vartheta}^{\beta_2,\gamma_2}_{\varepsilon,-f_2}\Big)(\mathfrak{r})\Big)+\varepsilon^{N+1}\boldsymbol{\rho}^{N}_{int2}(\varepsilon,\mathfrak{r})\\
&=\Big(\Big(\boldsymbol{\vartheta}^{\beta_{p+1},\gamma_{p+1}}_{\varepsilon,-f_{p+1}}\cdot\ldots\cdot\boldsymbol{\vartheta}^{\beta_2,\gamma_2}_{\varepsilon,-f_2}\Big)\cdot\boldsymbol{\vartheta}^{\beta_1,\gamma_1}_{\varepsilon,-f_1}\Big)(\mathfrak{r})+\varepsilon^{N+1}\boldsymbol{\rho}^{N,p+1}(\varepsilon,\mathfrak{r})\,.
\end{aligned}\tag{2.5.32}$$

In this formula, the second equality is obtained from the induction hypothesis, and the third equality is obtained using a Taylor expansion. Notice that this expansion is valid because of formulas (2.5.30) and (2.5.31) and since $\boldsymbol{\Xi}^{\beta_1,\gamma_1}_{\varepsilon,f_1}$ is well defined on the convex subset $\mathfrak{b}^{\#}\big(\mathfrak{r}_0,R'_{\mathfrak{r}_0}\big)$. The fourth equality is obtained by applying the case $p=1$, and the last equality by applying the generalization of Theorem 2.4.24, given by Lemma 2.4.28, with $g_\varepsilon=\boldsymbol{\nu}^{\beta_1,\gamma_1}_{\varepsilon,-f_1}$ and $\boldsymbol{\vartheta}^{\beta_{p+1},\gamma_{p+1}}_{\varepsilon,-f_{p+1}}\cdot\ldots\cdot\boldsymbol{\vartheta}^{\beta_2,\gamma_2}_{\varepsilon,-f_2}$.

The proof that $\boldsymbol{\rho}^{N,p+1}$ is in $\mathcal{C}^\infty_{\#}\Big([-\eta_{p+1},\eta_{p+1}]\times\mathfrak{b}^{\#}(\mathfrak{r}_0,R_{\mathfrak{r}_0})\Big)$ is very similar to the proof that $\boldsymbol{\rho}^{N}_{\boldsymbol{\Xi}^{i,j}_{\varepsilon,f}}$ is in $\mathcal{C}^\infty_{\#}\Big([-\bar\eta_2,\bar\eta_2]\times\mathfrak{b}^{\#}(\mathfrak{r}_0,R_{\mathfrak{r}_0})\Big)$ in Theorem 2.4.14. This ends the proof of Theorem 2.5.4. □

Now, we can consider the change of coordinate $\hat{\mathbf{r}}=\boldsymbol{\chi}^N_\varepsilon(\bar{\mathbf{r}})$ from $\mathfrak{b}^{\#}(\mathfrak{r}_0,R_{\mathfrak{r}_0})$ onto its range and formula (2.5.27) allows us to compute easily an expansion of the inverse change of coordinates. In order to obtain the expression of the Hamiltonian dynamical system in the Partial Lie Transform Coordinate System of order N, we need both the expressions of the Poisson Matrix and of the Hamiltonian function in this coordinate system.

Theorem 2.5.5. *Let* $\mathfrak{r}_0 \in \mathbb{R}^2 \times \mathbb{R} \times (0,+\infty)$ *and* $R_{\mathfrak{r}_0} > 0$ *be such that* $\overline{\mathfrak{b}^{\#}(\mathfrak{r}_0, R_{\mathfrak{r}_0})} \subset \mathbb{R}^2 \times \mathbb{R} \times (0,+\infty)$; $\bar{g}_1, \bar{g}_2, \ldots, \bar{g}_N \in \mathcal{A}\left(\mathbb{R}^3 \times (0,+\infty)\right) \cap \mathcal{Q}^{\infty}_{T,b}$; *and* $\hat{\mathcal{P}}_\varepsilon$ *be the Matrix which entries are given by :*

$$\hat{\mathcal{P}}^{k,l}_{\varepsilon}(\mathfrak{r}) = \left\{ \left(\boldsymbol{\chi}^N_{\varepsilon}\right)_k, \left(\boldsymbol{\chi}^N_{\varepsilon}\right)_l \right\}_{\bar{\mathbf{r}}} \left(\boldsymbol{\lambda}^N_{\varepsilon}(\mathfrak{r})\right). \tag{2.5.33}$$

Then, for any $\mathfrak{b}^{\#}(\mathfrak{r}^{\star}_0, R^{\star}_{\mathfrak{r}_0})$ *such that* $\overline{\mathfrak{b}^{\#}\left(\mathfrak{r}^{\star}_0, R^{\star}_{\mathfrak{r}_0}\right)} \subset \mathfrak{b}^{\#}(\mathfrak{r}_0, R_{\mathfrak{r}_0})$, *there exists a real number* $\bar{\eta}_{14} > 0$, *such that for any* $\varepsilon \in [-\bar{\eta}_{14}; \bar{\eta}_{14}]$,

$$\boldsymbol{\chi}^N_{\varepsilon}\left(\mathfrak{b}^{\#}\left(\mathfrak{r}^{\star}_0, R^{\star}_{\mathfrak{r}_0}\right)\right) \subset \mathfrak{b}^{\#}(\mathfrak{r}_0, R_{\mathfrak{r}_0}) \tag{2.5.34}$$

and for any $\mathfrak{r} \in \mathfrak{b}^{\#}(\mathfrak{r}_0, R_{\mathfrak{r}_0})$ *the following equality holds true :*

$$\forall i,j \in \{1,2,3,4\}, \ \hat{\mathcal{T}}^{i,j}_{\varepsilon}(\mathfrak{r}) = \bar{\mathcal{T}}^{i,j}_{\varepsilon}(\mathfrak{r}) + \varepsilon^{N+1} \rho^N_{\hat{\mathcal{T}}^{i,j}}(\varepsilon, \mathfrak{r}), \tag{2.5.35}$$

where $\rho^N_{\hat{\mathcal{T}}^{i,j}}$ *is in* $\mathcal{C}^{\infty}_{\#}\Big([-\bar{\eta}_{14}; \bar{\eta}_{14}] \times \mathfrak{b}^{\#}(\mathfrak{r}_0, R_0)\Big)$, *and* $\hat{\mathcal{T}}_\varepsilon$ *stands for the matrix satisfying :*

$$\hat{\mathcal{P}}_\varepsilon = \frac{1}{\varepsilon}\hat{\mathcal{T}}_\varepsilon. \tag{2.5.36}$$

Proof. In a first place, we will show by induction on $p \in \mathbb{N}^{\star}$ that for any $\mathfrak{b}^{\#}(\mathfrak{r}_0, R_{\mathfrak{r}_0})$ such that $\overline{\mathfrak{b}^{\#}(\mathfrak{r}_0, R_{\mathfrak{r}_0})} \subset \mathbb{R}^2 \times \mathbb{R} \times (0,+\infty)$; for any $\beta_1, \ldots, \beta_p \in \mathbb{N}$, for any $\gamma_1, \ldots, \gamma_p \in \mathbb{N}$, such that $\forall i \in \{1, \ldots, p\}, \beta_i\gamma_i \geq N$; for any $f_1,\ f_2, \ldots, f_p \in \mathcal{A}\left(\mathbb{R}^2 \times \mathbb{R} \times (0,+\infty)\right) \cap \mathcal{Q}^{\infty}_{T,b}$; there exists a real number $\eta_p > 0$ such that for any $\varepsilon \in [-\eta_p, \eta_p]$, $\boldsymbol{\vartheta}^{\beta_1,\gamma_1}_{\varepsilon,f_1} \circ \ldots \circ \boldsymbol{\vartheta}^{\beta_p,\gamma_p}_{\varepsilon,f_p}$ is well defined and analytic on $\mathfrak{b}^{\#}(\mathfrak{r}_0, R_{\mathfrak{r}_0})$ and the $k-$th component of $\boldsymbol{\vartheta}^{\beta_1,\gamma_1}_{\varepsilon,f_1} \circ \boldsymbol{\vartheta}^{\beta_2,\gamma_2}_{\varepsilon,f_2} \circ \ldots \circ \boldsymbol{\vartheta}^{\beta_p,\gamma_p}_{\varepsilon,f_p}$ is given by

$$\begin{aligned}\left(\boldsymbol{\vartheta}^{\beta_1,\gamma_1}_{\varepsilon,f_1} \circ \boldsymbol{\vartheta}^{\beta_2,\gamma_2}_{\varepsilon,f_2} \circ \ldots \circ \boldsymbol{\vartheta}^{\beta_p,\gamma_p}_{\varepsilon,f_p}\right)_k(\mathfrak{r}) = \left(\boldsymbol{\vartheta}^{\beta_p,\gamma_p}_{\varepsilon,f_p} \cdot \boldsymbol{\vartheta}^{\beta_{p-1},\gamma_{p-1}}_{\varepsilon,f_{p-1}} \cdot \ldots \cdot \boldsymbol{\vartheta}^{\beta_1,\gamma_1}_{\varepsilon,f_1} \cdot \bar{\mathfrak{r}}_k\right)(\mathfrak{r}) \\ + \varepsilon^{N+1}\boldsymbol{\rho}^{N,p}(\varepsilon, \mathfrak{r}),\end{aligned} \tag{2.5.37}$$

where $\boldsymbol{\rho}^{N,p}$ is in $\mathcal{C}^{\infty}_{\#}\Big([-\eta_p; \eta_p] \times \mathfrak{b}^{\#}(\mathfrak{r}_0, R_0)\Big)$.

For, $p = 1$, equality (2.5.37) is direct consequence of definition 2.4.7 and the analyticity is obvious (Notice that for $p = 1$ the remainder is zero).

Now, we assume the result for some fixed $p \geq 1$. Let $\mathfrak{b}^{\#}(\mathfrak{r}_0, R_{\mathfrak{r}_0})$ be such that $\overline{\mathfrak{b}^{\#}(\mathfrak{r}_0, R_{\mathfrak{r}_0})} \subset \mathbb{R}^2 \times \mathbb{R} \times (0,+\infty)$, $\beta_1, \ldots, \beta_{p+1} \in \mathbb{N}$, $\gamma_1, \ldots, \gamma_{p+1} \in \mathbb{N}$, such that for any $i \in \{1, \ldots, p+1\}$, $\beta_i\gamma_i \geq N$, and $f_1,\ f_2, \ldots, f_{p+1} \in \mathcal{A}\left(\mathbb{R}^2 \times \mathbb{R} \times (0,+\infty)\right) \cap \mathcal{Q}^{\infty}_{T,b}$.

Let $R_{\mathfrak{r}_0}$, and $R'_{\mathfrak{r}_0}$ be two real numbers such that $0 < R_{\mathfrak{r}_0} < R'_{\mathfrak{r}_0}$ and $\overline{\mathfrak{b}^{\#}\left(\mathfrak{r}_0, R'_{\mathfrak{r}_0}\right)} \subset \mathbb{R}^2 \times \mathbb{R} \times (0,+\infty)$. We will show that there exists a real number $\eta_{p+1} > 0$ such that for any $\varepsilon \in [-\eta_{p+1}, \eta_{p+1}]$, $\boldsymbol{\vartheta}^{\beta_1,\gamma_1}_{\varepsilon,f_1} \circ \boldsymbol{\vartheta}^{\beta_2,\gamma_2}_{\varepsilon,f_2} \ldots \circ \boldsymbol{\vartheta}^{\beta_{p+1},\gamma_{p+1}}_{\varepsilon,f_{p+1}}$ is well defined and analytic on $\mathfrak{b}^{\#}(\mathfrak{r}_0, R_{\mathfrak{r}_0})$. According to Lemma 2.4.18, there exists $\eta_1 > 0$ such that for any $\varepsilon \in [-\eta_1, \eta_1]$,

$$\boldsymbol{\vartheta}^{\beta_{p+1},\gamma_{p+1}}_{\varepsilon,f_{p+1}}\left(\mathfrak{b}^{\#}(\mathfrak{r}_0, R_{\mathfrak{r}_0})\right) \subset \mathfrak{b}^{\#}\left(\mathfrak{r}_0, R'_{\mathfrak{r}_0}\right).$$

Obviously, $\boldsymbol{\vartheta}^{\beta_{p+1},\gamma_{p+1}}_{\varepsilon,f_{p+1}}$ is analytic on $\mathfrak{b}^{\#}(\mathfrak{r}_0, R_{\mathfrak{r}_0})$. According to the induction assumption, there exists $\eta_p > 0$ such that for any $\varepsilon \in [-\eta_p, \eta_p]$, $\boldsymbol{\vartheta}^{\beta_1,\gamma_1}_{\varepsilon,f_1} \circ \boldsymbol{\vartheta}^{\beta_2,\gamma_2}_{\varepsilon,f_2} \circ \ldots \circ \boldsymbol{\vartheta}^{\beta_p,\gamma_p}_{\varepsilon,f_p}$ is well defined

and analytic on $\mathfrak{b}^{\#}\big(\mathfrak{r}_0, R'_{\mathfrak{r}_0}\big)$. Setting $\eta_{p+1} = \min(\eta_1, \eta_p)$, and according to Theorem 2.4.3, for any $\varepsilon \in [-\eta_{p+1}, \eta_{p+1}]$, $\boldsymbol{\vartheta}^{\beta_1,\gamma_1}_{\varepsilon,f_1} \circ \boldsymbol{\vartheta}^{\beta_2,\gamma_2}_{\varepsilon,f_2} \ldots \circ \boldsymbol{\vartheta}^{\beta_{p+1},\gamma_{p+1}}_{\varepsilon,f_{p+1}}$ is well defined and analytic on $\mathfrak{b}^{\#}(\mathfrak{r}_0, R_{\mathfrak{r}_0})$.

To end this induction, we will show that for any $\varepsilon \in [-\eta_{p+1}, \eta_{p+1}]$ and for any $\mathfrak{r} \in \mathfrak{b}^{\#}(\mathfrak{r}_0, R_{\mathfrak{r}_0})$:

$$\Big(\boldsymbol{\vartheta}^{\beta_1,\gamma_1}_{\varepsilon,f_1} \circ \boldsymbol{\vartheta}^{\beta_2,\gamma_2}_{\varepsilon,f_2} \circ \ldots \circ \boldsymbol{\vartheta}^{\beta_{p+1},\gamma_{p+1}}_{\varepsilon,f_{p+1}}\Big)_k(\mathfrak{r}) = \Big(\boldsymbol{\vartheta}^{\beta_{p+1},\gamma_{p+1}}_{\varepsilon,f_{p+1}} \cdot \boldsymbol{\vartheta}^{\beta_{p-1},\gamma_{p-1}}_{\varepsilon,f_{p-1}} \cdot \ldots \cdot \boldsymbol{\vartheta}^{\beta_1,\gamma_1}_{\varepsilon,f_1} \cdot \bar{\mathfrak{r}}_k\Big)(\mathfrak{r}) + \varepsilon^{N+1}\boldsymbol{\rho}^{N,p+1}(\varepsilon,\mathfrak{r}), \tag{2.5.38}$$

where $\boldsymbol{\rho}^{N,p+1}$ is is in $\mathcal{C}^{\infty}_{\#}\Big([-\eta_{p+1};\eta_{p+1}] \times \mathfrak{b}^{\#}(\mathfrak{r}_0, R_0)\Big)$.

According to the induction step, for any $\varepsilon \in [-\eta_p, \eta_p]$ the $k-$th component of $\boldsymbol{\vartheta}^{\beta_1,\gamma_1}_{\varepsilon,f_1} \circ \boldsymbol{\vartheta}^{\beta_2,\gamma_2}_{\varepsilon,f_2} \circ \ldots \circ \boldsymbol{\vartheta}^{\beta_p,\gamma_p}_{\varepsilon,f_p}$ is given by (2.5.37). Then we obtain for any $\varepsilon \in [-\eta_{p+1}, \eta_{p+1}]$ and for any $\mathfrak{r} \in \mathfrak{b}^{\#}(\mathfrak{r}_0, R_{\mathfrak{r}_0})$:

$$\begin{aligned}
&\Big(\boldsymbol{\vartheta}^{\beta_1,\gamma_1}_{\varepsilon,f_1} \circ \boldsymbol{\vartheta}^{\beta_2,\gamma_2}_{\varepsilon,f_2} \circ \ldots \circ \boldsymbol{\vartheta}^{\beta_{p+1},\gamma_{p+1}}_{\varepsilon,f_{p+1}}\Big)_k(\mathfrak{r}) \\
=&\Big(\boldsymbol{\vartheta}^{\beta_1,\gamma_1}_{\varepsilon,f_1} \circ \boldsymbol{\vartheta}^{\beta_2,\gamma_2}_{\varepsilon,f_2} \circ \ldots \circ \boldsymbol{\vartheta}^{\beta_p,\gamma_p}_{\varepsilon,f_p}\Big)_k\Big(\boldsymbol{\vartheta}^{\beta_{p+1},\gamma_{p+1}}_{\varepsilon,f_{p+1}}(\mathfrak{r})\Big) \\
=&\Big(\boldsymbol{\vartheta}^{\beta_p,\gamma_p}_{\varepsilon,f_p} \cdot \ldots \cdot \boldsymbol{\vartheta}^{\beta_1,\gamma_1}_{\varepsilon,f_1}\Big)_k\Big(\boldsymbol{\vartheta}^{\beta_{p+1},\gamma_{p+1}}_{\varepsilon,f_{p+1}}(\mathfrak{r})\Big) + \varepsilon^{N+1}\boldsymbol{\rho}^{N,p}\Big(\varepsilon, \boldsymbol{\vartheta}^{\beta_{p+1},\gamma_{p+1}}_{\varepsilon,f_{p+1}}(\mathfrak{r})\Big) \\
=&\boldsymbol{\vartheta}^{\beta_{p+1},\gamma_{p+1}}_{\varepsilon,f_{p+1}} \cdot \Big(\boldsymbol{\vartheta}^{\beta_p,\gamma_p}_{\varepsilon,f_p} \cdot \ldots \cdot \boldsymbol{\vartheta}^{\beta_1,\gamma_1}_{\varepsilon,f_1}\Big)_k(\mathfrak{r}) + \varepsilon^{N+1}\boldsymbol{\rho}^{N,p+1}(\varepsilon,\mathfrak{r}) \\
=&\Big(\boldsymbol{\vartheta}^{\beta_{p+1},\gamma_{p+1}}_{\varepsilon,f_{p+1}} \cdot \boldsymbol{\vartheta}^{\beta_p,\gamma_p}_{\varepsilon,f_p} \cdot \ldots \cdot \boldsymbol{\vartheta}^{\beta_1,\gamma_1}_{\varepsilon,f_1}\Big)_k(\mathfrak{r}) + \varepsilon^{N+1}\boldsymbol{\rho}^{N,p+1}(\varepsilon,\mathfrak{r}).
\end{aligned} \tag{2.5.39}$$

In the third equality we have used Theorem 2.4.24 with $g_\varepsilon = \Big(\boldsymbol{\vartheta}^{\beta_{p+1},\gamma_{p+1}}_{\varepsilon,f_{p+1}} \cdot \ldots \cdot \boldsymbol{\vartheta}^{\beta_1,\gamma_1}_{\varepsilon,f_1}\Big)_k - \mathfrak{r}_k$.

Since for $k = 1,\ 2,$ and 4,

$$\Big(\boldsymbol{\vartheta}^{\beta_1,\gamma_1}_{\varepsilon,f_1} \circ \boldsymbol{\vartheta}^{\beta_2,\gamma_2}_{\varepsilon,f_2} \circ \ldots \circ \boldsymbol{\vartheta}^{\beta_{p+1},\gamma_{p+1}}_{\varepsilon,f_{p+1}}\Big)_k \text{ and } \Big(\boldsymbol{\vartheta}^{\beta_{p+1},\gamma_{p+1}}_{\varepsilon,f_{p+1}} \cdot \boldsymbol{\vartheta}^{\beta_p,\gamma_p}_{\varepsilon,f_p} \cdot \ldots \cdot \boldsymbol{\vartheta}^{\beta_1,\gamma_1}_{\varepsilon,f_1}\Big)_k \tag{2.5.40}$$

are 2π-periodic, so is the remainder. Since for $k = 3$

$$\Big(\boldsymbol{\vartheta}^{\beta_1,\gamma_1}_{\varepsilon,f_1} \circ \boldsymbol{\vartheta}^{\beta_2,\gamma_2}_{\varepsilon,f_2} \circ \ldots \circ \boldsymbol{\vartheta}^{\beta_{p+1},\gamma_{p+1}}_{\varepsilon,f_{p+1}}\Big)_3\Big(\mathfrak{r}^{\#}\Big) = \Big(\boldsymbol{\vartheta}^{\beta_1,\gamma_1}_{\varepsilon,f_1} \circ \boldsymbol{\vartheta}^{\beta_2,\gamma_2}_{\varepsilon,f_2} \circ \ldots \circ \boldsymbol{\vartheta}^{\beta_{p+1},\gamma_{p+1}}_{\varepsilon,f_{p+1}}\Big)_3(\mathfrak{r}) + 2\pi, \tag{2.5.41}$$

$$\Big(\boldsymbol{\vartheta}^{\beta_{p+1},\gamma_{p+1}}_{\varepsilon,f_{p+1}} \cdot \boldsymbol{\vartheta}^{\beta_p,\gamma_p}_{\varepsilon,f_p} \cdot \ldots \cdot \boldsymbol{\vartheta}^{\beta_1,\gamma_1}_{\varepsilon,f_1}\Big)_3\Big(\mathfrak{r}^{\#}\Big) = \Big(\boldsymbol{\vartheta}^{\beta_{p+1},\gamma_{p+1}}_{\varepsilon,f_{p+1}} \cdot \boldsymbol{\vartheta}^{\beta_p,\gamma_p}_{\varepsilon,f_p} \cdot \ldots \cdot \boldsymbol{\vartheta}^{\beta_1,\gamma_1}_{\varepsilon,f_1}\Big)_3(\mathfrak{r}) + 2\pi, \tag{2.5.42}$$

the reminder is also 2π-periodic. This ends this first proof by induction.

Beside this, Lemma 2.4.26, yields :

$$\begin{aligned}
&\Big\{\boldsymbol{\vartheta}^{\beta_p,\gamma_p}_{\varepsilon,f_p} \cdot \boldsymbol{\vartheta}^{\beta_{p-1},\gamma_{p-1}}_{\varepsilon,f_{p-1}} \cdot \ldots \cdot \boldsymbol{\vartheta}^{\beta_1,\gamma_1}_{\varepsilon,f_1} \cdot \bar{\mathfrak{r}}_k, \boldsymbol{\vartheta}^{\beta_p,\gamma_p}_{\varepsilon,f_p} \cdot \boldsymbol{\vartheta}^{\beta_{p-1},\gamma_{p-1}}_{\varepsilon,f_{p-1}} \cdot \ldots \cdot \boldsymbol{\vartheta}^{\beta_1,\gamma_1}_{\varepsilon,f_1} \cdot \bar{\mathfrak{r}}_l\Big\}_{\bar{\mathfrak{r}}}(\mathfrak{r}) \\
&= \Big(\boldsymbol{\vartheta}^{\beta_p,\gamma_p}_{\varepsilon,f_p} \cdot \boldsymbol{\vartheta}^{\beta_{p-1},\gamma_{p-1}}_{\varepsilon,f_{p-1}} \cdot \ldots \cdot \boldsymbol{\vartheta}^{\beta_1,\gamma_1}_{\varepsilon,f_1} \cdot \{\bar{\mathfrak{r}}_k, \bar{\mathfrak{r}}_l\}_{\bar{\mathfrak{r}}}\Big)(\mathfrak{r}) + \varepsilon^N \boldsymbol{\rho}^{N,p}_2(\varepsilon,\mathfrak{r}),
\end{aligned} \tag{2.5.43}$$

with $\boldsymbol{\rho}^{N,p}_2$ 2π-periodic with respect to the penultimate variable.

Afterwards, the bilinearity of the Poisson Bracket, formulas (2.5.37) and (2.5.43) yield for any $\varepsilon \in [-\eta_p, \eta_p]$ and for all $\mathfrak{r} \in \mathfrak{b}^{\#}(\mathfrak{r}_0, R_{\mathfrak{r}_0})$:

$$\begin{aligned}&\left\{\left(\boldsymbol{\vartheta}_{\varepsilon,f_1}^{\beta_1,\gamma_1} \circ \boldsymbol{\vartheta}_{\varepsilon,f_2}^{\beta_2,\gamma_2} \circ \ldots \circ \boldsymbol{\vartheta}_{\varepsilon,f_p}^{\beta_p,\gamma_p}\right)_k, \left(\boldsymbol{\vartheta}_{\varepsilon,f_1}^{\beta_1,\gamma_1} \circ \boldsymbol{\vartheta}_{\varepsilon,f_2}^{\beta_2,\gamma_2} \circ \ldots \circ \boldsymbol{\vartheta}_{\varepsilon,f_p}^{\beta_p,\gamma_p}\right)_l\right\}_{\bar{\mathbf{r}}}(\mathfrak{r}) \\ &= \boldsymbol{\vartheta}_{\varepsilon,f_p}^{\beta_p,\gamma_p} \cdot \boldsymbol{\vartheta}_{\varepsilon,f_{p-1}}^{\beta_{p-1},\gamma_{p-1}} \cdot \ldots \cdot \boldsymbol{\vartheta}_{\varepsilon,f_1}^{\beta_1,\gamma_1} \cdot \{\bar{\mathbf{r}}_k, \bar{\mathbf{r}}_l\}_{\bar{\mathbf{r}}}(\mathfrak{r}) + \varepsilon^N \boldsymbol{\rho}^N(\varepsilon, \mathfrak{r}),\end{aligned} \tag{2.5.44}$$

with $\boldsymbol{\rho}^N$ 2π-periodic with respect to the penultimate variable.

Lastly formula (2.5.37), a Taylor expansion, and Lemma 2.4.28, yield that for any $p \in \mathbb{N}^\star$, there exists a real number $\eta_p^\star > 0$ such that for any $\varepsilon \in [-\eta_p^\star, \eta_p^\star]$, and for all $\mathfrak{r} \in \mathfrak{b}^{\#}(\mathfrak{r}_0, R_{\mathfrak{r}_0})$:

$$\begin{aligned}&\bar{\mathcal{T}}_\varepsilon^{k,l}\left(\boldsymbol{\vartheta}_{\varepsilon,f_1}^{\beta_1,\gamma_1} \circ \boldsymbol{\vartheta}_{\varepsilon,f_2}^{\beta_2,\gamma_2} \circ \ldots \circ \boldsymbol{\vartheta}_{\varepsilon,f_p}^{\beta_p,\gamma_p}(\mathfrak{r})\right) \\ &= \left(\boldsymbol{\vartheta}_{\varepsilon,f_p}^{\beta_p,\gamma_p} \cdot \ldots \cdot \boldsymbol{\vartheta}_{\varepsilon,f_1}^{\beta_1,\gamma_1} \cdot \bar{\mathcal{T}}_\varepsilon^{k,l}\right)(\mathfrak{r}) + \varepsilon^{N+1} \boldsymbol{\rho}_p^N(\varepsilon, \mathfrak{r})\end{aligned} \tag{2.5.45}$$

where $\boldsymbol{\rho}_p^N$ is 2π-periodic with respect to the penultimate variable. Setting $\bar{\eta}_{14} = \min(\eta_p, \eta_p^\star)$ and combining (2.5.44) and (2.5.45) yields the result. This ends the proof of Theorem 2.5.5. □

The way that map $\boldsymbol{\lambda}_\varepsilon^N$, which expression is given by (2.5.16), transforms functions is now tackled.

Theorem 2.5.6. *Let $\mathfrak{r}_0 \in \mathbb{R}^2 \times \mathbb{R} \times (0, +\infty)$, and $R_{\mathfrak{r}_0} > 0$ be such that $\overline{\mathfrak{b}^{\#}(\mathfrak{r}_0, R_{\mathfrak{r}_0})} \subset \mathbb{R}^2 \times \mathbb{R} \times (0, +\infty)$; $\bar{g}_1, \bar{g}_2, \ldots, \bar{g}_N \in \mathcal{Q}_{T,b}^\infty \cap \mathcal{A}(\mathbb{R}^2 \times \mathbb{R} \times (0, +\infty))$; $\bar{G} = \bar{G}(\varepsilon, \mathfrak{r}) \in \mathcal{C}_{\#}^\infty(I \times \mathbb{R}^2 \times \mathbb{R} \times (0, +\infty))$ where I is an interval containing 0 ; and $\hat{G}$ be defined by $\hat{G}(\varepsilon, \mathfrak{r}) = \bar{G}\left(\varepsilon, \boldsymbol{\lambda}_\varepsilon^N(\mathfrak{r})\right)$. Assume that $\bar{G}$ admits the following decomposition*

$$\bar{G} = \bar{G}^N + \varepsilon^{N+1} \iota_{N+1}, \tag{2.5.46}$$

where $\iota_{N+1} \in \mathcal{C}_{\#}^\infty\big(I \times \mathbb{R}^2 \times \mathbb{R} \times (0, +\infty)\big)$, $\bar{G}^N \in \mathcal{Q}_{T,b}^\infty \cap \mathcal{A}\big(\mathbb{R}^2 \times \mathbb{R} \times (0, +\infty)\big)$ for any $\varepsilon \in \mathbb{R}$ and $\varepsilon \mapsto \bar{G}^N(\varepsilon, \mathfrak{r})$ is in $\mathcal{C}^\infty(\mathbb{R})$ for any $\mathfrak{r} \in \mathbb{R}^2 \times \mathbb{R} \times (0, +\infty)$. Then, there exists a real number $\bar{\eta}_{20} > 0$ such that for any $\varepsilon \in [-\bar{\eta}_{20}; \bar{\eta}_{20}] \cap I$, and for any $\mathfrak{r} \in \mathfrak{b}^{\#}(\mathfrak{r}_0, R_{\mathfrak{r}_0})$:

$$\hat{G}(\varepsilon, \mathfrak{r}) = \left(\boldsymbol{\vartheta}_{\varepsilon,\bar{g}_1}^{\alpha_1,1} \cdot \ldots \cdot \boldsymbol{\vartheta}_{\varepsilon,\bar{g}_N}^{\alpha_N,N} \cdot \bar{G}^N\right)(\varepsilon, \mathfrak{r}) + \varepsilon^{N+1} \rho_{\bar{G}}^N(\varepsilon, \mathfrak{r}), \tag{2.5.47}$$

where $\rho_{\bar{G}}^N \in \mathcal{C}_{\#}^\infty\Big(([-\bar{\eta}_{20}; \bar{\eta}_{20}] \cap I) \times \mathfrak{b}^{\#}(\mathfrak{r}_0, R_{\mathfrak{r}_0})\Big)$.

Proof. Let $\mathfrak{r}_0 \in \mathbb{R}^2 \times \mathbb{R} \times (0, +\infty)$, $R_{\mathfrak{r}_0} > 0$ and $R'_{\mathfrak{r}_0}$ be a real number such that $0 < R_{\mathfrak{r}_0} < R'_{\mathfrak{r}_0}$ and $\overline{\mathfrak{b}^{\#}(\mathfrak{r}_0, R'_{\mathfrak{r}_0})} \subset \mathbb{R}^2 \times \mathbb{R} \times (0, +\infty)$. According to Lemma 2.5.1, there exists a real number $\eta' > 0$ such that $\forall \varepsilon \in [-\eta', \eta']$

$$\boldsymbol{\lambda}_\varepsilon^N\Big(\mathfrak{b}^{\#}(\mathfrak{r}_0, R_{\mathfrak{r}_0})\Big) \subset \mathfrak{b}^{\#}(\mathfrak{r}_0, R'_{\mathfrak{r}_0}). \tag{2.5.48}$$

According to Lemma 2.4.25 there exists a real number $\eta'' > 0$ such that $\forall \varepsilon \in [-\eta'', \eta'']$

$$\boldsymbol{\vartheta}_{\varepsilon,\bar{g}_1}^{\alpha_1,1} \cdot \boldsymbol{\vartheta}_{\varepsilon,\bar{g}_2}^{\alpha_2,2} \cdot \ldots \cdot \boldsymbol{\vartheta}_{\varepsilon,\bar{g}_N}^{\alpha_N,N}\Big(\mathfrak{b}^{\#}(\mathfrak{r}_0, R_{\mathfrak{r}_0})\Big) \subset \mathfrak{b}^{\#}(\mathfrak{r}_0, R'_{\mathfrak{r}_0}). \tag{2.5.49}$$

Let $\eta^\star = \min(\eta', \eta'')$. Then for any $\varepsilon \in [-\eta^\star, \eta^\star]$ both $\boldsymbol{\lambda}_\varepsilon^N\left(\mathfrak{b}^\#(\mathfrak{r}_0, R_{\mathbf{r}_0})\right)$ and $\boldsymbol{\vartheta}_{\varepsilon,\bar{g}_1}^{\alpha_1,1} \cdot \boldsymbol{\vartheta}_{\varepsilon,\bar{g}_2}^{\alpha_2,2} \cdot \ldots \cdot \boldsymbol{\vartheta}_{\varepsilon,\bar{g}_N}^{\alpha_N,N}\left(\mathfrak{b}^\#(\mathfrak{r}_0, R_{\mathbf{r}_0})\right)$ are included in $\mathfrak{b}^\#\left(\mathfrak{r}_0, R'_{\mathbf{r}_0}\right)$ which is convex, and consequently, applying a Taylor Theorem we obtain :

$$\begin{aligned}\bar{G}^N\Big(\varepsilon, \boldsymbol{\vartheta}_{\varepsilon,\bar{g}_1}^{\alpha_1,1} \cdot \boldsymbol{\vartheta}_{\varepsilon,\bar{g}_2}^{\alpha_2,2} \cdot \ldots \cdot \boldsymbol{\vartheta}_{\varepsilon,\bar{g}_N}^{\alpha_N,N}(\mathfrak{r}) + \varepsilon^{N+1}\boldsymbol{\rho}_{\boldsymbol{\lambda}}^N(\varepsilon,\mathfrak{r})\Big)& \\ = \bar{G}^N\Big(\varepsilon, \boldsymbol{\vartheta}_{\varepsilon,\bar{g}_1}^{\alpha_1,1} \cdot \boldsymbol{\vartheta}_{\varepsilon,\bar{g}_2}^{\alpha_2,2} \cdot \ldots \cdot \boldsymbol{\vartheta}_{\varepsilon,\bar{g}_N}^{\alpha_N,N}(\mathfrak{r})\Big) + \varepsilon^{N+1}\boldsymbol{\rho}_{int1}^N(\varepsilon,\mathfrak{r})\,.& \quad (2.5.50)\end{aligned}$$

Eventually, applying formula (2.5.27) of Theorem 2.5.4, and the extension, given in Lemma 2.4.28, of Theorem 2.4.24 with $g_\varepsilon = \bar{G}^N(\varepsilon,\cdot)$ and $\boldsymbol{\vartheta}_{\varepsilon,\bar{g}_1}^{\alpha_1,1} \cdot \boldsymbol{\vartheta}_{\varepsilon,\bar{g}_2}^{\alpha_2,2} \cdot \ldots \cdot \boldsymbol{\vartheta}_{\varepsilon,\bar{g}_N}^{\alpha_N,N}$ instead of $\boldsymbol{\vartheta}_{\varepsilon,f}^{i,j}$, there exists a real number $\bar{\eta}_{20}$, smaller than $\eta^\star$, such that for any $\varepsilon \in [-\bar{\eta}_{20}, \bar{\eta}_{20}] \cap I$:

$$\begin{aligned}\hat{G}(\varepsilon,\mathfrak{r}) =& \bar{G}\left(\varepsilon, \boldsymbol{\lambda}_\varepsilon^N(\mathfrak{r})\right)\\ =& \bar{G}\Big(\varepsilon, \boldsymbol{\vartheta}_{\varepsilon,\bar{g}_1}^{\alpha_1,1} \cdot \boldsymbol{\vartheta}_{\varepsilon,\bar{g}_2}^{\alpha_2,2} \cdot \ldots \cdot \boldsymbol{\vartheta}_{\varepsilon,\bar{g}_N}^{\alpha_N,N}(\mathfrak{r}) + \varepsilon^{N+1}\boldsymbol{\rho}_{\boldsymbol{\lambda}}^N(\varepsilon,\mathfrak{r})\Big)\\ =& \bar{G}^N\Big(\varepsilon, \boldsymbol{\vartheta}_{\varepsilon,\bar{g}_1}^{\alpha_1,1} \cdot \boldsymbol{\vartheta}_{\varepsilon,\bar{g}_2}^{\alpha_2,2} \cdot \ldots \cdot \boldsymbol{\vartheta}_{\varepsilon,\bar{g}_N}^{\alpha_N,N}(\mathfrak{r})\Big) + \varepsilon^{N+1}\boldsymbol{\rho}_{int1}^N(\varepsilon,\mathfrak{r})\\ =& \left(\boldsymbol{\vartheta}_{\varepsilon,\bar{g}_1}^{\alpha_1,1} \cdot \boldsymbol{\vartheta}_{\varepsilon,\bar{g}_2}^{\alpha_2,2} \cdot \ldots \cdot \boldsymbol{\vartheta}_{\varepsilon,\bar{g}_N}^{\alpha_N,N}\right) \cdot \bar{G}^N(\varepsilon,\mathfrak{r}) + \varepsilon^{N+1}\rho_{\bar{G}}^N(\varepsilon,\mathfrak{r})\,.\end{aligned} \quad (2.5.51)$$

Since $\bar{G} \in \mathcal{C}_\#^\infty\Big(([-\bar{\eta}_{20};\bar{\eta}_{20}] \cap I) \times \mathfrak{b}^\#(\mathfrak{r}_0, R_{\mathbf{r}_0})\Big)$, and since

$$\left(\boldsymbol{\vartheta}_{\varepsilon,\bar{g}_1}^{\alpha_1,1} \cdot \boldsymbol{\vartheta}_{\varepsilon,\bar{g}_2}^{\alpha_2,2} \cdot \ldots \cdot \boldsymbol{\vartheta}_{\varepsilon,\bar{g}_N}^{\alpha_N,N}\right) \cdot \bar{G}^N \in \mathcal{C}_\#^\infty\Big([-\bar{\eta}_{20};\bar{\eta}_{20}] \times \mathfrak{b}^\#(\mathfrak{r}_0, R_{\mathbf{r}_0})\Big)\,,$$

the remainder $\rho_{\bar{G}}^N$ is also 2π-periodic with respect to the penultimate variable. This ends the proof of Theorem 2.5.6. □

To end this subsection, we will give an useful expression of $\hat{G}(\varepsilon,\mathfrak{r})$ that we will use in the next subsection. For $p \in \mathbb{N}$, we define the subset $\mathcal{U}_p \subset \mathbb{N}^p$ by

$$\mathcal{U}_p = \left\{(m_1,\ldots,m_p) \in \mathbb{N}^p \text{ s.t. } \sum_{k=1}^p k m_k = p\right\}. \quad (2.5.52)$$

Proposition 2.5.7. *With the same notations and under the same assumptions as in Theorem 2.5.6, if $\bar{G}^N$ can be written as*

$$\bar{G}^N(\varepsilon,\mathfrak{r}) = \sum_{k=0}^N \bar{G}_k(\mathfrak{r})\,\varepsilon^k, \quad (2.5.53)$$

then, there exists a real number $\bar{\eta}_{21} > 0$ such that for any $\varepsilon \in [-\bar{\eta}_{21};\bar{\eta}_{21}] \cap I$ and for any $\mathfrak{r} \in \mathfrak{b}^\#(\mathfrak{r}_0, R_{\mathfrak{r}_0})$:

$$\hat{G}(\varepsilon,\mathfrak{r}) = \sum_{n=0}^N \left(\sum_{k=0}^n \mathbf{V}_{n-k}^\varepsilon \cdot \bar{G}_k\right)(\mathfrak{r})\,\varepsilon^n + \varepsilon^{N+1}\iota_{\bar{G}}^{N,\bullet}(\varepsilon,\mathfrak{r})\,, \quad (2.5.54)$$

where, for any $l \in \{0,\ldots,N\}$,

$$\mathbf{V}_l^\varepsilon = \sum_{(m_1,\ldots,m_l)\in\mathcal{U}_l} \frac{\left(\bar{\mathbf{X}}_{\varepsilon\bar{g}_1}^\varepsilon\right)^{m_1} \cdot \ldots \cdot \left(\bar{\mathbf{X}}_{\varepsilon\bar{g}_l}^\varepsilon\right)^{m_l} \cdot}{m_1!\ldots m_l!} \quad (2.5.55)$$

Proof. The proof is obvious. We just have to expand formula (2.5.47). □

2.5.2 The Partial Lie Transform Method

The results we set out in the former subsection will be used to set out what we call the Partial Lie Transform Method of order N. This method applies to Hamiltonian Function $\bar{H}_\varepsilon$, since its first term does not depend on the penultimate coordinate; i.e. $\bar{H}_0 \in \bar{\mathcal{K}}$, where

$$\overline{\mathcal{K}} = \left\{ \bar{f} = \bar{f}\left(\bar{\mathbf{r}}\right) \in \mathcal{C}^\infty\big(\mathbb{R}^2 \times \mathbb{R} \times (0,+\infty)\big) \text{ s.t. } \frac{\partial \bar{f}}{\partial \bar{r}_3} = 0 \right\}. \tag{2.5.56}$$

The goal of the Partial Lie Transform Method is to find $\bar{g}_1, \bar{g}_2, \ldots, \bar{g}_N \in \mathcal{Q}^\infty_{T,b} \cap \mathcal{A}\big(\mathbb{R}^2 \times \mathbb{R} \times (0,+\infty)\big)$ such that under the change of coordinates (2.5.2) the Hamiltonian Function does not depend, up to order N, on the penultimate coordinate; i.e. such that the first terms $\hat{H}_0, \hat{H}_1, \ldots, \hat{H}_N$ of the expansion of $\hat{H}_\varepsilon$, are in

$$\hat{\mathcal{K}} = \left\{ \hat{f} \in \mathcal{C}^\infty\big(\mathbb{R}^2 \times \mathbb{R} \times (0,+\infty)\big) \text{ s.t. } \frac{\partial \hat{f}}{\partial \hat{r}_3} = 0 \right\}. \tag{2.5.57}$$

In this case, we will say that the Hamiltonian function is under its partial normal form of order N.

We will start the construction of the algorithm. The matrix $\bar{\mathcal{T}}_\varepsilon$, defined by $\bar{\mathcal{P}}_\varepsilon = \frac{1}{\varepsilon}\bar{\mathcal{T}}_\varepsilon$, is given by :

$$\bar{\mathcal{T}}_\varepsilon\left(\mathfrak{r}_1, \mathfrak{r}_2\right) = \bar{\mathcal{T}}_0 + \varepsilon^2 \bar{\mathcal{T}}_2\left(\mathfrak{r}_1, \mathfrak{r}_2\right), \tag{2.5.58}$$

where

$$\bar{\mathcal{T}}_0 = \begin{bmatrix} 0 & 0 & 0 & 0 \\ 0 & 0 & 0 & 0 \\ 0 & 0 & 0 & 1 \\ 0 & 0 & -1 & 0 \end{bmatrix} \text{ and } \bar{\mathcal{T}}_2\left(\mathfrak{r}_1, \mathfrak{r}_2\right) = \begin{bmatrix} 0 & \frac{-1}{B(\mathfrak{r}_1,\mathfrak{r}_2)} & 0 & 0 \\ \frac{1}{B(\mathfrak{r}_1,\mathfrak{r}_2)} & 0 & 0 & 0 \\ 0 & 0 & 0 & 0 \\ 0 & 0 & 0 & 0 \end{bmatrix}. \tag{2.5.59}$$

Hence Hamiltonian vector fields $\bar{\mathbf{X}}^\varepsilon_{\varepsilon\bar{g}_i}$ defined by (2.4.3) are given by :

$$\bar{\mathbf{X}}^\varepsilon_{\varepsilon\bar{g}_i} = \bar{\mathcal{T}}_0 \nabla \bar{g}_i + \varepsilon^2 \bar{\mathcal{T}}_2 \nabla \bar{g}_i, \tag{2.5.60}$$

or equivalently by

$$\bar{\mathbf{X}}^\varepsilon_{\varepsilon\bar{g}_i} = \overline{\mathbf{M}}_i + \varepsilon^2 \overline{\mathbf{N}}_{i+2}, \tag{2.5.61}$$

where

$$\overline{\mathbf{M}}_i = \frac{\partial \bar{g}_i}{\partial \mathfrak{r}_4}\frac{\partial}{\partial \mathfrak{r}_3} - \frac{\partial \bar{g}_i}{\partial \mathfrak{r}_3}\frac{\partial}{\partial \mathfrak{r}_4} \text{ and } \overline{\mathbf{N}}_{i+2} = -\frac{1}{B\left(\mathfrak{r}_1, \mathfrak{r}_2\right)}\left(\frac{\partial \bar{g}_i}{\partial \mathfrak{r}_2}\frac{\partial}{\partial \mathfrak{r}_1} - \frac{\partial \bar{g}_i}{\partial \mathfrak{r}_1}\frac{\partial}{\partial \mathfrak{r}_2}\right). \tag{2.5.62}$$

The first result on which the method is based is the following theorem.

Theorem 2.5.8. *Let $\mathcal{M}_0\mathcal{C}^\infty_{per}$ be the space defined by*

$$\mathcal{M}_0\mathcal{C}^\infty_{per} = \left\{ u \in \mathcal{C}^\infty_{\#}\left(\mathbb{R}^2 \times \mathbb{R} \times (0,+\infty)\right) \text{ such that } \int_0^{2\pi} u\left(\mathfrak{r}\right) d\mathfrak{r}_3 = 0 \right\}, \tag{2.5.63}$$

and $\bar{H}_0$ be the function defined by $\bar{H}_0\left(\mathfrak{r}_1, \mathfrak{r}_2, \mathfrak{r}_4\right) = B\left(\mathfrak{r}_1, \mathfrak{r}_2\right)\mathfrak{r}_4$ (see formula (2.3.118) of corollary 2.3.23). Then, for any $\bar{u} \in \mathcal{A}\big(\mathbb{R}^2 \times \mathbb{R} \times (0,+\infty)\big) \cap \mathcal{Q}^\infty_{T,b} \cap \mathcal{M}_0\mathcal{C}^\infty_{per}$, the function

$$\bar{g}\left(\mathfrak{r}\right) = -\frac{1}{B\left(\mathfrak{r}_1, \mathfrak{r}_2\right)} \int_0^{\mathfrak{r}_3} \bar{u}\left(\mathfrak{r}'\right) d\mathfrak{r}'_3 \tag{2.5.64}$$

is solution of the PDE

$$\big(\bar{\mathcal{T}}_0 \nabla \bar{g}\big) \cdot \nabla \bar{H}_0 = \bar{u}, \tag{2.5.65}$$

and $\bar{g} \in \mathcal{A}\big(\mathbb{R}^2 \times \mathbb{R} \times (0,+\infty)\big) \cap \mathcal{Q}^\infty_{T,b}$ *(see Definition 2.4.2 and* (2.3.117)*).*

Proof. On the one hand, PDE (2.5.65) can be rewritten

$$-\, B\,(\mathfrak{r}_1, \mathfrak{r}_2)\, \frac{\partial \bar{g}}{\partial \mathfrak{r}_3}\,(\mathfrak{r}) = \bar{u}\,(\mathfrak{r})\,. \tag{2.5.66}$$

Consequently, the function $\bar{g}$ defined by formula (2.5.64) is solution of (2.5.65). Now, we need to check that this function is in $\mathcal{A}\big(\mathbb{R}^2 \times \mathbb{R} \times (0,+\infty)\big) \cap \mathcal{Q}^\infty_{T,b}$. Firstly, since $\mathcal{A}\big(\mathbb{R}^2 \times \mathbb{R} \times (0,+\infty)\big)$ is stable by integration, function $\bar{g}$ is clearly in $\mathcal{A}\big(\mathbb{R}^2 \times \mathbb{R} \times (0,+\infty)\big)$. On the other hand, since $\bar{u} \in \mathcal{Q}^\infty_{T,b} \cap \mathcal{M}_0\mathcal{C}^\infty_{per}$ function $\bar{g}$ is in $\mathcal{Q}^\infty_{T,b}$. □

Theorem 2.5.9. *Let* $\bar{H}_\varepsilon$ *be the Hamiltonian function expressed in the Darboux coordinate system and whose expansion of order* N *is given by Corollary 2.3.22. Then, there exists* $\hat{H}_1, \dots, \hat{H}_N \in \hat{\mathcal{K}} \cap \mathcal{A}\big(\mathbb{R}^2 \times \mathbb{R} \times (0,+\infty)\big) \cap \mathcal{Q}^\infty_{T,b}$ *and* $\bar{g}_1, \dots, \bar{g}_N \in \mathcal{A}\big(\mathbb{R}^2 \times \mathbb{R} \times (0,+\infty)\big) \cap \mathcal{Q}^\infty_{T,b}$ *such that for any* $\mathfrak{r}_0 \in \mathbb{R}^2 \times \mathbb{R} \times (0,+\infty)$*, for any* $R_{\mathfrak{r}_0}$ *and* $R'_{\mathfrak{r}_0}$ *such that* $0 < R_{\mathfrak{r}_0} < R'_{\mathfrak{r}_0}$ *and* $\overline{\mathfrak{b}^\#\big(\mathfrak{r}_0, R'_{\mathfrak{r}_0}\big)} \subset \mathbb{R}^2 \times \mathbb{R} \times (0,+\infty)$ *there exists a real number* $\bar{\eta}_{14} > 0$*, such that for any* $\varepsilon \in [-\bar{\eta}_{14}; \bar{\eta}_{14}]$*, function* $\boldsymbol{\chi}^N_\varepsilon$ *defined by* (2.5.2) *is well defined on* $\mathfrak{b}^\#(\mathfrak{r}_0, R_{\mathfrak{r}_0})$*,*

$$\overline{\boldsymbol{\chi}^N_\varepsilon\Big(\mathfrak{b}^\#(\mathfrak{r}_0, R_{\mathfrak{r}_0})\Big)} \subset \mathfrak{b}^\#\big(\mathfrak{r}_0, R'_{\mathfrak{r}_0}\big)\,, \tag{2.5.67}$$

function $\boldsymbol{\lambda}^N_\varepsilon$ *defined by* (2.5.16) *is well defined on* $\mathfrak{b}^\#\big(\mathfrak{r}_0, R'_{\mathfrak{r}_0}\big)$*,*

$$\overline{\boldsymbol{\lambda}^N_\varepsilon\Big(\mathfrak{b}^\#\big(\mathfrak{r}_0, R'_{\mathfrak{r}_0}\big)\Big)} \subset \mathbb{R}^2 \times \mathbb{R} \times (0,+\infty)\,, \tag{2.5.68}$$

and for any $\varepsilon \in [-\bar{\eta}_{14}; \bar{\eta}_{14}] \cap \mathbb{R}_+$ *function* $\hat{H}^N_\varepsilon$ *defined by* $\hat{H}^N_\varepsilon(\mathfrak{r}) = \bar{H}_\varepsilon\big(\boldsymbol{\lambda}^N_\varepsilon(\mathfrak{r})\big)$ *writes :*

$$\hat{H}^N_\varepsilon(\mathfrak{r}) = \sum_{k=0}^{n} \hat{H}_k(\mathfrak{r})\, \varepsilon^k + \varepsilon^{N+1} \iota^N_{\hat{H}}(\varepsilon, \mathfrak{r})\,, \tag{2.5.69}$$

where $\iota^N_{\hat{H}} \in \mathcal{C}^\infty_\# \Big([0; \bar{\eta}_{14}] \times \mathfrak{b}^\#\big(\mathfrak{r}_0, R'_{\mathfrak{r}_0}\big)\Big)$ *(see* (2.3.30)*).*

Remark 2.5.10. *In order to be precise, if we work on the Darboux Coordinate chart or on the Partial Lie Transform Coordinate chart we will write* $\bar{\mathfrak{r}}$*, instead of* $\mathfrak{r}$*, for* $\mathfrak{r}$ *in the Darboux coordinate chart; and* $\hat{\mathfrak{r}}$*, instead of* $\mathfrak{r}$*, for* $\mathfrak{r}$ *in the Partial Lie Transform coordinate chart. In Theorem 2.5.9, the periodic ball* $\mathfrak{b}^\#(\mathfrak{r}_0, R_{\mathfrak{r}_0})$ *is viewed as a subset of the open subset on which the Darboux Coordinate System is defined (precisely* $\mathbb{R}^2 \times \mathbb{R} \times (0,+\infty)$*), and* $\mathfrak{b}^\#\big(\mathfrak{r}_0, R'_{\mathfrak{r}_0}\big)$ *is viewed as a subset of the open subset on which the Partial Lie Transform Coordinate System is defined.*

Proof. Let $\bar{g}_1, \dots, \bar{g}_N \in \mathcal{A}\big(\mathbb{R}^2 \times \mathbb{R} \times (0,+\infty)\big) \cap \mathcal{Q}^\infty_{T,b}$. According to Lemma 2.5.1 and Theorem 2.5.3, there exists a real number $\bar{\eta}_{20} > 0$ such that for any $\varepsilon \in [-\bar{\eta}_{20}; \bar{\eta}_{20}]$, formulas (2.5.67) and (2.5.68) hold true. Moreover, according to Proposition 2.5.7, there exists a real number $\bar{\eta}_{21} > 0$ such that for any $\varepsilon \in [-\bar{\eta}_{21}; \bar{\eta}_{21}] \cap \mathbb{R}_+$ and for any $\hat{\mathfrak{r}} \in \mathfrak{b}^\#\big(\mathfrak{r}_0, R'_{\mathfrak{r}_0}\big)$,

$$\hat{H}^N_\varepsilon(\hat{\mathfrak{r}}) = \sum_{n=0}^{N} \left(\sum_{k=0}^{n} \mathbf{V}^\varepsilon_{n-k} \cdot \bar{H}_k \right)(\hat{\mathfrak{r}})\, \varepsilon^n + \varepsilon^{N+1} \iota^{N,\bullet}_{\bar{H}}(\varepsilon, \hat{\mathfrak{r}})\,, \tag{2.5.70}$$

where $\iota_{\hat{H}}^N \in \mathcal{C}^\infty_{\#}\Big([-\bar{\eta}_{21};\bar{\eta}_{21}]\cap\mathbb{R}_+\times\mathfrak{b}^{\#}\big(\mathfrak{r}_0,R'_{\mathfrak{r}_0}\big)\Big)$, and for any $l\in\{0,\dots,N\}$, $\mathbf{V}_l^\varepsilon$ is defined by formula (2.5.55).
The only possible values that m_l can have in formula (2.5.55) are 0 and 1. If $m_l=1$, then $m_1=m_2=\ldots=m_{l-1}=0$. Hence, the only term in the sum of the right hand side of (2.5.55) that involves function $\bar{g}_l$ is $\bar{\mathbf{X}}^\varepsilon_{\varepsilon\bar{g}_l}\cdot$. Consequently the only term of

$$\sum_{k=0}^{n}\mathbf{V}^\varepsilon_{n-k}\cdot\bar{H}_k \tag{2.5.71}$$

that involves function $\bar{g}_n$ is $\bar{\mathbf{X}}^\varepsilon_{\varepsilon\bar{g}_n}\cdot\bar{H}_0$.

Injecting formula (2.5.61) in the right hand side of (2.5.70), gathering terms of the same power of ε, and comparing the result with the desired form of $\hat{H}^N_\varepsilon(\hat{\mathbf{r}})$:

$$\hat{H}^N_\varepsilon(\hat{\mathbf{r}})=\bar{H}_0(\hat{r}_1,\hat{r}_2,\hat{r}_4)+\varepsilon\hat{H}_1(\hat{r}_1,\hat{r}_2,\hat{r}_4)+\ldots+\varepsilon^N\hat{H}_N(\hat{r}_1,\hat{r}_2,\hat{r}_4)+\varepsilon^{N+1}\iota_{\hat{H}}(\varepsilon,\hat{\mathbf{r}})\,, \tag{2.5.72}$$

we obtain that $\bar{g}_1$ must be such that

$$\hat{H}_1=\bar{H}_1+\big(\bar{\mathcal{T}}_0\nabla\bar{g}_1\big)\cdot\nabla\bar{H}_0, \tag{2.5.73}$$

and, for any $i\in\{2,\dots,N\}$, that $\bar{g}_i$ must satisfy

$$\hat{H}_i=\big(\bar{\mathcal{T}}_0\nabla\bar{g}_i\big)\cdot\nabla\bar{H}_0-\mathcal{V}\left(\bar{g}_1,\dots,\bar{g}_{i-1}\right), \tag{2.5.74}$$

with $\mathcal{V}\left(\bar{g}_1,\dots,\bar{g}_{i-1}\right)$ depending only on $\bar{g}_1,\dots,\bar{g}_{i-1}$ and their derivatives (and of course of the entries of the Poisson Matrix) and, consequently, is in $\mathcal{A}\big(\mathbb{R}^2\times\mathbb{R}\times(0,+\infty)\big)\cap\mathcal{Q}^\infty_{T,b}$.

Now, to end the proof, we need to check that using (2.5.73) and (2.5.74) we can build recursively $\hat{H}_1,\dots,\hat{H}_N$ and $\bar{g}_1,\dots,\bar{g}_N\in\mathcal{A}\big(\mathbb{R}^2\times\mathbb{R}\times(0,+\infty)\big)\cap\mathcal{Q}^\infty_{T,b}$ such that for any $i\in\{1,\dots,N\}$, $\hat{H}_i$ is in $\hat{\mathcal{K}}\cap\mathcal{A}\big(\mathbb{R}^2\times\mathbb{R}\times(0,+\infty)\big)\cap\mathcal{Q}^\infty_{T,b}$. We will prove it by induction on $i\in\{1,\dots,N\}$.

For $i=1$, setting

$$\hat{H}_1=\frac{1}{2\pi}\int_0^{2\pi}\bar{H}_1\,d\hat{r}_3\quad\text{and}\quad u_1=-\bar{H}_1+\frac{1}{2\pi}\int_0^{2\pi}\bar{H}_1\,d\hat{r}_3, \tag{2.5.75}$$

yields that $\hat{H}_1\in\hat{\mathcal{K}}\cap\mathcal{A}\big(\mathbb{R}^2\times\mathbb{R}\times(0,+\infty)\big)\cap\mathcal{Q}^\infty_{T,b}$ and $u_1\in\mathcal{A}\big(\mathbb{R}^2\times\mathbb{R}\times(0,+\infty)\big)\cap\mathcal{Q}^\infty_{T,b}\cap\mathcal{M}_0\mathcal{C}^\infty_{per}$. Hence, equation (2.5.73) yields

$$\big(\bar{\mathcal{T}}_0\nabla\bar{g}_1\big)\cdot\nabla\bar{H}_0=u_1, \tag{2.5.76}$$

and Theorem 2.5.8 gives $\bar{g}_1$ as a solution to this PDE.

Let $i\in\{1,\dots,N-1\}$. Assume the result for all $k\in\{1,\dots,i\}$. $\hat{H}_{i+1}$ is given by $\hat{H}_{i+1}=\big(\bar{\mathcal{T}}_0\nabla\bar{g}_{i+1}\big)\cdot\nabla\bar{H}_0-\mathcal{V}_{i+1}\left(\bar{g}_1,\dots,\bar{g}_i\right)$. Setting

$$\hat{H}_{i+1}=-\frac{1}{2\pi}\int_0^{2\pi}\mathcal{V}_{i+1}\left(\bar{g}_1,\dots,\bar{g}_i\right)d\hat{r}_3\in\hat{\mathcal{K}}\cap\mathcal{A}\big(\mathbb{R}^2\times\mathbb{R}\times(0,+\infty)\big)\cap\mathcal{Q}^\infty_{T,b}, \tag{2.5.77}$$

and

$$u_{i+1}=\mathcal{V}_{i+1}\left(\bar{g}_1,\dots,\bar{g}_i\right)-\frac{1}{2\pi}\int_0^{2\pi}\mathcal{V}\left(\bar{g}_1,\dots,\bar{g}_i\right)d\hat{r}_3$$
$$\in\mathcal{A}\big(\mathbb{R}^2\times\mathbb{R}\times(0,+\infty)\big)\cap\mathcal{Q}^\infty_{T,b}\cap\mathcal{M}_0\mathcal{C}^\infty_{per}, \tag{2.5.78}$$

transform this equation into

$$\left(\bar{\mathcal{T}}_0 \nabla \bar{g}_{i+1}\right) \cdot \nabla \bar{H}_0 = u_{i+1}. \tag{2.5.79}$$

Here again Theorem 2.5.8 gives $\bar{g}_{i+1}$ as a solution to this PDE. This ends the proof of Theorem 2.5.9. □

Theorem 2.5.9 and its proof makes up the Partial Lie Transform Algorithm. This algorithm can be summarized as follow :

Algorithm 2.5.11.

– *step 1 : Inject formula* (2.5.61) *in the right hand side of*

$$\hat{H}_\varepsilon^N(\hat{\mathbf{r}}) = \sum_{n=0}^{N} \left(\sum_{k=0}^{n} \mathbf{V}_{n-k}^\varepsilon \cdot \bar{H}_k \right)(\hat{\mathbf{r}})\, \varepsilon^n + \varepsilon^{N+1} \iota_{\bar{H}}^{N,\bullet}(\varepsilon, \hat{\mathbf{r}}), \tag{2.5.80}$$

where for any $l \in \{0, \ldots, N\}$, $\mathbf{V}_l^\varepsilon$ *is defined by formula* (2.5.55).

– *step 2 : Gather terms according to their power of* ε *and compare the result with the following desired expression :*

$$\hat{H}_\varepsilon^N(\hat{\mathbf{r}}) = \hat{H}_{\varepsilon,T}^N(\hat{r}_1, \hat{r}_2, \hat{r}_4) + \varepsilon^{N+1} \iota_{\hat{H}}^N(\varepsilon, \hat{\mathbf{r}}), \tag{2.5.81}$$

with

$$\hat{H}_{\varepsilon,T}^N(\hat{r}_1, \hat{r}_2, \hat{r}_4) = \bar{H}_0(\hat{r}_1, \hat{r}_2, \hat{r}_4) + \varepsilon \hat{H}_1(\hat{r}_1, \hat{r}_2, \hat{r}_4) + \ldots + \varepsilon^N \hat{H}_N(\hat{r}_1, \hat{r}_2, \hat{r}_4), \tag{2.5.82}$$

to obtain

$$\hat{H}_1 = \bar{H}_1 + \left(\bar{\mathcal{T}}_0 \nabla \bar{g}_1\right) \cdot \nabla \bar{H}_0 \tag{2.5.83}$$

and, for any $i \in \{1, \ldots, N\}$ *:*

$$\hat{H}_i = \left(\bar{\mathcal{T}}_0 \nabla \bar{g}_i\right) \cdot \nabla \bar{H}_0 - \mathcal{V}_i(\bar{g}_1, \ldots, \bar{g}_{i-1}). \tag{2.5.84}$$

– *step 3 : Set*

$$\hat{H}_1 = -\frac{1}{2\pi} \int_0^{2\pi} \bar{H}_1 \, d\hat{r}_3, \tag{2.5.85}$$

and get $\bar{g}_1$ *by solving*

$$\left(\bar{\mathcal{T}}_0 \nabla \bar{g}_1\right) \cdot \nabla \bar{H}_0 = \bar{H}_1 - \frac{1}{2\pi} \int_0^{2\pi} \bar{H}_1 \, d\hat{r}_3. \tag{2.5.86}$$

Then for $i \in \{1, \ldots, N\}$*, set*

$$\begin{aligned} \hat{H}_i &= -\frac{1}{2\pi} \int_0^{2\pi} \mathcal{V}_i\left(\bar{g}_1, \ldots, \bar{g}_{i-1}\right) d\hat{r}_3, \\ u_i &= \mathcal{V}_i\left(\bar{g}_1, \ldots, \bar{g}_{i-1}\right) - \frac{1}{2\pi} \int_0^{2\pi} \mathcal{V}_i\left(\bar{g}_1, \ldots, \bar{g}_{i-1}\right) d\hat{r}_3, \end{aligned} \tag{2.5.87}$$

and get $\bar{g}_i$ *by solving :*

$$\left(\bar{\mathcal{T}}_0 \nabla \bar{g}_i\right) \cdot \nabla \bar{H}_0 = u_i, \tag{2.5.88}$$

with the help of formula (2.5.64).

This Algorithm is given in detail up to $N = 5$ in Appendix B.2.

Applying this algorithm, we obtain functions $\bar{g}_i$ and hence the change of coordinates

$$\hat{\mathbf{r}} = \boldsymbol{\chi}_\varepsilon^N (\varepsilon, \bar{\mathbf{r}}), \tag{2.5.89}$$

where $\boldsymbol{\chi}_\varepsilon^N$ is defined by (2.5.2) and (2.4.46). Moreover, in the yielding coordinate system the Hamiltonian function writes

$$\hat{H}_\varepsilon^N(\hat{\mathbf{r}}) = \bar{H}_0(\hat{r}_1, \hat{r}_2, \hat{r}_4) + \sum_{n=0}^{N} \varepsilon^n \hat{H}_n(\hat{r}_1, \hat{r}_2, \hat{r}_4) + \varepsilon^{N+1} \iota_{\hat{H}}^N(\hat{\mathbf{r}}), \tag{2.5.90}$$

and the Poisson Matrix is given by formulas (2.5.35) and (2.5.36).

2.6 The Gyro-Kinetic Coordinate System - Proof of Theorem 2.1.3

In the present section, we begin by giving the following Theorem 2.6.1 from which the part of Theorem 2.1.3 that concerns any value of N is then deducted. In the next subsection, we prove Theorem 2.6.1 and finally, we consider the case when $N = 2$ to end the proof of Theorem 2.1.3.

Theorem 2.6.1. *Assume that the magnetic field B satisfies assumptions* (2.1.42) *and* (2.1.43) *and that all its derivatives are bounded. Let $\boldsymbol{\Upsilon}$ be the diffeomorphism of $\mathbb{R}^2 \times \mathbb{R} \times (0, +\infty)$, whose components are solutions to the system of PDEs* (2.3.11)*, whose third component is given by $\boldsymbol{\Upsilon}_3(\mathbf{x}, \theta, v) = \theta$ and which expansions of its components* 1, 2 *and* 4 *are given by Theorems 2.3.4, 2.3.10 and 2.3.11. Let N be a positive integer; and $\bar{g}_1$, $\ldots$, $\bar{g}_N$ and $\hat{H}_{\varepsilon,T}^N$ be the maps defined on $\mathbb{R}^2 \times \mathbb{R} \times (0, +\infty)$ and obtained by Algorithm 2.5.11. Then, for any open subset $\mathcal{O}_{\mathfrak{Pol}} = \mathfrak{b}^2(\mathbf{x}_0, R_{\mathbf{x}_0}) \times \mathbb{R} \times (a, b)$, for any $R'_{\mathbf{x}_0}$ such that $R'_{\mathbf{x}_0} > R_{\mathbf{x}_0}$, and for any (c, d) such that $\left[\frac{a^2}{2\|B\|_\infty}, \frac{b^2}{2}\right] \subset (c, d)$, there exists a real number $\eta \in (0, +\infty)$, such that for any $\varepsilon \in (0, \eta)$, there exists a real number $t_e^\varepsilon > \frac{\alpha_0}{\varepsilon}$, where $\alpha_0 > 0$ does not depend on ε, such that for any $(\mathbf{y}_0, \theta_0, k_0) \in \boldsymbol{\Upsilon}(\mathfrak{b}^2(\mathbf{x}_0, R_{\mathbf{x}_0}) \times \mathbb{R} \times (a, b))$, and for any $t \in (-t_e^\varepsilon, t_e^\varepsilon)$, the characteristic $(\mathbf{Y}^\varepsilon, \boldsymbol{\mathcal{K}}_{\mathfrak{Dar}}^\varepsilon, \Theta_{\mathfrak{Dar}}^\varepsilon)(t; \mathbf{y}_0, \theta_0, k_0)$ expressed in the Darboux Coordinate System $(\mathbf{y}, \theta, k) = \boldsymbol{\Upsilon}(\mathbf{x}, \theta, v)$ satisfies*

$$(\mathbf{Y}^\varepsilon, \boldsymbol{\mathcal{K}}_{\mathfrak{Dar}}^\varepsilon, \Theta_{\mathfrak{Dar}}^\varepsilon)(t; \mathbf{y}_0, \theta_0, k_0) \in \mathfrak{b}^2\big(\mathbf{x}_0, R'_{\mathbf{x}_0}\big) \times \mathbb{R} \times \left[\frac{a^2}{2\|B\|_\infty}, \frac{b^2}{2}\right]; \tag{2.6.1}$$

and such that the map $\boldsymbol{\chi}_\varepsilon^N$, defined by

$$\boldsymbol{\chi}_\varepsilon^N = \boldsymbol{\vartheta}_{\varepsilon,-\bar{g}_1}^{\alpha_1,1} \circ \boldsymbol{\vartheta}_{\varepsilon,-\bar{g}_2}^{\alpha_2,2} \circ \ldots \circ \boldsymbol{\vartheta}_{\varepsilon,-\bar{g}_N}^{\alpha_N,N}, \tag{2.6.2}$$

where for any $i \in \{1, \ldots, N\}$, the function $\boldsymbol{\vartheta}_{\varepsilon,-\bar{g}_i}^{\alpha_i,i}$ is defined on $\mathbb{R}^2 \times \mathbb{R} \times (0, +\infty)$ by formula (2.4.45) *and where the α_i are defined by* (2.5.1)*, is a diffeomorphism from*

$$\mathcal{O}_{\mathfrak{Dar}} = \mathfrak{b}^2\big(\mathbf{x}_0, R'_{\mathbf{x}_0}\big) \times \mathbb{R} \times (c, d), \tag{2.6.3}$$

onto its range.
Moreover, for any $\varepsilon \in (0, \eta)$, for any $t \in (-t_e^\varepsilon, t_e^\varepsilon)$, for any $(\mathbf{z}_0, \gamma_0, j_0) \in \boldsymbol{\chi}_\varepsilon^N \circ \boldsymbol{\Upsilon}(\mathfrak{b}^2(\mathbf{x}_0, R_{\mathbf{x}_0}) \times$

$\mathbb{R}\times(a,b))$, *the solution* $\left(\mathbf{Z}^{T,\#},\Gamma^{T,\#},\mathcal{J}^{T,\#}\right)=\left(\mathbf{Z}^{T,\#},\Gamma^{T,\#},\mathcal{J}^{T,\#}\right)(t,\mathbf{z}_0,\gamma_0,j_0)$ *of the following dynamical system, written within system of coordinates* $(\mathbf{z},\gamma,j)=\boldsymbol{\chi}_\varepsilon^N(\mathbf{y},\theta,k)$ *on* $\boldsymbol{\chi}_\varepsilon^N(\mathcal{O}_{\mathfrak{Dar}})$,

$$\frac{\partial\mathbf{Z}^{T,\#}}{\partial t}=-\frac{\varepsilon}{B\left(\mathbf{Z}^{T,\#}\right)}\begin{pmatrix}\dfrac{\partial\hat{H}^N_{\varepsilon,T}}{\partial z_2}\left(\mathbf{Z}^{T,\#},j_0\right)\\ -\dfrac{\partial\hat{H}^N_{\varepsilon,T}}{\partial z_1}\left(\mathbf{Z}^{T,\#},j_0\right)\end{pmatrix},\qquad \mathbf{Z}^{T,\#}(0;\mathbf{z}_0,j_0)=\mathbf{z}_0, \tag{2.6.4}$$

$$\frac{\partial\Gamma^{T,\#}}{\partial t}=-\frac{1}{\varepsilon}\frac{\partial\hat{H}^N_{\varepsilon,T}}{\partial j}\left(\mathbf{Z}^{T,\#},j_0\right),\qquad \mathbf{\Gamma}^{T,\#}(0;\mathbf{z}_0,j_0,\gamma_0)=\gamma_0, \tag{2.6.5}$$

$$\frac{\partial\mathcal{J}^{T,\#}}{\partial t}=0,\qquad \mathcal{J}^{T,\#}(0;\mathbf{z}_0,j_0)=j_0, \tag{2.6.6}$$

where $\hat{H}^N_{\varepsilon,T}$ *is defined by formula*(2.5.82)*, satisfies*

$$\left\|(\mathbf{Z}^{\#},\mathcal{J}^{\#})-(\mathbf{Z}^{T,\#},\mathcal{J}^{T,\#})\right\|_{\infty,\mathbf{init}^{\#}}\leq C\varepsilon^{N-1}, \tag{2.6.7}$$

where C *is a constant that does not depend on* ε*, where*

$$\|g\|_{\infty,\mathbf{init}^{\#}}=\sup_{(\mathbf{z}_0,j_0,\gamma_0)\in\boldsymbol{\chi}_\varepsilon^N\circ\boldsymbol{\Upsilon}(\mathfrak{b}^2(\mathbf{x}_0,R_{\mathbf{x}_0})\times\mathbb{R}\times(a,b))}\left|g(\mathbf{z}_0,j_0,\gamma_0)\right|, \tag{2.6.8}$$

and where $\left(\mathbf{Z}^{\#},\Gamma^{\#},\mathcal{J}^{\#}\right)=\boldsymbol{\chi}_\varepsilon^N(\mathbf{Y}^\varepsilon,\boldsymbol{\mathcal{K}}^\varepsilon_{\mathfrak{Dar}},\Theta^\varepsilon_{\mathfrak{Dar}})$ *corresponds to the expression of* $(\mathbf{Y}^\varepsilon,\boldsymbol{\mathcal{K}}^\varepsilon_{\mathfrak{Dar}},\Theta^\varepsilon_{\mathfrak{Dar}})$ *in the coordinate system* $(\mathbf{z},\gamma,j)$.

2.6.1 Proof of Theorem 2.1.3 for any fixed N

Once N is fixed, in view of definitions of $\mathcal{O}(\mathbf{x}_0,R_{\mathbf{x}_0};a,b)$ and $\boldsymbol{\mathcal{U}}_{\boldsymbol{\mathcal{D}}}$ and having in mind that $\boldsymbol{\Upsilon}$ and $\boldsymbol{\chi}_\varepsilon^N$ are the Darboux change of coordinate map and the Lie change of coordinate map, the proof of the first part of Theorem 2.1.3 is a direct consequence of Theorem 2.6.1, as soon as there exists a diffeomorphism

$$\boldsymbol{\chi}_\varepsilon^{N,\circ}\ :\ \mathfrak{b}^2\left(\mathbf{x}_0,R'_{\mathbf{x}_0}\right)\times(\mathbb{R}/2\pi\mathbb{Z})\times(c,d)\to\boldsymbol{\chi}_\varepsilon^{N,\circ}(\mathfrak{b}^2\left(\mathbf{x}_0,R'_{\mathbf{x}_0}\right)\times(\mathbb{R}/2\pi\mathbb{Z})\times(c,d)\big) \tag{2.6.9}$$

such that $\mathfrak{p}\circ\boldsymbol{\chi}_\varepsilon^N(t,\cdot)=\boldsymbol{\chi}_\varepsilon^{N,\circ}(t,\cdot)\circ\mathfrak{p}$.

Since the components 1, 2 and 4 of $\boldsymbol{\chi}_\varepsilon^N$ are 2π-periodic with respect to θ, and since the penultimate components satisfies

$$\left(\boldsymbol{\chi}_\varepsilon^N\right)_3(\mathbf{y},\theta+2\pi,k)=\left(\boldsymbol{\chi}_\varepsilon^N\right)_3(\mathbf{y},\theta,k)+2\pi, \tag{2.6.10}$$

it is obviously the case.

Notice also that map $\mathfrak{GG}_\varepsilon$ is given by

$$\mathfrak{GG}_\varepsilon=\boldsymbol{\chi}_\varepsilon^{N,\circ}\circ\boldsymbol{\Upsilon}\circ\mathfrak{Pol}. \tag{2.6.11}$$

2.6.2 Proof of Theorem 2.6.1

The proof of Theorem 2.6.1 consists essentially in showing that we are under the conditions of application of Theorem 2.4.1, and to apply it.

Once N is fixed, let $\hat{H}_1,\ldots,\hat{H}_N\in\hat{\mathcal{K}}\cap\mathcal{A}(\mathbb{R}^2\times\mathbb{R}\times(0,+\infty))\cap\mathcal{Q}^\infty_{T,b}$ and $\bar{g}_1,\ldots,\bar{g}_N\in\mathcal{A}(\mathbb{R}^2\times\mathbb{R}\times(0,+\infty))\cap\mathcal{Q}^\infty_{T,b}$ (see Definition 2.4.2 and (2.3.117)) be the functions obtained

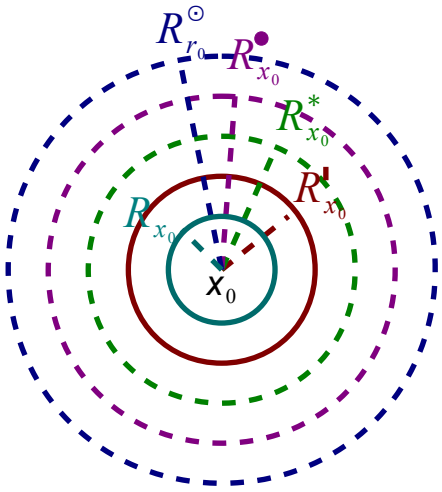

FIGURE 2.8 –

by applying Algorithm 2.5.11 ; $\mathcal{O}_{\mathfrak{Pol}} = \mathfrak{b}^2(\mathbf{x}_0, R_{\mathbf{x}_0}) \times \mathbb{R} \times (a,b)$; and $\mathcal{O}_{\mathfrak{Dar}} = \mathfrak{b}^2(\mathbf{x}_0, R'_{\mathbf{x}_0}) \times \mathbb{R} \times (c,d)$, where $R'_{\mathbf{x}_0} > R_{\mathbf{x}_0}$ and $\left[\frac{a^2}{2\|B\|_\infty}, \frac{b^2}{2}\right] \subset (c,d)$.

Let $\mathcal{O}^{\mathfrak{D},\star}_{\mathfrak{Int}} = \mathfrak{b}^2\left(\mathbf{x}_0, R^{\star}_{\mathbf{x}_0}\right) \times \mathbb{R} \times (c^\star, d^\star)$, $\mathcal{O}^{\mathfrak{D},\bullet}_{\mathfrak{Int}} = \mathfrak{b}^2\left(\mathbf{x}_0, R^{\bullet}_{\mathbf{x}_0}\right) \times \mathbb{R} \times (c^\bullet, d^\bullet)$; and $\mathcal{O}^{\mathfrak{D},\odot}_{\mathfrak{Int}} = \mathfrak{b}^2\left(\mathbf{x}_0, R^{\odot}_{\mathbf{x}_0}\right) \times \mathbb{R} \times (c^\odot, d^\odot)$, where $R^{\star}_{\mathbf{x}_0}$, $R^{\bullet}_{\mathbf{x}_0}$ and $R^{\odot}_{\mathbf{x}_0}$ are positive real numbers satisfying $0 < R'_{\mathbf{x}_0} < R^{\star}_{\mathbf{x}_0} < R^{\bullet}_{\mathbf{x}_0} < R^{\odot}_{\mathbf{x}_0}$ (see Figure 2.8), and

$$[c,d] \subset (c^\star, d^\star) \subset [c^\star, d^\star] \subset (c^\bullet, d^\bullet) \subset [c^\bullet, d^\bullet] \subset \left(c^\odot, d^\odot\right) \subset \left[c^\odot, d^\odot\right] \subset (0, +\infty)\,. \quad (2.6.12)$$

Firstly, we will show that the Lie change of coordinates map of order N $\boldsymbol{\chi}^N_\varepsilon$ is well defined on $\mathcal{O}^{\mathfrak{D},\odot}_{\mathfrak{Int}}$, that the inverse map $\boldsymbol{\lambda}^N_\varepsilon$ is well defined on $\mathcal{O}^{\mathfrak{D},\bullet}_{\mathfrak{Int}}$, and that the restriction of $\boldsymbol{\chi}^N_\varepsilon$ to $\mathcal{O}_{\mathfrak{Dar}}$ is a diffeomorphism whose range is included in $\mathcal{O}^{\mathfrak{D},\star}_{\mathfrak{Int}}$.
Applying Theorem 2.4.9 with $\mathfrak{C} = \mathfrak{b}^2\left(\mathbf{x}_0, R^{\odot}_{\mathbf{x}_0}\right) \times (c^\odot, d^\odot)$ and $\mathfrak{C}^{\#} = \mathcal{O}^{\mathfrak{D},\odot}_{\mathfrak{Int}}$ yields that for any positive integers i, j and for any function f in $\mathcal{C}^\infty_{\#}\left(\mathcal{O}^{\mathfrak{D},\odot}_{\mathfrak{Int}}\right) \cap \mathcal{C}^\infty_b\left(\mathcal{O}^{\mathfrak{D},\odot}_{\mathfrak{Int}}\right)$, there exists a real number η_1 such that for any $\varepsilon \in (-\eta_1, \eta_1)$ function $\boldsymbol{\vartheta}^{i,j}_{\varepsilon,f}$ defined by (2.4.46) is a diffeomorphism from $\mathcal{O}^{\mathfrak{D},\odot}_{\mathfrak{Int}}$ onto its range. Afterwards, a direct induction yields that there exists a real number η_N such that for any $\varepsilon \in (-\eta_N, \eta_N)$ the Partial Lie Transform map of order N is a diffeomorphism from $\mathcal{O}^{\mathfrak{D},\odot}_{\mathfrak{Int}}$ onto its range.

Now, by compacity, we can cover $\mathcal{O}^{\mathfrak{D},\bullet}_{\mathfrak{Int}}$ by a finite number $p^\bullet$ of periodic balls :

$$\mathcal{O}^{\mathfrak{D},\bullet}_{\mathfrak{Int}} = \bigcup_{k=1}^{p^\bullet} \mathfrak{b}^{\#}\left(\mathfrak{r}^k_0, R^{\bullet}_{\mathfrak{r}^k_0}\right), \quad (2.6.13)$$

such that for any $k \in \{1, \ldots, p^\bullet\}$, there exists $R^{\odot}_{\mathfrak{r}^k_0}$ such that $R^{\bullet}_{\mathfrak{r}^k_0} < R^{\odot}_{\mathfrak{r}^k_0}$ and $\overline{\mathfrak{b}^{\#}\left(\mathfrak{r}^k_0, R^{\odot}_{\mathfrak{r}^k_0}\right)} \subset \mathcal{O}^{\mathfrak{D},\odot}_{\mathfrak{Int}}$.

According to Lemma 2.5.1, for each $k \in \{1, \ldots, p^\bullet\}$, there exists a real number $\eta^\bullet_k$ such that for any $\varepsilon \in (-\eta^\bullet_k, \eta^\bullet_k)$

$$\mathfrak{b}^{\#}\left(\mathfrak{r}^k_0, R^{\bullet}_{\mathfrak{r}^k_0}\right) \subset \boldsymbol{\chi}^N_\varepsilon\left(\mathfrak{b}^{\#}\left(\mathfrak{r}^k_0, R^{\odot}_{\mathfrak{r}^k_0}\right)\right). \quad (2.6.14)$$

Consequently, for sufficiently small ε, $\boldsymbol{\lambda}_\varepsilon^N$ is well defined on $\mathcal{O}_{\mathfrak{Int}}^{\mathfrak{D},\bullet}$.

According to Theorems 2.5.4, 2.5.5, and 2.5.9, for any $k \in \{1,\dots,p^\bullet\}$, there exists a real number $\bar{\eta}_k$ such that for any $\varepsilon \in [-\bar{\eta}_k, \bar{\eta}_k]$, the inverse function $\boldsymbol{\lambda}_\varepsilon^N = \left(\boldsymbol{\chi}_\varepsilon^N\right)^{-1}$ of $\boldsymbol{\chi}_\varepsilon^N$ is analytic on $\mathfrak{b}^{\#}\left(\mathfrak{r}_0^k, R_{\mathfrak{r}_0^k}^\bullet\right)$ and expresses as

$$\boldsymbol{\lambda}_\varepsilon^N(\mathfrak{r}) = \boldsymbol{\vartheta}_{\varepsilon,\bar{g}_1}^{\alpha_1,1} \cdot \boldsymbol{\vartheta}_{\varepsilon,\bar{g}_2}^{\alpha_2,2} \cdot \ldots \cdot \boldsymbol{\vartheta}_{\varepsilon,\bar{g}_N}^{\alpha_N,N}(\mathfrak{r}) + \varepsilon^{N+1}\boldsymbol{\rho}_{\boldsymbol{\lambda}}^{N,k}(\varepsilon,\mathfrak{r}), \tag{2.6.15}$$

where $\boldsymbol{\rho}_{\boldsymbol{\lambda}}^{N,k}$ is in $\mathcal{C}_{\#}^\infty\left([-\bar{\eta}_k,\bar{\eta}_k] \times \mathfrak{b}^{\#}\left(\mathfrak{r}_0^k, R_{\mathfrak{r}_0^k}^\bullet\right)\right)$; the matrix $\hat{\mathcal{P}}_\varepsilon$, defined by (2.5.33), is well defined on $\mathfrak{b}^{\#}\left(\mathfrak{r}_0^k, R_{\mathfrak{r}_0^k}^\bullet\right)$ and

$$\forall i,j \in \{1,2,3,4\},\ \hat{\mathcal{T}}_\varepsilon^{i,j}(\mathfrak{r}) = \bar{\mathcal{T}}_\varepsilon^{i,j}(\mathfrak{r}) + \varepsilon^{N+1}\rho_{\hat{\mathcal{T}}^{i,j}}^{N,k}(\varepsilon,\mathfrak{r}), \tag{2.6.16}$$

where $\rho_{\hat{\mathcal{T}}^{i,j}}^{N,k}$ is in $\mathcal{C}_{\#}^\infty\left([-\bar{\eta}_k;\bar{\eta}_k] \times \mathfrak{b}^{\#}\left(\mathfrak{r}_0^k, R_{\mathfrak{r}_0^k}^\bullet\right)\right)$ and where $\hat{\mathcal{T}}_\varepsilon$ stands for the matrix satisfying (2.5.36); and, for any $\varepsilon \in [0,\bar{\eta}_k]$ the function $\hat{H}_\varepsilon^N$ defined by $\hat{H}_\varepsilon^N(\mathfrak{r}) = \bar{H}\left(\varepsilon, \boldsymbol{\lambda}_\varepsilon^N(\mathfrak{r})\right)$, is well defined on $\mathfrak{b}^{\#}\left(\mathfrak{r}_0^k, R_{\mathfrak{r}_0^k}^\bullet\right)$, and expresses

$$\hat{H}_\varepsilon^N = \bar{H}_0 + \sum_{n=0}^{N} \varepsilon^n \hat{H}_n + \varepsilon^{N+1}\iota_{PLH}^{N,k}, \tag{2.6.17}$$

where $\iota_{PLH}^{N,k}$ is in $\mathcal{C}_{\#}^\infty\left([0;\bar{\eta}_k] \times \mathfrak{b}^{\#}\left(\mathfrak{r}_0^k, R_{\mathfrak{r}_0^k}^\bullet\right)\right)$. Let $\bar{\eta} = \min\left(\bar{\eta}_1,\dots,\bar{\eta}_{p^\bullet},\eta_N,\eta_1^\bullet,\dots,\eta_{p^\bullet}^\bullet\right)$. Since the functions

$$\begin{array}{l} \boldsymbol{\lambda}_\varepsilon^N - \boldsymbol{\vartheta}_{\varepsilon,\bar{g}_1}^{\alpha_1,1} \cdot \boldsymbol{\vartheta}_{\varepsilon,\bar{g}_2}^{\alpha_2,2} \cdot \ldots \cdot \boldsymbol{\vartheta}_{\varepsilon,\bar{g}_N}^{\alpha_N,N}, \\ \hat{\mathcal{T}}_\varepsilon^{i,j} - \bar{\mathcal{T}}_\varepsilon^{i,j},\ i,j \in \{1,2,3,4\}, \end{array} \tag{2.6.18}$$

are in $\mathcal{C}_{\#}^\infty\left([-\bar{\eta};\bar{\eta}] \times \mathcal{O}_{\mathfrak{Int}}^{\mathfrak{D},\bullet}\right)$ and since the function

$$\hat{H}_\varepsilon - \bar{H}_0 - \sum_{n=0}^{N} \varepsilon^n \hat{H}_n, \tag{2.6.19}$$

is in $\mathcal{C}_{\#}^\infty\left([0;\bar{\eta}] \times \mathcal{O}_{\mathfrak{Int}}^{\mathfrak{D},\bullet}\right)$, functions $\boldsymbol{\rho}_{\boldsymbol{\lambda}}^N$, $\rho_{\hat{\mathcal{T}}^{i,j}}^N$ and ι_{PLH}^N, defined on $\mathcal{O}_{\mathfrak{Int}}^{\mathfrak{D},\bullet}$, and whose restrictions to each $\mathfrak{b}^{\#}\left(\mathfrak{r}_0^k, R_{\mathfrak{r}_0^k}^\bullet\right)$ are given by $\boldsymbol{\rho}_{\boldsymbol{\lambda}}^{N,k}$, $\rho_{\hat{\mathcal{T}}^{i,j}}^{N,k}$ and $\iota_{PLH}^{N,k}$, are well defined on $\mathcal{O}_{\mathfrak{Int}}^{\mathfrak{D},\bullet}$ and are in $\mathcal{C}_{\#}^\infty\left([-\bar{\eta};\bar{\eta}] \times \mathcal{O}_{\mathfrak{Int}}^{\mathfrak{D},\bullet}\right)$ for the two firsts and $\iota_{PLH}^N \in \mathcal{C}_{\#}^\infty\left([0;\bar{\eta}] \times \mathcal{O}_{\mathfrak{Int}}^{\mathfrak{D},\bullet}\right)$

In a similar way we can prove that the restriction of $\boldsymbol{\chi}_\varepsilon^N$ to $\mathcal{O}_{\mathfrak{Dar}}$ is a diffeomorphism whose range is included in $\mathcal{O}_{\mathfrak{Int}}^{\mathfrak{D},\star}$.

According to Theorems 2.3.24 and 2.3.25, there exists a real number $\eta' > 0$ and a real number $\alpha_0 > 0$, that does not depend on ε, such that for any $\varepsilon \in (-\eta',\eta')$,

$$\boldsymbol{\Upsilon}\left(\overline{\mathcal{O}_{\mathfrak{Pol}}}\right) \subset \mathfrak{b}^2\left(\mathbf{x}_0, R'_{\mathbf{x}_0}\right) \times \mathbb{R} \times \left[\frac{a^2}{2\left\|B\right\|_\infty}, \frac{b^2}{2}\right], \tag{2.6.20}$$

and such that for any $\varepsilon \in (0, \eta')$ there exists a real number $t_e^\varepsilon > \frac{\alpha_0}{\varepsilon}$ such that for any $t \in (-t_e^\varepsilon, t_e^\varepsilon)$ and for any $(\mathbf{y}, \theta, k) \in \boldsymbol{\Upsilon}\left(\overline{\mathcal{O}_{\mathfrak{Pol}}}\right)$,

$$\left(\mathbf{Y}^\varepsilon\left(t; \mathbf{y}, \theta, k\right), \mathcal{K}^\varepsilon_{\mathfrak{Dar}}\left(t; \mathbf{y}, \theta, k\right)\right) \in \mathfrak{b}^2\left(\mathbf{x}_0, R'_{\mathbf{x}_0}\right) \times \left[\frac{a^2}{2\left\|B\right\|_\infty}, \frac{b^2}{2}\right]. \tag{2.6.21}$$

Let $\mathcal{O}' = \boldsymbol{\chi}_\varepsilon^N \circ \boldsymbol{\Upsilon}\left(\mathcal{O}_{\mathfrak{Pol}}\right)$. Then, there exists a real number η'', such that for any $\varepsilon \in (-\eta'', \eta'')$,

$$\boldsymbol{\chi}_\varepsilon^N\left(\mathcal{O}_{\mathfrak{Dar}}\right) \subset \mathfrak{b}^2\left(\mathbf{x}_0, R^\star_{\mathbf{x}_0}\right) \times \mathbb{R} \times (c^\star, d^\star) = \mathcal{O}^{\mathfrak{D},\star}_{\mathfrak{Int}}, \tag{2.6.22}$$

and consequently such that

$$\bar{\mathcal{O}'} \subset \mathcal{O}^{\mathfrak{D},\star}_{\mathfrak{Int}}. \tag{2.6.23}$$

Eventually, (2.6.21) and inclusion (2.6.22) mean that the range by $\boldsymbol{\chi}_\varepsilon^N$ of the characteristics expressed in the Darboux coordinate system and provided with initial conditions in $\boldsymbol{\Upsilon}\left(\overline{\mathcal{O}_{\mathfrak{Pol}}}\right)$, or equivalently that the characteristics expressed in the Lie Coordinate System and provided with initial conditions in $\overline{\mathcal{O}'}$, belongs to $\mathcal{O}^{\mathfrak{D},\star}_{\mathfrak{Int}}$ (and hence to $\mathcal{O}^{\mathfrak{D},\bullet}_{\mathfrak{Int}}$), for any $t \in (-t_e^\varepsilon, t_e^\varepsilon)$.

Let

$$\eta = \min\left(\bar{\eta}, \eta', \eta''\right). \tag{2.6.24}$$

Choosing

$$R^\bullet_{\mathbf{x}_0} > 1 + R^\star_{\mathbf{x}_0} + \sqrt{2} \sup_{\varepsilon \in [-\eta, \eta]} \frac{\left\|\nabla \hat{H}^N_{\varepsilon,T}\right\|_\infty}{\left\|B\right\|_\infty}, \tag{2.6.25}$$

yields that we are under the conditions of application of Theorem 2.4.1. Applying this theorem yields the main part of Theorem 2.1.3.

2.6.3 Application with $N = 2$

Applying Algorithm 2.5.11 with $N = 2$, using results of Appendix B.2, yields

$$\bar{g}_1(\mathbf{y}, \theta, k) = \frac{\hat{c}(\theta) \cdot \nabla_{\mathbf{y}} B(\mathbf{y})}{3B(\mathbf{y})^3} \left(2B(\mathbf{y})\, k\right)^{\frac{3}{2}}, \tag{2.6.26}$$

$$\bar{g}_2(\mathbf{y}, \theta, k) = \frac{\left(2B(\mathbf{y})\, k\right)^2}{12B(\mathbf{y})^5} \hat{a}(\theta)\, \hat{c}(\theta) : \left[3B(\mathbf{y}) : \nabla\nabla B(\mathbf{y}) - \nabla B \nabla B(\mathbf{y})\right], \tag{2.6.27}$$

where

$$\nabla B \nabla B = \begin{pmatrix} \left(\frac{\partial B}{\partial x_1}\right)^2 & \frac{\partial B}{\partial x_1}\frac{\partial B}{\partial x_2} \\ \frac{\partial B}{\partial x_1}\frac{\partial B}{\partial x_2} & \left(\frac{\partial B}{\partial x_2}\right)^2 \end{pmatrix} \text{ and } \nabla\nabla B = \begin{pmatrix} \frac{\partial^2 B}{\partial x_1^2} & \frac{\partial^2 B}{\partial x_1 \partial x_2} \\ \frac{\partial^2 B}{\partial x_1 \partial x_2} & \frac{\partial^2 B}{\partial x_2^2} \end{pmatrix} \tag{2.6.28}$$

(Notice that, if u, v are two vectors and if A is a matrix, the notation $uv : A$ stands for $u^T A v$), and

$$\hat{H}_1\left(\mathbf{z}, j\right) = 0, \tag{2.6.29}$$

$$\hat{H}_2\left(\mathbf{z}, j\right) = \frac{j^2}{4B\left(\mathbf{z}\right)} \left[B\left(\mathbf{z}\right) \nabla^2_{\mathbf{x}} B\left(\mathbf{z}\right) - 3\left(\nabla_{\mathbf{x}} B\left(\mathbf{z}\right)\right)^2\right], \tag{2.6.30}$$

where

$$\nabla^2_{\mathbf{x}} B(\mathbf{x}) = \frac{\partial^2 B}{\partial x_1^2}(\mathbf{x}) + \frac{\partial^2 B}{\partial x_2^2}(\mathbf{x})\,, \tag{2.6.31}$$

$$\left(\nabla_{\mathbf{x}} B(\mathbf{x})\right)^2 = \nabla_{\mathbf{x}} B(\mathbf{x}) \cdot \nabla_{\mathbf{x}} B(\mathbf{x})\,. \tag{2.6.32}$$

Consequently, the dynamical system (2.1.67), (2.1.69), (2.1.68) approximates, with accuracy ε, the characteristics $(\mathbf{Z}, \Gamma, \mathcal{J}) = (\mathbf{Z}(t, \mathbf{z}_s, \gamma_s, j_s, s), \Gamma(t, \mathbf{z}_s, \gamma_s, j_s, s), \mathcal{J}(t, \mathbf{z}_s, \gamma_s, j_s, s)) = \mathcal{G}G(\mathbf{X}(t, \mathbf{x}_s, \mathbf{v}_s, s), \mathbf{V}(t, \mathbf{x}_s, \mathbf{v}_s, s))$, with $(\mathbf{X}, \mathbf{V})$ the solution of dynamical system (2.1.40)–(2.1.41). This ends the proof of the part of Theorem 2.1.3 concerning the application when $N = 2$. □

Chapitre 3

Application of Lie Transform Techniques for simulation of a charged particle beam

Sommaire

3.1 Introduction

In the same spirit of [18], we will consider non-relativistic long and thin beams. Within the general framework, if we neglect the collisions between particles, the particle density is obtained by solving a Vlasov-Maxwell system of equations. Here, in addition to consider a long and thin beam, we will consider a beam satisfying the following assumptions :

– The beam is steady-state : all partial derivatives with respect to time vanish.

– The beam is long and thin.
– The beam is propagating at constant velocity v_b along the propagation axis z.
– The beam is sufficiently long so that longitudinal self-consistent forces can be neglected.
– The external electric field is supposed to be independent of the time.
– The beam is axisymmetric.
– The initial distribution f_0 is concentrated in angular momentum.

Under the five first assumptions the $3D$ Vlasov-Maxwell system reduces itself to a $2D$ Vlasov-Poisson system in which the variable t does not represent from a physical point of view a time variable, but rather the longitudinal coordinate. The details about the derivation of this model can be found in [13]. Moreover, under all these assumptions it reduces even to a $1D$ axisymmetric Vlasov-Poisson system of the form :

$$\frac{\partial f_\varepsilon}{\partial t} + \frac{v_r}{\varepsilon}\frac{\partial f_\varepsilon}{\partial r} + \left(E^\varepsilon - \frac{r}{\varepsilon}\right)\frac{\partial f_\varepsilon}{\partial v_r} = 0, \tag{3.1.1}$$

$$-\frac{1}{r}\frac{\partial}{\partial r}\left(r\frac{\partial \phi_\varepsilon}{\partial r}\right) = \rho_\varepsilon(t,r), \quad E_\varepsilon = -\frac{\partial \phi^\varepsilon}{\partial r}, \tag{3.1.2}$$

$$\rho_\varepsilon(t,r) = \int_{\mathbb{R}} f_\varepsilon(t,r,v_r)\,dv_r, \tag{3.1.3}$$

$$E_\varepsilon(t,r=0) = 0, \quad \phi_\varepsilon(t,r=0) = 0, \tag{3.1.4}$$

$$f_\varepsilon(t=0,r,v_r) = f_0(r,v_r), \tag{3.1.5}$$

where $r \geq 0$ is the radial component of the projection of the position vector in the transverse plane to the propagation direction, $v_r \in \mathbb{R}$ is the projection of the transverse velocity in the transverse plan to the propagation direction, ε is the ratio between the characteristic transverse radius of the beam and the characteristic longitudinal length of the beam, $f_\varepsilon = f_\varepsilon(t,r,v_r)$ is the distribution function of the particles, $E_\varepsilon = E_\varepsilon(r,t)$ is the radial part of the transverse self-consistent electric field, and $-\frac{r}{\varepsilon}$ is the strong transverse external electric field. This system is naturally defined for $r \geq 0$ but we can extend it to $r \in \mathbb{R}$ by using the conventions $f_\varepsilon(t,r,v_r) = f_\varepsilon(t,-r,-v_r)$ and $E_\varepsilon(t,r) = -E_\varepsilon(t,-r)$. Details about the derivation of this model can be found in [18]. Moreover, in the same way as in [18] we will consider initial conditions for which the beam is confined. Such initial conditions can be found by solving envelope equations (see [13] for details about the obtention of such initial conditions).

The characteristics of (3.1.1) are given by

$$\frac{\partial \mathbf{R}^\varepsilon}{\partial t} = \frac{\mathbf{V}^\varepsilon_{\mathbf{r}}}{\varepsilon}, \qquad \mathbf{R}^\varepsilon(0,r,v_r) = r, \tag{3.1.6}$$

$$\frac{\partial \mathbf{V}^\varepsilon_r}{\partial t} = -\frac{\mathbf{R}^\varepsilon}{\varepsilon} + E_\varepsilon(\mathbf{R}^\varepsilon,t), \qquad \mathbf{V_r}^\varepsilon(0,r,v_r) = v_r. \tag{3.1.7}$$

Setting

$$H_\varepsilon(r,v_r,t) = \frac{v_r^2 + r^2}{2\varepsilon} + \phi_\varepsilon(r,t), \tag{3.1.8}$$

dynamical system (3.1.6)-(3.1.7) becomes :

$$\frac{\partial \mathbf{R}^\varepsilon}{\partial t} = \partial_{v_r} H_\varepsilon(\mathbf{R}^\varepsilon, \mathbf{V}^\varepsilon_r, t), \qquad \mathbf{R}^\varepsilon(0,r,v_r) = r, \tag{3.1.9}$$

$$\frac{\partial \mathbf{V}^\varepsilon_r}{\partial t} = -\partial_r H_\varepsilon(\mathbf{R}^\varepsilon, \mathbf{V}^\varepsilon_r, t), \qquad \mathbf{V_r}^\varepsilon(0,r,v_r) = v_r. \tag{3.1.10}$$

Consequently, the dynamical system that gives the characteristics is Hamiltonian.

Furthermore, dynamical system (3.1.6)-(3.1.7) corresponds to a perturbation of the dynamical system

$$\frac{\partial \mathbf{R}^{\varepsilon}_{\mathbf{Un}}}{\partial t} = \frac{\mathbf{V}^{\varepsilon}_{\mathbf{r,Un}}}{\varepsilon}, \qquad \mathbf{R}^{\varepsilon}_{\mathbf{Un}}(0, r, v_r) = r, \tag{3.1.11}$$

$$\frac{\partial \mathbf{V}^{\varepsilon}_{r,\mathbf{Un}}}{\partial t} = -\frac{\mathbf{R}^{\varepsilon}_{\mathbf{Un}}}{\varepsilon}, \qquad \mathbf{V}^{\varepsilon}_{r,\mathbf{Un}}(0, r, v_r) = v_r. \tag{3.1.12}$$

In other words, the Hamiltonian function (3.1.8) is a perturbation of the Hamiltonian function

$$H^{\mathbf{Un}}_{\varepsilon}(r, v_r, t) = \frac{v_r^2 + r^2}{2\varepsilon}, \tag{3.1.13}$$

associated to the dynamical system (3.1.11)-(3.1.12).

A well adapted coordinate system for the study of the dynamical system (3.1.11)-(3.1.12) is the (μ, θ) coordinate system defined by

$$\mu = \frac{r^2 + v_r^2}{2}. \tag{3.1.14}$$

and

$$r = \sqrt{2\mu}\cos(\theta), \tag{3.1.15}$$

$$v_r = \sqrt{2\mu}\sin(\theta). \tag{3.1.16}$$

Indeed, in this coordinate system the dynamical system (3.1.11)-(3.1.12) reads :

$$\frac{\partial \mathfrak{Mu}^{\varepsilon}_{\mathbf{Un}}}{\partial t} = 0, \qquad \mathfrak{Mu}^{\varepsilon}_{\mathbf{Un}}(0, \mu, \theta) = \mu, \tag{3.1.17}$$

$$\frac{\partial \mathbf{\Theta}^{\varepsilon}_{\mathbf{Un}}}{\partial t} = -\frac{1}{\varepsilon}, \qquad \mathbf{\Theta}^{\varepsilon}_{\mathbf{Un}}(0, \mu, \theta) = \theta. \tag{3.1.18}$$

As a consequence, solving this dynamical system in the new system of coordinates, reduces to find a trajectory in $\mathbb{R}$, in place of a trajectory in $\mathbb{R}^2$ when it is solved in the original system of coordinates.

Under the same change of coordinates, the Hamiltonian function associated to the dynamical system (3.1.6)-(3.1.7) becomes :

$$\bar{H}_{\varepsilon}(\mu, \theta, t) = \frac{\mu}{\varepsilon} + \phi_{\varepsilon}\left(\sqrt{2\mu}\cos(\theta), t\right), \tag{3.1.19}$$

and the dynamical system (3.1.6)-(3.1.7) reads :

$$\frac{\partial \mathfrak{Mu}^{\varepsilon}}{\partial t} = \sqrt{2\mathfrak{Mu}^{\varepsilon}}\sin(\mathbf{\Theta}^{\varepsilon}) E_{\varepsilon}\left(\sqrt{2\mathfrak{Mu}^{\varepsilon}}\cos(\mathbf{\Theta}^{\varepsilon}), t\right), \qquad \mathfrak{Mu}^{\varepsilon}(0, \mu, \theta) = \mu, \tag{3.1.20}$$

$$\frac{\partial \mathbf{\Theta}^{\varepsilon}}{\partial t} = -\frac{1}{\varepsilon} + \frac{\cos(\mathbf{\Theta}^{\varepsilon})}{\sqrt{2\mathfrak{Mu}^{\varepsilon}}} E_{\varepsilon}\left(\sqrt{2\mathfrak{Mu}^{\varepsilon}}\cos(\mathbf{\Theta}^{\varepsilon}), t\right), \qquad \mathbf{\Theta}^{\varepsilon}(0, \mu, \theta) = \theta. \tag{3.1.21}$$

Thus, we observe that $\mathfrak{Mu}^{\varepsilon}$ is no longer an invariant.

This kind of situation is very similar to the situation encountered in the Geometrical Gyrokinetic theory (see for instance Littlejohn [40, 41, 42], Brizard [5], Dubin *et al.* [11], Frieman & Chen [22], Hahm [29], Hahm, Lee & Brizard [31], Parra & Catto [50, 51, 52] and Quin *et al* [54]). In order to study this kind of situation, the idea is to make an infinitesimal change of coordinate $(\mu,\theta)\mapsto\left(\tilde{\mu},\tilde{\theta}\right)=\boldsymbol{\mathcal{L}}_{\varepsilon}^{t}\left(\mu,\theta\right)$ bringing the characteristics independent of $\tilde{\theta}$ and in which the characteristic associated with $\tilde{\mu}$ is an invariant.

The infinitesimal change of coordinates that we will construct belongs to the class of the Lie change of coordinates.

Definition 3.1.1. *A Lie Change of Coordinates is a formal change of coordinates of the form*

$$\boldsymbol{\mathcal{L}}_{\varepsilon}:\ (\mu,\theta,t)\mapsto\boldsymbol{\mathcal{L}}_{\varepsilon}\left(\mu,\theta,t\right)=\ldots\circ\bar{\varphi}_{\varepsilon^{n}}^{n}\circ\ldots\circ\bar{\varphi}_{\varepsilon}^{1}\left(\mu,\theta,t\right) \tag{3.1.22}$$

$$=\left(\boldsymbol{\mathcal{P}}\boldsymbol{\mathcal{L}}_{\varepsilon}\left(\mu,\theta,t\right),t\right), \tag{3.1.23}$$

where for each $n\in\mathbb{N}^{\star}$, $\bar{\varphi}_{\lambda}^{n}$ *is the flow of a vector field*

$$\bar{\mathbf{Z}}^{n}=\bar{Z}_{1}^{n}\partial_{\mu}+\bar{Z}_{2}^{n}\partial_{\theta}, \tag{3.1.24}$$

i.e., the solution of

$$\frac{\partial\bar{\varphi}_{\lambda}^{n,1}}{\partial\lambda}=\bar{Z}_{1}^{n}(\bar{\varphi}_{\lambda}^{n}), \tag{3.1.25}$$

$$\frac{\partial\bar{\varphi}_{\lambda}^{n,2}}{\partial\lambda}=\bar{Z}_{2}^{n}(\bar{\varphi}_{\lambda}^{n}),\qquad\bar{\varphi}_{0}(\mu,\theta,t)=(\mu,\theta,t), \tag{3.1.26}$$

$$\frac{\partial\bar{\varphi}_{\lambda}^{n,3}}{\partial\lambda}=0. \tag{3.1.27}$$

In this paper we will always denote by $\boldsymbol{\mathcal{P}}\varphi=(\varphi_{1},\varphi_{2})$ the projection of a function $\varphi=(\varphi_{1},\varphi_{2},\varphi_{3})$. In section 3.3, starting from the Hilbert expansions of the electric field E_{ε} and the electric potential ϕ_{ε}

$$E_{\varepsilon}=E_{0}+\varepsilon E_{1}+\varepsilon^{2}E_{2}+\ldots, \tag{3.1.28}$$

$$\phi_{\varepsilon}=\phi_{0}+\varepsilon\phi_{1}+\varepsilon^{2}\phi_{2}+\ldots, \tag{3.1.29}$$

we will develop and use a Lie Transform algorithm, based on the utilization of the Poincaré-Cartan one form, in order to give a constructive proof of the following Theorem :

Theorem 3.1.2. *There exists a Lie change of coordinates* $\boldsymbol{\mathcal{L}}_{\varepsilon}$ *such that in the yielding* $\left(\tilde{\mu},\tilde{\theta}\right)$ *coordinate system, given by* $(r,v_{r})\mapsto\left(\tilde{\mu},\tilde{\theta}\right)=\boldsymbol{\mathcal{P}}\boldsymbol{\mathcal{L}}_{\varepsilon}\left(\mathfrak{Pol}\left(r,v_{r}\right),t\right)$, *where*

$$\mathfrak{Pol}:\ \mathbb{R}^{2}\rightarrow(0,+\infty)\times(\mathbb{R}/(2\pi\mathbb{Z});\ (r,v_{r})\mapsto(\mu,\theta) \tag{3.1.30}$$

with θ *and* μ *given by formulas* (3.1.15)-(3.1.16)*, the system of equations* (3.1.1)-(3.1.5)

reads :

$$\frac{\partial \tilde{f}_\varepsilon}{\partial t}\left(\tilde{\mu},\tilde{\theta},t\right)+a_\varepsilon\left(\tilde{\mu},t\right)\frac{\partial \tilde{f}_\varepsilon}{\partial \tilde{\theta}}\left(\tilde{\mu},\tilde{\theta},t\right)=0, \tag{3.1.31}$$

$$-\frac{1}{r}\frac{\partial}{\partial r}\left(r\frac{\partial \phi^\varepsilon}{\partial r}\right)=\rho_\varepsilon\left(t,r\right),\quad E_\varepsilon=-\frac{\partial \phi_\varepsilon}{\partial r}, \tag{3.1.32}$$

$$\rho_\varepsilon\left(t,r\right)=\int_{\mathbf{D}_\varepsilon^t} h_r\left(\boldsymbol{\mathcal{P}}\boldsymbol{\mathcal{L}}_\varepsilon^{-1}\left(\tilde{\mu}',\tilde{\theta}',t\right)\right)\tilde{f}_\varepsilon\left(\tilde{\mu}',\tilde{\theta}',t\right)\left|\mathcal{J}_{\boldsymbol{\mathcal{P}}\boldsymbol{\mathcal{L}}_\varepsilon^{-1}}\left(\tilde{\mu}',\tilde{\theta}',t\right)\right|d\tilde{\mu}'d\tilde{\theta}', \tag{3.1.33}$$

$$E_\varepsilon\left(t,r=0\right)=0,\quad \phi_\varepsilon\left(t,r=0\right)=0, \tag{3.1.34}$$

$$\tilde{f}_\varepsilon\left(\tilde{\mu},\tilde{\theta},t=0\right)=f_0\left(\mathfrak{Pol}^{-1}\circ\boldsymbol{\mathcal{P}}\boldsymbol{\mathcal{L}}_\varepsilon^{-1}\left(\tilde{\mu},\tilde{\theta},t=0\right)\right), \tag{3.1.35}$$

where $\tilde{f}_\varepsilon$ *is the particle density expressed in the* $\left(\tilde{\mu},\tilde{\theta}\right)$ *coordinate system,* a_ε *is defined by* (3.3.89)*,* $h_r=h_r\left(\mu',\theta'\right)$ *is given by* $h_r\left(\mu',\theta'\right)=\delta\left(r-\sqrt{2\mu'}\cos\left(\theta'\right)\right)$*,* $\left|\mathcal{J}_{\boldsymbol{\mathcal{P}}\boldsymbol{\mathcal{L}}_\varepsilon^{-1}}\left(\tilde{\mu}',\tilde{\theta}',t\right)\right|$ *is the jacobian associated with* $\boldsymbol{\mathcal{P}}\boldsymbol{\mathcal{L}}_\varepsilon^{-1}$*, and* $\mathbf{D}_\varepsilon^t=\boldsymbol{\mathcal{P}}\boldsymbol{\mathcal{L}}_\varepsilon\left((0,+\infty)\times]-\pi,\pi],t\right)$*.*

Moreover, up to the second order, $\boldsymbol{\mathcal{L}}_\varepsilon$*,* $\boldsymbol{\mathcal{L}}_\varepsilon^{-1}$ *and* a_ε *admit the following expansions :*

$$\begin{aligned}\tilde{\mu}&=\mu+\varepsilon\bar{Z}_1^1\left(\mu,\theta,t\right)+\mathcal{O}\left(\varepsilon^2\right),\\ \tilde{\theta}&=\theta+\varepsilon\bar{Z}_2^1\left(\mu,\theta,t\right)+\mathcal{O}\left(\varepsilon^2\right),\end{aligned} \tag{3.1.36}$$

$$\begin{aligned}\mu&=\tilde{\mu}-\varepsilon\bar{Z}_1^1\left(\tilde{\mu},\tilde{\theta},t\right)+\mathcal{O}\left(\varepsilon^2\right),\\ \theta&=\tilde{\theta}-\varepsilon\bar{Z}_2^1\left(\tilde{\mu},\tilde{\theta},t\right)+\mathcal{O}\left(\varepsilon^2\right),\end{aligned} \tag{3.1.37}$$

where $\bar{Z}_1^1$ *and* $\bar{Z}_2^1$ *are given by formulas* (3.3.40) *and* (3.3.48)*, and* a_ε *admits the the following first order expansion :*

$$a_\varepsilon\left(\tilde{\mu},t\right)=-\frac{1}{\varepsilon}+\frac{1}{2\pi\sqrt{2\tilde{\mu}}}\int_{-\pi}^{\pi}\cos\left(\tilde{\theta}\right)E_0\left(\sqrt{2\tilde{\mu}}\cos\left(\tilde{\theta}\right),t\right)d\tilde{\theta}+\mathcal{O}\left(\varepsilon\right). \tag{3.1.38}$$

Remark 3.1.3. *In formulas* (3.1.36)*,* (3.1.37) *and* (3.1.38)*, we have only given second order expansions of the direct and the reciprocal Lie change of coordinates, and the first order expansion of* a_ε*. Nevertheless the algorithm developed in the proof of Theorem 3.1.2 allows us to obtain these expansions at any order.*

The change of coordinates $\boldsymbol{\mathcal{L}}_\varepsilon$ is formal in the sense that $\boldsymbol{\mathcal{L}}_\varepsilon$ corresponds to a composition of an infinite number of flows. Moreover the construction of $\boldsymbol{\mathcal{L}}_\varepsilon$ is based on Lie series expansions of each of these flows ; i.e., for any $n\in\mathbb{N}$ we will use the formal expansion

$$\bar{\varphi}_{\varepsilon^n}^n=\sum_{n\geq 0}\frac{\varepsilon^n}{n!}\mathbf{Z}^n\cdot.$$

See [48] (page 31) for more precisions about these series.

Making first order approximations in the characteristics and in the change of coordinates, we will use (3.1.31)-(3.1.35) in order to simulate the solution f_ε of (3.1.1)-(3.1.5). More precisely, approximating the change of coordinates by

$$\tilde{\mu}=\mu+\mathcal{O}\left(\varepsilon\right), \tag{3.1.39}$$

$$\tilde{\theta}=\theta+\mathcal{O}\left(\varepsilon\right), \tag{3.1.40}$$

the electric field and the electric potential by

$$E_\varepsilon = E_0 + \mathcal{O}(\varepsilon), \tag{3.1.41}$$

$$\phi_\varepsilon = \phi_0 + \mathcal{O}(\varepsilon), \tag{3.1.42}$$

the charge density as follow :

$$\begin{aligned}
&\mathbf{D}_\varepsilon^t = \boldsymbol{\mathcal{P}}\boldsymbol{\mathcal{L}}_\varepsilon\left(\mathbb{R}_+\times]-\pi,\pi],t\right) \simeq \boldsymbol{\mathcal{P}}\boldsymbol{\mathcal{L}}_0\left(\mathbb{R}_+\times]-\pi,\pi],t\right) = \mathbb{R}_+\times]-\pi,\pi],\\
&h_r\left(\boldsymbol{\mathcal{P}}\boldsymbol{\mathcal{L}}_\varepsilon^{-1}\left(\tilde{\mu}',\tilde{\theta}',t\right)\right) \simeq h_r\left(\boldsymbol{\mathcal{P}}\boldsymbol{\mathcal{L}}_0^{-1}\left(\tilde{\mu}',\tilde{\theta}',t\right)\right) = h_r\left(\tilde{\mu}',\tilde{\theta}'\right),\\
&\left|\mathcal{J}_{\boldsymbol{\mathcal{P}}\boldsymbol{\mathcal{L}}_\varepsilon^{-1}}\left(\tilde{\mu}',\tilde{\theta}',t\right)\right| \simeq \left|\mathcal{J}_{\boldsymbol{\mathcal{P}}\boldsymbol{\mathcal{L}}_0^{-1}}\left(\tilde{\mu}',\tilde{\theta}',t\right)\right| = 1,\\
&\rho_\varepsilon(t,r) \simeq \int_{\mathbb{R}_+\times]-\pi,\pi]} h_r\left(\tilde{\mu}',\tilde{\theta}'\right)\tilde{f}_\varepsilon\left(\tilde{\mu}',\tilde{\theta}',t'\right)d\tilde{\mu}'d\tilde{\theta}',
\end{aligned} \tag{3.1.43}$$

that is

$$\rho_\varepsilon(t,r) \simeq \int_{\mathbb{R}_+\times]-\pi,\pi]} \delta\left(r-\sqrt{2\tilde{\mu}'}\cos\left(\tilde{\theta}'\right)\right)\tilde{f}_\varepsilon\left(\tilde{\mu}',\tilde{\theta}',t\right)d\tilde{\mu}'d\tilde{\theta}'. \tag{3.1.44}$$

and a_ε by

$$a_\varepsilon(\tilde{\mu},t) \simeq -\frac{1}{\varepsilon} + \frac{1}{2\pi\sqrt{2\tilde{\mu}}}\int_{-\pi}^{\pi}\cos\left(\tilde{\theta}\right)E_0\left(\sqrt{2\tilde{\mu}}\cos\left(\tilde{\theta}\right),t\right)d\tilde{\theta}, \tag{3.1.45}$$

we obtain :

$$\frac{\partial\tilde{f}_\varepsilon}{\partial t} + \left(-\frac{1}{\varepsilon} + \frac{1}{2\pi\sqrt{2\tilde{\mu}}}\int_{-\pi}^{\pi}\cos\left(\tilde{\theta}\right)E_\varepsilon\left(\sqrt{2\tilde{\mu}}\cos\left(\tilde{\theta}\right),t\right)d\tilde{\theta}\right)\frac{\partial\tilde{f}_\varepsilon}{\partial\tilde{\theta}} = 0, \tag{3.1.46}$$

$$-\frac{1}{r}\frac{\partial}{\partial r}\left(r\frac{\partial\phi_\varepsilon}{\partial r}\right) = \int_{\mathbb{R}_+\times]-\pi,\pi]}\delta\left(r-\sqrt{2\tilde{\mu}'}\cos\left(\tilde{\theta}'\right)\right)\tilde{f}_\varepsilon\left(\tilde{\mu}',\tilde{\theta}',t\right)d\tilde{\mu}'d\tilde{\theta}', \tag{3.1.47}$$

$$E_\varepsilon = -\frac{\partial\phi_\varepsilon}{\partial r}, \tag{3.1.48}$$

$$E_\varepsilon(t,r=0) = 0, \quad \phi_\varepsilon(t,r=0) = 0, \tag{3.1.49}$$

$$\tilde{f}_\varepsilon\left(\tilde{\mu},\tilde{\theta},t=0\right) = f_0\left(\sqrt{2\tilde{\mu}}\cos\left(\tilde{\theta}\right),\sqrt{2\tilde{\mu}}\sin\left(\tilde{\theta}\right)\right). \tag{3.1.50}$$

We will give some remarks about this approximation in Subsection 3.3.5.

In the last section we will simulate (3.1.46)-(3.1.50) and then we will obtain an approximation of f_ε through :

$$f_\varepsilon(r,v_r,t) \simeq \tilde{f}_\varepsilon(\mu,\theta,t). \tag{3.1.51}$$

The numerical method that we will use to simulate (3.1.46)-(3.1.50) will be a Particle in Cell (PIC) method. I recall that a PIC method consists in the coupling of a particle method for the Vlasov equation, and a mesh method for the Poisson equation. The principle of the method is to discretize the distribution function by a set of macro-particles and to advance them in time by numerically solving the dynamical system giving the characteristics. As a consequence, solving this dynamical system in the new system of coordinates, reduces to find a trajectory in $\mathbb{R}$, in place of a trajectory in $\mathbb{R}^2$ when it is solved in the original system of coordinates.

The paper is organized as follows : in Section 3.2 we will construct an odd dimensional differential manifold well adapted to the study of (3.1.6)-(3.1.7) and we will give the mathematical tools necessary for the comprehension of the Lie Transform method we develop then. As a by product of this section we obtain that the non autonomous dynamical system we work with is characterized intrinsically by an autonomous dynamical system on the odd differential manifold we work within. Moreover, we will see that this autonomous dynamical system can also be characterized by the equivalence class of a differential one form called the Poincaré Cartan one form. Furthermore, we will introduce the Noether Theorem within this framework. This Theorem gives essentially an intuitive help for the comprehension of the Lie Transform method. In the third section, we will set out the Lie transform method and we will use it in order to derive the Lie Coordinate System and to prove Theorem 3.1.2. Finally, in the fourth and the fifth sections, we will implement and test the previously described numerical method based on the Lie transform method analysis.

3.2 Geometrical Tools

3.2.1 Characterization of the differential system (3.1.6)-(3.1.7) and of the Vlasov equation on an odd dimensional manifold

In the present subsection we will characterize intrinsically on an odd dimensional manifold differential systems of the form

$$\frac{\partial \mathbf{R}_G^\varepsilon}{\partial t} = \partial_{v_r} G_\varepsilon \left(\mathbf{R}_G^\varepsilon, \mathbf{V}_{r,G}^\varepsilon, t \right), \qquad \mathbf{R}_G^\varepsilon (0, r, v_r) = r, \tag{3.2.1}$$

$$\frac{\partial \mathbf{V}_{r,G}^\varepsilon}{\partial t} = -\partial_r G_\varepsilon \left(\mathbf{R}_G^\varepsilon, \mathbf{V}_{r,G}^\varepsilon, t \right), \qquad \mathbf{V}_{r,G}^\varepsilon (0, r, v_r) = v_r, \tag{3.2.2}$$

where $G_\varepsilon = G_\varepsilon(r, v_r, t)$ is a smooth function, and PDEs

$$\frac{\partial f_\varepsilon^G}{\partial t}(r, v_r, t) + \partial_{v_r} G_\varepsilon (r, v_r, t) \frac{\partial f_\varepsilon^G}{\partial r}(r, v_r, t) - \partial_r G_\varepsilon (r, v_r, t) \frac{\partial f_\varepsilon^G}{\partial v_r}(r, v_r, t) = 0 \tag{3.2.3}$$

of unknown f_ε^G, through a vector field $\boldsymbol{\tau}_G^\varepsilon$. Notice that if $G_\varepsilon = H_\varepsilon$, where H_ε is given by formula (3.1.8), dynamical system (3.2.1)-(3.2.2) and PDE (3.2.3) coincide with dynamical system (3.1.9)-(3.1.10) and PDE (3.1.1). The principal results are given in theorem 3.2.1 and 3.2.2.

Firstly, we need to build the manifold on which we will work. As a topological space we take $\mathcal{M} = \mathbb{R}^2 \times \mathbb{R}$ endowed with the (r, v_r, t) coordinate system and with its usual topology. Concerning the differential structure, we choose the differential atlas $\mathcal{A}$ which contains all the coordinate charts of the type $(\mathcal{U}, \varphi)$, where $\varphi : \mathcal{U} \to \mathbb{R}^3;\ (r, v_r, t) \mapsto (\boldsymbol{\mathcal{P}}\varphi(r, v_r, t), t)$, which are compatible with the global coordinate chart $(\mathcal{M}, \mathfrak{G})$, where $\mathfrak{G} : \mathcal{M} \to \mathbb{R}^3; (r, v_r, t) \mapsto \mathfrak{G}(r, v_r, t) = (r, v_r, t)$, and which leave the last coordinate t unchanged.

Defining the vector field $\mathbf{X}_G^\varepsilon$ by :

$$\mathbf{X}_G^\varepsilon = \partial_{v_r} G_\varepsilon \partial_r - \partial_r G_\varepsilon \partial_{v_r} + \partial_t, \tag{3.2.4}$$

and denoting by $\mathbf{F}^{\varepsilon}_{\lambda,G}$ its flow ; i.e., the solution of

$$\frac{\partial \mathbf{F}^{\varepsilon,1}_{\lambda,G}}{\partial \lambda} = \partial_{v_r} G_\varepsilon \left(\mathbf{F}^{\varepsilon}_{\lambda,G}\right), \qquad \mathbf{F}^{\varepsilon,1}_{0,G}(r,v_r,t) = r, \tag{3.2.5}$$

$$\frac{\partial \mathbf{F}^{\varepsilon,2}_{\lambda,G}}{\partial \lambda} = -\partial_{r} G_\varepsilon \left(\mathbf{F}^{\varepsilon}_{\lambda,G}\right), \qquad \mathbf{F}^{\varepsilon,2}_{0,G}(r,v_r,t) = v_r, \tag{3.2.6}$$

$$\frac{\partial \mathbf{F}^{\varepsilon,3}_{\lambda,G}}{\partial \lambda} = 1, \qquad \mathbf{F}^{\varepsilon,3}_{0,G}(r,v_r,t) = t, \tag{3.2.7}$$

we conclude that the trajectory associated with (3.2.1)-(3.2.2) corresponds to

$$\left(\mathbf{F}^{1,\varepsilon}_{t,G}\left(r,v_r,0\right), \mathbf{F}^{2,\varepsilon}_{t,G}\left(r,v_r,0\right)\right). \tag{3.2.8}$$

Now, we have enough material to characterize intrinsically the solution of (3.2.1)-(3.2.2).

Theorem 3.2.1. *Let $\boldsymbol{\tau}^{\varepsilon}_{G} : \mathcal{M} \to T\mathcal{M}$ be the vector field whose principal part in the (r, v_r, t) coordinate system is given by $\mathbf{X}^{\varepsilon}_{G}$, defined by formula (3.2.4), and let $\boldsymbol{\mathcal{F}}^{\varepsilon}_{\lambda,G}$ be its flow. Then, in every coordinate system $(\tilde{r}, \tilde{v}_r, t)$ belonging to $\mathcal{A}$ the trajectory associated with the dynamical system (3.1.6)-(3.1.7) is given by $\left(\tilde{\mathbf{F}}^{1,\varepsilon}_{t,G}\left(\tilde{r},\tilde{v_r},0\right), \tilde{\mathbf{F}}^{2,\varepsilon}_{t,G}\left(\tilde{r},\tilde{v_r},0\right)\right)$, where $\tilde{\mathbf{F}}^{\varepsilon}_{\lambda,G}$ corresponds to the representative of $\boldsymbol{\mathcal{F}}^{\varepsilon}_{\lambda,G}$ in the $(\tilde{r}, \tilde{v}_r, t)$ coordinate system, or equivalently to the flow of $\tilde{\mathbf{X}}^{\varepsilon}_{G}$, where $\tilde{\mathbf{X}}^{\varepsilon}_{G}$ corresponds to the representative of the principal part of $\boldsymbol{\tau}^{\varepsilon}_{G}$ in the $(\tilde{r}, \tilde{v}_r, t)$ coordinate system.*

Proof. Let $\mathbf{F}^{\varepsilon}_{\lambda,G}$ be the flow of $\mathbf{X}^{\varepsilon}_{G}$, where $\mathbf{X}^{\varepsilon}_{G}$ is given by (3.2.4). We denote by $\mathbf{R}^{\star} \equiv \mathbf{R}^{\star}\left(\lambda, r, v_r, t\right)$, $\mathbf{V}^{\star}_{r} \equiv \mathbf{V}^{\star}_{r}\left(\lambda, r, v_r, t\right)$ and $\mathbf{T}^{\star} \equiv \mathbf{T}^{\star}\left(\lambda, r, v_r, t\right)$ its components. Notice that $\mathbf{R}^{\star}$ and $\mathbf{V}^{\star}_{r}$ depends on the small parameter ε. But since this dependency does not play a role in this proof, we do not precise it in the notation. Then, (3.2.8) reads :

$$\begin{aligned} &\mathbf{R}^{\star}\left(t, r, v_r, 0\right) = \mathbf{R}_{G}\left(r, v_r, t\right), \\ &\mathbf{V}^{\star}_{r}\left(t, r, v_r, 0\right) = \mathbf{V}_{r,G}\left(r, v_r, t\right), \\ &\mathbf{T}^{\star}\left(t, r, v_r, 0\right) = t. \end{aligned} \tag{3.2.9}$$

Let

$$\psi \ : \ (r, v_r, t) \mapsto \left(\tilde{r}, \tilde{v}_r, \tilde{t}\right) = \left(\boldsymbol{\mathcal{P}}\psi\left(r, v_r, t\right), t\right)$$

be a change of coordinates such that $\tilde{t} = t$. We denote by $\tilde{\mathbf{R}}^{\star} \equiv \tilde{\mathbf{R}}^{\star}\left(\lambda, \tilde{r}, \tilde{v}_r, \tilde{t}\right)$, $\tilde{\mathbf{V}}^{\star}_{r} \equiv \tilde{\mathbf{V}}^{\star}_{\mathbf{r}}\left(\lambda, \tilde{r}, \tilde{v}_r, \tilde{t}\right)$ and $\tilde{\mathbf{T}}^{\star} \equiv \tilde{\mathbf{T}}^{\star}\left(\lambda, \tilde{r}, \tilde{v}_r, \tilde{t}\right)$ the components of $\tilde{\mathbf{F}}^{\varepsilon}_{\lambda,G}$; i.e., the components of the expression of the flow in the $\left(\tilde{r}, \tilde{v}_r, \tilde{t}\right)$ coordinate system. Then, the usual change of coordinates rules yield :

$$\begin{aligned} \tilde{\mathbf{R}}^{\star}\left(\lambda, \tilde{r}, \tilde{v}_r, \tilde{t}\right) &= \psi_1\Big(\mathbf{R}^{\star}\left(\lambda, \boldsymbol{\mathcal{P}}\psi^{-1}\left(\tilde{r}, \tilde{v}_r, \tilde{t}\right), \tilde{t}\right), \mathbf{V}^{\star}_{r}\left(\lambda, \boldsymbol{\mathcal{P}}\psi^{-1}\left(\tilde{r}, \tilde{v}_r, \tilde{t}\right), \tilde{t}\right), \\ &\qquad \mathbf{T}^{\star}\left(\lambda, \boldsymbol{\mathcal{P}}\psi^{-1}\left(\tilde{r}, \tilde{v}_r, \tilde{t}\right), \tilde{t}\right)\Big), \\ \tilde{\mathbf{V}}^{\star}_{\mathbf{r}}\left(\lambda, \tilde{r}, \tilde{v}_r, \tilde{t}\right) &= \psi_2\Big(\mathbf{R}^{\star}\left(\lambda, \boldsymbol{\mathcal{P}}\psi^{-1}\left(\tilde{r}, \tilde{v}_r, \tilde{t}\right), \tilde{t}\right), \mathbf{V}^{\star}_{r}\left(\lambda, \boldsymbol{\mathcal{P}}\psi^{-1}\left(\tilde{r}, \tilde{v}_r, \tilde{t}\right), \tilde{t}\right), \\ &\qquad \mathbf{T}^{\star}\left(\lambda, \boldsymbol{\mathcal{P}}\psi^{-1}\left(\tilde{r}, \tilde{v}_r, \tilde{t}\right), \tilde{t}\right)\Big), \\ \tilde{\mathbf{T}}^{\star}\left(\lambda, \tilde{r}, \tilde{v}_r, \tilde{t}\right) &= \mathbf{T}^{\star}\left(\lambda, \boldsymbol{\mathcal{P}}\psi^{-1}\left(\tilde{r}, \tilde{v}_r, \tilde{t}\right), \tilde{t}\right). \end{aligned} \tag{3.2.10}$$

On the other hand, let $\tilde{\mathbf{R}}_G \equiv \tilde{\mathbf{R}}_G(\tilde{r}, \tilde{v}_r, t)$ and $\tilde{\mathbf{V}}_{\mathbf{r},\mathbf{G}} \equiv \tilde{\mathbf{V}}_{\mathbf{r},\mathbf{G}}(\tilde{r}, \tilde{v}_r, t)$ be the components of the trajectory whose range by $\boldsymbol{\mathcal{P}}\psi^{-1}$ is the trajectory associate with $\mathbf{R}_G(r, v_r, t)$ and $\mathbf{V}_{r,G}(r, v_r, t)$; i.e., such that

$$\begin{aligned}
&\left(\tilde{\mathbf{R}}_G(\tilde{r}, \tilde{v}_r, t), \tilde{\mathbf{V}}_{r,G}(\tilde{r}, \tilde{v}_r, t)\right) \\
=&(\psi_1\left(\mathbf{R}_G\left(\boldsymbol{\mathcal{P}}\psi^{-1}(\tilde{r}, \tilde{v}_r, 0), t\right), \mathbf{V}_{r,G}\left(\boldsymbol{\mathcal{P}}\psi^{-1}(\tilde{r}, \tilde{v}_r, 0), t\right), t\right), \\
&\psi_2\left(\mathbf{R}_G\left(\boldsymbol{\mathcal{P}}\psi^{-1}(\tilde{r}, \tilde{v}_r, 0), t\right), \mathbf{V}_{r,G}\left(\boldsymbol{\mathcal{P}}\psi^{-1}(\tilde{r}, \tilde{v}_r, 0), t\right), t\right)).
\end{aligned}$$

To finish the proof, we have to show that

$$\left(\tilde{\mathbf{R}}^\star(t, \tilde{r}, \tilde{v}_r, 0), \tilde{\mathbf{V}}_r^\star(t, \tilde{r}, \tilde{v}_r, 0)\right) = \left(\tilde{\mathbf{R}}_G(\tilde{r}, \tilde{v}_r, t), \tilde{\mathbf{V}}_{r,G}(\tilde{r}, \tilde{v}_r, t)\right). \tag{3.2.11}$$

Differentiating

$$\tilde{\mathbf{T}}^\star\left(\lambda, \tilde{r}, \tilde{v}_r, \tilde{t}\right) = \mathbf{T}^\star\left(\lambda, \boldsymbol{\mathcal{P}}\psi^{-1}\left(\tilde{r}, \tilde{v}_r, \tilde{t}\right), \tilde{t}\right)$$

with respect to λ yields :

$$\frac{\partial \tilde{\mathbf{T}}^\star}{\partial \lambda} = 1$$

and consequently $\tilde{\mathbf{T}}^\star\left(\tilde{t}, r, v_r, 0\right) = \tilde{t}$. Hence, we obtain :

$$\begin{aligned}
&\left(\tilde{\mathbf{R}}^\star\left(\tilde{t}, \tilde{r}, \tilde{v}_r, 0\right), \tilde{\mathbf{V}}_{\mathbf{r}}^\star\left(\tilde{t}, \tilde{r}, \tilde{v}_r, 0\right)\right) \\
=&\Big(\psi_1\left(\mathbf{R}^\star\left(\tilde{t}, \boldsymbol{\mathcal{P}}\psi^{-1}(\tilde{r}, \tilde{v}_r, 0), 0\right), \mathbf{V}_r^\star\left(\tilde{t}, \boldsymbol{\mathcal{P}}\psi^{-1}(\tilde{r}, \tilde{v}_r, 0), 0\right), \tilde{t}\right), \\
&\quad \psi_2\left(\mathbf{R}^\star\left(\tilde{t}, \boldsymbol{\mathcal{P}}\psi^{-1}(\tilde{r}, \tilde{v}_r, 0), 0\right), \mathbf{V}_r^\star\left(\tilde{t}, \boldsymbol{\mathcal{P}}\psi^{-1}(\tilde{r}, \tilde{v}_r, 0), 0\right), \tilde{t}\right)\Big).
\end{aligned} \tag{3.2.12}$$

Finally, using (3.2.9) we obtain :

$$\begin{aligned}
&\left(\tilde{\mathbf{R}}^\star\left(\tilde{t}, \tilde{r}, \tilde{v}_r, 0\right), \tilde{\mathbf{V}}_{\mathbf{r}}^\star\left(\tilde{t}, \tilde{r}, \tilde{v}_r, 0\right)\right) \\
=&\Big(\psi_1\left(\mathbf{R}_G\left(\boldsymbol{\mathcal{P}}\psi^{-1}(\tilde{r}, \tilde{v}_r, 0), \tilde{t}\right), \mathbf{V}_{r,G}\left(\boldsymbol{\mathcal{P}}\psi^{-1}(\tilde{r}, \tilde{v}_r, 0), \tilde{t}\right), \tilde{t}\right), \\
&\quad \psi_2\left(\mathbf{R}_G\left(\boldsymbol{\mathcal{P}}\psi^{-1}(\tilde{r}, \tilde{v}_r, 0), \tilde{t}\right), \mathbf{V}_{r,G}\left(\boldsymbol{\mathcal{P}}\psi^{-1}(\tilde{r}, \tilde{v}_r, 0), \tilde{t}\right), \tilde{t}\right)\Big) \\
=&\left(\tilde{\mathbf{R}}_G\left(\tilde{r}, \tilde{v}_r, \tilde{t}\right), \tilde{\mathbf{V}}_{r,G}\left(\tilde{r}, \tilde{v}_r, \tilde{t}\right)\right)
\end{aligned} \tag{3.2.13}$$

This ends the proof of Theorem 3.2.1. □

Theorem 3.2.2. *Let $\boldsymbol{\tau}_G^\varepsilon : \mathcal{M} \to T\mathcal{M}$ be the vector field whose principal part in the (r, v_r, t) coordinate system is given by $\mathbf{X}_G^\varepsilon$, defined by formula (3.2.4). Then, in every coordinate system $(\tilde{r}, \tilde{v}_r, t)$ belonging to $\mathcal{A}$ the PDE (3.2.3) is given by*

$$i_{\tilde{\mathbf{X}}_G^\varepsilon} d\tilde{f}_\varepsilon^G = 0, \tag{3.2.14}$$

where $\tilde{\mathbf{X}}_G^\varepsilon$ and $\tilde{f}_\varepsilon^G$ correspond respectively to the representative of the principal part of $\boldsymbol{\tau}_G^\varepsilon$ and the representative of f_ε^G in the $(\tilde{r}, \tilde{v}_r, t)$ coordinate system.

Proof. Firstly in the (r, v_r, t) coordinate system $i_{\mathbf{X}_G^\varepsilon} df_\varepsilon^G$ reads :

$$\begin{aligned} i_{\mathbf{X}_G^\varepsilon} df_\varepsilon^G &= \left(\nabla_{(r,v_r,t)} f_\varepsilon^G\right)^T \mathbf{X}_G^\varepsilon \\ &= \frac{\partial f_\varepsilon^G}{\partial t} + X_G^{\varepsilon,1} \frac{\partial f_\varepsilon^G}{\partial r} + X_G^{\varepsilon,2} \frac{\partial f_\varepsilon^G}{\partial v_r} \\ &= \frac{\partial f_\varepsilon^G}{\partial t} + \partial_{v_r} G_\varepsilon \frac{\partial f_\varepsilon^G}{\partial r} - \partial_r G_\varepsilon \frac{\partial f_\varepsilon^G}{\partial v_r} \\ &= 0, \end{aligned}$$

and (3.2.14) is satisfied. Now, let $(\tilde{r}, \tilde{v}_r, t)$ be a coordinate system belonging to $\mathcal{A}$ and $(\mathcal{U}, \psi) \in \boldsymbol{\mathcal{A}}$ the corresponding coordinate chart. Then, the expression of $\boldsymbol{\tau}_G^\varepsilon$ is given by :

$$\tilde{\mathbf{X}}_G^\varepsilon (\tilde{r}, \tilde{v}_r, t) = \nabla_{(r,v_r,t)} \psi \left(\psi^{-1}(\tilde{r}, \tilde{v}_r, t)\right) \mathbf{X}_G^\varepsilon \left(\psi^{-1}(\tilde{r}, \tilde{v}_r, t)\right), \tag{3.2.15}$$

and the expression of the particle distribution is given by :

$$\tilde{f}_\varepsilon^G (\tilde{r}, \tilde{v}_r, t) = f_\varepsilon^G \left(\psi^{-1}(\tilde{r}, \tilde{v}_r, t)\right). \tag{3.2.16}$$

Consequently $i_{\tilde{\mathbf{X}}_G^\varepsilon} d\tilde{f}_\varepsilon^G$ reads :

$$\begin{aligned} & i_{\tilde{\mathbf{X}}_G^\varepsilon} d\tilde{f}_\varepsilon^G \\ =& \left(\nabla_{(\tilde{r},\tilde{v}_r,t)} \tilde{f}_\varepsilon^G\right)^T \tilde{\mathbf{X}}_G^\varepsilon \\ =& \Big(\left(\nabla_{(r,v_r,t)} \psi \left(\psi^{-1}(\tilde{r}, \tilde{v}_r, t)\right)\right)^{-T} \nabla_{(\tilde{r},\tilde{v}_r,t)} f_\varepsilon^G \left(\psi^{-1}(\tilde{r}, \tilde{v}_r, t)\right) \Big)^T \\ & \qquad \left(\nabla_{(r,v_r,t)} \psi \left(\psi^{-1}(\tilde{r}, \tilde{v}_r, t)\right) \mathbf{X}_G^\varepsilon \left(\psi^{-1}(\tilde{r}, \tilde{v}_r, t)\right)\right) \\ =& \left(\nabla_{(\tilde{r},\tilde{v}_r,t)} f_\varepsilon^G \left(\psi^{-1}(\tilde{r}, \tilde{v}_r, t)\right)\right)^T \mathbf{X}_G^\varepsilon \left(\psi^{-1}(\tilde{r}, \tilde{v}_r, t)\right) \\ =& 0, \end{aligned} \tag{3.2.17}$$

and (3.2.14) is satisfied.

□

Since the last coordinates of $\tilde{\mathbf{X}}_G^\varepsilon$ is always equal to 1, equation (3.2.14) reads also :

$$\frac{\partial \tilde{f}_\varepsilon^G}{\partial t} + \tilde{X}_G^{\varepsilon,1} \frac{\partial \tilde{f}_\varepsilon^G}{\partial \tilde{r}} + \tilde{X}_G^{\varepsilon,2} \frac{\partial \tilde{f}_\varepsilon^G}{\partial \tilde{v}_r} = 0. \tag{3.2.18}$$

3.2.2 The Poincaré Cartan one-form

Theorems 3.2.1 and 3.2.2 allow us to characterize intrinsically the differential system (3.2.1)-(3.2.2) and the PDE (3.2.3). More precisely, these Theorems ensure us that the differential system (3.2.1)-(3.2.2) and the PDE (3.2.3) are characterized intrinsically through the vector field $\boldsymbol{\tau}_G^\varepsilon$. Now, we will see that $\boldsymbol{\tau}_G^\varepsilon$ can also be characterized by an equation that involves a differential one form $\boldsymbol{\gamma}_G^\varepsilon$ called the Poincaré-Cartan one-form. We will essentially see that $\boldsymbol{\tau}_G^\varepsilon$ can be characterized as the direction vector of the eigenspace of $d\boldsymbol{\gamma}_G^\varepsilon$ associated with the eigenvalue 0 and whose last component is 1. In other words we will see that $\boldsymbol{\tau}_G^\varepsilon$ is the unique solution of $i_{\boldsymbol{\tau}_G^\varepsilon} d\boldsymbol{\gamma}_G^\varepsilon = 0$ satisfying $\boldsymbol{\tau}_{G,3}^\varepsilon = 1$. Afterwards, we will introduce the following equivalence relation on the one forms space : "$\boldsymbol{\alpha} \sim \boldsymbol{\beta}$ if and only if $\boldsymbol{\alpha} - \boldsymbol{\beta}$ is exact", and we will see that $\forall \boldsymbol{\beta}_G^\varepsilon \in [\boldsymbol{\gamma}_G^\varepsilon]$, where $[\boldsymbol{\gamma}_G^\varepsilon]$ stands for the equivalence class of $\boldsymbol{\gamma}_G^\varepsilon$, the vector field $\boldsymbol{\tau}_G^\varepsilon$ is characterized by $i_{\boldsymbol{\tau}_G^\varepsilon} d\boldsymbol{\beta}_G^\varepsilon = 0$ and $\boldsymbol{\tau}_{G,3}^\varepsilon = 1$. The main results are summarized in theorem 3.2.8.

Definition 3.2.3. *The Poincaré-Cartan 1-form $\boldsymbol{\gamma}_G^\varepsilon$ associated with the dynamical system* (3.2.1)-(3.2.2) *is the one-form whose expression in the (r, v_r, t) coordinate system is given by :*

$$\boldsymbol{\Gamma}_G^\varepsilon(r, v_r, t) = v_r dr - G_\varepsilon dt. \tag{3.2.19}$$

The matrix associated with the differential two-form $d\boldsymbol{\Gamma}_G^\varepsilon$ is given by

$$M_G^\varepsilon(r, v_r, t) = \begin{pmatrix} 0 & -1 & -\partial_r G_\varepsilon \\ 1 & 0 & -\partial_{v_r} G_\varepsilon \\ \partial_r G_\varepsilon & \partial_{v_r} G_\varepsilon & 0 \end{pmatrix} \tag{3.2.20}$$

Lemma 3.2.4. *Let $(\tilde{r}, \tilde{v}_r, t)$ be a coordinate system belonging to $\boldsymbol{\mathcal{A}}$ and $\tilde{M}_G^\varepsilon$ the matrix associated with the representative of $d\boldsymbol{\gamma}_G^\varepsilon$ in this coordinate system. Then,*

$$\mathbf{Ker}\left(\tilde{M}_G^\varepsilon(\tilde{r}, \tilde{v}_r, t)\right) = \mathbf{vect}\left(\tilde{\mathbf{X}}_G^\varepsilon(\tilde{r}, \tilde{v}_r, t)\right). \tag{3.2.21}$$

Proof. Let M_G^ε be the matrix defined by (3.2.20). Since M_G^ε is antisymmetric, its maximal rank is 2. As $\begin{pmatrix} 0 & -1 \\ 1 & 0 \end{pmatrix}$ is of rank 2, the rank of M_G^ε is exactly 2. Moreover,

$$i_{\mathbf{X}_G^\varepsilon} d\boldsymbol{\Gamma}_G^\varepsilon(r, v_r, t) = \left(\mathbf{X}_G^\varepsilon(r, v_r, t)\right)^T M_G^\varepsilon(r, v_r, t) = 0. \tag{3.2.22}$$

Since, $\forall (r, v_r, t)$, $\mathbf{X}_G^\varepsilon(r, v_r, t) \neq 0$ (the last component is 1) we have :

$$\mathbf{Ker}\left(M_G^\varepsilon(r, v_r, t)\right) = \mathbf{vect}\left(\mathbf{X}_G^\varepsilon(r, v_r, t)\right). \tag{3.2.23}$$

Let

$$\psi \ : \ (r, v_r, t) \mapsto \left(\tilde{r}, \tilde{v}_r, \tilde{t}\right) = \left(\boldsymbol{\mathcal{P}}\psi(r, v_r, t), t\right)$$

be a change of coordinates belonging in $\boldsymbol{\mathcal{A}}$ and $d\tilde{\boldsymbol{\Gamma}}_G^\varepsilon$ be the expression of $d\boldsymbol{\gamma}_G^\varepsilon$ in the $(\tilde{r}, \tilde{v}_r, t)$ coordinate system. Then, the usual change of coordinates rules for differential two-forms yield :

$$\left\langle d\tilde{\boldsymbol{\Gamma}}_G^\varepsilon(\tilde{r}, \tilde{v}_r, t); \tilde{\mathbf{u}}, \tilde{\mathbf{v}} \right\rangle = \left\langle d\boldsymbol{\Gamma}_G^\varepsilon\left(\psi^{-1}(\tilde{r}, \tilde{v}_r, t), t\right); d\psi^{-1}_{(\tilde{r}, \tilde{v}_r, t)} \cdot \tilde{\mathbf{u}}, d\psi^{-1}_{(\tilde{r}, \tilde{v}_r, t)} \cdot \tilde{\mathbf{v}} \right\rangle, \tag{3.2.24}$$

and consequently the expression of $\tilde{M}_G^\varepsilon$ is given by

$$\tilde{M}_G^\varepsilon(\tilde{r}, \tilde{v}_r, t) = \left(\nabla_{(\tilde{r}, \tilde{v}_r, t)} \psi^{-1}(\tilde{r}, \tilde{v}_r, t)\right)^T M_G^\varepsilon\left(\psi^{-1}(\tilde{r}, \tilde{v}_r, t)\right) \nabla_{(\tilde{r}, \tilde{v}_r, t)} \psi^{-1}(\tilde{r}, \tilde{v}_r, t). \tag{3.2.25}$$

Notice that formula (3.2.25) implies that $\tilde{M}_G^\varepsilon$ is of rank 2.

On an other hand the usual change of coordinates rule for vector fields yields that the representative of $\boldsymbol{\tau}_G^\varepsilon$ in the $(\tilde{r}, \tilde{v}_r, t)$ coordinate system is given by :

$$\tilde{\mathbf{X}}_G^\varepsilon(\tilde{r}, \tilde{v}_r, t) = \nabla_{(r, v_r, t)} \psi\left(\psi^{-1}(\tilde{r}, \tilde{v}_r, t)\right) \mathbf{X}_G^\varepsilon\left(\psi^{-1}(\tilde{r}, \tilde{v}_r, t)\right). \tag{3.2.26}$$

Consequently, the last component of $\tilde{\mathbf{X}}_G^\varepsilon$ is 1 and

$$\begin{aligned} i_{\tilde{\mathbf{X}}_G^\varepsilon} d\tilde{\mathbf{\Gamma}}^\varepsilon &= \left(\tilde{\mathbf{X}}_G^\varepsilon\left(\tilde{r},\tilde{v}_r,t\right)\right)^T \tilde{M}_G^\varepsilon\left(\tilde{r},\tilde{v}_r,t\right) \\ &= \left(\mathbf{X}_G^\varepsilon\left(\psi^{-1}\left(\tilde{r},\tilde{v}_r,t\right)\right)\right)^T M_G^\varepsilon\left(\psi^{-1}\left(\tilde{r},\tilde{v}_r,t\right)\right) \nabla_{(\tilde{r},\tilde{v}_r,t)}\psi^{-1}\left(\tilde{r},\tilde{v}_r,t\right) \\ &= 0. \end{aligned} \tag{3.2.27}$$

Hence,

$$\mathbf{Ker}\left(\tilde{M}_G^\varepsilon\left(\tilde{r},\tilde{v}_r,t\right)\right) = \mathbf{vect}\left(\tilde{\mathbf{X}}_G^\varepsilon\left(\tilde{r},\tilde{v}_r,t\right)\right). \tag{3.2.28}$$

This ends the proof of Lemma 3.2.4. □

In particular, lemma 3.2.4 implies that in every coordinate system the dimension of the kernel of $\tilde{M}_G^\varepsilon$ is equal to 1. Now, these kernels can be characterize intrinsically on the manifold as follow :

Definition 3.2.5. *The subspace* $\mathcal{V}_{(r,v_r,t)} = \left\{c\boldsymbol{\xi}_{(r,v_r,t)}/c \in \mathbb{R}\right\} \subset T_{(r,v_r,t)}\mathcal{M}$, *where* $\boldsymbol{\xi}_{(r,v_r,t)} \in T_{(r,v_r,t)}\mathcal{M}$ *is a vector satisfying* $\boldsymbol{\xi}_{(r,v_r,t)} \neq 0$ *and*

$$i_{\boldsymbol{\xi}_{(r,v_r,t)}}\left(d\boldsymbol{\gamma}_G^\varepsilon\right)(r,v_r,t) = 0, \tag{3.2.29}$$

is called the vortex line of $\boldsymbol{\gamma}_G^\varepsilon$ *at* (r,v_r,t).

Easy computations lead that the vortex line is well defined ; i.e., compatible with the differential structure. Moreover, Lemma 3.2.4 means that $\forall\,(r,v_r,t) \in \mathcal{M}$, $\boldsymbol{\tau}_G^\varepsilon(r,v_r,t)$ is the unique generator of $\mathcal{V}_{(r,v_r,t)}$ whose last component is 1.

Proposition 3.2.6. *Let* $(\tilde{r},\tilde{v}_r,t)$ *be local coordinates on* $\mathcal{M}$ *and let* $\tilde{\boldsymbol{X}}_G^\varepsilon$ *be the representative of* $\boldsymbol{\tau}_G^\varepsilon$ *in this coordinates system. Then,* $\tilde{\boldsymbol{X}}_G^\varepsilon$ *is the unique solution of the equation of unknown* $\tilde{\mathbf{Y}}^\varepsilon$

$$i_{\tilde{\mathbf{Y}}^\varepsilon} d\tilde{\mathbf{\Gamma}}_G^\varepsilon = 0 \tag{3.2.30}$$

that satisfies $\tilde{\mathbf{Y}}_3^\varepsilon = 1$.

Proposition 3.2.6 allows us to characterize intrinsically $\boldsymbol{\tau}_G^\varepsilon$ by using $\boldsymbol{\gamma}_G^\varepsilon$. In fact, as $d \circ d = 0$, replacing in (3.2.29) $\boldsymbol{\gamma}_G^\varepsilon$ by $\boldsymbol{\gamma}_G^\varepsilon + dS_\varepsilon$, where S_ε is a smooth function, yields the same result. As a consequence, we will introduce the following equivalence relation :

Definition 3.2.7. *Let* $\boldsymbol{\alpha}$ *and* $\boldsymbol{\beta}$ *be two differential one forms. We say that* $\boldsymbol{\alpha}$ *and* $\boldsymbol{\beta}$ *are equivalent if there exists a smooth function* S *such that* $\boldsymbol{\alpha} - \boldsymbol{\beta} = dS$. *We will denote by* $[\boldsymbol{\alpha}]$ *the equivalence class of* $\boldsymbol{\alpha}$.

Then we can generalize Proposition 3.2.6.

Theorem 3.2.8. *Let* $(\tilde{r},\tilde{v}_r,t)$ *be local coordinates on* $\mathcal{M}$, $\tilde{\boldsymbol{X}}_G^\varepsilon$ *the representative of* $\boldsymbol{\tau}_G^\varepsilon$ *in this coordinate system, and* $\boldsymbol{\beta}_G^\varepsilon \in [\boldsymbol{\gamma}_G^\varepsilon]$. *Then,* $\tilde{\boldsymbol{X}}_G^\varepsilon$ *is the unique solution of the equation of unknown* $\tilde{\mathbf{Y}}^\varepsilon$:

$$i_{\tilde{\mathbf{Y}}^\varepsilon} d\tilde{\boldsymbol{\beta}}_G^\varepsilon = 0, \tag{3.2.31}$$

that satisfies $\tilde{\mathbf{Y}}_3^\varepsilon = 1$, *where* $\tilde{\boldsymbol{\beta}}_G^\varepsilon$ *corresponds to the expression of* $\boldsymbol{\beta}_G^\varepsilon$ *in the* $(\tilde{r},\tilde{v}_r,t)$ *coordinate system.*

3.2.3 Noether's Theorem within this framework

As already said in the introduction, the dynamical system (3.1.6)-(3.1.7) is a perturbation of the dynamical system (3.1.11)-(3.1.12) and the (μ, θ) coordinate system is well adapted for the study of the dynamical system (3.1.11)-(3.1.12). The main argument discussed in the introduction was that in this coordinate system μ is an invariant of the trajectory. We will see in the next subsection that the Poincaré Cartan one-form associated with the dynamical system (3.1.6)-(3.1.7) is also a perturbation of the Poincaré Cartan one form associated with the dynamical system (3.1.11)-(3.1.12). Moreover, we will see that the non-exact part of the Poincaré Cartan one form associated with the dynamical system (3.1.11)-(3.1.12) does not depend on θ and consequently that it is invariant under the action of the flow of $\frac{\partial}{\partial\theta}$. Such flows are called symmetries of the Poincaré Cartan one form. The Noether's theorem connects such symmetries with invariants of the trajectory. Applying this Theorem in our case gives that $-\mu$ is the invariant corresponding to the flow of $\frac{\partial}{\partial\theta}$. Since the Poincaré Cartan one-form associated with the dynamical system (3.1.6)-(3.1.7) is a perturbation of the Poincaré Cartan one form associated with the dynamical system (3.1.11)-(3.1.12), the lowest order (in ε) of this one form, expressed in the (μ, θ) coordinate system, does not depend on θ. As a consequence, the flow of $\frac{\partial}{\partial\theta}$ is close to a symmetry. The goal of the Lie transform method, that we will introduce in the next section, is to find a coordinate system $(\tilde{\mu}, \tilde{\theta})$ close to the (μ, θ) coordinate system in which the flow of $\frac{\partial}{\partial\theta}$ is a symmetry and in which $-\tilde{\mu}$ is the corresponding invariant. The aim of this part is to introduce rigorously, within the framework of the Poincaré Cartan one form, these notions of symmetries, invariants and Noether's Theorem. The notions of symmetries and Noether's theorem can be written under a lot of forms. Indeed, there exists a lot of mathematical frameworks to study an Hamiltonian differential system and each of them provides an other formulation of the Noether's theorem. Nevertheless, in each of these mathematical frameworks a symmetry is a diffeomorphism, or a group of diffeomorphisms, leaving unchanged the principal object of the theory and the Noether's theorem connects these symmetries with the invariants of the trajectory. In this paper, according to Theorem 3.2.8, the principal object of the theory is the Poincaré-Cartan one form's equivalence class. Consequently, we will give the following definition of symmetries :

Definition 3.2.9. *Let $\mathcal{Y}$ be a vector field, $\mathcal{G}_\lambda$ its flow, and $\boldsymbol{\gamma}^\varepsilon_G$ the Poincaré Cartan one form associated with the dynamical system* (3.2.1)-(3.2.2)*. We will say that $(\mathcal{G}_\lambda)$ is a symmetry of $[\boldsymbol{\gamma}^\varepsilon_G]$ if for any λ for which $\mathcal{G}_\lambda$ is defined, $\mathcal{G}^\star_\lambda \boldsymbol{\gamma}^\varepsilon_G \in [\boldsymbol{\gamma}^\varepsilon_G]$; i.e., if $\mathcal{G}^\star_\lambda \boldsymbol{\gamma}^\varepsilon_G - \boldsymbol{\gamma}^\varepsilon_G$ is exact.*

This definition is well-posed with respect to the equivalence relation. Indeed, if $\boldsymbol{\beta}^\varepsilon_G \in [\boldsymbol{\gamma}^\varepsilon_G]$, then there exists a smooth function S^ε such that $\boldsymbol{\beta}^\varepsilon_G = \boldsymbol{\gamma}^\varepsilon_G + dS^\varepsilon$ and consequently if $\mathcal{G}_\lambda$ is a symmetry

$$\begin{aligned} \mathcal{G}^\star_\lambda \boldsymbol{\beta}^\varepsilon_G &= \mathcal{G}^\star_\lambda \left(\boldsymbol{\beta}^\varepsilon_G + dS^\varepsilon\right) \\ &= \mathcal{G}^\star_\lambda \boldsymbol{\gamma}^\varepsilon_G + d\mathcal{G}^\star_\lambda S^\varepsilon \\ &\in [\boldsymbol{\gamma}^\varepsilon_G]\,. \end{aligned} \tag{3.2.32}$$

Remark 3.2.10. *Easy computations lead to the fact that this definition of symmetry is well posed with respect to differential structure.*

On an other hand, a symmetry can be characterized by using directly the vector field that generates it.

Proposition 3.2.11. *Let $\mathcal{Y}$ be a vector field and $\mathcal{G}_\lambda$ its flow. Then, $\mathcal{G}_\lambda$ is a symmetry of $[\boldsymbol{\gamma}^\varepsilon_G]$ if and only if $\mathcal{L}_{\boldsymbol{\mathcal{Y}}} \boldsymbol{\gamma}^\varepsilon_G$ is exact.*

Proof. Assume that $\mathcal{G}_\lambda$ is a symmetry of $[\boldsymbol{\gamma}^\varepsilon_G]$. Then, there exists a smooth function P^ε_λ such that $\mathcal{G}^\star_\lambda \boldsymbol{\gamma}^\varepsilon_G - \boldsymbol{\gamma}^\varepsilon_G = dP^\varepsilon_\lambda$. As $\mathcal{G}^\star_0 \boldsymbol{\gamma}^\varepsilon_G = \boldsymbol{\gamma}^\varepsilon_G$, there exists a smooth function Q^ε_λ such that $\mathcal{G}^\star_\lambda \boldsymbol{\gamma}^\varepsilon_G - \boldsymbol{\gamma}^\varepsilon_G = \lambda dQ^\varepsilon_\lambda$. By definition of the Lie derivative, $\mathcal{L}_{\boldsymbol{\mathcal{Y}}} \boldsymbol{\gamma}^\varepsilon_G = \frac{\partial \mathcal{G}^\star_\lambda \boldsymbol{\gamma}^\varepsilon_G}{\partial \lambda} \mid_{\lambda=0} = dQ^\varepsilon_0$ and consequently $\mathcal{L}_{\boldsymbol{\mathcal{Y}}} \boldsymbol{\gamma}^\varepsilon_G$ is exact.

Reciprocally, if $\mathcal{L}_{\boldsymbol{\mathcal{Y}}} \boldsymbol{\gamma}^\varepsilon_G$ is exact ; i.e. if there exists a smooth function R^ε such that $\mathcal{L}_{\boldsymbol{\mathcal{Y}}} \boldsymbol{\gamma}^\varepsilon_G = dR^\varepsilon$, then, the usual formula

$$\frac{\partial}{\partial \lambda} \mathcal{G}^\star_\lambda \boldsymbol{\gamma}^\varepsilon_G \mid_{\lambda=\lambda_0} = \mathcal{G}^\star_{\lambda_0} \left(d i_{\boldsymbol{\mathcal{Y}}} \boldsymbol{\gamma}^\varepsilon_G + i_{\boldsymbol{\mathcal{Y}}} d \boldsymbol{\gamma}^\varepsilon_G \right) \tag{3.2.33}$$

and the Cartan formula

$$\mathcal{L}_{\boldsymbol{\mathcal{Y}}} \boldsymbol{\gamma}^\varepsilon_G = d i_{\boldsymbol{\mathcal{Y}}} \boldsymbol{\gamma}^\varepsilon_G + i_{\boldsymbol{\mathcal{Y}}} d \boldsymbol{\gamma}^\varepsilon_G \tag{3.2.34}$$

yield :

$$\begin{aligned} \frac{\partial}{\partial \lambda} \mathcal{G}^\star_\lambda \boldsymbol{\gamma}^\varepsilon_G &= \mathcal{G}^\star_\lambda \left(\mathcal{L}_{\boldsymbol{\mathcal{Y}}} \boldsymbol{\gamma}^\varepsilon_G \right) \\ &= \mathcal{G}^\star_\lambda \left(dR^\varepsilon \right) \\ &= d \left(\mathcal{G}^\star_\lambda R^\varepsilon \right). \end{aligned} \tag{3.2.35}$$

Finally an integration yields the result.

□

Now, we turn back to the notion of invariant.

Definition 3.2.12. *Let $\mathcal{I}$ be a smooth function on $\mathcal{M}$. We say that $\mathcal{I}$ is an invariant of* (3.2.1)-(3.2.2) *if and only if $i_{\boldsymbol{\tau}^\varepsilon_G} d\mathcal{I} = 0$.*

Remark 3.2.13. *Easy computations lead to the fact that this definition of invariant is well posed with respect to the differential structure.*

Having this material in hands, we can easily derive the Noether theorem within this framework.

Theorem 3.2.14. *Let $\boldsymbol{\mathcal{Y}}$ be a smooth vector field whose flow is a symmetry of $[\boldsymbol{\gamma}^\varepsilon_G]$. Let S^ε be a smooth function such that $\mathcal{L}_{\boldsymbol{\mathcal{Y}}} \boldsymbol{\gamma}^\varepsilon_G = dS^\varepsilon$. Then, $i_{\boldsymbol{\mathcal{Y}}} \boldsymbol{\gamma}^\varepsilon_G - S^\varepsilon$ is an invariant.*

Proof. The Cartan formula yields that $\mathcal{L}_{\boldsymbol{\mathcal{Y}}} \boldsymbol{\gamma}^\varepsilon_G = dS^\varepsilon$ is equivalent to

$$i_{\boldsymbol{\mathcal{Y}}} d \boldsymbol{\gamma}^\varepsilon_G + d i_{\boldsymbol{\mathcal{Y}}} \boldsymbol{\gamma}^\varepsilon_G = dS^\varepsilon. \tag{3.2.36}$$

Moreover, as $i_{\boldsymbol{\tau}^\varepsilon_G} d \boldsymbol{\gamma}^\varepsilon_G = 0$ we obtain :

$$\begin{aligned} i_{\boldsymbol{\tau}^\varepsilon_G} i_{\boldsymbol{\mathcal{Y}}} d \boldsymbol{\gamma}^\varepsilon_G &= \langle d \boldsymbol{\gamma}^\varepsilon_G ; \boldsymbol{\mathcal{Y}}, \boldsymbol{\tau}^\varepsilon_G \rangle \\ &= - \langle d \boldsymbol{\gamma}^\varepsilon_G ; \boldsymbol{\tau}^\varepsilon_G, \boldsymbol{\mathcal{Y}} \rangle \\ &= - \left\langle i_{\boldsymbol{\tau}^\varepsilon_G} d \boldsymbol{\gamma}^\varepsilon_G ; \boldsymbol{\mathcal{Y}} \right\rangle \\ &= 0. \end{aligned} \tag{3.2.37}$$

Consequently, applying $i_{\boldsymbol{\tau}^\varepsilon_G}$ at the both sides of (3.2.36) yields $i_{\boldsymbol{\tau}^\varepsilon_G} d \left(i_{\boldsymbol{\mathcal{Y}}} \boldsymbol{\gamma}^\varepsilon_G - S^\varepsilon \right) = 0$; i.e., $i_{\boldsymbol{\mathcal{Y}}} \boldsymbol{\gamma}^\varepsilon_G - S^\varepsilon$ is an invariant. □

Remark 3.2.15. *Notice that Theorem 3.2.14 is compatible with the relation of equivalence. Indeed, if* $\mathcal{L}_{\boldsymbol{\mathcal{Y}}}\boldsymbol{\gamma}_G^\varepsilon = dS^\varepsilon$*, then for any smooth function* σ^ε*,* $\mathcal{L}_{\boldsymbol{\mathcal{Y}}}\left(\boldsymbol{\gamma}_G^\varepsilon + d\sigma^\varepsilon\right) = d\left(S^\varepsilon + \mathcal{L}_{\boldsymbol{\mathcal{Y}}}\sigma^\varepsilon\right)$*. In other words* $\boldsymbol{\mathcal{Y}}$ *generates a symmetry of* $\boldsymbol{\gamma}_G^\varepsilon + d\sigma^\varepsilon$*. Moreover, the associated invariant is* $\left(\boldsymbol{\gamma}_G^\varepsilon + d\sigma^\varepsilon\right)\cdot\boldsymbol{\mathcal{Y}} - \left(S + L_{\boldsymbol{\mathcal{Y}}}\sigma^\varepsilon\right) = \boldsymbol{\gamma}_G^\varepsilon\cdot\boldsymbol{\mathcal{Y}} - S^\varepsilon$ *; i.e. the same invariant as the invariant associated to* $\boldsymbol{\gamma}^\varepsilon$*.*

Remark 3.2.16. *Easy computations lead to the fact that this Theorem is well posed with respect to the differential structure.*

Remark 3.2.17. *Definition 3.2.9 is a non-standard formulation of symmetry. A more popular approach, in cases where* G_ε *does not depend on* t*, is via momentum map (see for instance [44] or [45]). Within such framework, taking place on the symplectic manifold* $\left(\mathbb{R}^2, dr\wedge dv_r\right)$*, a symmetry associated with dynamical system* (3.2.1)-(3.2.2) *is a flow* ψ_t^F *of an Hamiltonian vector field* $\mathfrak{X}_F$ *satisfying* $G_\varepsilon\left(\psi_t^F\left(r,v_r\right)\right) = G_\varepsilon\left(r,v_r\right)$ *for any* $(r,v_r)\in\mathbb{R}^2$*. Constructing the vector field* $\mathbf{X}_F$ *on* $\mathcal{M}$ *by setting* $\mathbf{X}_F = \mathfrak{X}_F + 0\cdot\partial_t$*; i.e.,* $\mathbf{X}_F = \partial_{v_r}F\partial_r - \partial_r F\partial_{v_r}$*, we observe that* $\mathcal{L}_{\mathbf{X}_F}\boldsymbol{\gamma}_G^\varepsilon = d\left(-F + i_{\mathbf{X}_F}\boldsymbol{\gamma}_G^\varepsilon\right)$*. Hence, the flow of* $\mathbf{X}_F$ *is also a symmetry in the sense of definition 3.2.9. Notice that the corresponding invariant is well the momentum map* F*. Consequently definition 3.2.9 is well an extension of the classical definition of symmetry in cases where dynamical system* (3.2.1)-(3.2.2) *is non autonomous.*

3.2.4 Application at the differential system (3.1.6)-(3.1.7)

The non perturbed case (Dynamical system (3.1.11)-(3.1.12))

The solution of (3.1.11)-(3.1.12) is given by

$$\begin{pmatrix} \mathbf{R}_{\mathbf{Un}}^\varepsilon \\ \mathbf{V}_{\mathbf{r,Un}}^\varepsilon \end{pmatrix} = e^{\frac{t}{\varepsilon}N}\begin{pmatrix} r \\ v_r \end{pmatrix}, \tag{3.2.38}$$

where

$$N = \begin{bmatrix} 0 & -1 \\ 1 & 0 \end{bmatrix} \text{ and } e^{\frac{t}{\varepsilon}N} = \begin{bmatrix} \cos\left(\frac{t}{\varepsilon}\right) & -\sin\left(\frac{t}{\varepsilon}\right) \\ \sin\left(\frac{t}{\varepsilon}\right) & \cos\left(\frac{t}{\varepsilon}\right) \end{bmatrix}.$$

According to formula (3.2.38), the trajectories are circle of radius $\sqrt{r^2+v_r^2}$. Under the change of coordinates (3.1.15)-(3.1.16) dynamical system (3.1.11)-(3.1.12) reads :

$$\frac{\partial \mathfrak{Mu}_{\mathbf{Un}}^\varepsilon}{\partial t} = 0, \qquad \mathfrak{Mu}_{\mathbf{Un}}^\varepsilon\left(0,\mu,\theta\right) = \mu, \tag{3.2.39}$$

$$\frac{\partial \boldsymbol{\Theta}_{\mathbf{Un}}^\varepsilon}{\partial t} = -\frac{1}{\varepsilon}, \qquad \boldsymbol{\Theta}_{\mathbf{Un}}^\varepsilon\left(0,\mu,\theta\right) = \theta. \tag{3.2.40}$$

Making the change of coordinates (3.1.15)-(3.1.16) in the Poincaré Cartan one form, defined by (3.2.19) and with $G_\varepsilon = H_\varepsilon^{\mathbf{Un}}$ given by (3.1.13), yields :

$$\begin{aligned} \bar{\boldsymbol{\Gamma}}_{H^{\mathbf{Un}}}^\varepsilon &= \sin\left(\theta\right)\cos\left(\theta\right)d\mu - 2\mu\sin^2\left(\theta\right)d\theta - \frac{\mu}{\varepsilon}dt \\ &= -\mu d\theta - \frac{\mu}{\varepsilon}dt + d\left(\mu\sin\left(\theta\right)\cos\left(\theta\right)\right) \\ &= \bar{\boldsymbol{\beta}}_{H^{\mathbf{Un}}}^\varepsilon + d\left(\mu\sin\left(\theta\right)\cos\left(\theta\right)\right). \end{aligned} \tag{3.2.41}$$

The flow of $\frac{\partial}{\partial\theta}$ reads :

$$\bar{\mathcal{G}}_\lambda\left(\mu,\theta,t\right) = \left(\mu,\lambda+\theta,t\right). \tag{3.2.42}$$

As $\mathcal{L}_{\frac{\partial}{\partial\theta}}\bar{\boldsymbol{\beta}}_{H^{\mathbf{Un}}}^\varepsilon = 0$, proposition 3.2.11 yields that $\mathcal{G}_\lambda$ is a symmetry and Noether Theorem (Theorem 3.2.14) yields that $-\mu$ is the corresponding invariant.

The perturbed case (Dynamical system (3.1.6)-(3.1.7)**)**

Making the change of coordinates (3.1.15)-(3.1.16) in the Poincaré-Cartan one form, defined by (3.2.19) and with $G_\varepsilon = H_\varepsilon$, where H_ε is defined by (3.1.8), yields :

$$\begin{aligned}\bar{\mathbf{\Gamma}}^{\varepsilon}_{H_\varepsilon} &= \sin(\theta)\cos(\theta)\, d\mu - 2\mu\sin^2(\theta)\, d\theta - \left(\frac{\mu}{\varepsilon} + \phi_\varepsilon\left(\sqrt{2\mu}\cos(\theta), t\right)\right) dt \\ &= -\mu d\theta - \left(\frac{\mu}{\varepsilon} + \phi_\varepsilon\left(\sqrt{2\mu}\cos(\theta), t\right)\right) dt + d\left(\mu\sin(\theta)\cos(\theta)\right) \\ &= \bar{\boldsymbol{\beta}}^{\varepsilon}_{H_\varepsilon} + d\left(\mu\sin(\theta)\cos(\theta)\right).\end{aligned} \tag{3.2.43}$$

We remark that $\bar{\boldsymbol{\beta}}^{\varepsilon}_{H}$ defined by (3.2.43) is a perturbation of $\bar{\boldsymbol{\beta}}^{\varepsilon}_{H^{\mathbf{Un}}}$ defined by (3.2.41). Moreover, in this case the symmetry is broken ; i.e., $\bar{\mathcal{G}}_\lambda$ defined by (3.2.42) is no longer a symmetry.

3.2.5 Change of coordinates as the flow of a vector field

Change of coordinates in a one form

Let $\boldsymbol{\omega}$ be a one form defined on $\mathcal{M}$ and $\mathbf{\Omega}$ its expression in the (r, v_r, t) coordinate system. If $(r, v_r, t) \in \mathcal{M}$ and $\mathbf{u} \in \mathcal{TM}_{(r,v_r,t)}$, we will use the following notation for $\boldsymbol{\omega}$ evaluated at (r, v_r, t) and applied at $\mathbf{u}$:

$$\boldsymbol{\omega}_{(r,v_r,t)} \cdot \mathbf{u} =< \boldsymbol{\omega}(r, v_r, t); \mathbf{u} > . \tag{3.2.44}$$

Let $\psi : (r, v_r, t) \mapsto (\tilde{r}, \tilde{v}_r, t) = (\boldsymbol{\mathcal{P}}\psi(r, v_r, t), t)$ be a change of coordinates belonging in $\boldsymbol{\mathcal{A}}$ and $\tilde{\mathbf{\Omega}}$ the expression of $\boldsymbol{\omega}$ in the $(\tilde{r}, \tilde{v}_r, t)$ coordinate system. Then, $\tilde{\mathbf{\Omega}}$ is given by $(\psi^{-1})^\star\mathbf{\Omega}$, where $(\psi^{-1})^\star\mathbf{\Omega}$ is called the pullback of $\mathbf{\Omega}$ by ψ^{-1} and is computed as follow :

$$< \tilde{\mathbf{\Omega}}(\tilde{r}, \tilde{v}_r, t); \tilde{\mathbf{u}} >=< \mathbf{\Omega}(\psi^{-1}(\tilde{r}, \tilde{v}_r, t)); (d\psi^{-1})_{(\tilde{r},\tilde{v}_r,t)} \cdot \tilde{\mathbf{u}} > . \tag{3.2.45}$$

In term of coordinates, formula (3.2.45) means that $\tilde{\mathbf{\Omega}}(\tilde{r}, \tilde{v}_r, t)$ corresponds to the line vector

$$\begin{aligned}&\left[\tilde{\mathbf{\Omega}}_1(\tilde{r}, \tilde{v}_r, t), \tilde{\mathbf{\Omega}}_2(\tilde{r}, \tilde{v}_r, t), \tilde{\mathbf{\Omega}}_3(\tilde{r}, \tilde{v}_r, t)\right] \\ &= \left[\mathbf{\Omega}_1(\psi^{-1}(\tilde{r}, \tilde{v}_r, t)), \mathbf{\Omega}_2(\psi^{-1}(\tilde{r}, \tilde{v}_r, t)), \mathbf{\Omega}_3(\psi^{-1}(\tilde{r}, \tilde{v}_r, t))\right] \nabla_{(\tilde{r},\tilde{v}_r,t)}\psi^{-1}(\tilde{r}, \tilde{v}_r, t).\end{aligned} \tag{3.2.46}$$

Usually, we also use the notation :

$$\begin{aligned}\tilde{\mathbf{\Omega}}(\tilde{r}, \tilde{v}_r, t) &= (\psi^{-1})^\star\mathbf{\Omega}(\tilde{r}, \tilde{v}_r, t) \\ &= \tilde{\mathbf{\Omega}}_1(\tilde{r}, \tilde{v}_r, t)d\tilde{r} + \tilde{\mathbf{\Omega}}_2(\tilde{r}, \tilde{v}_r, t)d\tilde{v_r} + \tilde{\mathbf{\Omega}}_3(\tilde{r}, \tilde{v}_r, t)dt,\end{aligned} \tag{3.2.47}$$

where $\tilde{\mathbf{\Omega}}_1(\tilde{r}, \tilde{v}_r, t)$, $\tilde{\mathbf{\Omega}}_2(\tilde{r}, \tilde{v}_r, t)$ and $\tilde{\mathbf{\Omega}}_3(\tilde{r}, \tilde{v}_r, t)$ are given by formula (3.2.46).

Change of coordinates as the flow of a vector field.

Theorem 3.2.18. *Let $(\bar{r}, \bar{v}_r, t)$ be local coordinates on $\mathcal{M}$, $\boldsymbol{\mathcal{Z}}$ a vector field on $\mathcal{M}$, and $\boldsymbol{\omega}$ a one form on $\mathcal{M}$. Let $\bar{\mathbf{Z}}$ and $\bar{\mathbf{\Omega}}$ be their expressions in the $(\bar{r}, \bar{v}_r, t)$ coordinate system. Assume that the last coordinates of $\bar{\mathbf{Z}}$ is* 0*, i.e.*

$$\bar{\mathbf{Z}}(\bar{r}, \bar{v}_r, t) = \bar{Z}^1(\bar{r}, \bar{v}_r, t)\,\partial_{\bar{r}} + \bar{Z}^2(\bar{r}, \bar{v}_r, t)\,\partial_{\bar{v}_r}. \tag{3.2.48}$$

Let $\bar{\varphi}_\varepsilon$ be its flow; i.e. the solution of

$$\frac{\partial \bar{\varphi}^1_\varepsilon}{\partial \varepsilon} = \bar{Z}^1(\bar{\varphi}_\varepsilon), \tag{3.2.49}$$

$$\frac{\partial \bar{\varphi}^2_\varepsilon}{\partial \varepsilon} = \bar{Z}^2(\bar{\varphi}_\varepsilon), \qquad \bar{\varphi}_0(\bar{r}, \bar{v}_r, t) = (\bar{r}, \bar{v}_r, t), \tag{3.2.50}$$

$$\frac{\partial \bar{\varphi}^3_\varepsilon}{\partial \varepsilon} = 0. \tag{3.2.51}$$

Then, under the change of coordinates $(\bar{r}, \bar{v}_r, t) \mapsto (\tilde{r}, \tilde{v}_r, t) = \bar{\varphi}_\varepsilon(\bar{r}, \bar{v}_r, t)$, the expression $\tilde{\mathbf{\Omega}}_\varepsilon$ of $\boldsymbol{\omega}$ in the $(\tilde{r}, \tilde{v}_r, t)$ coordinate system admits the following expansion :

$$\begin{aligned}\tilde{\mathbf{\Omega}}_\varepsilon(\tilde{r}, \tilde{v}_r, t) = \bar{\mathbf{\Omega}}(\tilde{r}, \tilde{v}_r, t) - \varepsilon \mathcal{L}_{\bar{\mathbf{Z}}} \bar{\mathbf{\Omega}}(\tilde{r}, \tilde{v}_r, t) + \ldots + \frac{(-1)^n \varepsilon^n}{n!} \mathcal{L}^n_{\bar{\mathbf{Z}}} \bar{\mathbf{\Omega}}(\tilde{r}, \tilde{v}_r, t) \\ + \frac{\varepsilon^{n+1}}{n!} \int_0^1 (1-u)^n \frac{\partial^{n+1} \tilde{\mathbf{\Omega}}_\varepsilon}{\partial \varepsilon^{n+1}} \mid_{\varepsilon u} (\tilde{r}, \tilde{v}_r, t) du,\end{aligned} \tag{3.2.52}$$

where $\mathcal{L}^k_{\bar{\mathbf{Z}}} \bar{\mathbf{\Omega}}$ is defined recursively for $k \geq 1$ by

$$\mathcal{L}_{\bar{\mathbf{Z}}} \bar{\mathbf{\Omega}} = \left(\frac{\partial}{\partial \varepsilon} \left((\bar{\varphi}_\varepsilon)^\star \bar{\mathbf{\Omega}} \right) \right) \mid_{\varepsilon = 0} \tag{3.2.53}$$

and

$$\mathcal{L}^{k+1}_{\bar{\mathbf{Z}}} \bar{\mathbf{\Omega}} = \mathcal{L}_{\bar{\mathbf{Z}}} \left(\mathcal{L}^k_{\bar{\mathbf{Z}}} \bar{\mathbf{\Omega}} \right). \tag{3.2.54}$$

Moreover, the change of coordinates admits the following expansion in power of ε :

$$\begin{aligned}\tilde{r} =& \bar{r} + \varepsilon \bar{Z}^1 (\bar{r}, \bar{v}_r, t) + \ldots + \frac{\varepsilon^n}{n!} \left(\mathcal{L}^{n-1}_{\bar{\mathbf{Z}}} \bar{Z}^1 \right) (\bar{r}, \bar{v}_r, t) \\ & + \frac{\varepsilon^{n+1}}{n!} \int_0^1 (1-u)^n \frac{\partial^{n+1} \bar{\varphi}^1_\varepsilon}{\partial \varepsilon^{n+1}} \mid_{\varepsilon u} (\bar{r}, \bar{v}_r, t) \, du, \\ \tilde{v}_r =& \bar{v}_r + \varepsilon \bar{Z}^2 (\bar{r}, \bar{v}_r, t) + \ldots + \frac{\varepsilon^n}{n!} \left(\mathcal{L}^{n-1}_{\bar{\mathbf{Z}}} \bar{Z}^2 \right) (\bar{r}, \bar{v}_r, t) \\ & + \frac{\varepsilon^{n+1}}{n!} \int_0^1 (1-u)^n \frac{\partial^{n+1} \bar{\varphi}^2_\varepsilon}{\partial \varepsilon^{n+1}} \mid_{\varepsilon u} (\bar{r}, \bar{v}_r, t) \, du,\end{aligned} \tag{3.2.55}$$

and the reciprocal change of coordinates admits the following expansion :

$$\begin{aligned}\bar{r} =& \tilde{r} - \varepsilon \bar{Z}^1 (\tilde{r}, \tilde{v}_r, t) + \ldots + \frac{(-1)^n \varepsilon^n}{n!} \left(\mathcal{L}^{n-1}_{\bar{\mathbf{Z}}} \bar{Z}^1 \right) (\tilde{r}, \tilde{v}_r, t) \\ & + \frac{\varepsilon^{n+1}}{n!} \int_0^1 (1-u)^n \left(\frac{\partial^{n+1}}{\partial \varepsilon^{n+1}} \bar{\varphi}^1_{-\varepsilon} \right) \mid_{\varepsilon u} (\tilde{r}, \tilde{v}_r, t) \, du, \\ \bar{v}_r =& \tilde{v}_r - \varepsilon \bar{Z}^2 (\tilde{r}, \tilde{v}_r, t) + \ldots + \frac{(-1)^n \varepsilon^n}{n!} \left(\mathcal{L}^{n-1}_{\bar{\mathbf{Z}}} \bar{Z}^2 \right) (\tilde{r}, \tilde{v}_r, t) \\ & + \frac{\varepsilon^{n+1}}{n!} \int_0^1 (1-u)^n \left(\frac{\partial^{n+1}}{\partial \varepsilon^{n+1}} \bar{\varphi}^2_{-\varepsilon} \right) \mid_{\varepsilon u} (\tilde{r}, \tilde{v}_r, t) \, du.\end{aligned} \tag{3.2.56}$$

Proof. Let $(\bar{r}, \bar{v}_r, t)$ be local coordinates on $\mathcal{M}$, $\boldsymbol{\mathcal{Z}}$ a vector field on $\mathcal{M}$, and $\boldsymbol{\omega}$ a one form on $\mathcal{M}$. Let $\bar{\mathbf{Z}}$ and $\bar{\mathbf{\Omega}}$ be their expressions in the $(\bar{r}, \bar{v}_r, t)$ coordinates. We assume that the last coordinates of $\bar{\mathbf{Z}}$ is 0; i.e. that

$$\bar{\mathbf{Z}} = \bar{Z}^1 \partial_{\bar{r}} + \bar{Z}^2 \partial_{\bar{v}_r}. \tag{3.2.57}$$

Let $\bar{\varphi}_\varepsilon$ be its flow ; i.e. the solution of (3.2.49)-(3.2.51). According to formula (3.2.47), under the change of coordinates $(\bar{r}, \bar{v}_r, t) \mapsto (\tilde{r}, \tilde{v}_r, t) = \bar{\varphi}_\varepsilon(\bar{r}, \bar{v}_r, t)$, the expression of $\boldsymbol{\omega}$ in the $(\tilde{r}, \tilde{v}_r, t)$ coordinates is given by $\tilde{\boldsymbol{\Omega}}_\varepsilon = (\bar{\varphi}_\varepsilon^{-1})^\star \bar{\boldsymbol{\Omega}}$. A Taylor expansion in power of ε yields :

$$\begin{aligned}\tilde{\boldsymbol{\Omega}}_\varepsilon(\tilde{r}, \tilde{v}_r, t) = \tilde{\boldsymbol{\Omega}}_0(\tilde{r}, \tilde{v}_r, t) + \varepsilon \frac{\partial \tilde{\boldsymbol{\Omega}}_\varepsilon}{\partial \varepsilon} \mid_{\varepsilon=0} (\tilde{r}, \tilde{v}_r, t) + \ldots + \frac{\varepsilon^n}{n!} \frac{\partial^n \tilde{\boldsymbol{\Omega}}_\varepsilon}{\partial \varepsilon^n} \mid_{\varepsilon=0} (\tilde{r}, \tilde{v}_r, t) \\ + \frac{\varepsilon^{n+1}}{n!} \int_0^1 (1-u)^n \frac{\partial^{n+1} \tilde{\boldsymbol{\Omega}}_\varepsilon}{\partial \varepsilon^{n+1}} \mid_{\varepsilon u} (\tilde{r}, \tilde{v}_r, t) du.\end{aligned} \tag{3.2.58}$$

Notice that for each $k \in \{1, \ldots, n+1\}$ we have use the following notation :

$$\frac{\partial^k \tilde{\boldsymbol{\Omega}}_\varepsilon}{\partial \varepsilon^k} = \left[\frac{\partial^k \tilde{\boldsymbol{\Omega}}_\varepsilon^1}{\partial \varepsilon^k}, \frac{\partial^k \tilde{\boldsymbol{\Omega}}_\varepsilon^2}{\partial \varepsilon^k} \right]. \tag{3.2.59}$$

As $\tilde{\boldsymbol{\Omega}}_\varepsilon = (\bar{\varphi}_\varepsilon^{-1})^\star \bar{\boldsymbol{\Omega}}$, we have for each $k \in \{1, \ldots, n+1\}$

$$\frac{\partial^k \tilde{\boldsymbol{\Omega}}_\varepsilon}{\partial \varepsilon^k} \mid_{\varepsilon=0} = \left(\frac{\partial^k}{\partial \varepsilon^k} \left((\bar{\varphi}_\varepsilon^{-1})^\star \bar{\boldsymbol{\Omega}} \right) \right) \mid_{\varepsilon=0} . \tag{3.2.60}$$

By definition, the Lie derivative of $\bar{\boldsymbol{\Omega}}$ with respect to $-\bar{\mathbf{Z}}$ is given by

$$\mathcal{L}_{-\bar{\mathbf{Z}}} \bar{\boldsymbol{\Omega}} = \left(\frac{\partial}{\partial \varepsilon} \left((\bar{\varphi}_\varepsilon^{-1})^\star \bar{\boldsymbol{\Omega}} \right) \right) \mid_{\varepsilon=0} \tag{3.2.61}$$

and easy computations lead to

$$(-1)^k \mathcal{L}_{\bar{\mathbf{Z}}}^k \bar{\boldsymbol{\Omega}} = \mathcal{L}_{-\bar{\mathbf{Z}}}^k \bar{\boldsymbol{\Omega}} = \left(\frac{\partial^k}{\partial \varepsilon^k} \left((\bar{\varphi}_\varepsilon^{-1})^\star \bar{\boldsymbol{\Omega}} \right) \right) \mid_{\varepsilon=0}, \tag{3.2.62}$$

where $\mathcal{L}_{\bar{\mathbf{Z}}}^k \bar{\boldsymbol{\Omega}}$ is defined recursively by formulas (3.2.53)-(3.2.54). Injecting formulas (3.2.62) in (3.2.58) leads to formula (3.2.52).

In the same way, Taylor's expansions of the inverse of the flow ; i.e. of $\bar{\varphi}_{-\varepsilon}$, and of the flow ; i.e. $\bar{\varphi}_\varepsilon$, lead to formulas (3.2.55) and (3.2.56).

This ends the proof of Theorem 3.2.18.

□

3.3 Lie Transform Method

3.3.1 The Lie Change of Coordinates

Subsequently, we will denote by $\boldsymbol{\gamma}^\varepsilon$ the Poicarré-Cartan one form associated with the dynamical system (3.1.9)-(3.1.10). We will also denote by $\boldsymbol{\beta}^\varepsilon \in [\boldsymbol{\gamma}^\varepsilon]$ the one form whose expression in the (μ, θ, t) coordinate system, defined by (3.1.15)-(3.1.16), is given by (3.2.43) ;i.e., by

$$\bar{\boldsymbol{\beta}}^\varepsilon = -\mu d\theta - \left(\frac{\mu}{\varepsilon} + \phi_\varepsilon \left(\sqrt{2\mu} \cos(\theta), t \right) \right) dt. \tag{3.3.1}$$

Injecting the Hilbert expansion of the electric potential, given by (3.1.29), in (3.3.1) leads to the following Hilbert expansion of $\bar{\boldsymbol{\beta}}^\varepsilon$:

$$\bar{\boldsymbol{\beta}}^\varepsilon = \frac{1}{\varepsilon} \left(\bar{\boldsymbol{\beta}}_0 + \varepsilon \bar{\boldsymbol{\beta}}_1 + \varepsilon^2 \bar{\boldsymbol{\beta}}_2 + \ldots \right), \tag{3.3.2}$$

where

$$\begin{aligned}
\bar{\boldsymbol{\beta}}_0(\mu,\theta,t) &= -\mu dt,\\
\bar{\boldsymbol{\beta}}_1(\mu,\theta,t) &= -\mu d\theta - \phi_0\left(\sqrt{2\mu}\cos(\theta),t\right)dt,\\
\bar{\boldsymbol{\beta}}_2(\mu,\theta,t) &= -\phi_1\left(\sqrt{2\mu}\cos(\theta),t\right)dt,\\
&\vdots
\end{aligned} \tag{3.3.3}$$

According to definition 3.1.1, a Lie change of coordinate is a composite of flows of vector fields $\ldots,\bar{\mathbf{Z}}^3,\bar{\mathbf{Z}}^2,\bar{\mathbf{Z}}^1$ parametrized by $\ldots\varepsilon^3,\varepsilon^2,\varepsilon$. In the same way as in Theorem 3.2.18 we will give in the following Theorem an Hilbert expansion of the expression of $\boldsymbol{\beta}^\varepsilon$ in the Lie coordinate system. Notice that the expression of the Hilbert expansion of $\tilde{\boldsymbol{\beta}}^\varepsilon$ involves only the expressions of the vector fields $\bar{\mathbf{Z}}^1,\bar{\mathbf{Z}}^2,\bar{\mathbf{Z}}^3,\ldots$ and the expressions of the terms of the Hilbert expansion of $\bar{\boldsymbol{\beta}}^\varepsilon$.

Theorem 3.3.1. *Let $\boldsymbol{\gamma}^\varepsilon$ be the one form whose expression in the (r,v_r,t) coordinate system is defined by (3.2.19). Let $\boldsymbol{\beta}^\varepsilon\in[\boldsymbol{\gamma}^\varepsilon]$ be the one form whose expression in the (μ,θ,t) coordinate system, defined by (3.1.15)-(3.1.16), is given by (3.3.1). Let $\boldsymbol{\mathcal{L}}_\varepsilon:\ (\mu,\theta,t)\mapsto\left(\tilde{\mu},\tilde{\theta},t\right)$ be a Lie change of coordinates. Then the expression $\tilde{\boldsymbol{\beta}}^\varepsilon$ of $\boldsymbol{\beta}^\varepsilon$ in the Lie coordinates $\left(\tilde{\mu},\tilde{\theta},t\right)$ is given by :*

$$\tilde{\boldsymbol{\beta}}^\varepsilon\left(\tilde{\mu},\tilde{\theta},t\right)=\frac{1}{\varepsilon}\sum_{m\geq 0}\left(\sum_{k=0}^{m}\left(\bar{\boldsymbol{W}}_k\bar{\boldsymbol{\beta}}_{m-k}\right)\left(\tilde{\mu},\tilde{\theta},t\right)\right)\varepsilon^m, \tag{3.3.4}$$

where for each $k\in\mathbb{N}^\star$, $\bar{\boldsymbol{W}}_k$ is defined by

$$\bar{\boldsymbol{W}}_k=\sum_{n_1+2n_2+\ldots+kn_k=k}\frac{(-1)^{n_1}\ldots(-1)^{n_k}}{n_1!\ldots n_k!}\mathcal{L}_{\bar{\mathbf{Z}}^k}^{n_k}\ldots\mathcal{L}_{\bar{\mathbf{Z}}^1}^{n_1} \tag{3.3.5}$$

and $\bar{\boldsymbol{W}}_0=id$. Moreover, the change of coordinates admits the following expansion in power of ε :

$$\begin{aligned}
\left(\tilde{\mu},\tilde{\theta},t\right)&=\boldsymbol{\mathcal{L}}_\varepsilon(\mu,\theta,t)\\
&=\left(\sum_{k\geq 0}\varepsilon^k\left(\sum_{n_1+2n_2+\ldots+kn_k=k}\frac{\left(\bar{\mathbf{Z}}^1\right)^{n_1}\ldots\left(\bar{\mathbf{Z}}^k\right)^{n_k}}{n_1!\ldots n_k!}\right)(id)\right)(\mu,\theta,t),
\end{aligned} \tag{3.3.6}$$

and the reciprocal change of coordinates admits the following expansion :

$$\begin{aligned}
(\mu,\theta,t)&=\boldsymbol{\mathcal{L}}_\varepsilon^{-1}\left(\tilde{\mu},\tilde{\theta},t\right)\\
&=\left(\sum_{k\geq 0}\varepsilon^k\left(\sum_{n_1+2n_2+\ldots+kn_k=k}\frac{\left(-\bar{\mathbf{Z}}^1\right)^{n_1}\ldots\left(-\bar{\mathbf{Z}}^k\right)^{n_k}}{n_1!\ldots n_k!}\right)(id)\right)\left(\tilde{\mu},\tilde{\theta},t\right).
\end{aligned} \tag{3.3.7}$$

Proof. We will start the proof by proving formulas (3.3.6) and (3.3.7). Let $g = g(\mu, \theta, t)$ be a smooth function,

$$\mathbf{v} = \xi^1 \partial_\mu + \xi^2 \partial_\theta + \xi^3 \partial_t \tag{3.3.8}$$

a smooth vector field, and $\varphi_\varepsilon^{\mathbf{v}}$ its flow. Then, $(\varphi_\varepsilon^{\mathbf{v}})^\star g = g \circ \varphi_\varepsilon^{\mathbf{v}}$ admits the following Taylor expansion :

$$\left((\varphi_\varepsilon^{\mathbf{v}})^\star g\right)(\mu, \theta, t) = g(\mu, \theta, t) + \varepsilon \left(\mathbf{v} \cdot g\right)(\mu, \theta, t) + \ldots + \frac{\varepsilon^n}{n!} \left(\mathbf{v}^n \cdot g\right)(\mu, \theta, t) \tag{3.3.9}$$

$$+ \frac{\varepsilon^{n+1}}{n!} \int_0^1 (1-u)^n \frac{\partial^{n+1}}{\partial \varepsilon^{n+1}} \left(g\left(\varphi_\varepsilon^{\mathbf{v}}(\mu, \theta, t)\right)\right)|_{\varepsilon u} \, du, \tag{3.3.10}$$

where $\mathbf{v} \cdot g = \xi^1 \partial_\mu g + \xi^2 \partial_\theta g + \xi^3 \partial_t g$ and $\mathbf{v}^{k+1} \cdot g = \mathbf{v} \cdot (\mathbf{v}^k \cdot g)$. Writing formally the entire Taylor series in ε, we obtain :

$$\left((\varphi_\varepsilon^{\mathbf{v}})^\star g\right)(\mu, \theta, t) = \left(\left(\sum_{n \geq 0} \frac{\varepsilon^n}{n!} \mathbf{v}^k \cdot\right) g\right)(\mu, \theta, t). \tag{3.3.11}$$

The right hand side of (3.3.11) is usually called the Lie series for the action of the flow on g. The same result holds for vector valued function $G : \mathcal{M} \to \mathbb{R}^m, G = (G^1, \ldots, G^m)$, where we let $\mathbf{v}$ act component-wise on $G : \mathbf{v} \cdot G = (\mathbf{v} \cdot G^1, \ldots, \mathbf{v} \cdot G^m)$. In our case, the change of coordinates reads :

$$\begin{aligned}
\left(\tilde{\mu}, \tilde{\theta}, t\right) &= \boldsymbol{\mathcal{L}}_\varepsilon(\mu, \theta, t) \\
&= \ldots \circ \bar{\varphi}_{\varepsilon^n}^n \circ \ldots \circ \bar{\varphi}_{\varepsilon^1}^1 (\mu, \theta, t) \\
&= \left(\left(\ldots \circ \bar{\varphi}_{\varepsilon^n}^n \circ \ldots \circ \bar{\varphi}_{\varepsilon^1}^1\right)^\star (id)\right)(\mu, \theta, t) \\
&= \left(\left(\left(\bar{\varphi}_{\varepsilon^1}^1\right)^\star \circ \ldots \circ \left(\bar{\varphi}_{\varepsilon^n}^n\right)^\star \circ \ldots\right)(id)\right)(\mu, \theta, t).
\end{aligned} \tag{3.3.12}$$

According to formula (3.3.11), we have for each $n \in \mathbb{N}$ and for each vector valued function G :

$$\left(\left(\bar{\varphi}_{\varepsilon^k}^k\right)^\star G\right)(\mu, \theta, t) = \left(\left(\sum_{n_k \geq 0} \frac{\varepsilon^{k n_k}}{n_k!} (\bar{\mathbf{Z}}^k)^{n_k} \cdot\right) G\right)(\mu, \theta, t). \tag{3.3.13}$$

As a consequence, formula (3.3.12) can be rewritten :

$$\begin{aligned}
\boldsymbol{\mathcal{L}}_\varepsilon(\mu, \theta, t) &= \left(\left(\left(\sum_{n_1 \geq 0} \frac{\varepsilon^{n_1}}{n_1!} \left(\bar{\mathbf{Z}}^1\right)^{n_1}\right) \cdot \left(\sum_{n_1 \geq 0} \frac{\varepsilon^{2n_2}}{n_2!} \left(\bar{\mathbf{Z}}^2\right)^{n_2}\right) \cdot \ldots\right)(id)\right)(\mu, \theta, t) \\
&= \left(\left(\sum_{n_1, n_2, n_3, \ldots \geq 0} \frac{\varepsilon^{n_1 + 2n_2 + \ldots} \left(\bar{\mathbf{Z}}^1\right)^{n_1} \left(\bar{\mathbf{Z}}^2\right)^{n_2} \ldots}{n_1! n_2! \ldots} \cdot\right)(id)\right)(\mu, \theta, t).
\end{aligned} \tag{3.3.14}$$

Grouping together the terms with the same power of ε leads to formula (3.3.6). In the same way we obtain formula (3.3.7).

Now, we will prove formula (3.3.4). Let $\bar{\boldsymbol{\Omega}} = \bar{\boldsymbol{\Omega}}(\mu, \theta, t)$ be a differential one-form,

$$\mathbf{w} = w^1 \partial_\mu + w^2 \partial_\theta \tag{3.3.15}$$

a smooth vector field, and $\varphi_\varepsilon^{\mathbf{w}}$ its flow. Then, according to Theorem 3.2.18, $\left((\varphi_\varepsilon^{\mathbf{w}})^{-1}\right)^\star \bar{\mathbf{\Omega}}$ admits the following Taylor expansion :

$$\begin{aligned}&\left(\left((\varphi_\varepsilon^{\mathbf{w}})^{-1}\right)^\star \bar{\mathbf{\Omega}}\right)\left(\tilde{\mu},\tilde{\theta},t\right) = \bar{\mathbf{\Omega}}\left(\tilde{\mu},\tilde{\theta},t\right) - \varepsilon\mathcal{L}_{\mathbf{w}}\bar{\mathbf{\Omega}}\left(\tilde{\mu},\tilde{\theta},t\right) + \dots \\ &+ \frac{(-1)^n\,\varepsilon^n}{n!}\mathcal{L}_{\mathbf{w}}^n\bar{\mathbf{\Omega}}\left(\tilde{\mu},\tilde{\theta},t\right) + \frac{\varepsilon^{n+1}}{n!}\int_0^1 (1-u)^n \frac{\partial^{n+1}\tilde{\mathbf{\Omega}}_\varepsilon}{\partial\varepsilon^{n+1}}\,|_{\varepsilon u}\left(\tilde{\mu},\tilde{\theta},t\right)du\end{aligned} \tag{3.3.16}$$

Writing formally the entire Taylor series in ε, we obtain :

$$\left(\left((\varphi_\varepsilon^{\mathbf{w}})^{-1}\right)^\star \bar{\mathbf{\Omega}}\right)\left(\tilde{\mu},\tilde{\theta},t\right) = \left(\left(\sum_{n\geq 0}\frac{(-1)^n\,\varepsilon^n}{n!}\mathcal{L}_{\mathbf{w}}^n\right)\bar{\mathbf{\Omega}}\right)\left(\tilde{\mu},\tilde{\theta},t\right). \tag{3.3.17}$$

The right hand side of (3.3.17) is usually called the Lie series for the action of the flow on $\bar{\mathbf{\Omega}}$. Now, according to formula (3.2.47), the expression of $\boldsymbol{\beta}^\varepsilon$ in the Lie coordinate system is given by

$$\tilde{\boldsymbol{\beta}}^\varepsilon = \left(\boldsymbol{\mathcal{L}}_\varepsilon^{-1}\right)^\star \bar{\boldsymbol{\beta}}^\varepsilon. \tag{3.3.18}$$

Injecting (3.3.2) in (3.3.18) leads to :

$$\tilde{\boldsymbol{\beta}}^\varepsilon = \sum_{p\geq 0}\varepsilon^{p-1}\left(\boldsymbol{\mathcal{L}}_\varepsilon^{-1}\right)^\star \bar{\boldsymbol{\beta}}_p. \tag{3.3.19}$$

For each $p\in\mathbb{N}$ we obtain :

$$\begin{aligned}&\left(\left(\boldsymbol{\mathcal{L}}_\varepsilon^{-1}\right)^\star \bar{\boldsymbol{\beta}}_p\right)\left(\tilde{\mu},\tilde{\theta},t\right) \\ &= \left(\left(\left(\dots\circ\bar{\varphi}_{\varepsilon^n}^n\circ\dots\circ\bar{\varphi}_{\varepsilon^1}^1\right)^{-1}\right)^\star\bar{\boldsymbol{\beta}}_p\right)\left(\tilde{\mu},\tilde{\theta},t\right) \\ &= \left(\left(\dots\circ\left(\left(\bar{\varphi}_{\varepsilon^n}^n\right)^{-1}\right)^\star\circ\dots\circ\left(\left(\bar{\varphi}_{\varepsilon^1}^1\right)^{-1}\right)^\star\right)\bar{\boldsymbol{\beta}}_p\right)\left(\tilde{\mu},\tilde{\theta},t\right) \\ &= \left(\left(\dots\left(\sum_{n_2\geq 0}\frac{(-1)^{n_2}\,\varepsilon^{n_2}}{n_2!}\mathcal{L}_{\bar{\mathbf{Z}}^2}^{n_2}\right)\left(\sum_{n_1\geq 0}\frac{(-1)^{n_1}\,\varepsilon^{n_1}}{n_1!}\mathcal{L}_{\bar{\mathbf{Z}}^1}^{n_1}\right)\right)\bar{\boldsymbol{\beta}}_p\right)\left(\tilde{\mu},\tilde{\theta},t\right) \\ &= \left(\sum_{k\geq 0}\varepsilon^k\left(\sum_{n_1+2n_2+\dots+kn_k=k}(-1)^{n_1+\dots+n_k}\,\frac{\mathcal{L}_{\bar{\mathbf{Z}}^k}^{n_k}\dots\mathcal{L}_{\bar{\mathbf{Z}}^1}^{n_1}}{n_1!\dots n_k!}\right)\bar{\boldsymbol{\beta}}_p\right)\left(\tilde{\mu},\tilde{\theta},t\right).\end{aligned} \tag{3.3.20}$$

Injecting (3.3.20) in (3.3.19) and grouping together the terms with the same power of ε leads to formula (3.3.4).

This ends the proof of Theorem 3.3.1. □

We will denote by $\tilde{\boldsymbol{\beta}}_n$ the $(n-1)$th order of the Hilbert expansion (3.3.4) ; i.e.,

$$\tilde{\boldsymbol{\beta}}_n\left(\tilde{\mu},\tilde{\theta},t\right) = \sum_{k=0}^{n}\left(\bar{\boldsymbol{W}}_k\bar{\boldsymbol{\beta}}_{n-k}\right)\left(\tilde{\mu},\tilde{\theta},t\right). \tag{3.3.21}$$

3.3.2 The Lie Transform Method

The Lie Transform method consists to find a differential one-form $\tilde{\boldsymbol{\alpha}}_\varepsilon$ and a Lie change of coordinates $\boldsymbol{\mathcal{L}}_\varepsilon$ such that :

1. $\left(\boldsymbol{\mathcal{L}}_\varepsilon^{-1}\right)^\star \overline{\boldsymbol{\gamma}}^\varepsilon = \tilde{\boldsymbol{\alpha}}_\varepsilon + d\sigma_\varepsilon$,
2. $\tilde{\boldsymbol{\alpha}}_\varepsilon$ is under a normal form.

We will precise immediately our definition of normal forms. For this purpose, we will introduce the following linear spaces of smooth functions :

$$\mathcal{C}^\infty_{2\pi} = \left\{f \in \mathcal{C}^\infty\left((0,+\infty)\times\mathbb{R};\mathbb{R}\right);\ f \text{ is } 2\pi \text{ periodic with respect to } \theta\right\}, \tag{3.3.22}$$

$$\mathcal{D} = \left\{f \in \mathcal{C}^\infty_{2\pi};\ \frac{\partial f}{\partial \theta} = 0\right\}, \tag{3.3.23}$$

$$\mathcal{R} = \left\{f \in \mathcal{C}^\infty_{2\pi};\ \langle f\rangle = \frac{1}{2\pi}\int_0^{2\pi} f\left(\mu,\theta\right)d\theta = 0\right\}. \tag{3.3.24}$$

Notice also that $\mathcal{C}^\infty_{2\pi} = \mathcal{D}\oplus\mathcal{R}$.

Definition 3.3.2. *Let $\boldsymbol{\mathcal{L}}_\varepsilon$: $(\mu,\theta,t)\mapsto\left(\tilde{\mu},\tilde{\theta},t\right)$ be a Lie change of coordinates, $\tilde{\boldsymbol{\alpha}}_\varepsilon = \tilde{\boldsymbol{\alpha}}_\varepsilon\left(\tilde{\mu},\tilde{\theta},t\right)$ be a differential one form admitting a Hilbert expansion of the form :*

$$\tilde{\boldsymbol{\alpha}}_\varepsilon = \frac{1}{\varepsilon}\sum_{n\geq 0}\left(\tilde{\alpha}^1_n d\tilde{\mu} + \tilde{\alpha}^2_n d\tilde{\theta} + \tilde{\alpha}^3_n dt\right)\varepsilon^n, \tag{3.3.25}$$

and $\boldsymbol{\alpha}_\varepsilon = \boldsymbol{\alpha}_\varepsilon\left(\mu,\theta,t\right)$ the differential one form defined by $\boldsymbol{\alpha}_\varepsilon\left(\mu,\theta,t\right) = \tilde{\boldsymbol{\alpha}}_\varepsilon\left(\mu,\theta,t\right)$. We say that $\tilde{\boldsymbol{\alpha}}_\varepsilon$ is under a normal form if

$$\forall n\in\mathbb{N},\ \alpha^1_n \in \mathcal{D}, \tag{3.3.26}$$

$$\alpha^2_1 = -\mu,\ \text{and } \forall n\in\mathbb{N}\setminus\{1\},\ \alpha^2_n = 0, \tag{3.3.27}$$

$$\forall n\in\mathbb{N},\ \alpha^3_n \in \mathcal{D}. \tag{3.3.28}$$

This definition is made in order to have the following theorem :

Theorem 3.3.3. *Let $\boldsymbol{\mathcal{L}}_\varepsilon$: $(\mu,\theta,t)\mapsto\left(\tilde{\mu},\tilde{\theta},t\right)$ be a Lie change of coordinates and $\tilde{\boldsymbol{X}}^\varepsilon_H$ the expression of $\boldsymbol{\tau}^\varepsilon = \boldsymbol{\tau}^\varepsilon_H$ in the Lie coordinate system. Assume that there exists $\tilde{\boldsymbol{\alpha}}_\varepsilon \in [\tilde{\boldsymbol{\gamma}}^\varepsilon]$ which is under a normal form. Then, the first component of $\tilde{\mathbf{X}}^\varepsilon_H$ vanish, the second component is $\tilde{\theta}$ independent and is given by :*

$$\left(\tilde{X}^\varepsilon_H\right)^2 = \frac{\partial\tilde{\alpha}^3_\varepsilon}{\partial\tilde{\mu}} - \frac{\partial\tilde{\alpha}^1_\varepsilon}{\partial t}, \tag{3.3.29}$$

and the expression of the particle distribution in the Lie coordinate system satisfies :

$$\frac{\partial\tilde{f}_\varepsilon}{\partial t}\left(\tilde{\mu},\tilde{\theta},t\right) + \left(\tilde{X}^\varepsilon_H\right)^2\left(\tilde{\mu},t\right)\frac{\partial\tilde{f}_\varepsilon}{\partial\tilde{\theta}}\left(\tilde{\mu},\tilde{\theta},t\right) = 0. \tag{3.3.30}$$

Proof. Let $\boldsymbol{\mathcal{L}}_\varepsilon : \ (\mu,\theta,t) \mapsto \left(\tilde{\mu},\tilde{\theta},t\right)$ be a Lie change of coordinates and $\tilde{\boldsymbol{\alpha}}_\varepsilon \in [\tilde{\boldsymbol{\gamma}}^\varepsilon]$ which is under a normal form. According to Theorem 3.2.8 the expression of $\boldsymbol{\tau}^\varepsilon$ in the Lie coordinate system corresponds to the solution of

$$i_{\tilde{\mathbf{X}}_H^\varepsilon} d\tilde{\boldsymbol{\alpha}}_\varepsilon = 0 \tag{3.3.31}$$

that satisfies $\left(\tilde{X}_H^\varepsilon\right)^3 = 1$. Since all the components of $\tilde{\boldsymbol{\alpha}}_\varepsilon$ belong to $\mathcal{D}$, its differential is given by :

$$d\tilde{\boldsymbol{\alpha}}_\varepsilon = \frac{\partial \tilde{\alpha}_\varepsilon^1}{\partial t} dt \wedge d\tilde{\mu} - d\tilde{\mu} \wedge d\tilde{\theta} + \frac{\partial \tilde{\alpha}_\varepsilon^3}{\partial \tilde{\mu}} d\tilde{\mu} \wedge dt, \tag{3.3.32}$$

and consequently

$$\begin{aligned} & i_{\tilde{\mathbf{X}}_H^\varepsilon} d\tilde{\boldsymbol{\alpha}}_\varepsilon \\ &= \left(\frac{\partial \tilde{\alpha}_\varepsilon^1}{\partial t} - \frac{\partial \tilde{\alpha}_\varepsilon^3}{\partial \tilde{\mu}} + \left(\tilde{X}_H^\varepsilon\right)^2 \right) d\tilde{\mu} - \left(\tilde{X}_H^\varepsilon\right)^1 d\tilde{\theta} + \left(\left(\tilde{X}_H^\varepsilon\right)^1 \frac{\partial \tilde{\alpha}_\varepsilon^3}{\partial \tilde{\mu}} - \left(\tilde{X}_H^\varepsilon\right)^1 \right) dt \end{aligned} \tag{3.3.33}$$

Since $\tilde{\mathbf{X}}_H^\varepsilon$ satisfies (3.3.31), we obtain :

$$\left(\tilde{X}_H^\varepsilon\right)^1 = 0, \tag{3.3.34}$$

$$\frac{\partial \tilde{\alpha}_\varepsilon^1}{\partial t} - \frac{\partial \tilde{\alpha}_\varepsilon^3}{\partial \tilde{\mu}} + \left(\tilde{X}_H^\varepsilon\right)^2 = 0. \tag{3.3.35}$$

Since $\tilde{\alpha}_\varepsilon^1$ and $\tilde{\alpha}_\varepsilon^3$ lie in $\mathcal{D}$, equation (3.3.35) implies that $\left(\tilde{X}_H^\varepsilon\right)^2$ belongs to $\mathcal{D}$.

According to Theorem 3.2.2 the Vlasov equation reads

$$\frac{\partial \tilde{f}_\varepsilon}{\partial t}\left(\tilde{\mu},\tilde{\theta},t\right) + \left(\tilde{X}_H^\varepsilon\right)^2 (\tilde{\mu},t) \frac{\partial \tilde{f}_\varepsilon}{\partial \tilde{\theta}}\left(\tilde{\mu},\tilde{\theta},t\right) = 0. \tag{3.3.36}$$

This ends the proof of Theorem (3.3.3). □

Having this material in hand we can precise the objectives of the Lie Transform method. Let $\boldsymbol{\beta}^\varepsilon \in [\boldsymbol{\gamma}^\varepsilon]$ be the one form whose expression in the (μ,θ,t) coordinate system, defined by (3.1.15)-(3.1.16), is given by formula (3.3.1) and whose formal expansion in power of ε is given by (3.3.3). Let $\boldsymbol{\mathcal{L}}_\varepsilon : \ (\mu,\theta,t) \mapsto \left(\tilde{\mu},\tilde{\theta},t\right)$ be the unknown Lie Change of Coordinates and $\tilde{\boldsymbol{\beta}}^\varepsilon$ the expression of $\boldsymbol{\beta}^\varepsilon$ in this unknown Lie coordinate system. According to Proposition 3.3.1, $\tilde{\boldsymbol{\beta}}^\varepsilon$ admits the expansion in power of ε given by (3.3.4). The Lie Transform method consists to construct by induction the sequences of vector fields $\left(\bar{\mathbf{Z}}^n\right)_{n\in\mathbb{N}^\star}$ and the sequence of differential one forms $(\tilde{\boldsymbol{\alpha}}_n)_{n\in\mathbb{N}}$ such that for each $n \in \mathbb{N}^\star$

$$\frac{1}{\varepsilon}\left(\tilde{\boldsymbol{\alpha}}_0 + \varepsilon\tilde{\boldsymbol{\alpha}}_1 + \ldots + \varepsilon^n \tilde{\boldsymbol{\alpha}}_n\right) \in \left[\frac{1}{\varepsilon}\left(\tilde{\boldsymbol{\beta}}_0 + \varepsilon\tilde{\boldsymbol{\beta}}_1 + \ldots + \varepsilon^n \tilde{\boldsymbol{\beta}}_n\right)\right] \tag{3.3.37}$$

and such that the differential one form

$$\tilde{\boldsymbol{\alpha}}_\varepsilon^n = \frac{1}{\varepsilon}\sum_{k=0}^{n} \tilde{\boldsymbol{\alpha}}_k \varepsilon^k \tag{3.3.38}$$

is under a normal form.

Notice that by construction a Lie change of coordinate is infinitesimal and consequently the first term of the sequence defining $\tilde{\boldsymbol{\alpha}}_\varepsilon$ is given by

$$\tilde{\boldsymbol{\alpha}}_0 = -\tilde{\mu} dt. \tag{3.3.39}$$

Now, the constructive proof of the following Theorem constitutes the Lie Transform algorithm.

Theorem 3.3.4. *There exists a Lie change of coordinates $\boldsymbol{\mathcal{L}}_\varepsilon$ and a differential one form $\tilde{\boldsymbol{\alpha}}_\varepsilon$ such that $\tilde{\boldsymbol{\alpha}}_\varepsilon$ belongs to $[\boldsymbol{\gamma}^\varepsilon]$ and is under a normal form. Moreover the proof of this Theorem constitutes a constructive algorithm to build $\boldsymbol{\mathcal{L}}_\varepsilon$ and $\tilde{\boldsymbol{\alpha}}_\varepsilon$.*

3.3.3 The Lie Transform Algorithm : proof of Theorem 3.3.4

Lemma 3.3.5. *For any $\left(\bar{\mathbf{Z}}^n\right)_{n\geq 2} \in \mathcal{C}^\infty_{2\pi}$ and $\bar{Z}^1_2 \in \mathcal{C}^\infty_{2\pi}$, setting*

$$\begin{aligned}\bar{\mathbf{Z}}^1(\mu,\theta,t) = &\left(\phi_0\left(\sqrt{2\mu}\cos(\theta),t\right) - \frac{1}{2\pi}\int_{-\pi}^{\pi}\phi_0\left(\sqrt{2\mu}\cos(\theta),t\right)d\theta\right)\partial_\mu \\ &+ \bar{Z}^1_2\partial_\theta\end{aligned} \tag{3.3.40}$$

and

$$\tilde{\boldsymbol{\alpha}}_1 = -\tilde{\mu}d\tilde{\theta} - \left(\frac{1}{2\pi}\int_{-\pi}^{\pi}\phi_0\left(\sqrt{2\tilde{\mu}}\cos\left(\tilde{\theta}\right),t\right)d\tilde{\theta}\right)dt \tag{3.3.41}$$

yields that

$$\tilde{\boldsymbol{\alpha}}^1_\varepsilon = \frac{1}{\varepsilon}\left(\tilde{\boldsymbol{\alpha}}_0 + \varepsilon\tilde{\boldsymbol{\alpha}}_1\right) \in \left[\frac{1}{\varepsilon}\left(\tilde{\boldsymbol{\beta}}_0 + \varepsilon\tilde{\boldsymbol{\beta}}_1\right)\right] \tag{3.3.42}$$

and that $\tilde{\boldsymbol{\alpha}}^1_\varepsilon$ is under a normal form.

Proof. Applying formula (3.3.21) with $n = 1$ yields :

$$\tilde{\boldsymbol{\beta}}_1\left(\tilde{\mu},\tilde{\theta},t\right) = \bar{\boldsymbol{W}}_0\bar{\boldsymbol{\beta}}_1\left(\tilde{\mu},\tilde{\theta},t\right) + \bar{\boldsymbol{W}}_1\bar{\boldsymbol{\beta}}_0\left(\tilde{\mu},\tilde{\theta},t\right). \tag{3.3.43}$$

Computing $\bar{\boldsymbol{W}}_1$ with formula (3.3.5) and using Cartan Formula yields :

$$\bar{\boldsymbol{W}}_1 = -i_{\bar{\mathbf{Z}}^1}d - di_{\bar{\mathbf{Z}}^1}. \tag{3.3.44}$$

According to (3.3.44), the only non-exact contribution of $\bar{\boldsymbol{W}}_1$ is given by $-i_{\bar{\mathbf{Z}}^1}d$. Consequently, we just have to find $\tilde{\boldsymbol{\alpha}}_1$, S_1 and $\bar{\mathbf{Z}}^1$ such that :

$$\tilde{\boldsymbol{\alpha}}_1\left(\tilde{\mu},\tilde{\theta},t\right) = \bar{\boldsymbol{\beta}}_1\left(\tilde{\mu},\tilde{\theta},t\right) - \left(i_{\bar{\mathbf{Z}}^1}d\bar{\boldsymbol{\beta}}_0\right)\left(\tilde{\mu},\tilde{\theta},t\right) + \left(dS_1\right)\left(\tilde{\mu},\tilde{\theta},t\right), \tag{3.3.45}$$

and such that $\tilde{\boldsymbol{\alpha}}^1_\varepsilon = \frac{1}{\varepsilon}\left(\tilde{\boldsymbol{\alpha}}_0 + \varepsilon\tilde{\boldsymbol{\alpha}}_1\right)$ is under a normal form. Writing formula (3.3.45) in coordinates yields :

$$\begin{aligned}&\left(\frac{\partial S_1}{\partial\tilde{\mu}} - \tilde{\alpha}^1_1\right)d\tilde{\mu} + \left(\frac{\partial S_1}{\partial\tilde{\theta}} - \tilde{\alpha}^2_1 - \tilde{\mu}\right)d\tilde{\theta} + \\ &\left(\frac{\partial S_1}{\partial t} + \bar{Z}^1_1 - \phi_0\left(\sqrt{2\tilde{\mu}}\cos\left(\tilde{\theta}\right),t\right) - \tilde{\alpha}^3_1\right)dt = 0.\end{aligned} \tag{3.3.46}$$

Setting $\tilde{\alpha}_1^1 = 0,\ \tilde{\alpha}_1^2 = -\tilde{\mu},\ , \tilde{\alpha}_1^3 = -\frac{1}{2\pi}\int_{-\pi}^{\pi} \phi_0\left(\sqrt{2\tilde{\mu}}\cos\left(\tilde{\theta}\right), t\right) d\tilde{\theta}$,

$$\bar{Z}_1^1\left(\tilde{\mu},\tilde{\theta},t\right) = \phi_0\left(\sqrt{2\tilde{\mu}}\cos\left(\tilde{\theta}\right), t\right) - \frac{1}{2\pi}\int_{-\pi}^{\pi} \phi_0\left(\sqrt{2\tilde{\mu}}\cos\left(\tilde{\theta}\right), t\right) d\tilde{\theta} \tag{3.3.47}$$

and $S_1 = 0$ yields the result. This ends the proof of Lemma 3.3.5.

□

Theorem 3.3.6. *For any* $\left(\bar{\mathbf{Z}}^n\right)_{n\geq 3} \in \mathcal{C}^\infty_{2\pi}$, $\bar{Z}_1^{2,\mathcal{D}} \in \mathcal{D}$ *and* $\bar{Z}_2^2 \in \mathcal{C}^\infty_{2\pi}$, *setting*

$$\begin{aligned}\bar{Z}_2^1 = &\frac{1}{\sqrt{2\mu}}\int_0^\theta \cos\left(\theta'\right) E_0\left(\sqrt{2\mu}\cos\left(\theta'\right), t\right) d\theta' \\ &- \frac{\theta}{2\pi\sqrt{2\mu}}\int_{-\pi}^{\pi} \cos\left(\theta'\right) E_0\left(\sqrt{2\mu}\cos\left(\theta'\right), t\right) d\theta',\end{aligned} \tag{3.3.48}$$

$$\bar{Z}_1^{2,\mathcal{R}}\left(\tilde{\mu},\tilde{\theta},t\right) = \varrho_2\left(\tilde{\mu},\tilde{\theta},t\right) - \frac{1}{2\pi}\int_{-\pi}^{\pi} \varrho_2\left(\tilde{\mu},\tilde{\theta},t\right) d\tilde{\theta}, \tag{3.3.49}$$

where ϱ_2 *is defined by formula* (3.3.64), *and*

$$\tilde{\boldsymbol{\alpha}}_2 = \left(\bar{Z}_1^{2,\mathcal{D}} - \frac{1}{2\pi}\int_{-\pi}^{\pi} \varrho_2\left(\tilde{\mu},\tilde{\theta},t\right) d\tilde{\theta}\right) dt \tag{3.3.50}$$

yields that

$$\tilde{\boldsymbol{\alpha}}_\varepsilon^2 = \frac{1}{\varepsilon}\left(\tilde{\boldsymbol{\alpha}}_0 + \varepsilon\tilde{\boldsymbol{\alpha}}_1 + \varepsilon^2\tilde{\boldsymbol{\alpha}}_2\right) \in \left[\frac{1}{\varepsilon}\left(\tilde{\boldsymbol{\beta}}_0 + \varepsilon\tilde{\boldsymbol{\beta}}_1 + \varepsilon^2\tilde{\boldsymbol{\beta}}_2\right)\right] \tag{3.3.51}$$

and that $\tilde{\boldsymbol{\alpha}}_\varepsilon^2$ *is under a normal form.*

Proof. Applying formula (3.3.21) with $n = 2$ yields :

$$\tilde{\boldsymbol{\beta}}_2\left(\tilde{\mu},\tilde{\theta},t\right) = \bar{\boldsymbol{W}}_0\bar{\boldsymbol{\beta}}_2\left(\tilde{\mu},\tilde{\theta},t\right) + \bar{\boldsymbol{W}}_1\bar{\boldsymbol{\beta}}_1\left(\tilde{\mu},\tilde{\theta},t\right) + \bar{\boldsymbol{W}}_2\bar{\boldsymbol{\beta}}_0\left(\tilde{\mu},\tilde{\theta},t\right). \tag{3.3.52}$$

Computing $\bar{\boldsymbol{W}}_2$ with formula (3.3.5) and using Cartan Formula yields :

$$\bar{\boldsymbol{W}}_2 = -i_{\bar{\mathbf{Z}}^2}d - di_{\bar{\mathbf{Z}}^2} + \frac{1}{2}\left(i_{\bar{\mathbf{Z}}^1}di_{\bar{\mathbf{Z}}^1}d + di_{\bar{\mathbf{Z}}^1}\mathcal{L}_{\bar{\mathbf{Z}}^1}\right). \tag{3.3.53}$$

According to (3.3.53), the only non-exact contribution of $\bar{\boldsymbol{W}}_2$ is given by

$$-i_{\bar{\mathbf{Z}}^2}d + \frac{1}{2}i_{\bar{\mathbf{Z}}^1}di_{\bar{\mathbf{Z}}^1}d.$$

Consequently, we just have to find S_2, $\bar{Z}_2^1$ and $\bar{\mathbf{Z}}^2$ such that :

$$\begin{aligned}\tilde{\boldsymbol{\alpha}}_2\left(\tilde{\mu},\tilde{\theta},t\right) = &\bar{\boldsymbol{\beta}}_2\left(\tilde{\mu},\tilde{\theta},t\right) - \left(i_{\bar{\mathbf{Z}}^2}d\bar{\boldsymbol{\beta}}_0\right)\left(\tilde{\mu},\tilde{\theta},t\right) - \left(i_{\bar{\mathbf{Z}}^1}d\bar{\boldsymbol{\beta}}_1\right)\left(\tilde{\mu},\tilde{\theta},t\right) \\ &+ \frac{1}{2}\left(i_{\bar{\mathbf{Z}}^1}di_{\bar{\mathbf{Z}}^1}d\bar{\boldsymbol{\beta}}_0\right)\left(\tilde{\mu},\tilde{\theta},t\right) + \left(dS_2\right)\left(\tilde{\mu},\tilde{\theta},t\right).\end{aligned} \tag{3.3.54}$$

Writing the terms of formula (3.3.54) in coordinates yields :

$$\begin{aligned}
&i_{\bar{\mathbf{Z}}^2} d\bar{\boldsymbol{\beta}}_0 = -\bar{Z}_1^2 dt,\\
&i_{\bar{\mathbf{Z}}^1} d\bar{\boldsymbol{\beta}}_1 = \bar{Z}_2^1 d\tilde{\mu} - \bar{Z}_1^1 d\tilde{\theta} + \frac{\partial \phi_0}{\partial r}\left(\sqrt{2\tilde{\mu}}\cos(\tilde{\theta}), t\right)\\
&\qquad\qquad \left(\bar{Z}_2^1\sqrt{2\tilde{\mu}}\sin(\tilde{\theta}) - \bar{Z}_1^1\frac{\cos(\tilde{\theta})}{\sqrt{2\tilde{\mu}}}\right)dt,\\
&i_{\bar{\mathbf{Z}}^1} d i_{\bar{\mathbf{Z}}^1} d\bar{\boldsymbol{\beta}}_0 = -\left(\bar{Z}_1^1\frac{\partial \bar{Z}_1^1}{\partial \tilde{\mu}} + \bar{Z}_2^1\frac{\partial \bar{Z}_1^1}{\partial \tilde{\theta}}\right)dt.
\end{aligned} \tag{3.3.55}$$

Consequently, (3.3.54) reads :

$$\frac{\partial S_2}{\partial \tilde{\mu}} - \bar{Z}_2^1 - \tilde{\alpha}_2^1 = 0, \tag{3.3.56}$$

$$\frac{\partial S_2}{\partial \tilde{\theta}} + \bar{Z}_1^1 - \tilde{\alpha}_2^2 = 0, \tag{3.3.57}$$

and

$$\begin{aligned}
&\bar{Z}_1^2 - \tilde{\alpha}_2^3 + \frac{\partial S_2}{\partial t} - \phi_1\left(\sqrt{2\tilde{\mu}}\cos\left(\tilde{\theta}\right), t\right)\\
&- \left(\bar{Z}_2^1\sqrt{2\tilde{\mu}}\sin\left(\tilde{\theta}\right) - \bar{Z}_1^1\frac{\cos\left(\tilde{\theta}\right)}{\sqrt{2\tilde{\mu}}}\right)\frac{\partial \phi_0}{\partial r}\left(\sqrt{2\tilde{\mu}}\cos\left(\tilde{\theta}\right), t\right)\\
&- \frac{1}{2}\left(\bar{Z}_1^1\frac{\partial \bar{Z}_1^1}{\partial \tilde{\mu}} + \bar{Z}_2^1\frac{\partial \bar{Z}_1^1}{\partial \tilde{\theta}}\right) = 0
\end{aligned} \tag{3.3.58}$$

Since $\mathcal{C}^\infty_{2\pi} = \mathcal{D} \oplus \mathcal{R}$, we make the following decompositions :

$$S_2 = S_2^{\mathcal{D}} + S_2^{\mathcal{R}}, \tag{3.3.59}$$

$$\bar{Z}_2^1 = \bar{Z}_2^{1,\mathcal{D}} + \bar{Z}_2^{1,\mathcal{R}}, \tag{3.3.60}$$

$$\bar{Z}_1^2 = \bar{Z}_1^{2,\mathcal{D}} + \bar{Z}_1^{2,\mathcal{R}}. \tag{3.3.61}$$

Setting $\tilde{\alpha}_2^2 = 0$ in (3.3.57) implies

$$\frac{\partial S_2^{\mathcal{R}}}{\partial \tilde{\theta}} = -\bar{Z}_1^1. \tag{3.3.62}$$

Since $\bar{Z}_1^1 \in \mathcal{R}$, equation (3.3.62) has a solution in $\mathcal{R}$ and it is given by

$$\begin{aligned}
S_2^{\mathcal{R}} &= \int_0^\theta \left(-\bar{Z}_1^1(\mu, \theta', t)\right) d\theta' - \frac{1}{2\pi}\int_{-\pi}^{\pi}\left(-\bar{Z}_1^1(\mu, s, t)\right) ds\\
&= -\int_0^\theta \phi_0\left(\sqrt{2\mu}\cos\left(\theta'\right), t\right) d\theta' + \frac{\theta}{2\pi}\int_{-\pi}^{\pi}\phi_0\left(\sqrt{2\mu}\cos\left(\theta'\right), t\right) d\theta'.
\end{aligned} \tag{3.3.63}$$

Afterwards, setting $\bar{Z}_2^1 = \frac{\partial S_2^{\mathcal{R}}}{\partial \tilde{\mu}}$ (notice that this choice implies $\bar{Z}_2^1 = \bar{Z}_2^{1,\mathcal{R}}$) and $S_2^{\mathcal{D}} = 0$ in (3.3.56) implies $\tilde{\alpha}_2^1 = 0$.

Finally, let ϱ_2 be the function defined by

$$\begin{aligned}\varrho_2\left(\tilde{\mu},\tilde{\theta},t\right) &= -\frac{\partial S_2^{\mathcal{R}}}{\partial t} + \phi_1\left(\sqrt{2\tilde{\mu}}\cos\left(\tilde{\theta}\right),t\right) \\ &+ \left(\bar{Z}_2^1\sqrt{2\tilde{\mu}}\sin\left(\tilde{\theta}\right) - \bar{Z}_1^1\frac{\cos\left(\tilde{\theta}\right)}{\sqrt{2\tilde{\mu}}}\right)\frac{\partial\phi_0}{\partial r}\left(\sqrt{2\tilde{\mu}}\cos\left(\tilde{\theta}\right),t\right) \\ &+ \frac{1}{2}\left(\bar{Z}_1^1\frac{\partial\bar{Z}_1^1}{\partial\tilde{\mu}} + \bar{Z}_2^1\frac{\partial\bar{Z}_1^1}{\partial\tilde{\theta}}\right).\end{aligned} \tag{3.3.64}$$

Then, equation (3.3.58) reads :

$$\bar{Z}_1^2 - \tilde{\alpha}_2^3 - \varrho_2\left(\tilde{\mu},\tilde{\theta},t\right) = 0. \tag{3.3.65}$$

Setting

$$\bar{Z}_1^{2,\mathcal{R}}\left(\tilde{\mu},\tilde{\theta},t\right) = \varrho_2\left(\tilde{\mu},\tilde{\theta},t\right) - \frac{1}{2\pi}\int_{-\pi}^{\pi}\varrho_2\left(\tilde{\mu},\tilde{\theta},t\right)d\tilde{\theta} \tag{3.3.66}$$

remove the $\tilde{\theta}$ dependency in $\tilde{\alpha}_2^3$.

□

Remark 3.3.7. *Notice that at this level $\bar{Z}_1^{2,\mathcal{D}}$ is not fixed. But as soon as it will be fixed, $\tilde{\alpha}_2^3$ will also be fixed and will be equal to*

$$\tilde{\alpha}_2^3 = \bar{Z}_1^{2,\mathcal{D}} - \frac{1}{2\pi}\int_{-\pi}^{\pi}\varrho_2\left(\tilde{\mu},\tilde{\theta},t\right)d\tilde{\theta} \in \mathcal{D}.$$

Theorem 3.3.8. *For any $n \geq 2$, for any sequence $\left(\bar{\mathbf{Z}}^k\right)_{k\geq n+1} \in \mathcal{C}_{2\pi}^\infty$, for any $\bar{Z}_1^{n,\mathcal{D}} \in \mathcal{D}$ and for any $\bar{Z}_2^n \in \mathcal{C}_{2\pi}^\infty$, there exists $\left(\bar{\mathbf{Z}}^k\right)_{k\leq n-1} \in \mathcal{C}_{2\pi}^\infty$, $\bar{Z}_1^{n,\mathcal{R}} \in \mathcal{R}$ and $(\boldsymbol{\alpha}_k)_{0\leq k\leq n}$ such that*

$$\tilde{\boldsymbol{\alpha}}_\varepsilon^n = \frac{1}{\varepsilon}\left(\tilde{\boldsymbol{\alpha}}_0 + \varepsilon\tilde{\boldsymbol{\alpha}}_1 + \ldots + \varepsilon^n\tilde{\boldsymbol{\alpha}}_n\right) \in \left[\frac{1}{\varepsilon}\left(\tilde{\boldsymbol{\beta}}_0 + \varepsilon\tilde{\boldsymbol{\beta}}_1 + \ldots + \varepsilon^n\tilde{\boldsymbol{\beta}}_n\right)\right] \tag{3.3.67}$$

and such that $\tilde{\boldsymbol{\alpha}}_\varepsilon^n$ is under a normal form.

Proof. We will prove Theorem 3.3.8 by induction. The case $n = 2$ was treated in Theorem 3.3.6. Consequently, we pass directly to the induction step.

Let $n \geq 3$. Assume that $\bar{\mathbf{Z}}^1, \bar{\mathbf{Z}}^2, \ldots, \bar{\mathbf{Z}}^{n-2} \in \mathcal{C}_{2\pi}^\infty$ and $\bar{Z}_1^{n-1,\mathcal{R}} \in \mathcal{R}$ are fixed in such a way that

$$\tilde{\boldsymbol{\alpha}}_\varepsilon^{n-1} = \frac{1}{\varepsilon}\left(\tilde{\boldsymbol{\alpha}}_0 + \varepsilon\tilde{\boldsymbol{\alpha}}_1 + \ldots + \varepsilon^{n-1}\tilde{\boldsymbol{\alpha}}_{n-1}\right) \in \left[\frac{1}{\varepsilon}\left(\tilde{\boldsymbol{\beta}}_0 + \varepsilon\tilde{\boldsymbol{\beta}}_1 + \ldots + \varepsilon^{n-1}\tilde{\boldsymbol{\beta}}_{n-1}\right)\right] \tag{3.3.68}$$

and $\tilde{\boldsymbol{\alpha}}_\varepsilon^{n-1}$ is under a normal form. We will find $\bar{Z}_2^{n-1} \in \mathcal{C}_{2\pi}^\infty$, $\bar{Z}_1^{n-1,\mathcal{D}} \in \mathcal{D}$, $\bar{Z}_1^{n,\mathcal{R}} \in \mathcal{R}$ and $\tilde{\boldsymbol{\alpha}}_n$ such that :

$$\tilde{\boldsymbol{\alpha}}_\varepsilon^n = \frac{1}{\varepsilon}\left(\tilde{\boldsymbol{\alpha}}_0 + \varepsilon\tilde{\boldsymbol{\alpha}}_1 + \ldots + \varepsilon^n\tilde{\boldsymbol{\alpha}}_n\right) \in \left[\frac{1}{\varepsilon}\left(\tilde{\boldsymbol{\beta}}_0 + \varepsilon\tilde{\boldsymbol{\beta}}_1 + \ldots + \varepsilon^n\tilde{\boldsymbol{\beta}}_n\right)\right], \tag{3.3.69}$$

and such that $\tilde{\boldsymbol{\alpha}}_\varepsilon^n$ is under a normal form.

Formula (3.3.21) yields :

$$\tilde{\boldsymbol{\beta}}_n\left(\tilde{\mu},\tilde{\theta},t\right)=\sum_{k=0}^{n}\left(\bar{\boldsymbol{W}}_k\bar{\boldsymbol{\beta}}_{n-k}\right)(\tilde{\mu},\tilde{\theta},t),$$

where $\bar{\boldsymbol{W}}_n$ is given by (3.3.5). As in formula (3.3.5) (with $k=n$) $n_1+2n_2+\ldots+nn_n=n$, the only term depending on $\bar{\mathbf{Z}}^n$ in $\bar{\boldsymbol{W}}_n\bar{\boldsymbol{\beta}}_0$ is $-\mathcal{L}_{\bar{\mathbf{Z}}^n}\bar{\boldsymbol{\beta}}_0$, and the only term depending on $\bar{\mathbf{Z}}^{n-1}$ is $\mathcal{L}_{\bar{\mathbf{Z}}^{n-1}}\mathcal{L}_{\bar{\mathbf{Z}}^1}\bar{\boldsymbol{\beta}}_0$, and as in formula (3.3.5) (with $k=n-1$) $n_1+2n_2+\ldots+(n-1)n_{n-1}=n-1$, the only term depending on $\bar{\mathbf{Z}}^{n-1}$ in $\bar{\boldsymbol{W}}_{n-1}\bar{\boldsymbol{\beta}}_1$ is $-\mathcal{L}_{\bar{\mathbf{Z}}^{n-1}}\bar{\boldsymbol{\beta}}_1$. Consequently, the only terms in formula (3.3.21) depending on $\bar{\mathbf{Z}}^{n-1}$ and $\bar{\mathbf{Z}}^n$ are $-\mathcal{L}_{\bar{\mathbf{Z}}^n}\bar{\boldsymbol{\beta}}_0$, $\mathcal{L}_{\bar{\mathbf{Z}}^{n-1}}\mathcal{L}_{\bar{\mathbf{Z}}^1}\bar{\boldsymbol{\beta}}_0$ and $-\mathcal{L}_{\bar{\mathbf{Z}}^{n-1}}\bar{\boldsymbol{\beta}}_1$. Hence $\tilde{\boldsymbol{\beta}}_n$ reads :

$$\tilde{\boldsymbol{\beta}}_n=\bar{\boldsymbol{\beta}}_n-i_{\bar{\boldsymbol{Z}}^n}d\bar{\boldsymbol{\beta}}_0-i_{\bar{\boldsymbol{Z}}^{n-1}}d\bar{\boldsymbol{\beta}}_1+i_{\bar{\boldsymbol{Z}}^{n-1}}di_{\bar{\boldsymbol{Z}}^1}d\bar{\boldsymbol{\beta}}_0+\psi^n\left(\bar{\boldsymbol{Z}}^1,\ldots,\bar{\boldsymbol{Z}}^{n-2}\right)+\text{ something exact.}\tag{3.3.70}$$

Consequently, the job is reduced to find S_n, $\bar{Z}_2^{n-1}\in\mathcal{C}^\infty_{2\pi}$, $\bar{Z}_1^{n-1,\mathcal{D}}\in\mathcal{D}$, $\bar{Z}_1^{n,\mathcal{R}}\in\mathcal{R}$, and $\tilde{\boldsymbol{\alpha}}_n$ such that :

$$\tilde{\boldsymbol{\alpha}}_n=\bar{\boldsymbol{\beta}}_n-i_{\bar{\boldsymbol{Z}}^n}d\bar{\boldsymbol{\beta}}_0-i_{\bar{\boldsymbol{Z}}^{n-1}}d\bar{\boldsymbol{\beta}}_1+i_{\bar{\boldsymbol{Z}}^{n-1}}di_{\bar{\boldsymbol{Z}}^1}d\bar{\boldsymbol{\beta}}_0+\psi^n\left(\bar{\boldsymbol{Z}}^1,\ldots,\bar{\boldsymbol{Z}}^{n-2}\right)+dS_n,\tag{3.3.71}$$

and such that $\tilde{\boldsymbol{\alpha}}^n_\varepsilon$ satisfies (3.3.69). Writing formula (3.3.71) in coordinates yields :

$$\begin{aligned}
&i_{\bar{Z}^n}d\bar{\boldsymbol{\beta}}_0=-\bar{Z}_1^n dt,\\
&i_{\bar{Z}^{n-1}}d\bar{\boldsymbol{\beta}}_1=\bar{Z}_2^{n-1}d\tilde{\mu}-\bar{Z}_1^{n-1}d\tilde{\theta}\\
&\qquad\qquad+\frac{\partial\phi_0}{\partial r}\left(\sqrt{2\tilde{\mu}}\cos\left(\tilde{\theta}\right),t\right)\left(\bar{Z}_2^{n-1}\sqrt{2\tilde{\mu}}\sin\left(\tilde{\theta}\right)-\bar{Z}_1^{n-1}\frac{\cos\left(\tilde{\theta}\right)}{\sqrt{2\tilde{\mu}}}\right)dt,\\
&i_{\bar{Z}^{n-1}}di_{\bar{Z}^1}d\bar{\boldsymbol{\beta}}_0=-\left(\bar{Z}_1^{n-1}\frac{\partial\bar{Z}_1^1}{\partial\tilde{\mu}}+\bar{Z}_2^{n-1}\frac{\partial\bar{Z}_1^1}{\partial\tilde{\theta}}\right)dt.
\end{aligned}\tag{3.3.72}$$

Consequently, (3.3.71) reads :

$$\frac{\partial S_n}{\partial\tilde{\mu}}-\bar{Z}_2^{n-1}+\psi_1^n\left(\bar{\boldsymbol{Z}}^1,\ldots,\bar{\boldsymbol{Z}}^{n-2}\right)-\tilde{\alpha}_n^1=0,\tag{3.3.73}$$

$$\frac{\partial S_n}{\partial\tilde{\theta}}+\bar{Z}_1^{n-1}+\psi_2^n\left(\bar{\boldsymbol{Z}}^1,\ldots,\bar{\boldsymbol{Z}}^{n-2}\right)-\tilde{\alpha}_n^2=0,\tag{3.3.74}$$

and

$$\begin{aligned}
&\bar{Z}_1^n+\frac{\partial S_n}{\partial t}-\tilde{\alpha}_n^3-\phi_{n-1}\left(\sqrt{2\tilde{\mu}}\cos\left(\tilde{\theta}\right),t\right)\\
&-\left(\bar{Z}_2^{n-1}\sqrt{2\tilde{\mu}}\sin\left(\tilde{\theta}\right)-\bar{Z}_1^{n-1}\frac{\cos\left(\tilde{\theta}\right)}{\sqrt{2\tilde{\mu}}}\right)\frac{\partial\phi_0}{\partial r}\left(\sqrt{2\tilde{\mu}}\cos\left(\tilde{\theta}\right),t\right)\\
&+\psi_3^n\left(\bar{\boldsymbol{Z}}^1,\ldots,\bar{\boldsymbol{Z}}^{n-2}\right)-\left(\bar{Z}_1^{n-1}\frac{\partial\bar{Z}_1^1}{\partial\tilde{\mu}}+\bar{Z}_2^{n-1}\frac{\partial\bar{Z}_1^1}{\partial\tilde{\theta}}\right)=0
\end{aligned}\tag{3.3.75}$$

Since $\mathcal{C}^\infty_{2\pi}=\mathcal{D}\oplus\mathcal{R}$, we make the following decompositions :

$$S_n=S_n^{\mathcal{D}}+S_n^{\mathcal{R}},\tag{3.3.76}$$

$$\bar{Z}_2^{n-1}=\bar{Z}_2^{n-1,\mathcal{D}}+\bar{Z}_2^{n-1,\mathcal{R}},\tag{3.3.77}$$

$$\psi_2^n\left(\bar{\boldsymbol{Z}}^1,\ldots,\bar{\boldsymbol{Z}}^{n-2}\right)=\psi_2^{n,\mathcal{D}}\left(\bar{\boldsymbol{Z}}^1,\ldots,\bar{\boldsymbol{Z}}^{n-2}\right)+\psi_2^{n,\mathcal{R}}\left(\bar{\boldsymbol{Z}}^1,\ldots,\bar{\boldsymbol{Z}}^{n-2}\right).\tag{3.3.78}$$

Setting $\tilde{\alpha}_n^2 = 0$ in (3.3.74) implies

$$\frac{\partial S_n}{\partial \tilde{\theta}} + \bar{Z}_1^{n-1} + \psi_2^n \left(\bar{\boldsymbol{Z}}^1, \ldots, \bar{\boldsymbol{Z}}^{n-2} \right) = 0, \tag{3.3.79}$$

and consequently we set :

$$\frac{\partial S_n^{\mathcal{R}}}{\partial \tilde{\theta}} = -\bar{Z}_1^{n-1,\mathcal{R}} - \psi_2^{n,\mathcal{R}} \left(\bar{\boldsymbol{Z}}^1, \ldots, \bar{\boldsymbol{Z}}^{n-2} \right), \tag{3.3.80}$$

$$\bar{Z}_1^{n-1,\mathcal{D}} = -\psi_2^{n,\mathcal{D}} \left(\bar{\boldsymbol{Z}}^1, \ldots, \bar{\boldsymbol{Z}}^{n-2} \right). \tag{3.3.81}$$

Since $\bar{Z}_1^{n-1,\mathcal{R}} + \psi_2^{n,\mathcal{R}} \left(\bar{\boldsymbol{Z}}^1, \ldots, \bar{\boldsymbol{Z}}^{n-2} \right) \in \mathcal{R}$, equation (3.3.80) has a solution in $\mathcal{R}$.

Afterwards, setting $S_n^{\mathcal{D}} = 0$,

$$\bar{Z}_2^{n-1} = \frac{\partial S_n^{\mathcal{R}}}{\partial \tilde{\mu}} - \psi_1^{n,\mathcal{R}} \left(\bar{\boldsymbol{Z}}^1, \ldots, \bar{\boldsymbol{Z}}^{n-2} \right), \tag{3.3.82}$$

$$\tilde{\alpha}_n^1 = \psi_1^{n,\mathcal{D}} \left(\bar{\boldsymbol{Z}}^1, \ldots, \bar{\boldsymbol{Z}}^{n-2} \right), \tag{3.3.83}$$

solve equation (3.3.73).

Finally, let ϱ_n be the function defined by

$$\begin{aligned} \varrho_n \left(\tilde{\mu}, \tilde{\theta}, t \right) = & - \frac{\partial S_n}{\partial t} + \phi_{n-1} \left(\sqrt{2\tilde{\mu}} \cos\left(\tilde{\theta} \right), t \right) \\ & + \left(\bar{Z}_2^{n-1} \sqrt{2\tilde{\mu}} \sin\left(\tilde{\theta} \right) - \bar{Z}_1^{n-1} \frac{\cos\left(\tilde{\theta} \right)}{\sqrt{2\tilde{\mu}}} \right) \frac{\partial \phi_0}{\partial r} \left(\sqrt{2\tilde{\mu}} \cos\left(\tilde{\theta} \right), t \right) \\ & - \psi_3^n \left(\bar{\boldsymbol{Z}}^1, \ldots, \bar{\boldsymbol{Z}}^{n-2} \right) - \left(\bar{Z}_1^{n-1} \frac{\partial \bar{Z}_1^1}{\partial \tilde{\mu}} + \bar{Z}_2^{n-1} \frac{\partial \bar{Z}_1^1}{\partial \tilde{\theta}} \right) \end{aligned} \tag{3.3.84}$$

Then, equation (3.3.85) reads :

$$\bar{Z}_1^n - \tilde{\alpha}_n^3 - \varrho_n = 0. \tag{3.3.85}$$

Setting

$$\bar{Z}_1^{n,\mathcal{R}} = \varrho_n^{\mathcal{R}}, \tag{3.3.86}$$

$$\alpha_n^3 = -\varrho_n^{\mathcal{D}} + \bar{Z}_1^{n,\mathcal{D}} \tag{3.3.87}$$

remove the $\tilde{\theta}$ dependency in $\tilde{\alpha}_n^3$. This ends the induction step and the proof of Theorem 3.3.8. □

3.3.4 Proof of Theorem 3.1.2

Let $\boldsymbol{\mathcal{L}}_\varepsilon$ and $\tilde{\boldsymbol{\alpha}}_\varepsilon$ be the Lie change of coordinates and the normal form of $\boldsymbol{\gamma}^\varepsilon$ constructed in the proof of Theorem 3.3.4. According to Theorem (3.3.3) the expression of the particle distribution in the Lie coordinate system is given by :

$$\frac{\partial \tilde{f}_\varepsilon}{\partial t} + \left(\frac{\partial \tilde{\alpha}_\varepsilon^3}{\partial \tilde{\mu}} - \frac{\partial \tilde{\alpha}_\varepsilon^1}{\partial t} \right) \frac{\partial \tilde{f}_\varepsilon}{\partial t} = 0. \tag{3.3.88}$$

Setting

$$a_\varepsilon\left(\tilde{\mu},t\right)=\left(\frac{\partial\tilde{\alpha}_\varepsilon^3}{\partial\tilde{\mu}}\left(\tilde{\mu},t\right)-\frac{\partial\tilde{\alpha}_\varepsilon^1}{\partial t}\left(\tilde{\mu},t\right)\right) \tag{3.3.89}$$

yields formula (3.1.31). Moreover, the Hilbert expansion of a_ε is given by

$$a_\varepsilon\left(\tilde{\mu},t\right)=\frac{1}{\varepsilon}\sum_{n\geq 0}\left(\frac{\partial\tilde{\alpha}_n^3}{\partial\tilde{\mu}}\left(\tilde{\mu},t\right)-\frac{\partial\tilde{\alpha}_n^1}{\partial t}\left(\tilde{\mu},t\right)\right)\varepsilon^n. \tag{3.3.90}$$

According to formula 3.3.39, the first term of this Hilbert expansion is given by

$$a_0\left(\tilde{\mu},t\right)=-1, \tag{3.3.91}$$

and according to formula (3.3.41), the second term of the Hilbert expansion is given by

$$a_1\left(\tilde{\mu},t\right)=\frac{1}{2\pi\sqrt{2\tilde{\mu}}}\int_{-\pi}^{\pi}\cos\left(\tilde{\theta}\right)E_0\left(\sqrt{2\tilde{\mu}}\cos\left(\tilde{\theta}\right),t\right)d\tilde{\theta}. \tag{3.3.92}$$

Formulas (3.3.91) and (3.3.92) yield formula (3.1.38).

The Poisson equation expressed in the (r,v_r,t) coordinate system is given by (3.1.2) and the charge density by (3.1.3). In order to solve the Vlasov Equation (3.3.88) we need to express the charge density ρ_ε in terms of the particle density expressed in the Lie coordinate system. Let $\bar{f}_\varepsilon$ be the particle density expressed in the (μ,θ) coordinate system ; i.e.,

$$\bar{f}_\varepsilon\left(\mu,\theta,t\right)=f_\varepsilon\left(\mathfrak{Pol}^{-1}\left(\mu,\theta\right),t\right),\ \text{or equivalently} \tag{3.3.93}$$

$$f_\varepsilon\left(r,v_r,t\right)=\bar{f}_\varepsilon\left(\mathfrak{Pol}\left(r,v_r\right),t\right). \tag{3.3.94}$$

Then, the charge density ρ_ε, given by (3.1.3), can be rewritten as follow :

$$\begin{aligned}\rho_\varepsilon\left(t,r\right)&=\int_{\mathbb{R}}f_\varepsilon\left(r,v_r',t\right)dv_r'\\&=\int_{\mathbb{R}^2}f_\varepsilon\left(r',v_r',t\right)\delta\left(r-r'\right)dr'dv_r'\\&=\int_{\mathbb{R}_+\times]-\pi,\pi]}\bar{f}_\varepsilon\left(\mu',\theta',t\right)h_r\left(\mu',\theta'\right)d\mu'd\theta',\end{aligned}$$

where $h_r=h_r\left(\mu',\theta'\right)$ is defined by

$$h_r\left(\mu',\theta'\right)=\delta\left(r-\sqrt{2\mu'}\cos\left(\theta'\right)\right). \tag{3.3.95}$$

Let $\tilde{f}_\varepsilon$ the particle density expressed in the $\left(\tilde{\mu},\tilde{\theta},t\right)$ coordinate system ; i.e.,

$$\tilde{f}_\varepsilon\left(\tilde{\mu},\tilde{\theta},t\right)=\bar{f}_\varepsilon\left(\boldsymbol{\mathcal{L}}_\varepsilon^{-1}\left(\tilde{\mu},\tilde{\theta},t\right)\right),\ \text{or equivalently} \tag{3.3.96}$$

$$\bar{f}_\varepsilon\left(\mu,\theta,t\right)=\tilde{f}_\varepsilon\left(\boldsymbol{\mathcal{L}}_\varepsilon\left(\mu,\theta,t\right)\right), \tag{3.3.97}$$

$\mathbf{D}_\varepsilon^t=\boldsymbol{\mathcal{L}}_\varepsilon\left((0,+\infty)\times]-\pi,\pi],t\right)$ and $\left|\mathcal{J}_{\boldsymbol{\mathcal{L}}_\varepsilon^{-1}}\left(\tilde{\mu}',\tilde{\theta}',t'\right)\right|$ the jacobian associated with $\boldsymbol{\mathcal{L}}_\varepsilon^{-1}$. Then the charge density can be rewritten as follow :

$$\begin{aligned}\rho_\varepsilon\left(t,r\right)&=\int_{\boldsymbol{\mathcal{L}}_\varepsilon^{-1}\left(\mathbf{D}_\varepsilon^t\right)}\bar{f}_\varepsilon\left(\mu',\theta',t\right)h_r\left(\mu',\theta'\right)d\mu'd\theta'\\&=\int_{\mathbf{D}_\varepsilon^t}\tilde{f}_\varepsilon\left(\tilde{\mu}',\tilde{\theta}',t\right)h_r\left(\boldsymbol{\mathcal{P}}\boldsymbol{\mathcal{L}}_\varepsilon^{-1}\left(\tilde{\mu}',\tilde{\theta}',t\right)\right)\left|\mathcal{J}_{\boldsymbol{\mathcal{L}}_\varepsilon^{-1}}\left(\tilde{\mu}',\tilde{\theta}',t\right)\right|d\tilde{\mu}'d\tilde{\theta}'.\end{aligned}$$

Finally, Lemma 3.3.5 and Theorem 3.3.6 yields that :

$$\begin{aligned}\bar{\mathbf{Z}}^1(\mu,\theta,t) = &\Big(\phi_0(\sqrt{2\mu}\cos(\theta),t) - \frac{1}{2\pi}\int_{-\pi}^{\pi}\phi_0(\sqrt{2\mu}\cos(\theta),t)d\theta\Big)\partial_\mu \\ &+\Big(\frac{1}{\sqrt{2\mu}}\int_0^\theta \cos(\theta')\,E_0(\sqrt{2\mu}\cos(\theta'),t)d\theta' \\ &-\frac{\theta}{2\pi\sqrt{2\mu}}\int_{-\pi}^{\pi}\cos(\theta')\,E_0(\sqrt{2\mu}\cos(\theta'),t)d\theta'\Big)\partial_\theta.\end{aligned} \tag{3.3.98}$$

Applying formulas (3.3.6) and (3.3.7) and truncating at the second order yields formulas (3.1.36) and (3.1.37). This ends the proof of Theorem 3.1.2.

3.3.5 Truncated models and some remarks about their efficiency

As we saw in the previous Subsection, for a given $N \in \mathbb{N}^\star$ the vector fields $\bar{\mathbf{Z}}_1,\dots,\bar{\mathbf{Z}}_N$ allow us to construct the N first terms $\tilde{\boldsymbol{\alpha}}_0,\dots,\tilde{\boldsymbol{\alpha}}_N$ of the normal form $\tilde{\boldsymbol{\alpha}}_\varepsilon$. Hence, defining the partial Lie change of coordinates of order N by

$$\boldsymbol{\mathcal{L}}_\varepsilon^N = \bar{\varphi}_{\varepsilon^N}^N \circ \dots \circ \bar{\varphi}_{\varepsilon^1}^1 \tag{3.3.99}$$

and making the change of coordinates $\left(\tilde{\mu},\tilde{\theta},t\right) = \boldsymbol{\mathcal{L}}_\varepsilon^N(\mu,\theta,t)$ lead to a differential one form

$$\tilde{\boldsymbol{\alpha}}_\varepsilon^{T,N}\left(\tilde{\mu},\tilde{\theta},t\right) = \frac{1}{\varepsilon}\left(\sum_{n=0}^{N}\tilde{\boldsymbol{\alpha}}_n\left(\tilde{\mu},\tilde{\theta},t\right)\right) + \mathcal{O}\left(\varepsilon^N\right) \in \left[\tilde{\boldsymbol{\beta}}^\varepsilon\right]. \tag{3.3.100}$$

which is up to order N under the normal form. Consequently, Proposition 3.2.6 and Theorem 3.2.2 yield that the characteristics associated with the Vlasov equation (3.1.1) expressed in the partial Lie coordinate system of order N are given by :

$$\frac{\partial\tilde{\mathfrak{Mu}}_{T,N}^\varepsilon}{\partial t}\left(\tilde{\mu},\tilde{\theta},t\right) = \mathcal{O}\left(\varepsilon^N\right), \tag{3.3.101}$$

$$\frac{\partial\tilde{\Theta}_{T,N}^\varepsilon}{\partial t}\left(\tilde{\mu},\tilde{\theta},t\right) = \frac{1}{\varepsilon}\left(\sum_{n=0}^{N}a_n\left(\tilde{\mathfrak{Mu}}_{T,N}^\varepsilon,t\right)\varepsilon^n\right) + \mathcal{O}\left(\varepsilon^N\right), \tag{3.3.102}$$

$$\tilde{\mathfrak{Mu}}_{T,N}^\varepsilon\left(\tilde{\mu},\tilde{\theta},0\right) = \tilde{\mu}, \qquad \tilde{\Theta}_{T,N}^\varepsilon\left(\tilde{\mu},\tilde{\theta},0\right) = \tilde{\theta}. \tag{3.3.103}$$

Remark 3.3.9. *Notice that the reminders (the $\mathcal{O}\left(\varepsilon^N\right)$) depend to $\tilde{\mu}$, $\tilde{\theta}$ and t and that they are evaluated at the characteristics. By construction the vector fields $\bar{\mathbf{Z}}_1,\dots,\bar{\mathbf{Z}}_N$ are 2π periodic with respect to θ. Consequently we can easily deduce that the first component of $\boldsymbol{\mathcal{L}}_\varepsilon^N$ is 2π periodic with respect to θ, and that the second component satisfies*

$$\left(\boldsymbol{\mathcal{L}}_\varepsilon^N\right)_2(\tilde{\mu},\tilde{\theta}+2\pi,t) = \left(\boldsymbol{\mathcal{L}}_\varepsilon^N\right)_2(\tilde{\mu},\tilde{\theta},t) + 2\pi. \tag{3.3.104}$$

On the other hand, let $\boldsymbol{\tau}_H^\varepsilon$ be the vector field whose principal part in the (r,v_r,t) coordinate system is given by (3.2.4) (with $G = H_\varepsilon$). Then, its expression in the polar coordinate system (μ,θ,t) is given by

$$\begin{aligned}\bar{\mathbf{X}}_H^\varepsilon(\mu,\theta,t) = &\sqrt{2\mu}\sin(\theta)\,E^\varepsilon\left(\sqrt{2\mu}\cos(\theta),t\right)\partial_\mu \\ &+\left(-\frac{1}{\varepsilon}+\frac{\cos(\theta)}{\sqrt{2\mu}}E^\varepsilon\left(\sqrt{2\mu}\cos(\theta),t\right)\right)\partial_\mu + \partial_t\end{aligned} \tag{3.3.105}$$

and it is consequently 2π *periodic. Hence, the expression of* $\boldsymbol{\tau}_H^\varepsilon$ *in the* $\left(\tilde{\mu},\tilde{\theta},t\right)$ *coordinate system is* 2π *periodic with respect to* θ*. This implies that the reminders of* (3.3.101)-(3.3.102) *are* 2π *periodic with respect to* $\tilde{\theta}$ *and consequently bounded with respect to this variable.*

Remark 3.3.10. *Since we deal with confined beams, i.e., the initial condition* f_0 *is chosen in such a way that the beam is bounded, the characteristic* $\mathfrak{Mu}^\varepsilon$*, which corresponds for a given particle to the evolution of the half of the square of the modulus between the origin and the particle position in the phase space, is bounded. Hence if we observe the evolution of the beam up to a given time* $T \in (0,+\infty)$*, the usual change of coordinate rules for the characteristics yield that* $\tilde{\mathfrak{Mu}}^\varepsilon_{T,N}$ *is also bounded for* $t \in [0,T]$*. Finally, since the reminders of* (3.3.101)-(3.3.102) *are* 2π *periodic with respect to* $\tilde{\theta}$ *and since* $\tilde{\mathfrak{Mu}}^\varepsilon_{T,N}$ *is bounded for* $t \in [0,T]$*, we obtain for any positive real number* ν *and for any* $\varepsilon \in (0,\nu)$ *an estimation* $\left|\mathcal{O}\left(\varepsilon^N\right)\right| \leq C_N(T,\nu)\varepsilon^N$ *for the reminders. Integrating these estimations yields error terms bounded by* $C_N(T,\nu)\varepsilon^N T$*.*

Remark 3.3.11. $\boldsymbol{\mathcal{L}}_\varepsilon^N$ *admits the following expansion in power of* ε *:*

$$\boldsymbol{\mathcal{L}}_\varepsilon^N = \left(\sum_{k=0}^{N}\varepsilon^k\left(\sum_{n_1+2n_2+\ldots+kn_k=k}\frac{\left(\bar{\mathbf{Z}}^1\right)^{n_1}\ldots\left(\bar{\mathbf{Z}}^k\right)^{n_k}}{n_1!\ldots n_k!}\right)(id)\right)+\mathcal{O}\left(\varepsilon^{N+1}\right). \tag{3.3.106}$$

Hence, the partial Lie change of coordinates $\boldsymbol{\mathcal{L}}_\varepsilon^N$ *is an approximation of order* $N+1$ *of the Lie change of coordinates. Moreover, since the change of coordinates* $\left(\tilde{\mu},\tilde{\theta},t\right) = \boldsymbol{\mathcal{L}}_\varepsilon^N(\mu,\theta,t)$ *produces a* $\mathcal{O}\left(\varepsilon^N\right)$ *error term in the right hand side of* (3.3.101)-(3.3.102)*, it produces a* $\mathcal{O}\left(\varepsilon^N\right)$ *error term in the characteristics. Hence, for numerical simulations it is sufficient to truncate* (3.3.106) *at order* N*. That is what we do in our simulations for* $N=1$*.*

Remark 3.3.12. *As a consequence of the previous Remarks and since approximation* (3.1.46) *is obtained by making the change of coordinates* $\boldsymbol{\mathcal{L}}_\varepsilon^1$*, the error term in the characteristics is bounded by* $C_1(\nu,T)\varepsilon T$ *for any positive real numbers* T *and* ν*, and for any* $\varepsilon \in (0,\nu)$ *and* $t \in (0,T)$*. Hence, for small time* T *of simulation the accuracy is of order* ε*. For longer times the accuracy is rather* $\mathcal{O}(1)$*. Nevertheless, we will observe numerically in Subsection 3.5 that for longer times of simulation the dynamics (fast rotation+slow filamentation) characterizing the evolution of the shape of the beam is close, but that the filaments are longer and wider. We will give more explanations in Subsection 3.5.*

3.4 Description of the numerical method

In this section, we will describe the PIC method that we will use in order to simulate equations (3.1.46)-(3.1.50) with the initial condition

$$f_0(r,v_r) = \frac{n_0}{\sqrt{2\pi}v_{th}}\exp\left(-\frac{v_r^2}{2v_{th}^2}\right)\chi_{[-0,75;0,75]}(r). \tag{3.4.1}$$

As usual in a PIC method, $\tilde{f}_\varepsilon$ will be approximated by the following Dirac mass sum :

$$\tilde{f}_\varepsilon^N\left(\tilde{\mu},\tilde{\theta},t\right) = \sum_{k=1}^{N}\omega_k\delta\left(\tilde{\mu}-\tilde{\mathfrak{Mu}}_k^\varepsilon(t)\right)\delta\left(\tilde{\theta}-\tilde{\Theta}_k^\varepsilon(t)\right) \tag{3.4.2}$$

where $\left(\tilde{\mathfrak{Mu}}_k^{\varepsilon}(t), \tilde{\Theta}_k^{\varepsilon}(t)\right)$ is the position in the $\left(\tilde{\mu}, \tilde{\theta}, t\right)$ coordinate system of macro-particle k which moves along a characteristic curve of the first order PDE (3.1.46). Hence the job is reduced to compute the macro-particle positions $\left(\tilde{\mathfrak{Mu}}_k^{\varepsilon,l+1}, \tilde{\Theta}_k^{\varepsilon,l+1}\right)$ at time $t_{l+1} = t_l + \Delta t$, knowing their positions $\left(\tilde{\mathfrak{Mu}}_k^{\varepsilon,l}, \tilde{\Theta}_k^{\varepsilon,l}\right)$ at time t_l, by solving the following differential system :

$$\frac{d\tilde{\mathfrak{Mu}}_k^{\varepsilon}}{dt}(t) = 0, \tag{3.4.3}$$

$$\frac{d\tilde{\Theta}_k^{\varepsilon}}{dt}(t) = -\frac{1}{\varepsilon} + \frac{1}{2\pi\sqrt{2\tilde{\mathfrak{Mu}}_k^{\varepsilon}(t)}} \int_{-\pi}^{\pi} \cos\left(\tilde{\theta}'\right) E_{\varepsilon}\left(\sqrt{2\tilde{\mathfrak{Mu}}_k^{\varepsilon}(t)}\cos\left(\tilde{\theta}'\right), t\right) d\tilde{\theta}', \tag{3.4.4}$$

$$\tilde{\Theta}_k^{\varepsilon}(t_l) = \tilde{\Theta}_k^{\varepsilon,l}, \qquad \tilde{\mathfrak{Mu}}_k^{\varepsilon}(t_l) = \tilde{\mathfrak{Mu}}_k^{\varepsilon,l}. \tag{3.4.5}$$

According to (3.4.3), for each $t \in \mathbb{R}_+$ and for each $k \in \{1, \ldots, N\}$, $\tilde{\mathfrak{Mu}}_k^{\varepsilon}(t) = \tilde{\mu}_k^0$ and the job is also reduced to integrate for each time step the equation

$$\frac{d\tilde{\Theta}_k^{\varepsilon}}{dt}(t) = -\frac{1}{\varepsilon} + \frac{1}{2\pi\sqrt{2\tilde{\mu}_k^0}} \int_{-\pi}^{\pi} \cos\left(\tilde{\theta}'\right) E_{\varepsilon}\left(\sqrt{2\tilde{\mu}_k^0}\cos\left(\tilde{\theta}'\right), t\right) d\tilde{\theta}', \tag{3.4.6}$$

$$\tilde{\Theta}_k^{\varepsilon}(t_l) = \tilde{\Theta}_k^{\varepsilon,l}. \tag{3.4.7}$$

Notice also that as $\theta \mapsto E_{\varepsilon}\left(\sqrt{2\tilde{\mu}}\cos\left(\tilde{\theta}\right), t\right)$ is an even function, the above integral can be replaced by

$$4\int_0^{\frac{\pi}{2}} \cos\left(\tilde{\theta}'\right) E_{\varepsilon}\left(\sqrt{2\tilde{\mu}}\cos\left(\tilde{\theta}'\right), t\right) d\tilde{\theta}'. \tag{3.4.8}$$

The first step of the computation of $\tilde{\Theta}_k^{\varepsilon,l+1}$ consists in replacing the integral above by p-node quadrature formula. As we approximate the integral of a periodic function over one period, the trapezoidal rule is optimal and will yield very accurate results for as few quadrature points as are needed to resolve the oscillations of the function.

Then, the equation for $\tilde{\Theta}_k^{\varepsilon,l+1}$ becomes

$$\frac{d\tilde{\Theta}_k^{\varepsilon}}{dt}(t) = -\frac{1}{\varepsilon} + \frac{2}{\pi\sqrt{2\tilde{\mu}_k^0}} \sum_{m=1}^{p} \Lambda_m \cos(\sigma_m) E_{\varepsilon}\left(\sqrt{2\tilde{\mu}_k^0}\cos(\sigma_m), t\right). \tag{3.4.9}$$

$$\tilde{\Theta}_k^{\varepsilon}(t_l) = \tilde{\Theta}_k^{\varepsilon,l}, \tag{3.4.10}$$

where $(\sigma_m)_{m=0}^p$ is a grid of $[0, \frac{\pi}{2}]$.

3.4.1 Expression of the initial condition in the Lie coordinates

The first step consists to replace the initial condition (3.4.1) by

$$f_0^N(r, v_r) = \sum_{k=1}^{N} \omega_k \delta\left(r - R_k^0\right) \delta\left(v_r - V_{r,k}^0\right), \tag{3.4.11}$$

where $(R_k^0)_{1\leq k\leq N}$ are uniformly distributed in $[-0,75;0,75]$ and $(V_{r,k}^0)_{1\leq k\leq N}$ are normally distributed.

Using the following expression for θ

$$\theta = \begin{cases} \arctan\left(\frac{v_r}{r}\right) \text{ if } r > 0 \\ \arctan\left(\frac{v_r}{r}\right) + \pi \text{ if } r < 0 \text{ and } v_r \geq 0 \\ \arctan\left(\frac{v_r}{r}\right) - \pi \text{ if } r < 0 \text{ and } v_r < 0 \\ \frac{\pi}{2} \text{ if } r = 0 \text{ and } v_r > 0 \\ -\frac{\pi}{2} \text{ if } r = 0 \text{ and } v_r < 0 \end{cases} \tag{3.4.12}$$

and formula (3.1.14) for μ (Notice that formula (3.4.12) works only for $\mu \neq 0$. If $\mu = 0$ we set $\theta = 0$) we obtain the expression of the initial condition in the (μ, θ, t) coordinate system

$$\bar{f}_0^N(\mu,\theta) = \sum_{k=1}^{N} \omega_k \delta\left(\mu - \mathfrak{M}\mathfrak{u}_k^0\right) \delta\left(\theta - \Theta_k^0\right). \tag{3.4.13}$$

Finally, using for each $1 \leq k \leq N$ the first order approximation (3.1.39)-(3.1.40) of the Lie change of coordinates, we obtain :

$$\begin{aligned} \tilde{\mu}_k^0 &= \mathfrak{M}\mathfrak{u}_k^0, \\ \tilde{\Theta}_k^0 &= \Theta_k^0. \end{aligned} \tag{3.4.14}$$

Consequently, the expression of initial condition in the Lie coordinate system is given by :

$$\tilde{f}_0^N\left(\tilde{\mu},\tilde{\theta}\right) = \sum_{k=1}^{N} \omega_k \delta\left(\tilde{\mu} - \tilde{\mu}_k^0\right) \delta\left(\tilde{\theta} - \tilde{\Theta}_k^0\right). \tag{3.4.15}$$

3.4.2 Numerical Resolution of (3.1.47)

Because of the form of the right hand side in (3.4.9), all along the algorithm we need to compute values of the electric field E_ε generated by a given macro-particle distribution

$$\left(\tilde{\mu}_k^0, \tilde{\Theta}_k^\varepsilon(t)\right)_{k=1,\ldots,N}.$$

Firstly, in order to solve (3.1.47) on $[-L, L]$ (L will be precise afterwards), we will proceed as follow. Injecting (3.4.2) in the right hand side of (3.1.47), and denoting by ρ_ε^N the yielding expression, we obtain :

$$\rho_\varepsilon^N(t,r) = \sum_{k=1}^{N} \omega_k \delta\left(r - \sqrt{2\tilde{\mu}_k^0}\cos\left(\tilde{\Theta}_k^\varepsilon(t)\right)\right). \tag{3.4.16}$$

Now, let $(r_k)_{k=0,\ldots,m_P}$ be an uniform one-dimensional mesh of $[0, L]$. In order to obtain an expression of the right hand side of (3.1.47) on the grid, we will regularize (3.4.16) with first order spline

$$\rho_\varepsilon^h(t,r) = \sum_{k=1}^{N} \omega_k S^1\left(r - \sqrt{2\tilde{\mu}_k^0}\cos\left(\tilde{\Theta}_k^\varepsilon(t)\right)\right). \tag{3.4.17}$$

Afterwards, solving

$$\frac{\partial}{\partial r} r E_\varepsilon = r \rho_\varepsilon^h \tag{3.4.18}$$

on $(r_k)_{k=0,\dots,m_P}$, by integrating this equation with the trapezoidal rule, yields the expression of the electric field E_ε on the grid. We denote by $\left(E_\varepsilon^k\right)_{k=1,\dots,m_p}$ these values. Notice that according to (3.1.4), $E_\varepsilon^0 = 0$. On the other hand, using the fact that E_ε is even, we obtain the following expression for the electric field on $[-L, L]$:

$$E_\varepsilon^h(r,t) = dr_P \sum_{k=0}^{m_P} E_\varepsilon^k \left(S^1(r - r_k) - S^1(r + r_k) \right), \tag{3.4.19}$$

where $dr_P = (r_1 - r_0)/m_P$. At the end, in order to obtain the electric field E_ε at the macro particle $\left(\tilde{\mu}_k^0, \tilde{\Theta}_k^\varepsilon(t)\right)$, we just have to evaluate the above expression at $\sqrt{2\tilde{\mu}_k^0}\cos(\tilde{\Theta}_k^\varepsilon(t))$.

3.4.3 Numerical Resolution of (3.4.9)-(3.4.10)

We solve (3.4.9)-(3.4.10) using the classical Runge-Kutta 4 method which gives the following scheme when applied to the computation of the approximation y^{l+1} of the value of y solution to $\frac{dy}{dt} = K(t,y)$ at time $t_l + \Delta t$ knowing its approximation y^l at time t_l :

$$\begin{aligned}
&t_{l,1} = t_l, \quad y^{l,1} = y^l, \\
&t_{l,2} = t_l + \frac{\Delta t}{2}, \quad y^{l,2} = y^l + \frac{1}{2} I^1, \quad \text{with } I^1 = \Delta t K(t_{l,1}, y^{l,1}), \\
&t_{l,3} = t_l + \frac{\Delta t}{2}, \quad y^{l,3} = y^l + \frac{1}{2} I^2, \quad \text{with } I^2 = \Delta t K(t_{l,2}, y^{l,2}), \\
&t_{l,4} = t_l + \Delta t, \quad y^{l,4} = y^l + I^3, \quad \text{with } I^3 = \Delta t K(t_{l,3}, y^{l,3}),
\end{aligned} \tag{3.4.20}$$

$$y^{l+1} = y^l + \frac{1}{6} I^1 + \frac{1}{3} I^2 + \frac{1}{3} I^3 + \frac{1}{6} I^4, \text{ with } I^4 = \Delta t K(t_{l,4}, y^{l,4}).$$

Now, we will apply this scheme to our problem. So, the first step consists in computing $\left(\tilde{\Theta}_k^{\varepsilon,l,2}\right)_{1 \le k \le N}$ as follows :

$$\begin{aligned}
&\tilde{\Theta}_k^{\varepsilon,l,2} = \tilde{\Theta}_k^{\varepsilon,l} + \frac{1}{2} I^1, \text{ with} \\
&I^1 = \Delta t \left(-\frac{1}{\varepsilon} + \frac{2}{\pi \sqrt{2\tilde{\mu}_k^0}} \sum_{m=1}^{p} \Lambda_m \cos(\sigma_m) E_\varepsilon \left(\sqrt{2\tilde{\mu}_k^0} \cos(\sigma_m), t_{l,1} \right) \right),
\end{aligned} \tag{3.4.21}$$

where the value of $E_\varepsilon \left(\sqrt{2\tilde{\mu}_k^0} \cos(\sigma_m), t_{l,1} \right)$ has been computed solving equation (3.1.47) associated with the particle distribution $\left(\Theta_k^{\varepsilon,l}\right)_{k=1,\dots,N}$ by the procedure described in subsection (3.4.2).

The second step of the Runge-Kutta method consists in computing $\tilde{\Theta}_k^{\varepsilon,l,3}$ defined by

$$\begin{aligned}
&\tilde{\Theta}_k^{\varepsilon,l,3} = \tilde{\Theta}_k^{\varepsilon,l} + \frac{1}{2} I^2, \text{ with} \\
&I^2 = \Delta t \left(-\frac{1}{\varepsilon} + \frac{2}{\pi \sqrt{2\tilde{\mu}_k^0}} \sum_{m=1}^{p} \Lambda_m \cos(\sigma_m) E_\varepsilon \left(\sqrt{2\tilde{\mu}_k^0} \cos(\sigma_m), t_{l,2} \right) \right),
\end{aligned} \tag{3.4.22}$$

where the value of $E_\varepsilon\left(\sqrt{2\tilde{\mu}_k^0}\cos(\sigma_m), t_{l,2}\right)$ is computed as previously from the $\left(\Theta_k^{\varepsilon,l,2}\right)_{k=1,\dots,N}$ particle distribution.

Then we compute

$$\begin{aligned}
&\tilde{\Theta}_k^{\varepsilon,l,4} = \tilde{\Theta}_k^{\varepsilon,l} + I^3, \text{ with}\\
&I^3 = \Delta t\left(-\frac{1}{\varepsilon} + \frac{2}{\pi\sqrt{2\tilde{\mu}_k^0}}\sum_{m=1}^{p}\Lambda_m\cos(\sigma_m)\,E_\varepsilon\left(\sqrt{2\tilde{\mu}_k^0}\cos(\sigma_m), t_{l,3}\right)\right),
\end{aligned} \tag{3.4.23}$$

where $E_\varepsilon\left(\sqrt{2\tilde{\mu}_k^0}\cos(\sigma_m), t_{l,3}\right)$ is computed from particle positions $\left(\Theta_k^{\varepsilon,l,3}\right)_{k=1,\dots,N}$.

Finally, $\tilde{\Theta}_k^{\varepsilon,l+1}$ is obtained by the following formula :

$$\begin{aligned}
&\tilde{\Theta}_k^{\varepsilon,l+1} = \tilde{\Theta}_k^{\varepsilon,l} + \frac{1}{6}I^1 + \frac{1}{3}I^2 + \frac{1}{3}I^3 + \frac{1}{6}I^4, \text{ with}\\
&I^4 = \Delta t\left(-\frac{1}{\varepsilon} + \frac{2}{\pi\sqrt{2\tilde{\mu}_k^0}}\sum_{m=1}^{p}\Lambda_m\cos(\sigma_m)\,E_\varepsilon\left(\sqrt{2\tilde{\mu}_k^0}\cos(\sigma_m), t_{l+1}\right)\right),
\end{aligned} \tag{3.4.24}$$

where I^1, I^2 and I^3 are defined above and where $E_\varepsilon\left(\sqrt{2\tilde{\mu}_k^0}\cos(\sigma_m), t_{l+1}\right)$ is computed from particle positions $\left(\Theta_k^{\varepsilon,l,4}\right)_{k=1,\dots,N}$.

3.4.4 Expression of the particle density in the (r, v_r, t) coordinate system

Finally, using the previous algorithm, when we come to the desired time $t_f = m_f\Delta t$ of simulation we need to go back in the (r, v_r, t) coordinate system. Firstly, we go back in the (μ, θ, t) coordinate system. Applying for each $1 \le k \le N$ the first order approximation (3.1.39)-(3.1.40) of the Lie change of coordinates we obtain :

$$\begin{aligned}
\mathfrak{Mu}_k^{\varepsilon,m_f} &= \tilde{\mu}_k^0,\\
\Theta_k^{\varepsilon,m_f} &= \tilde{\Theta}_k^{\varepsilon,m_f}.
\end{aligned} \tag{3.4.25}$$

Afterwards, using formula (3.1.15)-(3.1.16) we obtain the particle density expressed in the (r, v_r, t) coordinate system.

3.5 Numerical simulations

For the numerical simulations we take a thermal velocity $v_{th} = 0.0727518214392$, an initial mass density $n_0 = 1$, a number $N = 1\cdot10^4$ of macro particles, constant weights $\omega_k = \omega = \frac{1}{N}$ in 3.4.2, a 18-node composed trapezoidal quadrature formula for the computation of (3.4.8), $L = 1.5$ and $m_P = 128$ for the Poisson mesh, a small parameter $\varepsilon = 10^{-3}$, a time step $\Delta t = \varepsilon\sqrt{\varepsilon}$ and a Box-Muller method in order to generate the initial condition. As no analytical solution is available, we will compare our result with a standard PIC method (see [18]). The simulation results are given in figures 4.1, 3.2 and 3.3.

Remark 3.5.1. *From Figure 4.1 one can see the announced property of accuracy for small times of simulations.*

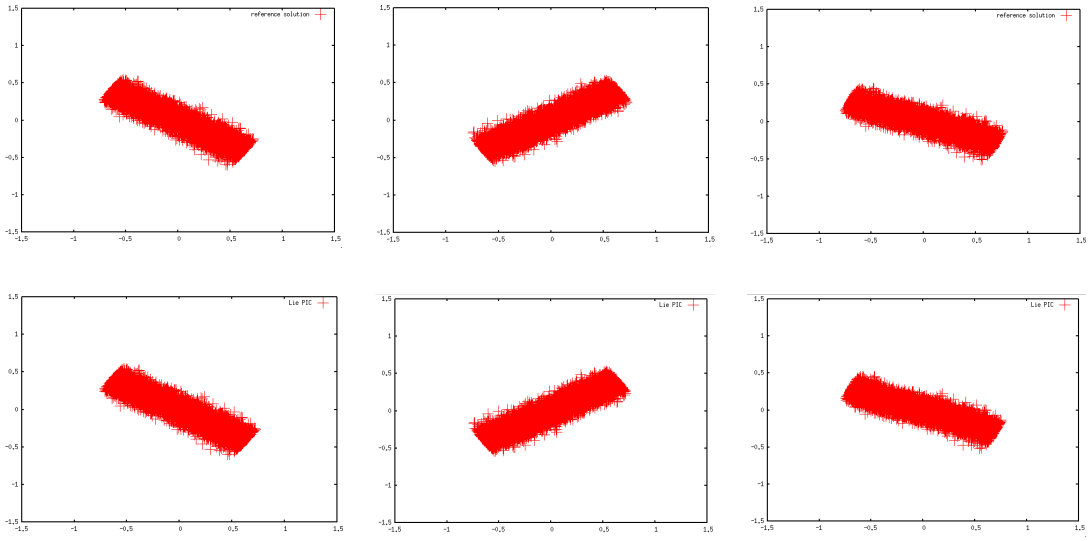

FIGURE 3.1 – Beam simulation with an usual PIC method and a Lie PIC method for $\varepsilon = 0.001$. Left : beam at time 0.001, center : beam at time 0.1, right : beam at time 1. Top : Simulation provided with the usual PIC method, bottom : Simulation provided with the Lie PIC method.

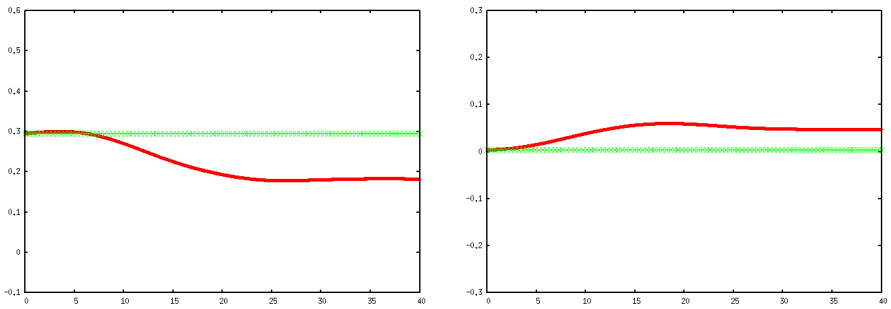

FIGURE 3.2 – Evolution of μ up to time 40 with an usual PIC method and a Lie PIC method for $\varepsilon = 0.001$. Green : with the Lie PIC method, red : with the usual PIC method. Left : with initial condition $\mu = 0.2948404402060960$, right : with initial condition $\mu = 4.22461332489106316 \cdot 10^{-3}$

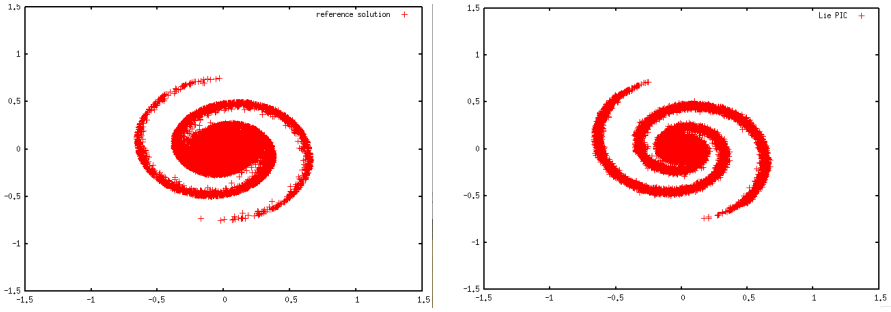

FIGURE 3.3 – Beam simulation at time 35 with an usual PIC method and a Lie PIC method for $\varepsilon = 0.001$. Left : with an usual PIC method, right : with the Lie PIC method.

Remark 3.5.2. *From Figure 3.2 one can see the evolution of μ for two given particles : one close to the center of the beam and the other close to the extremity of the beam.*

Remark 3.5.3. *In Figure 3.3 we observe that for longer times of simulation the dynamics characterizing the evolution of the shape of the beam (fast rotation+slow filamentation) is close to the reference solution but that the filaments are longer and wider. The reason is the following : we have made first order truncations in the dynamical system giving the characteristics and in the change of coordinates. Within the framework of these first order truncations, the electric field is truncated at the first order and the square of the modulus between the origin and the particles position in the phase space become constant. The filamentation is due to the fact that the electric field is larger at the extremity of the beam as at the center. Moreover, without these truncations the particles of the extremity move toward the center of the beam. With these truncations the distance between the particles and the origin remain constant and consequently since the electric field is larger when one moves away from the center of the beam the phenomena of filamentation begins earlier and the filaments are wider.*

3.6 Conclusions and perspectives

In this paper we have shown that we can adapt the geometrical techniques used for the derivation of the gyrokinetic coordinates to the case of a charged particle beam under the paraxial axisymetric approximation. In particular, these geometrical techniques are compatible with our way of doing the scaling. This paper is a first step in the application of these geometrical method, within our way to do the scaling (see Frénod & Sonnendrucker [21]), to the Vlasov Poisson equations modeling strongly magnetized plasmas. In particular, the derivation and the numerical simulations of these equations within our way to do the scaling, will allow us to compare the efficiently of this method with the other techniques of homogenization like the two scale methods. Probably, in order to eliminate a variable and to increase the time step, it will also be possible to combine the both methods. The numerical results are not only accurate but also promising, if one consider that they are only based on lowest order approximation of the electric field.

Acknowledgements

I would like to thank E. Frénod and S. A. Hirstoaga for fruitful discussions we had together.

Chapitre 4

An exponential integrator for a Vlasov-Poisson system with strong magnetic field

4.1 Introduction

In this paper we introduce a new numerical scheme in order to simulate efficiently in time the following four dimensional Vlasov equation when the parameter ε vanishes

$$\partial_t f^\varepsilon + \mathbf{v}\cdot\nabla_{\mathbf{x}} f^\varepsilon + \left(\mathbf{\Xi}^\varepsilon + \frac{1}{\varepsilon}\mathbf{v}^\perp\right)\cdot\nabla_{\mathbf{v}} f^\varepsilon = 0, \tag{4.1.1}$$

$$f^\varepsilon\left(\mathbf{x},\mathbf{v},t=0\right) = f_0\left(\mathbf{x},\mathbf{v}\right), \tag{4.1.2}$$

where $\mathbf{x} = (x_1, x_2)$ stands for the position variable, $\mathbf{v} = (v_1, v_2)$ for the velocity variable, $\mathbf{v}^\perp$ for $(v_2, -v_1)$, $f^\varepsilon \equiv f^\varepsilon(\mathbf{x},\mathbf{v},t)$ is the distribution function, f_0 is given, $\mathbf{\Xi}^\varepsilon \equiv \mathbf{\Xi}^\varepsilon(\mathbf{x},t)$ corresponds to the electric field and ε is a small parameter. Weak-$*$ and two-scale limits when ε goes to zero of this equation can rigorously be obtained following the method introduced in [19]. We notice that equations (4.1.1)-(4.1.2) can be obtained from the the six dimensional drift-kinetic regime by taking a constant magnetic field in the x_3-direction and an electric field evolving in the orthogonal plane to the magnetic field.

The main application will be the case when the electric field $\mathbf{\Xi}^\varepsilon$ is obtained by solving the Poisson equation. In this case we will rather denote by $\mathbf{E}^\varepsilon$ the electric field and thus, we will have to solve the following nonlinear system of equations :

$$\partial_t f^\varepsilon + \mathbf{v}\cdot\nabla_{\mathbf{x}} f^\varepsilon + \left(\mathbf{E}^\varepsilon + \frac{1}{\varepsilon}\mathbf{v}^\perp\right)\cdot\nabla_{\mathbf{v}} f^\varepsilon = 0, \tag{4.1.3}$$

$$\mathbf{E}^\varepsilon\left(\mathbf{x},t\right) = -\nabla_{\mathbf{x}}\phi^\varepsilon, \quad -\Delta_{\mathbf{x}}\phi^\varepsilon = \int_{\mathbb{R}^2} f^\varepsilon d\mathbf{v} - n_i, \tag{4.1.4}$$

$$f^\varepsilon\left(\mathbf{x},\mathbf{v},t=0\right) = f_0\left(\mathbf{x},\mathbf{v}\right), \tag{4.1.5}$$

where ϕ^ε is the electric potential and n_i is the background ion density.

We will also test our scheme when the electric field in (4.1.1) is given by

$$\mathbf{\Xi}^\varepsilon\left(\mathbf{x},t\right) = \begin{pmatrix} 2x_1 + x_2 \\ x_1 + 2x_2 \end{pmatrix}, \tag{4.1.6}$$

since in this case we are able to compute the solution to (4.1.1)-(4.1.2).

In this work we perform the numerical solution of the Vlasov equation (4.1.1) by particle methods, which consist in approximating the distribution function by a finite number of macroparticles. The trajectories of these particles are computed from the characteristic curves

$$\frac{\mathrm{d}\mathbf{X}^{\varepsilon}}{\mathrm{d}t} = \mathbf{V}^{\varepsilon}, \qquad \mathbf{X}^{\varepsilon}(0) = \mathbf{x}_0, \tag{4.1.7}$$

$$\frac{\mathrm{d}\mathbf{V}^{\varepsilon}}{\mathrm{d}t} = \frac{1}{\varepsilon}\left(\mathbf{V}^{\varepsilon}\right)^{\perp} + \mathbf{\Xi}^{\varepsilon}\left(\mathbf{X}^{\varepsilon}, t\right), \qquad \mathbf{V}^{\varepsilon}(0) = \mathbf{v}_0, \tag{4.1.8}$$

of the Vlasov equation. This method produces satisfying results for (4.1.1)-(4.1.2) with a small number of macro-particles (see [4]).

When the electric field $\mathbf{\Xi}^{\varepsilon}$ vanishes, the trajectory associated with (4.1.7)-(4.1.8) is a circle of center $\mathbf{c}_0 = \mathbf{x}_0 + \varepsilon\mathbf{v}_0^{\perp}$ and of radius $\varepsilon|\mathbf{v}_0|$. Otherwise, the dynamical system (4.1.7)-(4.1.8) can be viewed as a perturbation of the system obtained when the electric field is zero. Hence, in the general case of an electric field depending on position and time, the evolution of the position of a given particle is a combination of two disparate in time motions : a slow evolution of what was the center of the circle in the case where $\mathbf{\Xi}^{\varepsilon}$ is zero, usually called the Guiding Center, and a fast rotation of period about $2\pi\varepsilon$ with a small radius around it (see Fig. 4.1). We refer to Lee [38] and Dubin et all [11] for comprehensive physical viewpoint reviews about such questions. Consequently, if one wants to do accurate simulation of the problem (4.1.3)-(4.1.5) using classical numerical schemes, one needs small time steps, in particular smaller than $2\pi\varepsilon$. Another way is to use simpler (not stiff) models instead of (4.1.3)-(4.1.5), which can be simulated using larger time steps. Nevertheless, in this case, such models (as the Guiding Center) need to incorporate information about the self-consistent electric field acting on particles position and the additional effect generated by particles oscillations. The usual way to do this is to use technics based on Asymptotic Analysis and Homogenization Methods leading to a limit equation in which the mutual influence of the particles can be expressed in terms of their apparent motion, and afterwards to simulate this limit equation. We refer to Frénod & Sonnendrücker [19, 20], Frénod, Raviart & Sonnendrücker [17], Golse & Saint-Raymond [26] and Ghendrih, Hauray & Nouri [25] for a theoretical point of view on these questions, and Frénod, Salvarani & Sonnendrücker [18] for numerical applications of such technics. The contribution of this paper is to propose an alternative to such methods allowing to make direct simulations of (4.1.1)-(4.1.2) and (4.1.3)-(4.1.5) with a large time step with respect to $2\pi\varepsilon$.

We mention also the paper of Crouseilles, Lemou & Méhats [10] in which the authors deal with the same kind of problems. They consider an "augmented" kinetic equation, where they separate the two scales t/ε and t. The fast time scale is represented by a variable τ and the stiffness of the equation is concentrated in the right hand side of the augmented kinetic equation. Then, reinterpreting the singularly perturbed term as a "collision" operator in the collisionless context the authors construct an Asymptotic Preserving numerical scheme based on a micro-macro decomposition.

The stiffness of equations (4.1.7)-(4.1.8) comes from the velocity equation and therefore we are interested in solving the following type of ODE

$$u'(t) = \frac{u^{\perp}(t)}{\varepsilon} + F\left(t, u(t)\right), \qquad u(0) = u_0 \tag{4.1.9}$$

where ε is a small parameter and where F represents a nonlinear term playing the role of the electric field. Consequently, as already said, classical numerical schemes require very small time step to capture the stiff behavior. As done in [15], in this paper, we propose a

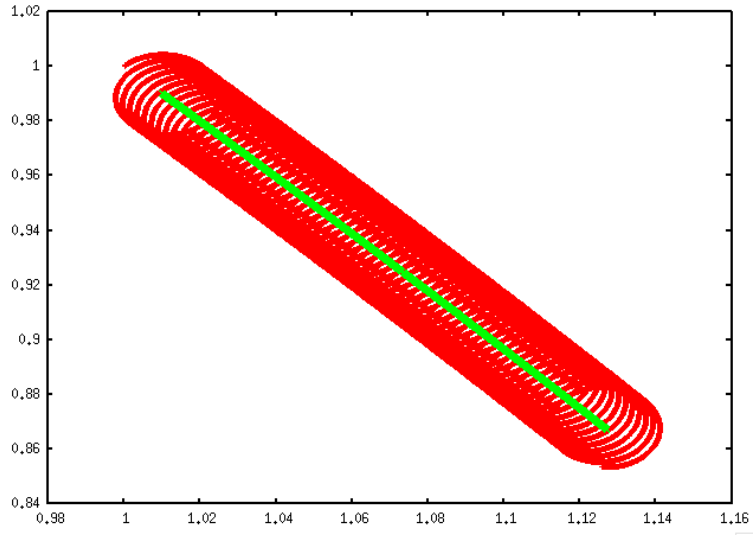

FIGURE 4.1 – Illustration of formula (4.1.11) in the case when the electric field is given by (4.1.6), $\varepsilon = 0.01$, and $(\mathbf{x}_0, \mathbf{v}_0) = (1, 1, 1, 1)$. In green the evolution of the Guiding Center and in red the position's evolution. The final time of simulation is $t = 4$.

method which is based on an exponential integrator in velocity. An exponential integrator consists in solving exactly the linear (stiff) part by using a variation-of-constants formula leading to

$$u(t) = e^{\frac{t}{\varepsilon}} u_0 + \int_0^t e^{(t-\tau)/\varepsilon} F(\tau, u(\tau))\, d\tau. \tag{4.1.10}$$

It will be interesting to consider the following Guiding Center decomposition

$$\mathbf{X}^\varepsilon(t) = \mathbf{C}^\varepsilon(t) - \varepsilon (\mathbf{V}^\varepsilon(t))^\perp. \tag{4.1.11}$$

The paper is organized as follows. In Section 4.2 we recall briefly the main steps of the Particle-In-Cell (PIC) method for solving the Vlasov-Poisson system in which we are interested. Then, Section 4.3 is devoted to the construction of the exponential integrator, named the ETD-PIC algorithm, for advancing in time the particles' position and velocity. In Section 4.4 we write the algorithm in terms of the Guiding Center position. Eventually, in Section 4.5, we implement and test our method on the cases presented above.

4.2 A Particle-In-Cell method

The numerical scheme that we describe in the next section is proposed in the framework of a Particle-In-Cell method. A PIC method consists first in approximating the initial condition f_0 (see (4.1.2)) by the following Dirac mass sum

$$f_0^{N_p}(\mathbf{x}, \mathbf{v}) = \sum_{k=1}^{N_p} \omega_k \delta(\mathbf{x} - \mathbf{x}_{k,0})\, \delta(\mathbf{v} - \mathbf{v}_{k,0}), \tag{4.2.1}$$

where $\{(\mathbf{x}_{k,0}, \mathbf{v}_{k,0})\}_{k=1}^{N_p}$ is a beam of N_p macroparticles distributed in the four dimensional phase space according to the density function f_0. Afterwards, one approximates the solution

of (4.1.1)-(4.1.2), by

$$f_{N_p}^{\varepsilon}(\mathbf{x},\mathbf{v},t)=\sum_{k=1}^{N_p}\omega_k\delta\left(\mathbf{x}-\mathbf{X}_k^{\varepsilon}(t)\right)\delta\left(\mathbf{v}-\mathbf{V}_k^{\varepsilon}(t)\right), \tag{4.2.2}$$

where $\left(\mathbf{X}_k^{\varepsilon}(t),\mathbf{V}_k^{\varepsilon}(t)\right)$ is the position in phase space of macroparticle k moving along a characteristic curve of equation

$$\frac{\mathrm{d}\mathbf{X}_k^{\varepsilon}}{\mathrm{d}t}=\mathbf{V}_k^{\varepsilon}, \tag{4.2.3}$$

$$\frac{\mathrm{d}\mathbf{V}_k^{\varepsilon}}{\mathrm{d}t}=\frac{1}{\varepsilon}\left(\mathbf{V}_k^{\varepsilon}\right)^{\perp}+\mathbf{\Xi}^{\varepsilon}\left(\mathbf{X}_k^{\varepsilon},t\right), \tag{4.2.4}$$

$$\mathbf{X}_k^{\varepsilon}(0)=\mathbf{x}_{k,0},\qquad \mathbf{V}_k^{\varepsilon}(0)=\mathbf{v}_{k,0}. \tag{4.2.5}$$

Therefore, the problem consists in finding the positions and velocities $\left(\mathbf{X}_{k,n+1}^{\varepsilon},\mathbf{V}_{k,n+1}^{\varepsilon}\right)$ at time t_{n+1} from their values at time t_n, by solving (4.2.3)-(4.2.4) with the initial condition $\left(\mathbf{X}_{k,n}^{\varepsilon},\mathbf{V}_{k,n}^{\varepsilon}\right)$.

When the problem (4.2.3)-(4.2.4) is coupled to the Poisson equation, the electric field term in (4.2.4) is numerically computed in a macroparticle position at time t as follows :

1. Construct a spatial grid (the Poisson grid).
2. Compute on this grid

$$\rho^S(\mathbf{x},t)=\sum_{k=1}^{N_p}\omega_k\mathbf{S}\left(\mathbf{x}-\mathbf{X}_k^{\varepsilon}(t)\right), \tag{4.2.6}$$

   where $\mathbf{S}$ is a first order two dimensional spline.
3. Solve the Poisson equation $-\Delta_{\mathbf{x}}\phi(\mathbf{x},t)=\rho^S(\mathbf{x},t)-n_i$ on this grid and deduce the expression of the grid electric field.
4. Interpolate the grid electric field with the same first order spline yielding the density ρ^S in order to obtain the electric field at the macroparticle position.

Eventually, an important question in the PIC method is the numerical integration of the dynamical system (4.2.3)-(4.2.4). Here is the contribution of this paper, to propose an accurate numerical scheme when using large time steps compared to the fast oscillation. We thus introduce in the next section a method based on exponential time differencing, following the same ideas as in [15].

4.3 The exponential integrator in velocity for the Particle-In-Cell method

Before to describe the exponential integrator that we have implemented for solving (4.2.3)-(4.2.4) in the framework of the PIC algorithm, we first detail the exponential time differencing (ETD) method for solving the stiff velocity equation (4.2.4).

4.3.1 The exponential integrator in velocity

One way to solve efficiently stiff ODEs is to use an exponential time differencing approach (see [8, 15] and the references therein). Such a scheme is recognized to solve the

stiff part exactly and therefore to avoid slow simulation with small time steps. In order to write down the scheme in our case we follow the steps in [8]. Let M be the matrix defined by

$$M = \begin{pmatrix} 0 & 1 \\ -1 & 0 \end{pmatrix}, \tag{4.3.1}$$

and let

$$e^{\tau M} = \begin{pmatrix} \cos(\tau) & \sin(\tau) \\ -\sin(\tau) & \cos(\tau) \end{pmatrix}, \tag{4.3.2}$$

be the exponential of M. As already said in Introduction, the dynamical system giving the characteristics of the Vlasov equation (4.1.1) is given by (4.1.7)-(4.1.8) Then, multiplying (4.1.8) by $e^{-\frac{\tau}{\varepsilon}M}$, we obtain

$$\frac{\mathrm{d}}{\mathrm{d}\tau}\left(e^{-\frac{\tau}{\varepsilon}M}\mathbf{V}^{\varepsilon}(\tau)\right) = e^{-\frac{\tau}{\varepsilon}M}\left(-\frac{1}{\varepsilon}M\mathbf{V}^{\varepsilon}\right) + e^{-\frac{\tau}{\varepsilon}M}\frac{\mathrm{d}\mathbf{V}^{\varepsilon}}{\mathrm{d}\tau} \tag{4.3.3}$$

$$= e^{-\frac{\tau}{\varepsilon}M}\boldsymbol{\Xi}^{\varepsilon}\left(\mathbf{X}^{\varepsilon},\tau\right). \tag{4.3.4}$$

Integrating this equality between s and t (where $s<t$) yields

$$\mathbf{V}^{\varepsilon}(t) = e^{\frac{t-s}{\varepsilon}M}\mathbf{V}^{\varepsilon}(s) + e^{\frac{t-s}{\varepsilon}M}\int_s^t e^{\frac{s-\tau}{\varepsilon}M}\boldsymbol{\Xi}^{\varepsilon}\left(\mathbf{X}^{\varepsilon}(\tau),\tau\right)d\tau. \tag{4.3.5}$$

Concerning the position equation, an integration between s and t of (4.1.7) yields

$$\mathbf{X}^{\varepsilon}(t) = \mathbf{X}^{\varepsilon}(s) + \int_s^t \mathbf{V}^{\varepsilon}(\tau)\,d\tau. \tag{4.3.6}$$

Equation (4.3.5) has the merit to solve exactly the stiff part in the velocity equation and thus, we are left with the numerical treatement of the integral term.

4.3.2 The ETD-PIC method with large time steps

In this section we establish and describe our time-stepping scheme following Section 4.2 in [15]. We write (4.3.5)-(4.3.6) with $s=t_n$ and $t=t_{n+1}=t_n+\Delta t$ in order to specify how the solution is computed at time t_{n+1} from its known value at time t_n. We are thus faced with the numerical computation of two integrals from t_n to t_{n+1}.
Since we want to build a scheme with a time step Δt much larger than the fast oscillation, we first need to find the unique positive integer N and the unique real $r\in[0,2\pi\varepsilon)$ such that

$$\Delta t = N\cdot(2\pi\varepsilon) + r. \tag{4.3.7}$$

The derivation of the scheme, the Algorithm 4.3.5, is based on the following approximations.

Approximation 4.3.1. *We have*

$$\int_{t_n}^{t_n+N\cdot(2\pi\varepsilon)} e^{\frac{t_n-\tau}{\varepsilon}M}\boldsymbol{\Xi}^{\varepsilon}\left(\mathbf{X}^{\varepsilon}(\tau),\tau\right)d\tau \simeq N\cdot\boldsymbol{\mathcal{I}}_1^{\varepsilon}, \tag{4.3.8}$$

where $\boldsymbol{\mathcal{I}}_1^{\varepsilon}$ *is defined by*

$$\boldsymbol{\mathcal{I}}_1^{\varepsilon} = \int_{t_n}^{t_n+2\pi\varepsilon} e^{\frac{t_n-\tau}{\varepsilon}M}\boldsymbol{\Xi}^{\varepsilon}\left(\mathbf{X}^{\varepsilon}(\tau),\tau\right)d\tau. \tag{4.3.9}$$

Approximation 4.3.2. *We have*

$$\int_{t_n}^{t_n+N\cdot(2\pi\varepsilon)} \mathbf{V}^\varepsilon(\tau)\,d\tau \simeq N\cdot\boldsymbol{\mathcal{J}}_1^\varepsilon, \tag{4.3.10}$$

where $\boldsymbol{\mathcal{J}}_1^\varepsilon$ *is defined by*

$$\boldsymbol{\mathcal{J}}_1^\varepsilon = \int_{t_n}^{t_n+2\pi\varepsilon} \mathbf{V}^\varepsilon(\tau)\,d\tau. \tag{4.3.11}$$

Remark 4.3.3. *Approximations 4.3.1 and 4.3.2 are valid if we made the assumptions that the velocity and the electric field evaluated at the particle position are quasi-periodic (with the same period close to* $2\pi\varepsilon$*) and that this period does not change significantly in time. We will see in the next section that the assumption of quasi-periodicity and small variations in the period of the particle electric field only is enough to validate approximations 4.3.1 and 4.3.2.*

Lemma 4.3.4. *Under Approximations 4.3.1 and 4.3.2 we obtain*

$$\begin{pmatrix} \mathbf{X}^\varepsilon(t_n+N\cdot(2\pi\varepsilon)) \\ \mathbf{V}^\varepsilon(t_n+N\cdot(2\pi\varepsilon)) \end{pmatrix} \simeq \begin{pmatrix} \mathbf{X}_n^\varepsilon \\ \mathbf{V}_n^\varepsilon \end{pmatrix} + N\cdot\begin{pmatrix} \mathbf{X}^\varepsilon(t_n+2\pi\varepsilon)-\mathbf{X}_n^\varepsilon \\ \mathbf{V}^\varepsilon(t_n+2\pi\varepsilon)-\mathbf{V}_n^\varepsilon \end{pmatrix}. \tag{4.3.12}$$

Proof. Applying formulas (4.3.5) and (4.3.6) with $s=t_n$ and $t=t_n+2\pi\varepsilon$ we obtain

$$\begin{pmatrix} \mathbf{X}^\varepsilon(t_n+2\pi\varepsilon) \\ \mathbf{V}^\varepsilon(t_n+2\pi\varepsilon) \end{pmatrix} = \begin{pmatrix} \mathbf{X}_n^\varepsilon \\ \mathbf{V}_n^\varepsilon \end{pmatrix} + \begin{pmatrix} \boldsymbol{\mathcal{J}}_1^\varepsilon \\ \boldsymbol{\mathcal{I}}_1^\varepsilon \end{pmatrix}. \tag{4.3.13}$$

Applying again formulas (4.3.5) and (4.3.6) with $s=t_n$ and $t=t_n+N\cdot(2\pi\varepsilon)$ yields

$$\begin{pmatrix} \mathbf{X}^\varepsilon(t_n+N\cdot(2\pi\varepsilon)) \\ \mathbf{V}^\varepsilon(t_n+N\cdot(2\pi\varepsilon)) \end{pmatrix} = \begin{pmatrix} \mathbf{X}_n^\varepsilon \\ \mathbf{V}_n^\varepsilon \end{pmatrix} + \int_{t_n}^{t_n+N\cdot(2\pi\varepsilon)} \begin{pmatrix} \mathbf{V}^\varepsilon(\tau) \\ e^{\frac{t_n-\tau}{\varepsilon}M}\boldsymbol{\Xi}^\varepsilon(\mathbf{X}^\varepsilon(\tau),\tau) \end{pmatrix} d\tau. \tag{4.3.14}$$

Injecting (4.3.10) and (4.3.8) in (4.3.14), we obtain

$$\begin{pmatrix} \mathbf{X}^\varepsilon(t_n+N\cdot(2\pi\varepsilon)) \\ \mathbf{V}^\varepsilon(t_n+N\cdot(2\pi\varepsilon)) \end{pmatrix} \simeq \begin{pmatrix} \mathbf{X}_n^\varepsilon \\ \mathbf{V}_n^\varepsilon \end{pmatrix} + N\cdot\begin{pmatrix} \boldsymbol{\mathcal{J}}_1^\varepsilon \\ \boldsymbol{\mathcal{I}}_1^\varepsilon \end{pmatrix}. \tag{4.3.15}$$

Injecting (4.3.13) in (4.3.15) we obtain (4.3.12). This ends the proof of Lemma 4.3.4. □

Using Lemma 4.3.4, we deduce the following algorithm to compute $\left(\mathbf{X}_{n+1}^\varepsilon, \mathbf{V}_{n+1}^\varepsilon\right)$ from $(\mathbf{X}_n^\varepsilon, \mathbf{V}_n^\varepsilon)$:

Algorithm 4.3.5. *Assume that* $(\mathbf{X}_n^\varepsilon, \mathbf{V}_n^\varepsilon)$ *the solution of* (4.1.7)-(4.1.8) *at time* t_n *is given.*

1. *Compute* $(\mathbf{X}^\varepsilon(t_n+2\pi\varepsilon), \mathbf{V}^\varepsilon(t_n+2\pi\varepsilon))$ *by using a fine Runge-Kutta solver with initial condition* $(\mathbf{X}_n^\varepsilon, \mathbf{V}_n^\varepsilon)$.
2. *Compute* $(\mathbf{X}^\varepsilon(t_n+N\cdot(2\pi\varepsilon)), \mathbf{V}^\varepsilon(t_n+N\cdot(2\pi\varepsilon)))$ *thanks to formula* (4.3.12)*, i.e., by setting*

$$\begin{pmatrix} \mathbf{X}^\varepsilon(t_n+N\cdot(2\pi\varepsilon)) \\ \mathbf{V}^\varepsilon(t_n+N\cdot(2\pi\varepsilon)) \end{pmatrix} = \begin{pmatrix} \mathbf{X}_n^\varepsilon \\ \mathbf{V}_n^\varepsilon \end{pmatrix} + N\cdot\begin{pmatrix} \mathbf{X}^\varepsilon(t_n+2\pi\varepsilon)-\mathbf{X}_n^\varepsilon \\ \mathbf{V}^\varepsilon(t_n+2\pi\varepsilon)-\mathbf{V}_n^\varepsilon \end{pmatrix}. \tag{4.3.16}$$

3. *Compute* $(\mathbf{X}^\varepsilon, \mathbf{V}^\varepsilon)$ *at time* t_{n+1} *by using a fine Runge-Kutta solver with initial condition* $(\mathbf{X}^\varepsilon, \mathbf{V}^\varepsilon)$ *at time* $t_n+N\cdot(2\pi\varepsilon)$*, obtained at the previous step.*

See Fig. 4.6 for a schematic description of the algorithm.

4.4 Link with the Guiding Center Decomposition

We have seen in Introduction that the time evolution of a particle's position following (4.1.7) can be split into two parts : the slow motion of the Guiding Center $\mathbf{C}^\varepsilon$ (see formula (4.1.11)) and a fast oscillation around it. Therefore, in this section, we are interested to see what gives for the numerical evolution of the Guiding Center the approximation obtained in (4.3.12).

With this attempt, we first recall the formula giving the Guiding Center position

$$\mathbf{C}^\varepsilon(t) = \mathbf{X}^\varepsilon(t) + \varepsilon\left(\mathbf{V}^\varepsilon(t)\right)^\perp. \tag{4.4.1}$$

Then, it is an easy fact to see that the rule in (4.3.16) is equivalent to

$$\begin{pmatrix} \mathbf{C}^\varepsilon(t_n + N\cdot(2\pi\varepsilon)) \\ \mathbf{V}^\varepsilon(t_n + N\cdot(2\pi\varepsilon)) \end{pmatrix} = \begin{pmatrix} \mathbf{C}_n^\varepsilon \\ \mathbf{V}_n^\varepsilon \end{pmatrix} + N\cdot\begin{pmatrix} \mathbf{C}^\varepsilon(t_n + 2\pi\varepsilon) - \mathbf{C}_n^\varepsilon \\ \mathbf{V}^\varepsilon(t_n + 2\pi\varepsilon) - \mathbf{V}_n^\varepsilon \end{pmatrix}. \tag{4.4.2}$$

In the following, we see that the rule for the Guiding Center in (4.4.2) may be obtained directly from the evolution of $\mathbf{C}^\varepsilon$ under an approximation similar to that in (4.3.8).

To this end, we derive in time (4.4.1) and making use of equations (4.1.7)-(4.1.8) leads to

$$\frac{\mathrm{d}\mathbf{C}^\varepsilon}{\mathrm{d}t}(t) = \varepsilon M\boldsymbol{\Xi}^\varepsilon\left(\mathbf{X}^\varepsilon(t), t\right), \tag{4.4.3}$$

where $M\boldsymbol{\Xi}^\varepsilon$ is $\left(\boldsymbol{\Xi}^\varepsilon\right)^\perp = (\Xi_2^\varepsilon, -\Xi_1^\varepsilon)$. Thus, we see that the Guiding Center experiences a slow motion in time. Then, we integrate this equation between s and t (where $s < t$)

$$\mathbf{C}^\varepsilon(t) = \mathbf{C}^\varepsilon(s) + \varepsilon M\int_s^t \boldsymbol{\Xi}^\varepsilon\left(\mathbf{X}^\varepsilon(\tau), \tau\right) d\tau, \tag{4.4.4}$$

and using this equality with $s = t_n$ and $t = t_n + N\cdot(2\pi\varepsilon)$ yields

$$\mathbf{C}^\varepsilon(t_n + N\cdot(2\pi\varepsilon)) = \mathbf{C}_n^\varepsilon + \varepsilon M\int_{t_n}^{t_n+N\cdot(2\pi\varepsilon)} \boldsymbol{\Xi}^\varepsilon\left(\mathbf{X}^\varepsilon(\tau), \tau\right) d\tau. \tag{4.4.5}$$

Therefore, proceeding as in Section 4.3.2, under the assumption

$$\int_{t_n}^{t_n+N\cdot(2\pi\varepsilon)} \boldsymbol{\Xi}^\varepsilon\left(\mathbf{X}^\varepsilon(\tau), \tau\right) d\tau \simeq N\cdot\int_{t_n}^{t_n+2\pi\varepsilon} \boldsymbol{\Xi}^\varepsilon\left(\mathbf{X}^\varepsilon(\tau), \tau\right) d\tau \tag{4.4.6}$$

we deduce from (4.4.5) that

$$\mathbf{C}^\varepsilon(t_n + N\cdot(2\pi\varepsilon)) \simeq \mathbf{C}_n^\varepsilon + N\cdot\left(\mathbf{C}^\varepsilon(t_n + 2\pi\varepsilon) - \mathbf{C}_n^\varepsilon\right). \tag{4.4.7}$$

In conclusion, assuming that the period of the electric field *only* does not change significantly in time leads the approximation (4.3.12) to be valid. Indeed, this assumption allows us to use the approximations in (4.4.6) and in (4.3.8) since $\tau \to e^{\frac{t_n-\tau}{\varepsilon}M}$ is $2\pi\varepsilon$-periodic. Then, following the lines of the proof of Lemma 4.3.4, we obtain that (4.4.2) is satisfied as an approximation, and thus that the approximation (4.3.12) is valid.

Let us notice that the scheme giving the Guiding Center evolution is crucial since it gives an idea about the qualitative behavior of the long time position's evolution. Indeed, being almost free of fast oscillations, the evolution of $\mathbf{C}^\varepsilon$ gives the curvature of the macroscopic evolution of the particle position (see Figs. 4.1 and 4.2). In the case of equations (4.1.1), (4.1.2), (4.1.6), developed in Section 4.5.1, this macroscopic evolution is periodic and the macroscopic (large) period can be explicitly computed, being about $2\pi/\varepsilon$.

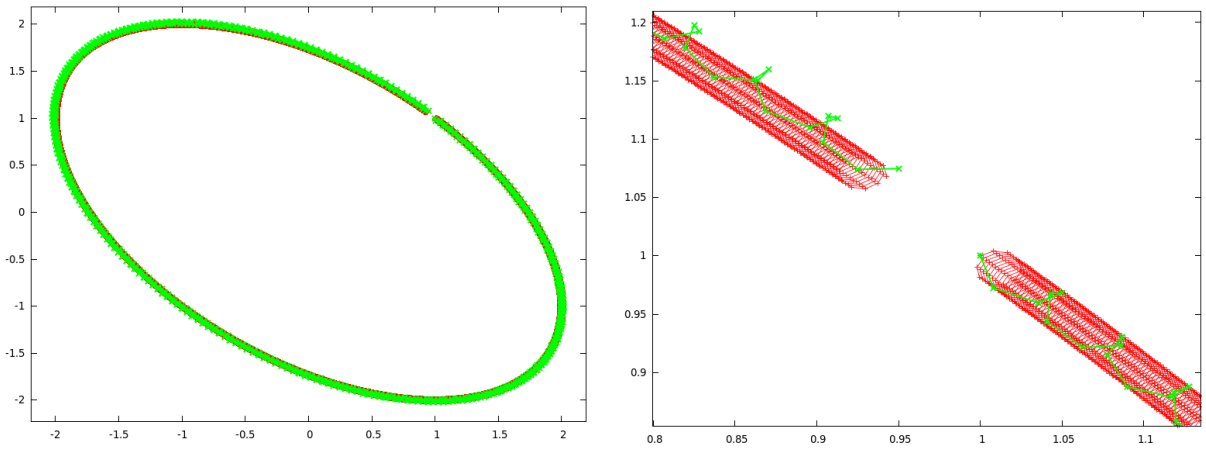

FIGURE 4.2 – The linear case in Section 4.5.1 with $\varepsilon = 0.01$ and the initial condition $(1, 1, 1, 1)$: the position's evolution in time until $t = 360$; the entire trajectory (left) and a zoom at the begining of the dynamics (right) ; In green the result of the ETD scheme using a time step $\Delta t = 30\varepsilon$ and in red the analytic solution (4.5.1)

4.5 Validation of the numerical method

We now validate our algorithm in the test cases presented in Introduction. In the linear Vlasov test case (4.1.1), (4.1.2), (4.1.6) we will take a number $N_p = 10^4$ of macroparticles (see (4.2.1) and (4.2.2)), and in the Vlasov-Poisson test case, in order to have a number of particles per cell which is about 100 (see subsection 4.5.2 for the construction of the Poisson mesh), we take a number $N_p = 2 \cdot 10^5$ of macroparticles. Moreover, in the first and the last step of the ETD-PIC method we take a time step equal to $\varepsilon\sqrt{\varepsilon}$.

4.5.1 The linear case

In this section we consider the Vlasov equation (4.1.1)-(4.1.2) provided with the electric field $\mathbf{\Xi}^\varepsilon$ given by (4.1.6). In order to test our algorithm it will be interesting to localize the initial conditions for which the fast oscillations disappear. This domain is usually called the slow manifold. Hence, in Section 4.5.1) we compute an analytic expression of the solution. This analytic solution will allow us to compute the slow manifold. Thus, in Section 4.5.1 we will compare the ETD-PIC method with a reference solution obtained with different initial conditions.

Analytic solution

Let ε be such that $0 < \varepsilon < \sqrt{1 - \frac{\sqrt{3}}{2}} \simeq 0.366$. Then, the solution of (4.1.7)-(4.1.8) is given by :

$$\begin{aligned}
X_1^\varepsilon(t;\mathbf{x}_0,\mathbf{v}_0) =& K_1^\varepsilon\left(\cos(a_\varepsilon t) - \frac{a_\varepsilon}{\varepsilon}\sin(a_\varepsilon t)\right) + K_2^\varepsilon\left(\sin(a_\varepsilon t) + \frac{a_\varepsilon}{\varepsilon}\cos(a_\varepsilon t)\right) \\
&+ K_3^\varepsilon\left(\cos(b_\varepsilon t) - \frac{b_\varepsilon}{\varepsilon}\sin(b_\varepsilon t)\right) + K_4^\varepsilon\left(\sin(b_\varepsilon t) + \frac{b_\varepsilon}{\varepsilon}\cos(b_\varepsilon t)\right), \\
X_2^\varepsilon(t;\mathbf{x}_0,\mathbf{v}_0) =& -K_1^\varepsilon u_\varepsilon\cos(a_\varepsilon t) - K_2^\varepsilon u_\varepsilon\sin(a_\varepsilon t) - K_3^\varepsilon v_\varepsilon\cos(b_\varepsilon t) - K_4^\varepsilon v_\varepsilon\sin(b_\varepsilon t), \\
V_1^\varepsilon(t;\mathbf{x}_0,\mathbf{v}_0) =& -K_1^\varepsilon a_\varepsilon\left(\frac{a_\varepsilon}{\varepsilon}\cos(a_\varepsilon t) + \sin(a_\varepsilon t)\right) + K_2^\varepsilon a_\varepsilon\left(\cos(a_\varepsilon t) - \frac{a_\varepsilon}{\varepsilon}\sin(a_\varepsilon t)\right) \\
&- K_3^\varepsilon b_\varepsilon\left(\frac{b_\varepsilon}{\varepsilon}\cos(b_\varepsilon t) + \sin(b_\varepsilon t)\right) + K_4^\varepsilon b_\varepsilon\left(\cos(b_\varepsilon t) - \frac{b_\varepsilon}{\varepsilon}\sin(b_\varepsilon t)\right), \\
V_2^\varepsilon(t;\mathbf{x}_0,\mathbf{v}_0) =& K_1^\varepsilon a_\varepsilon u_\varepsilon\sin(a_\varepsilon t) - K_2^\varepsilon a_\varepsilon u_\varepsilon\cos(a_\varepsilon t) + K_3^\varepsilon b_\varepsilon v_\varepsilon\sin(b_\varepsilon t) - K_4^\varepsilon b_\varepsilon v_\varepsilon\cos(b_\varepsilon t),
\end{aligned} \tag{4.5.1}$$

where

$$a_\varepsilon = \sqrt{\frac{1 - 4\varepsilon^2 - \sqrt{1 - 8\varepsilon^2 + 4\varepsilon^4}}{2\varepsilon^2}}, \tag{4.5.2}$$

$$b_\varepsilon = \sqrt{\frac{1 - 4\varepsilon^2 + \sqrt{1 - 8\varepsilon^2 + 4\varepsilon^4}}{2\varepsilon^2}}, \tag{4.5.3}$$

$$\begin{aligned}
u_\varepsilon &= 2 + a_\varepsilon^2, \\
v_\varepsilon &= 2 + b_\varepsilon^2, \\
w_\varepsilon &= 1 + \frac{a_\varepsilon^2}{\varepsilon^2}, \\
x_\varepsilon &= a_\varepsilon^2 - b_\varepsilon^2,
\end{aligned} \tag{4.5.4}$$

and

$$\begin{pmatrix} K_1^\varepsilon \\ K_2^\varepsilon \\ K_3^\varepsilon \\ K_4^\varepsilon \end{pmatrix} = \begin{pmatrix} \frac{\varepsilon^2 v_\varepsilon}{(2-\varepsilon^2)x_\varepsilon} & -\frac{1}{u_\varepsilon} + \frac{\varepsilon^2 v_\varepsilon w_\varepsilon}{(2-\varepsilon^2)x_\varepsilon u_\varepsilon} & -\frac{\varepsilon v_\varepsilon}{(2-\varepsilon^2)x_\varepsilon} & 0 \\ \frac{\varepsilon}{a_\varepsilon} + \frac{\varepsilon^3}{(2-\varepsilon^2)a_\varepsilon} - \frac{2\varepsilon u_\varepsilon}{x_\varepsilon a_\varepsilon(2-\varepsilon^2)} & -\frac{\varepsilon v_\varepsilon}{u_\varepsilon a_\varepsilon x_\varepsilon}\left(1 + \frac{\varepsilon^2 w_\varepsilon}{2-\varepsilon^2}\right) & \frac{\varepsilon^2 v_\varepsilon}{(2-\varepsilon^2)a_\varepsilon x_\varepsilon} & -\frac{1}{a_\varepsilon x_\varepsilon} \\ -\frac{\varepsilon^2 u_\varepsilon}{(2-\varepsilon^2)x_\varepsilon} & -\frac{\varepsilon^2 w_\varepsilon}{(2-\varepsilon^2)x_\varepsilon} & \frac{\varepsilon u_\varepsilon}{(2-\varepsilon^2)x_\varepsilon} & 0 \\ \frac{2\varepsilon u_\varepsilon}{(2-\varepsilon^2)b_\varepsilon x_\varepsilon} & \frac{\varepsilon}{b_\varepsilon x_\varepsilon} + \frac{\varepsilon^3 w_\varepsilon}{(2-\varepsilon^2)b_\varepsilon x_\varepsilon} & -\frac{\varepsilon^2 u_\varepsilon}{(2-\varepsilon^2)b_\varepsilon x_\varepsilon} & \frac{1}{b_\varepsilon x_\varepsilon} \end{pmatrix} \begin{pmatrix} x_{0,1} \\ x_{0,2} \\ v_{0,1} \\ v_{0,2} \end{pmatrix}. \tag{4.5.5}$$

We can thus observe that, in addition to the fast oscillations of period $\frac{2\pi}{b_\varepsilon} \sim 2\pi\varepsilon$, the solution of (4.1.7)-(4.1.8) contains slow oscillations of period $\frac{2\pi}{a_\varepsilon} \sim \frac{2\pi}{\sqrt{3}\varepsilon}$.

In this case, the slow manifold corresponds to the intersection between the hyperplanes $\{(\mathbf{x}_0,\mathbf{v}_0)$ such that $K_3^\varepsilon(\mathbf{x}_0,\mathbf{v}_0) = 0\}$ and $\{(\mathbf{x}_0,\mathbf{v}_0)$ such that $K_4^\varepsilon(\mathbf{x}_0,\mathbf{v}_0) = 0\}$. Since the two hyperplanes are different, the intersection is of dimension two. Straightforward computations yield that

$$\left\{ \begin{pmatrix} 1 \\ -\frac{u_\varepsilon}{w_\varepsilon} \\ 0 \\ -\frac{2\varepsilon u_\varepsilon}{2-\varepsilon^2} + \frac{\varepsilon u_\varepsilon}{w_\varepsilon} + \frac{\varepsilon^3 u_\varepsilon}{2-\varepsilon^2} \end{pmatrix}, \begin{pmatrix} 1 \\ 0 \\ \varepsilon \\ -\frac{2\varepsilon u_\varepsilon}{2-\varepsilon^2} + \frac{\varepsilon^3 u_\varepsilon}{2-\varepsilon^2} \end{pmatrix} \right\} \tag{4.5.6}$$

form a basis of this vectorial space. Subsequently we will denote by $\boldsymbol{\mathcal{D}}_2$ this space.

Numerical simulations

In this section we compare the ETD-PIC method with a reference solution obtained with a fourth order Runge-Kutta scheme. We consider two different kinds of initial condition f_0. The first one is with one macroparticle, alternatively located on, close to, and far from the slow manifold. In the second case, we consider a beam of macroparticles and we compute the maximum in time of the mean of the Euclidean errors.

Considering one particle alternatively on, close to, and far from the slow manifold means that we take initial conditions

$$f_0^i(\mathbf{x},\mathbf{v}) = \delta\left(\mathbf{x}-\mathbf{x}_0^i\right)\delta\left(\mathbf{v}-\mathbf{v}_0^i\right), \tag{4.5.7}$$

where $i=1,2,3$, and $\left(\mathbf{x}_0^1,\mathbf{v}_0^1\right)$ is on the slow manifold, $\left(\mathbf{x}_0^2,\mathbf{v}_0^2\right)$ is close to the slow manifold, and $\left(\mathbf{x}_0^3,\mathbf{v}_0^3\right)$ is far from the slow manifold. For the numerical simulations we will take

$$\begin{aligned}
\left(\mathbf{x}_0^1,\mathbf{v}_0^1\right) &= \left(1,0,\varepsilon,-\frac{2\varepsilon u_\varepsilon}{2-\varepsilon^2}+\frac{\varepsilon^3 u_\varepsilon}{2-\varepsilon^2}\right),\\
\left(\mathbf{x}_0^2,\mathbf{v}_0^2\right) &= \left(1,-\frac{u_\varepsilon}{w_\varepsilon},\varepsilon\frac{w_\varepsilon}{u_\varepsilon},-\frac{2\varepsilon u_\varepsilon}{2-\varepsilon^2}+\varepsilon\frac{w_\varepsilon}{u_\varepsilon}+\frac{\varepsilon^3 u_\varepsilon}{2-\varepsilon^2}\right),\\
\left(\mathbf{x}_0^3,\mathbf{v}_0^3\right) &= (1,1,1,1).
\end{aligned} \tag{4.5.8}$$

Using general formulas for the distances to the slow manifold $\boldsymbol{\mathcal{D}}_2$ from these particles, we obtain the following specific values in Table 4.1.

	$\varepsilon=0.01$	$\varepsilon=0.005$	$\varepsilon=0.001$	$\varepsilon=0.0005$	$\varepsilon=0.0001$
$i=1$	0.00000000	0.00000000	0.00000000	0.00000000	0.00000000
$i=2$	0.01999800	0.00999975	0.00199999	0.00099984	0.00018878
$i=3$	1.41477865	1.41435495	1.41421923	1.41421509	1.41422155

TABLE 4.1 – Euclidean distance between the slow manifold and $\left(\mathbf{x}_0^i,\mathbf{v}_0^i\right)_{i\in\{1,2,3\}}$ in (4.5.8), and for $\varepsilon=0.01$, $\varepsilon=0.005$, $\varepsilon=0.001$, $\varepsilon=0.0005$, and $\varepsilon=0.0001$.

Denoting by $\left(\mathbf{X}^\varepsilon(t),\mathbf{V}^\varepsilon(t)\right)$ the result of the ETD-PIC method, and by $\left(\mathbf{X}_{\text{ref}}^\varepsilon(t),\mathbf{V}_{\text{ref}}^\varepsilon(t)\right)$ the reference solution, we compute the global Euclidean errors

$$e_n^M = \max_{k\in\{0,\dots,n\}} \left\|\left(\mathbf{X}^\varepsilon,\mathbf{V}^\varepsilon\right)(t_k) - \left(\mathbf{X}_{\text{ref}}^\varepsilon,\mathbf{V}_{\text{ref}}^\varepsilon\right)(t_k)\right\|_2, \tag{4.5.9}$$

where $n\in\mathbb{N}$ corresponds to the ratio between the final time of simulation and the time step Δt, at final time 10 for several values of ε and of Δt (See Figs. 4.3 and 4.4).

Second, we consider the following initial condition

$$f_0(\mathbf{x},\mathbf{v}) = \frac{1}{8\pi^2 v_{th}^2}\left(1+\eta\cos\left(k_{x_1}x_1+k_{x_2}x_2\right)\right)\boldsymbol{\chi}(\mathbf{x})\exp\left(-\frac{v_1^2+v_2^2}{2v_{th}^2}\right), \tag{4.5.10}$$

with $k_{x_1}=0,\ k_{x_2}=0.5,\ v_{th}=1,\ \eta=0.1$, and

$$\boldsymbol{\chi}(\mathbf{x}) = \chi_{[0,1]}(x_1)\,\chi_{[0,4\pi]}(x_2), \tag{4.5.11}$$

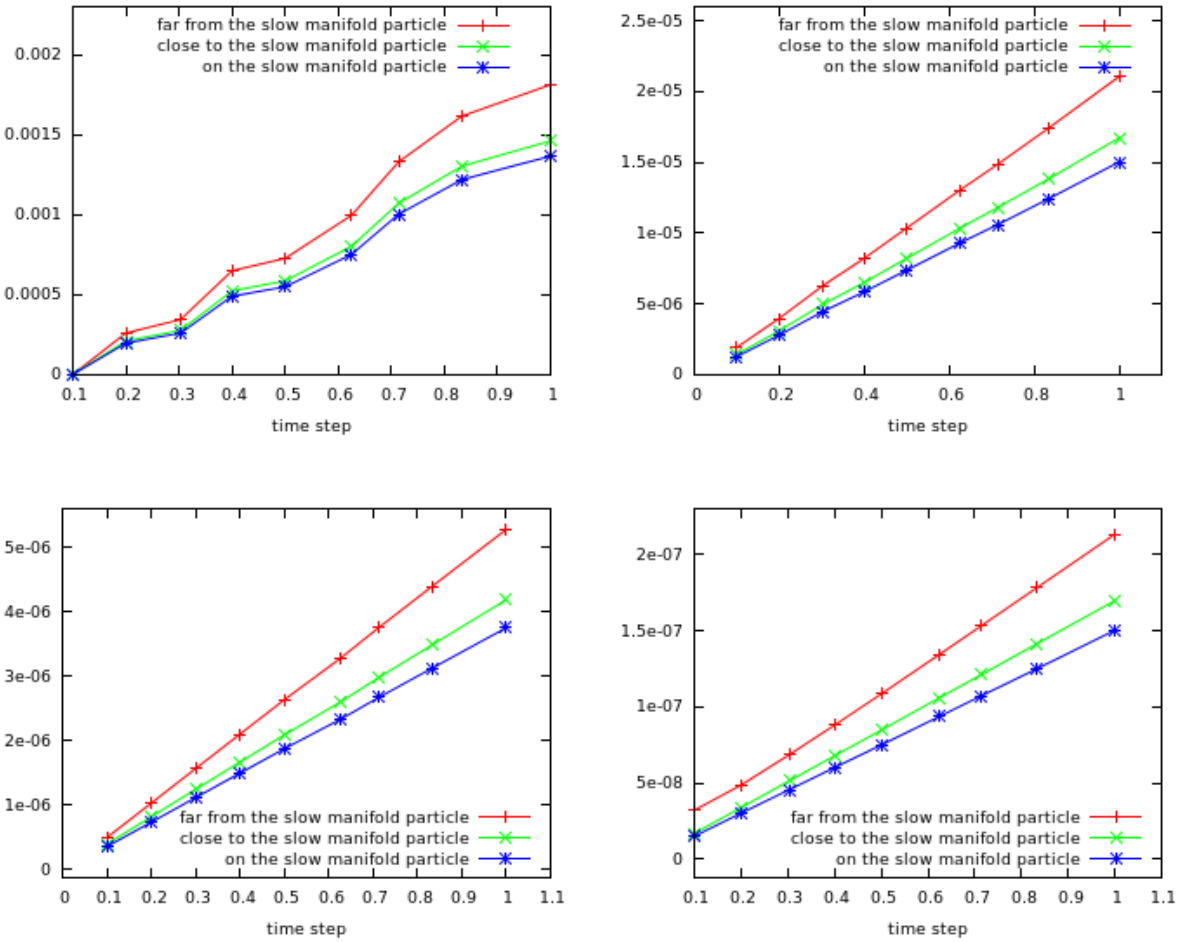

FIGURE 4.3 – Global Euclidean errors of the ETD-PIC method at time 10 for four values of ε (on the top : $\varepsilon = 0.01$ (left) and $\varepsilon = 0.001$ (right) ; on the bottom : $\varepsilon = 0.0005$ (left) and $\varepsilon = 0.0001$ (right)), obtained with three initial conditions differently positioned with regard to the slow manifold $\boldsymbol{\mathcal{D}}_2$

and we compute the maximum of the mean of the Euclidean errors

$$\mathcal{M}e_n^M = \max_{k\in\{0,\dots,n\}} \left(\frac{1}{N_p} \sum_{j=1}^{N_p} \left\| \left(\mathbf{X}_j^\varepsilon, \mathbf{V}_j^\varepsilon\right)(t_k) - \left(\mathbf{X}_{j,\mathrm{ref}}^\varepsilon, \mathbf{V}_{j,\mathrm{ref}}^\varepsilon\right)(t_k) \right\|_2 \right), \tag{4.5.12}$$

at final time 10 for several values of ε and of Δt (see Fig. 4.5).

Comments about the numerical results

As it can be see on the schematic description of the error given in Fig. 4.6, the numerical error consists of two parts : the error made in the macroscopic periodic evolution (the curvature error), denoted by E_C, and the error made by replacing the real fast period of oscillation by $2\pi\varepsilon$ or by $2\pi/b_\varepsilon$, denoted by E_P. When we take as initial condition f_0^1 the fast oscillations disappear and thus E_P is zero. Then, if we take as initial condition f_0^2 or f_0^3, we expect that the error is bigger for a particle off the slow manifold ; this point of view is in accordance with our numerical results (see Figs. 4.3 and 4.4). Notice also that

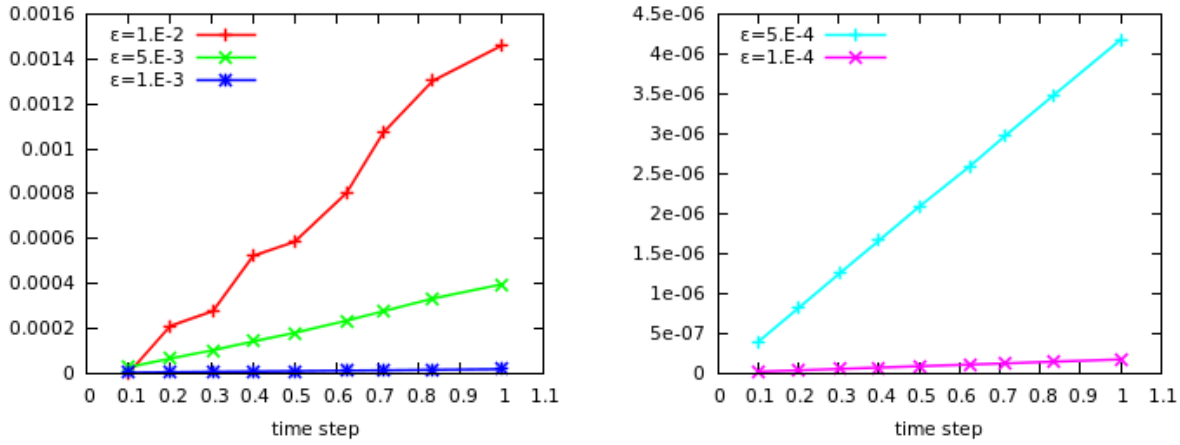

FIGURE 4.4 – Global Euclidean errors of the ETD-PIC method at time 10 for several values of ε, obtained with an initial condition close to the slow manifold

since the guiding center varies slowly (the magnitude of the period of oscillation is $1/\varepsilon$), the error E_C made at the final time of simulation $t = 10$ is small.

We observe from Figs. 4.3, 4.4, and 4.5 that the ETD-PIC scheme is uniformly accurate when ε goes to zero. This was numerically verified as well for one single particle (as those in (4.5.8)) as for the beam in formula (4.5.10).

4.5.2 The Vlasov-Poisson test case

In the present section we consider the Vlasov-Poisson equation (4.1.3)-(4.1.5), where the initial condition is given by

$$f_0(\mathbf{x},\mathbf{v}) = \frac{1}{2\pi v_{th}^2}\left(1+\eta\sin\left(k_{x_1}x+k_{x_2}y\right)\right)\exp\left(-\frac{v_1^2+v_2^2}{2v_{th}^2}\right). \tag{4.5.13}$$

In a first place (section 4.5.2) we describe the reference solution we use. Then, in section (4.5.2) we compare the ETD-PIC method with this reference solution.

Reference solution

We solve numerically (4.1.3)-(4.1.5) by using periodic conditions on the space domain. We take $v_{th} = 1, \eta = 0.1$, $k_{x_1} = 0$, $k_{x_2} = 0.5$, and

$$\mathbf{\Omega_x} = [0;T_{x_1}]\times[0;T_{x_2}], \tag{4.5.14}$$

where $T_{x_1} = 1$ and $T_{x_2} = 4\pi$. Therefore, since

$$\int_{\mathbf{\Omega_x}\times\mathbb{R}^2} f_0(\mathbf{x},\mathbf{v})\,d\mathbf{x}d\mathbf{v} = T_{x_1}T_{x_2}, \tag{4.5.15}$$

we take constant weights

$$\omega_i = \frac{T_{x_1}T_{x_2}}{N_p} \tag{4.5.16}$$

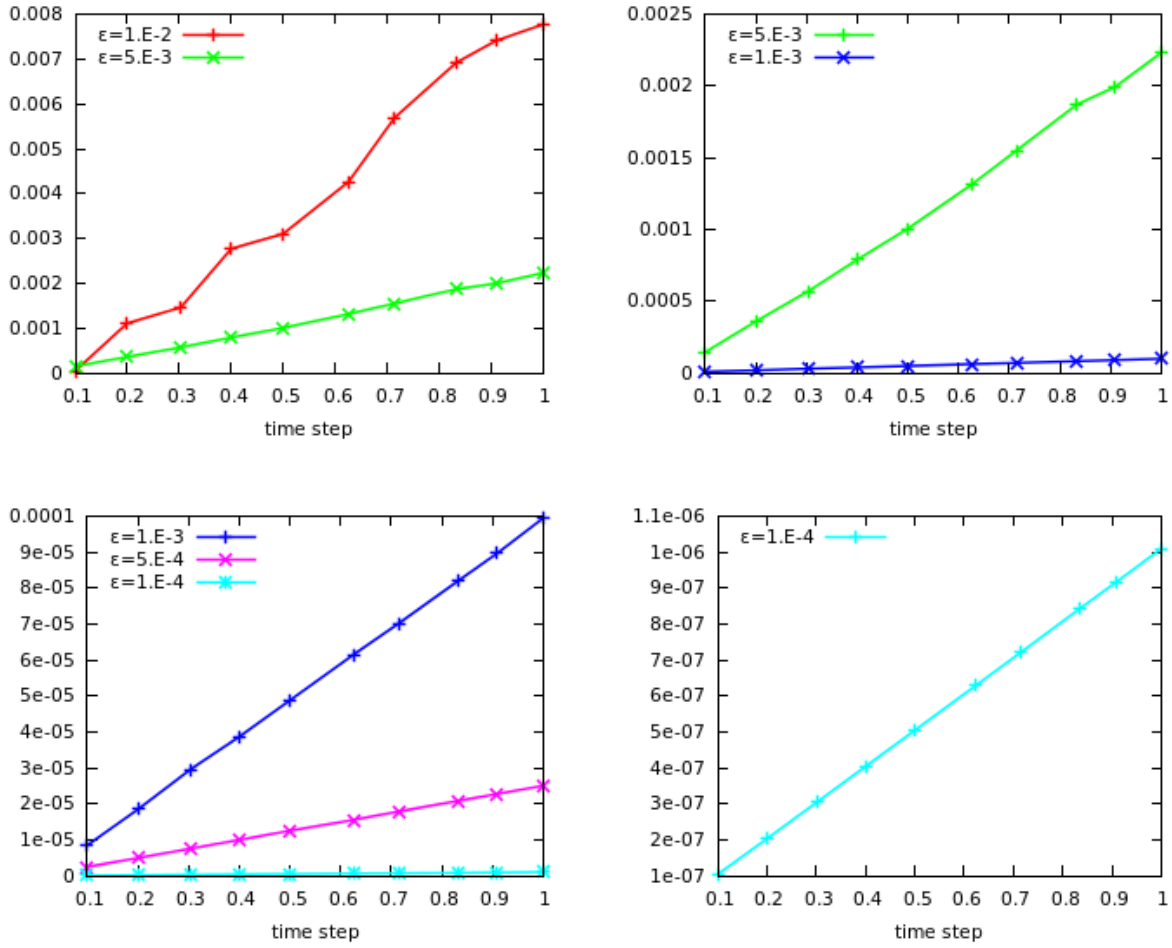

FIGURE 4.5 – Maximum at time 10 of the mean of the Euclidean errors of the ETD-PIC method for several values of ε, obtained with the initial condition f_0 defined by (4.5.10)

in (4.2.1) and (4.2.2), and $n_i = 1$ in (4.1.4). In this way, we obtain

$$\int_{\mathbf{\Omega_x}\times\mathbb{R}^2} f_0(\mathbf{x},\mathbf{v})\,d\mathbf{x}d\mathbf{v} = \int_{\mathbf{\Omega_x}\times\mathbb{R}^2} f_0^{N_p}(\mathbf{x},\mathbf{v})\,d\mathbf{x}d\mathbf{v} = T_{x_1}T_{x_2}, \tag{4.5.17}$$

ensuring the mass conservation, and

$$\int_{\mathbf{\Omega_x}} \left(\rho^S(\mathbf{x},t) - n_i\right) d\mathbf{x} = 0, \tag{4.5.18}$$

ensuring the neutrality condition.
For the construction of the reference solution, we use the usual fourth order Runge-Kutta scheme for the advection and an usual Fast Fourier Transform method with 2^4 cells in the x_1-direction and 2^7 cells in the x_2-direction to solve the Poisson equation. The time step of the Runge-Kutta solver for computing the reference solution is $\Delta t = \varepsilon\sqrt{\varepsilon}$.

Comments

In Fig. 4.7 we have computed the maximum of the mean of the Euclidean errors (see formula (4.5.12)) at final time 4 for several values of ε and of Δt. In this nonlinear case, the uniform accuracy, when ε goes to zero, of the ETD-PIC scheme is still observed.

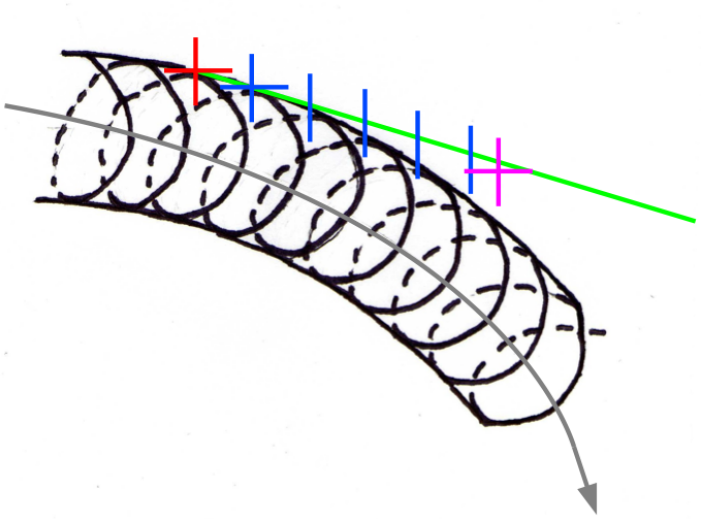

FIGURE 4.6 – Schematic description of the error made by the ETD-PIC algorithm. The red cross corresponds to the initial condition, the blue cross corresponds to the result of the ETD-PIC algorithm's first step, the vertical lines correspond to the result of the algorithm's second step, and the purple cross corresponds to what we obtain by applying the algorithm's last step.

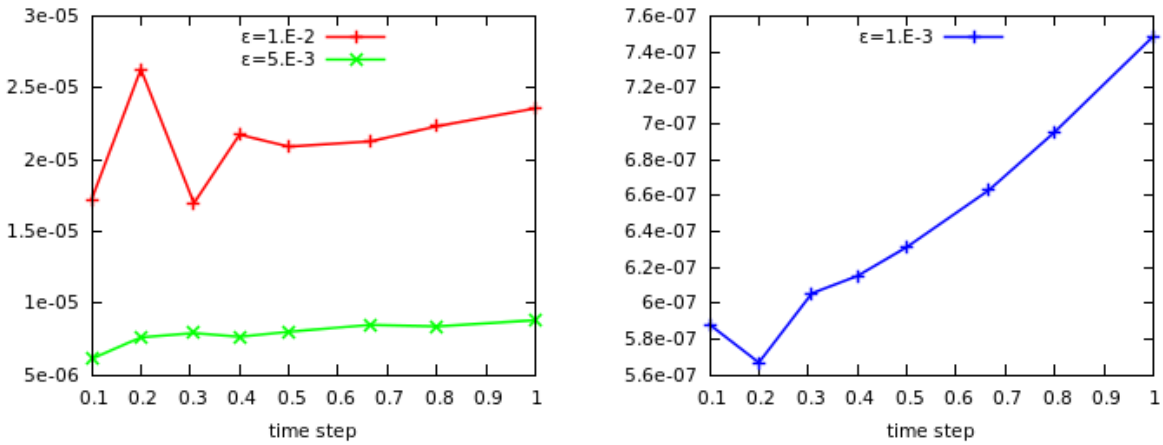

FIGURE 4.7 – Vlasov Poisson case with $\varepsilon = 0.01$, $\varepsilon = 0.005$, and $\varepsilon = 0.001$, ETD-PIC method : the maximum at time 4 of the mean of the Euclidean errors for initial particles distributed according to (4.5.13)

Chapitre 5

Conclusion générale et perspectives

Nous avons étudié dans ce manuscrit différentes méthodes théoriques et numériques pour simuler à coût réduit le comportement des plasmas ou des faisceaux de particules chargées sous l'action d'un champ magnétique fort.

Le point de départ du chapitre 1 correspond aux travaux de Littlejohn [40, 41, 42]. Ces travaux ont apporté un éclairage nouveau sur l'approximation centre-guide. Son approche, intégrant des concepts mathématiques de haut niveau (mécanique hamiltonienne, géométrie différentielle, géométrie symplectique), a permis de clarifier les travaux antérieurs (voir Kruskal [37], Gardner [24], Northrop [46], Northrop & Rome [47]). Cette théorie est une grande réussite et elle a été largement utilisée par les physiciens pour en déduire des modèles dérivés (*Modèle Rayon de Larmor fini, modèle de Drift-Kinetic, modèle Gyro-Cinétique quasi neutre, etc.,* voir Brizard [5], Dubin *et al.* [11], Frieman & Chen [22], Hahm [29], Hahm, Lee & Brizard [31], Parra & Catto [50, 51, 52]). Néanmoins, la théorie qui en résulte reste une théorie physique, formelle d'un point de vue mathématique, et qui n'est pas directement abordable pour les mathématiciens. Les travaux que nous avons réalisés dans le chapitre 2 sont une première étape pour rendre cette théorie accessible aux mathématiciens appliqués et aux informaticiens. Comme dans [40], nous nous sommes restreints à un système dynamique hamiltonien $\mathcal{SP}_\varepsilon$ décrivant le mouvement d'une particule chargée sous l'action d'un champ magnétique fort dont la direction est constante. Au terme de ce chapitre, nous avons obtenu pour tout entier N un système de coordonnées et un système dynamique Hamiltonien $\mathcal{TSP}_\varepsilon^N$ tels que :

- Le système dynamique hamiltonien $\mathcal{TSP}_\varepsilon^N$ satisfait les conditions d'application du théorème 2.1.2.
- Les trajectoires obtenues en résolvant $\mathcal{TSP}_\varepsilon^N$ approchent avec une précision ε^N, et pendant un intervalle de temps de largeur $1/\varepsilon$, les trajectoires du système $\mathcal{SP}_\varepsilon$ (écrit dans le nouveau système de coordonnées).

Afin d'obtenir des modèles réduits plus réalistes, plusieurs généralisations sont nécessaires :

1. Le passage en $3D$ (en position et en vitesse).
2. Adapter les techniques que nous avons introduites pour des géométries de champ magnétique plus complexes, comme par exemple celles présentées dans l'introduction.
3. Dériver ces modèles en tenant compte du champ électrique auto-consistant.

Nous avons par ailleurs adapté les techniques géométriques utilisées pour dériver les coordonnées gyro-cinétiques à un faisceau de particules chargées axisymétrique dans le cadre de l'approximation paraxiale. Nous avons alors appliqué une méthode PIC pour simuler les équations obtenues. D'un point de vue des trajectoires, la situation présente

beaucoup de similitudes avec celle d'un faisceau de particules sous l'action d'un champ magnétique fort, lorsque l'on considère que le rayon de Larmor est de magnitude 1. La principale difficulté est que le rayon de giration des particules n'est pas négligeable. Ainsi, contrairement à la situation où le rayon de Larmor est petit, le calcul du champ électrique auto-consistant dépend fortement du rayon de giration.

Plusieurs extensions sont donc envisageables. Afin d'obtenir des résultats plus précis en temps long, il faut tronquer les changements de coordonnées et le terme d'advection à un ordre supérieur. Ensuite il semble naturel de passer à l'équation de Vlasov dans le régime Rayon de Larmor Fini.

Dans le quatrième et dernier chapitre, nous introduisons un nouveau schéma numérique dont l'objectif est de simuler l'équation de Vlasov $2D$ (en position et en vitesse) dans le régime Drift-Kinetic en utilisant un pas de temps plus grand que la période d'oscillation des caractéristiques. Ce schéma, appliqué dans le cadre d'une méthode particulaire, est basé sur un intégrateur exponentiel en vitesse. Nous avons validé notre algorithme dans le cas d'un champ électrique externe linéaire et dans le cas où le champ électrique est obtenu en résolvant une équation de Poisson. Dans les deux situations cela donne des résultats très satisfaisants.

Deux principales extensions de ce travail sont envisagées. Premièrement, tester notre schéma dans le cadre du régime rayon de Larmor fini, avec des conditions périodiques assurant le confinement. La seconde extension consiste à adapter notre schéma pour des géométries toroïdales.

Mes autres perspectives concernent les méthodes d'homogénéisation deux-échelles et les méthodes numériques basées sur des intégrateurs variationnels symplectiques.

Dans l'introduction nous avons déterminé la limite deux échelles de l'équation de Vlasov-Poisson $2D$ dans le régime Drift-Kinetic. Nous avons vu que la limite deux échelles ne dépendait pas du champ électrique auto-consistant. Ainsi, la limite deux-échelles ne permet pas de capter les effets dus à la composante orthogonale au champ magnétique du champ électrique. Afin de capter ces effets il semble donc indispensable de dériver l'approximation deux-échelles d'ordre 1.

Obtenir la limite deux échelles du système de Vlasov-Maxwell est une autre perspective. Les principaux ingrédients pour déterminer cette limite sont le lemme d'Aubin-Lions et des estimations portant sur les moments de la fonction de distribution. Ces estimations sont fortement liées aux estimations nécessaires pour démontrer les résultats d'existence de solutions faibles pour le problème de Vlasov-Poisson. Il apparait donc raisonnable d'essayer de reproduire des arguments similaires en se basant sur les résultats ad-hoc des équations de Vlasov-Maxwell.

Un intégrateur variationnel symplectique conserve exactement une structure symplectique associée à un Lagrangien discret. En plus de conserver les volumes dans l'espace des phases, un intégrateur variationnel permet de conserver les invariants avec une grande précision. Ce genre de schéma semble particulièrement adapté aux régimes que nous avons considérés dans cette thèse.

Annexe A

Annexe relative au chapitre 1

Dans cette annexe, nous allons appliquer la méthode PIC (présentée dans l'introduction) au système de Vlasov-Poisson $4D$ avec des conditions initiales qui correspondent à une perturbation périodique de l'équilibre thermodynamique. Le phénomène physique ainsi observé, est appelé l'amortissement Landau.

A.1 Présentation de l'équation

Considérons l'équation de Vlasov Poisson $4D$ suivante :

$$\frac{\partial f}{\partial t} + \mathbf{v} \cdot \nabla_{\mathbf{x}} f + \mathbf{E}(\mathbf{x}, t) \cdot \nabla_{\mathbf{v}} f = 0, \tag{A.1.1}$$

$$\mathbf{E} = -\nabla \phi, \qquad -\Delta \phi = \rho - 1, \tag{A.1.2}$$

$$\rho = \int_{\mathbb{R}^3} f(\mathbf{x}, \mathbf{v}, t)\, d\mathbf{v}, \tag{A.1.3}$$

$$f(t = 0, \mathbf{x}, \mathbf{v}) = f_0(\mathbf{x}, \mathbf{v}), \tag{A.1.4}$$

où f_0 est donnée par

$$f_0(\mathbf{x}, \mathbf{v}) = \frac{1}{2\pi v_{th}^2 T_1 T_2} \big(1 + \varepsilon \cos(k_1 x_1 + k_2 x_2)\big) \exp\left(-\frac{v_1^2 + v_2^2}{2 v_{th}^2}\right), \tag{A.1.5}$$

avec $T_1 = 2\pi/k_1$ et $T_2 = 2\pi/k_2$. Pour résoudre numériquement (A.1.1)-(A.1.4) nous utilisons des conditions périodiques en espace. Plus précisément, nous nous plaçons sur $\mathbf{\Omega_x}$ définit par :

$$\mathbf{\Omega_x} = (\mathbb{R} \setminus [0, T_{x_1}]) \times (\mathbb{R} \setminus [0, T_{x_2}]). \tag{A.1.6}$$

Comme nous l'avons vu dans l'introduction, le second membre de l'équation de Poisson (A.1.2) est constitué de la densité d'électrons ρ et de la densité d'ions supposée constante égale à 1. Ce fond d'ions neutralisant assure la condition de neutralité du plasma. D'un point de vue mathématique, ce fond d'ions neutralisant est indispensable. En effet, si ϕ est périodique, ses dérivées le sont également, ce qui implique que l'intégrale sur $[0, T_{x_1}] \times [0, T_{x_2}]$ du second membre de l'équation de Poisson doit être nulle.

Remarque A.1.1. *On peut bien évidemment argumenter contre la pertinence des conditions aux limites périodiques. Néanmoins, cette façon de procéder est certainement la plus simple pour avoir accès à une géométrie confinée. Elle évite des effets très complexes a gérer numériquement tels que la dispersion à l'infini.*

Le choix de la condition initiale (A.1.5) nécessite également quelques explications. Le paramètre ε est un petit paramètre. Par conséquent, la condition initiale (A.1.5) correspond à une perturbation périodique de la fonction de distribution représentant le plasma à l'équilibre thermodynamique.

Remarque A.1.2. *L'équilibre thermodynamique est un équilibre stable : lorsqu'on lui applique une petite perturbation, la répartition des électrons s'égalise et le champ électrique créé par le plasma tend vers zéro (de façon exponentielle en temps) au fur et à mesure que la neutralité électrique est rétablie. Ce phénomène surprenant est connue sous le nom d'amortissement Landau et a été mis en évidence en* 1946 *par le physicien du même nom. Il a été démontré pour la première fois dans un cadre non-linéaire, en temps infini, et avec un taux exponentiel par C. Mouhot et C. Villani.*

A.2 Résolution numérique

A.2.1 Spécification des différentes étapes de la méthode PIC

Dans le cadre de l'équation de Vlasov $4D$ (A.1.1) les N macro-particules sont avancées le long des caractéristiques en résolvant les équations différentielles :

$$\frac{d\mathbf{x}_k}{dt} = \mathbf{v}_k, \tag{A.2.1}$$

$$\frac{d\mathbf{v}_k}{dt} = \mathbf{E}\left(\mathbf{x}_k, t\right), \tag{A.2.2}$$

$$\mathbf{x}_k(0) = \mathbf{x}_k^0, \quad \mathbf{v}_k(0) = \mathbf{v}_k^0 \tag{A.2.3}$$

Pour les simulations, nous présenterons les résultats numériques obtenus avec un schéma Runge-Kutta d'ordre 4 et un schéma de Verlet. Le premier de ces schémas est présenté dans l'introduction. Le schéma de Verlet, pour passer du temps t_n au temps $t_{n+1} = t_n + \Delta t$ est donné par :

$$\mathbf{v}_k^{n+\frac{1}{2}} = \mathbf{v}_k^n + \frac{\Delta t}{2}\mathbf{E}^n\left(\mathbf{x}_k^n\right), \tag{A.2.4}$$

$$\mathbf{x}_k^{n+1} = \mathbf{x}_k^n + \Delta t \mathbf{v}_k^{n+\frac{1}{2}} \tag{A.2.5}$$

$$\mathbf{v}_k^{n+1} = \mathbf{v}_k^{n+\frac{1}{2}} + \frac{\Delta t}{2}\mathbf{E}^{n+1}\left(\mathbf{x}_k^{n+1}\right). \tag{A.2.6}$$

La dernière étape nécessite la connaissance du champ électrique à l'instant t_{n+1}. Ce champ électrique est obtenu en déposant les positions des particules obtenues à l'étape (A.2.5) puis, en résolvant l'équation de Poisson.

Concernant l'initialisation, nous avons utilisé la méthode d'inversion de la fonction des densités cumulées, présentée dans [3] (page 79). Il s'agit d'une méthode pseudo-aléatoire. La seule différence est que nous avons généré les positions avec une méthode d'inversion de la fonction de répartition.

Pour la résolution de l'équation de Poisson, nous avons utilisé une grille uniforme de $[0, T_1] \times [0, T_2]$ de pas $\Delta x_1 = T_1/N_1$ dans la direction x_1 et $\Delta x_2 = T_2/N_2$ dans la direction x_2. Cependant, en raison de la périodicité, nous n'avons considéré que les noeuds dans $\mathbf{\Omega}'_{\mathbf{x}} = [0, T_1 - \Delta x_1] \times [0, T_2 - \Delta x_2]$.

L'étape de déposition est optimisée en faisant une boucle sur l'ensemble des particules, en les localisant, puis en ajoutant la contribution de chaque particule aux quatre noeuds de la maille dans laquelle la particule se trouve. Il faut également tenir compte des conditions de périodicité (voir Figure A.1).

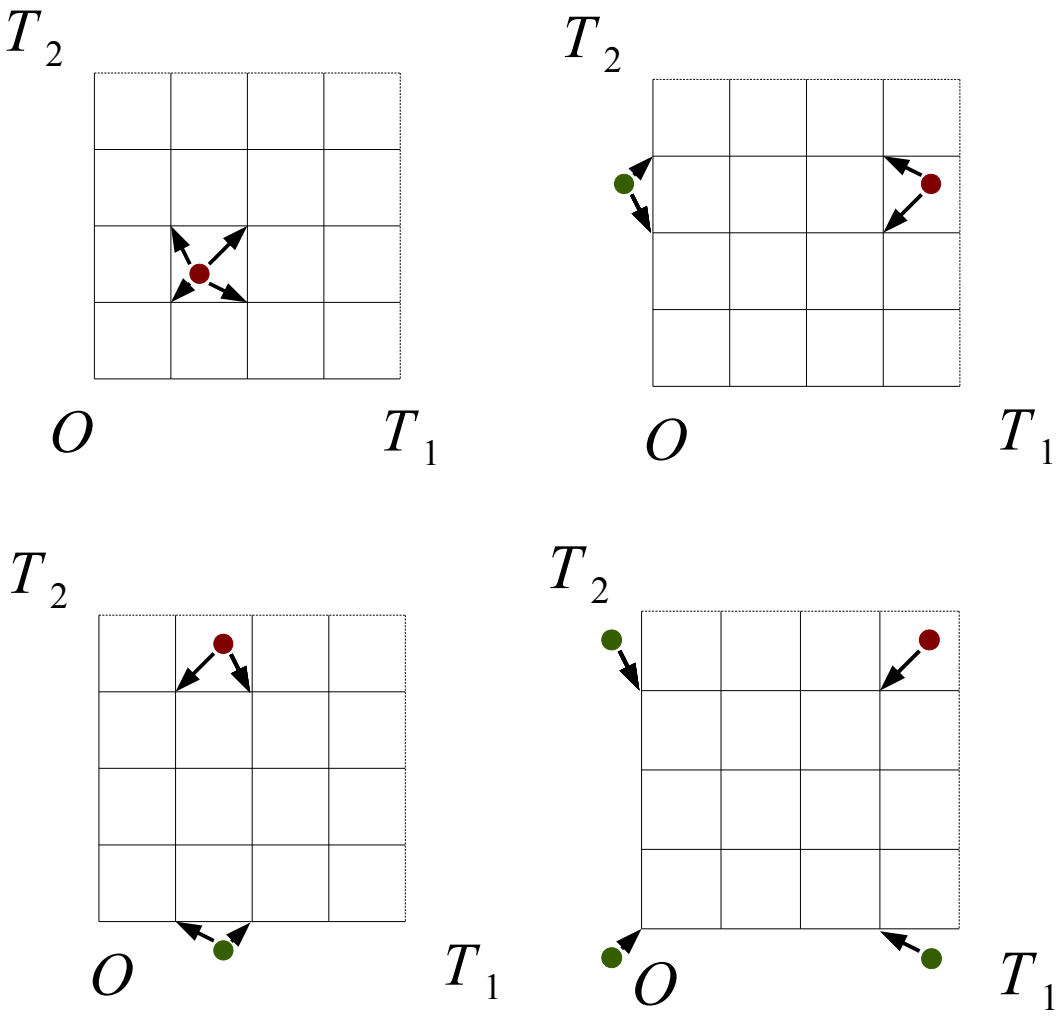

FIGURE A.1 – En haut à gauche : la particule est située au centre du maillage et elle apporte une contribution aux 4 noeuds de la maille dans laquelle elle se trouve. Sur les autres figures : la particule dans le maillage apporte des contributions via les conditions de périodicité.

A.2.2 Principe de la résolution numérique de l'équation de Poisson

Coefficients de Fourier du potentiel électrique

Supposons la fonction de distribution f donnée, et déterminons les coefficients de Fourier de ϕ en fonction de ceux du second membre de l'équation de Poisson :

$$-\Delta\phi = g, \tag{A.2.7}$$

où g est défini par

$$g = \int_{\mathbb{R}^2} f d\mathbf{v} - 1. \tag{A.2.8}$$

La première étape consiste à associer à ϕ et à g leurs développements en série de Fourier :

$$\begin{aligned} \phi(\mathbf{x}) &= \sum_{(n_1,n_2)\in\mathbb{Z}^2} \hat{\phi}_{n_1,n_2} \exp\left(-2i\pi\frac{n_1}{T_1}x_1\right)\exp\left(-2i\pi\frac{n_2}{T_2}x_2\right), \\ g(\mathbf{x}) &= \sum_{(n_1,n_2)\in\mathbb{Z}^2} \hat{g}_{n_1,n_2} \exp\left(-2i\pi\frac{n_1}{T_1}x_1\right)\exp\left(-2i\pi\frac{n_2}{T_2}x_2\right). \end{aligned} \tag{A.2.9}$$

En injectant ces développements dans (A.2.7), puis en procédant par identification, on en déduit que les coefficients de Fourier de ϕ sont donnés par :

$$\begin{aligned} &\hat{\phi}_{0,0} = 0, \\ &\forall (n_1,n_2) \in \mathbb{Z}^2 \setminus (0,0),\ \hat{\phi}_{n_1,n_2} = \frac{\hat{g}_{n_1,n_2}}{\left(\frac{2\pi n_1}{T_1}\right)^2 + \left(\frac{2\pi n_2}{T_2}\right)^2}. \end{aligned} \tag{A.2.10}$$

En notant $\mathbf{E} = (E_1, E_2)$, et en utilisant la relation $\mathbf{E} = -\nabla\phi$, on obtient également les coefficients de Fourier du champ électrique en fonction de ceux de g.

Transformé de Fourier Discrète

Soient N_1 et N_2 deux entiers strictement positifs et $\mathbf{\Pi}_{N_1,N_2}$ l'espace des suites bi-périodiques sur $\mathbb{C}$ défini par :

$$\mathbf{\Pi}_{N_1,N_2} = \left\{ (\mathbf{x}_{n_1,n_2})_{(n_1,n_2)\in\mathbb{Z}^2},\ \ \forall (n_1,n_2)\in\mathbb{Z}^2,\ \mathbf{x}_{n_1+N_1,n_2+N_2} = \mathbf{x}_{n_1,n_2} \right\}.$$

Toutes les suites de cet espace sont entièrement déterminées par les valeurs prisent par $\mathbf{x}_{n_1,n_2}$ pour $0 \le n_1 \le N_1 - 1$ et $0 \le n_2 \le N_2 - 1$.

Definition A.2.1. *La transformé de Fourier discrète d'ordre (N_1, N_2) est l'application $\mathcal{F}_{N_1,N_2} : \mathbf{\Pi}_{N_1,N_2} \to \mathbf{\Pi}_{N_1,N_2}$ définie par $\mathbf{y} = \mathcal{F}_{N_1,N_2}(\mathbf{x})$, où*

$$\mathbf{y}_{m_1,m_2} = \sum_{n_1=0}^{N_1-1}\sum_{n_2=0}^{N_2-1} \mathbf{x}_{n_1,n_2}\xi_{N_1}^{n_1m_1}\xi_{N_2}^{n_2m_2}, \tag{A.2.11}$$

avec $\xi_{N_1} = \exp\left(\frac{2i\pi}{N_1}\right)$ et $\xi_{N_2} = \exp\left(\frac{2i\pi}{N_2}\right)$.

Théorème A.2.2. *$\mathcal{F}_{N_1,N_2}$ est un automorphisme de $\mathbf{\Pi}_{N_1,N_2}$ dont l'inverse $\mathcal{F}^{-1}_{N_1,N_2}$ est donné par :*

$$\mathbf{x}_{m_1,m_2} = \frac{1}{N_1N_2}\sum_{n_1=0}^{N_1-1}\sum_{n_2=0}^{N_2-1} \mathbf{y}_{n_1,n_2}\xi_{N_1}^{-n_1m_1}\xi_{N_2}^{-n_2m_2}. \tag{A.2.12}$$

Approximation numérique des coefficients de Fourier

On approxime les coefficients de Fourier en utilisant une méthode des rectangles à gauche. On obtient alors l'approximation suivante :

$$\hat{g}_{m_1,m_2} \approx \hat{h}_{m_1,m_2} = \frac{1}{N_1 N_2} \sum_{n_1=0}^{N_1-1} \sum_{n_2=0}^{N_2-1} g\left(x_{1,n_1}, x_{2,n_2}\right) \exp\left(2i\pi \frac{m_1}{N_1} n_1\right) \exp\left(2i\pi \frac{m_2}{N_2} n_2\right), \tag{A.2.13}$$

où $\left\{\left(x_{1,n_1}, x_{2,n_2}\right)\right\}$ correspond aux noeuds du maillage définis dans la section (A.2.1).

Remarque A.2.3. *La suite $\hat{h}_{m_1,m_2}$ est un élément de $\mathbf{\Pi}_{N_1,N_2}$. En effet, un calcul direct donne $\hat{h}_{m_1+N_1,m_2+N_2} = \hat{h}_{m_1,m_2}$ pour tout $(m_1, m_2) \in \mathbb{Z}^2$.*

Soit S_{N_1,N_2} l'espace des fonctions engendrées par :

$$\left\{ \exp\left(2i\pi \frac{m_1}{T_1} x\right) \exp\left(2i\pi \frac{m_2}{T_2} y\right),\ (m_1, m_2) \in A_{N_1,N_2} \right\},$$

$$A_{N_1,N_2} = \left\{ (m_1, m_2),\ -\frac{N_1}{2} < m_1 \leq \frac{N_1}{2}, -\frac{N_2}{2} < m_2 \leq \frac{N_2}{2} \right\}. \tag{A.2.14}$$

Lemma A.2.4. *Si la fonction g est un élément de S_{N_1,N_2} alors :*
- $\forall (m_1, m_2) \notin A_{N_1,N_2}$, $\hat{g}_{m_1,m_2} = 0$.
- $\forall (m_1, m_2) \in A_{N_1,N_2}$ *la formule* (A.2.13) *est exacte.*

Résolution numérique de l'équation de Poisson

Soit Υ^{N_1,N_2} l'application qui a une fonction g associe la suite $\Upsilon^{N_1,N_2}(g) \in \mathbf{\Pi}_{N_1,N_2}$ définie par :
- $\forall (n_1, n_2) \in A_{N_1,N_2}$, $\Upsilon^{N_1,N_2}(g) = \hat{g}_{n_1,n_2}$.
- Les autres éléments sont obtenus par (N_1, N_2)-périodicité.

Le principe de la résolution numérique est le suivant :

1. A partir des valeurs de g sur le maillage, on détermine $\Upsilon^{N_1,N_2}(g)$ en utilisant $\mathcal{F}^{-1}_{N_1,N_2}$.
2. En utilisant les formules (A.2.10), on obtient $\Upsilon^{N_1,N_2}(\phi)$.
3. En appliquant $\mathcal{F}_{N_1,N_2}$ à $\Upsilon^{N_1,N_2}(\phi)$, on obtient une approximation de ϕ sur le maillage.

Lorsque g est un élément de S_{N_1,N_2}, ce schéma est exact.

Remarque A.2.5. *La seconde étape doit être traitée avec prudence. En effet, $\Upsilon^{N_1,N_2}(\phi)$ correspond à l'extension périodique des coefficients de Fourier $\hat{\phi}_{n_1,n_2}$ pour $(n_1, n_2) \in A_{N_1,N_2}$. Dans la seconde étape, il est donc nécessaire d'utiliser les formules* (A.2.10) *pour $(n_1, n_2) \in A_{N_1,N_2}$.*

A.3 Résultats numériques

Pour les simulations numériques nous prenons un nombre $N = 2 \cdot 10^5$ de particules, une répartition initiale de particules donnée par

$$f_0(\mathbf{x}, \mathbf{v}) = \frac{1}{2\pi v_{th}} \left(1 + \varepsilon \cos\left(k_1 x_1 + k_2 x_2\right)\right) \exp\left(-\frac{v_x^2 + v_y^2}{2v_{th}}\right), \tag{A.3.1}$$

où $k_1 = 0,\ k_2 = 0.5,\ v_{th} = 1$, $\varepsilon = 0.1$, un pas de temps $\Delta t = 10^{-3}$, des périodes $T_1 = 1$ et $T_2 = 4\pi$, des poids constants égaux à $1/N$, et nous fixons $N_1 = 2^4$ et $N_2 = 2^7$. Ce choix de paramètres correspond à une perturbation dans la direction x_2 de l'équilibre thermodynamique.

Le test numérique consiste à vérifier que la seconde composante du champ électrique décroit vers 0 de façon exponentielle en temps. En linéarisant l'équation de Vlasov-Poisson, on peut montrer (voir [60] et [3]) que la seconde composante du champ électrique peut être approximée par

$$E_2(\mathbf{x}, t) \simeq E_0 \exp(\gamma t) \sin(k_2 x_2 - \omega t), \tag{A.3.2}$$

où $\gamma = -0.151$ et $\omega = 1.323$. Notons que ceci n'est pas la solution complète, car nous n'avons considéré que le mode dominant du développement en série de Fourier du champ électrique. Néanmoins, il s'avère qu'après environ une période en temps, ceci représente une excellente approximation de E_2 car les autres modes deviennent très rapidement négligeables devant le mode dominant.

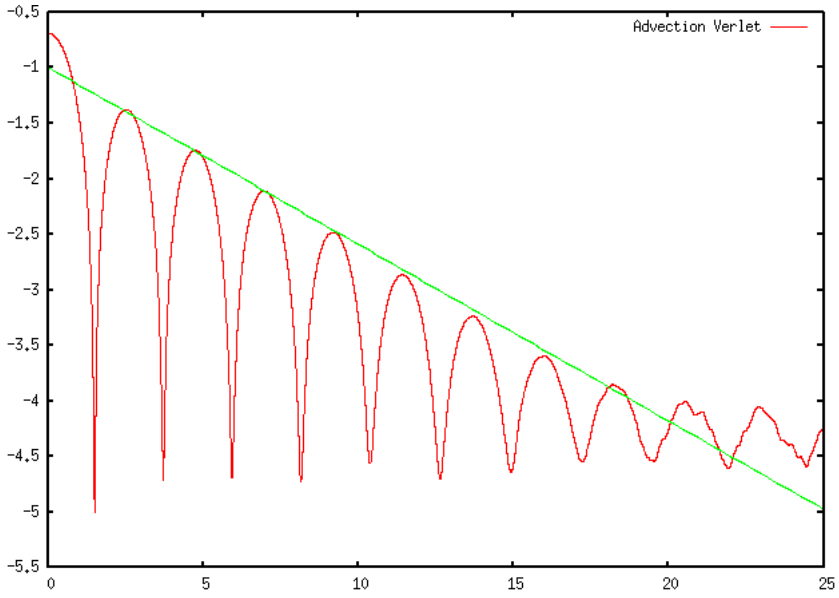

FIGURE A.2 – Advection avec un algorithme de Verlet. En rouge : Evolution de $\ln(\|E_2\|_{L^2})$ en fonction du temps. En vert : la droite $-0.159t - 1$.

Sur les figures (A.2) et (A.3) nous voyons le logarithme de la norme 2 de la seconde composante du champ électrique. On a également tracé la pente correspondant à l'amortissement. Numériquement, le coefficient directeur est plutôt de l'ordre de -0.159. On remarque également que pour un temps de l'ordre de 18 l'amortissement est interrompu. Il s'agit là d'un phénomène purement numérique lié au bruit numérique inhérent à une méthode PIC. Ce bruit correspond à l'erreur commise en approximant la fonction de distribution par des réalisations aléatoires de la loi de probabilité associée à cette fonction. Il peut être réduit en augmentant le nombre de particules ou en utilisant une méthode δf (voir [60]). Plus la solution est proche de l'état d'équilibre, plus les résultats obtenus avec la méthode δf seront précis. La Figure (A.4) illustre le gain obtenu en utilisant une méthode δf. Sur la figure (A.5) nous voyons que lorsque la perturbation de l'équilibre est

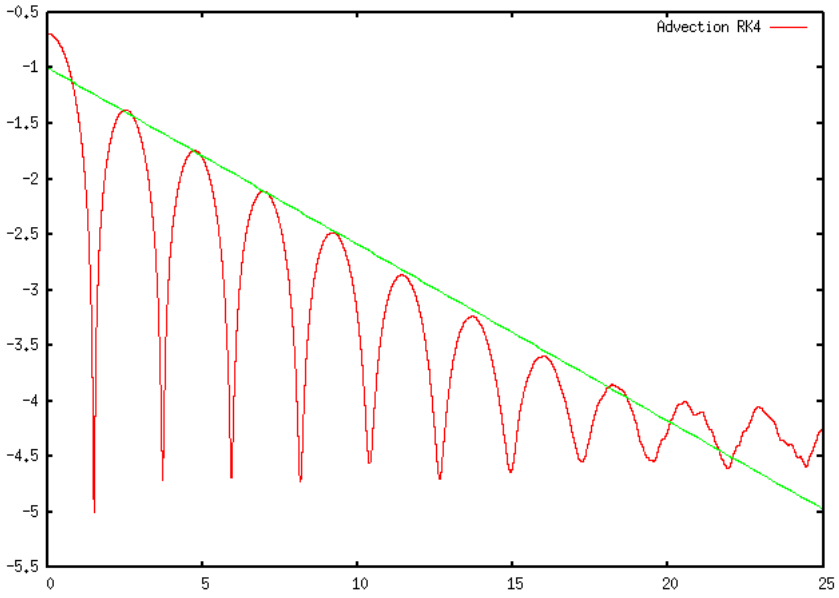

FIGURE A.3 – Advection avec un algorithme Runge Kutta d'ordre 4. En rouge : Evolution de $\ln\left(\|E_2\|_{L^2}\right)$ en fonction du temps. En vert : la droite $-0.159t - 1$.

plus faible ($\varepsilon = 10^{-3}$) les résultats sont plus précis. En particulier l'amortissement a lieu sur un intervalle de temps plus large.

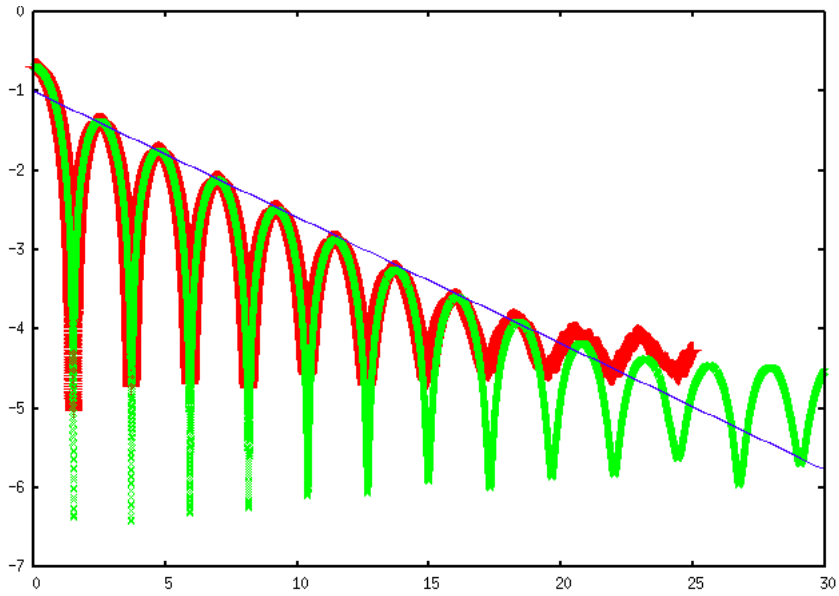

FIGURE A.4 – En rouge : Evolution de $\ln(\|E_2\|_{L^2})$ obtenue avec un algorithme $RK4$. En vert : Le même algorithme avec une correction δf.

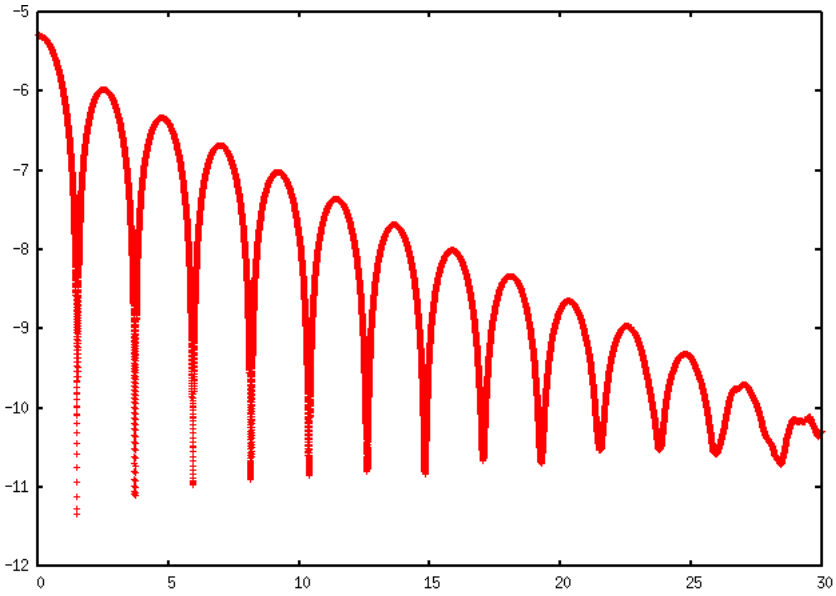

FIGURE A.5 – Algorithme δf avec $\varepsilon = 10^{-3}$

Annexe B

Annexe relative au chapitre 2

B.1 Example of non-symplectic Hamiltonian vector field flow

In this Appendix, we exhibit an example of a flow - of parameter ε - of Hamiltonian vector field, which - since the Poisson Matrix does depend on ε - is not symplectic.

Let $\varepsilon \in]-1, +\infty[$. Consider on $\mathbb{R}^4$ endowed with coordinate system $\mathbf{x} = (x_1, x_2, x_3, x_4)$ the symplectic two-form $\omega_\varepsilon \in \Omega^2\left(\mathbb{R}^4\right)$, given by

$$\omega_\varepsilon(\mathbf{x}) = \frac{1}{1+\varepsilon} dx_1 \wedge dx_2 + \frac{1}{2+\varepsilon} dx_3 \wedge dx_4. \tag{B.1.1}$$

The associated Poisson Matrix is given by

$$J_\varepsilon(\mathbf{x}) = \begin{pmatrix} 0 & 1+\varepsilon & 0 & 0 \\ -(1+\varepsilon) & 0 & 0 & 0 \\ 0 & 0 & 0 & 2+\varepsilon \\ 0 & 0 & -(2+\varepsilon) & 0 \end{pmatrix}. \tag{B.1.2}$$

Now, let $G(\mathbf{x}) = x_1 x_3$. The Hamiltonian vector field generated by G is given by

$$\mathbf{X}_G(\mathbf{x}) = J_\varepsilon(\mathbf{x}) \nabla_{\mathbf{x}} G(\mathbf{x}) = \begin{pmatrix} 0 \\ -(1+\varepsilon) x_3 \\ 0 \\ -(2+\varepsilon) x_1 \end{pmatrix}. \tag{B.1.3}$$

The flow of this Hamiltonian vector field, denoted by φ_ε, is given by

$$\varphi_\varepsilon(\mathbf{x}) = \left(x_1, x_2 - \left(\varepsilon + \frac{\varepsilon^2}{2}\right) x_3, x_3, x_4 - \left(2\varepsilon + \frac{\varepsilon^2}{2}\right) x_1\right). \tag{B.1.4}$$

Now, if we make the change of coordinate $\mathbf{x} \mapsto \mathbf{z} = \varphi_\varepsilon(\mathbf{x})$, the Poisson Matrix in the coordinate system $\mathbf{z}$ reads

$$\begin{pmatrix} 0 & 1+\varepsilon & 0 & 0 \\ -(1+\varepsilon) & 0 & 0 & \frac{\varepsilon^2}{2} \\ 0 & 0 & 0 & 2+\varepsilon \\ 0 & -\frac{\varepsilon^2}{2} & -(2+\varepsilon) & 0 \end{pmatrix}. \tag{B.1.5}$$

Thus, although φ_ε is the flow of an Hamiltonian vector field, φ_ε is not symplectic.

B.2 Algorithm 2.5.11 detailed up to $N = 5$

In this Appendix, we apply Algorithm 2.5.11 for $N = 1,\ 2,\ 3,\ 4$ and 5. The computations are led using Sage software. We first need to compute $\mathbf{V}_0^\varepsilon$, $\mathbf{V}_1^\varepsilon$, $\mathbf{V}_2^\varepsilon$, $\mathbf{V}_3^\varepsilon$, $\mathbf{V}_4^\varepsilon$ and $\mathbf{V}_5^\varepsilon$ with formula (2.5.55). The first step consists in expressing $\mathcal{U}_1$, $\mathcal{U}_2$, $\mathcal{U}_3$, $\mathcal{U}_4$ and $\mathcal{U}_5$.

$$
\begin{aligned}
\mathcal{U}_2 &= \left\{(m_1,m_2)\in\mathbb{N}^2 \text{ s.t. } m_1+2m_2=2\right\} = \left\{(0,1)\,;(2,0)\right\},\\
\mathcal{U}_3 &= \left\{(m_1,m_2,m_3)\in\mathbb{N}^3 \text{ s.t. } m_1+2m_2+3m_3=3\right\}\\
&= \left\{(0,0,1)\,;(1,1,0)\,;(3,0,0)\right\},\\
\mathcal{U}_4 &= \left\{(m_1,m_2,m_3,m_4)\in\mathbb{N}^4 \text{ s.t. } m_1+2m_2+3m_3+4m_4=4\right\}\\
&= \left\{(0,0,0,1)\,;(1,0,1,0)\,;(0,2,0,0)\,;(2,1,0,0)\,;(4,0,0,0)\right\},\\
\mathcal{U}_5 &= \left\{(m_1,m_2,m_3,m_4,m_5)\in\mathbb{N}^5 \text{ s.t. } m_1+2m_2+3m_3+4m_4+5m_5=5\right\}\\
&= \Big\{\ (0,0,0,0,1)\,;(1,0,0,1,0)\,;(0,1,1,0,0)\,;(2,0,1,0,0)\,;\\
&\qquad (1,2,0,0,0)\,;(3,1,0,0,0)\,;(5,0,0,0,0)\ \Big\}
\end{aligned}
\tag{B.2.1}
$$

Then, applying formula (2.5.55) yields :

$$
\begin{aligned}
\mathbf{V}_0^\varepsilon &= id,\\
\mathbf{V}_1^\varepsilon &= \bar{\mathbf{X}}^\varepsilon_{\varepsilon\bar{g}_1}\cdot\\
&= \overline{\mathbf{M}}_1 + \varepsilon^2\overline{\mathbf{N}}_3,\\
\mathbf{V}_2^\varepsilon &= \frac{1}{2}\left(\bar{\mathbf{X}}^\varepsilon_{\varepsilon\bar{g}_1}\right)^2\cdot + \bar{\mathbf{X}}^\varepsilon_{\varepsilon\bar{g}_2}\cdot\\
&= \left(\overline{\mathbf{M}}_2 + \frac{1}{2}\overline{\mathbf{M}}_1^2\right) + \varepsilon^2\left(\overline{\mathbf{N}}_4 + \frac{1}{2}\overline{\mathbf{M}}_1\overline{\mathbf{N}}_3 + \frac{1}{2}\overline{\mathbf{N}}_3\overline{\mathbf{M}}_1\right) + \varepsilon^4\frac{1}{2}\overline{\mathbf{N}}_3\\
\mathbf{V}_3^\varepsilon &= \frac{1}{6}\left(\bar{\mathbf{X}}^\varepsilon_{\varepsilon\bar{g}_1}\right)^3\cdot + \bar{\mathbf{X}}^\varepsilon_{\varepsilon\bar{g}_1}\cdot\,\bar{\mathbf{X}}^\varepsilon_{\varepsilon\bar{g}_2}\cdot + \bar{\mathbf{X}}^\varepsilon_{\varepsilon\bar{g}_3}\cdot\\
&= \left(\overline{\mathbf{M}}_3 + \overline{\mathbf{M}}_1\overline{\mathbf{M}}_2 + \frac{1}{6}\overline{\mathbf{M}}_1^3\right)\\
&\quad + \varepsilon^2\left(\overline{\mathbf{N}}_5 + \overline{\mathbf{M}}_1\overline{\mathbf{N}}_4 + \overline{\mathbf{N}}_3\overline{\mathbf{M}}_2 + \frac{1}{6}\overline{\mathbf{M}}_1\overline{\mathbf{N}}_3\overline{\mathbf{M}}_1 + \frac{1}{6}\overline{\mathbf{M}}_1^2\overline{\mathbf{N}}_3 + \frac{1}{6}\overline{\mathbf{N}}_3\overline{\mathbf{M}}_1^2\right)\\
&\quad + \varepsilon^4\left(\overline{\mathbf{N}}_3\overline{\mathbf{N}}_4 + \frac{1}{6}\overline{\mathbf{M}}_1\overline{\mathbf{N}}_3^2 + \frac{1}{6}\overline{\mathbf{N}}_3\overline{\mathbf{M}}_1\overline{\mathbf{N}}_3 + \frac{1}{6}\overline{\mathbf{N}}_3^2\overline{\mathbf{M}}_1\right)\\
&\quad + \frac{1}{6}\varepsilon^6\overline{\mathbf{N}}_3^3
\end{aligned}
\tag{B.2.2}
$$

$$
\begin{aligned}
\mathbf{V}_4^{\varepsilon} &= \bar{\mathbf{X}}^{\varepsilon}_{\varepsilon\bar{g}_4}\cdot + \bar{\mathbf{X}}^{\varepsilon}_{\varepsilon\bar{g}_1}\cdot \bar{\mathbf{X}}^{\varepsilon}_{\varepsilon\bar{g}_3}\cdot + \frac{1}{2}\left(\bar{\mathbf{X}}^{\varepsilon}_{\varepsilon\bar{g}_2}\right)^2\cdot + \frac{1}{2}\left(\bar{\mathbf{X}}^{\varepsilon}_{\varepsilon\bar{g}_1}\right)^2\cdot \bar{\mathbf{X}}^{\varepsilon}_{\varepsilon\bar{g}_2}\cdot + \frac{1}{24}\left(\bar{\mathbf{X}}^{\varepsilon}_{\varepsilon\bar{g}_1}\right)^4\cdot \\
&= \left(\overline{\mathbf{M}}_4 + \overline{\mathbf{M}}_1\overline{\mathbf{M}}_3 + \frac{1}{2}\overline{\mathbf{M}}_1^2\overline{\mathbf{M}}_2 + \frac{1}{2}\overline{\mathbf{M}}_2^2 + \frac{1}{24}\overline{\mathbf{M}}_1^4\right) \\
&\quad + \varepsilon^2\Big(\overline{\mathbf{N}}_6 + \overline{\mathbf{M}}_1\overline{\mathbf{N}}_5 + \frac{1}{2}\overline{\mathbf{M}}_2\overline{\mathbf{N}}_4 + \overline{\mathbf{N}}_3\overline{\mathbf{M}}_3 + \frac{1}{2}\overline{\mathbf{N}}_4\overline{\mathbf{M}}_2 + \frac{1}{2}\overline{\mathbf{M}}_1^2\overline{\mathbf{N}}_4 + \frac{1}{2}\overline{\mathbf{M}}_1\overline{\mathbf{N}}_3\overline{\mathbf{M}}_2 + \frac{1}{2}\overline{\mathbf{N}}_3\overline{\mathbf{M}}_1\overline{\mathbf{M}}_2 \\
&\qquad + \frac{1}{24}\overline{\mathbf{M}}_1^3\overline{\mathbf{N}}_3 + \frac{1}{24}\overline{\mathbf{M}}_1^2\overline{\mathbf{N}}_3\overline{\mathbf{M}}_1 + \frac{1}{24}\overline{\mathbf{M}}_1\overline{\mathbf{N}}_3\overline{\mathbf{M}}_1^2 \\
&\qquad + \frac{1}{24}\overline{\mathbf{N}}_3\overline{\mathbf{M}}_1^3\Big) \\
&\quad + \varepsilon^4\Big(\overline{\mathbf{N}}_3\overline{\mathbf{N}}_5 + \frac{1}{2}\overline{\mathbf{N}}_4^2 + \frac{1}{2}\overline{\mathbf{M}}_1\overline{\mathbf{N}}_3\overline{\mathbf{N}}_4 + \frac{1}{2}\overline{\mathbf{N}}_3\overline{\mathbf{M}}_1\overline{\mathbf{N}}_4 + \frac{1}{2}\overline{\mathbf{N}}_3^2\overline{\mathbf{M}}_2 \\
&\qquad + \frac{1}{24}\overline{\mathbf{M}}_1^2\overline{\mathbf{N}}_3^2 + \frac{1}{24}\overline{\mathbf{M}}_1\overline{\mathbf{N}}_3\overline{\mathbf{M}}_1 N_3 + \frac{1}{24}\overline{\mathbf{M}}_1\overline{\mathbf{N}}_3^2\overline{\mathbf{M}}_1 + \frac{1}{24}\overline{\mathbf{N}}_3\overline{\mathbf{M}}_1^2\overline{\mathbf{N}}_3 + \frac{1}{24}\overline{\mathbf{N}}_3\overline{\mathbf{M}}_1\overline{\mathbf{N}}_3\overline{\mathbf{M}}_1 \\
&\qquad + \frac{1}{24}\overline{\mathbf{N}}_3^2\overline{\mathbf{M}}_1^2\Big) \\
&\quad + \varepsilon^6\Big(\frac{1}{2}\overline{\mathbf{N}}_3^2\overline{\mathbf{N}}_4 + \frac{1}{24}\overline{\mathbf{M}}_1\overline{\mathbf{N}}_3^3 + \frac{1}{24}\overline{\mathbf{N}}_3\overline{\mathbf{M}}_1\overline{\mathbf{N}}_3^2 + \frac{1}{24}\overline{\mathbf{N}}_3^2\overline{\mathbf{M}}_1\overline{\mathbf{N}}_3 + \frac{1}{24}\overline{\mathbf{N}}_3^3\overline{\mathbf{M}}_1\Big) \\
&\quad + \varepsilon^8\frac{1}{24}\overline{\mathbf{N}}_3^4
\end{aligned}
\tag{B.2.3}
$$

$$
\begin{aligned}
\mathbf{V}_5^\varepsilon &= \bar{\mathbf{X}}^\varepsilon_{\varepsilon\bar{g}_5}\cdot + \bar{\mathbf{X}}^\varepsilon_{\varepsilon\bar{g}_1}\cdot \bar{\mathbf{X}}^\varepsilon_{\varepsilon\bar{g}_4}\cdot + \bar{\mathbf{X}}^\varepsilon_{\varepsilon\bar{g}_2}\cdot \bar{\mathbf{X}}^\varepsilon_{\varepsilon\bar{g}_3}\cdot + \left(\bar{\mathbf{X}}^\varepsilon_{\varepsilon\bar{g}_1}\right)^2\cdot \bar{\mathbf{X}}^\varepsilon_{\varepsilon\bar{g}_3}\cdot \\
&\quad + \frac{1}{2}\bar{\mathbf{X}}^\varepsilon_{\varepsilon\bar{g}_1}\cdot \left(\bar{\mathbf{X}}^\varepsilon_{\varepsilon\bar{g}_2}\right)^2\cdot + \frac{1}{6}\left(\bar{\mathbf{X}}^\varepsilon_{\varepsilon\bar{g}_1}\right)^3\cdot \bar{\mathbf{X}}^\varepsilon_{\varepsilon\bar{g}_2} + \frac{1}{120}\left(\bar{\mathbf{X}}^\varepsilon_{\varepsilon\bar{g}_1}\right)^5\cdot \\
&= \Big(\overline{\mathbf{M}}_5 + \overline{\mathbf{M}}_1\overline{\mathbf{M}}_4 + \overline{\mathbf{M}}_2\overline{\mathbf{M}}_3 + \overline{\mathbf{M}}_1^2\overline{\mathbf{M}}_3 + \frac{1}{2}\overline{\mathbf{M}}_1\overline{\mathbf{M}}_2^2 + \frac{1}{6}\overline{\mathbf{M}}_1^3\overline{\mathbf{M}}_2 + \frac{1}{120}\overline{\mathbf{M}}_1^5\Big) \\
&\quad + \varepsilon^2\Big(\frac{1}{120}\overline{\mathbf{N}}_3\overline{\mathbf{M}}_1^4 + \frac{1}{120}\overline{\mathbf{M}}_1\overline{\mathbf{N}}_3\overline{\mathbf{M}}_1^3 + \frac{1}{120}\overline{\mathbf{M}}_1^2\overline{\mathbf{N}}_3\overline{\mathbf{M}}_1^2 + \overline{\mathbf{N}}_7 + \overline{\mathbf{M}}_1\overline{\mathbf{N}}_6 + \overline{\mathbf{M}}_2\overline{\mathbf{N}}_5 \\
&\qquad + \overline{\mathbf{N}}_3\overline{\mathbf{M}}_4 + \overline{\mathbf{N}}_4\overline{\mathbf{M}}_3 + \overline{\mathbf{M}}_1^2\overline{\mathbf{N}}_5 + \overline{\mathbf{M}}_1\overline{\mathbf{N}}_3\overline{\mathbf{M}}_3 + \frac{1}{2}\overline{\mathbf{M}}_1\overline{\mathbf{M}}_2\overline{\mathbf{N}}_4 + \frac{1}{2}\overline{\mathbf{M}}_1\overline{\mathbf{N}}_4\overline{\mathbf{M}}_2 \\
&\qquad + \overline{\mathbf{N}}_3\overline{\mathbf{M}}_1\overline{\mathbf{M}}_3 + \frac{1}{2}\overline{\mathbf{N}}_3\overline{\mathbf{M}}_2^2 + \frac{1}{6}\overline{\mathbf{M}}_1^3\overline{\mathbf{N}}_4 + \frac{1}{6}\overline{\mathbf{M}}_1^2\overline{\mathbf{N}}_3\overline{\mathbf{M}}_2 \\
&\qquad + \frac{1}{6}\overline{\mathbf{M}}_1\overline{\mathbf{N}}_3\overline{\mathbf{M}}_1\overline{\mathbf{M}}_2 + \frac{1}{6}\overline{\mathbf{N}}_3\overline{\mathbf{M}}_1^2\overline{\mathbf{M}}_2 + \frac{1}{120}\overline{\mathbf{M}}_1^4\overline{\mathbf{N}}_3 + \frac{1}{120}\overline{\mathbf{M}}_1^3\overline{\mathbf{N}}_3\overline{\mathbf{M}}_1\Big) \\
&\quad + \varepsilon^4\Big(\overline{\mathbf{N}}_3\overline{\mathbf{N}}_6 + \overline{\mathbf{N}}_4\overline{\mathbf{N}}_5 + \overline{\mathbf{M}}_1\overline{\mathbf{N}}_3\overline{\mathbf{N}}_5 + \frac{1}{2}\overline{\mathbf{M}}_1\overline{\mathbf{N}}_4^2\overline{\mathbf{N}}_3\overline{\mathbf{M}}_1\overline{\mathbf{N}}_5 + \frac{1}{2}\overline{\mathbf{N}}_3\overline{\mathbf{M}}_2\overline{\mathbf{N}}_4 + \overline{\mathbf{N}}_3^2\overline{\mathbf{M}}_3 \\
&\qquad + \frac{1}{2}\overline{\mathbf{N}}_3\overline{\mathbf{N}}_4\overline{\mathbf{M}}_2 + \frac{1}{6}\overline{\mathbf{M}}_1^2\overline{\mathbf{N}}_3\overline{\mathbf{N}}_4 + \frac{1}{6}\overline{\mathbf{M}}_1\overline{\mathbf{N}}_3^2\overline{\mathbf{M}}_2 + \frac{1}{6}\overline{\mathbf{N}}_3\overline{\mathbf{M}}_1^2N_4 + \frac{1}{6}\overline{\mathbf{N}}_3\overline{\mathbf{M}}_1\overline{\mathbf{N}}_3\overline{\mathbf{M}}_2 \\
&\qquad + \frac{1}{6}\overline{\mathbf{N}}_3^2\overline{\mathbf{M}}_1\overline{\mathbf{M}}_2 + \frac{1}{120}\overline{\mathbf{M}}_1^3\overline{\mathbf{N}}_3^2 + \frac{1}{120}\overline{\mathbf{M}}_1^2\overline{\mathbf{N}}_3\overline{\mathbf{M}}_1\overline{\mathbf{N}}_3 \\
&\qquad + \frac{1}{120}\overline{\mathbf{M}}_1\overline{\mathbf{N}}_3\overline{\mathbf{M}}_1^2\overline{\mathbf{N}}_3 + \frac{1}{120}\overline{\mathbf{M}}_1\overline{\mathbf{N}}_3\overline{\mathbf{M}}_1\overline{\mathbf{N}}_3\overline{\mathbf{M}}_1 + \frac{1}{120}\overline{\mathbf{M}}_1^2\overline{\mathbf{N}}_3^2\overline{\mathbf{M}}_1 \\
&\qquad + \frac{1}{120}\overline{\mathbf{M}}_1\overline{\mathbf{N}}_3^2\overline{\mathbf{M}}_1^2 + \frac{1}{120}\overline{\mathbf{N}}_3\overline{\mathbf{M}}_1^3\overline{\mathbf{N}}_3 + \frac{1}{120}\overline{\mathbf{N}}_3\overline{\mathbf{M}}_1^2\overline{\mathbf{N}}_3\overline{\mathbf{M}}_1 \\
&\qquad + \frac{1}{6}\overline{\mathbf{M}}_1\overline{\mathbf{N}}_3\overline{\mathbf{M}}_1\overline{\mathbf{N}}_4 + \frac{1}{120}\overline{\mathbf{N}}_3\overline{\mathbf{M}}_1\overline{\mathbf{N}}_3\overline{\mathbf{M}}_1^2 + \frac{1}{120}\overline{\mathbf{N}}_3^2\overline{\mathbf{M}}_1^3\Big) \\
&\quad + \varepsilon^6\Big(\overline{\mathbf{N}}_3^2\overline{\mathbf{N}}_5 + \frac{1}{2}\overline{\mathbf{N}}_3\overline{\mathbf{N}}_4^2 + \frac{1}{6}\overline{\mathbf{M}}_1\overline{\mathbf{N}}_3^2\overline{\mathbf{N}}_4 + \frac{1}{6}\overline{\mathbf{N}}_3\overline{\mathbf{M}}_1\overline{\mathbf{N}}_3\overline{\mathbf{N}}_4 + \frac{1}{6}\overline{\mathbf{N}}_3^2\overline{\mathbf{M}}_1\overline{\mathbf{N}}_4 + \frac{1}{6}\overline{\mathbf{N}}_3^3\overline{\mathbf{M}}_2 \\
&\qquad + \frac{1}{120}\overline{\mathbf{M}}_1^2\overline{\mathbf{N}}_3^3 + \frac{1}{120}\overline{\mathbf{M}}_1\overline{\mathbf{N}}_3\overline{\mathbf{M}}_1\overline{\mathbf{N}}_3^2 + \frac{1}{120}\overline{\mathbf{M}}_1\overline{\mathbf{N}}_3^2\overline{\mathbf{M}}_1\overline{\mathbf{N}}_3 \\
&\qquad + \frac{1}{120}\overline{\mathbf{M}}_1\overline{\mathbf{N}}_3^3\overline{\mathbf{M}}_1 + + \frac{1}{120}\overline{\mathbf{N}}_3\overline{\mathbf{M}}_1^2\overline{\mathbf{N}}_3^2 + \frac{1}{120}\overline{\mathbf{N}}_3\overline{\mathbf{M}}_1\overline{\mathbf{N}}_3\overline{\mathbf{M}}_1\overline{\mathbf{N}}_3 \\
&\qquad + \frac{1}{120}\overline{\mathbf{N}}_3\overline{\mathbf{M}}_1\overline{\mathbf{N}}_3^2\overline{\mathbf{M}}_1 + \frac{1}{120}\overline{\mathbf{N}}_3^2\overline{\mathbf{M}}_1^2\overline{\mathbf{N}}_3 + \frac{1}{120}\overline{\mathbf{N}}_3^2\overline{\mathbf{M}}_1\overline{\mathbf{N}}_3\overline{\mathbf{M}}_1 + \frac{1}{120}\overline{\mathbf{N}}_3^3\overline{\mathbf{M}}_1^2\Big) \\
&\quad + \varepsilon^8\Big(\frac{1}{6}\overline{\mathbf{N}}_3^3\overline{\mathbf{N}}_4 + \frac{1}{120}\overline{\mathbf{M}}_1\overline{\mathbf{N}}_3^4 + \frac{1}{120}\overline{\mathbf{N}}_3\overline{\mathbf{M}}_1\overline{\mathbf{N}}_3^3 \\
&\qquad + \frac{1}{120}\overline{\mathbf{N}}_3^2\overline{\mathbf{M}}_1\overline{\mathbf{N}}_3^2 + \frac{1}{120}\overline{\mathbf{N}}_3^3\overline{\mathbf{M}}_1\overline{\mathbf{N}}_3 + \frac{1}{120}\overline{\mathbf{N}}_3^4\overline{\mathbf{M}}_1\Big) \\
&\quad + \varepsilon^{10}\frac{1}{120}\overline{\mathbf{N}}_3^5
\end{aligned}
\tag{B.2.4}
$$

Hence, the expansions in power of ε of $\mathbf{V}_1^\varepsilon$, $\mathbf{V}_2^\varepsilon$, $\mathbf{V}_3^\varepsilon$, $\mathbf{V}_4^\varepsilon$ and $\mathbf{V}_5^\varepsilon$ and the dependency with respect to the differential operators $\overline{\mathbf{M}}_i$ and $\overline{\mathbf{N}}_j$ of each term of these expansions can

be summarized by :

$$
\begin{aligned}
\mathbf{V}_1^\varepsilon &= \mathbf{V}_1^0\left(\overline{\mathbf{M}}_1\right) + \varepsilon^2 \mathbf{V}_1^2\left(\overline{\mathbf{N}}_3\right), \\
\mathbf{V}_2^\varepsilon &= \mathbf{V}_2^0\left(\overline{\mathbf{M}}_1, \overline{\mathbf{M}}_2\right) + \varepsilon^2 \mathbf{V}_2^2\left(\overline{\mathbf{M}}_1, \overline{\mathbf{N}}_3, \overline{\mathbf{N}}_4\right) + \varepsilon^4 \mathbf{V}_2^4\left(\overline{\mathbf{N}}_3\right), \\
\mathbf{V}_3^\varepsilon &= \mathbf{V}_3^0\left(\overline{\mathbf{M}}_1, \overline{\mathbf{M}}_2, \overline{\mathbf{M}}_3\right) + \varepsilon^2 \mathbf{V}_3^2\left(\overline{\mathbf{M}}_1, \overline{\mathbf{M}}_2, \overline{\mathbf{N}}_3, \overline{\mathbf{N}}_4, \overline{\mathbf{N}}_5\right) + \varepsilon^4 \mathbf{V}_3^4\left(\overline{\mathbf{M}}_1, \overline{\mathbf{N}}_3, \overline{\mathbf{N}}_4\right) \\
&\quad + \varepsilon^6 \mathbf{V}_3^6\left(\overline{\mathbf{N}}_3\right), \\
\mathbf{V}_4^\varepsilon &= \mathbf{V}_4^0\left(\overline{\mathbf{M}}_1, \overline{\mathbf{M}}_2, \overline{\mathbf{M}}_3, \overline{\mathbf{M}}_4\right) + \varepsilon^2 \mathbf{V}_4^2\left(\overline{\mathbf{M}}_1, \overline{\mathbf{M}}_2, \overline{\mathbf{M}}_3, \overline{\mathbf{N}}_3, \overline{\mathbf{N}}_4, \overline{\mathbf{N}}_5, \overline{\mathbf{N}}_6\right) \\
&\quad + \varepsilon^4 \mathbf{V}_4^4\left(\overline{\mathbf{M}}_1, \overline{\mathbf{M}}_2, \overline{\mathbf{N}}_3, \overline{\mathbf{N}}_4, \overline{\mathbf{N}}_5\right) + \varepsilon^6 \mathbf{V}_4^6\left(\overline{\mathbf{M}}_1, \overline{\mathbf{N}}_3, \overline{\mathbf{N}}_4\right) + \varepsilon^8 \mathbf{V}_4^8\left(\overline{\mathbf{N}}_3\right), \\
\mathbf{V}_5^\varepsilon &= \mathbf{V}_5^0\left(\overline{\mathbf{M}}_1, \overline{\mathbf{M}}_2, \overline{\mathbf{M}}_3, \overline{\mathbf{M}}_4, \overline{\mathbf{M}}_5\right) + \varepsilon^2 \mathbf{V}_5^2\left(\overline{\mathbf{M}}_1, \overline{\mathbf{M}}_2, \overline{\mathbf{M}}_3, \overline{\mathbf{M}}_4, \overline{\mathbf{N}}_3, \overline{\mathbf{N}}_4, \overline{\mathbf{N}}_5, \overline{\mathbf{N}}_6, \overline{\mathbf{N}}_7\right) \\
&\quad + \varepsilon^4 \mathbf{V}_5^4\left(\overline{\mathbf{M}}_1, \overline{\mathbf{M}}_2, \overline{\mathbf{M}}_3, \overline{\mathbf{N}}_3, \overline{\mathbf{N}}_4, \overline{\mathbf{N}}_5, \overline{\mathbf{N}}_6\right) + \varepsilon^6 \mathbf{V}_5^6\left(\overline{\mathbf{M}}_1, \overline{\mathbf{M}}_2, \overline{\mathbf{N}}_3, \overline{\mathbf{N}}_4, \overline{\mathbf{N}}_5\right) \\
&\quad + \varepsilon^8 \mathbf{V}_5^8\left(\overline{\mathbf{M}}_1, \overline{\mathbf{N}}_3, \overline{\mathbf{N}}_4\right) + \varepsilon^{10} \mathbf{V}_5^{10}\left(\overline{\mathbf{N}}_3\right).
\end{aligned}
\tag{B.2.5}
$$

B.2.1 Formulas for $N = 1$

In the present subsection we will apply algorithm 2.5.11 with $N = 1$. The first step of the algorithm consists in injecting the expression of $\mathbf{V}_1^\varepsilon$ in

$$
\hat{H}_\varepsilon^1(\hat{\mathbf{r}}) = \sum_{n=0}^{1} \left(\sum_{k=0}^{n} \mathbf{V}_{n-k}^\varepsilon \cdot \bar{H}_k \right)(\hat{\mathbf{r}})\, \varepsilon^n + \varepsilon^2 \iota_{\bar{H}}^{1,\bullet}(\varepsilon, \hat{\mathbf{r}}), . \tag{B.2.6}
$$

Applying the second step of the algorithm, we obtain :

$$
\hat{H}_\varepsilon^1(\hat{\mathbf{r}}) = \bar{H}_0(\hat{\mathbf{r}}) + \varepsilon \left(\bar{H}_1(\hat{\mathbf{r}}) + \mathbf{V}_1^0\big(\overline{\mathbf{M}}_1\big) \cdot \bar{H}_0(\hat{\mathbf{r}}) \right) + \varepsilon^3 \mathbf{V}_1^2\left(\overline{\mathbf{M}}_1\right) \cdot \bar{H}_0(\hat{\mathbf{r}}) + \varepsilon^2 \iota_{\bar{H}}^{1,\bullet}(\varepsilon, \hat{\mathbf{r}}), \tag{B.2.7}
$$

that have to be compared with the desired expression :

$$
\hat{H}_\varepsilon^1(\hat{\mathbf{r}}) = \bar{H}_0(\hat{\mathbf{r}}) + \varepsilon \hat{H}_1(\hat{\mathbf{r}}) + \varepsilon^2 \iota_{\hat{H}}^1(\varepsilon, \hat{\mathbf{r}}), \tag{B.2.8}
$$

to get

$$
\hat{H}_1(\hat{\mathbf{r}}) = \left(\bar{\mathcal{T}}_0 \nabla \bar{g}_1\right) \cdot \nabla \bar{H}_0(\hat{\mathbf{r}}) + \bar{H}_1(\hat{\mathbf{r}}). \tag{B.2.9}
$$

Eventually, applying the last step of the algorithm, we set

$$
\hat{H}_1(\hat{\mathbf{r}}) = \frac{1}{2\pi} \int_0^{2\pi} \bar{H}_1(\hat{\mathbf{r}})\, d\hat{r}_3, \tag{B.2.10}
$$

$$
u_1(\hat{\mathbf{r}}) = -\bar{H}_1(\hat{\mathbf{r}}) + \frac{1}{2\pi} \int_0^{2\pi} \bar{H}_1(\hat{\mathbf{r}})\, d\hat{r}_3, \tag{B.2.11}
$$

and then we solve equation $\left(\bar{\mathcal{T}}_0 \nabla \bar{g}_1\right) \cdot \nabla \bar{H}_0(\hat{\mathbf{r}}) = u_1$ by setting

$$
\bar{g}_1(\bar{\mathbf{r}}) = -\frac{1}{B(\hat{r}_1, \hat{r}_2)} \int_0^{\bar{r}_3} u_1(\bar{r}_1, \bar{r}_2, s, \bar{r}_4)\, ds. \tag{B.2.12}
$$

B.2.2 Formulas for $N = 2$

In this subsection we will apply algorithm 2.5.11 with $N = 2$. The first step of the algorithm consists in injecting expressions of $\mathbf{V}_1^\varepsilon$ and $\mathbf{V}_2^\varepsilon$ in

$$
\hat{H}_\varepsilon^2(\hat{\mathbf{r}}) = \sum_{n=0}^{2} \left(\sum_{k=0}^{n} \mathbf{V}_{n-k}^\varepsilon \cdot \bar{H}_k \right)(\hat{\mathbf{r}})\, \varepsilon^n + \varepsilon^3 \iota_{\bar{H}}^{2,\bullet}(\varepsilon, \hat{\mathbf{r}}). \tag{B.2.13}
$$

Ordering terms according to their power of ε (second step of the algorithm) we obtain :

$$\begin{aligned}\hat{H}^2_\varepsilon(\hat{\mathbf{r}}) = \bar{H}_0(\hat{\mathbf{r}}) &+ \varepsilon\left(\bar{H}_1(\hat{\mathbf{r}}) + \mathbf{V}^0_1(\overline{\mathbf{M}}_1)\cdot\bar{H}_0(\hat{\mathbf{r}})\right)\\ &+ \varepsilon^2\Big(\mathbf{V}^0_2(\overline{\mathbf{M}}_1,\overline{\mathbf{M}}_2)\cdot\bar{H}_0(\hat{\mathbf{r}}) + \mathbf{V}^0_1(\overline{\mathbf{M}}_1)\cdot\bar{H}_1(\hat{\mathbf{r}}) + \bar{H}_2(\hat{\mathbf{r}})\Big)\\ &+ \varepsilon^3\Big(\mathbf{V}^2_1(\overline{\mathbf{M}}_1)\cdot\bar{H}_0(\hat{\mathbf{r}})\Big)\\ &+ \varepsilon^4\left(\mathbf{V}^2_2(\overline{\mathbf{M}}_1,\overline{\mathbf{N}}_3,\overline{\mathbf{N}}_4)\cdot\bar{H}_0 + \mathbf{V}^2_1(\overline{\mathbf{N}}_3)\cdot\bar{H}_1\right)\\ &+ \varepsilon^6\Big(\mathbf{V}^4_2(\overline{\mathbf{N}}_3)\cdot\bar{H}_0\Big)\\ &+ \varepsilon^3\iota^{2,\bullet}_{\bar{H}}(\varepsilon,\hat{\mathbf{r}})\,,\end{aligned} \tag{B.2.14}$$

that we compare to

$$\hat{H}^2_\varepsilon(\hat{\mathbf{r}}) = \bar{H}_0(\hat{\mathbf{r}}) + \varepsilon\hat{H}_1(\hat{\mathbf{r}}) + \varepsilon^2\hat{H}_2(\hat{\mathbf{r}}) + \varepsilon^3\iota^2_{\hat{H}}(\varepsilon,\hat{\mathbf{r}})\,, \tag{B.2.15}$$

to deduce

$$\begin{aligned}\hat{H}_1(\hat{\mathbf{r}}) &= \left(\bar{\mathcal{T}}_0\nabla\bar{g}_1\right)\cdot\nabla\bar{H}_0(\hat{\mathbf{r}}) + \bar{H}_1(\hat{\mathbf{r}})\,,\\ \hat{H}_2(\hat{\mathbf{r}}) &= \left(\bar{\mathcal{T}}_0\nabla\bar{g}_2\right)\cdot\nabla\bar{H}_0(\hat{\mathbf{r}}) + \mathcal{V}_2(g_1)(\hat{\mathbf{r}})\,,\end{aligned} \tag{B.2.16}$$

with

$$\mathcal{V}_2(g_1) = \frac{1}{2}\overline{\mathbf{M}}^2_1\cdot\bar{H}_0 + \mathbf{V}^0_1(\overline{\mathbf{M}}_1)\cdot\bar{H}_1 + \bar{H}_2. \tag{B.2.17}$$

The last step of the algorithm consists in solving iteratively equations (B.2.16) with $\bar{g}_1$, $\bar{g}_2$, $\hat{H}_1$ and $\hat{H}_2$ as unknowns. The first equation was tackled in subsection B.2.1 in which we obtain $\bar{g}_1$ and $\hat{H}_1$. So the job is reduced to solve the second equation of (B.2.16). Setting

$$\hat{H}_2(\hat{\mathbf{r}}) = -\frac{1}{2\pi}\int_0^{2\pi}\mathcal{V}_2(g_1)(\hat{\mathbf{r}})\,d\hat{r}_3, \tag{B.2.18}$$

we just have to solve

$$\left(\bar{\mathcal{T}}_0\nabla\bar{g}_2\right)\cdot\nabla\bar{H}_0(\hat{\mathbf{r}}) = u_2, \tag{B.2.19}$$

where u_2 is given by

$$u_2(\hat{\mathbf{r}}) = \mathcal{V}_2(g_1)(\hat{\mathbf{r}}) - \frac{1}{2\pi}\int_0^{2\pi}\mathcal{V}_2(g_1)(\hat{\mathbf{r}})\,d\hat{r}_3. \tag{B.2.20}$$

Hence we obtain

$$\bar{g}_2(\bar{\mathbf{r}}) = -\frac{1}{B(\hat{r}_1,\hat{r}_2)}\int_0^{\bar{r}_3}u_2(\bar{r}_1,\bar{r}_2,s,\bar{r}_4)\,ds. \tag{B.2.21}$$

B.2.3 Formulas for $N = 3$

In this subsection we will apply algorithm 2.5.11 with $N = 3$. The first step of the algorithm consists in injecting expressions of $\mathbf{V}^\varepsilon_1$, $\mathbf{V}^\varepsilon_2$ and $\mathbf{V}^\varepsilon_3$ in

$$\hat{H}^3_\varepsilon(\hat{\mathbf{r}}) = \sum_{n=0}^{3}\left(\sum_{k=0}^{n}\mathbf{V}^\varepsilon_{n-k}\cdot\bar{H}_k\right)(\hat{\mathbf{r}})\,\varepsilon^n + \varepsilon^4\iota^{3,\bullet}_{\bar{H}}(\varepsilon,\hat{\mathbf{r}})\,. \tag{B.2.22}$$

Ordering terms according to their power of ε (second step of the algorithm) we obtain :

$$\begin{aligned}
\hat{H}^3_\varepsilon(\hat{\mathbf{r}}) = \bar{H}_0(\hat{\mathbf{r}}) &+ \varepsilon\left(\bar{H}_1(\hat{\mathbf{r}}) + \mathbf{V}^0_1\big(\overline{\mathbf{M}}_1\big)\cdot\bar{H}_0(\hat{\mathbf{r}})\right)\\
&+ \varepsilon^2\Big(\mathbf{V}^0_2\big(\overline{\mathbf{M}}_1,\overline{\mathbf{M}}_2\big)\cdot\bar{H}_0(\hat{\mathbf{r}}) + \mathbf{V}^0_1\big(\overline{\mathbf{M}}_1\big)\cdot\bar{H}_1(\hat{\mathbf{r}}) + \bar{H}_2(\hat{\mathbf{r}})\Big)\\
&+ \varepsilon^3\Big(\mathbf{V}^2_1\big(\overline{\mathbf{M}}_1\big)\cdot\bar{H}_0(\hat{\mathbf{r}}) + \mathbf{V}^0_3\big(\overline{\mathbf{M}}_1,\overline{\mathbf{M}}_2,\overline{\mathbf{M}}_3\big)\cdot\bar{H}_0(\hat{\mathbf{r}})\\
&\qquad + \mathbf{V}^0_2\big(\overline{\mathbf{M}}_1,\overline{\mathbf{M}}_2\big)\cdot\bar{H}_1(\hat{\mathbf{r}}) + \mathbf{V}^0_1\big(\overline{\mathbf{M}}_1\big)\cdot\bar{H}_2(\hat{\mathbf{r}}) + \bar{H}_3(\hat{\mathbf{r}})\Big)\\
&+ \varepsilon^4\left(\mathbf{V}^2_2\big(\overline{\mathbf{M}}_1,\overline{\mathbf{N}}_3,\overline{\mathbf{N}}_4\big)\cdot\bar{H}_0(\hat{\mathbf{r}}) + \mathbf{V}^2_1\big(\overline{\mathbf{N}}_3\big)\cdot\bar{H}_1(\hat{\mathbf{r}})\right)\\
&+ \varepsilon^6\Big(\mathbf{V}^4_2\big(\overline{\mathbf{N}}_3\big)\cdot\bar{H}_0(\hat{\mathbf{r}})\Big)\\
&+ \varepsilon^7\Big(\mathbf{V}^4_3\big(\overline{\mathbf{M}}_1,\overline{\mathbf{N}}_3,\overline{\mathbf{N}}_4\big)\cdot\bar{H}_0(\hat{\mathbf{r}}) + \mathbf{V}^4_2\big(\overline{\mathbf{N}}_3\big)\cdot\bar{H}_1(\hat{\mathbf{r}})\Big)\\
&+ \varepsilon^9\Big(\mathbf{V}^6_3\big(\overline{\mathbf{N}}_3\big)\cdot\bar{H}_0(\hat{\mathbf{r}})\Big)\\
&+ \varepsilon^4\iota^{3,\bullet}_{\bar{H}}(\varepsilon,\hat{\mathbf{r}}),
\end{aligned} \tag{B.2.23}$$

that is compared to

$$\hat{H}^3_\varepsilon(\hat{\mathbf{r}}) = \bar{H}_0(\hat{\mathbf{r}}) + \varepsilon\hat{H}_1(\hat{\mathbf{r}}) + \varepsilon^2\hat{H}_2(\hat{\mathbf{r}}) + \varepsilon^3\hat{H}_3(\hat{\mathbf{r}}) + \varepsilon^4\iota^3_{\hat{H}}(\varepsilon,\hat{\mathbf{r}}), \tag{B.2.24}$$

so that $\hat{H}_1$ and $\hat{H}_2$ are given by formulas (B.2.16) and $\hat{H}_3$ is given by :

$$\hat{H}_3(\hat{\mathbf{r}}) = \big(\bar{\mathcal{T}}_0\nabla\bar{g}_3\big)\cdot\nabla\bar{H}_0(\hat{\mathbf{r}}) + \mathcal{V}_3(g_1,g_2)(\hat{\mathbf{r}}), \tag{B.2.25}$$

with

$$\mathcal{V}_3(g_1,g_2) = \overline{\mathbf{M}}_1\overline{\mathbf{M}}_2\cdot\bar{H}_0(\hat{\mathbf{r}}) + \frac{1}{6}\overline{\mathbf{M}}^3_1\cdot\bar{H}_0(\hat{\mathbf{r}}) + \mathbf{V}^2_1\big(\overline{\mathbf{M}}_1\big)\cdot\bar{H}_0 \tag{B.2.26}$$

$$+ \mathbf{V}^0_2\big(\overline{\mathbf{M}}_1,\overline{\mathbf{M}}_2\big)\cdot\bar{H}_1 + \mathbf{V}^0_1\big(\overline{\mathbf{M}}_1\big)\cdot\bar{H}_2 + \bar{H}_3. \tag{B.2.27}$$

Eventually the last step of the algorithm consists in solving iteratively the equations (B.2.16) and (B.2.25). The two firsts were tackled in subsection B.2.1 and B.2.2 in which we obtain $\bar{g}_1$, $\bar{g}_2$, $\bar{H}_1$ and $\hat{H}_2$. So the job is reduced to solve equation (B.2.25). Setting

$$\hat{H}_3(\hat{\mathbf{r}}) = -\frac{1}{2\pi}\int_0^{2\pi}\mathcal{V}_3(g_1,g_2)(\hat{\mathbf{r}})\,d\hat{r}_3, \tag{B.2.28}$$

we just have to solve PDE

$$\big(\bar{\mathcal{T}}_0\nabla\bar{g}_3\big)\cdot\nabla\bar{H}_0(\hat{\mathbf{r}}) = u_3, \tag{B.2.29}$$

where u_3 is given by

$$u_3(\hat{\mathbf{r}}) = \mathcal{V}_3(g_1,g_2)(\hat{\mathbf{r}}) - \frac{1}{2\pi}\int_0^{2\pi}\mathcal{V}_3(g_1,g_2)(\hat{\mathbf{r}})\,d\hat{r}_3. \tag{B.2.30}$$

Hence we obtain

$$\bar{g}_3(\bar{\mathbf{r}}) = -\frac{1}{B(\hat{r}_1,\hat{r}_2)}\int_0^{\bar{r}_3}u_3(\bar{r}_1,\bar{r}_2,s,\bar{r}_4)\,ds. \tag{B.2.31}$$

B.2.4 Formulas for $N = 4$

Now we will apply algorithm 2.5.11 with $N = 4$. The first step of the algorithm consists to inject the expression of $\mathbf{V}_1^\varepsilon$, $\mathbf{V}_2^\varepsilon$, $\mathbf{V}_3^\varepsilon$ and $\mathbf{V}_4^\varepsilon$ in

$$\hat{H}_\varepsilon^4(\hat{\mathbf{r}}) = \sum_{n=0}^{4} \left(\sum_{k=0}^{n} \mathbf{V}_{n-k}^\varepsilon \cdot \bar{H}_k \right)(\hat{\mathbf{r}})\, \varepsilon^n + \varepsilon^5 \iota_{\bar{H}}^{4,\bullet}(\varepsilon, \hat{\mathbf{r}}) \tag{B.2.32}$$

According to the second step of the algorithm we order the terms according to their power of ε and we obtain :

$$\begin{aligned}
\hat{H}_\varepsilon^4(\hat{\mathbf{r}}) = {} & \bar{H}_0(\hat{\mathbf{r}}) + \varepsilon \left(\bar{H}_1(\hat{\mathbf{r}}) + \mathbf{V}_1^0(\overline{\mathbf{M}}_1) \cdot \bar{H}_0(\hat{\mathbf{r}}) \right) \\
& + \varepsilon^2 \Big(\mathbf{V}_2^0(\overline{\mathbf{M}}_1, \overline{\mathbf{M}}_2) \cdot \bar{H}_0(\hat{\mathbf{r}}) + \mathbf{V}_1^0(\overline{\mathbf{M}}_1) \cdot \bar{H}_1(\hat{\mathbf{r}}) + \bar{H}_2(\hat{\mathbf{r}}) \Big) \\
& + \varepsilon^3 \Big(\mathbf{V}_1^2(\overline{\mathbf{M}}_1) \cdot \bar{H}_0(\hat{\mathbf{r}}) + \mathbf{V}_3^0(\overline{\mathbf{M}}_1, \overline{\mathbf{M}}_2, \overline{\mathbf{M}}_3) \cdot \bar{H}_0(\hat{\mathbf{r}}) \\
& \qquad + \mathbf{V}_2^0(\overline{\mathbf{M}}_1, \overline{\mathbf{M}}_2) \cdot \bar{H}_1(\hat{\mathbf{r}}) + \mathbf{V}_1^0(\overline{\mathbf{M}}_1) \cdot \bar{H}_2(\hat{\mathbf{r}}) + \bar{H}_3(\hat{\mathbf{r}}) \Big) \\
& + \varepsilon^4 \Big(\mathbf{V}_2^2(\overline{\mathbf{M}}_1, \overline{\mathbf{N}}_3, \overline{\mathbf{N}}_4) \cdot \bar{H}_0(\hat{\mathbf{r}}) + \mathbf{V}_1^2(\overline{\mathbf{N}}_3) \cdot \bar{H}_1(\hat{\mathbf{r}}) \\
& \qquad + \mathbf{V}_3^0(\overline{\mathbf{M}}_1, \overline{\mathbf{M}}_2, \overline{\mathbf{M}}_3) \cdot \bar{H}_1(\hat{\mathbf{r}}) + \mathbf{V}_4^0(\overline{\mathbf{M}}_1, \overline{\mathbf{M}}_2, \overline{\mathbf{M}}_3, \overline{\mathbf{M}}_4) \cdot \bar{H}_0(\hat{\mathbf{r}}) \\
& \qquad + \mathbf{V}_2^0(\overline{\mathbf{M}}_1, \overline{\mathbf{M}}_2) \cdot \bar{H}_2(\hat{\mathbf{r}}) + \mathbf{V}_1^0(\overline{\mathbf{M}}_1) \cdot \bar{H}_3(\hat{\mathbf{r}}) + \bar{H}_4(\hat{\mathbf{r}}) \Big) \\
& + \varepsilon^5 \Big(\mathbf{V}_3^2(\overline{\mathbf{M}}_1, \overline{\mathbf{M}}_2, \overline{\mathbf{N}}_3, \overline{\mathbf{N}}_4, \overline{\mathbf{N}}_5) \cdot \bar{H}_0(\hat{\mathbf{r}}) + \mathbf{V}_2^2(\overline{\mathbf{M}}_1, \overline{\mathbf{N}}_3, \overline{\mathbf{N}}_4) \cdot \bar{H}_1(\hat{\mathbf{r}}) \\
& \qquad + \mathbf{V}_1^2(\overline{\mathbf{N}}_3) \cdot \bar{H}_2(\hat{\mathbf{r}}) \Big) \\
& + \varepsilon^6 \Big(\mathbf{V}_2^4(\overline{\mathbf{N}}_3) \cdot \bar{H}_0(\hat{\mathbf{r}}) + \mathbf{V}_4^2(\overline{\mathbf{M}}_1, \overline{\mathbf{M}}_2, \overline{\mathbf{M}}_3, \overline{\mathbf{N}}_3, \overline{\mathbf{N}}_4, \overline{\mathbf{N}}_5, \overline{\mathbf{N}}_6) \cdot \bar{H}_0(\hat{\mathbf{r}}) \\
& \qquad + \mathbf{V}_3^2(\overline{\mathbf{M}}_1, \overline{\mathbf{M}}_2, \overline{\mathbf{N}}_3, \overline{\mathbf{N}}_4, \overline{\mathbf{N}}_5) \cdot \bar{H}_1(\hat{\mathbf{r}}) + \mathbf{V}_2^2(\overline{\mathbf{M}}_1, \overline{\mathbf{N}}_3, \overline{\mathbf{N}}_4) \cdot \bar{H}_2(\hat{\mathbf{r}}) \\
& \qquad + \mathbf{V}_1^2(\overline{\mathbf{N}}_3) \cdot \bar{H}_3(\hat{\mathbf{r}}) \Big) \\
& + \varepsilon^7 \Big(\mathbf{V}_3^4(\overline{\mathbf{M}}_1, \overline{\mathbf{N}}_3, \overline{\mathbf{N}}_4) \cdot \bar{H}_0(\hat{\mathbf{r}}) + \mathbf{V}_2^4(\overline{\mathbf{N}}_3) \cdot \bar{H}_1(\hat{\mathbf{r}}) \Big) \\
& + \varepsilon^8 \Big(\mathbf{V}_4^4(\overline{\mathbf{M}}_1, \overline{\mathbf{M}}_2, \overline{\mathbf{N}}_3, \overline{\mathbf{N}}_4, \overline{\mathbf{N}}_5) \cdot \bar{H}_0(\hat{\mathbf{r}}) + \mathbf{V}_3^4(\overline{\mathbf{M}}_1, \overline{\mathbf{N}}_3, \overline{\mathbf{N}}_4) \cdot \bar{H}_1(\hat{\mathbf{r}}) \\
& \qquad + \mathbf{V}_2^4(\overline{\mathbf{N}}_3) \cdot \bar{H}_2(\hat{\mathbf{r}}) \Big) \\
& + \varepsilon^9 \Big(\mathbf{V}_3^6(\overline{\mathbf{N}}_3) \cdot \bar{H}_0(\hat{\mathbf{r}}) \Big) \\
& + \varepsilon^{10} \left(\mathbf{V}_4^6(\overline{\mathbf{M}}_1, \overline{\mathbf{N}}_3, \overline{\mathbf{N}}_4) \cdot \bar{H}_0(\hat{\mathbf{r}}) + \mathbf{V}_3^6(\overline{\mathbf{N}}_3) \cdot \bar{H}_1(\hat{\mathbf{r}}) \right) \\
& + \varepsilon^{12} \left(\mathbf{V}_4^8(\overline{\mathbf{N}}_3) \cdot \bar{H}_0(\hat{\mathbf{r}}) \right) \\
& + \varepsilon^5 \iota_{\bar{H}}^{4,\bullet}(\varepsilon, \hat{\mathbf{r}})\,.
\end{aligned} \tag{B.2.33}$$

We compare this expansion with the following desired form

$$\begin{aligned}
\hat{H}^4_\varepsilon(\hat{\mathbf{r}}) &= \bar{H}_0(\hat{\mathbf{r}}) + \varepsilon\hat{H}_1(\hat{\mathbf{r}}) + \varepsilon^2\hat{H}_2(\hat{\mathbf{r}}) + \varepsilon^3\hat{H}_3(\hat{\mathbf{r}}) + \varepsilon^4\hat{H}_4(\hat{\mathbf{r}}) + \varepsilon^5\iota^4_{\hat{H}}(\varepsilon,\hat{\mathbf{r}}) \\
&= \bar{H}_0(\hat{\mathbf{r}}) + \varepsilon\left(\bar{H}_1(\hat{\mathbf{r}}) + \overline{\mathbf{M}}_1\cdot\bar{H}_0(\hat{\mathbf{r}})\right) \\
&\quad + \varepsilon^2\Big(\mathbf{V}^0_2(\overline{\mathbf{M}}_1,\overline{\mathbf{M}}_2)\cdot\bar{H}_0(\hat{\mathbf{r}}) + \mathbf{V}^0_1(\overline{\mathbf{M}}_1)\cdot\bar{H}_1(\hat{\mathbf{r}}) + \bar{H}_2(\hat{\mathbf{r}})\Big) \\
&\quad + \varepsilon^3\Big(\mathbf{V}^2_1(\overline{\mathbf{M}}_1)\cdot\bar{H}_0(\hat{\mathbf{r}}) + \mathbf{V}^0_3(\overline{\mathbf{M}}_1,\overline{\mathbf{M}}_2,\overline{\mathbf{M}}_3)\cdot\bar{H}_0(\hat{\mathbf{r}}) \\
&\qquad + \mathbf{V}^0_2(\overline{\mathbf{M}}_1,\overline{\mathbf{M}}_2)\cdot\bar{H}_1(\hat{\mathbf{r}}) + \mathbf{V}^0_1(\overline{\mathbf{M}}_1)\cdot\bar{H}_2(\hat{\mathbf{r}}) + \bar{H}_3(\hat{\mathbf{r}})\Big) \\
&\quad + \varepsilon^4\Big(\mathbf{V}^2_2(\overline{\mathbf{M}}_1,\overline{\mathbf{N}}_3,\overline{\mathbf{N}}_4)\cdot\bar{H}_0(\hat{\mathbf{r}}) + \mathbf{V}^2_1(\overline{\mathbf{N}}_3)\cdot\bar{H}_1(\hat{\mathbf{r}}) \\
&\qquad + \mathbf{V}^0_3(\overline{\mathbf{M}}_1,\overline{\mathbf{M}}_2,\overline{\mathbf{M}}_3)\cdot\bar{H}_1(\hat{\mathbf{r}}) + \overline{\mathbf{M}}_4\cdot\bar{H}_0(\hat{\mathbf{r}}) + \overline{\mathbf{M}}_1\overline{\mathbf{M}}_3\cdot\bar{H}_0(\hat{\mathbf{r}}) \\
&\qquad + \frac{1}{2}\overline{\mathbf{M}}^2_1\overline{\mathbf{M}}_2\cdot\bar{H}_0(\hat{\mathbf{r}}) + \frac{1}{2}\overline{\mathbf{M}}^2_2\cdot\bar{H}_0(\hat{\mathbf{r}}) + \frac{1}{24}\overline{\mathbf{M}}^4_1\cdot\bar{H}_0(\hat{\mathbf{r}}) \\
&\qquad + \mathbf{V}^0_2(\overline{\mathbf{M}}_1,\overline{\mathbf{M}}_2)\cdot\bar{H}_2(\hat{\mathbf{r}}) + \mathbf{V}^0_1(\overline{\mathbf{M}}_1)\cdot\bar{H}_3(\hat{\mathbf{r}}) + \bar{H}_4(\hat{\mathbf{r}})\Big) \\
&\quad + \varepsilon^5\iota^4_{\hat{H}}(\varepsilon,\hat{\mathbf{r}})\,.
\end{aligned} \tag{B.2.34}$$

Hence, we obtain that $\hat{H}_1$ and $\hat{H}_2$ are given by formulas (B.2.16), $\hat{H}_3$ by formula (B.2.25) and $\hat{H}_4$ by :

$$\hat{H}_4(\hat{\mathbf{r}}) = \left(\bar{\mathcal{T}}_0\nabla\bar{g}_4\right)\cdot\nabla\bar{H}_0(\hat{\mathbf{r}}) + \mathcal{V}_4(g_1,g_2,g_3)(\hat{\mathbf{r}}) \tag{B.2.35}$$

with

$$\begin{aligned}
\mathcal{V}_4(g_1,g_2,g_3) &= \mathbf{V}^2_2(\overline{\mathbf{M}}_1,\overline{\mathbf{N}}_3,\overline{\mathbf{N}}_4)\cdot\bar{H}_0 + \mathbf{V}^2_1(\overline{\mathbf{N}}_3)\cdot\bar{H}_1 \\
&\quad + \mathbf{V}^0_3(\overline{\mathbf{M}}_1,\overline{\mathbf{M}}_2,\overline{\mathbf{M}}_3)\cdot\bar{H}_1 + \overline{\mathbf{M}}_1\overline{\mathbf{M}}_3\cdot\bar{H}_0 \\
&\quad + \frac{1}{2}\overline{\mathbf{M}}^2_1\overline{\mathbf{M}}_2\cdot\bar{H}_0 + \frac{1}{2}\overline{\mathbf{M}}^2_2\cdot\bar{H}_0 + \frac{1}{24}\overline{\mathbf{M}}^4_1\cdot\bar{H}_0 \\
&\quad + \mathbf{V}^0_2(\overline{\mathbf{M}}_1,\overline{\mathbf{M}}_2)\cdot\bar{H}_2 + \mathbf{V}^0_1(\overline{\mathbf{M}}_1)\cdot\bar{H}_3 + \bar{H}_4\Big)
\end{aligned} \tag{B.2.36}$$

Now, the last step of the algorithm consists in solving equations (B.2.16), (B.2.25) and (B.2.35) wit $\bar{g}_1$, $\bar{g}_2$, $\bar{g}_3$, $\bar{g}_4$, $\hat{H}_1$, $\hat{H}_2$, $\hat{H}_3$ and $\hat{H}_4$ as unknowns. The three first equations were processed in subsection B.2.1, B.2.2 and B.2.3 in which we obtain the expressions of $\bar{g}_1$, $\bar{g}_2$, $\bar{g}_3$, $\hat{H}_1$, $\hat{H}_2$, and $\hat{H}_3$. So we just have to solve equation (B.2.35). Setting

$$\hat{H}_4(\hat{\mathbf{r}}) = -\frac{1}{2\pi}\int_0^{2\pi}\mathcal{V}_4(g_1,g_2,g_3)(\hat{\mathbf{r}})\,d\hat{r}_3 \tag{B.2.37}$$

the job is reduced to solve PDE

$$\left(\bar{\mathcal{T}}_0\nabla\bar{g}_4\right)\cdot\nabla\bar{H}_0(\hat{\mathbf{r}}) = u_4, \tag{B.2.38}$$

with $\bar{g}_4$ as unknown, where u_4 is given by

$$u_4(\hat{\mathbf{r}}) = \mathcal{V}_4(g_1,g_2,g_3)(\hat{\mathbf{r}}) - \frac{1}{2\pi}\int_0^{2\pi}\mathcal{V}_4(g_1,g_2,g_3)(\hat{\mathbf{r}})\,d\hat{r}_3. \tag{B.2.39}$$

Hence we obtain :

$$\bar{g}_4(\bar{\mathbf{r}}) = -\frac{1}{B(\hat{r}_1,\hat{r}_2)}\int_0^{\bar{r}_3}u_4(\bar{r}_1,\bar{r}_2,s,\bar{r}_4)\,ds \tag{B.2.40}$$

B.2.5 Formulas for $N = 5$

Presently we will apply algorithm 2.5.11 with $N = 5$. The first step of the algorithm consists to inject the expression of $\mathbf{V}_1^\varepsilon$, $\mathbf{V}_2^\varepsilon$, $\mathbf{V}_3^\varepsilon$, $\mathbf{V}_4^\varepsilon$ and $\mathbf{V}_5^\varepsilon$ in

$$\hat{H}_\varepsilon^5(\hat{\mathbf{r}}) = \sum_{n=0}^{5} \left(\sum_{k=0}^{n} \mathbf{V}_{n-k}^\varepsilon \cdot \bar{H}_k \right) (\hat{\mathbf{r}})\, \varepsilon^n + \varepsilon^6 \iota_{\vec{H}}^{5,\bullet}(\varepsilon, \hat{\mathbf{r}}) \tag{B.2.41}$$

According to the second step of the algorithm we order the terms according to their power of ε and we obtain :

$$
\begin{aligned}
\hat{H}^5_\varepsilon(\hat{\mathbf{r}}) &= \sum_{n=0}^{5}\left(\sum_{k=0}^{n}\mathbf{V}^{\varepsilon}_{n-k}\cdot\bar{H}_k\right)(\hat{\mathbf{r}})\,\varepsilon^n+\varepsilon^6\iota^5_{\hat{H}}(\varepsilon,\hat{\mathbf{r}})\\
&=\bar{H}_0(\hat{\mathbf{r}})+\varepsilon\left(\bar{H}_1(\hat{\mathbf{r}})+\mathbf{V}^0_1\big(\overline{\mathbf{M}}_1\big)\cdot\bar{H}_0(\hat{\mathbf{r}})\right)\\
&\quad+\varepsilon^2\Big(\mathbf{V}^0_2\big(\overline{\mathbf{M}}_1,\overline{\mathbf{M}}_2\big)\cdot\bar{H}_0(\hat{\mathbf{r}})+\mathbf{V}^0_1\big(\overline{\mathbf{M}}_1\big)\cdot\bar{H}_1(\hat{\mathbf{r}})+\bar{H}_2(\hat{\mathbf{r}})\Big)\\
&\quad+\varepsilon^3\Big(\mathbf{V}^2_1\big(\overline{\mathbf{M}}_1\big)\cdot\bar{H}_0(\hat{\mathbf{r}})+\mathbf{V}^0_3\big(\overline{\mathbf{M}}_1,\overline{\mathbf{M}}_2,\overline{\mathbf{M}}_3\big)\cdot\bar{H}_0(\hat{\mathbf{r}})\\
&\qquad+\mathbf{V}^0_2\big(\overline{\mathbf{M}}_1,\overline{\mathbf{M}}_2\big)\cdot\bar{H}_1(\hat{\mathbf{r}})+\mathbf{V}^0_1\big(\overline{\mathbf{M}}_1\big)\cdot\bar{H}_2(\hat{\mathbf{r}})+\bar{H}_3(\hat{\mathbf{r}})\Big)\\
&\quad+\varepsilon^4\Big(\mathbf{V}^2_2\big(\overline{\mathbf{M}}_1,\overline{\mathbf{N}}_3,\overline{\mathbf{N}}_4\big)\cdot\bar{H}_0(\hat{\mathbf{r}})+\mathbf{V}^2_1\big(\overline{\mathbf{N}}_3\big)\cdot\bar{H}_1(\hat{\mathbf{r}})\\
&\qquad+\mathbf{V}^0_3\big(\overline{\mathbf{M}}_1,\overline{\mathbf{M}}_2,\overline{\mathbf{M}}_3\big)\cdot\bar{H}_1(\hat{\mathbf{r}})+\mathbf{V}^0_4\big(\overline{\mathbf{M}}_1,\overline{\mathbf{M}}_2,\overline{\mathbf{M}}_3,\overline{\mathbf{M}}_4\big)\cdot\bar{H}_0(\hat{\mathbf{r}})\\
&\qquad+\mathbf{V}^0_2\big(\overline{\mathbf{M}}_1,\overline{\mathbf{M}}_2\big)\cdot\bar{H}_2(\hat{\mathbf{r}})+\mathbf{V}^0_1\big(\overline{\mathbf{M}}_1\big)\cdot\bar{H}_3(\hat{\mathbf{r}})+\bar{H}_4(\hat{\mathbf{r}})\Big)\\
&\quad+\varepsilon^5\Big(\mathbf{V}^2_3\big(\overline{\mathbf{M}}_1,\overline{\mathbf{M}}_2,\overline{\mathbf{N}}_3,\overline{\mathbf{N}}_4,\overline{\mathbf{N}}_5\big)\cdot\bar{H}_0(\hat{\mathbf{r}})+\mathbf{V}^2_2\big(\overline{\mathbf{M}}_1,\overline{\mathbf{N}}_3,\overline{\mathbf{N}}_4\big)\cdot\bar{H}_1(\hat{\mathbf{r}})+\mathbf{V}^2_1\big(\overline{\mathbf{N}}_3\big)\cdot\bar{H}_2(\hat{\mathbf{r}})\\
&\qquad\mathbf{V}^0_5\big(\overline{\mathbf{M}}_1,\overline{\mathbf{M}}_2,\overline{\mathbf{M}}_3,\overline{\mathbf{M}}_4,\overline{\mathbf{M}}_5\big)\,\bar{H}_0(\hat{\mathbf{r}})+\mathbf{V}^0_4\big(\overline{\mathbf{M}}_1,\overline{\mathbf{M}}_2,\overline{\mathbf{M}}_3,\overline{\mathbf{M}}_4\big)\cdot\bar{H}_1(\hat{\mathbf{r}})\\
&\qquad\mathbf{V}^0_3\big(\overline{\mathbf{M}}_1,\overline{\mathbf{M}}_2,\overline{\mathbf{M}}_3\big)\cdot\bar{H}_2(\hat{\mathbf{r}})+\mathbf{V}^0_2\big(\overline{\mathbf{M}}_1,\overline{\mathbf{M}}_2\big)\cdot\bar{H}_3(\hat{\mathbf{r}})\\
&\qquad\mathbf{V}^0_1\big(\overline{\mathbf{M}}_1\big)\cdot\bar{H}_4(\hat{\mathbf{r}})+\bar{H}_5(\hat{\mathbf{r}})\Big)\\
&\quad+\varepsilon^6\Big(\mathbf{V}^4_2\big(\overline{\mathbf{N}}_3\big)\cdot\bar{H}_0(\hat{\mathbf{r}})+\mathbf{V}^2_4\big(\overline{\mathbf{M}}_1,\overline{\mathbf{M}}_2,\overline{\mathbf{M}}_3,\overline{\mathbf{N}}_3,\overline{\mathbf{N}}_4,\overline{\mathbf{N}}_5,\overline{\mathbf{N}}_6\big)\cdot\bar{H}_0(\hat{\mathbf{r}})\\
&\qquad+\mathbf{V}^2_3\big(\overline{\mathbf{M}}_1,\overline{\mathbf{M}}_2,\overline{\mathbf{N}}_3,\overline{\mathbf{N}}_4,\overline{\mathbf{N}}_5\big)\cdot\bar{H}_1(\hat{\mathbf{r}})+\mathbf{V}^2_2\big(\overline{\mathbf{M}}_1,\overline{\mathbf{N}}_3,\overline{\mathbf{N}}_4\big)\cdot\bar{H}_2(\hat{\mathbf{r}})\\
&\qquad+\mathbf{V}^2_1\big(\overline{\mathbf{N}}_3\big)\cdot\bar{H}_3(\hat{\mathbf{r}})\Big)\\
&\quad+\varepsilon^7\Big(\mathbf{V}^4_3\big(\overline{\mathbf{M}}_1,\overline{\mathbf{N}}_3,\overline{\mathbf{N}}_4\big)\cdot\bar{H}_0(\hat{\mathbf{r}})+\mathbf{V}^4_2\big(\overline{\mathbf{N}}_3\big)\cdot\bar{H}_1(\hat{\mathbf{r}})\\
&\qquad+\mathbf{V}^2_5\big(\overline{\mathbf{M}}_1,\overline{\mathbf{M}}_2,\overline{\mathbf{M}}_3,\overline{\mathbf{M}}_4,\overline{\mathbf{N}}_3,\overline{\mathbf{N}}_4,\overline{\mathbf{N}}_5,\overline{\mathbf{N}}_6,\overline{\mathbf{N}}_7\big)\cdot\bar{H}_0(\hat{\mathbf{r}})\\
&\qquad+\mathbf{V}^2_4\big(\overline{\mathbf{M}}_1,\overline{\mathbf{M}}_2,\overline{\mathbf{M}}_3,\overline{\mathbf{N}}_3,\overline{\mathbf{N}}_4,\overline{\mathbf{N}}_5,\overline{\mathbf{N}}_6\big)\cdot\bar{H}_1(\hat{\mathbf{r}})+\mathbf{V}^2_3\big(\overline{\mathbf{M}}_1,\overline{\mathbf{M}}_2,\overline{\mathbf{N}}_3,\overline{\mathbf{N}}_4,\overline{\mathbf{N}}_5\big)\cdot\bar{H}_2(\hat{\mathbf{r}})\\
&\qquad+\mathbf{V}^2_2\big(\overline{\mathbf{M}}_1,\overline{\mathbf{N}}_3,\overline{\mathbf{N}}_4\big)\cdot\bar{H}_3(\hat{\mathbf{r}})+\mathbf{V}^2_1\big(\overline{\mathbf{N}}_3\big)\cdot\bar{H}_4(\hat{\mathbf{r}})\Big)\\
&\quad+\varepsilon^8\Big(\mathbf{V}^4_4\big(\overline{\mathbf{M}}_1,\overline{\mathbf{M}}_2,\overline{\mathbf{N}}_3,\overline{\mathbf{N}}_4,\overline{\mathbf{N}}_5\big)\cdot\bar{H}_0(\hat{\mathbf{r}})+\mathbf{V}^4_3\big(\overline{\mathbf{M}}_1,\overline{\mathbf{N}}_3,\overline{\mathbf{N}}_4\big)\cdot\bar{H}_1(\hat{\mathbf{r}})+\mathbf{V}^4_2\big(\overline{\mathbf{N}}_3\big)\cdot\bar{H}_2(\hat{\mathbf{r}})\Big)\\
&\quad+\varepsilon^9\Big(\mathbf{V}^6_3\big(\overline{\mathbf{N}}_3\big)\cdot\bar{H}_0(\hat{\mathbf{r}})+\mathbf{V}^4_5\big(\overline{\mathbf{M}}_1,\overline{\mathbf{M}}_2,\overline{\mathbf{M}}_3,\overline{\mathbf{N}}_3,\overline{\mathbf{N}}_4,\overline{\mathbf{N}}_5,\overline{\mathbf{N}}_6\big)\cdot\bar{H}_0(\hat{\mathbf{r}})\\
&\qquad+\mathbf{V}^4_4\big(\overline{\mathbf{M}}_1,\overline{\mathbf{M}}_2,\overline{\mathbf{N}}_3,\overline{\mathbf{N}}_4,\overline{\mathbf{N}}_5\big)\cdot\bar{H}_1(\hat{\mathbf{r}})\\
&\qquad+\mathbf{V}^4_3\big(\overline{\mathbf{M}}_1,\overline{\mathbf{N}}_3,\overline{\mathbf{N}}_4\big)\cdot\bar{H}_2(\hat{\mathbf{r}})+\mathbf{V}^4_2\big(\overline{\mathbf{N}}_3\big)\cdot\bar{H}_4(\hat{\mathbf{r}})\Big)\\
&\quad+\varepsilon^{10}\big(\mathbf{V}^6_4\big(\overline{\mathbf{M}}_1,\overline{\mathbf{N}}_3,\overline{\mathbf{N}}_4\big)\cdot\bar{H}_0(\hat{\mathbf{r}})+\mathbf{V}^6_3\big(\overline{\mathbf{N}}_3\big)\cdot\bar{H}_1(\hat{\mathbf{r}})\big)\\
&\quad+\varepsilon^{11}\Big(\mathbf{V}^6_5\big(\overline{\mathbf{M}}_1,\overline{\mathbf{M}}_2,\overline{\mathbf{N}}_3,\overline{\mathbf{N}}_4,\overline{\mathbf{N}}_5\big)\cdot\bar{H}_0(\hat{\mathbf{r}})+\mathbf{V}^6_4\big(\overline{\mathbf{M}}_1,\overline{\mathbf{N}}_3,\overline{\mathbf{N}}_4\big)\cdot\bar{H}_1(\hat{\mathbf{r}})\\
&\qquad+\mathbf{V}^6_3\big(\overline{\mathbf{N}}_3\big)\cdot\bar{H}_3(\hat{\mathbf{r}})\Big)\\
&\quad+\varepsilon^{12}\big(\mathbf{V}^8_4\big(\overline{\mathbf{N}}_3\big)\cdot\bar{H}_0(\hat{\mathbf{r}})\big)\\
&\quad+\varepsilon^{13}\Big(\mathbf{V}^8_5\big(\overline{\mathbf{M}}_1,\overline{\mathbf{N}}_3,\overline{\mathbf{N}}_4\big)\cdot\bar{H}_0(\hat{\mathbf{r}})+\mathbf{V}^8_4\big(\overline{\mathbf{N}}_3\big)\cdot\bar{H}_1(\hat{\mathbf{r}})\Big)\\
&\quad+\varepsilon^{15}\Big(\mathbf{V}^{10}_5\big(\overline{\mathbf{N}}_3\big)\cdot\bar{H}_0(\hat{\mathbf{r}})\Big)\\
&\quad+\varepsilon^6\iota^{5,\bullet}_{\hat{H}}(\varepsilon,\hat{\mathbf{r}})\,,
\end{aligned}
\tag{B.2.42}
$$

that is compared with

$$
\hat{H}^5_\varepsilon(\hat{\mathbf{r}})=\bar{H}_0(\hat{\mathbf{r}})+\varepsilon\hat{H}_1(\hat{\mathbf{r}})+\varepsilon^2\hat{H}_2(\hat{\mathbf{r}})+\varepsilon^3\hat{H}_3(\hat{\mathbf{r}})+\varepsilon^4\hat{H}_4(\hat{\mathbf{r}})+\varepsilon^5\hat{H}_5(\hat{\mathbf{r}})+\varepsilon^6\iota^5_{\hat{H}}(\varepsilon,\hat{\mathbf{r}})\,,
\tag{B.2.43}
$$

so that $\hat{H}_1$ and $\hat{H}_2$ are given by formulas (B.2.16), $\hat{H}_3$ by formula (B.2.25), $\hat{H}_4$ by formula (B.2.35) and $\hat{H}_5$ by :

$$\hat{H}_5(\hat{\mathbf{r}}) = \big(\bar{\mathcal{T}}_0 \nabla \bar{g}_5\big) \cdot \nabla \bar{H}_0(\hat{\mathbf{r}}) + \mathcal{V}_5(g_1, g_2, g_3, g_4)(\hat{\mathbf{r}})\,, \tag{B.2.44}$$

with

$$\begin{aligned}
\mathcal{V}_5(g_1, g_2, g_3, g_4) = {} & \mathbf{V}_3^2\big(\overline{\mathbf{M}}_1, \overline{\mathbf{M}}_2, \overline{\mathbf{N}}_3, \overline{\mathbf{N}}_4, \overline{\mathbf{N}}_5\big) \cdot \bar{H}_0 + \mathbf{V}_2^2\big(\overline{\mathbf{M}}_1, \overline{\mathbf{N}}_3, \overline{\mathbf{N}}_4\big) \cdot \bar{H}_1 \\
& + \mathbf{V}_1^2\big(\overline{\mathbf{N}}_3\big) \cdot \bar{H}_2 + \overline{\mathbf{M}}_1 \overline{\mathbf{M}}_4 \cdot \bar{H}_0 + \overline{\mathbf{M}}_2 \overline{\mathbf{M}}_3 \cdot \bar{H}_0 + \overline{\mathbf{M}}_1^2 \overline{\mathbf{M}}_3 \cdot \bar{H}_0 \\
& + \frac{1}{2} \overline{\mathbf{M}}_1 \overline{\mathbf{M}}_2^2 \cdot \bar{H}_0 + \frac{1}{6} \overline{\mathbf{M}}_1^3 \overline{\mathbf{M}}_2 \cdot \bar{H}_0 + \frac{1}{120} \overline{\mathbf{M}}_1^5 \cdot \bar{H}_0 \\
& + \mathbf{V}_4^0\big(\overline{\mathbf{M}}_1, \overline{\mathbf{M}}_2, \overline{\mathbf{M}}_3, \overline{\mathbf{M}}_4\big) \cdot \bar{H}_1 \\
& + \mathbf{V}_3^0\big(\overline{\mathbf{M}}_1, \overline{\mathbf{M}}_2, \overline{\mathbf{M}}_3\big) \cdot \bar{H}_2 + \mathbf{V}_2^0\big(\overline{\mathbf{M}}_1, \overline{\mathbf{M}}_2\big) \cdot \bar{H}_3 \\
& + \mathbf{V}_1^0\big(\overline{\mathbf{M}}_1\big) \cdot \bar{H}_4 + \bar{H}_5.
\end{aligned} \tag{B.2.45}$$

Finally the last step of the algorithm consists to solve iteratively the equations (B.2.16), (B.2.25), (B.2.35) and (B.2.44) of unknowns $\bar{g}_1$, $\bar{g}_2$, $\bar{g}_3$, $\bar{g}_4$, $\bar{g}_5$, $\hat{H}_1$, $\hat{H}_2$, $\hat{H}_3$, $\hat{H}_4$, and $\hat{H}_5$. The fourth first equations were tackled in subsection B.2.1, B.2.2, B.2.3 and B.2.4 in which we obtain $\bar{g}_1$, $\bar{g}_2$, $\bar{g}_3$, $\bar{g}_4$, $\hat{H}_1$, $\hat{H}_2$, $\hat{H}_3$ and $\hat{H}_4$. So we just have to solve equation (B.2.44). Setting

$$\hat{H}_5(\hat{\mathbf{r}}) = -\frac{1}{2\pi} \int_0^{2\pi} \mathcal{V}_5(g_1, g_2, g_3, g_4)(\hat{\mathbf{r}})\, d\hat{r}_3, \tag{B.2.46}$$

the job is reduced to solve the PDE

$$\big(\bar{\mathcal{T}}_0 \nabla \bar{g}_5\big) \cdot \nabla \bar{H}_0(\hat{\mathbf{r}}) = u_5, \tag{B.2.47}$$

with $\bar{g}_5$ as unknown, where u_5 is given by

$$u_5(\hat{\mathbf{r}}) = \mathcal{V}_5(g_1, g_2, g_3, g_4)(\hat{\mathbf{r}}) - \frac{1}{2\pi} \int_0^{2\pi} \mathcal{V}_5(g_1, g_2, g_3, g_4)(\hat{\mathbf{r}})\, d\hat{r}_3. \tag{B.2.48}$$

We obtain

$$\bar{g}_5(\bar{\mathbf{r}}) = -\frac{1}{B(\hat{r}_1, \hat{r}_2)} \int_0^{\bar{r}_3} u_5(\bar{r}_1, \bar{r}_2, s, \bar{r}_4)\, ds. \tag{B.2.49}$$

Références bibliographiques

[1] R. Abraham, J. Marsden, and T. Ratiu. *Manifolds, Tensor Analysis, and Applications*. Springer, 1988.

[2] C. Bardos and P. Degond. Global existence for the vlasov-poisson equation in 3 space variables with small initial data. *Annales de l'I.H.P.*, 2(2) :101–118, 1985.

[3] R. Barthelmé. *Le problème de conservation de la charge dans le couplage des équations de Vlasov et de Maxwell*. PhD thesis, Université de Strasbourg, 2005.

[4] C.K. Birdsall and A.B. Langdon. *Plasma Physics via Computer Simulation*. Institute of Physics, Bristol and Philadelphia, 1991.

[5] J. A. Brizard. Nonlinear gyrokinetic Vlasov equation for toroidally rotating axisymmetric tokamaks. *Physics of Plasmas*, 2(2) :459–471, 1995.

[6] L Brouwer. Über abbildung von mannigfaltigkeiten. *Mathematische Annalen*, 71 :97–115, 1912.

[7] H. Cartan. *Théorie élémentaire des fonctions analytiques d'une ou plusieurs variables complexes*. Hermann, 1997.

[8] S. M. Cox and P. C. Matthews. Exponential time differencing for stiff systems. *J. Comput. Phys.*, 176 :430–455, 2002.

[9] A. Crestetto. *Optimisation de méthodes numériques pour la physique des plasmas. Application aux faisceaux de particules chargées*. PhD thesis, Inria Nancy et Université de Strasbourg, 2012.

[10] N. Crouseilles, M. Lemou, and F. Méhats. Asymptotic preserving schemes for highly oscillatory kinetic equations. *J. Comp. Phys.*, 248 :287–308, 2013.

[11] D. H. E. Dubin, J. A. Krommes, C. Oberman, and W. W. Lee. Nonlinear gyrokinetic equations. *Physics of Fluids*, XXVI(12) :3524–3535, 1983.

[12] F. Filbet. *Contribution à l'analyse et la simulation numérique de l'équation de Vlasov*. PhD thesis, Université Henri Poincaré, Nancy, 2001.

[13] F. Filbet and E. Sonnendrücker. Modeling and numerical simulation of space charge dominated beams in the paraxial approximation. *Mathematical Models and Methods in Applied Sciences*, 16(5) :763–791, 2006.

[14] E. Frénod, S. A. Hirstoaga, and M. Gutnic. First order Two-Scale Particle-In-Cell Method for Vlasov Equation. *Esaim : Proceedings*, 38 :348–360, 2011.

[15] E. Frénod, S. A. Hirstoaga, and E. Sonnendrücker. An exponential integrator for a highly oscillatory Vlasov equation. *Discrete Contin. Dyn. Syst. Ser. S*, 2013 (In Press).

[16] E. Frénod and M. Lutz. The Gyro-Kinetic Approximation : an attempt at explaining the method based on Darboux Algorithm and Lie Transform. *Proceeding of Inria Fusion Summer School, September 2011, JLLL, UPMC*.

[17] E. Frénod, P. A. Raviart, and E. Sonnendrücker. Asymptotic expansion of the Vlasov equation in a large external magnetic field. *J. Math. Pures et Appl.*, 80(8) :815–843, 2001.

[18] E. Frénod, F. Salvarani, and E. Sonnendrücker. Long time simulation of a beam in a periodic focusing channel via a two-scale PIC-method. *Mathematical Models and Methods in Applied Sciences*, 19(2) :175–197, 2009.

[19] E. Frénod and E. Sonnendrücker. Homogenization of the Vlasov equation and of the Vlasov-Poisson system with a strong external magnetic field. *Asymp. Anal.*, 18(3,4) :193–214, Dec. 1998.

[20] E. Frénod and E. Sonnendrücker. Long time behavior of the two dimensionnal Vlasov equation with a strong external magnetic field. *Math. Models Methods Appl. Sci.*, 10(4) :539–553, 2000.

[21] E. Frénod and E. Sonnendrücker. The Finite Larmor Radius Approximation. *SIAM J. Math. Anal.*, 32(6) :1227–1247, 2001.

[22] E. A. Frieman and L. Chen. Nonlinear gyrokinetic equations for low-frequency electromagnetic waves in general plasma equilibria. *Physics of Fluids*, 25(3) :502–508, 1982.

[23] X. Garbet, Y. Idomura, L. Villard, and T. H. Watanabe. Gyrokinetic simulations of turbulent transport. *Nuclear Fusion*, 50(4) :043002, 2010.

[24] C. S. Gardner. Adiabatic invariants of periodic classical systems. *Physical Rieview*, 115, 1959.

[25] P. Ghendrih, M. Hauray, and A. Nouri. Derivation of a gyrokinetic model. Existence and uniqueness of specific stationary solutions. *ArXiv e-prints*, April 2010.

[26] F. Golse and L. Saint Raymond. The Vlasov-Poisson system with strong magnetic field. *J. Math. Pures. Appl.*, 78 :791–817, 1999.

[27] V. Grandgirard, M. Brunetti, P. Bertrand, N. Besse, X. Garbet, P. Ghendrih, G. Manfredi, Y. Sarazin, O. Sauter, E. Sonnendrücker, J. Vaclavik, and L. Villard. A drift-kinetic semi-lagrangian 4d code for ion turbulence simulation. *Journal of Computational Physics*, 217(2) :395 – 423, 2006.

[28] V. Grandgirard, Y. Sarazin, P Angelino, A. Bottino, N. Crouseilles, G. Darmet, G. Dif-Pradalier, X. Garbet, Ph. Ghendrih, S. Jolliet, G. Latu, E. Sonnendrücker, and L. Villard. Global full-f gyrokinetic simulations of plasma turbulence. *Plasma Physics and Controlled Fusion*, 49(12B) :B173, 2007.

[29] T. S. Hahm. Nonlinear gyrokinetic equations for tokamak microturbulence. *Physics of Fluids*, 31(9) :2670–2673, 1988.

[30] T. S. Hahm. Nonlinear gyrokinetic equations for turbulence in core transport barriers. *Physics of Plasmas*, 3(12) :4658–4664, 1996.

[31] T. S. Hahm, W. W. Lee, and A. Brizard. Nonlinear gyrokinetic theory for finite-beta plasmas. *Physics of Fluids*, 31(7) :1940–1948, 1988.

[32] T. S. Hahm, Lu Wang, and J. Madsen. Fully electromagnetic nonlinear gyrokinetic equations for tokamak edge turbulence. *Physics of Plasmas*, 16(2) :022305, 2009.

[33] E. Horst. On the classical solution of the initial value problem for the unmodified non-linear vlasov equation. *Math. Meth. in the Appl. Sci.*, 3 :229–248, 1981.

[34] V.I. Istratescu. *Fixed Point Theory an Introduction*. Kluwer Academic Publishers,, 2001.

[35] G. Kawamura and A. Fukuyama. Refinement of the gyrokinetic equations for edge plasmas with large flow shears. *Physics of Plasmas*, 15(4) :042304, 2008.

[36] S. Krantz and H. Parks. *A Primer of Real Analytic Functions*. BirkhÃd'user, 2002.

[37] M. D. Kruskal. *Plasma Physics*, chapter Elementary Orbit and Drift Theory. International Atomic Energy Agency, Vienna, 1965.

[38] W. W. Lee. Gyrokinetic approach in particle simulation. *Phys. Fluids*, 26(2) :556–562, 1983.

[39] Perthame B. Lions, J.-L. Propagation of moments and regularity for the 3-dimensional Vlasov-Poisson system. *Inventiones mathematicae*, 105 :415–430, 1991.

[40] R. G. Littlejohn. A guiding center Hamiltonian : A new approach. *Journal of Mathematical Physics*, 20(12) :2445–2458, 1979.

[41] R. G. Littlejohn. Hamiltonian formulation of guiding center motion. *Physics of Fluids*, 24(9) :1730–1749, 1981.

[42] R. G. Littlejohn. Hamiltonian perturbation theory in noncanonical coordinates. *Journal of Mathematical Physics*, 23(5) :742–747, 1982.

[43] G. Loeper. Uniqueness of the solution to the Vlasov-Poisson system with bounded density. *Journal de Mathematiques Pures et Appliquées*, 86 :68–79, 2005.

[44] Jerrold E. Marsden and Tudor S. Ratiu. *Introduction to Mechanics and Symmetry : A Basic Exposition of Classical Mechanical Systems*. Springer, 1999.

[45] K. R. Meyer and D. Hall, G. R.and Offin. *Introduction to hamiltonian dynamical systems and the N-Body Problem*, volume 90 of *Applied Mathematical Sciences*. Springer, 1979.

[46] T. G. Northrop. The guiding center approximation to charged particle motion. *Annals of Physics*, 15(1) :79–101, 1961.

[47] T. G. Northrop and J. A. Rome. Extensions of guiding center motion to higher order. *Physics of Fluids*, 21(3) :384–389, 1978.

[48] P. J. Olver. *Applications of Lie groups to differential equations*. Graduate Texts in Mathematics. Springer, 2000.

[49] C. Pallard. Moment propagation for weak solutions to the vlasov-poisson system. *Communications in Partial Differential Equations*, 37(7) :1273–1285, 2012.

[50] F. I. Parra and P. J. Catto. Limitations of gyrokinetics on transport time scales. *Plasma Physics and Controlled Fusion*, 50(6) :065014, 2008.

[51] F. I. Parra and P. J. Catto. Gyrokinetic equivalence. *Plasma Physics and Controlled Fusion*, 51(6) :065002, 2009.

[52] F. I. Parra and P. J. Catto. Turbulent transport of toroidal angular momentum in low flow gyrokinetics. *Plasma Physics and Controlled Fusion*, 52(4) :045004, 2010.

[53] K. Pfaffelmoser. Global classical solutions of the Vlasov-Poisson system in three dimensions for general initial data. *J. Diff. Eqns*, 95 :281–303, 1992.

[54] H. Qin, R. H. Cohen, W. M. Nevins, and X. Q. Xu. General gyrokinetic equations for edge plasmas. *Contributions to Plasma Physics*, 46(7-9) :477–489, 2006.

[55] H. Qin, R. H. Cohen, W. M. Nevins, and X. Q. Xu. Geometric gyrokinetic theory for edge plasmas. *Physics of Plasmas*, 14(5) :056110, 2007.

[56] H. Qin, X. Guan, and W. M. Tang. Variational symplectic algorithm for guiding center dynamics and its application in tokamak geometry. *Physics of Plasmas*, 16, 2009.

[57] J. M. Rax. *Physique des plasmas-Cours et applications*. Dunod, 2005.

[58] G. Rein. *Collisionless Kinetic Equations from Astrophysic–The Vlasov-Poisson system*. Elsevier, 2005.

[59] Tomas Roubicek. *Nonlinear Partial Differential Equations with Applications*, volume 153 of *International Series of Numerical Mathematics*. Birkhauser, 2010.

[60] E. Sonnendrücker. *Approximation numérique des équations de Vlasov-Maxwell*, 2008.

[61] S. Ukai and T. Okabe. On classical solutions in the large in time two-dimensional Vlasov's equation. *J. Math.*, 15 :245–261, 1978.

[62] C. Villani. *Landau Damping, Notes de cours du CEMRACS*, 2010.

Mathieu Lutz

Étude mathématique et numérique d'un modèle gyrocinétique incluant des effets électromagnétiques pour la simulation d'un plasma de Tokamak.

Résumé

Cette thèse propose différentes méthodes théoriques et numériques pour simuler à coût réduit le comportement des plasmas ou des faisceaux de particules chargées sous l'action d'un champ magnétique fort. Outre le champ magnétique externe, chaque particule est soumise à champ électromagnétique créé par les particules elles-mêmes. Dans les modèles cinétiques, les particules sont représentées par une fonction de distribution f(x,v,t) qui vérifie l'équation de Vlasov. Afin de déterminer le champ électromagnétique, cette équation est couplée aux équations de Maxwell ou de Poisson. L'aspect champ magnétique fort est alors pris en compte par un adimensionnement adéquat qui fait apparaître un paramètre de perturbation singulière $1/\varepsilon$.

Equation de Vlasov – Modélisation des plasmas – Modèles gyro-cinétiques – Rayon de Larmor fini – Approximation centre-guide – Simulations numériques – Méthodes PIC – Schémas ETD – Méthodes numériques multi-échelles

Résumé en anglais

This thesis is devoted to the study of charged particle beams under the action of strong magnetic fields. In addition to the external magnetic field, each particle is submitted to an electromagnetic field created by the particles themselves. In kinetic models, the particles are represented by a distribution function f(x,v,t) solution of the Vlasov equation. To determine the electromagnetic field, this equation is coupled with the Maxwell equations or with the Poisson equation. The strong magnetic field assumption is translated by a scaling wich introduces a singular perturbation parameter $1/\varepsilon$.

Vlasov-Poisson Equation – Plasma modeling – Gyro-kinetic – Finite Larmor Radius – Guiding-Center Approximation – Numerical Simulations – Particle-In-Cell – ETD Schemes– Multiscale numerical model